AD-A275 588

DTIC ACCESSION NUMBER

LEVEL

INVENTORY

①

AGARD-LS-194

DOCUMENT IDENTIFICATION

Dec 93

DISTRIBUTION STATEMENT A

Approved for public release.
Distribution Unlimited

DISTRIBUTION STATEMENT

ACCESSION FOR
NTIS	GRA&I	☑
DTIC	TRAC	☐
UNANNOUNCED		☐
JUSTIFICATION		

BY
DISTRIBUTION/
AVAILABILITY CODES
| DISTRIBUTION | AVAILABILITY AND/OR SPECIAL |
| A-1 | |

DISTRIBUTION STAMP

DTIC QUALITY INSPECTED 5

DTIC
ELECTE
FEB 9 1994
C D

DATE ACCESSIONED

DATE RETURNED

DATE RECEIVED IN DTIC

9403208

23170

REGISTERED OR CERTIFIED NUMBER

DTIC FORM 70A

DOCUMENT PROCESSING SHEET

PREVIOUS EDITIONS MAY BE USED UNTIL
STOCK IS EXHAUSTED

94 2 01 014

AGARD

ADVISORY GROUP FOR AEROSPACE RESEARCH & DEVELOPMENT

7 RUE ANCELLE 92200 NEUILLY SUR SEINE FRANCE

AGARD LECTURE SERIES 104

Research and Development of Ram/Scramjets and Turboramjets in Russia

(La Recherche et le Développement des Statoréacteurs,
des Statoréacteurs à Combustion Supersonique
et des Turbostatoréacteurs en Russie)

*The material in this publication was assembled to support a Lecture Series
under the sponsorship of the Propulsion and Energetics Panel and the
Consultant and Exchange Programme of AGARD presented on
1st—2nd December 1993 in Laurel, Maryland, United States,
13th—14th January 1994 in Köln, Germany and 17th—18th January 1994
in Paris, France.*

NORTH ATLANTIC TREATY ORGANIZATION

AGARD

ADVISORY GROUP FOR AEROSPACE RESEARCH & DEVELOPMENT

7 RUE ANCELLE 92200 NEUILLY SUR SEINE FRANCE

AGARD LECTURE SERIES 194

Research and Development of Ram/Scramjets and Turboramjets in Russia

(La Recherche et le Développement des Statoréacteurs,
des Statoréacteurs à Combustion Supersonique
et des Turbostatoréacteurs en Russie)

North Atlantic Treaty Organization
Organisation du Traité de l'Atlantique Nord

94 2 01 014

The Mission of AGARD

According to its Charter, the mission of AGARD is to bring together the leading personalities of the NATO nations in the fields of science and technology relating to aerospace for the following purposes:

— Recommending effective ways for the member nations to use their research and development capabilities for the common benefit of the NATO community;

— Providing scientific and technical advice and assistance to the Military Committee in the field of aerospace research and development (with particular regard to its military application);

— Continuously stimulating advances in the aerospace sciences relevant to strengthening the common defence posture;

— Improving the co-operation among member nations in aerospace research and development;

— Exchange of scientific and technical information;

— Providing assistance to member nations for the purpose of increasing their scientific and technical potential;

— Rendering scientific and technical assistance, as requested, to other NATO bodies and to member nations in connection with research and development problems in the aerospace field.

The highest authority within AGARD is the National Delegates Board consisting of officially appointed senior representatives from each member nation. The mission of AGARD is carried out through the Panels which are composed of experts appointed by the National Delegates, the Consultant and Exchange Programme and the Aerospace Applications Studies Programme. The results of AGARD work are reported to the member nations and the NATO Authorities through the AGARD series of publications of which this is one.

Participation in AGARD activities is by invitation only and is normally limited to citizens of the NATO nations.

Abstract

Russia has a long tradition of achievement in ramjet research and development. This tradition, and aspirations toward new and effective products, have led to establish Russian priority in the ramjet field.

This Lecture Series will present and discuss the scientific problems of the development of ramjets/scramjets and turboramjets.

Some specific aspects of liquid/solid ramjet development, the concepts of LH2 high efficiency RAM combustors, the results of full scale turboramjet testing, scramjet or CFD analyses and their ground flight tests will be studied.

This Lecture Series, endorsed by the Propulsion and Energetics Panel of AGARD, has been implemented by the Consultant and Exchange programme.

Abrégé

Il existe en Russie une longue tradition de réalisations dans le domaine de la recherche et le développement des statoréacteurs. Ces traditions et ces ambitions de produits nouveaux et efficaces ont contribué à l'établissement de la primauté russe dans le domaine des statoréacteurs.

Ce cycle de conférences présente et expose les problèmes scientifiques posés par le développement des statoréacteurs, des statoréacteurs à combustion supersonique et des turboréacteurs.

La conférence étudiéra certaines particularités du développement des statoréacteurs liquide/solide, les concepts des chambres de combustion RAM LH2 à rendement élevé, les résultats des essais des turboréacteurs à grandeur réelle, les statoréacteurs à combustion supersonique, les analyses à l'aide de l'aérodynamique numérique et les essais au sol.

Ce cycle de conférences est présenté dans le cadre du programme des Consultants et des Echanges, sous l'égide du Panel AGARD de Propulsion et d'Energétique.

List of Authors/Speakers

Lecture Series Director: Prof. V. Sosounov
CIAM (Central Institute of
Aviation Motors)
Aviamotornaya Street 2
111250 Moscow
Russia

Dr V. Kopchenov
CIAM (Central Institute of
Aviation Motors)
Aviamotornaya Street 2
111250 Moscow
Russia

Dr A. Roudakov
CIAM (Central Institute of
Aviation Motors)
Aviamotornaya Street 2
111250 Moscow
Russia

Dr M.M. Tskhovrebov
CIAM (Central Institute of
Aviation Motors)
Aviamotornaya Street 2
111250 Moscow
Russia

Contents

INTRODUCTION AND OVERVIEW

by

Prof., D.Sc. V.SOSOUNOV
CIAM (Central Institute of Aviation Motors)
2, Aviamotornaya St.
111250 MOSCOW
RUSSIA

SUMMARY OF LECTURE SERIES.

Ramjets, turboramjets and scramjets are studied very intensively in many advanced countries as very effective propulsion for missiles and high velocity planes including aerospace planes during their acceleration in the atmosphere.

All these types of airbreathing engines have the similar elements: ram ducts. That fact allows us to unite the discussion on R & D problems of all these engines in the frame of the Lecture Series.

Russia has quite large experience in research and development of high velocity airbreathing engines for unmanned vehicles and future aero- and aerospace planes. This experience is connected first of all with ramjets or combined engines having ramjet duct, and also with the use of solid, liquid and hydrogen fuels.

The traditions of ramjet development go back to prewar period and to the afterwar aspiration to new achievements which led to well known Russian priority in ramjet field. The short historical overview as well as the survey of the contemporary state of high speed engines R & D in Russia are given in this overview lecture.

The following part of Lecture Series is devoted to discuss the result of R & D of solid propellant ramrockets, liquid fuel ramjets and experimental hydrogen ram combustors.

The next lectures are devoted to turboramjets. The results of the large program of investigation of the features and performance of experimental full scaled turboramjets developed at CIAM are discussed. The second stage of aerospace plane acceleration to Mach number 10 - 12 (and more) many connect now with the use of scramjet engines, which are studied in the next two parts of Lecture Series. In the first of them the features and performances of scramjets and also the result of their ground and flight tests are discussed. The last part of Lecture Series is devoted to Scramjet CFD methods and analyses results review.

NOMENCLATURE

D,d - diameter;
H - altitude;
H_u - mass heat of combustion;
H_v - volumetric heat of combustion;
I - mass specific impulse;
I_v - volumetric specific impulse;
L - length;
M - mach number;
P - pressure;
T - temperature;
t - time;
v - flight velocity;
V - volume;
w - air, gas velocity;

ABBREVIATIONS

ABE - airbreathing engines;
ASP - aerospace plane;
ATR - airturborocket;
DMSCRJ - dual mode scramjet;
FD - flying distance;
FV - flying vehicle;
I - mass specific impulse;
JP - hydrocarbon fuel, kerosene;
J_v - volumetric specific impulse;
LFRJ - liquid fuel ramjet;
LH_2 - liquid hydrogen;
LR - liquid rocket;
PR - pressure ratio;
PS - propulsion system;
RJ - ramjet engine;
SCRJ - scramjet;
SCRJ-R - scram-rocket engine;
SFC - specific fuel consumption;
SPRR - solid propellant ramrocket;
SR - solid rocket;
SSTO - Single stage to orbit ASP;
TF - turbofan;
TRJ - turboramjet engine;
TSTO - Two stage to orbit ASP.

1. INTRODUCTION

It is well know that the use of ram/scramjet principle permit to broaden the sphere of airbreathing engines application to the high and hypersonic flight speeds area especially when using H_2- fuel (Fig. 1.1).

Ram propulsion can be divided into three groups which characterized by type of engine, fuels and application (Fig. 1.2):

1. Ramjets or ramrockets for missiles which equipped with power boosters. They use liquid fuels (LFRJ) or solid propellants (SPRR). The possible Mach number flight range extends from 1,5 - 2 to 3 - 4,5.

2 Combined engines (TRJ, ATR and others) with ram duct. The gasturbine core engine of them usually is switching off near the flight Mach number of 3. The maximum flight Mach number of ram duct work extends up to 4 - 4,5 by using of kerosene and up to 6 - 7 by using cryogenic (LH_2) fuel which has big cooling capacity. Their application may be on hypersonic cruise aircraft or on aerospace planes for the first stage of their acceleration.

3. Supersonic combustion ramjets using LH_2 have the operating Mach number range from 5 - 6 (dual mode sub/supersonic combustion SCRJ: from 3 - 4) up to 10 - 15 and more if the oxygen boosting is used. The application of such engines may be realized on hypersonic cruise or aerospace planes. Scramjets can power hypersonic cruise missiles when using heavy liquid fuels, for instance endothermic hydrocarbon fuels. In such case the FV cooling problems restrict the maximum value of flight Mach number on 6 - 7 limit.

The first group of ram propulsion is in quite wide service or under development on different missiles, but the second and the third groups of engines are on different stages of scientific study, research and development.

Unlike the aviation gasturbine engines the use of ram propulsion connects with application of different kinds of fuels: from common kerosene to slush, solid propellants and cryogenic fuels, such as LH_2 and CH_4. This problem must be overviewed [12].

Mendeleev Table of chemical elements gives us only 7 elements with the mass heat of combustion Hu > 25 MJ/kg (Fig. 1.3). Hydrogen, beryllium and boron have the most mass heat of combustion, and boron, beryllium, carbon and metals: aluminium and magnesium - the most volumetric heat of combustion.

The mass heat of combustion Hu is preferable for large-size FV and volumetric Hv - for small-size FV (so called "low-volume"), as by the geometric similarity the relative vehicle volume is proportional to the characteristic size:

V ~ D (Fig. 1.4). Here boron is beyond the concurrence.

The above mentioned elements can be used as fuels directly either in chemical compounds or mechanical mixtures each with other (Fig. 1.5).

For the manned FV it is practically reasonable to use hydrogen and hydrocarbons as fuels. In the past (in the 50s) they attempted to use the borohydrides in the aircraft but the toxicity of these fuels and the viscous boron oxide formation while burning made attempts unreal.

For small unmanned FV, that is for ramjet powered missiles, more heavy fuels are suitable such as heavy and synthetic hydrocarbons, solid fuels with metals (Al, Mg) or boron as the components. It is possible, in principle, to use the boron as a powder, or as a slush of boron powder in kerosene, or as a liquid hydrocarbon chemical compound.

The above mentioned three ram propulsion groups are overviewed below.

2. RAM PROPULSION FOR MISSILES

Short Historical Review

Ramjet as the simplest type of airbreathing engine which has low value of fuel consumption during the flight in the atmosphere in comparison with rocket engine long since attract the attention of scientists and engineers in many countries.

The first ramjet idea was offered in France by Rene Lorin in 1913 [1]. In Russia the base of ramjet airbreathing engine theory was developed in 1929 by B.S. Stechkin [2], who became afterwards famous scientist in the aviation gasturbine engine field, academician.

The first actions devoted to development of experimental ramjets began in Russia before the War II. At the beginning of 30s Professor Yu.A. Pobedonostsev was testing the ramjets on artillery projectiles. The first development and flight testing of subsonic ramjet were done by engineer I. Merkulov in 1939. The engine was attached to the flying-bed aircraft and ignited in flight.

At the War II end period the work on ramjet development was continued, and in 1944 it was been concentrated at special Design Bureau headed by Chief Designer M.M. Bondaryuk. M.M. Bondaryuk who had the great talent as a designer-organizer and scientist has created high qualified team, scientific and

designer's school, that permitted to develop some effective ramjet-systems and afterwards to summarize the ramjet development experience in some books, one of which, written by M.M. Bondaryuk and S.M. Iljashenko, [3] is well known in the world.

The scientific heritage of M.M. Bondaryuk is quite broad (Fig. 1.6):
- development of basic ramjet theory, methods of its calculation and design;
- study of duct gas dynamics: supersonic intakes, ram combustors, controlled jet nozzles;
- effective fuel-air mixing, flame stabilization and combustion;
- research of different energy sources: chemical and nuclear;
- methodology of ramjets development, ground and flight testing.

Pre-war initial activity, the Bondaryuk Design Bureau actions, the activity of the following Design Bureaus, the powerful CIAM, Ts$_{AGI}$ and other institutes scientific support have created the great Russian traditions and priority in ramjets field.

Later in 60s - 80s the developments of ramjets ramrockets systems were carried out in several Design Bureaus.

The basic knowledge on ramjets and ramrockets one can have got from references [1...6].

First Ramjet Generations

The description of ramjet missile generations given by B. Crispin [8] divided the generations by the grade of propulsion/missile dart integration (Fig. 1.7).

The first generation of missile has the ramjet nacelles outside the dart. Russia has not missiles of such types. The second generation of missiles has integrated ramjet and missile dart, but boosters are mounted externally in tandem or parallel position.

Russian operational surface to air missile of second generation SA-4 GANEF* using kerosene ramjet is well know [21]. It has circular intake with long forebody and shorter air duct between inlet and combustion chamber than the missile with tip intake. This layout is better for guidance system arrangement and maintenance but there are some troubles by flight on big angles of

---

* NATO code

---

attack. Ramjet of this missile was developed at Bondaryuk Bureau.

There is not so known another Russian ramjet missile of the second generation: the "Burya" Mach 3 class large cruise missile (Fig. 1.8). The cruise missile was designed for an intercontinental range and had the total weight of 130-ton class [10]. Two liquid boosters were installed under missile's delta wing. The ramjet engine, designed by M.M. Bondaryuk, was integrated in the fuselage of 19 meters length and had a tip intake, connected with the combustion chamber by a long cylindrical duct. Around the duct was displaced a ring-shaped kerosene tank.

The ramjet had 3-shock high efficient inlet and subsequent launches showed reliable action of ignition system and efficient fuel burning.

The "Burya" cruise missile development began in 1954, and since 1957 were carried out many launches, but despite of successful flight tests this splendid project was stopped after successful launch of the Russian R7 intercontinental ballistic missile.

Despite of its cancellation the "Burya" project gave the large technology experience especially in ramjet field.

New Generation of Full Integrated Ramjets

The first missile of the third generation which used low volume full integrated ram/rocket construction was the Russian low altitude surface-to-air system ZRK-SD Kub (3M9) well know as SA-6 "Gainful" in NATO code [21].

Shown in the Fig. 1.7 and 1.9 the missile SA-6 has an integral ram/rocket propulsion. The solid propellant insert booster grain accelerates the missile for 4 second to a speed of Mach 1.5. Then after ejection of booster rocket nozzle missile is propelled by a solid-propellant ramrocket sustainer, which is fed with ram air from four inlets installed along the dart. For 22.5 seconds maximum speed is reached, according to Mach number of 2.8 [21].

Being for the long time in worldwide service the SA-6 missile was developed by the Toropov Design Bureau in cooperation with TsAGI, CIAM and other organizations and in the middle of 60s has gone to mass production [9].

The SA-6 missile has opened the new stage of ramjet propulsion development. Now the low volume integral ram/rockets become more compatible with rocket propulsion on different

types of missiles. The SA-6 is now the unique ram propulsion system using solid propellant ramrocket type as the sustainer.

The low volume ramjet propulsion of integral type is characterized by four main principles (Fig. 1.10):

1. Full integration of propulsion and flying vehicle in unit dart. One, two, four intakes are installed laterally an the dart.

2. Ram combustor and booster (grain or case with grain) are combined.

3. Use of liquid or solid fuels with high value of volumetric heat of combustion.

4. Use of ejection action of sustained solid propellant in ramrocket to increase the front area specific thrust.

As it has been shown (see Fig. 1.4) the SPRR using heavy solid propellants with high volumetric heat capacity are more suitable for rather small missiles needed more simple operation conditions. But the last requirement may lead to SPRR appliance on much more bigger vehicles.

The examples of third generation of air-to-surface missiles with integral liquid fuel ramjets are shown in the Fig. 1.11 [9]: Russian Kh-31P, French ASMP, both are in service, and French/Germanic ANC is in development stage. The solidity of these missiles construction is very impressive.

The common view of Russian Kh-31P missile is shown in the Fig. 1.12. There was developed in Russia another bigger anti ship missile with rocket/ramjet propulsion system: so called ASM - MSS, which has air launch and surface launch variants [22]. The ASM - MSS as well as the Kh - 31P propulsion systems were developed by Soyuz Turaevo Machine Design Bureau, the successor of the Bondaryuk Design Bureau.

R&D of Integral Ramjet/Ramrocket Problems

As the integral ramjets/ramrockets are the new combined systems, there are many variants of their construction and many problems of their development and testing.

We will not touch upon an aerodynamic problems and intakes arrangement peculiarities because it is not the subject of this lecture series. Many such problems were described in details in the previous AGARD Lecture Series No 136, 1984. The engine internal processes are of our main interest.

Some scientific problems of integral solid propellant ramrockets development must be analyzed, such as:

- Integration of ram- combustor and booster.

- Energy capabilities of different ramjet solid propellants and their application.

- Effectiveness of gasified fuel combustion in ram combustor and fuel supply devices [20].

- Methodology of model and full scaled ram/rocket systems ground testing [20].

- Possibilities of ramrocket improving by fuel flow rate control ... and others.

Some problems of integral liquid fuel ramjets development must be studied:

- The integration of ramjet combustor and solid rocket booster.

- Duct flow instability during the ejection of booster case.

- Fuel supply devices and effectiveness of combustion in ramjet.

- Efficient adaptive control of ramjet on different trajectories of flight.

The integral ramjet/ramrocket systems are one of the most promising propulsion for missiles of different type. Longer range, adaptive value of thrust by flight at different altitudes, bigger mean trajectory speed of missile, that are the main advantages given by integral ram propulsion.

3. PROPULSION FOR HIGH VELOCITY FLIGHT

Creation possibility of reusable aerospace systems (two stage variant) and their ABF propulsion was under intensive study from the beginning of 60s. However only at last years the progress in aviation, astronautics, propulsion, materials made real the programs of research and development in this field. The tempting goal to create in the next century the aerospace system (especially single stage one) inspired scientists and designers in many countries. The ASP projects have been proposed in the USA, the UK, Germany, Russia and are developing in some other countries (France, Japan, and other).

New goals gave the power impulse to research and development of combined and ramjet engines for high supersonic and hypersonic speed flight. The results of theoretical and experimental research of such types engines which was conducted in CIAM and other organizations in Russia at 60 - 90s, are the base experience for start of new stage of practical action [11]. This experience includes:

- conceptual theoretical investigations of aerospace planes and their combined propulsion systems of different type using liquid hydrogen;

- the works round directed on developing and investigation of experimental turboramjets using hydrocarbon fuels;

- experimental works complex intended to solve practical problems of using LH_2 in airbreathing engines, such as hydrogen supply and effective burning, developing of turbofan engine using cryogenic fuels: hydrogen and methane, flights of experimental "hydrogen" aircraft with this engine;

- the search of rational scramjet types, mathematical modeling of processes in its ducts, model scramjets research on ground test facilities, the first flight tests of model scramjets.

Propulsion System Concepts for Aerospace Plane

The CIAM with TsAGI and other aviation industry organizations [14] carry out investigations of propulsion systems for various types of aerospace vehicles (Fig. 1.13):

- single stage earth-to-orbit vehicles (similar "NASP");

- two stage vehicles (similar "Sanger");

- two stage vehicles (orbit plane launch from subsonic heavy aircraft). These vehicles are intended for transport of payload to near-earth orbit [11].

The single stage earth-to-orbit vehicle can be provided with alternative propulsion systems such as ATR with gas generator of expander cycles; turboramjet, turbofanramjet - for first phase of acceleration (O < M < 3-6). For greater Mach numbers (from M = 3...5 to M = 12...15) application of scramjet-rocket is assumed. Further, up to orbit velocities vehicle will be powered by liquid rocket engines.

For the first stage of two stage vehicles such types of engines as turboramjet with through-flow-cycle or combined turbojet+dual mode scramjet can be proposed. The second stage of TSTO is powered with liquid rocket engines.

The first stage of two-stage vehicle based on subsonic aircraft "MRIA" is powered by turbofan engines D18T. For second stage liquid rocket engine are envisaged.

The final choice of PS for aerospace plane must be done on base of analysis and optimization of various concepts and some practical consideration.

For efficiency analysis of alternative propulsion system concepts the complex program (vehicle synthesis and analysis) was created in CIAM. This software complex makes it possible the optimization of following components:

- acceleration-climb trajectory with account to limitations for dynamic pressure, aerothermodynamic, acceleration loads, etc.;

- operation regimes of engines (fuel/air ratio, range of Mach numbers);

- main engine cycle parameters;

- engine and vehicle matching parameters (thrust to total weight ratio, wing loading, engine static thrust per unit inlet area, inlet to wing area ratio)

The modern mathematical methods of optimization are used.

Engine Types for the First Stage of ASP Acceleration

The propulsion of ASP on the first stage of acceleration up to M = 5-7 can not be realized with engines of conventional type by two reasons.

The first is more broad region of flight Mach number. The use of combined engine must be the necessity

The second is the use of LH_2-fuel on ASP. The unique properties of LH_2, such as great heat of combustion, big cooling capacity and high energy capacity as a working medium, allow us to study and develop a great number of new types of LH_2 - ABE with complex thermodynamic cycles having a substantially better characteristics and parameters - specific thrust, specific impulse, thrust/weight ratio, maximum flight speed, and with possibilities of engine components cooling

All such engines must be provided by ram duct. From the end of 50-s in various countries and companies (in CIAM also) there was an intensive work for searching the optimal types of combined propulsion system using conventional fuel and LH_2 for high Mach number cruise FV and ASP. The principal review of this problem was done in monograph [6] and some results were published in many previous and contemporary works, for example [15], [16].

Typical schemes of engines for ASP acceleration up to M = 5...7, for landing, maneuvering and for ferrying are shown in Fig. 1.14. The variants of airturborocket, turbofan and turboramjet engines are studied on present time. The choice of engine type depend on many factors: working range, required dimension-mass and thrust-fuel consumption performance, technology capabilities.

CIAM Experimental Turboramjets [11] [17] [18]

The ground tests of experimental full-scale turboramjets were carried out at CIAM in 70-80s. The experimental turboramjet engines was assembled from units of soviet series produced TJ and TF engines (Fig. 1.15). The deep theoretical researches of turboramjet performances, structures and application possibilities were carried out before experimental work beginning [7].

Experimental investigations was carried out at CIAM special cell with high speed flight conditions simulation (M_{max} = 4-4,5). This cell was equipped with inlet air heating and ejector exhaust systems. Experimental turboramjets testing parameters of inlet air were T = 288-1000 K, P = 0.1-0.2 MPa.

The main goals of experimental research were:
- complex study of operation,
- afterburner and ramjet combustor operation,
- engines switching modes (M = 3) and operation stability,
- windmilling mode,
- passage hydraulic characteristics
- power output possibilities,
- ramjet operation mode characteristics (M > 2.5),
- ramjet combustor and nozzle cooling at M = 3.5-4.5,
- cooling system impact on thrust and SFC,
- structure heat state and transmission operability.

In Fig. 1.16 are shown the results of turboramjet transient mode experimental research. This process is needed of special control of bypass switching device and engine nozzle area to avoid unstable operation and surge of engine.

This work was intended for cruise FV using conventional JP-fuel. But inspire of this matter the experience gained in this unique experimental round may be very useful by solving ASP power system problems.

LH$_2$ - Use in ABE and FV Experience

We have realized some programs to solve the problems of using hydrogen in ABE devoted to subsonic and supersonic FV. These programs were coordinated by CIAM as the head organization. Main results were discussed in previous author papers [12] [13]. Here they will be briefly overviewed:

1). The investigations round of model afterburning and ramjet direct-flow combustion chambers with H_2 - gasifying fuel diffusion combustion in subsonic flow with solving such problems as:
- flame stabilization behind fuel nozzle edge;
- ignition and flame spread to all nozzle;
- increase of nozzles number and chamber length reduction;
- separate combustion without confluence of flames;
- uniform spread of fuels and air in chamber section.

While meeting this conditions the combustion chamber using the hydrogen can be made 2-2.5 times as short as a combustor using the kerosene with high burning completeness (Fig. 1.17).

2). R&D of LH$_2$ - engine fuel feed system as a complex of systems and aggregates which functions are full feeding and control of the engine at all stages of its operation. Two classes of such systems were researched: open loop and closed loop schemes. The first one was developed and applied to experimental LH$_2$ - engine of Samara Scientific-Production Association (SSPA) "Trud".

3). The creation of experimental LH$_2$-turbofan NK-88 at the Design bureau of academician N.D. Kuznetsov (SSPA "Trud") with CIAM co-operation. This engine based on the NK-8-2U turbofan which is used on Tu-154 aircraft. It has such main hydrogen aggregates (Fig. 1.18): turbopump, heat exchanger - LH$_2$ gasificator, multi-nozzle combustion chamber equipped with special H$_2$-air nozzle modules of selected type, and also special hydrogen equipment: tubes, valves, container, safety protection system and so on. The NK-88 can be easily converted for running on the liquid natural gas (methane).

4). The creation of experimental "hydrogen" aircraft Tu-155 in design bureau of academician A.A. Tupolev using one NK-88 turbofan. Special tank, fuel supply and safety protection systems, airfield complex were developed.

The Tu-155 aircraft (Fig. 1.19) in the rear fuselage part has a special section in which the liquid hydrogen tank of volume 18 m^3 and fuel systems are located. For the sake of safety in case of possible hydrogen leakage the fuel section is either filled with nitrogen or continuously purged with air from the conditioning system of the aircraft. The aircraft has a helium system too,

which is used for pipeline scavenging as well as for valve control of hydrogen fuel system.

Flying tests were carried out after completion of the durable ground bench tests of the engine and the individual elements of the fuel system and also functional check of the whole aboard hydrogen complex with a running engine as a whole.

The Tu-155 with one engine using the hydrogen, made its first historic flight on April 15, 1988. The first flight lasted 21 minutes. The following test flights lasted twice as much. Next year on January 18, 1989 the same modified aircraft named as Tu-156 has made the first flight with one engine NK-89 running on liquid methane.

Successful flight tests of the experimental vehicles showed the validity of the accepted technical principles and approaches for their developing. In such a way the investigations on using the alternative fuels in the aviation being under way in Russia for more than twenty recent years have given the practical results.

The experience on hydrogen engines, their special components, aircraft and air field systems obtained in above mentioned works can be used in development of ASP first stage acceleration combined propulsion systems, such as turboramjets and others.

4. SCRAMJET - NEW STAGE OF RAM ENGINES DEVELOPMENT

Russian traditions in ramjets helped to carry on theoretical and experimental works on scramjets using hydrogen as a fuel.

Hydrogen scramjet supposed to be one of the most perspective engines for hypersonic vehicles and aerospace planes in particular for SSTO. In the Fig. 1.20 are shown some results of study of two SSTO vehicle concepts: with and without scramjet engine (DMSCRJ). The analysis allows us to conclude that a successful design of single stage earth-to-orbit with acceptable value of payload can be fulfilled only when using scramjet engine in combined propulsion system.

However, for scramjet creating it is necessary to solve a set of large-scale problems:

- optimum engine-aircraft integration,
- high combustion efficiency with supersonic gas velocity being in the combustor,
- heat protection and cooling in high-enthalpy gas flow,

- advanced material technology,
- flight Mach number range extension.

The last factor is of very importance because of strong influence of scramjet flight Mach number working range on flight effectiveness of ASP. So it is necessary to choice of suitable scramjet scheme (Fig. 1.21). Scramjet with fixed flow passage geometry having more simple and realizable construction takes transparent advantage. But it has the relatively narrow flight Mach number range from $M = 6...7$ to $M = 13...15$.

The flight Mach number range extension may be obtained as the engine with more flexible operating process, for example, with the variable flow passage geometry is used. In particular, the dual-mode scramjet (ramjet/scramjet) application allows us to reduce the low limit of Mach number range from $M = 6...7$ to $M = 3...4$.

At high flight Mach number $(M > 10)$ the scramjets effectiveness may be oxygen boosting. The hydrogen-oxygen scramjet specific impulse is lower a little then that one of hydrogen scramjet, but volumetric impulse of the first engine by $M = 12-20$ is $2...3$ times greater. Thus, oxygen application may be the acceptable meaning to reduce fuel tank mass and volume and to increase the aerospace plane effectiveness.

The study of scramjets development problems can be made by three main directions: CFD analyzes, ground testing, use of flight laboratories and experimental flying vehicles.

Computer Analysis of In-Scramjet Processes

Because of test possibilities limitation and difficulties of measurements in high speed/enthalpy flows the computer analysis of scramjet behaviour became of great importance. It served as a powerful stimulus in CFD development.

The program complex for the computation of the two- and three-dimensional scramjet duct flow field is developed with the use of the modular structures of software. The flow region is divided into elements: forebody, inlet, cowl, combustor, nozzle and afterbody. That software complex, which will be described in these Lecture Series, below also includes the possibility for the optimization of scramjet elements, for example, nozzle - afterbody. There is the 2-D or axisymmetric unified "nose-to-tail" flow field model.

The mixing enhancement in scramjet chamber may be reached with the aid of the 3-dimensional effect. The mixing of the hydrogen jet from elliptical or rectangular nozzle with the stream is more intensive, then in the case of axisymmetric nozzle.

The example of calculation of the 3-D hydrogen jets and air stream turbulent mixing with burning in the rectangular channel is shown in Fig. 1.22. The results are obtained with the use of parabolized Navier-Stokes equations.

One of the greet problems is that of cooling the scramjet structures under high enthalpy gas flow operation.

At the example of the fuel supplying strut CFD analyzes it is shown that maximum heat flux is in region of shock waves interaction and boundary layer separation. The fact that one cannot predict location of laminar-to-turbulent transition makes to provide cooling for the greater heating rates with margin.

So, complete experimental study of the processes of mixing, burning and heat transfer to scramjet combustor elements is of great necessity.

Scramjet Models Ground Testing

The scramjet ground testing pulls out very difficult and expensive requirements: high pressure and enthalpy airflow and LH_2 or GH_2 fuel supply, huge amount of air supply for exhausted system with ejector to achieve high altitude conditions and so on. These requirements become extremely hard when using free jet test method. So, the existent scramjet test facilities with continuous air supply are intended for testing rather small SCRJ-modules by not very high Mach numbers, less that eight. The special field of testing are the shock tubes in which the test duration is very short to study some SCRJ working processes.

CIAM has some SCRJ-test facilities which can provide the testing the models up to 200x200 mm and 300x300 mm size with Mach number simulation up to 6-8. These facilities allows us to test models both in the free stream flow and with the connected duct.

In the Fig. 1.23 is shown one of that facilities. It consist of altitude chamber, electrical and fire air heaters, nozzle, thrust meter system, ejector and exhausted section system. Two type of heaters give capability to estimate effect of air composition in engine inlet. The facility has such capabilities: simulated Mach number - up to 8;

hot air flow rate - 25 kg/s; total air temperature and pressure - up to 2500 K and 20 MPa; hydrogen flow rate - up to 1.4 kg/s and oxygen - up to 10 kg/s. These parameters can be increased by test cell modernization because of whole energetic supply of CIAM experimental center is very large.

There were designed at CIAM and manufactured in co-operation with Turaevo "Soyuz" Design Bureau two models of dual mode scramjet: axisymmetric and 2-D one (Fig. 1.24). The model inlets were of three-shock-wave, fixed geometry type with design Mach number M = 6. Gaseous H_2 is used as a fuel. Axisymmetric DMSCRJ is intended to testing on flight laboratory. The sizes of models were: $0.2x0.2m^2$ of 2D and inlet diameter 0.223m of axisymmetric one. Both the models were thoroughly studied in free jet, and the results were widely published [11].

Scramjet Models Flight Test

Flight tests are of very great importance not only for comparison the ground and flight testing results but because of the joint work of many specialist developing engine, fuel supply and control systems, on-board LH_2 tank, ground and on-board telemetry systems, ground infrastructure and launch system, mobile hydrogen refueling complex, rocket booster and its in-flight control and so on. All these specialists intended to rich the common practical goal. Such complicated work gave us integral experience and made the stirring effect.

The many years program of flight lab development and test preparation was carried out by the CIAM in co-operation with Air Force, missile Design Bureau "Fakel", engine Design Bureau "Soyuz", control system Design Bureau "Temp" and the other organizations of industry.

As the flight test model was used the CIAM axisymmetric scramjet (Fig. 1.24) and as a booster system was chosen one of old ground-to-air missile. The scramjet flight laboratory on the start position is shown in Fig. 1.25.

The first flight test was carried out in Kazakhstan at the end of 1991 and the second one with participation of France party at the end of 1992. Both flight tests were successful. The results of scramjet flight testing are analyzed in these Lecture Series.

The use of hypersonic flight laboratories and small unmanned research vehicles with scramjets seems to be very fruitful because of

financial restrictions, from one side, and the availability of powerful rocket boosters as the result of demilitarization, from other side.

In that situation the CIAM and other Russian organization experience and scientific-technological achievements in scramjet testing field become especially valuable.

5. SCIENTIFIC SUPPORT OF ENGINES R&D IN RUSSIA

The creation problem of principle new propulsion for high speed flight vehicles, for example ASP, is extremely hard and complex and requires the participation of great number of scientific and design organizations and even international cooperation.

The R & D organization of such PS in Russia has the important peculiarities, which are in the significant concentration of scientific and experimental investigations in research institutes, that become really co-operation of developing organizations with design bureaus (Fig. 1.26). The design bureaus in a lesser degree conduct the investigations and work at design and development of engines the initial conception of which are produced in co-operation with institutes.

The leading institutes of aviation industry are: Central Aerohydrodynamic Institute "TsAGI" (aerodynamic of FV and PS, airframe durability); Central Institute of Aviation Motors "CIAM" (all engine problems); All-Russia Institute of Aviation Materials "VIAM" (materials for airframes, engines and all FV systems). Institutes work together each with other and with aircraft and engine design bureaus. Under contracts the investigation are conducted as in institutes of the Russian Academies of Science and Engineering and in educational institution laboratories.

The head organization devoted on aviation engines of all types is CIAM, the large-scale scientific center. The main directions of CIAM activity are:
- fundamental investigation on gas dynamics, combustion and heat exchange, structural durability, theory of control;
- research in the field of ABE theory and optimization of advanced engines performances;
- fundamental and applied investigations of advanced engine components and systems;
- experimental investigations of the demonstrators and of all Russian engines under development, of its components and systems;
- engines certification.

The structure of CIAM consisting of the Moscow center and out of town Test-Research Center is the following:

Moscow Scientific-Research Center includes a number of scientific-research departments, powerful computer center, test facilities for testing units and small engines. Test and Research Center has full scale altitude-pressure cells for testing engines of all type and facilities for testing full scale engine components; powerful energy complex with compressors and exhausters, cooling and drain stations and other systems, industrial strength testing center. This is the biggest in Europe engine test center.

Above described scientific support system is very effective but it is in need of centralizes financial support. Now this system is modifying by the influence of market economic tendency.

CONCLUSION

The Russian traditions of ramjet study and development, the big series of research programs devoted on turboramjets, hydrogen fueled engines and FV, scramjets ground and flight tests constitute the large scientific-technological value.

The international discussion on these achievements may be very fruitful for all the participants.

ACKNOWLEDGMENTS

Author is indebted to his colleagues Dr. M. Mikhechko, Mrs. M. Sapronova and Mrs. L. Zhemuranova for their permanent assistance.

REFERENCES

1. Lorin R., Une experience simple relative au propulseur a reaction directe. Aerophile, Paris, 1913.

2. Стечкин Б.С. Теория воздушного реактивного двигателя. "Техника воздушного флота", М., 1929.

3. Бондарюк М.М., Ильяшенко С.М. Прямоточные воздушно-реактивные двигатели. М., Оборонгиз. 1958. 392 с.

4. Jet Propulsion Engines. Vol. XII High Speed Aerodynamics and Jet Propulsion. Editor: O.E.Lancaster. Princeton Univ. Press, 1959. Русский перевод: Воениздат. М., 1962, 668 с.

5. Зуев В.С., Макарон В.С. Теория прямоточных и ракетно-прямоточных двигателей. М.,"Машиностроение", 1971, 368 с.

6. Курзинер Р.И. Реактивные двигатели для больших сверхзвуковых скоростей полета (Основы теории). М., "Машиностроение", 1977, 216 с.

7. Теория двухконтурных турбореактивных двигателей. Под ред. д-ра техн. наук, проф. В.А. Сосунова. М., "Машиностроение", 1979, 432 с.

8. B. Grispin. Introduction and Overview. Ramjet and Ramrocket Propulsion Systems for Missiles. AGARD Lecture Series No. 136. 1984.

9. JALW - ISSUE 11, 12.

10. J.M. Lenorovitz. Russians Detail 1950-s Cruise Missile Effort. Aviation Week & Space Technology. November 2, 1992.

11. V. Sosounov. Study of Propulsion for High Velocity Flight. X ISABE, 1991. Nottingham, UK.

12. V. Sosounov. Some Aspects of Hydrogen and Other Alternative Fuels for Application in Air-Breathing Engines. IX ISABE, 1989, Athens, Greece.

13. Sosounov V.A., Orlov V.N. Experimental Turbofan Using Liquid Hydrogen and Liquid Natural Gas as Fuel. AIAA Paper 90-2421. 26th Joint Propulsion Conference, 1990. Orlando, Fl.

14. А. Туполев, Г. Загайнов, Д. Огородников, В. Чепкин. К Марсу на ... самолете. "Правда" N 159, 4 июля 1991.

15. J. Bendot. Composite Engines for Application to a Single-Stage-to-Orbit Vehicle. NASA CR-2613, 1975.

16. K. Sakata, M. Minoda, R. Yanagi, H. Nouse. Hypersonic Turbomachinery-Based Air-Breathing Engines for the Earth-to-Orbit Vehicle. AIAA J. of Propulsion, vol. 7, No. 1, 1991, pp. 108-114.

17. Sosounov V.A., Tschovrebov M.M., Solonin V.I., Palkin V.A. The Study of Experimental Turboramjets. AIAA Paper 92-3720, 28th Joint Propulsion Conference, July, 1992. Nashville, TN.

18. V.A. Sosounov, V.I. Solonin, M.M. Tschovrebov, P.A. Kadjarduzov and V.A. Palkin. The Study of Experimental Turboramjets: Heat state and Cooling Problems. AIAA Paper 93-1989, 29th Joint Propulsion Conference, July, 1993. Monterey, CA.

19. А.А.Туполев. "Ту" летает на водороде. "Наука и жизнь" N 1, 1989. М., изд."Правда".

20. Ю.М. Аннушкин, В.А. Сосунов. Исследование диффузионного процесса горения и аэродинамики течений в воздушной камере сгорания ракетно-прямоточных двигателей. Части I и II. Под редакцией В.А. Сосунова. М., ЦИАМ. 1969. 314 с.

21. Jane's Land-Based Air Defense. Fifth edition. 1992-93.

22. Aviation Week & Space Technology / August 24, 1992, p.64.
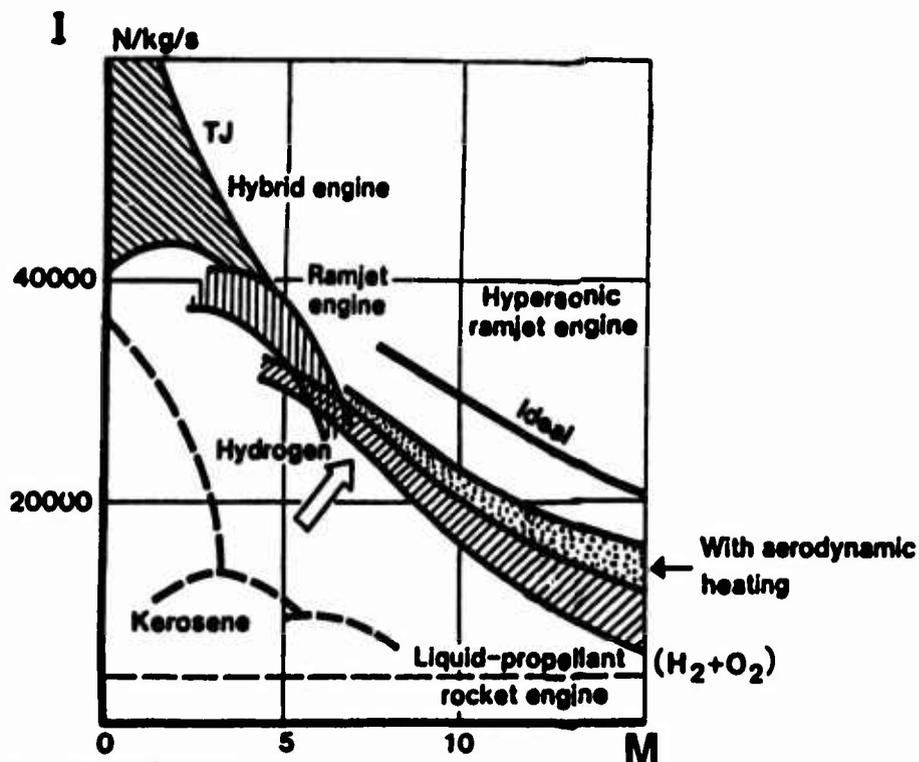
Fig. 1.1

Ram engines - propulsion
for high velocity flight [12].

Fig. 1.2.   Ram Propulsion.

Only 7 elements have
Hu > 25 MJ/kg
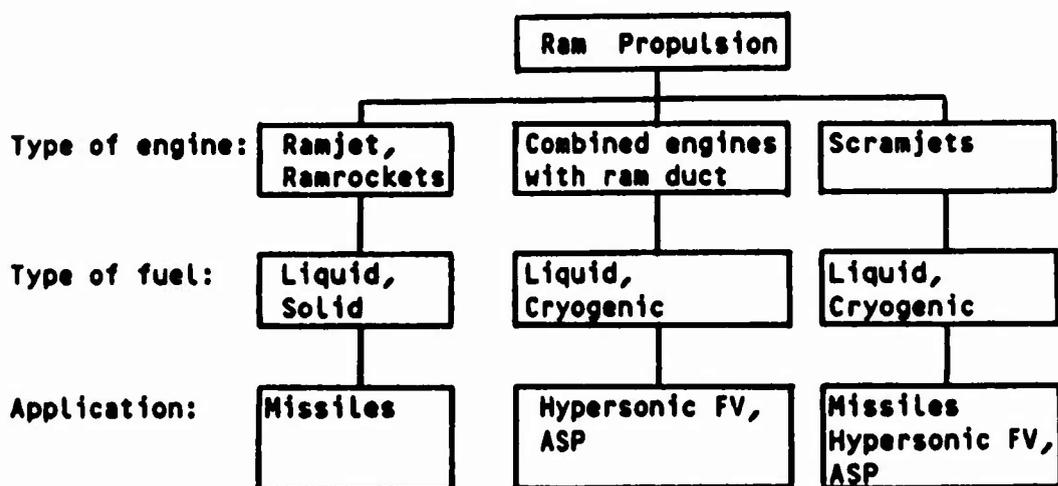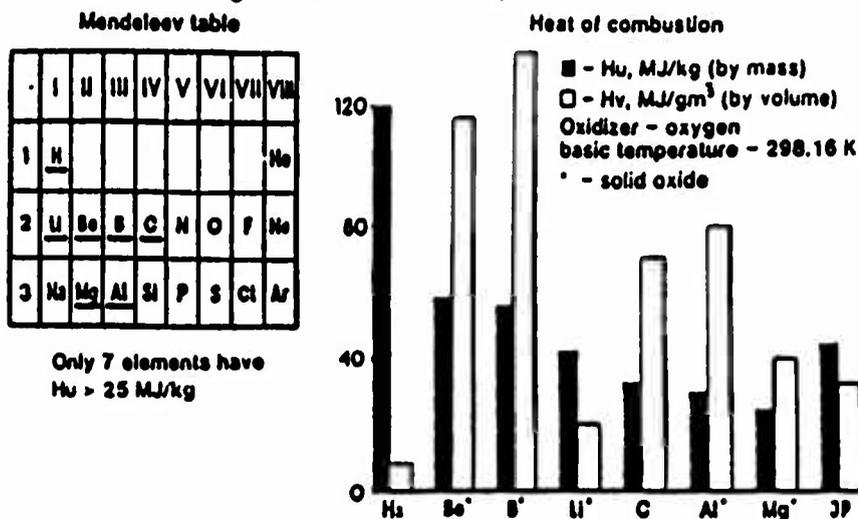
Fig. 1.3.   Basic combustible elements [12].
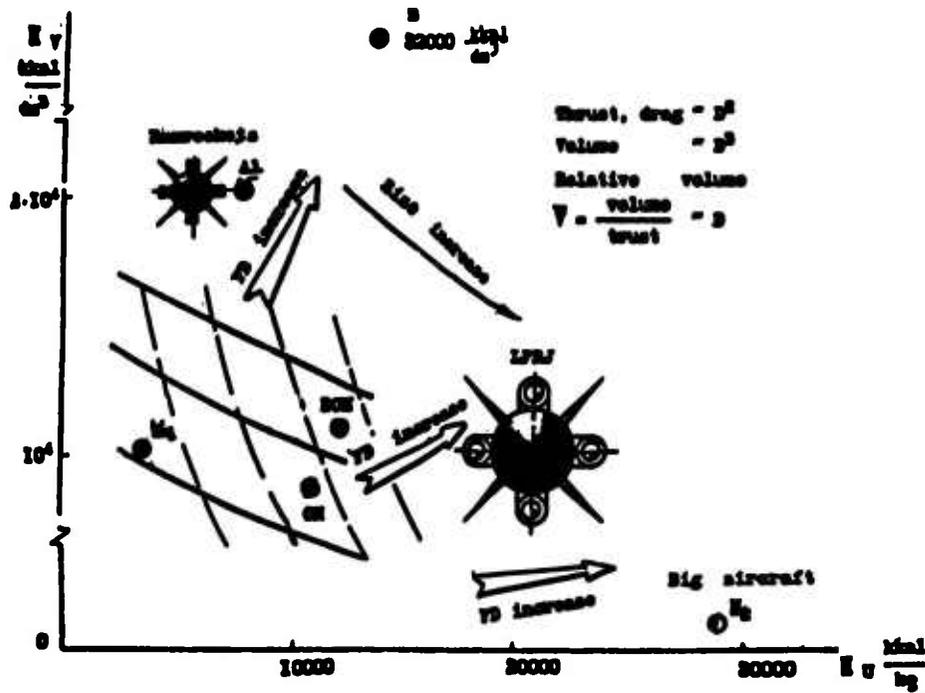
Fig. 1.4.   Fuels and the FV size.

Practically used elements
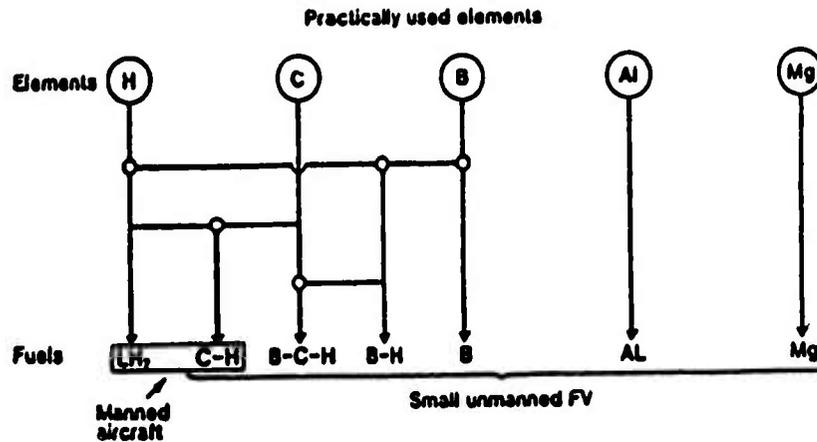
Fig. 1.5.   Potential chemical Fuels [12].

* Classification and fields of use
* Basis of ramjet theory and design
* Duct gas dynamics (intakes, combustion
  chambers, jet nozzles)
* Fuel - air mixing and combustion
* Chemical and nuclear energy sources
* Development and test metodology

Fig. 1.6. Solentific heritage of M.M.Bondaryuk
          in ramjet field. (1940 - 1969).
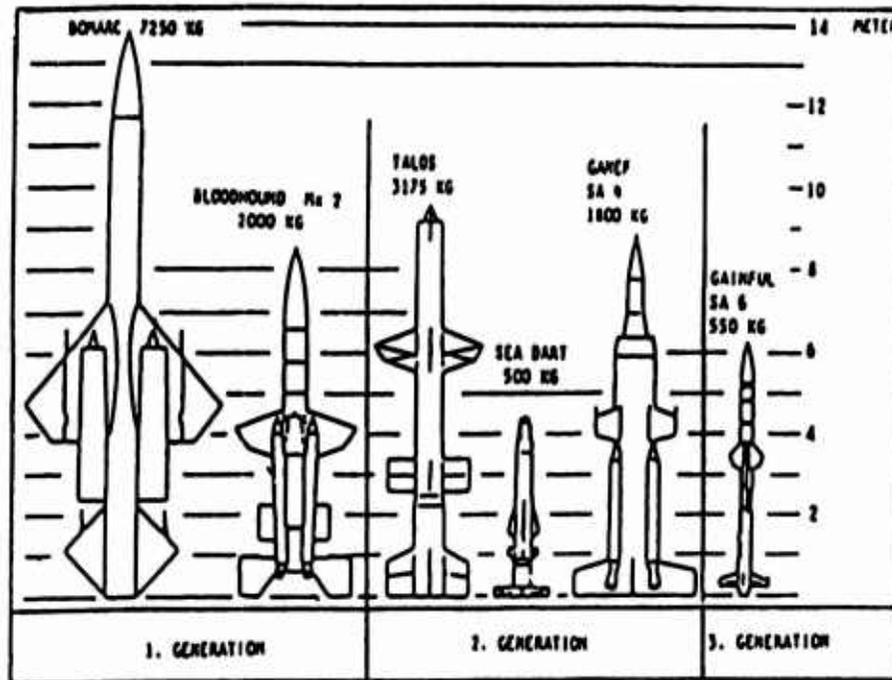
Fig. 1.7.   Ramjet Generations [8].
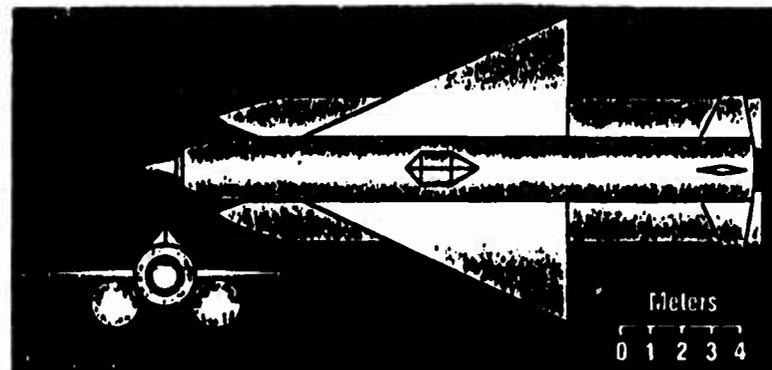
Fig. 1.8.   The "Burya" Mach 3 – class Russian
cruise missile with ramjet [9], [10].
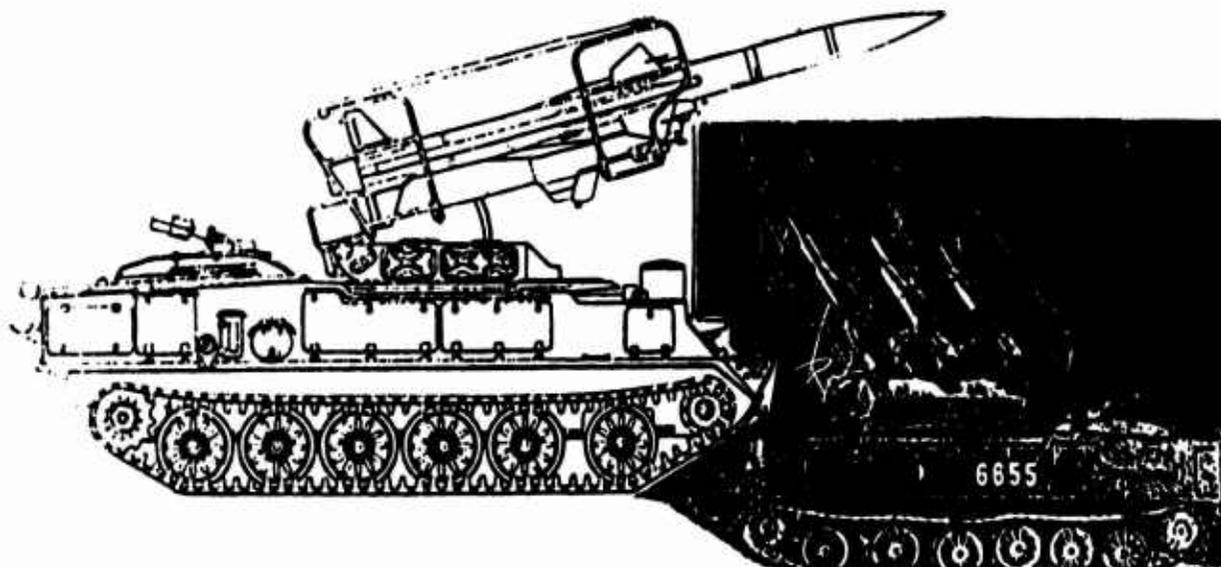
Fig. 1.9.   The Surface-to-air Russian missile SA – 6.
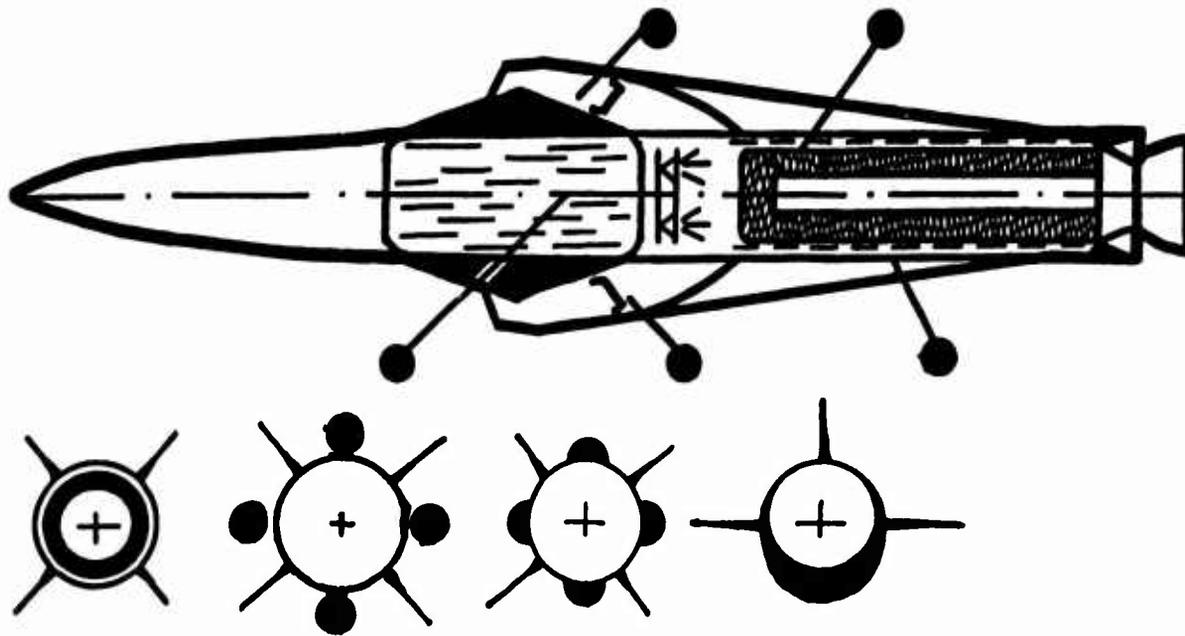
- Full integration of PS and FV
- Ram combuster and booster combined
- Heavy (solid) fuels
- Ramrocket type (ejection effect)

Fig. 1.10. Low volume Ramjet - new generation.
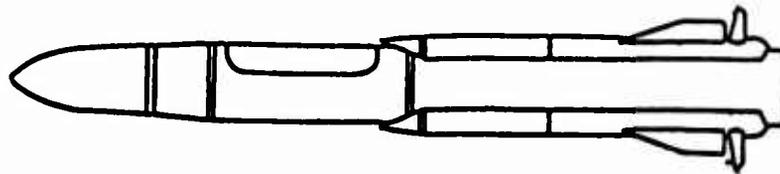
Kh - 31P (Russia) 720 kq, 1983.

ASMP (Frauce) 860 kq, 1986.
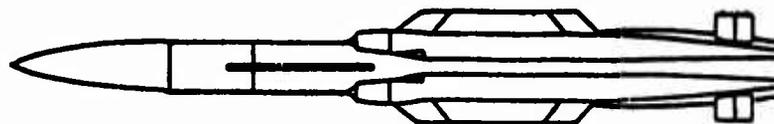
ANS (International) 650 kq, 2000.

Fig. 1.11. New ramjets of 3-d generation for
air-to-surface missiles [9].

Fig. 12.   The Kh-31P air-to-surface [9]

MAIN TYPES OF PROPULSION

ATR_gg − TURBOROCKET WITH GG
ATR_ex − TURBOEXPANDER
TRJ − TURBORAMJET
SCRJ − SCRAMJET (DM−DUAL, MODE)
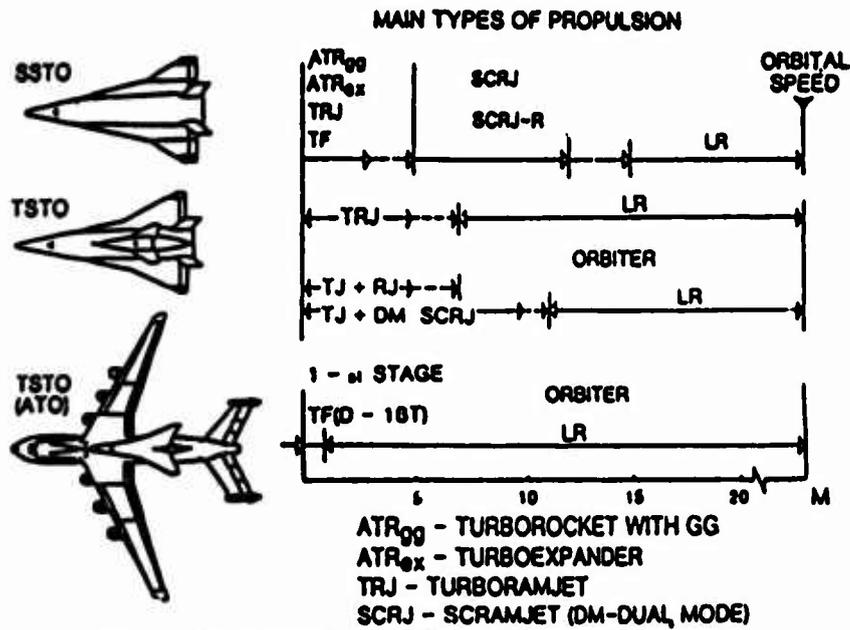
Fig. 1.13. Propulsion system concepts [11].
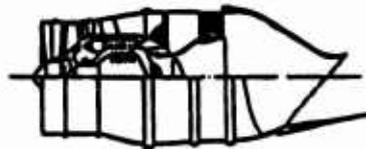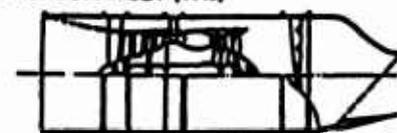
Fig. 1.14. Engines for the first stage of ASP
acceleration and for hupersonic FV [11].

Fig. 1.15. CIAM experimental turboramjet engine [11].

Turbojet mode

Ramjet mode

Cooling air

Different engine control during transient mode

TJ COMPRESSOR MAP

PR

CORRECTED AIRFLOW
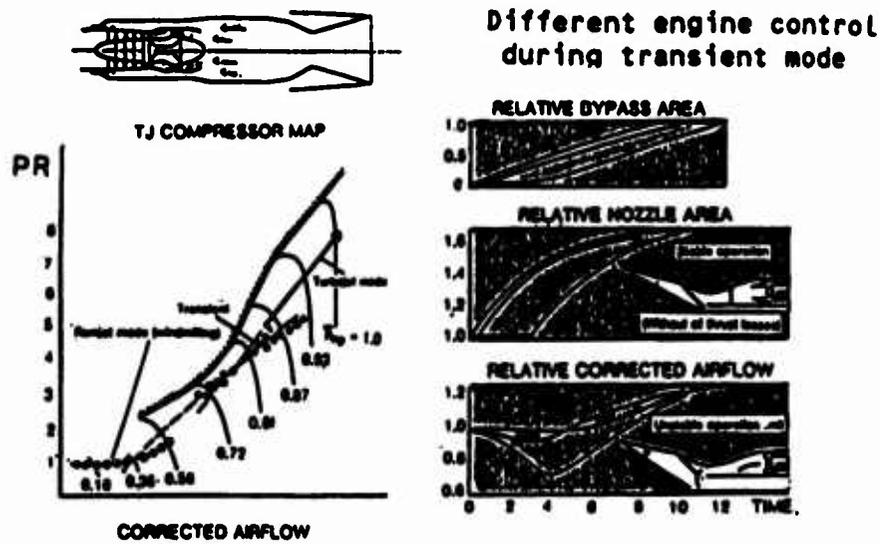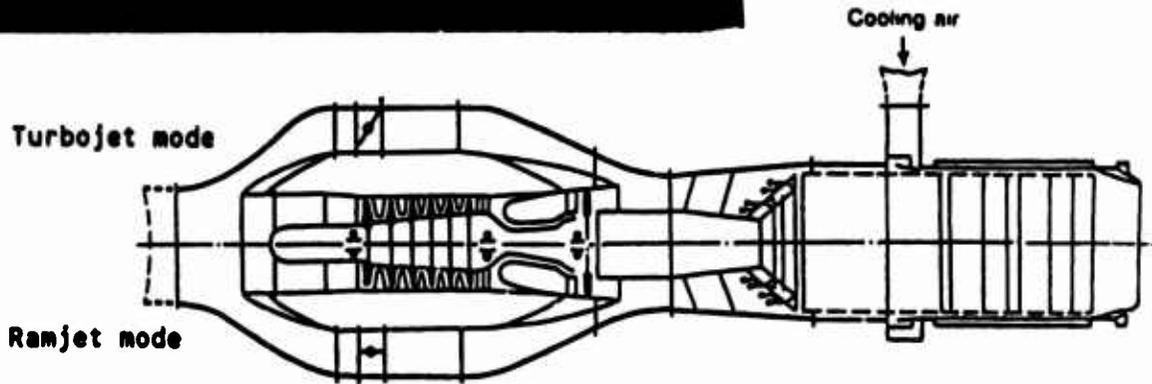
Fig. 1.16. Study of turboramjet transient mode [11].

$L_{komb} = (2 - 2.5)L_{kam}$
● JP – homogenized mixture combustion
● H_2 – gaseous fuel diffusion combustion
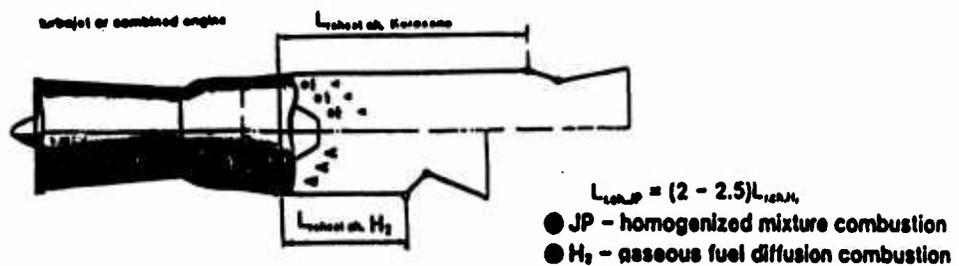
Fig. 1.17. Hydrogen afterburner – ram combustion chamber [12].
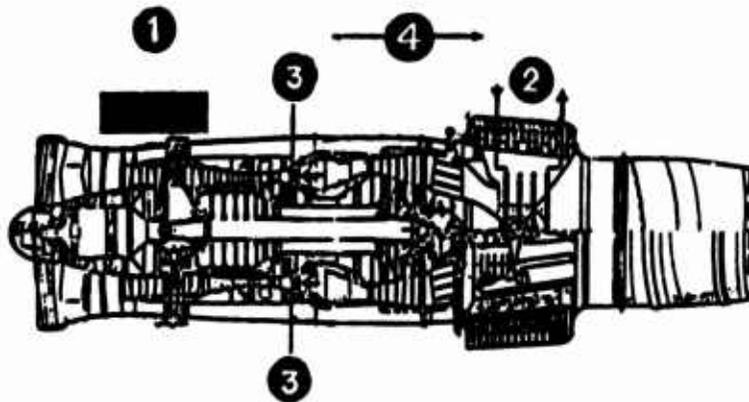
Fig. 1.18. Basic hydrogen aggregates of the NK-88 engines.
1-turbopump;   2-heat   exchanger-gasificator;
3-hydrogen combustion chamber; 4-special cryogenic
equipment including automatic control system [13].
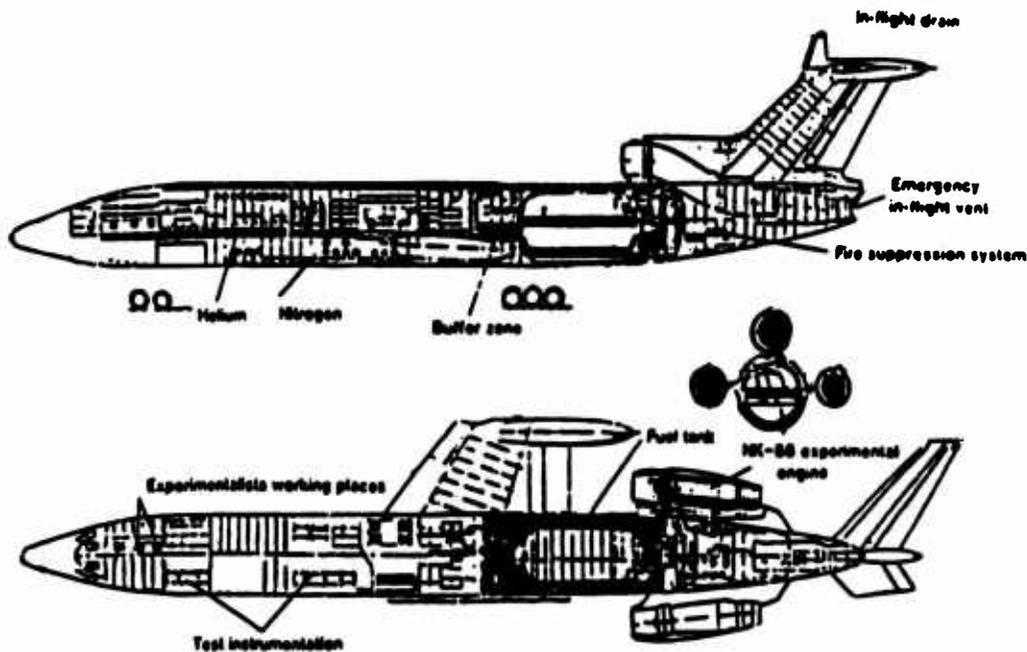
Fig. 1.19. The Tu-155 LH_2 - aircraft layout [19].
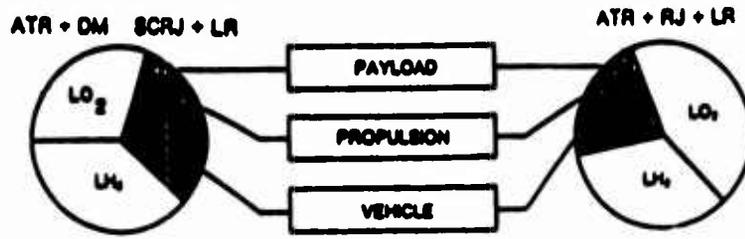
Fig. 1.20. Mass efficiency of SSTO [11].
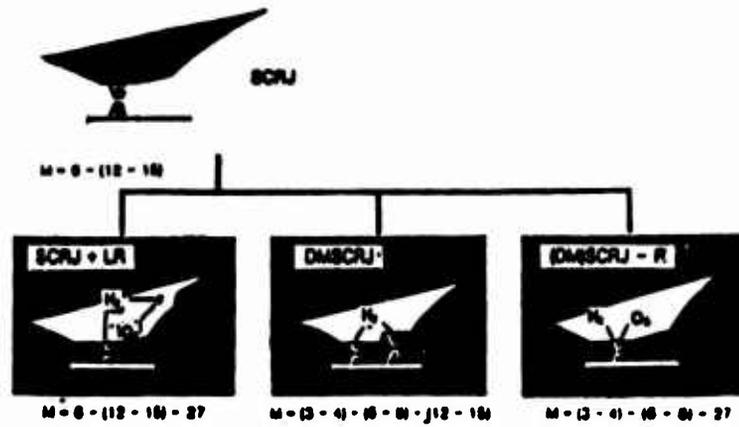
Fig. 1.21. Scramjet engine types [11].
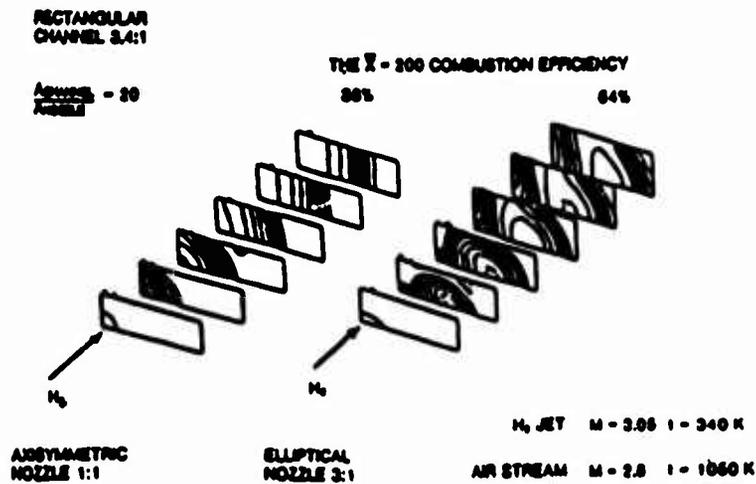
Fig. 1.22. The numerical 3-D simulation of the turbulent
mixing with combustion of the supersonic flows
in rectangular channel [11].
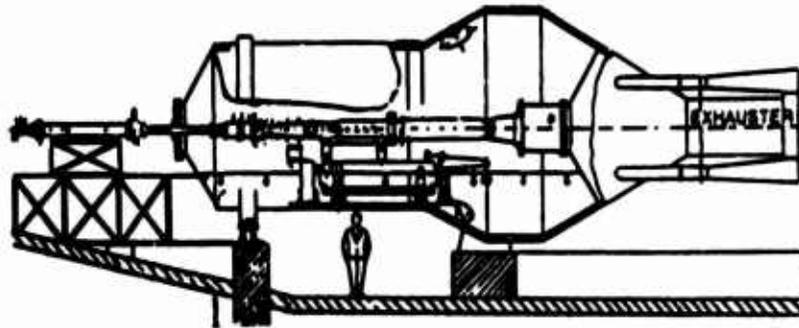
Fig. 1.23. Scramjet test facility [11].

$M_c = 2.5 - 6(8)$
$T_c = 800 - 2100 K$
$A = 2 - 5 kg/s$
Fuel H_2, C_xH_y

DUAL MODE
SCRAMJETS

AXISYMMETRIC
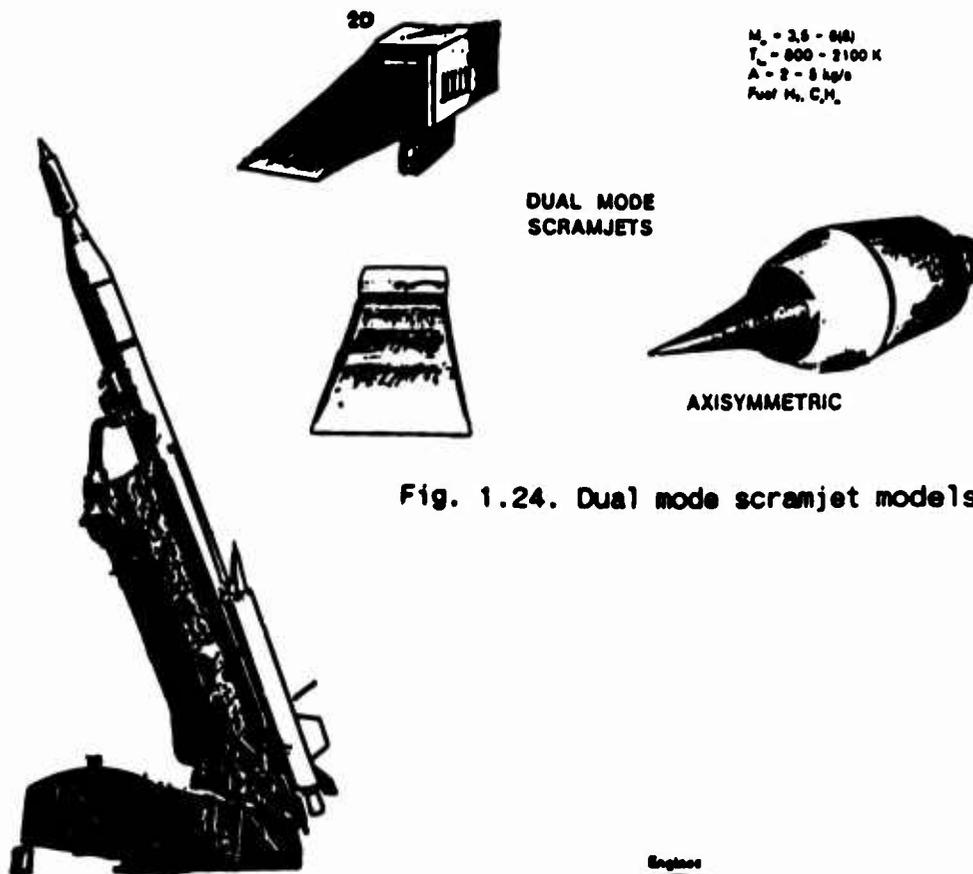
Fig. 1.24. Dual mode scramjet models [11].

Fig. 1.25.   Scramjet flight laboratory on the
start position
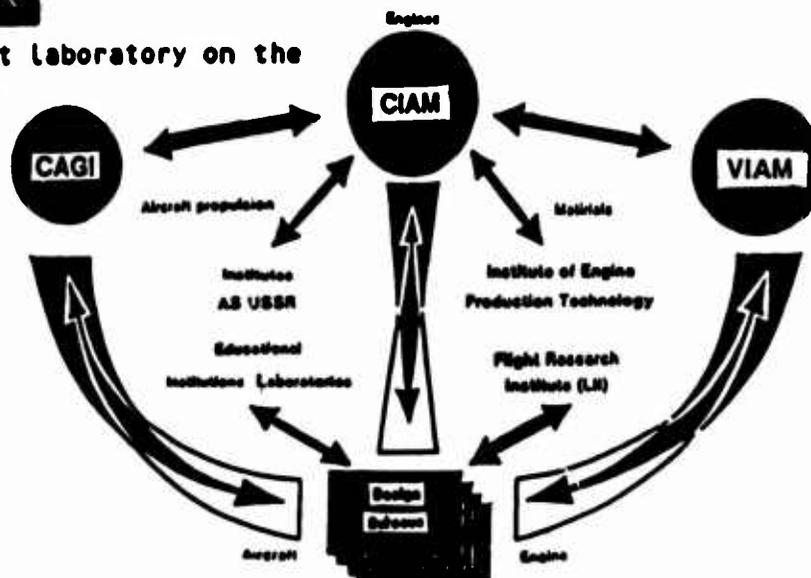
Fig. 1.26. R&D of propulsion in Russia [11].

TURBORAMJET ENGINES - TYPES AND PERFORMANCES

by
Dr M.M.TSKHOVREBOV
CIAM (Central Institute of Aviation Motors)
2, Aviamotornaya st.,
111250 MOSCOW,
RUSSIA

ABSTRACT

In this, first of the two reports on Turboramjet Engines, some properties of variable cycle propulsion plants based on a combination of ramjet and various turbine - type engines are considered. Various jet engine type thrust performance vs flight Mach number are represented. Turboramjet engine (TRE) are classified according to the manner of energy transfer to the ramjet parts. The defining principles of essential TRE propulsion plant working parameters and dimensions defining principles with taking into account of flight vehicle requirements, are considered. TRE various types thrust performance are presented.

A Comparative effectiveness study of various types combined propulsion plants for future hypersonic transport planes and TSTO first stage with LH2 fuel is given. A preference is shown for the turboramjet engine as a universal multimode propulsion plar... Interrelations of TRE configuration and working parameters with the change to ramjet operation mode process is considered. Optimisation of operation modes changing conditions as an approach to the governing principles of a combined engine working process is given.

NOMENCLATURE AND ABBREVIATIONS

A	- area.
ABE	- air-breathing engine.
ARCC	- augmented-ramjet combustion chamber.
ASP	- airspace plane.
ATOS	- airplane-to-orbite system.
ATR	- gas generator type turborocket engine.
a	- air-to-fuel stoichiometry ratio coefficient.
$b = \dfrac{m+1}{m}$	- relative airflow in RJ duct or TF outer duct.
Cp	- vehicle aerodynamic drag coefficient related to the wing area.
Dp	- vehicle aerodynamic drag.
Ep	- vehicle mechanical energy.
fin to air	- ratio of free stream cross section area to air inlet area.
H	- flight altitude.
He	- flight "energetic altitude" (the ratio of vehicle mechanical energy to vehicle weight).
HST	- hypersonic transport airplane.
h	- efficiency.
hin	- air inlet efficiency.
ha	- acceleration efficiency.
hoa	- overall acceleration efficiency.
k	- adiabatic exponent.

L/D	- lift to drag ratio.
M	- Mach number.
Mo	- optimum for transition to RJ operation mode flight M.
Mx	- flow M at the ARCC inlet.
m	- bypass ratio.
P	- pressure.
Pa	- ambient air pressure.
PS	- propulsion system.
PRC	- compressor pressure ratio.
RJ	- ramjet engine.
SFC	- specific fuel consumption.
Sin	- intake recovery coefficient.
T	- temperature, K. - engine thrust.
Ta	- ambient air temperature, K.
Ts	- engine specific thrust.
t	- time.
TF	- turbofan engine.
TF(A)	- augmented turbofan.
TF(A)s	- TF with bypass reheat.
TFRJ	- turboramjet with TF as a core.
TFRJs	- TRE with TF as a core and bypass ARCC.
TJ	- turbojet engine.
TRE	- turboramjet engine.
TRJ	- TRE with TJ as a core.
TSTO	- two stage to orbite ASP.
(T/W)	- thrust to weight ratio.
V	- flight speed.
Vx	- flow velocity at ARCCinlet.
W	- engine weight.
w	- mass airflow.
Wp	- vehicle weight.

SUBSCRIPTS

a	- acceleration.
c	- compressor.
cor	- corrected parameters.
cr	- cruise.
f	- fan.
g	- turbine inlet.
in	- intake, inlet.
n	- nozzle.
r	- ARCC, reheat.
R, rj	- ramjet operation mode.
s	- specific parameters, separate.
T, tj	- turbojet (gasturbine) operation mode.
t	- sum, summary; total.
x	- ARCC inlet.
o	- sea level static conditions; optimum.
*	- critical parameters.

INTRODUCTION

The air traffic role in modern life is increasingly important. The overall number of passengers per year exceeded one billion just at the end of the last decade. World political and economical situation development broadens relations between countries. One can foresee the tendency to a growing share of long range passenger aircraft in the world airliner fleet. Passenger traffic growth at the beginning of 21 st century, in conjuction with increasing needs in long range transport require more attention to higher flight speeds [1,2].

Today the flight speed range of air transport is limited by technical economic factors to the subsonic area mainly. Transcontinental and transonic flights require a lot of time. Given the expected increase in air transportation and established practice of "comfortable" flight-time for a passenger of no more than 2...3 hours, we may infer the prospective development of a supersonic passenger aircraft of a new generation (M = 2 - 2.5) and in the distant future we shall require air transport at hypersonic speeds, which could enable flights on the longest routes within a minimum time (Fig.1).

Flight speed increase leads to flight time reduction and hence improves travel comfort, particularly on intercontinental routes. However, while the transition from subsonic to supersonic speed of Mach 2-3 at a flight range of 10.000-12.000 km reduces flight time by 10 hours, a further speed increase up to Mach 5 - 6 results in a time saving of about one hour.

For an appreciation of the maximum flight speed of future airliners it is suitable to consider results of modelling of a one-day business trip concept [3] (leaving home not earlier than 07.00 and returning home after a business meeting not later than 24.00 at the same day). Analysis has shown that even at Mach 6, the overall amount of possible routes between the twelve most important political-economic world centres is already approaching the practical limit (Fig.2).

The development of an effective aerospace plane (ASP) for launch of commercial loads is needed to continue to open up the near-Earth space for peaceful goals. The key factor in low cost launch is the use of reusable launch from an Airplane-To-Orbit System (ATOS) with horizontal take-off/landing and a fuel-efficient air breathing engine. The rise of ATOS or TSTO first stage speed from subsonic to hypersonic of Mach 6 - 7 enable an increase in the relative mass load of about 2 - 3 times [2].

The present development of ATOS on the basis of a subsonic launcher can be considered as precedent for the parallel development of an advanced hypersonic transport (HTS) and a hypersonic launcher for ATOS in the future (Fig.2). The key problem of development of the hypersonic propulsion system (PS) will be better resolved when using the 'double application engine' concept for development of an engine of HST and ATOS. In this case, the propulsion system for various aviation system missions will keep their distinctions according to the mission, including cooling system, relative size of an inlet and nozzle, integration with airframe, etc. In this connection the possibility of using the TurboRamjet is of substantial interest [5].

1. VARIABLE CYCLE COMBINED PROPULSION SYSTEMS

In developing the supersonic or hypersonic power plant, the main factor in defining its configuration is a wide range of operating conditions. Engine efficiency in cruise flight is ensured by optimising thermodynamic parameters, which considerably change depending on flight speed and altitude. On the other hand, a significant requirement for the power plant of a high-speed aircraft is providing high thrust for acceleration, which at high Mach flight numbers is determined by the air flow.

A typical property of a turbojet is the lowering of the pressure increase and the corrected air flow in the turbocompressor part with an increase in flight speed (Fig.3). Specific thrust parameters of the augmented turbo jet approach ramjet specific parameters at flight Mach numbers 3...3.5. At higher flight speeds RJ gives higher than TJ specific thrust at equal air-to-fuel coefficients (Fig.4). Corrected air flow in RJ with variable inlet and nozzle can be maintained constant over a wide flight speed range. As a result the Rj thrust rises with Mach number more rapidly than turbojet thrust. Then at M numbers higher than 3...4 RJ thrust exceeds augmented TJ thrust, and in this flight speed region RJ can be more ef fective than TJ.

Together with augmented TJ performance degradation it is very difficult to provide TJ operability at flight M numbers higher than 3.5...4. In Fig.5 are represented the air temperatures at compressor inlet Tin and outlet Tc vs Mach number at various pressure ratio design values PRC, and typical temperature level, admitted by materials thermodurability.

It is seen that, when maximum air temperature is limited to a value of 1100...1200K by requirements of structure thermodurability, then maximum flight Mach numbers for augmented TJ are limited approximately to M = 3.5...4, whilst RJ can operate up to M = 4.5. Taking into account the absence of rotating parts in RJ and its structure and flameholder fuel cooling possibility, one can conclude that possible maximum flight speeds for RJ exceed M = 5. Attractive RJ properties are structural simplicity and low specific (relative to cross section) weight [4]. But at low flight speeds RJ has poor efficiency. Then in engines designed for a wide operating flight speed range it is necessary to combine high TJ efficiency at M numbers up to 3...3.5 with RJ satisfactory specific parameters at M > 3.5...4.

Combining in a single propulsion plant the TJ and RJ engines gives the possibility to obtain the ABE type class, which are operable and effective up to M = 4...5 and higher. A combined turboramjet engine (TRE) is, in essence, a bypass ABE, in which a high pressure inner part represents the TJ or TF (gasturbine part), and a low

pressure external part - RJ (ramjet part). Depending on the engine type, some of its structural elements can be common to both parts. Usually in these engines afterburning chambers represent the combustion chambers of RJ too, which are formed by switching out the TJ part by means of special devices and feeding fuel only to RJ combustion chambers.

Selection of one or another type of engine is to a great extent determined by the requirements of a hypersonic aircraft. A change in these requirements can significantly change the optimum powerplant design. For example, at high aircraft thrust-to-take-off weight ratio and with stringent requirements for the specific weight of an engine, powerplants with air-turbo-rocket engines (ATR) may have certain advantages; however they have low fuel efficiency, particularly at low flight speed.

Turbocompressor engines of more sophisticated cycles, using hydrogen's high cooling and working capacity (air cooling at the engine entry, steam-hydrogen turbine) enable extension of the flight speed range of use and have higher efficiency, but higher weight too, as compared to the rather simple gas-generator ATR.

Problems of matching the essentially different operating modes in combination with the more stringent requirements on noise levels, sonic boom intensity and detrimental emission create a very complicated problem for the development of the multimode hypersonic power plant.

There is a need when using variable cycle engines (VCE) to match conflicting ecological and thrust characteristic requirements. Usually a VCE is a bypass engine with variable geometry components [7]. Adding the ramjet to such engine types allows developement of a combined variable cycle power plant with a very wide range of performance.

When there is a considerable amount of subsonic cruise flight (for instance flight over populated territory, subsonic hold, emergency situation in case of supersonic or hypersonic transport aircraft) there are severe requirements for high fuel efficiency in the mentioned modes. In this case, the advantageous will be the power plant with the turbojet (TJ) or turbofan (TF) (VCE), whose fuel efficiency in the throttle cruise modes is much higher as compared to the steam-hydrogen (regenerative) ATR.

2. TRE TYPES

The TRE features depend on its design. Therefore the TRE type selection depends on the vehicle mission. The multitude of TRE types can be split up according to the principle of using the engine gasturbine part "free power" to compress air in the ramjet part in order to increase the engine thrust at take-off and low flight speeds [9].

The TRE without energy transfer to the ramjet part is just a mechanical combination of turbojet and ramjet engines (Fig.6). Their thrust performances are obtained by adding together the performances of gasturbine and ramjet parts. The relative airflow in the ramjet is the part equal to

$$b = \frac{Wrj}{Wtj + Wrj} = \frac{m}{m + 1}$$

In the gas-turbine operating mode, that is to say when the ramjet part is switched off (b=0), such an engine has a TJ or TF with afterburning (TJ(A) or TF(A)) performance, while in the ramjet mode, when the TJ is switched off (b = 1) it has ramjet engine (RJ) performance. If there is a separate combustor in the ramjet part then the parts are independent. This allows switching on the ramjet in transonic flight to increase the total thrust of the engine (TRJs and some other types on Fig.6). Thus, in the TRE of this type, simultaneous (parallel) operation of the parts is realized.

For better performance of the engine in the ramjet mode the switched-off part should be shut off by special devices such as doors, louvres, moving centre body etc.

The drawback of TRE types with separate combustion chamber and without energy transfer to RJ part consists in larger dimensions, complexity and higher structure weight, which is a necessity for the parallel arrangement of two combustion chambers with variable nozzles. The most simple, compact and advanced in this group of types is the TRJ with separate gas-turbine and ramjet channels (TRJs), especially when using a "stoichio-metric" TJ.

A group of TRE types without energy transfer to the ramjet part at low flight speeds includes also the TRJ with, common to both TJ and RJ parts, an afterburning ramjet combustion chamber (ARCC). In this case the TJ is intended for charging the ARCC at low and moderate flight speeds. Thanks to the consecutive layout of the TJ and ARCC, the RJ operation mode changes with flight speed increase from TJ mode to the ramjet mode. The TRJ principle feature is the impossibility of simultaneous (joint) operation mode at low and moderate flight speeds due to the large pressure difference in TJ and RJ channels. Hence the necessity to shut off the ramjet duct in the gas-turbine operation mode with a special device and a specific control mode when switching to RJ.

The need to isolate the switched off TJ at high M numbers may be the result of consist in the influence of kinetic heating on the structure. Hence, if structural durability and oil system operability are sufficient, then, along with switching to RJ mode it is possible to transfer the TJ to windmilling or idling and use it for driving accessories. Usually in this mode only a small part of the airflow passes through the TJ part (b -> 1), and thrust performance difference from that of pure RJ is rather small. Then joint operation and windmilling modes are nearly the same as RJ mode operation. The TRJ has advantages from the point of view of dimensions, weight and simplicity.

In TRE with energy transfer to the ramjet part (Fig.6), the free power produced by the gasturbine engine is used to increase pressure of the air supplied to the ramjet. As a

result both parts of the engine can be involved in operation within the whole range of speeds and altitudes of flight. These types are essentially the development of the TRJs and TRJ by application of a bladed (or jet) compressor to increase air pressure in the ramjet part.

In the TRE types with energy transfer by ejector, the active operating fluid is the airflow from the fan or turbine. These TRE types in principle don't need the shut off device for the RJ part channel. For effective operation at take-off and low flight speed conditions in which one can obtain some effect from ejection, it is necessary to take some constructive measures. Among these there are: lowering the turbine or fan passage exit area for maintaining high active gas parameters; using a narrowed mixing chamber and special mixer for reducing the losses; using ARCC with a large cross section for reducing losses lowering and, consequently, using the diffuser with large area ratio before ARCC. The necessity of these measures, leading to engine complexity, higher weight and dimensions, is conditioned by the low efficiency of a jet compressor when its dimensions are limited. As a result the TRE types with ejection have no practical advantages over the types with energy transfer to RJ part by turbofan.

The TRE with energy transfer by fan (TFRJ) doesn't differ principally from augmented turbo fans with separate primary and secondary flows TF(A)s or with mixing flows TF(A) (Fig.6). Their special feature is the change to RJ operation mode with turbofan windmilling at high flight speeds (b -> 1). In this connection the windmilling turbofan drag presents an important factor. Multimode operation and the use of a windmilling turbofan to drive accessories are the important advantages of the TFRJ. In the case a high design fan pressure ratio, which changes windmilling performance for the worse, or if the TF is isolated from kinetic heating in the RJ mode operating conditions as a result of reliability requirements, it is necessary to include into the engine structure a passage around the fan to bypass the airflow at high flight M numbers. For the same reasons as in the case of TRJ, this passage should be closed by a special device in low flight speed conditions.

TRE types with energy transfer and a separate combustion chamber for the RJ part inherently have a compact configuration because of parallel arrangement of both parts. But these types require closing of gas turbine passage exit in the RJ operation mode to maintain thrust performance. TRE types with common ARCC don't need such closing, but are longer and need a wider range of nozzle flap movement.

The expediency of using the TRE on the basis of TJ or TF is defined by the vehicle mission. If high fuel efficiency at low flight speeds is required (Fig.7) along with good performance when cruising at M = 4...5 then the TF as the basic engine is preferable; if the mean requirement is for high performance at maximum flight speeds, then it is expedient to analyse the possibility of using the TRE types on base of TJ. It is possible to make the TFRJ structure with slightly less length and weight than the TRJ with equal design thrust [4].

The main merits of the TFRJ are:

- effective performance over a wide range of flight conditions;

- lower noise level at take-off and low flight speedcondition;

- wide range of thrust variations at constant air-flow.

3. TRE DESIGN PARAMETERS AND DIMENSIONS

The independent selection of gas turbine part and ramjet part sizes (a fan/compressor inlet area Af or Ac and an ARCC or ramjet burner cross section area Ax) is a common feature of the combined engines (Fig.8).

In general:

- a size of inlet area Ain is determined by the design thrust value at the maximum flight speed and optimised by the influence on the flight range and externaldrag at transonic flight speed;

- a size of the fan (compressor) area Ac is determined bearing in mind ecological requirements: namely, by a design thrust at transonic flightspeed (sonic boom limitations) or at take-off (noise level limitations); for engines with lower dry specific thrust (TFRJ) the subsonic cruisethrust can be the determinating factor (Fig.7);

-the size of ARCC cross section area Ax is determinedby the flight speed at which a transition to ramjetmode is realized and is optimised taking into consideration matching of TJ, TF and RJ operation modes;

-the size of nozzle exit area An is optimised takinginto consideration nozzle efficiency at maximum flight speed (Fig.9), external drag at trasonic flight speed and nozzle weight.

Selection of the design by-pass ratio is of important role in developing a multimode engine. The less the by-pass ratio, the closer the TF(A) performance to those of the TJ(A). With by-pass ratio rising TF(A) properties approach those of the RJ (Fig.10).

It is possible to base the choice of the reasonable by-pass ratio value, for example, of the HST engine on the following considerations. When the design bypass ratio m is raised at given cycle parameters, the optimum fan pressure ratio and engine core airflow decrease. This decreasing relaxes the core airflow steepness influence and leads to increasing of total engine airflow at supersonic flight speeds. As a result, the relative engine thrust at maximum augmented ratings T/T_o increases.

The corresponding SFC also increases, but usually this does not lead to a significant increase of required fuel amount, because of a simultaneous increase of excessive thrust and a higher acceleration rate. At high supersonic speed flight (M > 3.5) the engine must run according to

the RJ cycle, which can be realized more simply with larger dimensions of the external low pressure passage, that is, higher design by-pass ratio. Its increase in this case decreases the need for special mechanization of the passage and an additional by-pass duct. The fuel efficiency at subsonic cruise is also improved.

For example, for a bypass ratio of order m = 3 fan pressure ratio values are PRCfo = 2...2.5. The high pass capacity of such low pressure ratio fans over a wide range of rotating speeds is one of the main factors that determine the possibility of creation of the TFRJ (or TFRJs) types of TRE, which can be transferred to RJ operation mode with fan windmilling at high flight speeds.

Increase in design bypass ratio results in an increase in engine air flow and its cross sectional dimensions. For aircraft of moderate supersonic flight speeds (M = 2...2.5) this is one of the reasons for selecting low by-pass ratio values. For high supersonic flight speeds (M > 3) the relative cross sectional dimensions of an inlet and diverging nozzle rise considerably (Fig.11), whereby a significant increase in the by-pass ratio within the range determined by the dimensions of the power plant entry and exit can be possible.

As to the subsonic cruise part of flight, which is inherent to heavy-weight supersonic vehicles, the fuel economy considerations also require the choice of higher by-pass ratios, but with upper limits nearly m = 4 because of substantial decrease of engine dry thrust.

In Fig.12 the typical TFRJ performance inter-relations are represented, which should be considered when making the choice of design bypass ratio. In this case the "critical" factor is the engine dry thrust at subsonic cruise. The requirements for the design take-off (or transonic) thrust and thrust value at cruise with maximum hypersonic speed are provided for by the corresponding design dimensions of inlet, fan and ARCC in the whole range of engine parameters considered. With higher design bypass ratios, fan dimension increases but this has no influence on fuel efficiency at hypersonic cruise, slightly affects on engine weight W and leads to higher fuel efficiency at subsonic cruise. However subsonic dry thrust decreases. Increasing bypass ratio higher than some limiting value would require greater engine dimensions and weight and lead to engine oversizing relative to other flight conditions. In this case the maximum bypass ratio, at which the dry thrust corresponds to the required level, is the expedient design value.

Thus, for multimode vehicle engines with high supersonic flight speed adoption of relatively high design bypass ratios may be the rational decision. The optimum bypass ratio values depend on the engine cycle parameters, aircraft aerodynamic characteristics, distances of flight segments with supersonic and subsonic speed etc.

It is possible to use a similar approach when defining the optimum correlation between the dimensions of the RJ and TJ parts of TRJ. This correlation one can express as the ratio of the ARCC section area to the area of

compressor inlet. The choice of each of them is to some extent mutually independent, and is defined by required thrust values at RJ and TJ (for example at take-off) operation modes. At rather low Ax/Ac ratios the engine would be oversized for TJ mode of operation, while at the high values - for RJ mode (Fig.13). At some ratio value both areas and engine weight W are minimized, and it is possible to consider this value as an optimum.

4. COMBINED ENGINE TYPES COMPARISON

The analysis of mission performance and advantages of some various combined ABE concepts was conducted for two advanced hypersonic aircraft:- ATOS launcher with stage separation at Mach 6;- HST with cruise speed Mach 6 (Fig.14).

Liquid hydrogen fuel is used. The using of LH2 enables us to consider a wide variety of engine concepts as it is of great heating value, high cooling capacity and high working capacity when expanding in a turbine [4].

The transition of aviation to new types of energy sources is historically inevitable. In some decades switch-over from a transport-energy system based on oil and other fossil energy sources to a system operating with a new energy source will take place. Synthetic hydrocarbon fuel will fill the shortage of oil fuel for some period of time. A prospective aviation fuel will be liquid hydrogen, having no raw materials limits. Global restorable sources of primary energy are used to obtain it. Passing to hydrogen energetics will resolve the ecological problems resulting from the wide application of hydrocarbon fuels.

The energy properties of traditional and alternative fuels are represented on Fig.15. The fuels, obtained on base of oil, casing head oil gas (ACF) and natural gas (AMF) rather slightly differ in mass calorific value, but significantly differ in volume calorific value and cooling capacity.

Liquid hydrogen as a future aviation fuel offers a complex of unique properties against a conventional kerosene - the heat value is higher by a factor of 2.8, the cooling capacity - by a factor of 15...20. LH2 is ecologically clean as a fuel. These properties, along with its reproducibility as an energy carrier raise the question of developing widely spread air transport of global importance, bringing aviation transport to high supersonic and hypersonic possibilities.

In our country, wide-scale experiments on using cryogenic fuels in aviation we are carried out, including flight testing. The Tu-155 experimental aircraft successfully made its first flight on April 15, 1988. The NK-88 hydrogen engine was mounted in the right engine nacelle. The engine was developed by the design bureau of N.D.Kouznetsov. The engine has a special fuel feed and control system with gasifying and heating of the hydrogen and a modified combustion chamber.

It took about ten years to develop all the required techniques including the investigation and experiments.

The Tu-155 aircraft can also use liquefied natural gas (liquid methane) as a fuel. The liquid methane engine was also developed in the design bureau of N.D.Kouznetsov. The Tu-155 experimental aircraft made the first flight in aviation history using liquified natural gas on January 18, 1989.

Flight tests of the Tu-155 confirmed the reality of developing a production passenger aircraft with cryogenic fuel [10].

For both above mentioned hypersonic missions in the comparison analysis the climb and acceleration trajectory was practically identical and flight at maximum speed was conducted at an altitude outside the atmospheric ozone maximum concentration area (Fig.16).

The efficiency criterion for the ATOS power plant was the relative mass of the second stage. For the HST with commercial load mass constant for all variants, the criterion was take-off weight. For the last mission airplane (HST), two flight concepts were considered—only with hypersonic cruise and combined subsonic (about 20 percent of total range) and hypersonic cruise. The combined mission reflects the possibility of flight speed reduction over populated territory for sonic boom impact elimination.

The following engine concepts are discussed (Fig.17).

1. Turboramjet engine (TRJ). TRJ consists of the TJ and RJ parts and has a common afterburner - ramjetcombustion chamber (ARCC) and ramjet channel with shut-off device. The TJ has a compressor with moderate pressure ratio and high temperature turbine (Tg max up to 2000 K). The variation of TRJ with a separate combustion chamber of the RJ part (TRJs) was also considered. The independence of the TJ and RJ parts in TRJs provides parallel operation of the parts at low and moderate flight speed with higher thrust performance.

2. Turbofanramjet engine (TFRJ), which, in essence, is a high temperature, variable geometry turbofan. The selection of a design by-pass ratio value at higher level improves matching of the TF and RJ sizes and transition of the engine to windmilling fan mode at high flight M numbers.

3. Regenerative Airturborocket engine (RATR) with transition to RJ mode at high M. Its compressor is driven by a turbine working on gaseous hydrogen, heating of which is performed in the heat exchanger, located in the combustion chamber. Because of heat regeneration the SFC of the engine is nearly equal to the SFC of the TFRJ at operation with the same maximum fuel-to-air ratio, but the RATR has higher thrust-to-weight ratio because of lowpumping work of a liquid fuel. The turbine inlet temperature is 1200 K.

4. Airturborocket engine (ATR) with transition to RJmode at high flight M. The oxygen/hydrogen burner (gas-generator) provides a high pressure, fuel rich flow to the uncooled turbine. This fuel rich flow is then mixed with the compressor discharge flow and burned in the combustion chamber. The turbine inlet temperature is 1200 K.

The variable geometry inlet and nozzle performance efficiencies are the same for all engine types. Design fan (compressor) pressure ratio in the cases of TFRJ, RATR and ATR was selected nearly the same. For this reason the thrust characteristics of TFRJ and RATR are nearly similar (Fig.18). The SFC of the ATR is more than 2 times higher in comparison with other engine types because of the use of onboard oxygen. It was decided, that all engines would operate on RJ mode at flight speed higher than Mach 3.5.

TFRJ has the highest fuel efficiency in subsonic cruise flight. In accordance with higher propulsive efficiency its dry thrust SFC is about 25 - 35 percent lower in comparison with TRJ and about 2-3 times - in comparison with RATR (for very high fuel consumption the ATR engine cannot be a competitor at these flight regimes). (Fig.19). However, the low dry specific thrust of the TFRJ at minimum SFC condition may lead to a decrease of subsonic cruise flight speed and altitude or to an increase of engine size and propulsion system weight. It should be noted that the range of RATR throttling performance is limited by heat exchanger over-heating.

For the engines considered one can recognize some interdependence between the engine thrust-to-weight ratio (TWR) and SFC in subsonic cruise flight. The ATR has a highest TWR. The RATR has a TWR about 10 - 15 percent lower in comparison with the ATR because of heat exchanger weight and lower working medium flow in the turbine. The TRJ and TFRJ have a TWR about 1.5 - 2 times lower (Fig.20).

The results of mission performance analysis are presented in Fig.21a,b. The highest second stage mass corresponds to ATOS launcher with RATR propulsion plant in accordance with good engine TWR and relatively low fuel consumption at maximum thrust rating (Fig.21a). The second stage mass of only about 5 - 7 percent lower corresponds to the system with TFRJ or TRJ. The lowest second stage mass corresponds to ATR (about 12 - 14 percent lower in comparison with turboramjets) because of worse fuel consumption which cannot be compensated by low engine weight.

The mission performance results for HST are substantially influenced by the presence of subsonic cruise. In the case

of fully hypersonic cruise the lowest HST take-off weight corresponds to the RATR power plant. Effectiveness of other engine types is somewhat lower and nearly equal (TOGW is higher by 18...20%). (Fig.21b). If combined subsonic and hypersonic cruise is considered (subsonic part is about 20 percent of total range), then turboramjet engines reveal the lowest take-off weight (TFRJ gives nearly 5% advantage in comparison with TRJ). Take-off weight with RATR engines is about 1.8 times higher than with turboramjets. Taking into account take-off noise limitations, the advantages of TFRJ are even greater. Thus, TRJ and TFRJ could be considered as universal multimode engine types of hypersonic (up to nearly Mach 6) aircraft of different missions.

5. TRE OPERATION MODE CHANGING CONDITIONS OPTIMISATION

At some flight M numbers the specific parameters of turbine and ramjet engines converge. On the other hand, TJ corrected airflow decreases with inlet air temperature increase, while in the case of RJ it is possible to maintain the corrected airflow constant. As a result the RJ thrust increases vs M number more rapidly, than of the augmented TJ type engines.

The high sensitivity of supersonic vehicles to the weight of components requires identification of propulsion system control methods which provide maximum vehicle effectiveness. For accurate resolution of such problems variation methods are normally used. As a result of different variation of the combined ABE thrust and SFC vs M number when operating on TJ or RJ modes there is some flight speed during the acceleration trajectory, which provides maximum efficiency for transition to RJ operation according to some criteria.

Usually it is required to provide:

- minimum time spent for acceleration;

- minimum fuel required for the acceleration part of the flight trajectory (for example, for TSTO first stage);

- maximum flight range (for example, for HST).

Only in particular cases does the optimum flight M number Mo for transition of operating mode correspond to the flight speed at which specific thrust parameters of TJ and RJ are equal to one another.

It should be mentioned, that it is possible to define the appropriate flight M number for mode changing from another point of view (for example, on the basis of minimum dynamic influence on the vehicle or minimum change of variable geometry components or from higher life considerations, etc.). However the above mentioned principle criteria are important for TRE working process analysis.

5.1. Defining the Mo

To obtain the corresponding equations we made the following assumptions [8]:

- changes of operation mode from TJ to RJ is instantaneous

- The acceleration trajectory is given;

- the air-to-fuel ratio at each trajectory point is optimum in accordance with the above mentioned cri-teria.

If the thrust vector is directed towards the tangent to flight trajectory, then the acceleration flight time from point (M1, H1) to point (M2, H2) of the trajectory:

$$t = \int_{He1}^{He2} \frac{Wp}{V(Tsum - D_p)} dHe$$

where Wp, V, Dp and vehicle propulsion system summary thrust Tsum vary vs M(He). If M1 < Mot < M2, then one can find the optimum value Mot (for time criteria) by resolving the equation:

$$tmin = \int_{He1}^{Heo} \frac{Wp}{V(Tsumtj - Dptj)} dHe$$

$$+ \int_{Heo}^{He2} \frac{Wp}{V(Tsumrj - Dprj)} dHe \qquad (1)$$

where "energetic altitude" Heo corresponds to Mot. Minimum value of the (1) right part corresponds to minimum values of functions under the integral. These values correspond to an engine operating at maximum rating in each point of the trajectory. Because engine thrust when operating in the RJ mode increases vs M more rapidly than in the TJ mode, then the minimum value of the right part (1) corresponds to the value of variable integration limit Heo, at which functions under the integral for TJ and RJ modes of operation are equal. Geometry interpretation is represented in Fig.22. The summary area under the curves of functions under the integral, which is proportional to the time spent for acceleration, would be minimum where the Heo value (or Mo) corresponds to the point of intersection of the curves.

Transfer to RJ mode of operation is accomplished at rather high M numbers, when additional inlet drag decreases substantially. Then one can neglect the difference in overall vehicle aerodynamic drag at TJ and RJ operating modes in trajectory point Mot. Consequently, the Mot value corresponds practically, to the condition when engine thrust values associated with TJ and RJ operating modes become equal.

$$Ttj = Trj.$$

Combined ABE always has some structural elements common to both parts (inlet, ARCC, external casing etc.) with characteristic cross section area A.

Then equation for Mot definition is:

$$\frac{Tstj}{Tsrj} \cdot \frac{(Wcor/A)rj}{(Wcor/A)tj} = 0 \quad (2)$$

Then, the Mot value depends on the gas turbine part cycle parameters, engine control law, correlation of both engine parts dimensions (for example, Ax/Ac), but it is independent of flight trajectory and vehicle drag parameters.

If with increasing flight M, the first member of the left part of (2) decreases and the second increases, which is inherent to TRE, then the Mot value would be between the M numbers corresponding to equal values of specific thrust Ts and airflow (Mw) when operating in TJ and RJ modes:

Mw < Mot < Mτs or Mw > Mot > Mτs.

If Ax/Ac increases at constant (Wcor/A)rj the ratio

Tstj/Tsrj

in equation (2) increases too, i.e. Mot value decreases.

Acting in the same way as previously, one can conclude that the Mog number (transition to the RJ operating mode which provides minimum fuel consumption), corresponds to the flight speed when the relative to excess thrust SFC values for both operation modes are becoming equal to one another. The equation for Mog number definition is as follows [8]: ·

$$\frac{Tsrj - \dfrac{d.U(Mog)}{(Wcor/A)rj}}{Tstj - \dfrac{d.U(Mog)}{(Wcor/A)tj}} = \frac{atj}{arj} \quad (3)$$

Where the values

$$\frac{d(U\,Mog)}{(Wcor/A)}$$

in the left part represent the ratio of the vehicle aerodynamic drag to the summary airflow of the whole powerplant (specific vehicle aerodynamic drag).

The value d is proportional to the vehicle drag coefficient and inversely proportional to the sum of engine section areas A for all propulsion sectors of the powerplant:

$$d = \frac{KPo}{2} \cdot \frac{Cp}{Asum/S} \cdot \left(\frac{Ta}{To}\right)^{0.5}$$

where Asum is the sum of areas A, S the wing area.

Included in equation (3) the flight M number function U(M) looks as follows:

$$U(m) = \frac{M^2 \cdot \left[1 + \frac{k-1}{2} \cdot M^2(1 - h_{in})\right]^{\frac{k}{k-1}}}{\left[1 + \frac{k-1}{2} \cdot M^2\right]^{\frac{k+1}{2(k-1)}}}$$

where intake efficiency hin is the ratio of airflow kinetic energy after isentropic expansion from behind the intake section to that of the free-stream air-flow. The intake recovery Sin values vs M and typical hin values are represented in Fig.23.

Thus, unlike the Mot number, the Mog depends also on the vehicle aerodynamic perfection and its (T/W) ratio, which is reflected by value d. If air-to-fuel ratios a on both operation modes are equal, then with value d decreasing, the Mog number approaches the value at which specific thrust values in both operating modes become equal. With value d increasing, the Mog approaches the value at which airflow values in both operating modes are become equal. So, depending on cycle parameters, dimension correlation and engine control law, with d increase the Mog number can either increase or decrease. The latter is more likely.

Using a similar approach an equation was obtain for defining the Mol number, corresponding to maximum range [8].

Being subjected to the influence of the same factors as that of the Mog number, the Mol value additionally depends on the trajectory altitude (dynamic pressure) at the point of transfer to the RJ mode, the wing loading factor and on the range factor (i.e. on vehicle L/D, overall engine efficiency, flight speed at cruise). With improving the vehicle quality at cruise (increasing L/D or engine overall efficiency) the Mol number approaches Mog , because it is profitable to redistribute the onboard fuel in favour of the cruise part of the flight.

As was represented, the Mo numbers depend on the variation of specific thrust and airflow in both TJ and RJ operation modes.

The TRE propulsion plant transition to the RJ mode process depends on correlation between the airflow characteristics of the variable geometry inlet and of both combined engine parts.

As an illustration, in Fig.24 are represented the typical variations of maximum possible airflow in inlet at constant altitude vs flight M number (lines for Ain1 and Ain2, and for this example it is known that Ain1 > Ain2), and also the curves of maximum airflow capacity for the TJ (curve "T") and RJ (curve "R") engine parts. One can see that the real propulsion plant airflow variation vs flight speed would be defined by the correlation between the air inlet and the engine part dimensions (i.e. fan or compressor and ARCC cross section areas).

If the engine airflow in the transition to the RJ mode proceeding is defined by the ARCC airflow capacity and is not limited by the variable inlet, that is more specific to the TRJ with its rather high specific thrust values in the TJ operation mode, then suitable power plant governing corresponds to maintaining the TJ part maximum rating (curve "T") up to point 1 at Mol, in which the transition to RJ mode of operation takes place. Then between points 2...3 the airflow corresponds to the ARCC maximum capacity, and at higher flight M numbers is limited by the maximum inlet airflow capacity. In this trajectory part the

best engine performances are provided by a corresponding decrease of the critical sections of inlet and nozzle.

For the TFRJ type of TRE (with rather low specific thrust in the TJ mode) the transition to RJ operation mode process is to a greater extent characterized by the limiting of the engine airflow by the inlet flow capacity (line Ain2 on Fig.24). In this case the transition to RJ mode process consists of gradual derating of the TJ(TF) part in some range of flight M number up to TJ(TF) switch off. In the transition proceeding the air-to-fuel ratio in the ARCC should be maintained at maximum rating. The power plant control law in this process is defined by the accordance of the inlet and engine variable geometry elements with the condition of providing the minimum pressure losses and the necessary surge margin. The transition begins at flight M number, when the engine airflow approaches the limit of the inlet airflow capacity (point 4), and finishes with the TJ part approaching windmilling mode. In this case the optimum Mo numbers on various "energetic" criteria coincide.

5.2. Mo numbers for TRJ

The influence of various factors on Mo number analysis was performed for TRJ (Fig.25) on the basis of the equations obtained.

The minimum time spent for vehicle acceleration corresponds to the maintenance of minimum air-to-fuel ratio values along the acceleration trajectory. The range of possible Mot numbers is limited by values of Mw and MTs. The equal engine nozzle pressure ratio expansion values in both operation modes correspond to the latter.

The Mw number, at which the airflow values in both operating modes become equal, depends on the engine's design cycle parameters, its control law and the correlation of the engine part dimensions.

In Fig.26 as an example the typical MTs and Mw number variations vs design engine compressor pressure ratio are represented. If we increase the compressor work by opening the nozzle, the curves for MTs and Mw draw together because of a decrease in TJ operating mode specific thrust and an increase in airflow. This is illustrated by curves corresponding to critical nozzle area increase by 20% (An* = 1.2). The curves mentioned in Fig.26 correspond to equal corrected stream velocity at ARCC inlet for both operation modes. Increasing the airflow and stream velocity at the ARCC inlet in the RJ operating mode decreases the Mw numbers.

To define the engine ratings corresponding to minimum fuel spent during the vehicle acceleration phase one can use the idea of "instant acceleration efficiency" as the ratio of vehicle mechanical energy increment to engine thrust work within infinitesimal time, which, bearing in mind the approximate correlation for the vehicle mechanical energy deriva- tive on time equals [8]:

$$ha = \frac{dEp}{Tsum.V.dt} = 1 - \frac{Dp}{Tsum}$$

The ha efficiency characterizes the part of the useful engine thrust work which transmits to the vehicle mechanical energy

Similarly, by defining the instant overall acceleration efficiency hoa as the ratio of vehicle mechanical energy increment to the energy of fuel spent in the propulsion plant within infinitesimal time one can obtain that hoa equals the product of engine overall efficiency and instant acceleration efficiency:

$$hoa = ho.a = ho.\quad \mathcal{A} - \left(\frac{Dp}{Tsum}\right)$$

The minimum fuel spent in the vehicle acceleration phase corresponds to such engine control laws, when at each acceleration trajectory point the maximum possible hoa value is provided. Such propulsion governing corresponds to the minimization of SFC related to excessive thrust. These minimum points displace to the right (on lower air-to-fuel ratio values) along the engine rating curve SFC(T) relatively to usual SFC (relative to inner thrust) minimum points. From the fuel-spent point of view, in practically possible cases the optimum engine rating in the supersonic part of the acceleration trajectory coincides with the maximum (afterburning) ratings [8].

TRJ Mo number calculations were performed at constant values of air-to-fuel ratio (a = 1.2), ambient air and turbine inlet gas temperatures.

Fig.27 shows the dependence of Mo numbers on design compressor pressure ratio. The presence of maximum points on curves for Mot and Mog is explained by compressor pressure ratio variation contrary influence on specific thrust and air-flow on TJ operation mode. When increasing the design turbine inlet temperature value the maximum Mo numbers displace to the higher design compressor pressure ratios, and the Mo numbers themselves increase because of, mainly, the relative decrease of ARCC dimensions and corresponding decrease of thrust in the RJ operation mode (Fig.28). If it is possible to increase the compressor work while maintaining its efficiency at the initial level then the optimum Mo values also rise because airflow and thrust increase in the TJ operation mode. This is presented in Fig.27 by curves corresponding to the nozzle throat area increase by 20% (An* = 1.2).As follows from the Fig.27, at typical values of d = 45...90 kPa the Mog values are close to the Mot values, being somewhat higher than the latter. The curve for Mol number (dotted with points line) practically is analogous to the corresponding curve for Mog numbers.

The dependence of Mot and Mog numbers on the ratio of the ARCC cross section area to the compressor inlet area is shown in Fig.29. The optimum Mo numbers decrease when the Ax/Ac value increases and are lower than the TJ "degeneration" Mach numbers. When the air-to-fuel ratio is given, then the main factor by which, in a powerplant with variable geometry inlet and nozzle, one can vary thrust performance in RJ operation mode is the airflow. Increasing the flow velocity at the ARCC inlet while

maintaining the inlet efficiency leads to thrust increase in the RJ operation mode and consequently to Mo number decrease (Fig.30), in spite of the somewhat worse engine specific parameters. This enables forcing of the TRJ on air-flow capacity in the RJ mode as a method for lowering the flight M number for transition to RJ operation mode.

TRJ performance analysis has revealed that typically optimum Mach numbers for transition to RJ flight lie in the range of 2.5...3.5 and because of higher airflow in the RJ mode as a rule the Mo number is lower than the TJ "degeneration" flight Mach number, i.e. at Mo there is a difference in total pressure values behind the TJ and RJ engine parts in favor of the first. In this case, adequate control of the propulsion system is needed to provide stable operation in the transition mode.

CONCLUSION

Theoretical investigations and computational modelling of air breathing powerplants for $M = 4...6$ have included the classification and performance analysis of various types of turboramjet engine. An approach to the theoretical design and construction of the engine configuration was produced. Comparative analysis of the merits of various ABE types being installed on future hypersonic vehicles with cruise and acceleration flight trajectories has revealed the advantages of TRJ and TFRJ as universal variable cycle engines for high flight Mach numbers. Optimisation of specific TRE transition mode conditions along with other investigation results give an approach to engine governing in the operating modes and the basis for formulating the requirements for experimental TRE and the problems of their investigation.

REFERENCES

1. Д.А.Огородников, М.М.Цховребов. Авиационные двигатели XXI века. Техника воздушного флота. 1(487), 1990.

2. Г.С.Бюшгенс. Авиация в XXI веке. Техника воздушного флота. 1(487), 1990.

3. L.M.Shkadov, V.I.Babkin, M.M.Tskhovrebov, "Civil aviation - the ways of progress in XXI century". Rep. on Airshow Canada Symposium. Vancouver, aug. 1991.

·4. Р.И.Курзинер. Реактивные двигатели для больших сверх звуковых скоростей полета. М. Маш. 1989.

5. Турбопрямоточные двигатели для гиперзвуковых скоростей полета. Под ред. В.А.Сосунова, М.М.Цховребова. Вопросы авиационной науки и техники. Серия Авиационное двигателестроение. Вып.3, 1993. М., ЦИАМ.

6. M.M.Tskhovrebov, V.A.Palkin, "Combined engines for hypersonic flight". ICAS - -92-3.1.3. 18-th ICAS Congress, 21-25 September, 1992, Beijing, PRC.

7. N.Yu.Rotmistrov, M.M.Tskhovrebov, "Variable - cycle engines for boosting-cruising vehicles". IAF-88-249. Report at IAF congress, Bangalore, India, 1988.

8. М.М.Цховребов. Об оптимальных числах М перехода комбинированного двигателя на прямоточный режим работы. Труды ЦИАМ, 1972, N 542.

9. Теория двухконтурных турбореактивных двигателей. Под ред. С.М.Шляхтенко, В.А.Сосунова. М. Маш. 1979.

10. V.A.Sosounov, "Some Aspects of Hydrogen and other Alternative Fuels for Application in Air - breathing engines". IX ISABE, Athens, Greece, September 3-8, 1989.

Fig 1 Commercial transport propulsion plants [1]
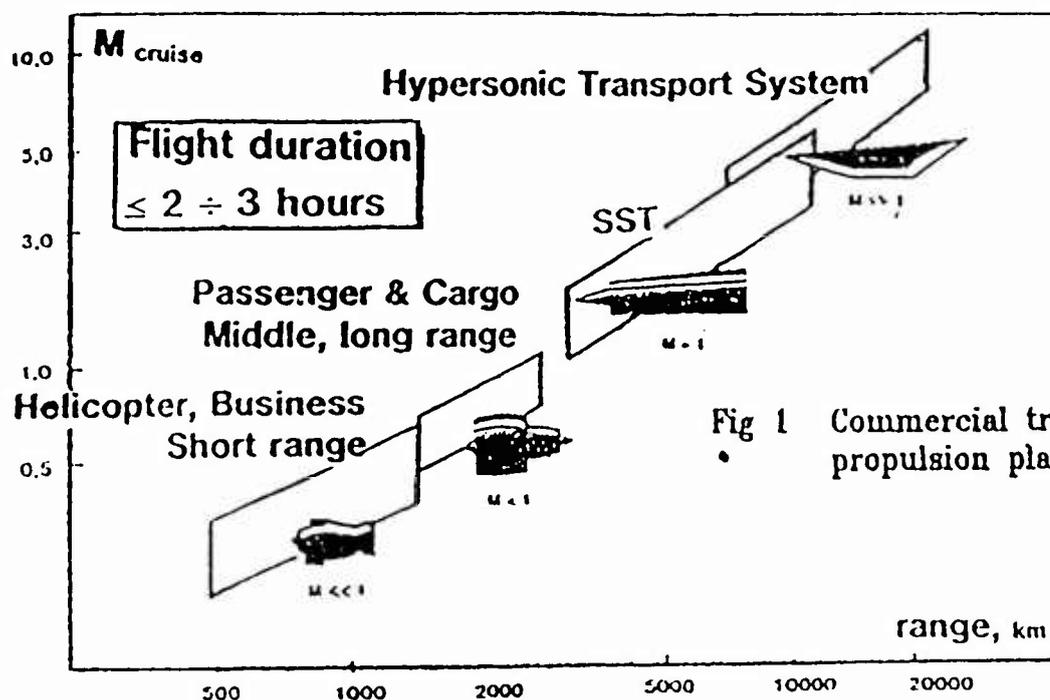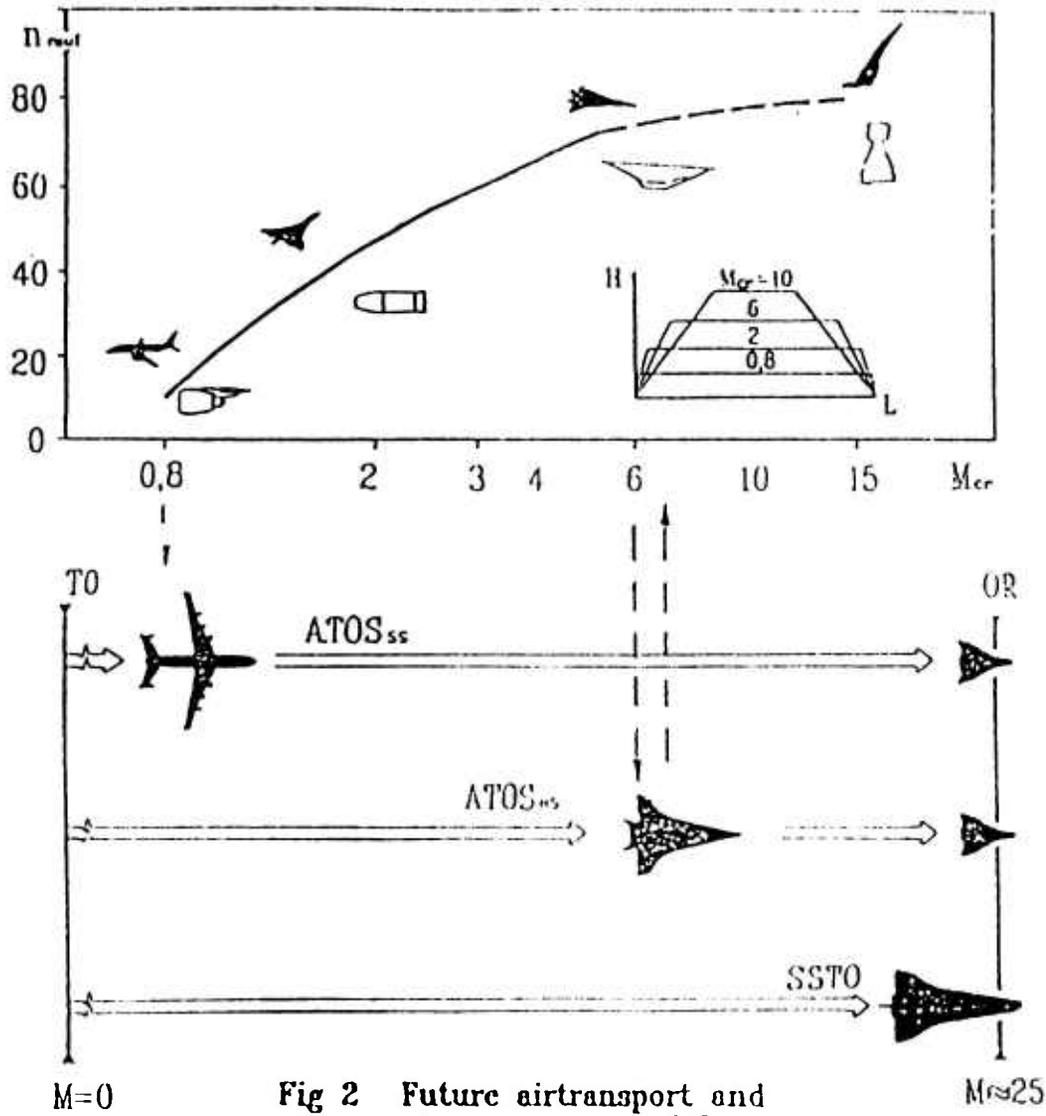
Fig 2   Future airtransport and
         airspace systems [6]
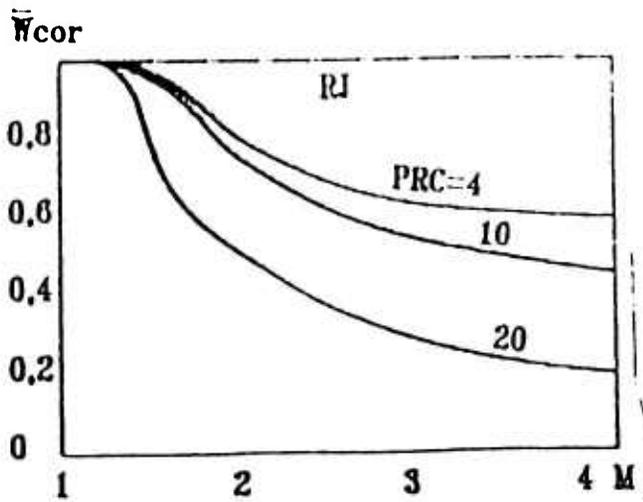
Fig 3   TJ correctedairflow vs flight
         M number [4]
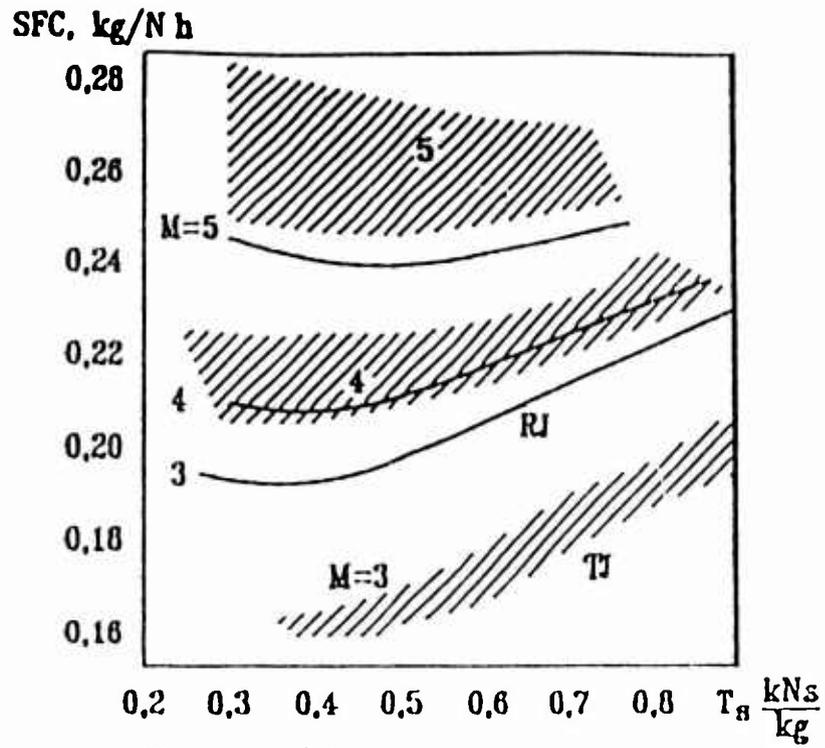
Fig 4   TJ(A) and RJ performance
comparison [4]
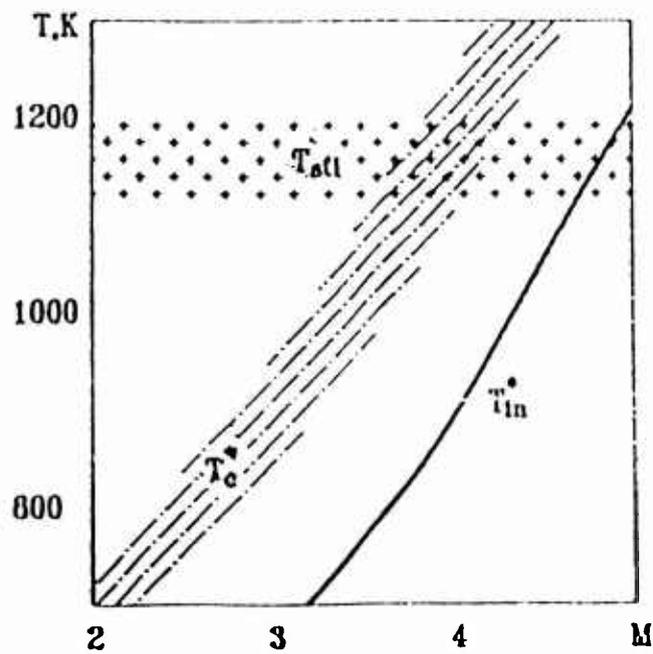
Fig 5   Compressor inlet and outlet
temperatures vs flight M number [4]
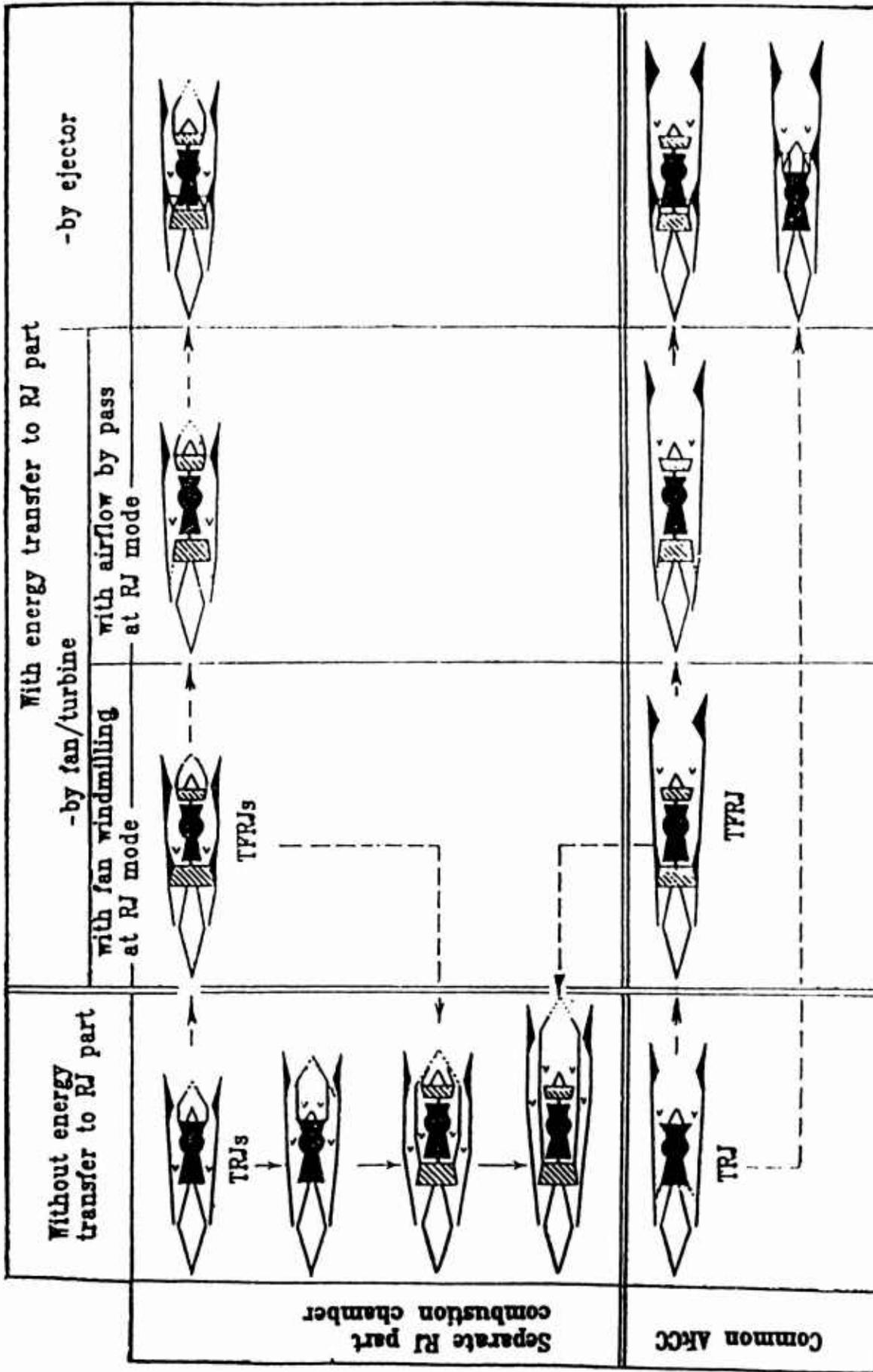
Fig 6   TRE types classification [9]
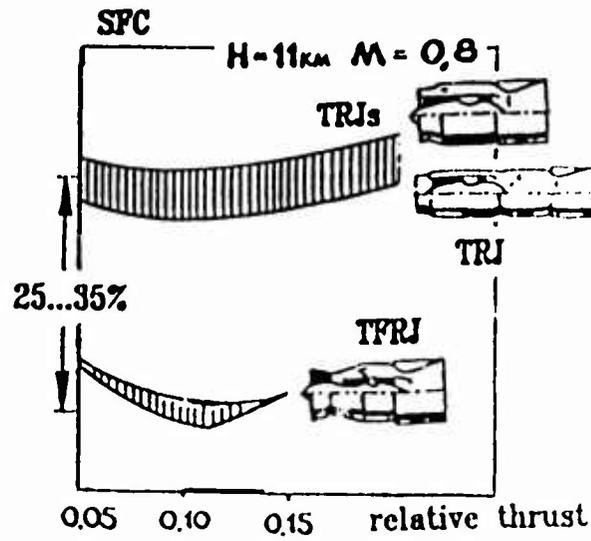
Fig 7   Engines subsonic performance [5]
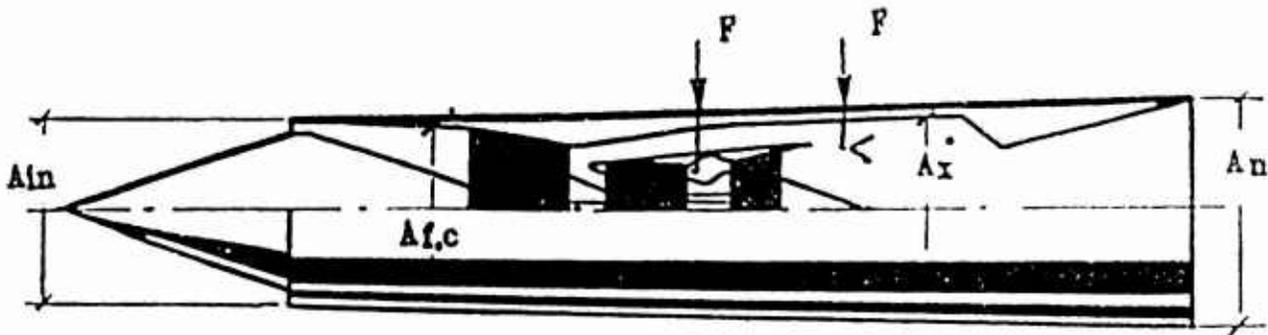
Fig 8   TRE characteristic sections [5]

Fig 9

Spesific thrust
variation vs PS
outlet/inlet
areas ratio [5]
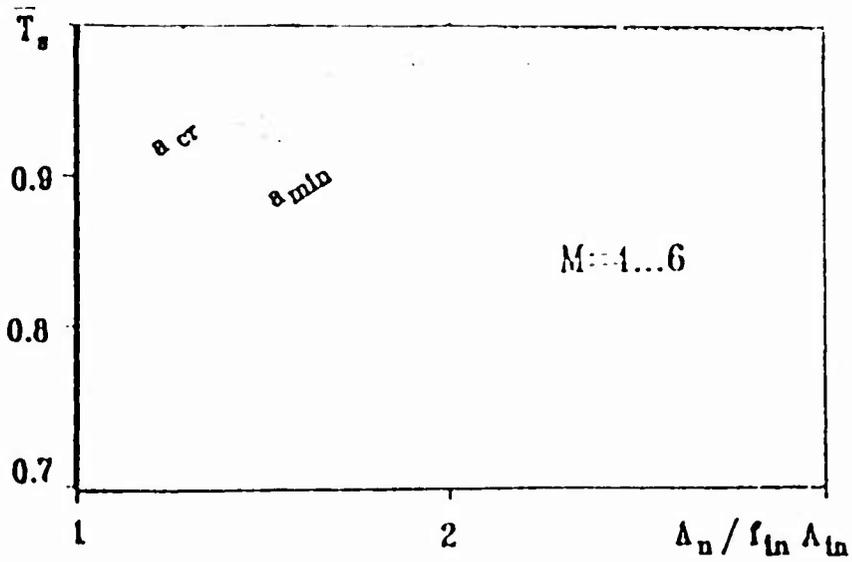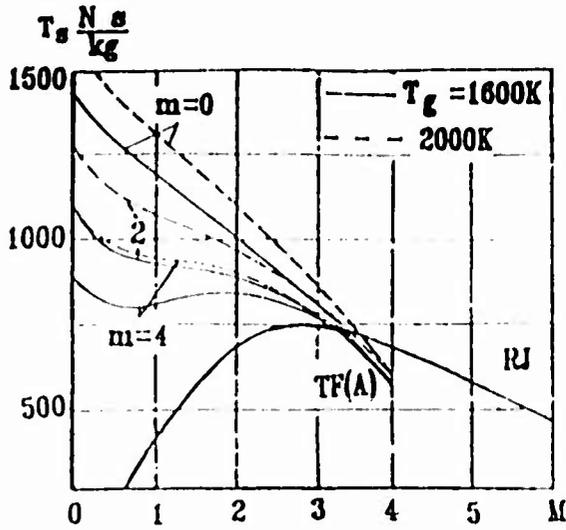
Fig 10   Turbofan and Ramjet specific
          thrust comparison [5,9]
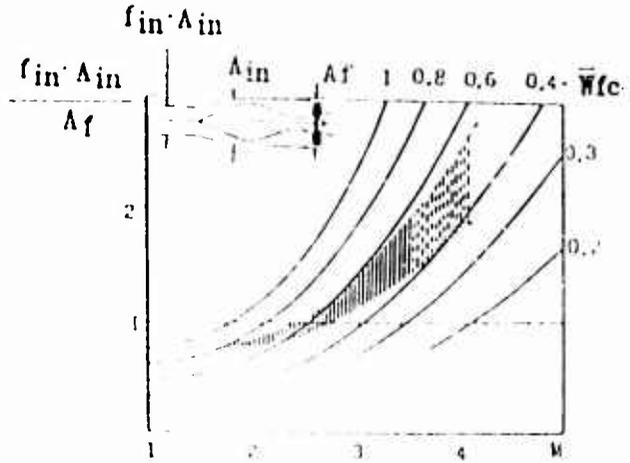
Fig. 11   Fan(compressor) and intake
           dimensions comparison [6]
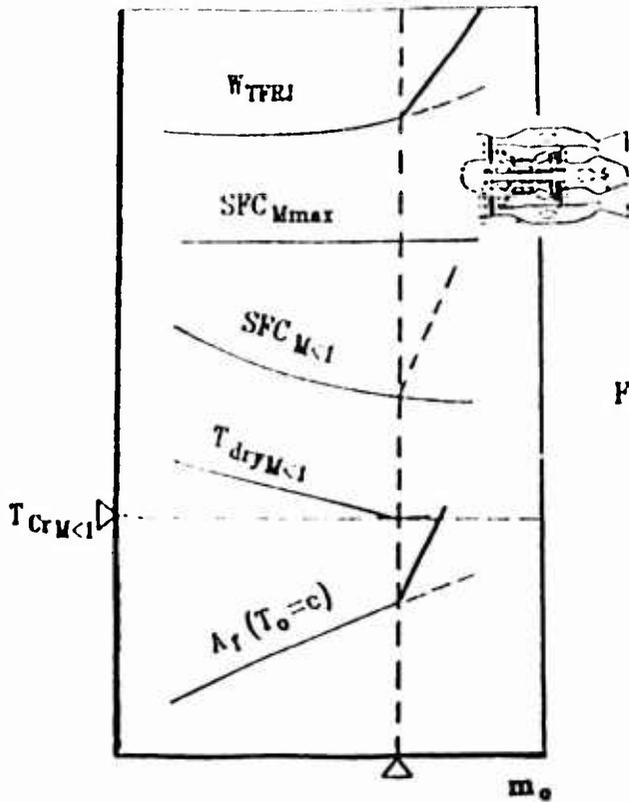
Fig 12   Design bypass ratio
          definition [5]
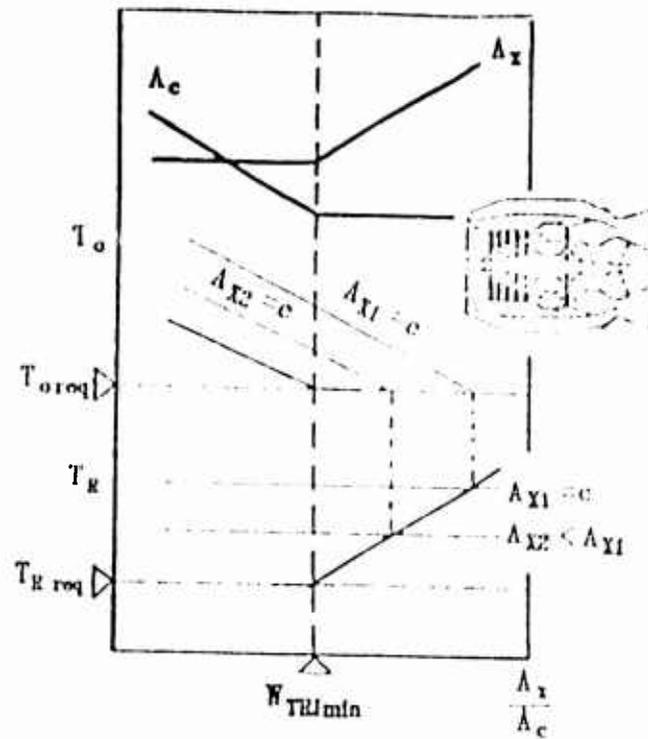
Fig. 13 Design area ratio
definition [5]
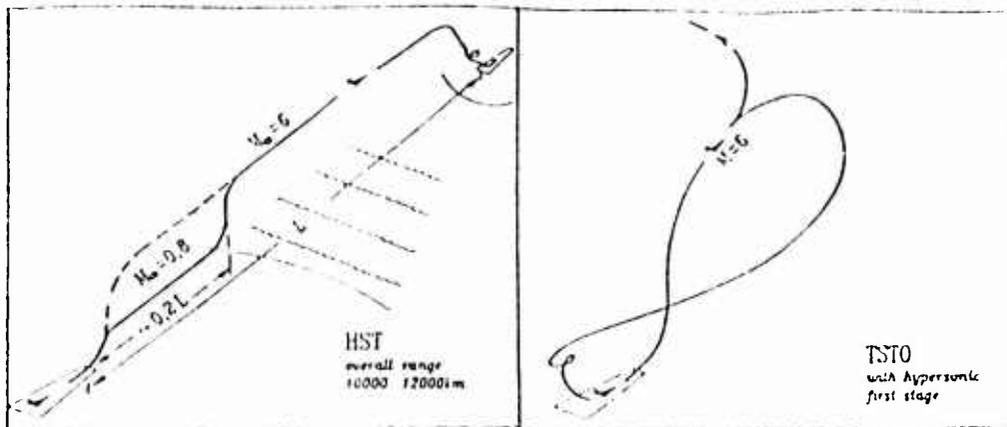
Fig 14 The flight profiles of ATOS
(TSTO) and HST [6]
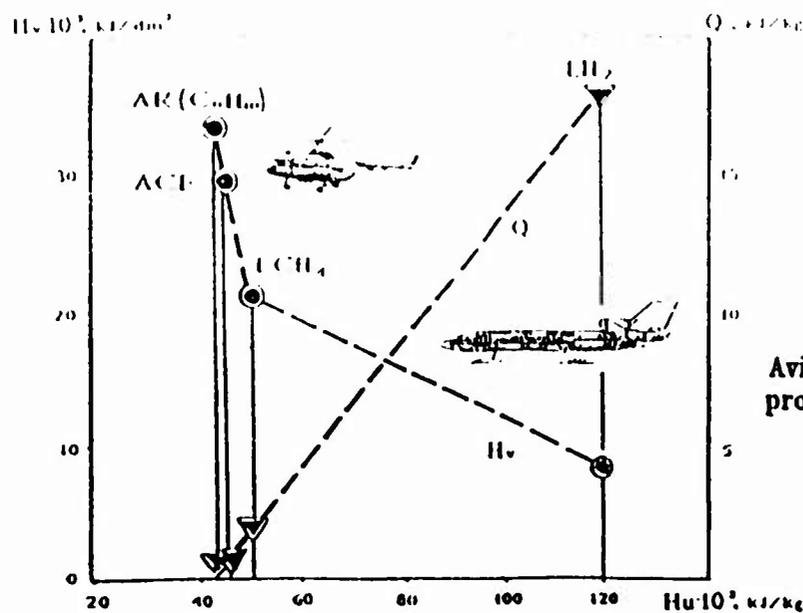
Fig 15

Aviation fuels mean
properties [3]
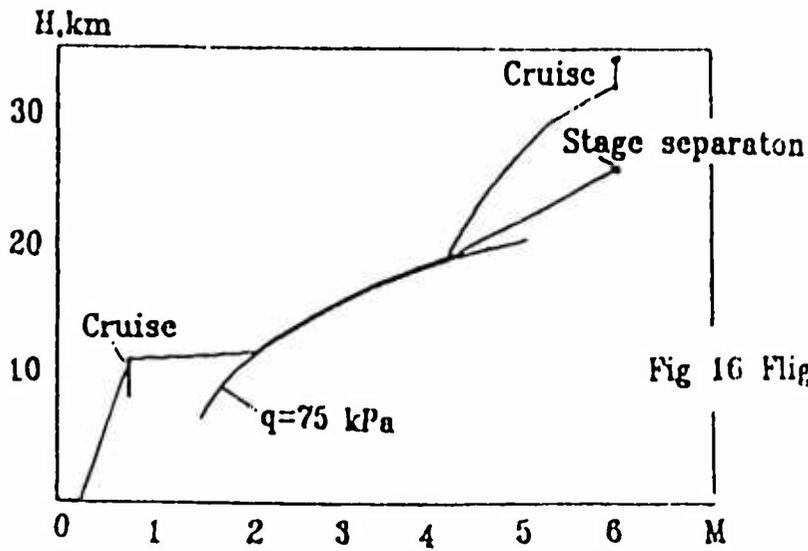
Fig 16 Flight trajectories[6]
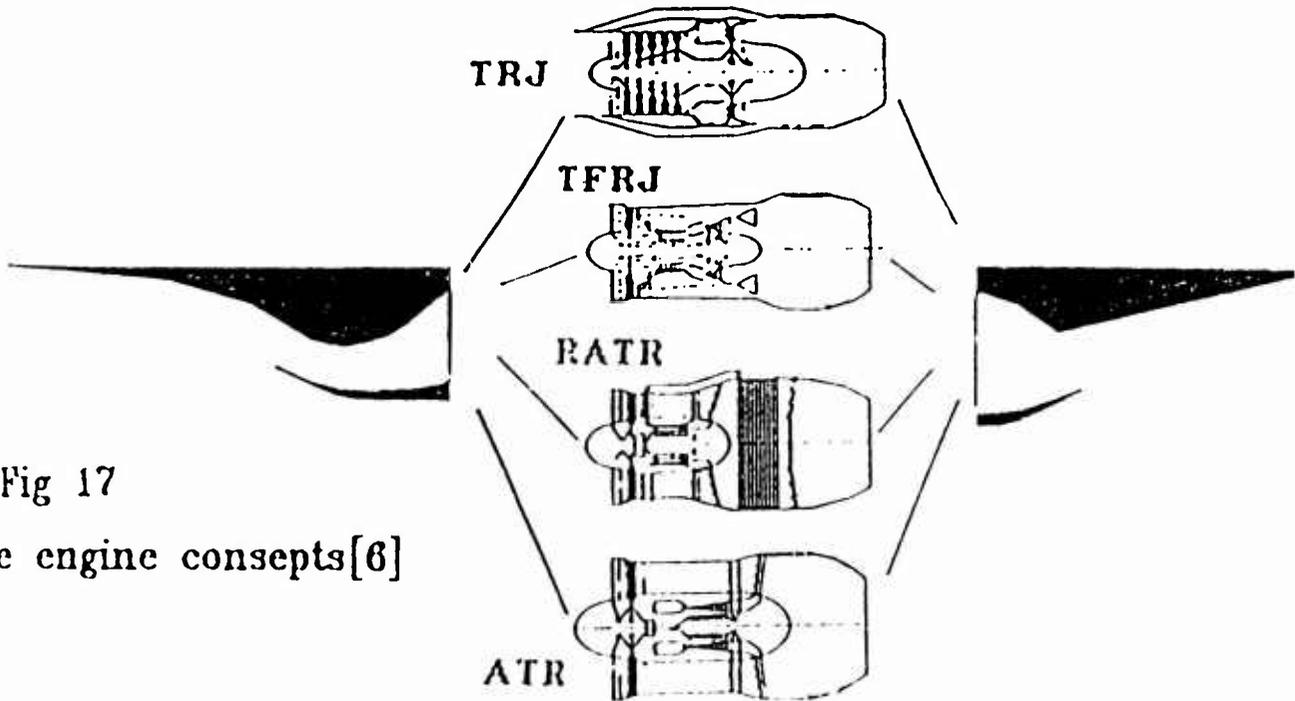
Fig 17

The engine consepts[6]
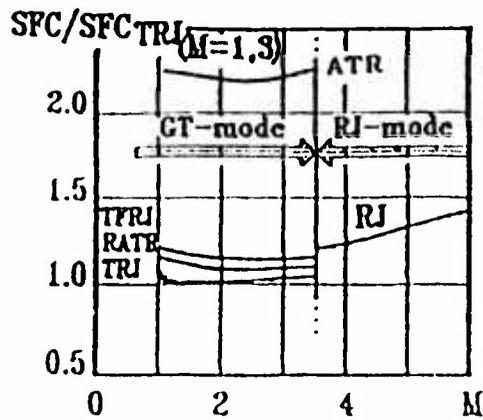
Fig 18 The engines' performance
characteristics[6]
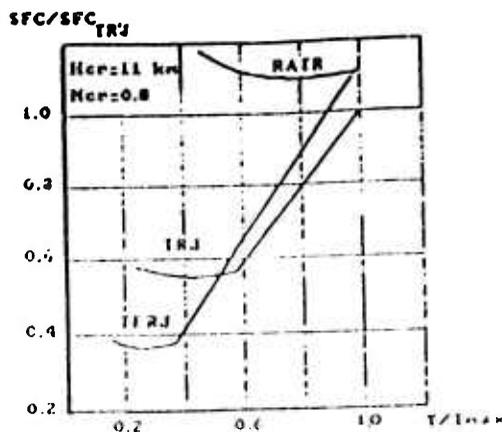
Fig 19 The engines' relative SFC[6]
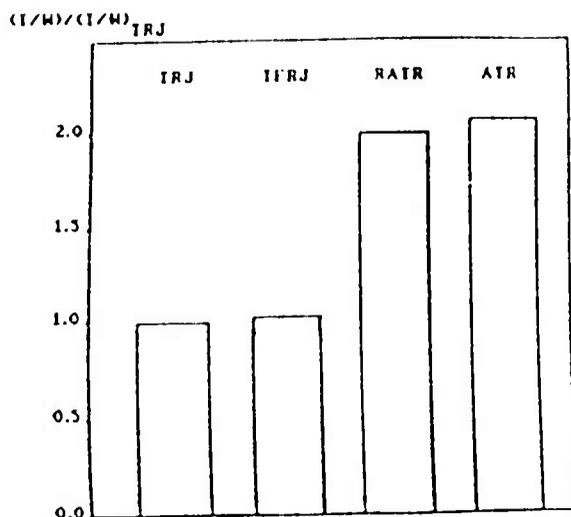
Fig 20 The engines' relative
thrust-to-weight
ratio at transonic
flight speed[6]
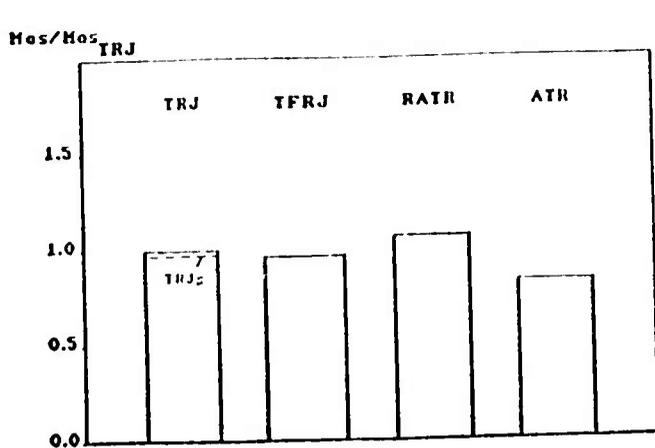
Fig 21a TSTO second stage relative mass[6]
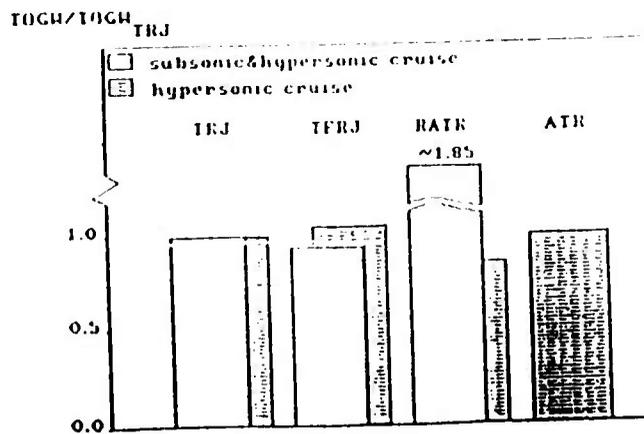
Fig 21b The relative TOGW of HST[6]
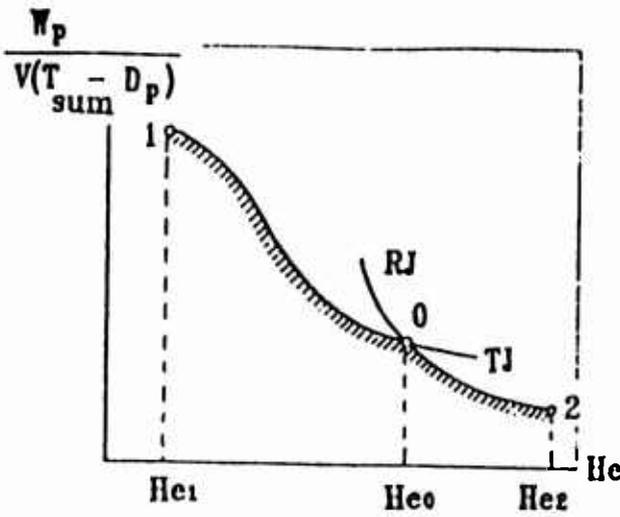
Fig 22 Defining flight Mo
number [8]
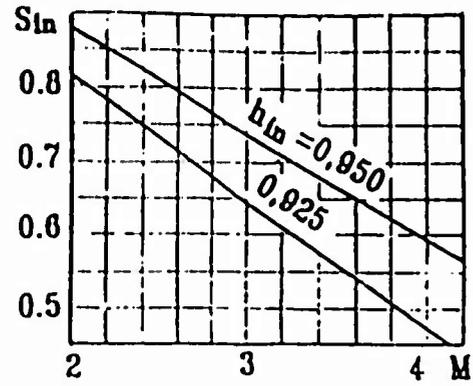
Fig 23 Intake pressure recovery
coefficient vs M number
and intake efficiency [8]
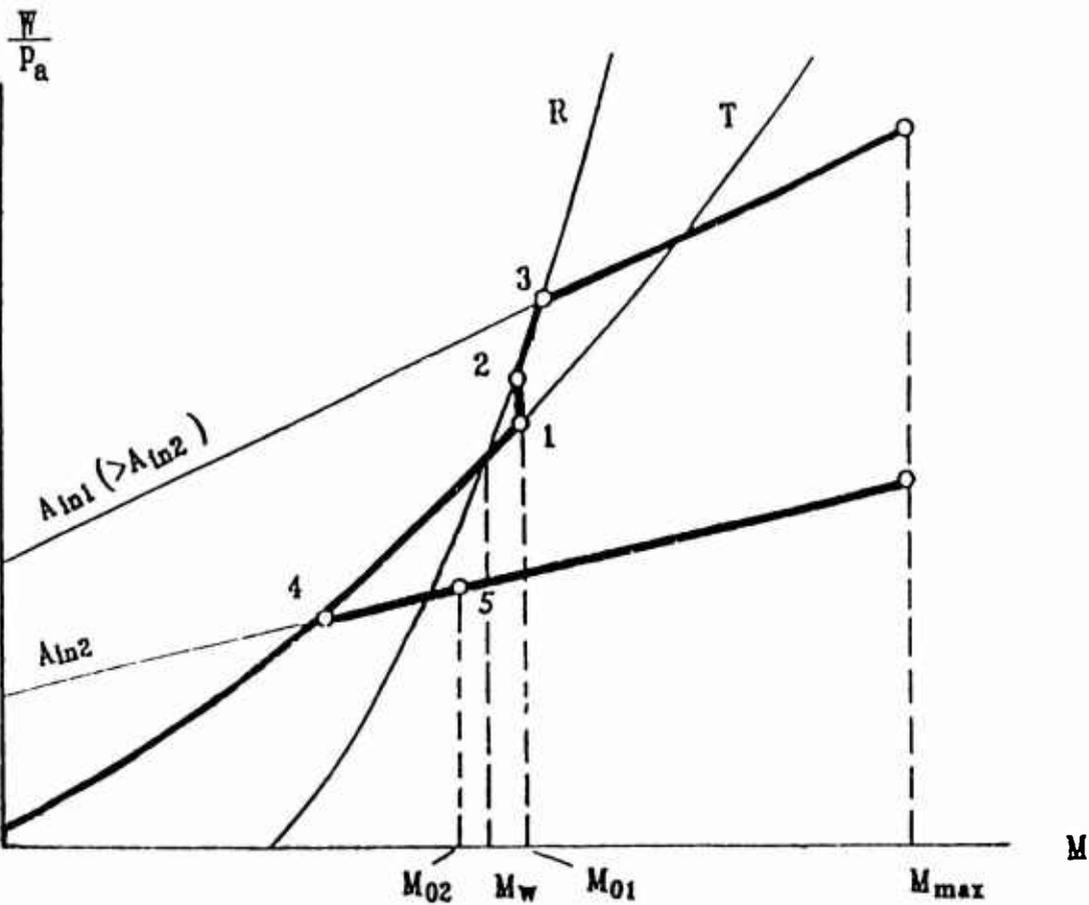
Fig 24 The TRE airflow variation at
transition to RJ operating mode [5]
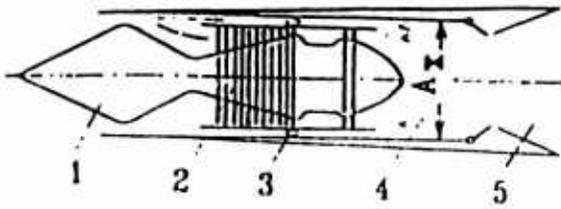
Fig 25 TRJ layout [8]

1-variable common inlet;
2-TJ; 3-RJ duct shut-off device;
4-common ARCC;
5-variable nozzle
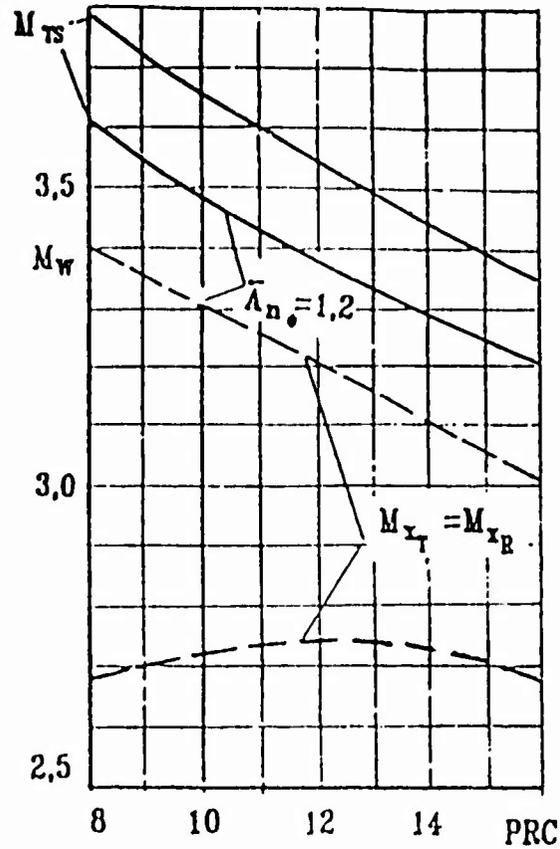
Fig 26 M_{TS} and $\dot{M}_W$ numbers vs design PRC [8]
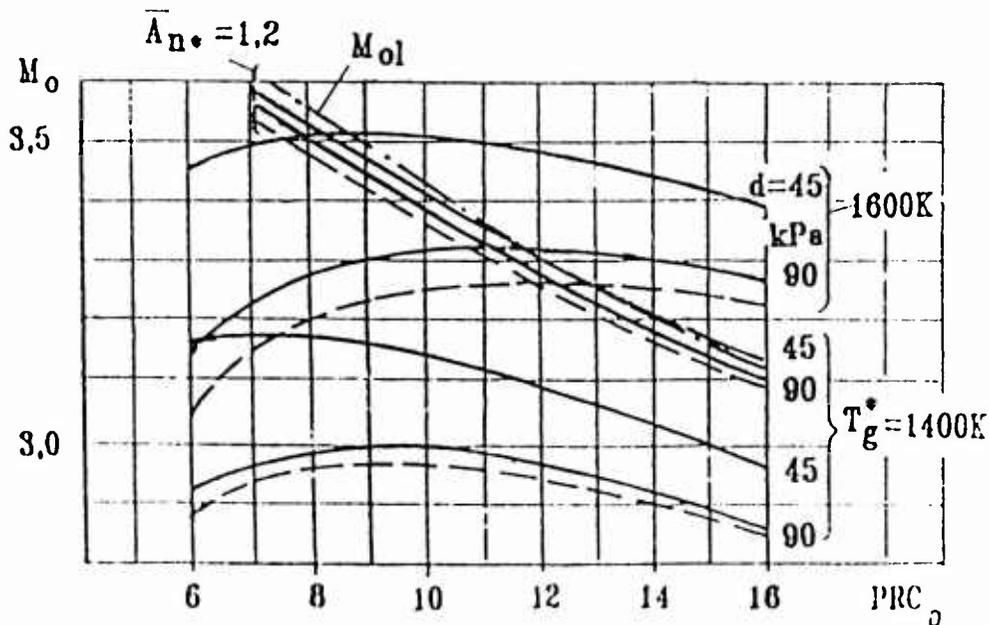
Fig 27 M_0 numbers vs design PRC [8]

——— M_{og}

———— M_{ot}

Fig 28 Mo numbers vs turbine inlet temperature [8]
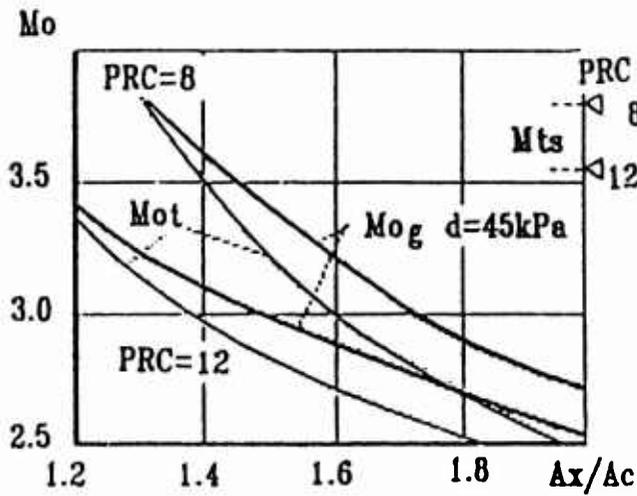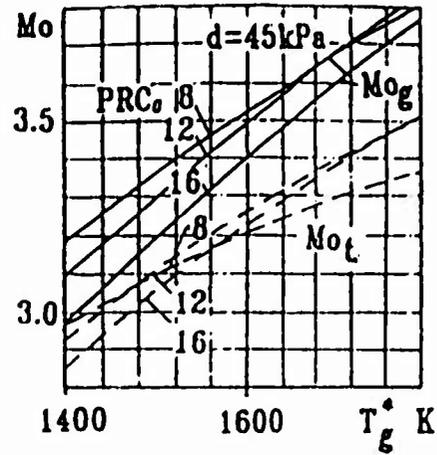
Fig 29 Mo numbers vs ARCC/compressor areas ratio [8]
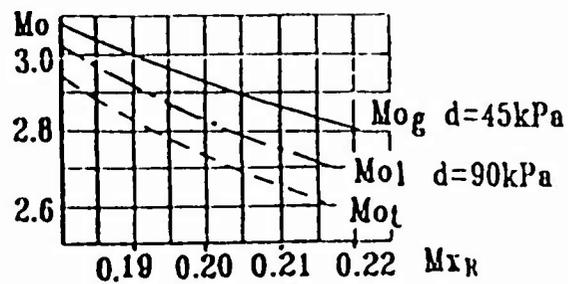
Fig 30 Mo numbers vs ARCC inlet flow velocity at RJ operating mode [8]

RESEARCH AND DEVELOPMENT OF RAMJETS/RAMROCKETS
PART I. INTEGRAL SOLID PROPELLANT RAMROCKETS

by
Prof., D. Sc. V. Sosounov
CIAM (Central Institute of Aviation Motors)
2, Aviamotornaya St.
111250, Moscow,
Russia

INTRODUCTION/SUMMARY

Solid propellant ramrockets (SPRR) combines the exclusive operational advantages of solid rockets with high fuel efficiency as being air - breathing type of engine.

The specific feature of SPRR which differs from liquid fuel ramjet is the arrangement of ram - combustor in which the products of primary burning of solid propellant inside the gas generator are injected through some nozzles and reburn (fig. 2.1). By this process not only the heat is released but some ejection effect appears which increases the front area specific engine thrust. So the direction gas generator nozzles axes must be arranged mainly along the main ram combustion chamber airflow.

The second feature of SPRR combustion process is that the gasified products of primary burning gas generator reburn in ram combustor as turbulent or quasi turbulent gas flames. Usually there is no need in some special flameholders.

All these special features lead to some peculiarities of inserted booster case or grain arrange it and to rather complicated gasified fuel supply devices.

The third special (negative) feature of SPRR is the constant or programmed fuel supply rate during the flight. So the problem of SPRR fuel flow rate control arises.

This lecture contains such items of discussion:
- Integration of SPRR with booster rocket engine.
- Energy capabilities of different ramjet solid propellants and their application.
- Effectiveness of fuel secondary combustion in ram combustor.
- Model and full scaled ramrockets ground testing.
- Fuel flow rate control in ramrockets.

NOMENCLATURE

A - area;

a - velocity of sound;
$C_F = F_a/q_0$ - thrust coefficient;
D, d - diameter;
F - thrust;
$F_a = F/A_{in}$ - frontal area specific thrust;
$F_s = F/G_a$ - specific engine thrust (per 1 kg/s airflow);
G - mass flow rate;
H - altitude;
$Ht = Hu/(1+L_0)$ - max heat capacity of combustion products (by $\alpha = 1$)
Hu - mass heat of combustion;
Hv - volumetric heat of combustion;
I - mass specific impulse;
I_v - volumetric specific impulse;
L - length;
L_0 - stoichiometric ratio;
M - Mach number;
m - mass;
N - number of nozzles, injectors, holes;
P - pressure;
$q = \rho v^2/2$ - dynamic pressure;
$q(\lambda) = A^*/A$ - ratio of critical to current cross-section;
Q - heat of combustion without air;
R - gas constant;
r - range;
T - temperature;
t - time;
V - volume;
v - flight velocity;
w - air, gas velocity;
$\alpha = G_a/L_0 G_f$ - equivalence air-fuel ratio (air excess coefficient);
β - equivalence fuel-air ratio ($\beta = 1/\alpha$);
ε - erosive burning augmentation ratio;
η - fuel combustion completeness;
η_s - secondary combustion completeness;
$\lambda = w/a^*$ - dimensionless velocity coefficient;
μ - relative fuel mass;
ν - burning rate pressure exponent;
ρ - density;
σ - pressure recovery factor;

INDICES

a - air;
b - burner, combustor;
c - corrected;

cb - central body;
eq - equivalent;
f   - fuel;
fl   - flame;
g   - gas;
gg - gas generator exit;
n   - nozzle;
p   - propellant;
t   - total;
o   - nominal value, infinity;
opt - optimal;
( )* - critical value;
($^-$) - relative value, mean value;
| | - references placed at the end of lecture;
I   - booster stage;
II   - sustain stage;

ABBREVIATIONS

ABE   - air breathing engines;
GG   - gas generator;
LFRJ   - liquid fuel ramjet;
LR   - liquid rocket;
PR   - pressure ratio;
PS   - propulsion system;
RJ   - ramjet engine;
SPRR - solid propellant ramrocket;
SR   - solid rocket;

I. INTEGRATION OF SOLID PROPELLANT RAMROCKET WITH BOOSTER AND MISSILE IMPROVEMENT

Since the SA-6 missile was put into operation in 1967 solid propellant ram rockets (SPRR) have been largely improved in different countries. The investigations were pursued mainly in the following directions (Fig. 2.2):

-increase of ramjet propellant energetic;

-improvement of a booster;

-development of different ways of propellant consumption control.

Thus, it was shown that the use of boron instead of magnesium and aluminium provided 1.5 increase of gas generator propellants mass combustion heat and more than double increase volume combustion heat. The formulas of special propellants having an index of a power in combustion law $v = 0.5 - 0.7$ and meant for use in gas generators with solid propellant consumption control have also been developed.

Booster improvement has been performed mainly using grains bonded to the combustion chamber walls according to cast technology adopted in solid propellant rocket engines (SR). This allows to increase volume filling of a booster combustor by 7% in comparison with insert grains. The intensive studies of nozzleless boosters are being conducted and the practical results in them introduction for aviation missiles SPRR have already been obtained. Their main advantage is the absence of jettisonable structural components that is of great importance for this class of missiles.

Great attention was being given and is currently being given to investigation and development of different ways of solid propellant consumption control on cruising regime. Especially that concerns the problem connected with the development of the effective and reliable design of controller allowing to perform control according to arbitrary program. Just the absence of such structure restrained till lately the use of SPRR on air-to-air missiles. Now there are certain achievements in this field.

Introduction of all these achievements allows to improve substantially thrust - economical performance of SPRR and to widen the area of their application.

Integration of solid propellant ram rockets with booster engine

It is preferable to use integral SPRR on small or medium air-to-air and ground-to-air missiles. The principle of integration of solid propellant booster and cruising ramjet in a common configuration allowed to realize in the best way the combination of simplicity, reliability and small size of a solid propellant booster with the high fuel efficiency of the simplest engine of air-breathing type. In this case placing the solid propellant of the booster engine in the ramjet combustor is due to the overall small volume of these engines. That is an important factor under conditions of strict overall dimensions limitation, which are characteristic for aviation missiles and small guided anti-aircraft missiles.

In the most full measure the low volume factor takes place in SPRR due to relatively high density and ejective effect of its propellant. In range of flight Mach number of 2-4 typical for advanced aviation missiles the integral SPRR has 2-4 times as much specific impulse than the rocket engine has at sea level. That is defining factor for long-range missiles. The cruising SPRR running for a long time allows the missile to develop high averaged speed on its trajectory and provides its high efficiency. Placing the solid propellant booster in the combustor of integral ramjet permits to reduce the volume of propulsion system (PS) by 30-40% in comparison with scheme of tandem arrange and jettisonable booster.

According to structural indications the booster SR of integral SPRR with a common combustor can be classified in the following way (Fig. 2.3):

- the booster SR with insert grain and ejectable nozzle (PS of the SA-6 missile can be considered as an example);
- the booster SR with case bonded grain and ejectable nozzle (an example is PS of ASALM);
- the nozzleless booster [1,2,3].

The design of integral ramjet with booster grain placed directly in a ramjet combustor has been studied in the USA from 1974 (ASALM program and others). In this case grain is either inserted or filled into ramjet combustor. The variants when grain is placed simultaneously in combustor and inlet diffuser of ramjet engine are also considered

In all considered cases after SR burn-out, its nozzle, cowlings and plugs are ejected or fired downward. The necessity of structural components ejecting on the transient regime is one of substantial basic drawbacks of the studied PS schemes for aviation missiles.

In order to eliminate these drawbacks United Technologies' Chemical Systems division proposed a new concept of integral ramjet arrangement - using the nozzleless SR.

Till 1976 all programs on integral ramjet called for using only the booster SR with ejectable nozzle. Such engines were ground and flight tested. As a result, the most part of problems concerning development of integral ramjet was solved though at the expense of mass and structure complexity increase, reliability reduction and PS cost growth. The main difficulty, which couldn't be overcome in any way, consisted in danger to entail damage of carrier aircraft by ejected from the engine components of an SR booster. The logic solution of this problem was the use of a nozzleless SR booster.

The application of a nozzleless SR booster simplifies the missile and reduces its cost, and the main thing consists in elimination of ejectable components that fly around the aircraft during the missile launch and also in elimination of a danger connected with the fall of these components on the ground.

Details of nozzleless boosters development

The feature of a nozzleless SR is the absence of a nozzle and a rear bottom in their

common understanding. The nozzle is formed by the solid propellant grain itself. Grain burning is realized on the duct surface in a radial direction The throat is at the end of grain duct, but it can move upstream and downstream during grain burning. The typical scheme of a nozzleless SR is shown in Fig. 2.3.

Application of nozzleless SR and integral ramjet is conditioned by a number of advantages in comparison with a standard engine with a nozzle. These advantages include:

- operational merits (absence of ejectable structural components);
- structure simplicity;
- higher reliability;
- low cost

Naturally the nozzle absence causes noticeable reduction of the nozzleless SR thrust specific impulse in comparison with the engine having nozzle. Real specific impulse of a nozzleless engine is usually equal to 75 - 85% (in the best case it can achieve up to 90%) of the engine with a nozzle thrust specific impulse value. The difference is explained by not only the absence of a contoured nozzle. Performance degradation also takes place because of low operating pressure in combustor during the second half of engine operation. Though engine operation starts at high pressure, during the process of grain burn-out pressure can drop to 15% from its maximum value. In this case the engine thrust can vary differently depending on the index of a power ν in the equation of solid propellant grain burning:

$$G_p = K \rho_p S P^\nu, \qquad (1)$$

where

G_p - gasified propellant consumption, kg/s;
K - coefficient, m/s;
ρ_p - propellant density, kg/m³;
S - burning surface, m²;
P - pressure in gas generator, kPa.

The nozzleless SR booster thrust in such case can be constant (at $\nu = 0.5$), can change progressively (at $\nu < 0.5$) or degressively (at $\nu > 0.5$) as it is show in Fig. 2.4.

With given engine overall dimensions the less specific thrust impulse of a nozzleless SR can be compensated by the propellant mass increase due to filling the propellant into the volume that earlier was occupied by the nozzle unit. When the parameters of a nozzleless SR are chosen rationally, its full thrust impulse can be equal or even higher than one of an SR with a nozzle.

True, the mass of a grain loaded nozzleless engine in this case will be slightly greater.

The ideal propellant for a nozzleless SR significantly differs from the propellant for the engine with a nozzle. With the exception of engines with high length-to-diameter ratio (L/D $\geq$ 15) the burning rate of propellant used in a nozzleless engine must be substantially higher in order to exclude long-duration non-effective propellant burning at low pressure. Physical-mechanical characteristics of a nozzleless SR propellant also must be higher. At low operating temperatures the ability of grain to deform without destruction has to be very good to provide optimum values of the coefficient, which characterizes the filling of combustor with the propellant. At high operating temperatures the propellant used in a nozzleless SR must have high allowable shearing strength so that grain could sustain large loads conditioned by high pressure difference between front and rear parts of engine combustor.

One of the consequences of such higher requirements to characteristics nozzleless SR propellants is the fact that the propellants themselves become more expensive, but not as much to lose gain in cost of development and manufacture of a nozzleless SR in comparison with a standard SR. It also must be taken into account that structure of nozzleless SR grains is substantially simpler and, hence, these grains are less expensive in production than grains of standard SR.

Consumption thrust characteristics of a nozzleless SR depend on used solid propellant properties, such as gas constant and temperature of combustion products (R, T), propellant densities (ρ_p), burning rate (U_p), coefficient v, dimensions of engine (L, D) and environmental conditions (pressure, grain temperature etc.).

Design of interballistic and thrust characteristics of nozzleless SR must be performed with taken account of larger number of factors than for SR with a nozzle. Among them the following ones should be marked.
1. Erosion burning of solid rocket propellant under condition of gas stream speeds change from zero up to supersonic.
2. Unsteadiness of grain burning process.
3. Non-efficiency of propellant burning, especially when it is metallized because the particles residence time in combustor is very short.
4. Movement of throat section during grain burning.
5. Two-phase flow.

6. Changing of solid propellant grain duct contour and the duct diameter including throat section.

Importance of above mentioned factors is different in the beginning, the middle and the end of engine operation.

Availability of the sustainer ramjet nozzle favours the performance improvement of nozzleless SR integrated with SPRR.

In order to define the characteristics of nozzleless SR there were developed programs of parameters calculation in quasi-stationary and non-stationary tasks.

Taking account of solid propellant erosion burning becomes the important part of these programs. For this we use criterion functions of the form:

$$\varepsilon = \varepsilon_0 + B \left(\frac{\rho_g \, w_g}{\rho_p \, U_{po}} \, C_{fo} \right)^{\mu}.$$

where
ε - coefficient of solid propellant erosion burning $\varepsilon = U_p / U_{po}$;
U_{po} - propellant burning rate when burning surface blowing over by gas stream is absent;
U_p - propellant burning rate under conditions of gas stream blowing over;
ρ_g - gas density;
w_g - gas stream velocity;
C_{fo} - friction coefficient on the plate without blow - in:

$$C_{fo} = 0.0592 \, Re_d^{-0.2};$$

Re_d - Reynolds number for which defining the grain duct diameter d is used as a typical size;
ε_0, B, μ - parameters, which are defined experimentally.

In Fig. 2.5 there are shown typical criterion functions on erosion burning for mixed and double-base solid rocket propellants with indications of a nozzleless SR and an SR with nozzle operation areas. If for the SR with a nozzle erosion propellant burning practically is not admitted: $\varepsilon \leq 1.10$ - 1.15, then for the nozzleless SR the area of operating to ε practically is unlimited. It should be noticed that mixed solid propellants are subjected to erosion burning in a larger measure than double-base ones.

Application of nozzleless SR under certain conditions, as assessments show, can allow to reduce the total cost of the engine by 10 - 20%

to increase maximum flight speed at the end of booster operation by 5 - 15% and eliminates the necessity of nozzle ejecting during transition to cruise regime.

2. RAMROCKET SOLID PROPELLANTS AND THEIR APPLICATION

The possibility of using significantly different fuels and oxidizers in solid propellants of ramrockets requires the development of special methods to reveal energetic potential of the propellant in the propulsion-vehicle system with allowance for specific conditions of the missile application.

For propellants of SPRR there is no any single energetic index under which the propellant may be selected. Many things depend on specific dimension - mass restrictions and condition of application. In the general case the energetic potentials of solid propellants of ramrockets are characterized by the following main indices: a volumetric combustion heat - Hv; a mass combustion heat - Hu; a density - ρ_p; a stoichiometric coefficient - L_0; a natural impulse of the first burning products following out of the gas generator - I_{gg}, as well as a heat capacity $H_1 = Hu/(1 + L_0)$ determining the maximum heat release per 1 kg fuel - air mixture in stoichiometric ratio ($\alpha = 1$).

All these indices in some extent or another have influence on three main parameters of ramrockets: a thrust coefficient (C_F), volumetric and mass specific impulse (I_v and I) and finally on the flight missiles operation.

Propellants for SPRR are considered in references |1 - 3|.For the most detailed review see |4|.

SPRR propellants

It will be remembered that the propellant composition of SPRR can theoretically changed from the composition typical for SR propellant containing up to 70 - 80% oxidizer) to ramjet solid fuels without an oxidizer. For integral SPRR, which are initially accelerated by SR booster and SPRR operates on a sustain regime, the solid propellants containing ultimately a large number of fuel components (to 75 -85%) and the minimum quantity of the oxidizer (15 - 25%).

Solid propellants of ramrockets have as a rule three main components an oxidizer, a metallic fuel and a fuel binder. Nitrate natrium $NaNO_3$ and nitrate kalium KNO_3, perchlorates,

for example, ammonium of perchlorate NH_4ClO_4 are used as oxidizer. For the advanced boron-containing fuels the fluorine - base oxidizers (fluoroplastics, fluorine rubbers) are also considered. Different hydrocarbons (naphthalene $C_{10}H_8$, paraffin $C_{16}H_{54}$, rubber, etc.) are used as binders. The solid compounds such as B - C - H (carboron) etc. refer to advanced binders. magnesium, aluminium, their alloys and metalloid boron are generally used as metallic fuels.

Fig. 2.6 compares a general picture of solid propellant development with liquid fuels. From all possible variety of propellants one may select the following characteristic groups of the propellants, to a great extent differing in properties and energetic characteristics (Hv, Hu, H_1, ρ, L_0, etc.):
a) "magnesium" propellants containing up to 60 - 70% magnesium (are labelled "Mg" in Fig. 2.6);
b) "aluminium" propellants containing up to 60% aluminium ("Al");
c) "hydrocarbon" propellants containing up to 60% hydrocarbon fuels ("C - H");
d) "carboron" propellants containing up to 60% carboron ("B - C - H");
e) "boron" propellants containing unbonded boron up to 30 - 55% ("B").

These propellants are characterized by growing values of heat of combustion Hv and Hu. There is a great number of propellants of intermediate compositions.

To reveal the most effective propellants, the energetic potentials of a sequence of theoretical propellant receipts were analyzed around which the conclusion can be drawn regarding the effectiveness of one component introduction or another.

The composition and the main properties of the characteristic propellants are tabulate in Table 1 and 2.

The given typical series of propellants makes it possible to find out the effectiveness of the mutual replacement of different components: metals (Mg, Al) and metalloid - B, hydrocarbon and boron containing binders when using either nitrate natrium (up to 20%) or ammonium of perchlorate (20 - 25%) as oxidizer. The quantity of metal and fuel binder is varied from 60% to 15 - 20%. Naphthalene and paraffin represent a set of hydrocarbon compounds with ultimately low (6.3%) and ultimately high (14.8%) hydrogen content by mass. Aluminium - magnesium alloy Al/Mg (AMA) is often used in propellants of ramrockets.

To analyze energetic potentials of significantly different propellants of ramrockets within the range of flight velocities and altitudes (M < 5 - 6 and H < 30 - 35 km) in which the missiles with ramrockets operate already, the following simplest method of the specific parameters comparison of ramrockets has been suggested. The method of the propellant mass redistribution between the booster and sustainer stages of the propulsion system and vehicle and the comparison method of the missile sustained flight range on the characteristic trajectories under typical dimension - mass restrictions of the missile armament.

Comparison of Ramrocket Specific Parameters

The specific parameters of ramrockets are calculated by the internal thrust with full heat generation in a combustor on a design nozzle flow discharge regime using the standard characteristic of the intake. The coefficient of the thrust is related to the intake entry area.

Fig. 2.7 compares the specific parameters of ramrockets; C_F, I_v, I of solid propellants (Table 1) at different coefficients of air excess (α) in the engine.

As known, the ramrockets may operate stablely both in the $\alpha > 1$ regime area and in the $\alpha < 1$ area.

It is obvious that C_F is increased with decrease in the coefficient of air excess for all propellants. On the regime of $\alpha = 1$ the C_F highest coefficient of thrust is observed with the magnesium - base propellant "1", having the lowest stoichiometric coefficient of $L_0 = 3.89$.

In the $\alpha > 1$ operation regime area the lowest values of the specific impulses Iv and I are noted for the magnesium - base propellant "1" and the highest ones - for the unbounded boron - base propellant "9".

For more illustrative comparison of the combustion heat of Hu and Hv propellants with I and I_v specific impulses transform the diagram (Fig. 2.7), relating all the propellants to the parameters of propellant "1" at the same values of C_F (Fig. 2.8).

This Figure shows such peculiarities: 1) The C_F value for the magnesium-, aluminium-, hydrocarbon - base propellants (1, 2, 3, 6) is approximately characterized by the gas temperature level (particularly, at high value of α) and a chemical composition of combustion

products, dissociation etc. have an influence to a small extent.

The curves of the appropriate propellants in Fig. 2.8 prove to be near - vertical. Contrary to this group of propellants, "boron" propellants (8, 9) have the advantage that permits a significant increase in the engine efficiency namely, the increase in I (propellant 8) or I_v (propellant 9) to be obtained at moderate coefficient of thrust. This feature of boron propellants is caused by the absence of dissociation at low temperatures and their outstanding energetic indices are realized to a great extent. At high values of C_F and gas temperatures the boron propellants approach their indices to the other as the processes of dissociation and phase transition among them show up much stronger.

Evaluation of Flight Range

Perform in the first approximation a comparative evaluation of the missile flight range, using the different propellants, for two characteristic flight trajectories: low - efficient low (H≈0) and highest - efficient high trajectories on which the maximum range may be achieved.

Although a supersonic flight at low altitude is rather inefficient because of high aerodynamic drag of a vehicle, however, such a flight is a great interest in view of the difficulty of a missile detection.

On the efficient high trajectories the range is described by the known equation

$$r = Kv \, I \, \ln \frac{1}{1-\mu_{II}}$$

and at the low flight trajectory is described by the simplest relation:

$$r = v \, t \, .$$

Here $K = L/D$ is lift to drag ratio.

It will be remembered that the flight for the maximum range is made on the regime of the K_{max}, maximum L/D ratio with gradual climbing and continuous decrease in aerodynamic drag in flight time namely, the flight takes place with a gradual decrease in propellant flow rate caused by a reduction in vehicle weight with a propellant utilization. At low flight trajectory the propellant flow rate remains unchanged as the drag and thrust retained practically constant (although the vehicle is also lightened). It is physically associated with the fact that at low altitude the

flight occurs with ultimately low angle of attack and in this area the change in vehicle mass does not affect practically the drag and the required thrust.

Next turn our attention to the comparison results of energetic potentials of propellants on the vehicle

Comparison at the missile mass = idem (Fig. 2.9)

Fig. 2.9 gives the diagram of the relative change of flight range and volume of fuel tank for a case of an equal of a missile mass. The diagram is given under changes of the engine α coefficient. As previously, propellant "1" is taken as a basic one. It is typical that, if the missile mass is retained, the regularities in change of the range both for low and high trajectories are the same.

As we see, the most range $\bar{r} = 1.92$ proportional to the H_u change with some decrease in the $\bar{V}_t = 0.96$ tank volume can be provided by bonded boron - base propellant "9". The carboron - base propellant "8" may theoretically also provide a significant increase in range $\bar{r}$ up to 1.86 however, a considerable enlargement of the fuel tank volume ($\bar{V}_t = 1.3$) is required by reason of lesser density. Although aluminium - base propellant "2" has the $\bar{V}_t = 0.8$ ultimately small volume of tank, the range increment does not exceed 15 - 18%.

The most energy - consuming boron - base propellants even if markedly decrease their effectiveness on augmented regimes $\alpha = 1$, however, they have some advantages over the others (when complete combustion of a propellant is considered).

Comparison at the missile volume = idem (Fig. 2.10)

This case evidently conforms to a great extent to modern concept of the armament development - the retention of sizes, launcher dimension of different carriers (aircraft, ship, stationary or mobile complex, etc.). In this case using the different propellants of ramrockets, more complicated regularities are observed.

Fig. 2.10 illustrates the diagram of the mutual change in range $\bar{r}$ and total mass m of a missile with $\mu_{II} = 0.2 - 0.6$ parametric changing the relative mass of sustain propellant and constant mass of a booster $\mu_I = 0.3$ for C_I thrust

coefficient level appropriate to an initial 3 on propellant "1" for low and high trajectory.

In these conditions of comparison the most range $\bar{r} = 1.7$ with 2 - 4% increase in missile mass may be provided by unbonded - boron propellant "9". In this case the $\bar{r}$ change practically agrees with a growth in volumetric impulse of $I_v = 1.73$ (Hv = 2). Rather minor change in density of this propellant ($\rho_p = 1.04$) led to a small variation in missile mass by stage of the propulsion system and, as a consequence, to rather slight difference in missile flight range both for low and high trajectories.

Propellant "10" with 30% Al and 30% B by its energetic potentials is most close to propellant "9" while slightly gives way to the letter in range and missile mass.

Propellant "2" with 60% Al among examined propellants at relative small reserve of onboard fuel ($\mu_{II} = 0.2$) may provided a stable increase in flight range on any sustain trajectories and all selected operation regimes of the engine $\alpha = 1$ up to $\mu_{II} = 0.6$.

Carboron - base propellant "8" has rather good indices of a range and mass especially at large reserve of onboard fuel ($\mu_{II} = 0.5 - 0.6$) on the economic altitude regimes with the $\alpha = 2 - 3$ coefficient of air excess.

The propellants with high content hydrocarbons (3, 4, 6, 7) against propellant "1" may provide the $\bar{r}$ increase to 10 - 20% with simultaneous reduction in missile mass by 10 - 15%.

As a whole, performed energetic analysis of the propellant propulsion system - vehicle system testifies rather high potentials of the ramrockets development when using boron - base solid propellants as well as aluminium - base propellants.

Although recently the boron - base solid propellants became a subject of a close consideration in the investigations of Russia, United States, Germany, however, when developing the real objects with SPRR, the designers and scientists had to deal with solid propellants of which the main fuels are well - proved magnesium, aluminium and different hydrocarbons.

The results of operating process investigation program in combustion of model

and fuel scale ramrockets on the standard solid
propellants with different content of magnesium,
aluminium - magnesium alloy and hydrocarbons
are given in the following sections. The
investigations have been carried out in CIAM
when creating and developing the specific SPRR
of supersonic missiles. The composition and the
basic characteristics of these propellants listed in
Table 3 somewhat differ from the propellants
taken for the theoretical calculation and shown in
Table 1 and 2.

3. EFFECTIVENESS OF FUEL SECONDARY COMBUSTION IN RAM COMBUSTOR

The process of gasified in SPRR gas
generator propellant secondary combustion is a
new problem that has not studied very well. The
effectiveness of such secondary combustion
defines propellant energy complete use and
influences by high grade on the final missile
effectiveness. We must be in need to study
physical base of this processes, then develop the
working methodology to summarize all
experimental results, and to give
recommendations on effective secondary
combustion process organization in ramrocket
engines.

In the 60s the large program of theoretical
investigations, model experimental studies and
full scaled demonstrators ground testing was
fulfilled in Russia. For studying and development
of propellants, engines, missiles test cells many
institutes design bureaus were involved, despite of
the only one missile with SPRR now in service -
SA-6, large experience in such type of engine was
gained. Many ideas and results from this round of
works influenced on the another field -
combustion of gasified fuel - hydrogen, methane
in ram combustors of combined engines (see the
forth lecture of this series).

The most important scientific results of
diffusion combustion process in ramrockets study
was described in the monograph, edited by
author [8][1] In two next parts of this lecture will
be given briefly some results from this book.

Quasi Gaseous Diffusion Combustion Mode

The specific of SPRR which differs from
SR or LFRJ engines is the reheat chamber in
which the products of first stage propellant
burning in gas generator going as hot jets must be

reburned with high efficiency and must produced
some injection effect. These features define the
out lines of combustion chamber and gas
generator nozzles device which must direct the
hot fuel jets mainly in axial direction. The high
temperature of the gasified propellant jets, i.e.
1700 - 2500 K, provides self - ignition and stable
burning.

In the Fig. 2.11 are shown the equilibrium
composition of combustion products for different
typical propellants. It is not so much of hart
(condensed) components: 10 - 30 %. Mostly it is
soot in very small particles: 0.03 - 0.3 mkm. The
burning of such small soot particles must be
quick because of high temperature in flame. Last
part of magnesium after the burning and
evaporation in gas generator can have the size of
particles less than 10 - 25 mkm and must have
the secondary combustion distance by estimation
no more than 40 - 250 mm, i.e. rather small.

Two factors of subsequent experimental
series show us that kinetic factors were not the
limitation in the secondary combustion process in
SPRR combustion chambers:
1) High temperature working region: the air
excess coefficient was no more than $\alpha = 2 - 3$.
2) Most experimental objects: models and full
scaled, were big enough ($D_h > 500$ mm, $L_h > 500$
- 1000 mm), so the kinetic burning was not
visible for practical purposes.

So we assume such a model of burning
process in SPRR:
1. The primary combustion products in gas
generator after ejection reburned in air as
turbulent diffusion flame, as pure gas flame.
2. Gas and condensed phases are in full
kinematics and thermal equilibrium.
3. All combustible elements, gaseous and
condensed, burned in the narrow flame front,
which is the shape of stoichiometric conditions
($\alpha_{fl} = 1$).

The picture of such quasi gaseous flames of
two jets flowing from gas generator through two
nozzles: $d = 21$ mm and 10.5 mm is shown in
Fig. 2.12. Two times bigger nozzles give two
times longer flame, showing quasi gaseous
diffusion flame effect.

In the overwhelming majority of cases in
ram rocket the process of propellant secondary
combustion in air will be mainly determined by
the diffusion mixing of the fuel jet with the air.

The combustor length required for full
propellant combustion is determined by the
length of the diffusion flame generated in a

turbulent jet of the gas generator propellant combustion products. That is why the model of a quasi-gas diffusion flame can form a basis for the SPRR combustor length determination.

From the semi-empirical theor of the turbulent mixing it is known that the density of an inert gas turbulent jet mixing with an unclosed co-current air flow is determined by the relationships of mixing flows velocities and densities. When the reactable mixture of the gas generator propellant incomplete combustion products mixes with co-current air flow, the unclosed flame length also will depend on a stoichiometric mixture ratio L_0 determining the relative air amount which will diffuse to the jet axis at the end of the unclosed flame. Pressure gradient along combustor (at constant mixture flow through the combustor outlet section) also will influence the gas generator propellant reactable combustion products mixing SPRR with the air stream in the space limited by the SPRR combustor walls. Mixing under such conditions results in the diffusion flame lengthening at a less air excess coefficient α than its average value α_0 in a turbulent jet at the unclosed flame end which is determined from the empirical relationship for $L_0 = 4-6$:

$$\bar{\alpha}_0 = 2.5 + 1.5/L_0$$

At $\alpha = \bar{\alpha}_0$ the outer boundaries of the combustion products turbulent jet will reach the combustor wall simultaneously with combustion completion in the flame on the jet axis (Fig. 2.13). At $\alpha < \bar{\alpha}_0$ the jet outer boundaries reached the wall before completion of combustion on the flame jet axis. At $\alpha \to 1.0$ the flame length must theoretically tend to infinity, because the entire amount of the air has to mix with gas generator propellant.

Thus, the ram combustor length, required for the gas generator propellant full combustion depends on a large number of parameters. The most important of them are:
a) engine operating regime determined by an air excess coefficient value α and by an air inlet temperature T_0;
b) specification of used propellant determining the value L_0 and the gas generator specific impulse I_{gg};
c) relative critical values of the engine exhaust nozzle area and gas generator nozzle (or sum of nozzles)

$$\bar{A}_n^* = A_n^*/A_h \quad \text{and} \quad \bar{A}_{gg}^* = A_{gg}^*/A_h .$$

Reference is the inlet combustion chamber area.

The pattern of these parameters effect on the flame length, determined by calculation for the number of propellants, is shown in Fig. 2.14. As one can see, the rise of T_0 and L_0 results in the largest increase of the flame length. This results from decreasing the relative velocity of mixing gas generator gas flows and air at T_0 increase. I_{gg} rise causes the flame length decrease due to mixing flows relative velocity increase. An air excess coefficient when $\alpha > 1.0$ reduces the flame length with α rise due to reduction of the diffusing air required amount at completion of combustion on the jet axis and when $\alpha < 1.0$ the value of L_n reduces because of lack of air to combustion.

Idealized Ramrocket Outline

The calculations show that at high flight speeds when $T_0 \geq 500 - 600$ K, $L_0 > 1.5$ and $\alpha \approx 1$ the combustor length-to-diameter ratio (L_h/D_h) becomes very high: of the order of few tens and even hundreds of relative length. To reduce an SPRR combustor length it makes sense to substitute one flame for a large number of diffusion flames that can be achieved by using a multi-nozzle gas generator. Fig. 2.15 shows the circumference of a combustor of single-nozzle gas generator which is equivalent to a multi-nozzle one in terms of the diffusion flame. The scheme of the corresponding single-nozzle SPRR is shown in this figure too.

By the equivalent length $\bar{L}_{eq}$ a combustor of the SPRR with a multi-nozzle gas generator one should mean the SPRR combustor relative length of a single-nozzle engine which is equivalent to multi-nozzle by all other parameter:

$$\bar{L}_{eq} = \frac{L_h}{D_{eq}} = \frac{L_h}{D_h}\sqrt{\frac{N_n}{1-\bar{d}_{cb}^2}} . \qquad (2)$$

where $\bar{d}_{cb} = d_{cb}/D_h$ - relative diameter of the SPRR centre body; N_n - nozzle number of the gas generator.

So by the given diameter and length of SPRR ram combustor we can arrange many nozzles of gas generator, the $\bar{L}_{eq}$, become big, the secondary burning completeness growth much time (2).

One can see that nozzle increase at given required values of L_h/D_h can result in substantial increase of $\bar{L}_{eq}$ and, hence, in a possible realization of the $L_n = L_h$ required value at given value of L_h/D_h including low L_h/D_h values.

Experimental data confirm the possibility of using this method for the combustion length choice.

Summarizing of Secondary Combustion Effectiveness in Different SPRR on the Base of Equivalent combustor length

If Q_{gg} is the heat of primary combustion in gas generator, so the effectiveness of secondary combustion in ram burner η_s, can be expressed by

$$\eta_s = \frac{\eta - \bar{Q}_{gg}}{1 - \bar{Q}_{gg}},$$

where η_s - is the effectiveness of propellant combustion in engine, $\bar{Q}_{gg} = Q_{gg}/Hu$ - is relative heat of primary combustion.

A numerous experiments showed, the combustion efficiency depends on length of flame $\bar{L}_{fl} = L_{fl}/D_b$ (Fig. 2.14). These results allow us in engineering definition of a problem at engine operating regime, propellant specification and flight condition changes that only the flame length to be determined and using the experimental relation $\eta_s = f(L_{fl}/D_b)$ or $\eta_s - f(\bar{L}_{eq})$ to estimate the efficiency of propellant secondary ram combustion. Numerous investigations have given us such generalized dependence (Fig. 2.16). On the base of such generalized dependence there was developed the methodology of calculating secondary combustion completeness η_s of SPRR ram combustor. This methodology made as a special software takes into account engine size and construction (L_b, T_b, N_n, $\overset{\bullet}{A}_n$, $\overset{\bullet}{A}_{gg}$), type of propellant ($I_{gg}$, L_o), flight and engine parameters, Mach number, T_o, air excess coefficient α. Of course this method need in uniform spread of gasified fuel through the combustion chamber cross section.

Two examples of application of this method are given below.

In the Fig. 2.17 the propellant combustion efficiency versus air excess coefficient α and flight speed is plotted. Decrease of η value at $\alpha \to 1$ is a natural result of flame length L_{fl} rise and combustion efficiency reduction at flight speed increase as a result of T_o growth, the mixing gas and air flows velocities decrease.

In the Fig. 2.18 the characteristics of two multi-nozzle SPRR are compared. The first has short camber length L_{b1} or has small number of nozzles N_1, so its relative equivalent length L_{eq_1} is low. The second one has the same diameter but four times bigger chamber length $L_{b2} = 4L_{b1}$, or its gas generator has 16 times greater nozzle number: $N_2 = 16N_1$ at the same length $L_{b2} = L_{b1}$. So the second SPRR has four times bigger equivalent length $L_{eq2} = 4L_{eq1}$. As we can see in the Fig. 2.18 the both SPRR tried on the same missile with regime optimization give essential different results: "long" equivalent chamber (or multi-nozzle) have very high propellant efficiency, bigger specific impulse, low α - coefficient and as result bigger maximum Mach number.

So effective SPRR must be multi-nozzle one.

4. RAMROCKETS GROUND TESTING

Types of SPRR Mixing Devices

In the Fig. 2.19 are shown possible SPRR mixing devices divided in 6 groups.

The first group of engine does not concern SPRR proper because these engine have no gas generator, but have practically open grain of propellant. They can be used in some small missiles, drones and so on.

The second group (II, III, IV) is characterized by medium number of gas generator nozzles ($N_n = 10 - 30$). They are simple and light, but have rather low burning efficiency. They can be used on medium size missiles with long combustion chamber, by medium Mach number. For instance, such type device has the Russian surface-to-air missile SA 6 "Gainful".

The third group (V, VI) - "super" multi-nozzle devices. They are complicated, have rather big duct pressure losses. But they have very short chamber with high burning efficiency even at the high Mach number flight. So such SPRR might be applied on big-sized, high Mach number with high specific impulse vehicles.

Most of above mentioned type of SPRR nozzle devices were experimental studied on CIAM test facilities.

Ground Test Facility

Most of experiments were conducted on connected pipe facilities (Fig. 2.20). Their actions are well known and clear from the Fig. 2.20. But

many-many methodology particularities we introduced to have high accuracy in such measurements as fuel flow, Impulse (thrust), air flow, heat flux, fuel combustion efficiency etc.

Ground Test Development of SA 6 SPRR

In the 1950-60s the whole program of SA 6 missile and especially its engine development was the epic work because it finished by the creation the first in the world full integrated ram rocket first using sustain solid propellant.

Here I want present only some results showing the process of SPRR itself development (no intake, no real nozzle, no flight tests etc.).

We have started with open grain engine scheme, which seemed to us to be more simple (Fig. 2.21). As it will be shown below the result was not very good. It was decided to use SPRR scheme of engine with gas generator.

In the Fig. 2.22 is shown the prototype of SA 6 SPRR with variants of propellant nozzle devices (N_n = 1 - 4 - 12). The fourth right was the best (see later). The results of combustion completeness for both variants: Fig. 2.21 and 2.22 are shown in Fig. 2.23.

These experimental data obtained with magnesium propellant CH-1 show:

1) Using open end grain give rather bed result - combustion completeness is not more than 0.7.

2) Using better of mixing devices by open grain can rise the combustion completeness on 5 - 10 %.

3) The high level of combustion efficiency can be achieved in the scheme of SPRR with gas generator (η_g = 0.9 - 0.95).

4) The rational choice of number and position of gas generator nozzles (by the given chamber length) can achieve the calculating data of generalized dependence (see curve 1 in Fig. 2.23).

5) The № 4 nozzle device was the best.

The developing the combustion process of SA 6 missile SPRR promote achieve its excellent quality.

Multi-Nozzle Complicated Devices

For special purposes, such as:
1) big size of SPRR (D_b),
2) relative short combustion chamber (L_b/D_b = 1 - 2),
3) high level of specific impulse and combustion efficiency,
4) high flight Mach number

we must use multi-nozzle devices of pylon or mixed type (Fig. 2.19). The number of nozzles in such devices might be of 100 - 200 and more.

There was realized the program of detailed study of such nozzle devices (Fig. 2.24). The object was to developed SPRR with short combustor and very high combustion efficiency. Many variants were studied. The Fig. 2.25 shows:

1) The high secondary combustion efficiency η_s = 0.8 - 0.9 may be achieved at the combustor length L_b/D_b = 1 - 1.5.

2) Under the uniform spread of fuel in air the experimental data are near to calculated curves derived from the generalized dependence.

3) The generalized dependence can be applied to multi-nozzle of SPRR having N_n from 1 to 100 -200 under requirement of uniform spread fuel in air.

5. SOLID PROPELLANT RAM ROCKET WITH CONTROLLED PROPELLANT CONSUMPTION

The problem on the necessity of a solid propellant consumption control in SPRR has arisen since a moment SPRR came into use. The main tasks of the fuel consumption control in ramjets generally are:
- the provision of the maximum values of the ballistic missile efficiency criterion on the whole of flight regimes;
- the restriction in propulsion operation based upon the condition of the intake surge prevention;
- the restriction in propulsion operation based upon the condition of the engine and missile elements strength (the inlet temperature and dynamic pressure limits);
- the restriction in engine operation based upon the stable propellant burning provision.

The optimization of the ballistic missile efficiency criterion is the most significant task from all the above mentioned for SPRR. Depending on a missile mission, the efficiency criterion may be a launch range[2] or a flying range[3] (for air-to-air missiles) or a flying range and average missile velocity (for air-to-surface missiles), etc. Algorithm and program of the propellant consumption control are selected accordingly chosen criterion.

---

[2] A launch range is a distance between a missile carrier and a target at the moment of the missile launch.
[3] A flying range is a distance between a missile carrier and a target at the moment of its destruction.

Unlike liquid fuel ramjets in which a liquid fuel consumption is controlled by a throttling, the solid propellant consumption control in SPRR on cruising regime is a difficult technical problem comparable with the problem of a propellant consumption control in SR (by the way they are solved by the same manners).

The necessity of control is caused by the fact that non-variable thrust SPRR significantly yields to a variable-thrust engine in efficiency, when it is moving along the trajectory with variable H and M. The loss value depends on the range of missile flight altitude and velocity variations, namely, the sizes of area of the use by H and M. The greatest variation range of these parameters is typical air-to-air and air-to-ground aviation missiles and guided anti-aircraft missiles. Fig. 2.26 illustrates the typical area of the use for air-to-air medium range missile.

For this missile the flight Mach number and altitude are varied within the ranges of M = 0.8-3.6 and H = 0-25 km, and the optimum value of the solid propellant consumption varies 3-5 times ($G_p = G_{pmax}/G_{pmin} = 3-5$). The problem is further complicated by the fact that for air-to-air and guided anti-aircraft missiles the flight path is not known previously in most cases as it is defined by a specific combat situation.

The method of control of the cruising propellant consumption in an integrated SPRR depends on a degree of a missile flight path definiteness. So, in the extreme case of the path regularity the optimum program of the propellant consumption control may be previously calculated and built into a solid propellant grain structure by setting the shape of grain surface (for grains made by the cast technology) or by manufacturing the grain as a set of individual layers having different burning rate (for grains made by the pressing technology, Fig. 2.27). If the missile can fly alone several paths (previously known), the control process becomes complicated as for each path it is necessary to realize its optimum program of propellant consumption control. Fig. 2.28 gives an example of a partial solution of this problem. The SPRR has a seven-chamber gas generator. Each chamber is equipped with its own igniter. That allows to realize the required optimum program of the propellant consumption control, depending on a path, by means of a certain choice of sequence of separate chambers operation. In so doing, all logic operations are performed on a carrier board and transmitted to the missile at the moment of launch.

The method of the propellant consumption control by means of changing the area of the gas generator nozzle throat is the most perfect but the most difficult simultaneously. Fig. 2.29 shows the example of realizing such a method. Here, the area of the gas generator nozzle throat is set by the position of a conic-shape center body. The equilibrium position of the center body depends on the command pressure value of the liquid supplied to the sealed chamber of the regulator.

From the continuity equation (see equation (1))

$$G_p = K \rho_p S P_{gg}^v = n \frac{P_{gg} A_{gg}^*}{\sqrt{T_{gg}}}$$

it follows

$$P_{gg} = \left(\frac{K S_p S \sqrt{T_{gg}}}{n A_{gg}^*} \right)^{\frac{1}{1-v}} = \left(\frac{B}{A_{gg}^*} \right)^{\frac{1}{1-v}} ,$$

where

n - coefficient of flow rate,

A_{gg}^* - area of the gas generator nozzle throat,

Tgg - combustion products temperature.

So the solid propellant consumption is equal to

$$G_p = K \rho_p S \left(\frac{b}{A_{gg}^*} \right)^{\frac{v}{1-v}}$$

The properties of a system, using such a control method, are basically determined by a sensitivity of the solid propellant burning rate to the pressure l

$$P_{gg} = \frac{P_{gg \, max}}{P_{gg \, min}} = \bar{G}_p^{\frac{1}{v}}$$

The special propellants with rather high values of $v = 0.5-0.8$ are developed for this purpose (as a rule, $v = 0.2-0.3$ for usual propellants).

The system of the arbitrary control allows automatically to optimize the propellant consumption during the missile flight along any non pre known path and also to parry the effect of initial grain temperature. The difficulty of this system realization consists in a selection of thermal and erosion resistance materials for a center body and "cavity" of gas generator nozzle. At present the prototypes of such control system have been developed and are being developed.

Onboard power sources are required for their function as well as rather sophisticated electronic devices, generating the control signal depending on the flight condition. As a result, the passive mass and dimensions of controllable propulsion increase. Therefore, the use of the arbitrary control is reasonable in the case when a significant propellant save is obtained, namely, the ballistic missile efficiency is improved.

The inter-engine parameters control of SPRR is considered the simplest. In this case the control system measures air flow through the engine, being a function of the form:

$$G_a = P_{bin} f(\alpha, T_{to}, A_n^*);$$

and establishes a propellant consumption appropriating to the optimum value of the air excess coefficient

$$G_p = \frac{G_a}{\alpha_{opt} L_0},$$

where
P_{bin} - static pressure at the combustion chamber,

T_{to} - total temperature at engine intake,

A_n^* - engine nozzle critical section area.

The optimum value of air excess coefficient may be calculated based on a total mathematical model of the engine-missile system. Fig. 2.30 gives the example of such a calculation for air-to-air medium-range missile. The flying range is rather as a criterion of the ballistic efficiency.

Fig. 2.30 illustrates the flying range at different altitudes against α It is seen that for each altitude there is its own value of α range of a missile. In the real missile flight the current flight altitude H either is measured directly or is determined by a static air pressure value at the combustion chamber inlet P_{bin}. Value G_p is achieved by the setting and maintaining of the gas generator pressure P_{gg} by a flow regulator (Fig. 2.29).

The considered system of the automatic control is the simplest. There are more sophisticated systems including the elements of the missile dynamics (for example, the axial overloading) into control algorithms. The calculative investigations showed that the arbitrary control might provide the gain in the ballistic efficiency to 40%.

CONCLUSION

The first full integration missile with ramjet using solid propellant SA-6 till our time it is the only one SPRR missile in operation. Meanwhile many missiles using liquid fuel are under operation. But the main advantage of SPRR over them remained: it is the "solidity" of its propellant, and subsequently exclusive operability.

Scientific and developments programmes of SPRR are going in many countries: USA, Germany, Russia and other, most of these objects are experimental. It is necessary to mention the results the scientific investigations in some country of the boron, as one of the most promised combustible element and other new untraditional solutions.

The author believe that the accumulated "global" SPRR experience and also Russian theoretical and practical achievements is SPRR well lead to creation a new generation of untraditional effective missiles examples using solid propellants.

ACKNOWLEDGEMENTS

REFERENCES

1. D.P. Harry. Status of Nozzleless Solid Rocket Motor Internal Ballistics Analysis. AIAA Paper № 77-910, 12.VII.1977.

2. I.M. Procinsky, W.R. Smith. Nozzleless Boosters for Integral Rocket Ramjet Systems. AIAA Paper № 80-1277, 30.VI.-2.VIII.1980.

3. C.D. Mikkelsen, G.P. Roys. Application of the Saderholm Erosive Burning Model to Nozzleless Solid Propellant Rocket Motors. AIAA Paper № 82-1146, 21-23.VII.1982.

4. С. Сарнер. Химия ракетных топлив. М.: Мир, 1969. 488с.

5. И. Глассмэн, Дж.В. Черик. Ракетно-прямоточные двигатели. В кн.: Ракетные двигатели. т. XII. под ред. О. Ланкастера. М., 1962. 576-608с.

6. Р.И. Курзинер. Реактивные двигатели для больших сверхзвуковых скоростей полета. М.: Машиностроение, 1977. 212с.

7. Hans.-L. Besser. Solid Propellant Ramrockets. Ramjet and Ramrocket Propulsion Systems for missiles. AGARD lecture series, № 136, 1984.

8. Ю.М. Аннушкин, В.А. Сосунов. Исследование диффузионного процесса горения и аэродинамики течений в воздушной камере сгорания ракетно-претоточных двигателей. Части I и II. Под редакцией В.А. Сосунова. М., ЦИАМ. 1964. 314 с.

Table 1. Composition of typical ramrocket solid fuels (%)

Propellant №	Fuel						Binder-fuel			Oxidant	
	Mg	Mg/Al	Al	Al/B	B	C	$C_{10}H_8$	$C_{26}H_{54}$	BCH	$NaNO_3$	NH_4ClO_4
1	60						20			20	
2		60					20			20	
3	20						60			20	
4			20				60			20	
5		60					20			20	
6			20					60		20	
7			15					60		25	
8			20						60	20	
9					55			20			25
10			30		30			20			20

Table 2. Characteristics of propellants

Propellant №	$\bar{Hv}$	$\bar{Hu}$	$\bar{\rho_p}$	Lo	$\dfrac{Hu}{1+L_0}$ kJ/kg
1	1	1	1	3.89	4444
2	1.47	1.18	1.25	4.49	4653
3	1.05	1.26	0.83	7.93	3064
4	1.17	1.32	0.88	8.13	3136
5	1.21	1.09	1.11	4.18	4563
6	1.09	1.46	0.75	9.5	3011
7	1.05	1.44	0.73	9.5	2985
8	1.43	1.86	0.77	7.55	4739
9	2.00	1.92	1.04	7.88	4690
10	1.81	1.66	1.08	6.70	4700

Reference: Propellant №1: $60Mg + 20(C_{10}H_8) + 20(NaNO_3)$
$Hu = 21730$ kJ/kg
$Hv = 33855$ kJ/dm³
$\rho_p = 1.56$ kg/dm³

Table3. Standard propellants composition.

Propellant	TT-1	CH-1	TT-3	Л-24	ЛК-6Т
ingredients, %					
Mg	37.5	65	19.6	15.25	17.25
Al	-	-	-	15.25	17.25
C	17.41	9.38	33.2	30.6	32
H	2.08	0.62	5	4.5	4.8
O	31.62	14.45	25.9	20.8	17.8
Cl	-	-	11	9	7.4
N	11.28	3.63	5.3	4	3.5
Na	-	6.92	-	-	-
Zn	0.11	-	-	-	-
parameters					
Hu kJ/kg	16325	18690	19507	22144	24697
Qgg kJ/kg	6488	4081	3893	5525	4111
Lo	2.32	2.8	4.87	5.14	5.87
I^*_{gg} m/s	1226	981	1226	1275	127.5
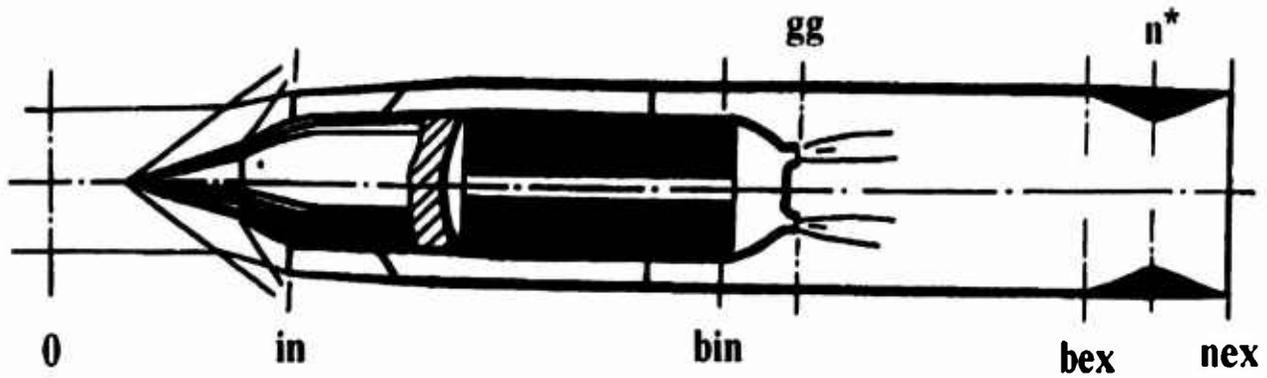
Fig. 2.1. SPRR layout with main cross section.
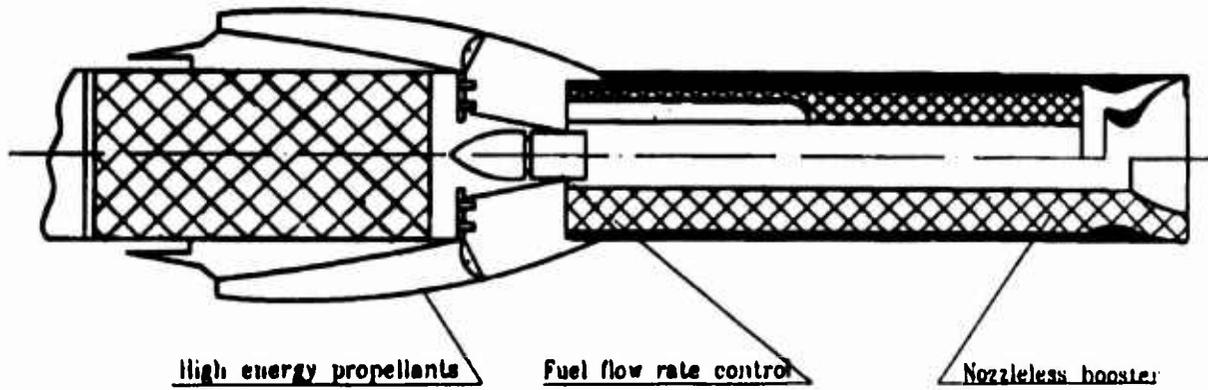
Fig. 2.2. Solid propellant ramrocket improving.
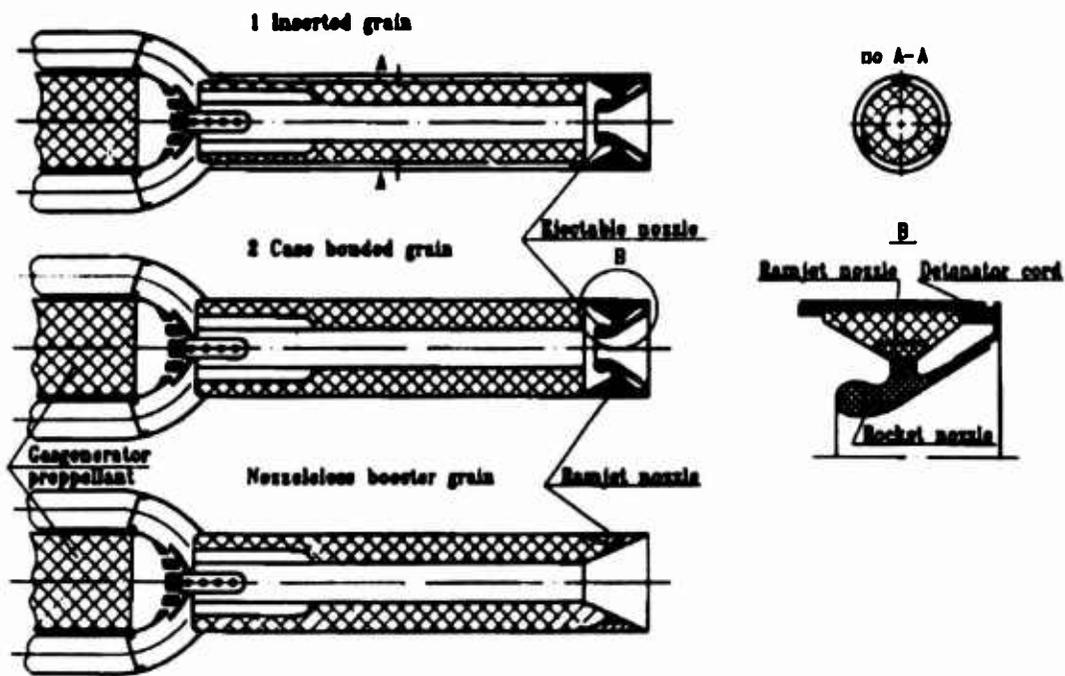
Fig. 2.3. Integration of ram combuster and booster.
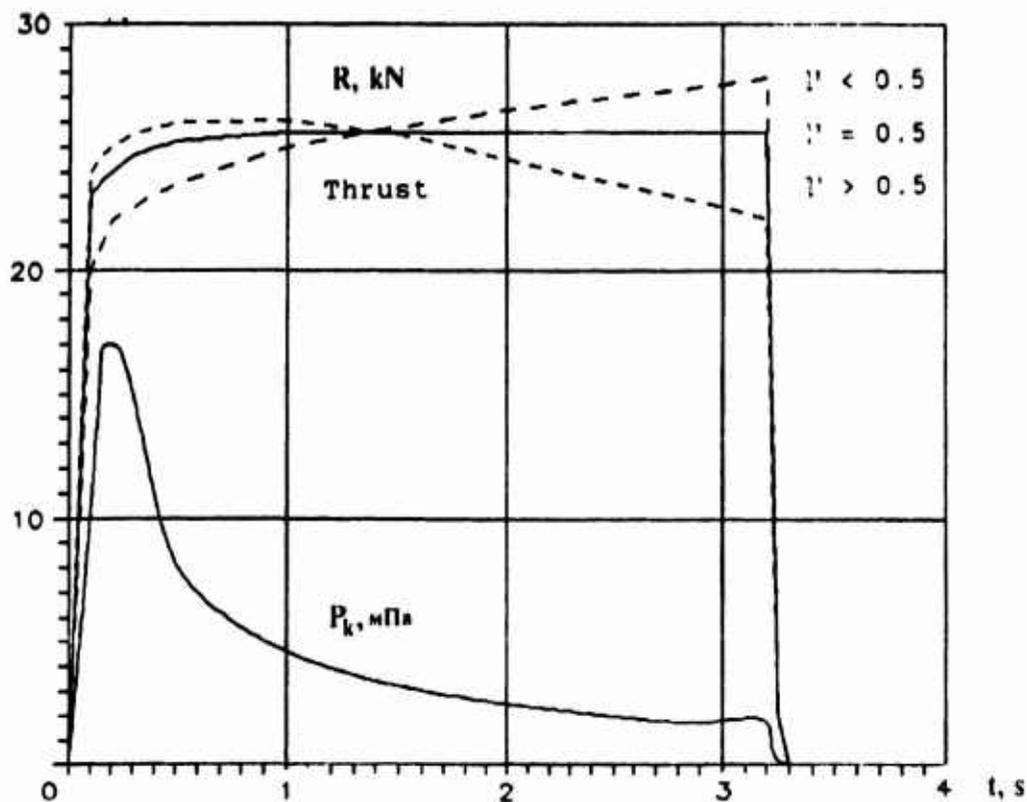
Fig. 2.4. Thrust and chamber pressure of nozzleless solid rocket motor.
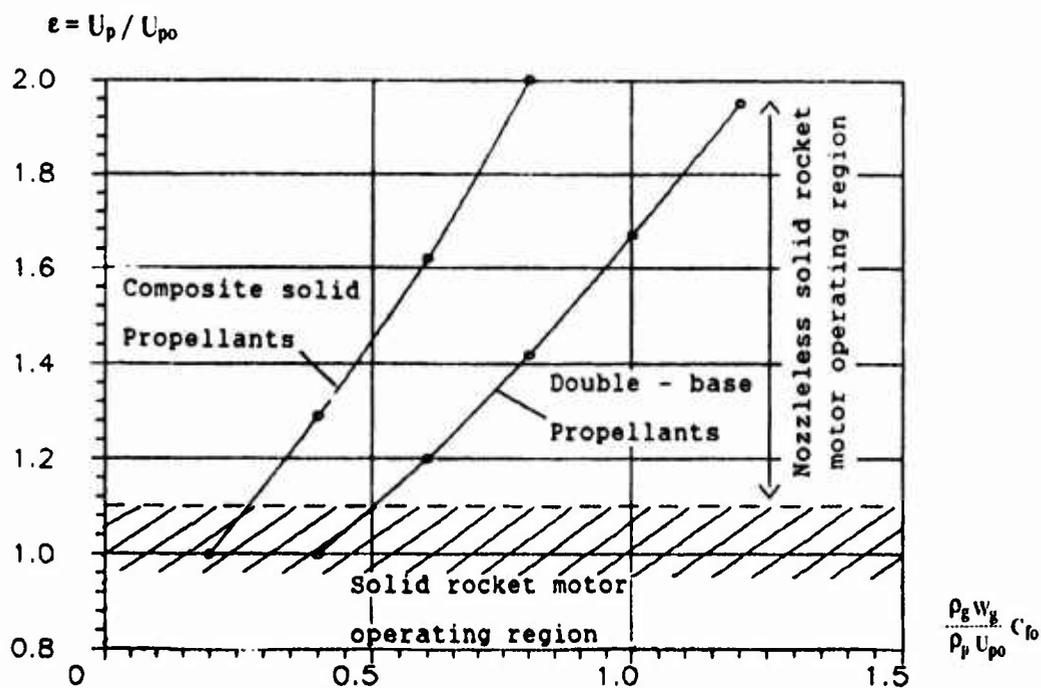
Fig. 2.5. Erosive burning of solid propellants.
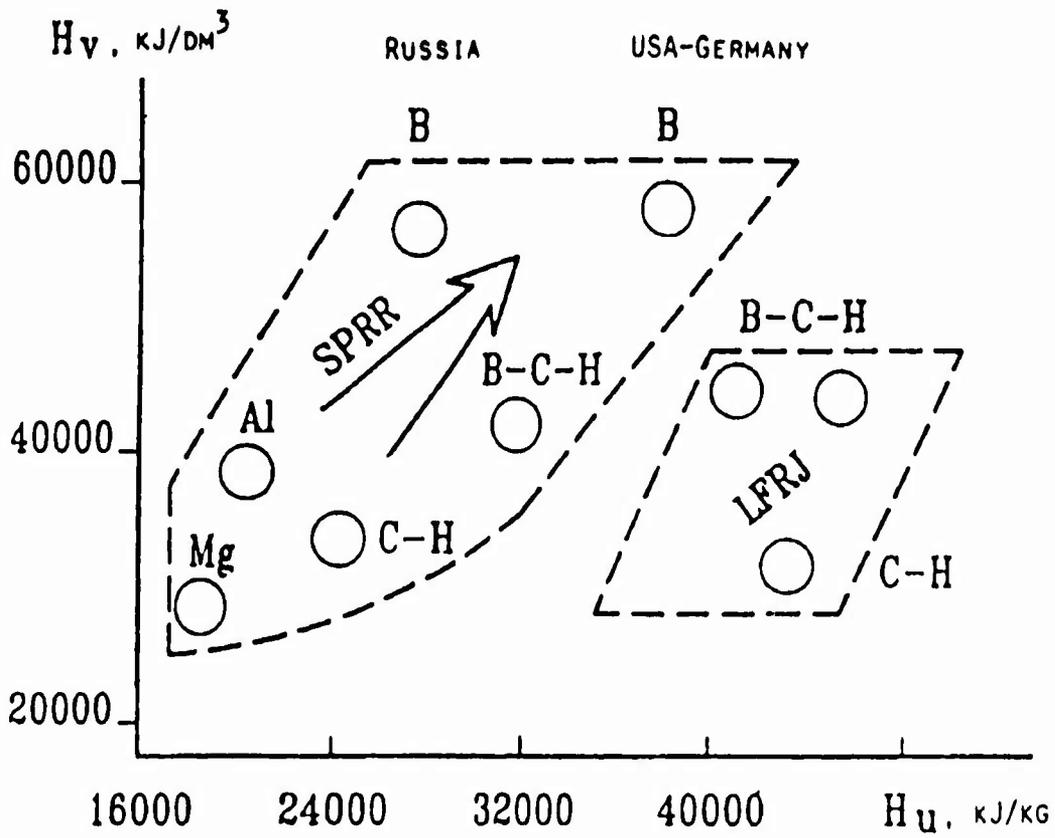
Fig. 2.6. SPRR propellants evolution.
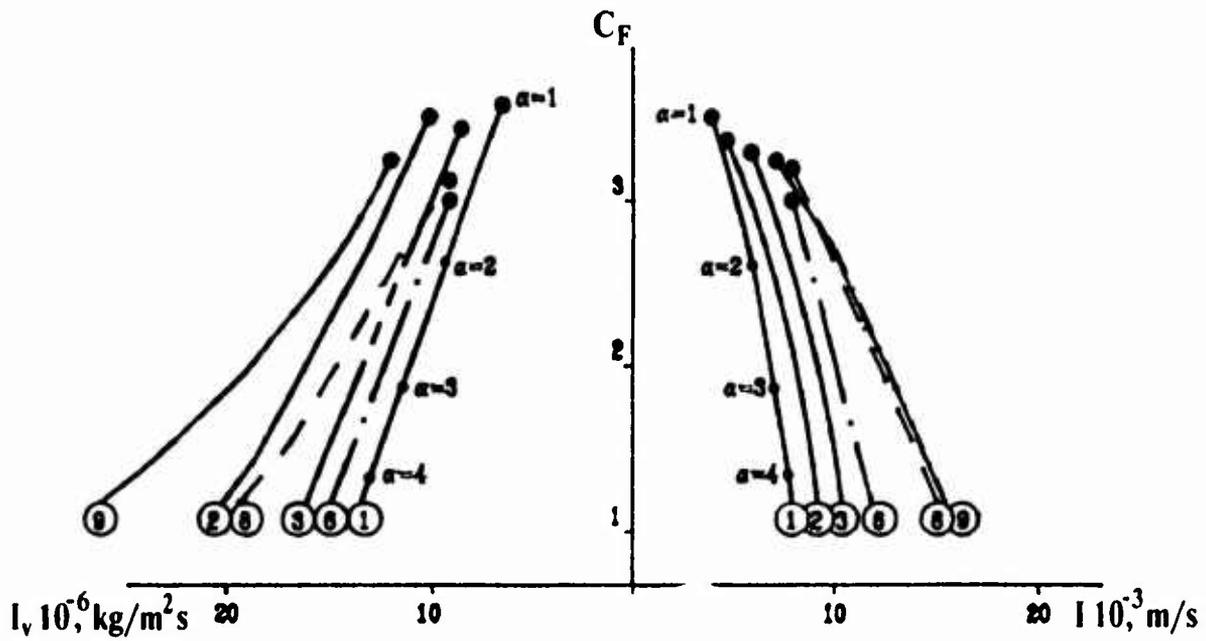
Fig. 2.7. The comparison of different solid propellants for ramjets by some specific characteristics (first).
M = 2; H = 0;
№№ of propellants see table 1.
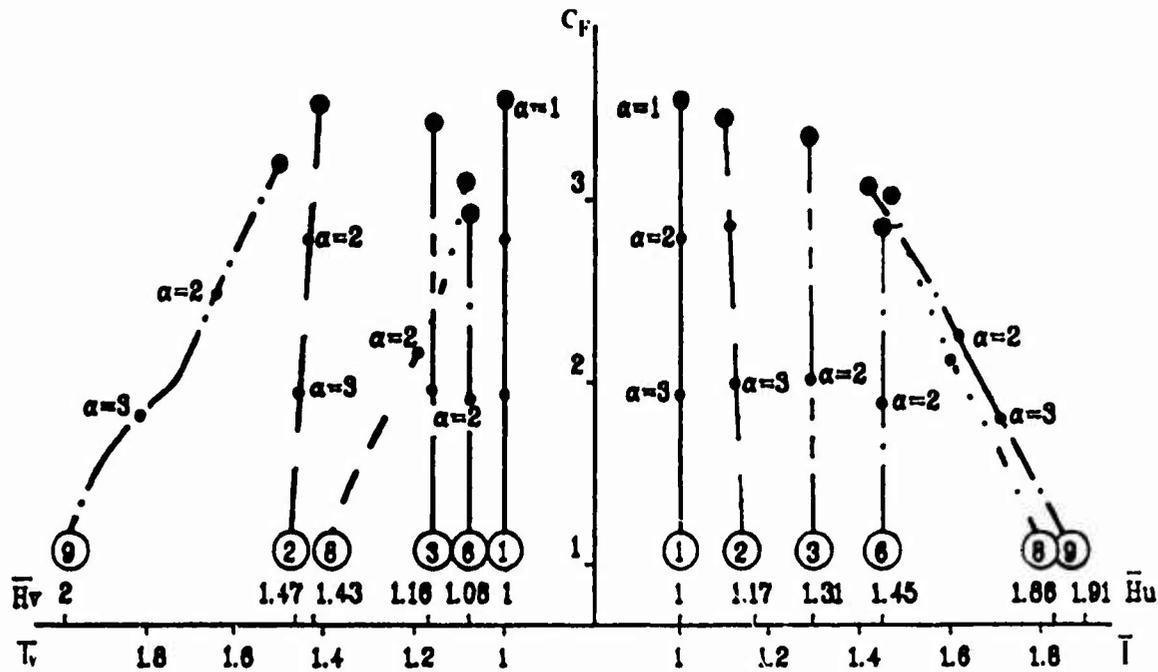
Fig. 2.8. The comparison of different solid propellants for ramjets by some specific characteristics (second).
M = 2; H = 0;
№№ of propellants see table 1
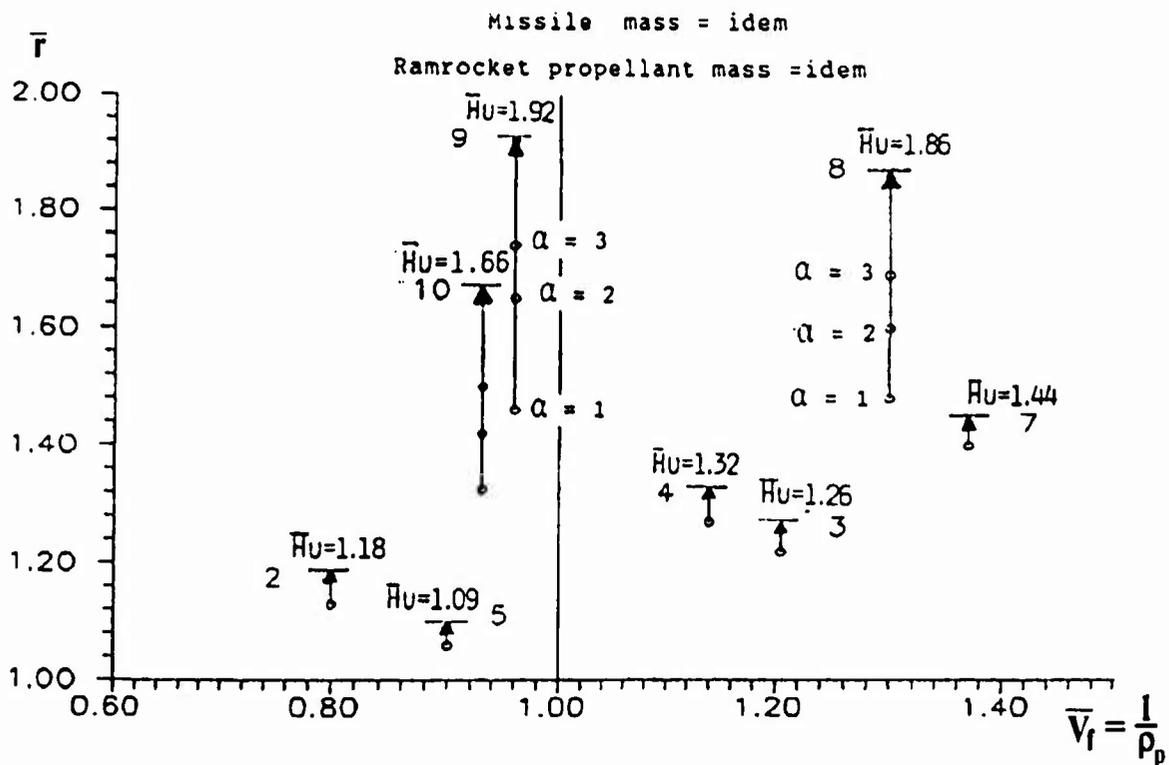
Fig. 2.9. Relative values missile range and propellant volume by use of different propellants and by missile mass=idem.
M=var; H=var.
№№ of propellants see table 1.
Reference propellant № 1.
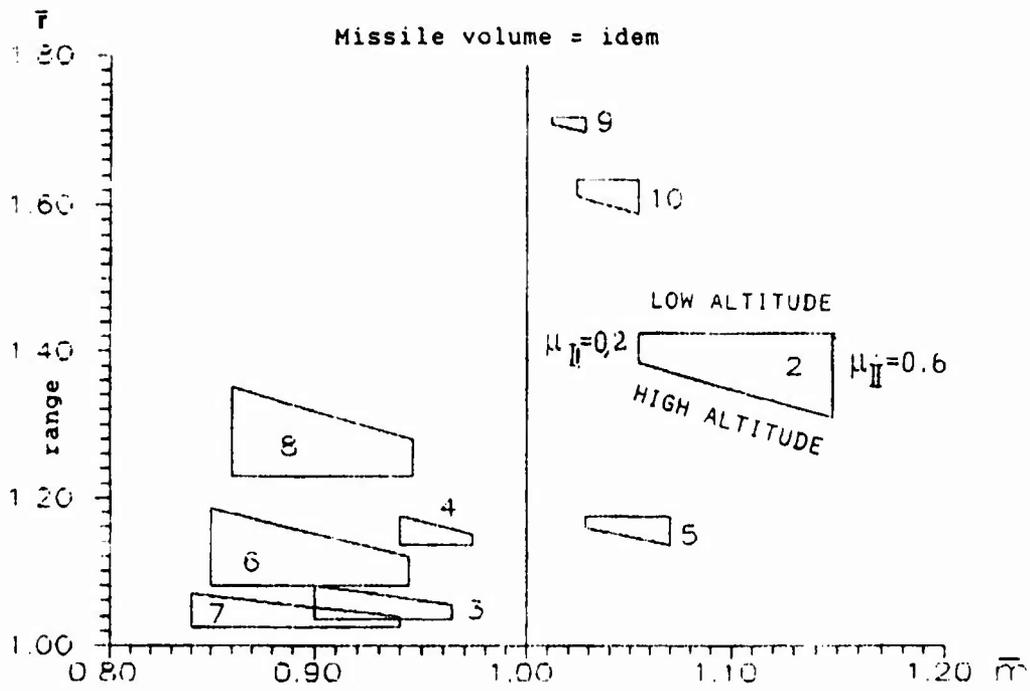
Fig. 2.10. Relative values of missile range and missile mass by use of different propellants and by missile volume idem.

$M=2$; $\mu_I=0.3$; $\mu_{II}=0.2-0.6$; $\alpha=3$.

№№ of propellants see table 1.

Reference propellant № 1.
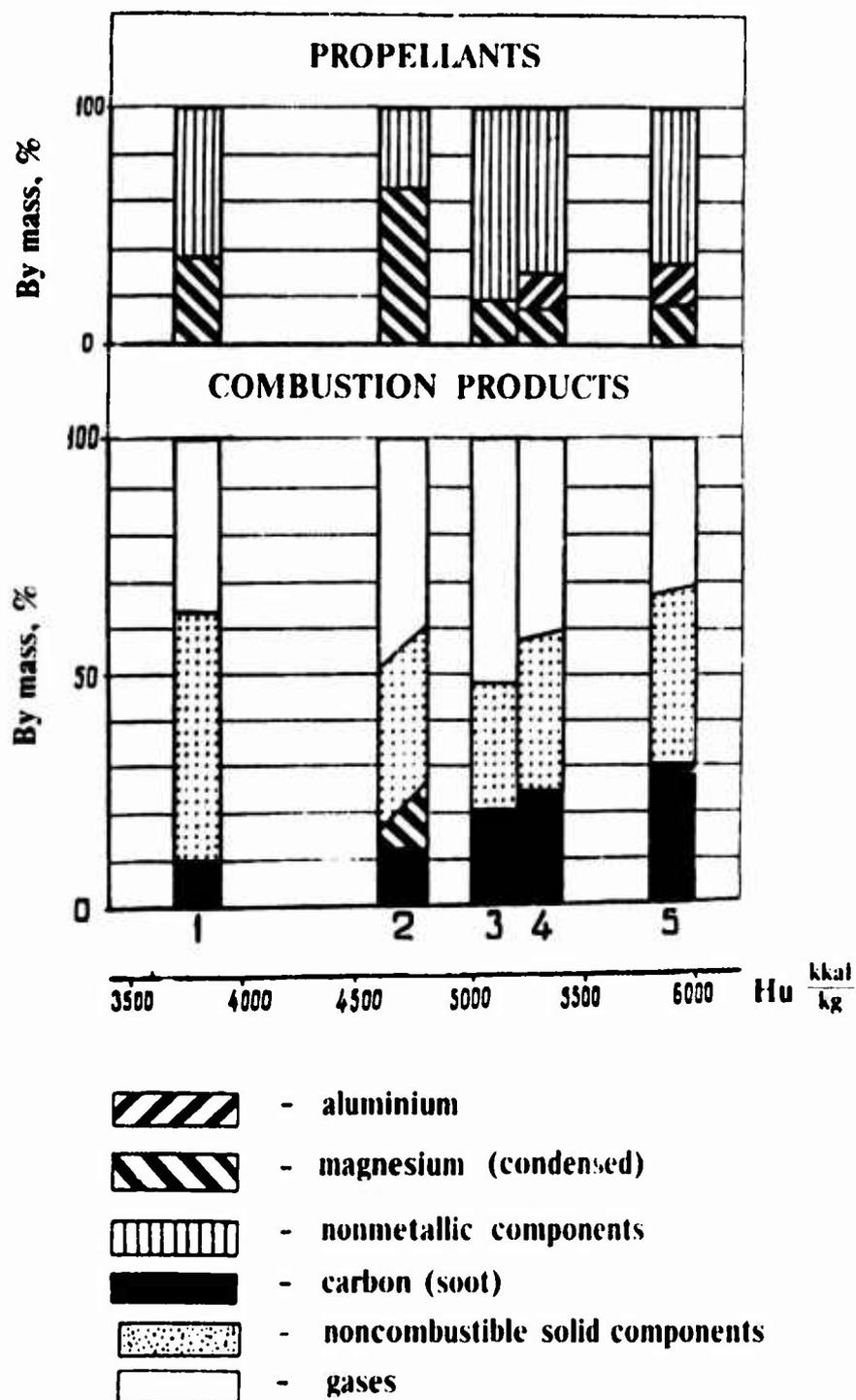
Fig. 2.11. Metal contents in different SPRR propellants and equilibrium composition of their combustion products in gas generator. [8]
Propellants: 1 - TT-1, 2 - CH-1, 3-TT-3, 4 - Л-24, 5 - ЛК-6К (see table 3)

$$\frac{P_{gg}}{P_o} = 28$$
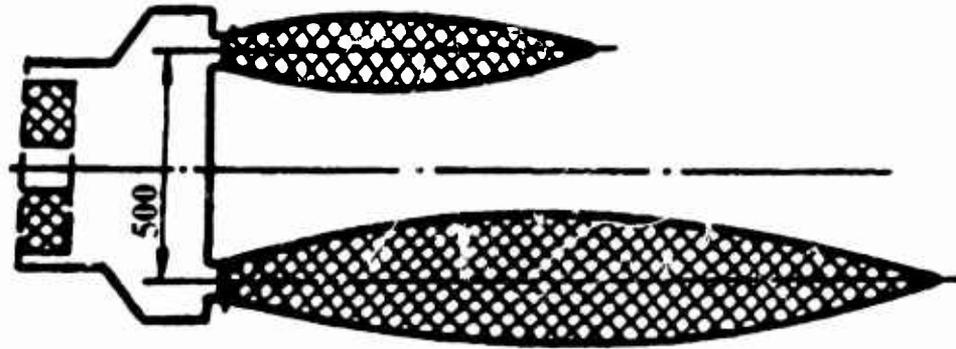
$$\frac{P_{gg}}{P_o} = 20$$

Fig. 2.12. Flames from two times differing nozzle diameters of gas generator by the outflow to the atmosphere. [8].
Propellant: Л-24
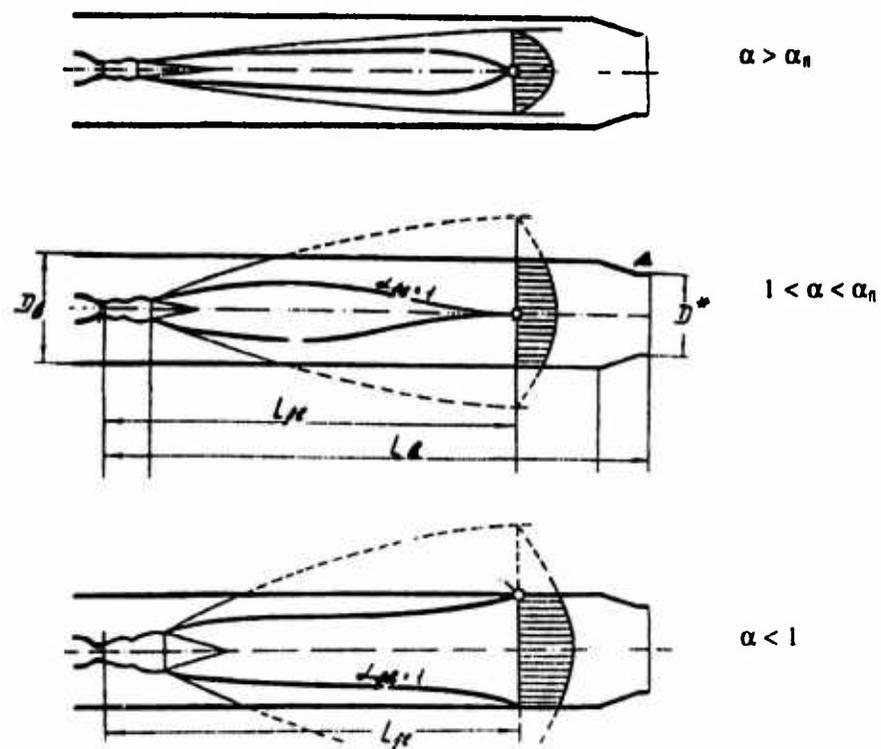
Fig. 2.13. The modification of gas generators flames form by changing air excess coefficient α.
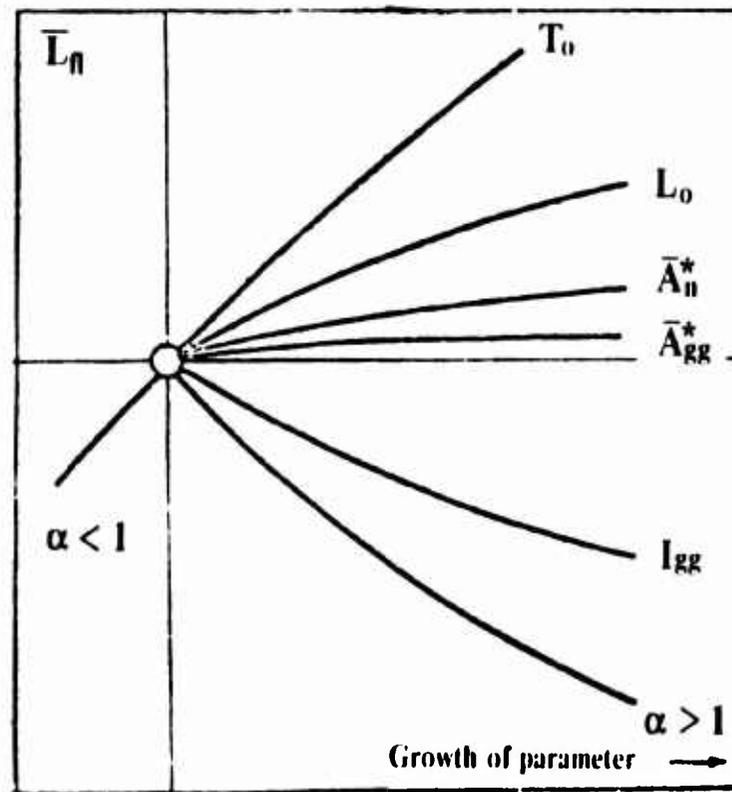
Fig. 2.14 The relative influence of different parameters on diffusion flame length by secondary burning in ram/chamber of the products of propellant primary burning in one nozzle gas generator SPRR [8].
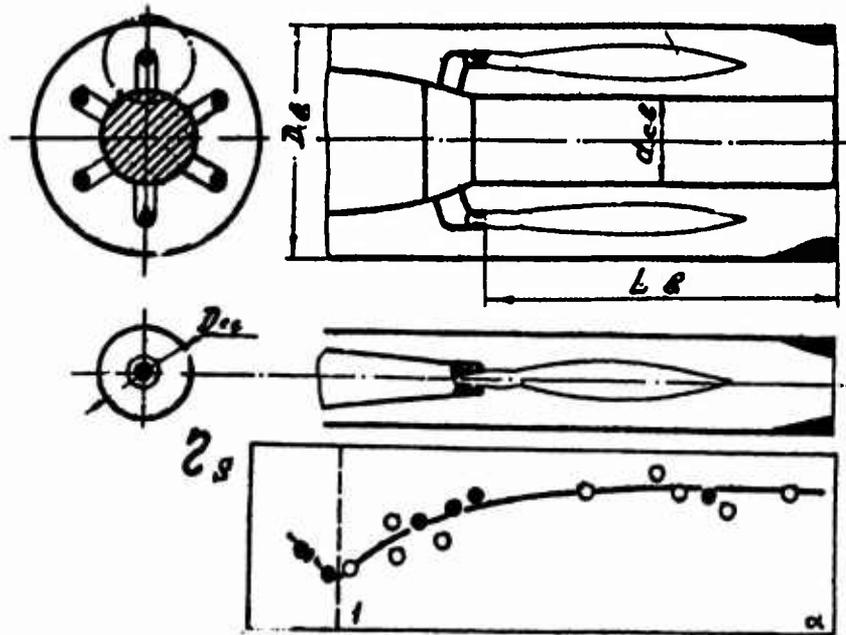
Fig 2.15. Multi-nozzle and equivalent one-nozzle SPRR, having the same equivalent relative combustor chamber length and the same fuel combustion efficiency at the same α value [8].

O one-nozzle SPRR, ● multi-nozzle SPRR
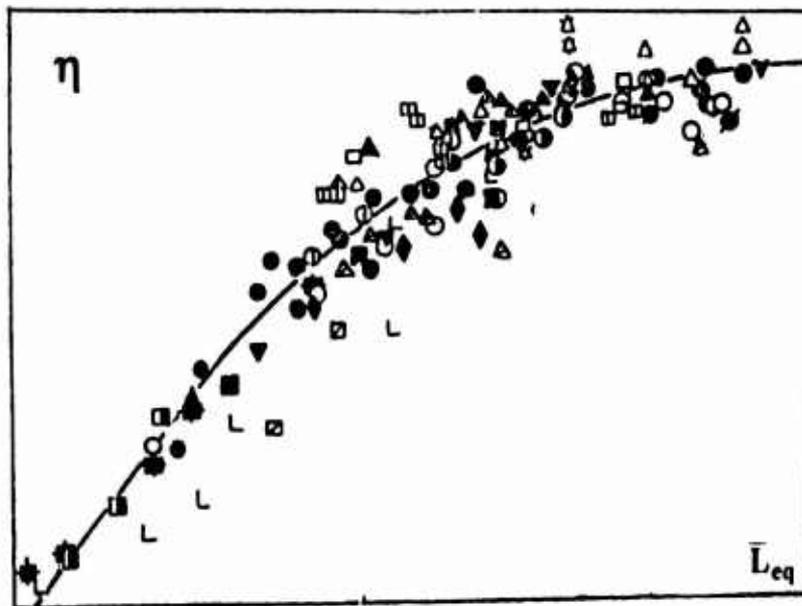
Fig 2.16 The Generalized dependence of secondary ram combustion from relative equivalence combustor length[8].
Absolute testing date:
fuels - see table 3.
$D_h = 100 - 1100$ mm,
$L_h = 400 - 2800 (4000)$ mm,
$N_n = 1 - 228$,
$\alpha = 0,74 - 2,5$,
$T_o = 288 - 1150$ K.
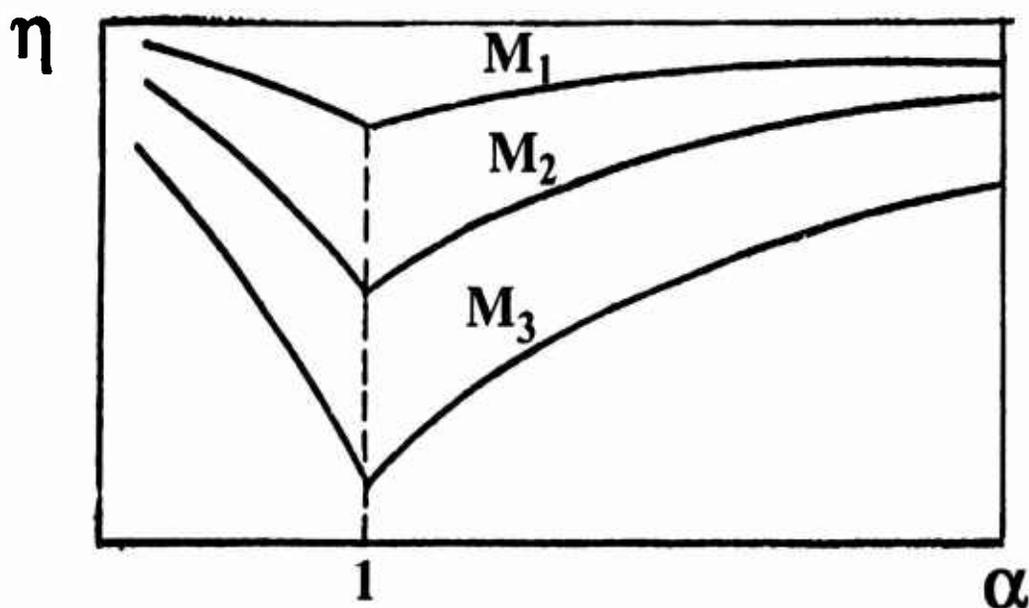
Fig 2.17. The complete SPRR propellant combustion effectiveness in dependence of air excess coefficient α by different flight Mach Number (calculation data).
M₃ > M₂ > M₁ (T_ot3 > T_ot2 > T_ot1)

$$M_3 > M_2 > M_1 \ (T_{ot3} > T_{ot2} > T_{ot1})$$
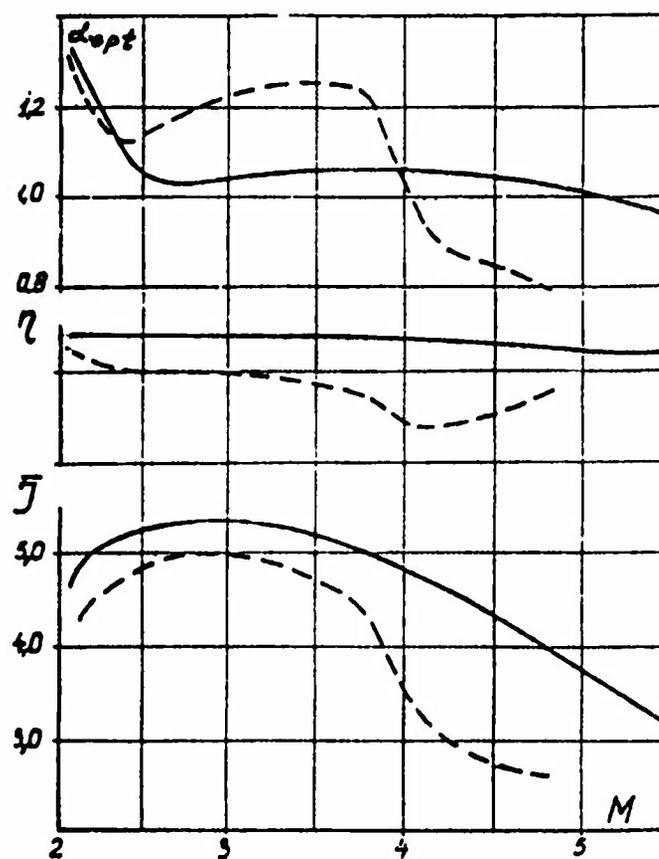
Fig. 2.18 The comparison of two SPRR in flight
- - - L_{eq1}, —— $L_{eq2} = 4L_{eq1}$, [8] (calculation)

	Type of mixer
I	Open grain
II	Rear device
III	Conical device
IV	Circular device
V	Pylon nozzle device
VI	Mixed type
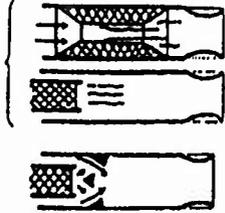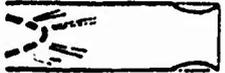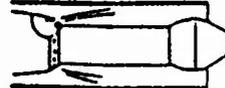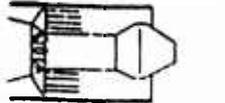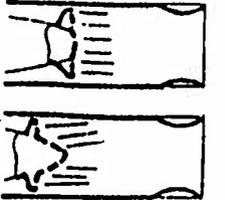
Fig. 2.19. Possible SPRR mixing devices. [8]
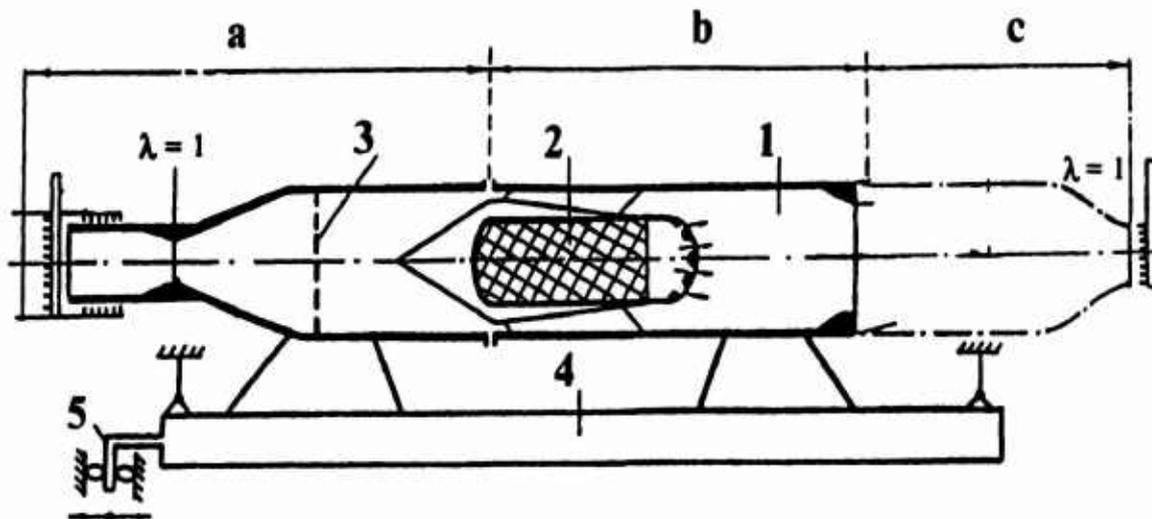
Fig. 2.20 Test-bed to SPRR with connected pipe testing.
a - test-bed inlet device.
b - engine (without intakes, and supersonic nozzle part).
c - detachable "cold" calibration device.
1. - secondary combustion chamber.
2. - gas generator with propellant grain
3. - net for uniforming the flow.
4. - moving platform for thrust measurement
5. - device for thrust measurement

mixer   water

$\phi 324$

$l_b = 1485 - 1540$

Mixers

№ 1

2

3

4

6

7

8

9
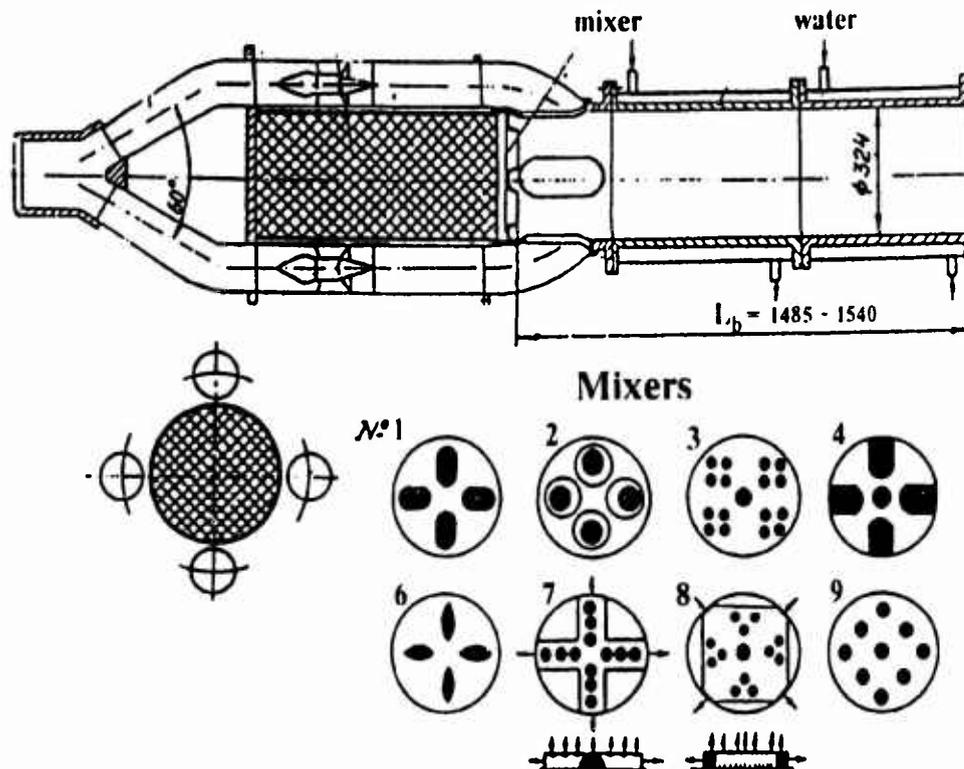
Fig. 2.21 Experimental engine of SA6 type with the open grain propellant with number of different mixing devices.[8].
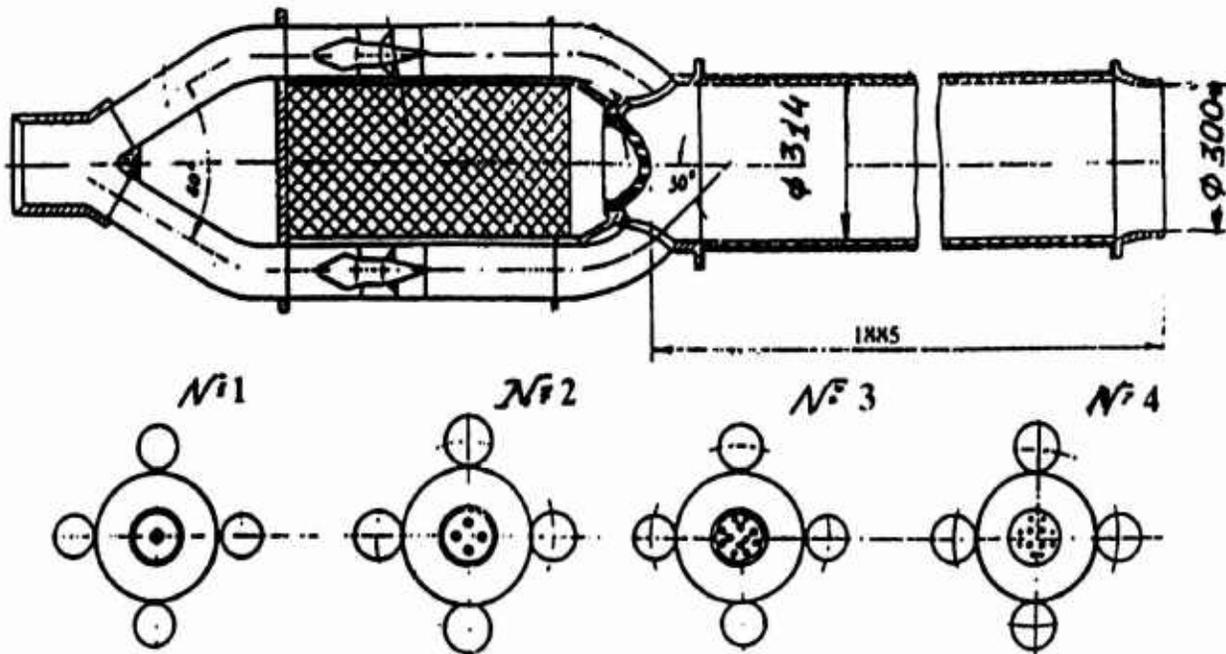
Fig 2.22 The tests prototype of SA6 missile SPRR with four variants of propellant nozzle devices[8].
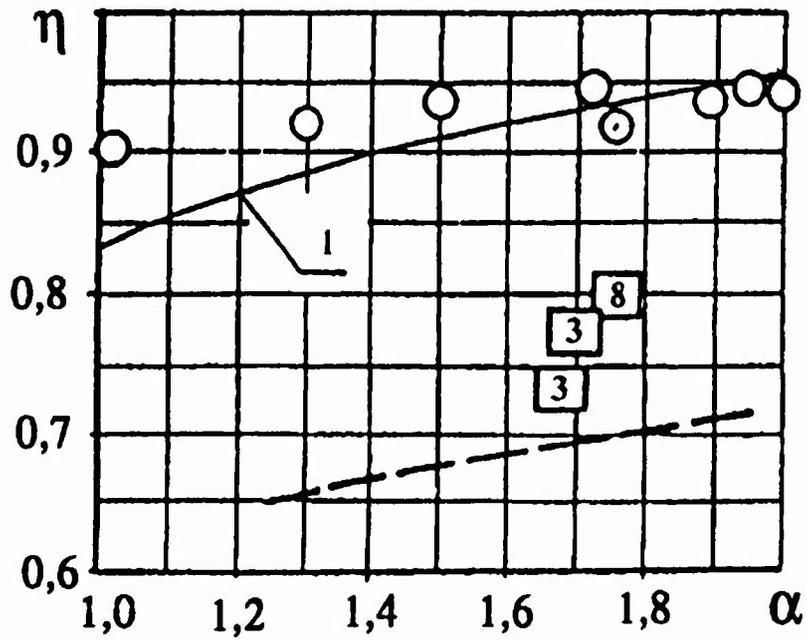
Fig 2.23. Combustion completeness for fig 2.21, 2.22 variants [8]. Fuel CH-1 (Table 3). $T_0 = 450 \div 500K$.
---- open end grain without mixer
3, 8 - open grain with mixers №3, and 8
OO - grain in gas generator, Nn = 12 (variant N4)
1 - calculation for $\overline{L}_{eq} \approx 21$.
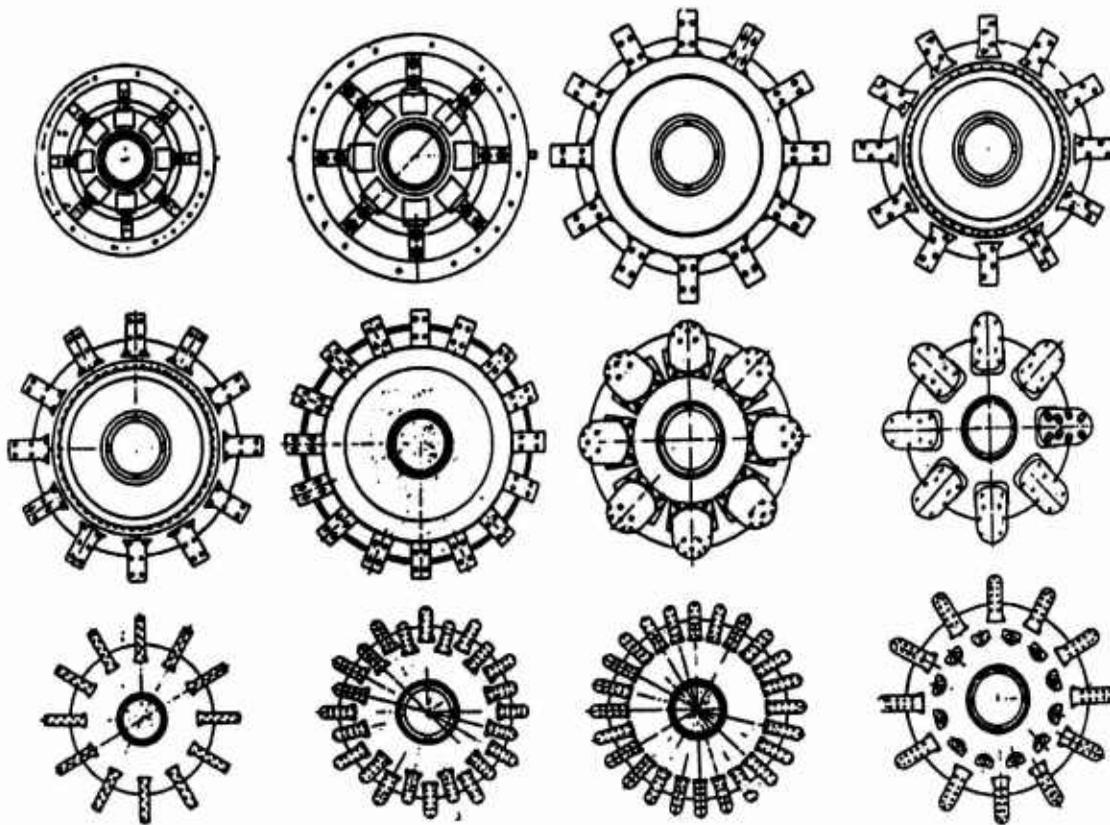
Fig 2.24 Experimental nozzle devices of pylon and mixed types.
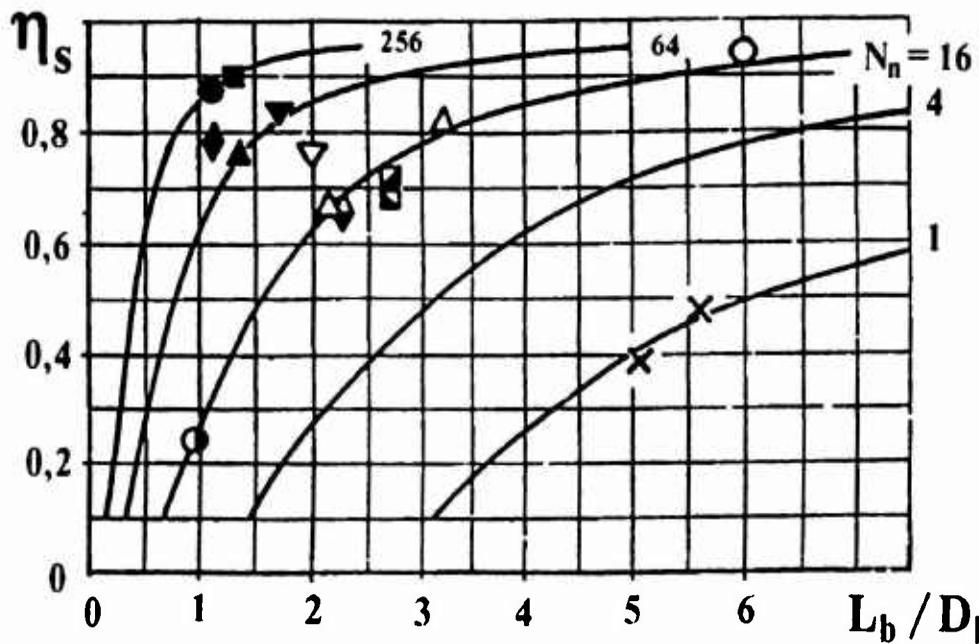
Fig 2.25. Secondary combustion effectiveness in dependence of relative combustor length and of gas generator nozzle number [8] $\alpha \approx 1,3$; $T_0 \approx 500K$.

H,km
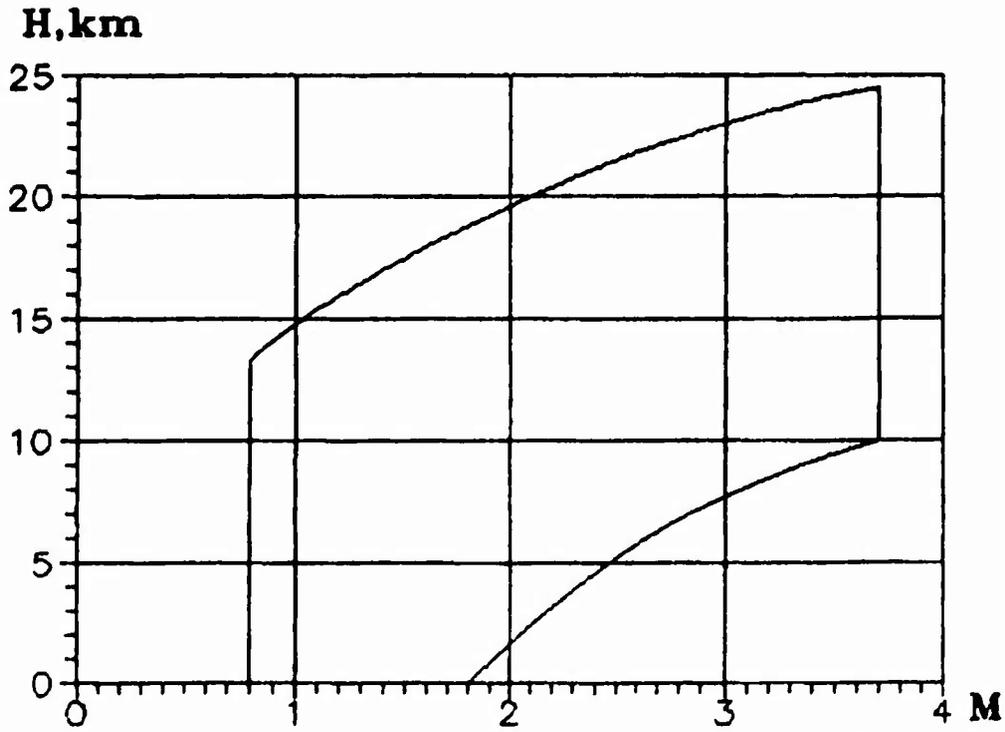
Fig. 2.26. Typical flight zone of middle-range air-to-air missile.
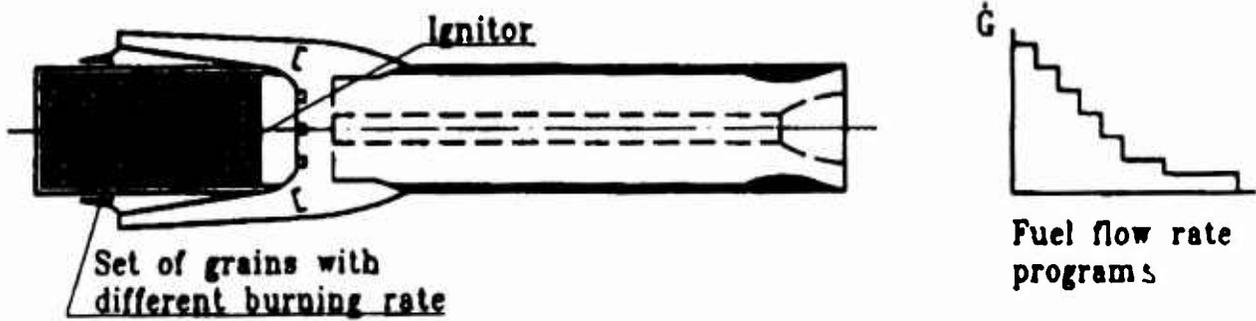
Fig. 2.27. Integral SPRR with fixed fuel flow rate programme.
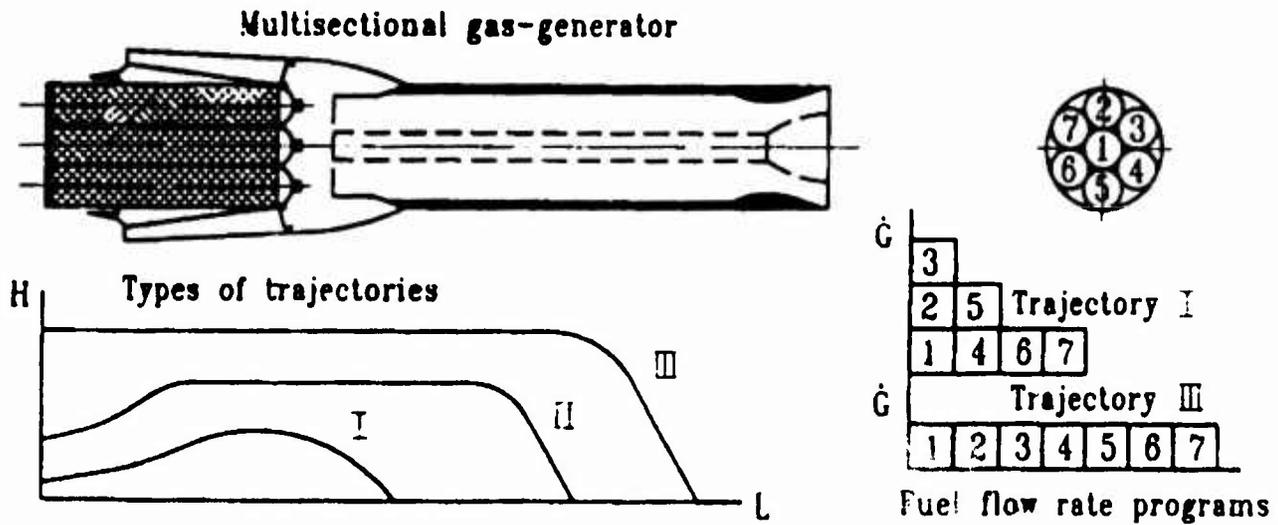
Fig. 2.28. Integral SPRR with discrete fuel flow rate control.

$$\dot{G} = A\ P^{\nu}; \quad \nu = 0.5-0.8 \text{ (usually } 0.2-0.3)$$

flow governor
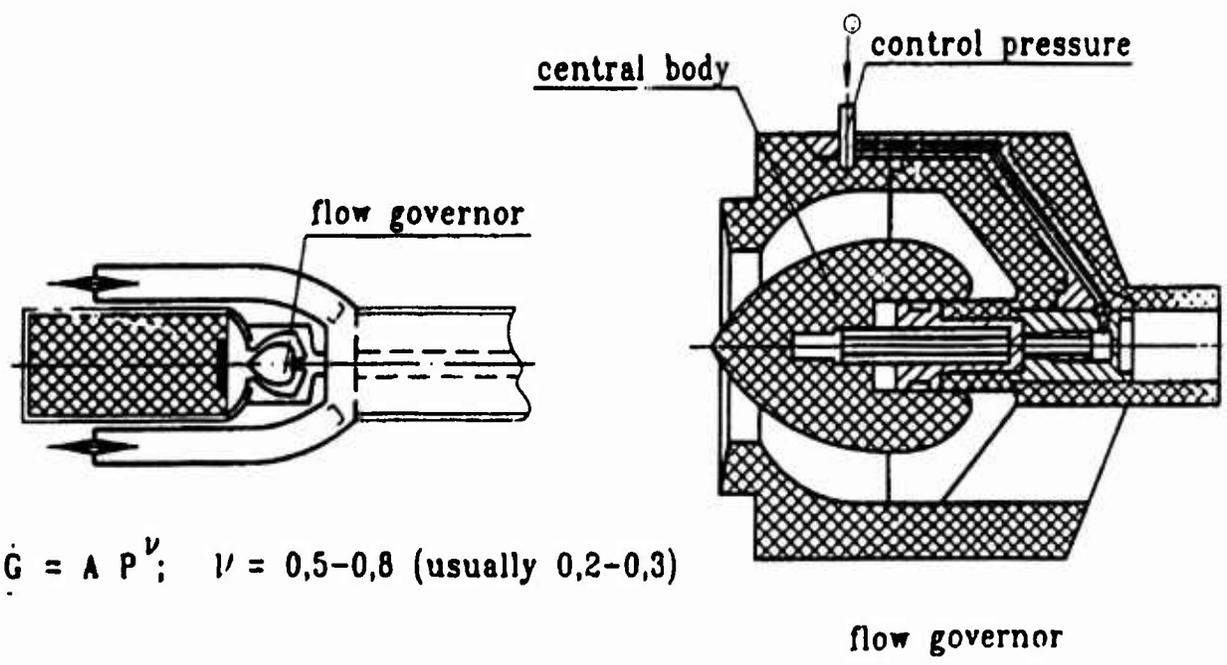
Fig. 2.29. Integral SPRR with flexible fuel flow control.
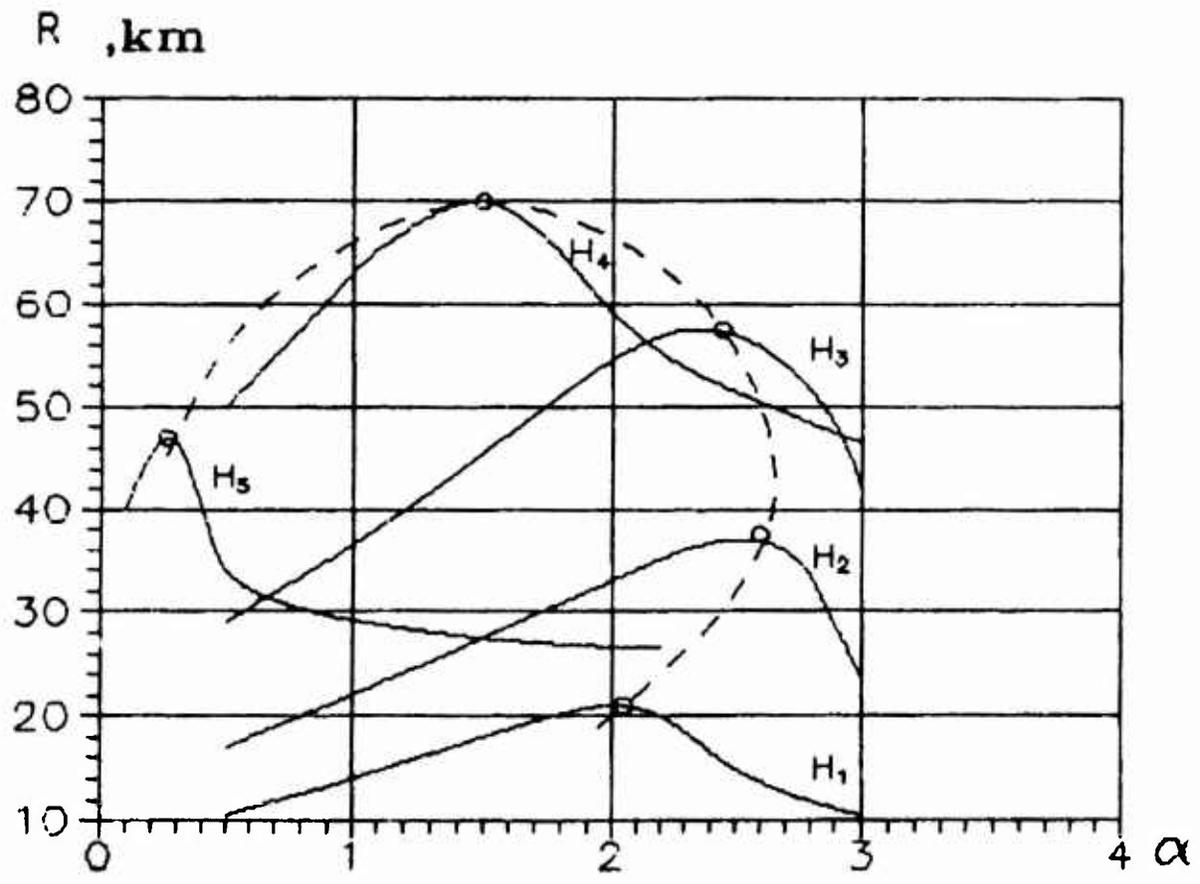
Fig. 2.30. Typical dependence of flight range of air-to-air missile on air excess coefficient at different altitude
$$H_1 < H_2 < ... < H_5.$$
---- optimal value of α.

SOME PROBLEMS OF SCRAMJET PROPULSION FOR AEROSPACEPLANES
PART I. -- SCRAMJET: AIMS AND FEATURES

by
Dr A.ROUDAKOV
CIAM (Central Institute of Aviation Motors)
111250 MOSCOW
RUSSIA

Introduction.

This lecture topic is problems of scramjet propulsion for single-stage aerospace planes. The aerospace plane main destination is acceleration of some pay load up to orbital speed. It defined a requirement to propulsion system to be frugal in the wide flight speed range under conditions of propulsion mass limitation and thrust compared with flight vehicle weight. In accordance with modern estimations, real hydrogen fuel scramjet specific impulse may be in several times more than that of rocket engine in the wide flight speed range, from $Mf = 5...6$ up to $Mf = 15. .20$. But hydrogen scramjet propulsion requires significant air ram connected with high heating of vehicle structure, large hydrogen tanks (and vehicle), special forms of flying vehicle. As a result scramjet advantage as well as any other air breathing engine advantage over the modern liquid rocket engines is not doubtless.

Nevertheless scramjets can provide good efficiency of aerospace plane if each scramjet element and units are developed very carefully and have high performances. In other case scramjet may lose competition with liquid rocket engines and full scale scramjet will be never created.

Theoretical and experimental investigations, ground and flight model test have demonstrated possibility of supersonic combustion ramjet for hypersonic flights. But we must carry out serious investigations to obtain high efficiency of scramjet elements and scramjet propulsion as a whole to be sure of scramjet success in aerospace plane competition with liquid rocket engine.

In this lecture I shall try to repeat nothing known from books and shall try to use only last study results known only to a small number of scientists.

The authors of this paper are the CIAM scientists: Dr. L.Gogish, dr. V.Krjutchenko, dr. N.Dulepov, dr. V. Semenov, dr. Yu. Shikhman and me.

Some Features of Scramjet

Nowadays all space objects are being accelerated by launch systems based on chemical rocket engines. These engines' technologies are enough completed and they permit to carry out some space experiments and investigations, to create some space communication system, to use space vehicles for some unique technology, but not high propulsive economies of chemical rocket engines requires to create multi-stage launch systems contented many one used components. It leads to high launch cost, to bad influence on ecology, to the earth surface and the space pollution by lost parts of rockets.

Modern chemical rocket engine efficiency is near to its limit and excludes possibility to create future effective one-stage multi-used rocket launch systems for variable aims.

Some years ago many scientists and specialists hoped on nuclear rocket engines that may give propulsive efficiency 1.5...2 times more than modern chemical rocket engines, but problems of ecology and safety compelled to give up hope to use nuclear rocket engines in near future launch systems.

At present many scientists pay their attention for problems of metastable substances used as rocket engine propulsive. These substances have energetic performances in many times better than chemical rocket propulsive, but practical realization of metastable propulsive rocket engine has many hard problems. Solution time of these problems is not clear now.

Now single possibility to increase sig-nificantly launch systems efficiency and to decrease

cost of to-space transportation operations is air breathing engines using. Air breathing engines modern technology level, modern materials, scientific background of gasdynamics and technology permit to design projects of one-stage multi-use wing launch system to accelerate space objects to orbit and to give back that to the earth surface. This system will use all aviation technology, existent runways and all ground aviation systems. These wing launch vehicles with air breathing propulsion are named the Aerospace Planes.

The main advantage of air breathing engines over rocket engines is atmospheric air using as oxidizer and work-substance of jet nozzle. That permits to decrease consumption of on-board propellant in several times. Besides of air breathing engines using leads to economical atmospheric flight possibility. As a result air-breathing propulsion launches system is transformed to aerospace plane capable to make some maneuver in atmosphere practically without additional propellant consumption. This capability will give new important quality: to come to orbit of any declination practically from any point of the earth surface and in any time moment. This quality is practically impossible for rocket launch system due to large additional propellant consumption.

In accordance to many experts opinion air-breathing technology may permit to create aerospace plane as new kind of aircraft, new kind of launch system, to open new stage of space using for wide aims' kinds in next century beginning.

The main success of airbreathing propulsion technology needed for aerospace plane is connected with supersonic ramjet concept. The scramjet is single kind of air breathing engine capable to operate at hypersonic flight speed accordant to flight Mach number -- $M_f > 7$. Scramjets have the widest operating flight speed range: $dM_f \cong 9$ in accordance to very strict estimations and $dM_f > 19$ in accordance to optimistic estimates. These scramjet qualities determine importance of it's application to aerospace plane in comparison with other air breathing engines.

Only engines of liquid air circle may compete with scramjet in width of operating speed range but liquid air circle engines achieve the best efficiency in mutual operating with scramjets.

At present idea of supersonic flow combustion engine can be admitted as realized due to many ground experiments and due to two flight tests of scramjet model. But wide and serious scientific and technology researches must be carried out, many problems of gasdynamics, combustion, high temperature materials must be soluted for creation of scramjet to obtain necessary aerospace plane propulsion efficiency. The scramjet concepts must be corrected and optimized continuously on base of new results of computational and experimental researches.

The main part of thrust of any air jet engine is the difference between nozzle jet momentum and intake air momentum:

$$R \ (\dot{m}_a + \dot{m}_p)V_n - \dot{m}_aV_f;$$

there are R -- thrust, $\dot{m}_a$ -- air mass flow, $\dot{m}_p$ -- propulsive mass flow, V_f -- flight speed, V_n -- nozzle jet speed. Pressure intake/nozzle difference influence is not taken into account in this formula.

As a rule m_p value is only several percent from m_a. Nozzle jet speed is defined by energy supplied to flow due to combustion. This energy is comparable with intake air flow energy under hypersonic flight conditions in case of the best fuel - hydrogen - even. For example ratio of combustion energy to intake air flow energy is less than 0.5 if flight Mach number is more than 11.5. Therefore nozzle jet velocity is more than flight velocity at several percent only, if $M_f > 15$ (See Fig. 1.1.) This simple result leads to very important effect the small losses of air momentum give significant decrease of thrust and specific impulse.

Fig. 1.2 shows influences of various losses on scramjet specific impulse. These curves were computed for some real losses:
-- stognatic pressure intake ratio in accordance three shock wave intake;
-- relative nozzle momentum losses are equal to 0.03,
-- nozzle intake area ratio -- 3;
-- combustion perfection -- 98;
-- relative flow losses in combustor -- .02

Some small variations of scramjet part parameters are very significant for propulsion performances. This significance increases if flight speed increases.

Some ideal hypothetical scramjet is capable to operate up to orbital flight speed but real losses in scramjets duct lead to zero thrust at $M_f \cong 23$. Real scramjet specific impulse is less than that of rocket engine if $M_f > 19$. The rocket engine uses more dense propellant and it is capable to operate in high altitude to decrease flight vehicle drag force. It must be taken into account to compare the rocket engine and the scramjet as aerospace plane propulsion. Practically, classic scramjet is not better than rocket engine at $M_f > 15...17$.

As a rule aerospace plane propulsion concept estimation is not a simple task. Very careful computational analysis and trajectory optimization are needed to estimate propulsion efficiency correctly Specific impulse or some another engine parameter is not enough for real estimation of engine and

propulsion efficiency.

Hypersonic intake and nozzle are all down surface of the plane. Intake and nozzle configurations influence on either scramjet propulsion performances or outside plane aerodynamics. Nozzle/intake area ratio is very important for either scramjet high flight Mach number performances or plain transonic performances. For these reasons nozzle/intake area ratio, intake and nozzle configurations must be chosen on base of total vehicle optimization.

Practically all performances of scramjet influence on the plane configuration, sizes, dry mass and other parameters. It causes very hard and important problem in design of aerospace plane and its propulsion. It may be the most significant problem of aerospace plane/propulsion integration.

Some examples of scramjet parameters influence on propulsion performances and aerospace plane efficiencies are being suggested to your attention.

Influence of fuel injection technique, fuel and combustion properties on scramjet performances.

Scramjet for aerospace planes must provide sufficient thrust and efficiency in the wide range of flight speed. A scramjet with fixed structure will have small mass and simple technology, so it is desirable. But its thrust decreases quickly with increase of flight speed.

For flight Mach number more than 10...12 required thrust may be provided with significant fuel excess. Excessive part of hydrogen doesn't release chemical energy. It only increases propulsive mass through the nozzle. Hydrogen is best fuel for aerospace plane engines, due to its high heat capacity and cooling capacity. But usage of hydrogen as passive propulsive mass doesn't seem valid, because of very low density of liquid hydrogen that results in necessary large tank. One may suggest to substitute it by any non reactive substance.

Really, physical properties of additional substance may influence on gas expansion processes in the nozzle and may lead to changes in the engine performances.

Furthermore, the scramjet performance can be improved by the fuel impulse utilization. The fuel will have high pressure and good enthalpy if it will be used after pump for the cooling of gas flow passage. Therefore injector fuel impulse may be compared with difference of exhaust and inlet impulses. The value of fuel impulse depends on fuel substance properties also

A set of additional substances was selected to find out the effect of physical processes in the scramjet gas flow passage on its performance and to propose for future detailed investigations some substances, application of which may provide actual advantages and which are valid in terms of economics and ecology. Passive additions were considered: inert gases (He,Ne,Ar,Kr,Xe), nitrogen (N_2), water (H_2O). Besides the effect of 8/9 excessive hydrogen by oxygen change was studied in order to supply additional enthalpy into the air flow.

It is assumed, that fuel components are heated in combustion chamber cooling system and mixed in gas generator and injected into scramjet combustion chamber through gas generator nozzles tangentially to air flow.

In case of oxygen application, fuel injectors are converted into micro rocket engines and scramjet is converted into combined cycle air breathing-rocket engine, i.e. rocket scramjet.

Some computational investigations of additional fuel component properties effect on the real scramjet main performances were carried out on the basis of equations describing one-dimensional imperfect gas flow (accounting heat capacity/temperature relation, equilibrium chemical reaction, dissociation and recombination reactions). The scramjets performances were computed accounting some inlet and nozzles total pressure losses. Besides, nozzle area expansion ratio was supposed restricted and constant.

Statement of the problem

Pure hydrogen (monopropellant) scramjet thrust efficiency performances were compared with that of bipropellant scramjet, provided that hydrogen consumption in the first engine ($m^{(1)}$) was equal to the sum of hydrogen consumption ($m_h^{(2)}$) and additional component consumption ($m_e^{(2)}$) in the second engine:

$$\dot{m}^{(1)} = \dot{m}_h^{(2)} + \dot{m}_e^{(2)} \qquad (1)$$

All other conditions were the same, i.e. the same scramjet geometry, flight conditions, efficiency of engine units and so on. These conditions lead to equality of air flow rates through both scramjets:

$$\dot{m}_a^{(1)} = \dot{m}_a^{(2)} = \dot{m}_a \qquad (2)$$

All the results were obtained on condition the hydrogen part, reacting with air, was the same in every case. That is, for usage of any additional non reactive substance, the reacting part of hydrogen was kept the same

$$\dot{m}_{H}^{(2)} \quad \dot{m}_a \quad L_{aH}$$

where L_{aH} 34 3 -- stoichiometric mixture ratio of air-hydrogen reaction

Introducing additional fuel component mass flow ratio

$$B_e = \dot{m}_e^{(2)} L_{aH} \quad \dot{m}_a$$

expression (1) may be written

$$B_e = B_H^{(1)} - 1 \tag{3}$$

for all the considered additional substances but for oxygen ($B_H^{(1)} = B^{(1)} = B^{(2)} = B$ -- total fuel mass flow ratio for the first and for the second engines)

Additional oxygen consumption was selected such that hydrogen-air-oxygen mixture was sustained stoichiometric

$$\dot{m}^{(1)} -- \dot{m}_{eo}^{(2)} \quad \dot{m}_a \quad L_{aH} \cdot \dot{m}_{eo}^{(2)} \quad L_{oH} \tag{4}$$

where $\dot{m}_{eo}^{(2)}$ -- oxygen consumption, $L_{oH} =$ 7 94 stoichiometric mixture ratio of oxygen-hydrogen reaction

Expression (4) may be written

$$B_{eo} = (B -- 1)L_{oH} \quad (L_{oH} + 1) \tag{5}$$

or

$$B_{eo} = 8(B -- 1) 9 \tag{6}$$

Total fuel (propellant) mass consumption in the bipropellant scramjet was always kept equal to the hydrogen consumption in the monopropellant scramjet (see eq 1) Therefore

$$B_H^{(1)} = B_H^{(2)} + B_e = B \tag{7}$$

Computations of scramjet performances were carried out with the aid of the program, computation procedure of which is based on the solution of one-dimensional gas dynamics equations, accounting equilibrium chemical reactions, air and combustion gases dissociation The computations were carried out in the flight Mach number range M 8 20 with the following assumptions

- flight path corresponds to the constant air ram value q 75 kPa;

- air inlet characteristics are shown in Fig. 1 3 as flight Mach number dependent relationships for inlet total pressure recovery factor P_i and mass flow factor F_i $F_a F_t$ (where F_a -- captured air flow area, F_t -- inlet throat area);

- the combustion chamber is expanding, expansion ratio $F_e F_t$ 1.2,

- fuel component tank temperature values

correspond to boiling temperature values at the see-level pressure with the exception of water ,

- nozzle exhaust area -- inlet throat area ratio F_e $F_e F_t$ 30,

- nozzle impulse factor I_e 0 97,

- fuel components are heated in combustion chamber cooling system to total temperature $1000 K$, mixed in gas generator chamber and injected into combustion chamber tangentially to air flow through gas generator nozzles.

- for hydrogen-oxygen fuel components gas generator is a liquid-hydrogen-oxygen micro rocket engine and scramjet is a rocket scramjet engine.

- gas generator nozzle exhaust area -- throat area ratio F_{ge} $F_{ge} F_{gt}$ 10,

- gas generator nozzle impulse factor I_{ge} 0 98

Fig 1 4 shows the effects of relative additional component consumption on gas generator exhaust specific impulse I_g for different components The value d is defined as

$$d \quad \dot{m}_e^{(2)} \quad (\dot{m}_H^{(2)} + \dot{m}_e^{(2)})$$

The relationships between d and B can be obtained from previous formulas for non reactive component

$$d \quad 1 - 1 B$$

and for oxygen

$$d \quad (1 - 1 B) (1 + 1 L_o)$$

For non reactive components the distinction between impulses for different components and impulse decrease with increase of impulse value are explained by effect of gas mixture molecule mass on nozzle exhaust impulse I_g It is known, that for fixed gas total temperature nozzle exhaust impulse depends mainly on gas molecule mass ($I_g \sim 1 (\mu)^{1/2}$) For this reason the substitution of excessive part of hydrogen by gas with the molecule mass higher than that of hydrogen (see table 1) leads to increase of mixture molecule mass and, consequently, to decrease of gas generator impulse

The highest impulse for hydrogen-oxygen components is explained by energy release in chemical reaction between hydrogen and oxygen in gas generator combustion chamber

Hydrogen-oxygen gas generator nozzle exhaust specific impulse is presented in Fig 1 5 for different hydrogen total temperature T_H The value B is gas generator equivalence fuel ratio

$$B_{HO} = \dot{m}_H^{(2)} L_{oH} \quad \dot{m}_{eo}^{(2)}$$

Note, that in case of $T_H \geq 1000\ K$ pure hydrogen gas generator impulse is higher than that of the hydrogen - oxygen gas generator and in case of $T_H = 500\ K$ vice versa.

Fig. 1.6 shows effect of gas generator impulse Ig on pure hydrogen fuel scramjet specific impulse Im. Dashed lines correspond to normal fuel injection $(Ig = 0)$, and continuous lines correspond to tangential fuel injection $(Ig\ 0)$. One can see, that fuel impulse has an essential influence on scramjet impulse. For example, at $M = 12$ and $B = 2.5$ the increase of scramjet impulse is about $1.2\ kN\ s/kg\ (20\%)$.

Scramjet mass and density specific impulses, obtained for neon application as additional fuel component with total bipropellant fuel consumption ratio $B = 1.43;\ 2.5;\ 5$, are shown in Fig. 1.7 and Fig. 1.8. For comparison pure hydrogen fuel scramjet impulses are given. One can see, that specific impulse (Fig. 1.7) for bipropellant fuel with neon is somewhat lower in the considered range of flight Mach number $(M = 7...20)$. Density impulse (Fig. 1.8) is significantly higher, if compared with that for pure hydrogen fuel. So at $M = 12$ for pure hydrogen engine and $B = 2.5$, specific impulse $Ig = 8.2\ kNs/kg$ and density impulse $Iv = 1.18\ MN\ s/cub.m$, i.e. replacement of hydrogen excessive part with neon results in specific impulse reduction by 12% and double density impulse increase.

Engine thrust changes exactly like specific impulse because comparison of mono- and bipropellant fuels is made at the equal fuel flow rates. That is why thrust versus M relationships are omitted here and hereinafter.

Replacement of hydrogen excessive part by helium (Fig. 1.9 and Fig. 1.10) changes scramjet performances less significantly. Specific impulses of hydrogen-helium and pure hydrogen scramjets practically coincide. Density impulse increase is not so significant due to the comparable densities of liquid helium and hydrogen.

If fuels with the other inert gases (Ar,Kr,Xe) are used, scramjet performances are close to that of the hydrogen-neon scramjet.

In Fig. 1.11 and Fig. 1.12 engine performances for bipropellant fuel are compared with that for monopropellant hydrogen fuel (total fuel flow ratio being $B\ 2.5$). Increments of specific impulse $I = I_m -- I_{mH}$ and of density impulse $I_v = I_v -- I_{vH}$, corresponding the considered gas, are shown.

It can be seen that values of specific impulse, corresponding to helium, are approximately $1.0\ kN\ s/kg$ higher than that corresponding to neon, that makes 10...30% in the Mach number range $M = 9...16$. Specific impulses corresponding to Ar,Xe are $0.1...0.3\ kN\ s/kg$ lower than that corresponding to Ne, that makes 2...3%. But density impulse corresponding to He is $0.1...0.5\ MN\ s/cub.m$ (20...30%) lower than that, corresponding to Ne, inspite of the higher values of specific impulse.

That is explained by the fact that Ne density is one order higher and that results in 1.7 times higher density of bipropellant fuel with Ne compared to fuel with He. Values of density impulse for Ne,Ar,Kr and Xe nearly coincide. Density impulse curves for Ar and Kr lie between the curves for Ne and Xe and are omitted in Fig. 1.12. The marked features are typical for bipropellant fuels with different percentage of inert gases. When total fuel flow ratio (B) increases, absolute values of increments Im and Iv increase too, and vice versa.

Specific impulse - fuel composition relationship, chemical energy supply being constant and all the engine parameters being identical, is explained by properties of real combustion gases.

In reality combustion gases heat capacity increases with temperature growth and the combustion gases are partly dissociated. It particularly regards to water vapor and nitrogen.

Fig. 1.13 shows relative specific heat capasity of N, H, O, Ar - temperature curves. Relative specific heat of each gas is the ratio of its specific heat and that at temperature $400\ K$. One can see significant heat capacity increase of nitrogen and particularly of water with temperature raise. Argon heat capacity is constant in wide range of temperatures, argon (as well as other inert gases) is practically ideal gas. Inconstancy of heat capacity results in lower kinetic energy increase of real gases molecules compared to that of ideal gases, in case of heating. Some kinetic energy increase delay occurs, part of kinetic energy is realized in the nozzle at lower pressure. As a result effectiveness of engine thermodynamics cycle degrades.

Another significant feature is nozzle performance dependence (for fixed nozzle expansion ratio) on adiabatic index of combustion gas mixture. The higher adiabatic index - the higher the conversion factor of total gas enthalpy into exhaust jet kinetic energy in the nozzle. Inert monoatomic gases are practically ideal gases, their heat capacities are practically constant, they can not dissociate, their adiabatic indexes are the highest $(= 1.67)$.

At last, scramjet performances depend on gas generator exhaust impulse (Fig. 1.6), the value of that depends on propellant composition (Fig. 1.4).

In case of excessive hydrogen replacement

with inert monoatomic gas, gas mixture in the nozzle becomes closer to ideal gas, its adiabatic index increases and one should expect specific impulse increase But lower inert gas heat capacity compared with that of hydrogen (especially for Ne and heavier gases) results in higher gas mixture temperatures

In consequence, non-ideality effect of water and nitrogen, forming essential part in the nozzle exhaust flow, becomes stronger

The effect of these two factors (adiabatic index and heat capacity) is shown in Fig 1 14 and Fig 1 15, obtained at the condition of normal fuel injection $(lg \quad 0)$ into combustion chamber One can see, that the effect of the second factor is stronger than that of the first factor (except the case of part helium application and $B \quad 2.5$)

The effect of the third factor (gas generator impulse) increases the distinction between the impulses of monopropellant hydrogen fuel scramjet and of bipropellant fuel scramjet (compare Fig 1 14 and Fig 1 11) because of the gas generator impulse for hydrogen fuel is higher than that for inert gas and hydrogen mixture (see Fig 1 4)

In consequence, in case of tangentially injected fuel, specific impulse of bipropellant scramjet appears lower than that of pure hydrogen scramjet for any inert gases as fuel additio But dencity impulse of bipropellant scramjet is higher than that of hydrogen scramjet for tangential (Fig 1 12) and normal (Fig 1 15) fuel injection (especially for Ne and heavier gases, Fig 1 12)

This effect, in spite of its specific impulse reduction, may be very useful in practice, because it permits to reduce the needed volume and dry mass of tanks

Effect of real-gas-mixture properties influence on the engine performances is observed also when non-monoatomic substances are used as additional components of the fuel Fig 1 16 and Fig 1 17 (like Fig 1 11 and Fig 1 12) for the case of tangentially injected fuel and Fig 1 18 and Fig 1 19 (like Fig 1 14 and Fig 1 15) for the case of normal fuel injection show the results, when water, nitrogen and oxygen were used as additional components The results of water and nitrogen application are worse compared to that of neon in the both cases It can be explained by non-ideal properties of water and nitrogen inconstancy of heat capacity and low value of adiabatic index.

Replacement of excessive hydrogen part by oxygen and hydrogen in stoichiometric ratio is significantly more effective in the case of tangential gas generator gas injection than in the case of normal fuel

propellant injection One can see, that for the case of tangential injection hydrogen-oxygen scramjet has the highest values of density impulse for the all considered Mach numbers and the highest values of specific impulse in Mach number range $9 \quad 16$ at B 2.5 Note, that by normal injection the highest value of density impulse corresponds to neon-hydrogen fuel scramjet and specific impulse of hydrogen-oxygen scramjet is higher than that of hydrogen scramjet only for $M \quad 9.5$

The specific impulse increase of hydrogen-oxygen scramjet is achieved by additional chemical energy, that is provided by hydrogen and oxygen But specific impulse increases slightly, because the part of water in the nozzle gas mixture increases and temperature raise shows non-ideal properties of nitrogen and water In the case of tangential fuel injection the effect of non-ideality appears lower than in case of normal fuel injection, because tangential fuel injection leads to gas velocity increase (gas temperature decrease) in combustion chamber and, in consequence, the larger part of additional chemical energy is converted into exhaust jet kinetic energy In Fig 1 20 and Fig 1 21 specific and density impulses of hydrogen-oxygen scramjet at tangential fuel injection are compared with that of pure hydrogen scramjet for different values of $B \quad 1.43, 2.5, 5$ Note, specific impulse of hydrogen-oxygen scramjet is higher then that of hydrogen scramjet at $B \quad 5$ and $M \quad 6.20$

Fig 1 22 differs from Fig 1 20 only by values of gas generator exhaust impulse lg In Fig 1 20 they correspond to the hydrogen temperature at gas generator chamber inlet $T \quad 1000K$, while in Fig 1 22 they correspond to $T \quad 2000K$ (see Fig 1 5) One can see, that inspite of higher gas generator impulse for pure hydrogen scramjet $(lg \quad 6.9 \, kNs \, kg)$ specific impulse of hydrogen-oxygen scramjet is higher than that of hydrogen scramjet in the wide flight Mach number range (for $B \quad 2.5$ at $M \quad 8.12$)

Previously mentioned effects of gas mixture reality influence on exhaust velocity from nozzle are small, but essential for scramjets at high speeds It is known, that in high flight speeds, thrust of any air-breathing engine is defined by the small difference of two large values exhaust and inlet impulses Even slight change in exhaust velocity may result in significant change of thrust and specific impulse of the engine It complicates the quality of investigations of scramjet for aerospace planes and requires as detailed computations as possible

Carried out computations could not take into account possible effect of the additional substance on spatial effects in the engine passage. Besides, problems of engine construction cooling in case of bipropellant fuel application were not considered. Accounting of these effects requires more complicated

model of processes in a scramjet. As for aerospace planes, to estimate the engine effectiveness would require detailed computations of the plane trajectory, particularly, tank volume effects on the aerodynamics must be accounted. Due to these reasons one cannot conclude that application of additional substances instead of excessive hydrogen is absolutely advantageous. No doubt, the problem is worth carrying out more deep investigations

Some conclusions

Tangential injection of fuel gives significant improvement of scramjet performances and must be applied on aerospace plane scramjet propulsion

Some additional fuel component effects on hydrogen scramjet performances show significance of small differences of propellant and combustion products properties

It seems attractive to use oxygen as additional fuel component. oxygen's application allows to increase as density impulse (1 5 2 times), as well as specific impulse (by 3 10%) of engine and to reduce the needed tank volume and tank dry mass

Some inert gases application is interesting also

More sure results of scramjets modifications comparison may be received by the aerospace plane trajectory optimization methods

Trajectory Efficiency Analysis of Oxygen Boosted Scramjet.

Computational efficiency analysis of single stage aerospace planes (ASP) was carried out to compare two propulsion system (PS) concepts

-- the first PS uses classical scramjet (SCRJ) operating only on hydrogen fuel,
-- the second PS uses on-board oxygen boosted scramjet (SCRJ-R)

Efficiency analysis of two PS concepts -- on basis of SCRJ and SCRJ-R -- was conducted for an example of hypothetical single-stage ground starting ASP with start mass of 280 t. The ASP is designed to launch the payload on near-earth circular orbit (H = 200 km) with inclination angle of 51 deg. The latitude of starting place -- 47 deg. The additional characteristical velocity needed to orbit maneuver and re-entry starting was taken equal to 120 m/s. The ascent trajectory was determined with following constraints on vehicle motion parameters
-- maximum dynamic pressure allowed - 75 kPa,
-- maximum longitudinal acceleration - 3g,
-- maximum cross acceleration - 1,5g
-- maximum trajectory angle 35 degrees

The optimization of ascent trajectory was conducted with account to these and some other limitations on different phases of motion. The aerodynamic scheme of hypothetical ASP can be defined as wing body without horizontal tail. The bottom nose part of the fuselage forms engine compression surface, and fuselage afterbody is used for nozzle gases expansion

For efficiency comparison of various PS unified model was accepted. The following mass and volumetric characteristics were assumed

Mass Characteristics

a) Propulsion system

-- specific mass of thrust loaded structure panels. 16 kg/sq m,
-- specific mass of SCRJ (SCRJ-R) cooled panels. 20 kg/sq m,
-- specific mass of air entry and nozzle panels. 20 kg/sq m,
-- specific mass of LR, 0 0009 kg/N, -
-- specific mass of ATR, 0 004 kg/N

b) Airframe

-- fuselage structure specific mass, 23 kg/sq m,
-- wing structure specific mass, 30 kg/sq m,
-- fin structure specific mass, 35 kg/sq m,
-- hydrogen tanks specific mass, 18 kg/sq m,
-- oxygen tanks relative mass, 0 015,
-- constant mass (crew, equipment, undercarriage, etc), 19 t

Geometrical Characteristics

1-- wing span to length ratio, 0 44,
-- basic wing leading edge sweep angle, 52 deg.
-- strake leading edge sweep angle, 83 deg.
-- wing profile thickness, 0 05,
-- wing fineness ratio, 1 83,

The wing loading and disposable fuel capacity were determined by solving two equations

-- the equation of vehicle existence (mass balance),
-- the equation of matching the required and disposable vehicle volume

Airframe modelling was assumed for comparative evaluation of alternative PS versions and design parameters. In accordance with this airframe modelling, the absolute sizes of vehicle (length, wing surface, etc) are changing in some limits while relative paramaters (span to length ratio, relative

maximum fuselage area, sweep angle, aspect ratio, etc.) remain unchanged. Thus the aerodynamic characteristics also remain constant.

Aerodynamic Characteristics of Aerospaceplane (ASP)

Aerodynamic characteristics of the ASP were determined by mathematical modelling method. It is known that the possibility to obtain experimental data for hypersonic velocities range is limited by aerodynamic facilities capacity. At the same time the CFD (computational fluid dynamics) methods used for large computational investigations connected with optimization of ASP propulsion system (PS) require very great computer resources. Therefore the engineering method published in was used for evaluation of aerodynamic forces and moments acting on vehicle at hypersonic flight speeds.

The friction forces, heats flux and equilibrium wall temperature are defined on base of some boundary layer model. This model permit to determin gas parameters on viscous boundary layer on base of Newton and Prandtl-Mayer theories, theory of tangent cones and wedges and takes into account entropy effect and hypersonic viscous interaction. The corresponded algorithms and computer codes were described in

The method based on supersonic potential theory, on slender body theory and on some empirical dependencies was used to determine approximetly profile drag force, polar slope at subsonic, transsonic and moderate hypersonic flight speeds.

In Fig. 1.23 - 1.26 are shown the configuration and aerodynamic characteristics of ASP considered in this paper are shown as drag force factor and lift force factor dependencies on Mach number and angle of attack. Maximum aerodynamic fineness (Kmax) and corresponding angle of attack versus

flight Mach number are shown too.

The results of aerodynamic characteristics computations were confirmed by flight experiments of Bouran Space Vehicle program and hypersonic scramjet test flights.

Propulsion System Concepts

Two concepts of propulsion system are considered:

- the first PS based on scramjet,
- the second PS based on scramjet-rocket

They are identified as SCRJ concept and SCRJ-R concept

These combined PS concepts consist on following engine types

-- In the first acceleration phase (M<5) air-turbo-rocket engine (ATR) operating on oxygen-hydrogen fuel is used.
-- In the second phase from M=5 SCRJ or SCRJ-R are used

-- In the third (final) phase of acceleration oxygen-hydrogen Liquid Rocket Engine (LRE) is operating with space specific impulse equal to 4576 m/s and oxygen/hydrogen flow ratio equal to 7.

SCRJ/LRE or (SCRJ-R)/LRE transition flight Mach number were optimazed for highest payload mass

Optimum Propulsion Operating Modes of SCRJ and SCRJ-R.

The values of ATR effective specific impulse along the ascent trajectory depending on Mach number and flight altitude are listed in Table 1

ATR Performances

Table 1

H, km	0.00	0.00	0.33	11.80	15.50	18.50	21.60
Jsp, km/s	20.59	20.12	21.75	21.65	21.30	20.90	21.80
T, K	288	295	380	600	880	1075	1250

The operating modes and flight speed range on diverse hases of erospaceplane acceleration trajectory were chosen in three ways: they could be set, or defined from the "combustion chamber choking" condition or optimized. So the operating mode of ATR on the first phase of trajectory (M < 5) was set by choosing air excess air coefficient equal to 1.0. The operating mode of SCRJ and SCRJ-R were

optimized for all operating part of trajectiry, but limitation of SCRJ combustor choking requied to chois air excess at Mf < 7 without optimisation practicaly

The operating mode of SCRJ-R may be optimized in the whole range of Mach numbers. It was characterized by two parameters: total air excess coefficient and oxygen-fuel excess coefficient in

gasgenerator.

The results of computational study of optimum operating modes are shown: for SCRJ - in

Table 2, for SCRJ-R in Table 3. In the tables the values of total effective thrust, of specific impulse and of angle of attack along the flight trajectory are given

Scramjet Performances

Table 2.

M	5	6	7	8	11	12	14
H, km	21.6	24.0	25.8	27.8	32.3	35.0	48.3
air/fuel ratio	2.78	1.5	1.0	1.0	0.9	0.8	0.6
R, kN	1100	1447	1800	1953	1400	1140	475
Isp, km/s	35.2	31.0	26.0	22.8	12.9	9.8	3 8

Scramjet--Rocket Performances

Table 3

M	5	6	10	11	12	13	15.2
H, km	21.6	24.0	30.6	32.3	35.0	40.4	53.6
air/fuel ratio	1.60	1.20	1 10	1.10	1.15	0.90	0.80
O/H ration of preborner	0.30	0.00	0.00	0.00	0.05	0 05	0.70
R, kN	1900	1947	1600	1314	1139	947	2437
Isp, km/s	12.00	32.87	16.40	12.90	9.40	7.10	4.30

As a result of optimization of SCRJ hypersonic operating mode, the air excess coefficient remains constant and is equal to 1.0 at acceleration phase from M = 7 to M = 10. (Table 2.) Futher with the speed increasing SCRJ operates on a fuel enriched by hydrogen.

Optimization of SCRJ-R operation modes gives following results: in the concluding acceleration phase (M = 12...15) for providing high thrust values engine may operate on oxygen enriched propellant

In moderate hypersonic speed range (6 < M < 11) corresponding to constant dynamic pressure q = 75 kPa the optimum chosen on payload criterion is represented by highly economical operating mode without on-board oxygen supply

The results of computational optimization of

Mach number range for SCRJ and SCRJ-R effective operation show that optimum transition Mach number (to LRE) makes up: for SCRJ 14 and for SCRJ-R 15.2

The simultaneous operation is also useful: of LRE and ATRgg in transsonic flight range, of LRE and SCRJ -- by Mach numbers 13.6...14.0 and of LRE and SCRJ-R by Mach numbers 14 8 15 2

Comparative Evaluation of Flight Performances of Aerospaceplane with SCRJ and SCRJ-R.

Basic aerospaceplane flight performances with two PS concepts -- SCRJ and SCRJ-R -- are shown in Table 4

SCRJ and SCRJ-R Performances   *Table 4.*

Flight performances parameters		PS concepts	
		SCRJ	SCRJ--R
PS -- ASP the main parameters	Start accelaration, m/sq. s	6.25	6.25
	Start relative loading, kg/sq.m	603	620
	Landing relative loading, kg/sq.m	192	203
Mass ballance parameters, tonns	Pay load mass	1.4	4.6
	Mass in orbit	91.1	93.8
	Propulsion mass	20.1	20.9
	Air fraim mass	39.0	37.9
	Tank mass	9.4	9.1
Propellents mass, tonns	Oxygen for ATR--gg	15.7	15.7
	Hydrogen for ATR--gg	15.7	15.7
	Oxygen for SCRJ--R	----	21.3
	Hydrogen for SCRJ/SCRJ--R	45.6	43.8
	Oxygen for LR	101.5	82.5
	Hydrogen for LR	14.43	11.8
	Total oxygen	117.3	119.5
	Total hydrogen	76.1	71.3
Geometrical parameters	Vehicle length, m	65.7	64.8
	Wings span, m	29.1	28.7
	Vehicle valume, cub.m	1564	1500
Flight performances	Accent time, s	1345	1340
	Accent distance, km	4351	4428
	Speed losses due to drag, m/s	3367	3210

One can see from Table 4 that SCRJ thrust augmentaton (use of SCRJ-R) allows to diminish aerospaceplane volume what is particularly important under conditions of high tanks and airframe elements specific mass.

So using SCRJ-R instead of SCRJ allows to reduce total hydrogen mass by 5 t, aerospaceplane volume by 64 cub.m, aerospaceplane wetted surface by 43 sq.m, airframe and tanks mass by 1.5 t. All these improvements ensure launching into near-earth orbit 4.5...5t of payload, i.e. some three times greater than the payload launched when using SCRJ only.

Some Conclusions.

1 A 4-5 t payload may be launched to the near-earth orbit (H=20 km, i=51 deg) by aerospaceplane with starting mass of 280 t using oxygen boosted SCRJ, i.e. SCRJ-R. This payload mass is three times greater than that launched by ASP with not oxygen SCRJ

2. Optimum Mach number for transition to LRE operation mode is for SCRJ - 14 and for SCRJ-R - 15.2

Using oxygen as additional fuel component leads to larger the effective operating diapason of SCRJ-R in comparison with not oxygen SCRJ that

3 Using of SCRJ-R permits to increase volumetric efficiency of aerospaceplane and to reduce it's structure mass.

Bibliograthy

1. Курзинер Р.И. "Реактивные двигатели для больших сверхзвуковых скоростей полета" М. *Машиностроение*, 1989.

2. Sosounov V. "Study of Propulsion for High Velocity Flight" *ISABE*, 1991.

3. Escher W.J.D., Teeter R.R., Rice E.E. "Airbreathing and Rocket Propulsion Synergism: Enabling Measures for Tomorrow's Orbital Transports" *AIAA Paper*. 86-1680, 1986

4. Bendot J. "Composite Engines for Application to a Single-Stage-to-Orbit Vehicle" *NASA CR-2613*, 1975.

5. Murthy S.N.B., Czysz P.A. "Energy Analysis of High speed Vehicle Systems" *AIAA Paper*, 90-0089,1990.

6. Hewitt F.A., Ward B.D. "Advanced Airobreathing Powerplant for Hypersonic Vehicles" *ISABE 89*-7107, 1989.

7. Heppenheimer. "The National Aerospace Plane" *Pasha Publikations,* 1989.

8. Czysz P.A. "Thermodynamic Spectrum of Airobreathing Propulsion" *SAE T.P.* 881203, 1988

9. Saber A.J. and Chen X. "H2/Air Subsystems Combustion Kinetics in Aerospaceplan Powerplants" *IAF*-91- 276, 1991.

10. Robert A. Jones, Caleman du P., Donaldson "From Earth to Orbitin at Single Stage" *Aerospace America*, August 1987. Vol. 25, No. 8.

11. Rudakov A., Krutchenko V. "Additional Fuel Component Application for Hydrogen Scramjet Boosting" *SAE T.P.* 900990, 1990.

12. Hewitt F.A., Ward B.D. (Rolls-Royce) "Advanced Airbreathing Powerplant for Hypersonic Vehicles" *ISABE* 89 -- 7107, 1989

13. Kors D. (Aerojet Propulsion Division). "Design Cosiderations for Combined Air Breathing-Rocket Propulsion systems" *AIAA Paper* No. 90-5216,1990.

14. Варгафтик Н.Б. "Справочник по теплофизическим свойствам газов и жидкостей" М. *Физматгиз*, 1972.

15. Schetz T.A. and Billig F.S. "Studies oi Scramjet Flowfields" *AIAA Paper* No. 87- 2161, 1987

16. Billig F.S. "Combustion Processes in Supersonic Flow" *Jet Propulsion*, Vol. 4, No. 3, 1988

17. Pouliquen M.F., Doublier M., Scherer D "Combined Engines for Future Launchers" *AIAA Paper*. 88-2823, 1988.

18. Roudakov A., Dulepov N. et.al. "Analysis of Efficiency of System with Oxygen Liquifaction and Accumulation for Improvement of Aerospaceplane Performances" *IAF*-91-270, 1991.

19. Czisz P.A. "Space Transportation Systems Requirments Derived from the Propulsion Perforance" *IAF*-92-0858.

20. Vinogradov V., Stepanov V. "Numerical and Experimental Investigation of Airframe-Integrated Inlet for High Velocities". *AIAA Paper* 89-2679, 1989

21 Pouliquen M "Propulsion of Space Transportation System", Paris, 1991

22. Wolf D.M., Daum A., et.al "Air-Borne Launching with Existing technology", *IAF-93*-V.3.615, 1993

23. Billant C, Boueldleu E., Wagner A., "Radiance: A High Staging Speed Airbreathing First Stage TSTO Launcher", *IAF-93*-V.3.616, 1993

24 Roudakov A, Novelli Ph, et al , "Flight testing an Axisymmetric scramjet - Russian Recent Advances." *IAF- 93*-S.4.485, 1993
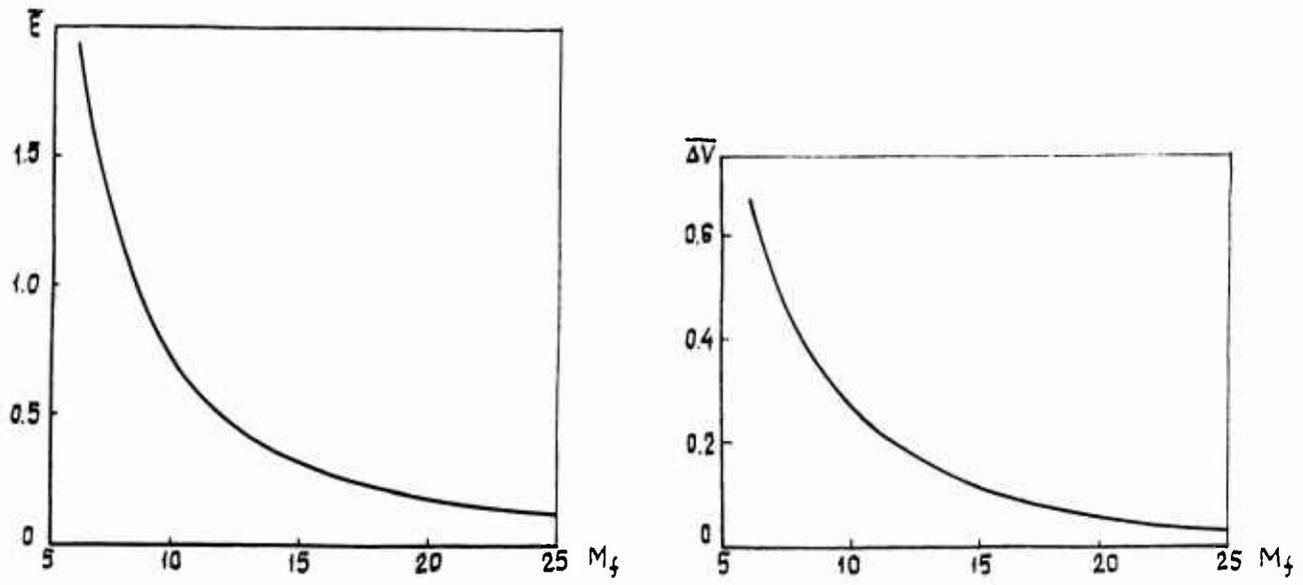
Fig 1 1 Relative energy of hydrogen combustion and theoretical relative limit
of flow velocity increase for scramjet
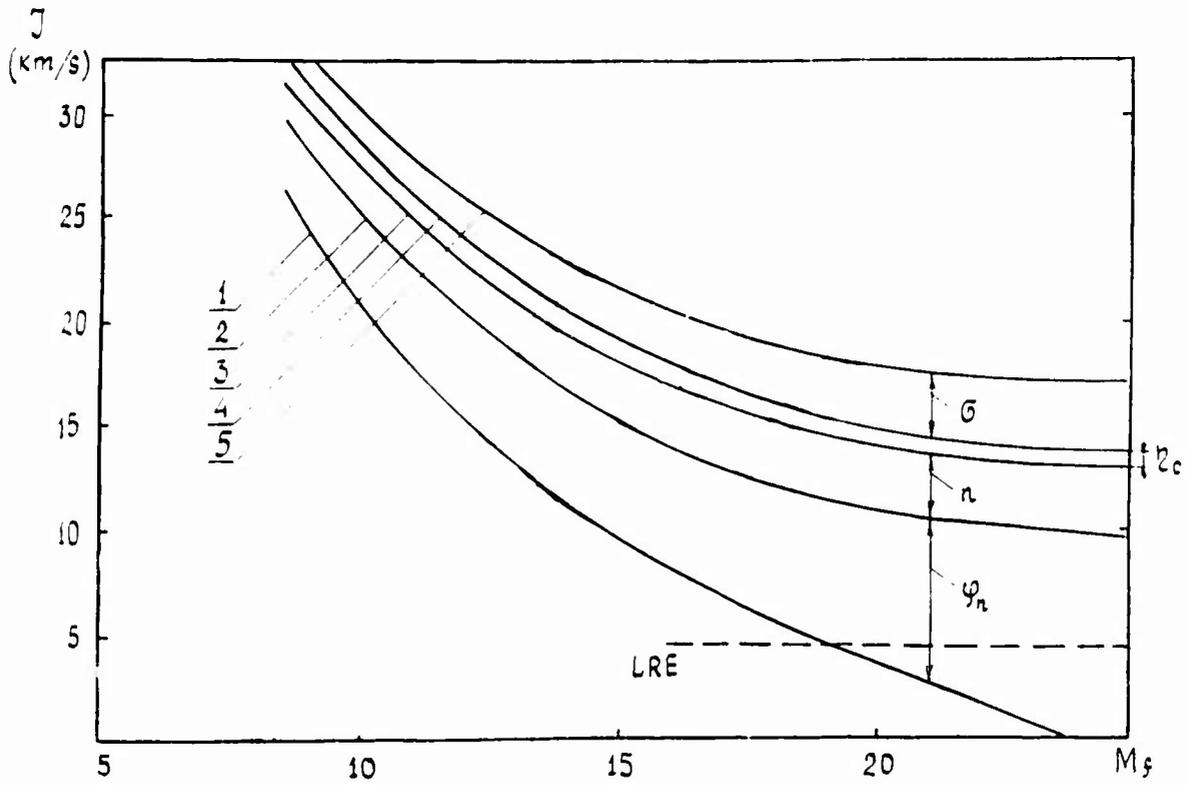
Fig 1 2 Influence of various losses on scramjet specific impulse along the
flight path
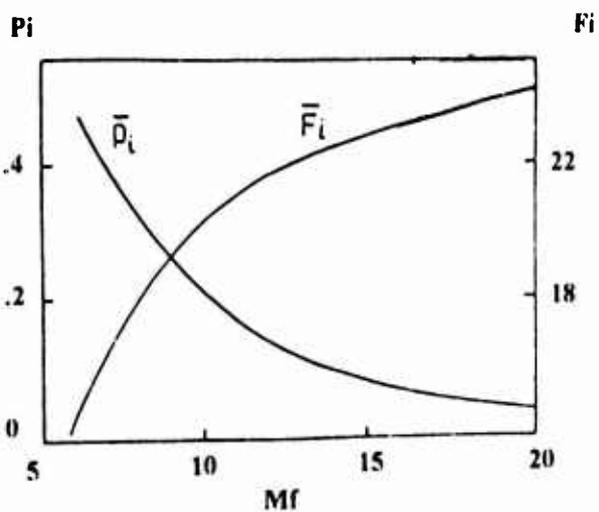
Fig. 1.3. Inlet performances.
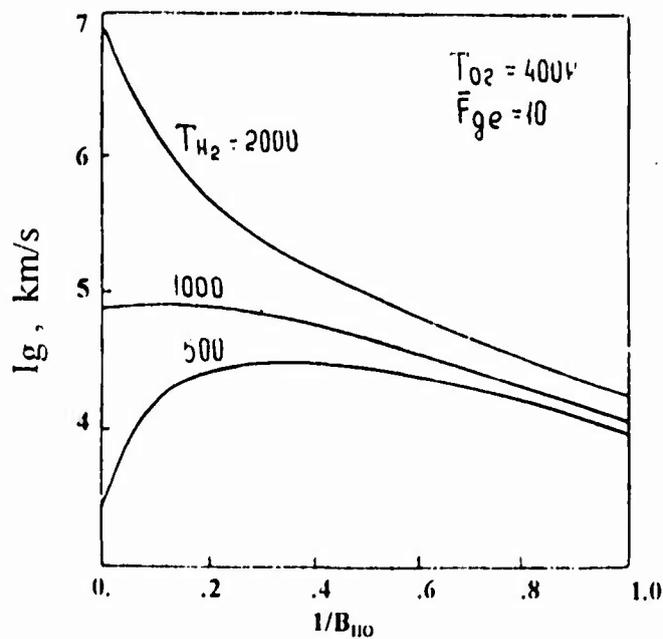
Fig. 1.5. Hydrogen oxygen gas exhaust specific impulse.
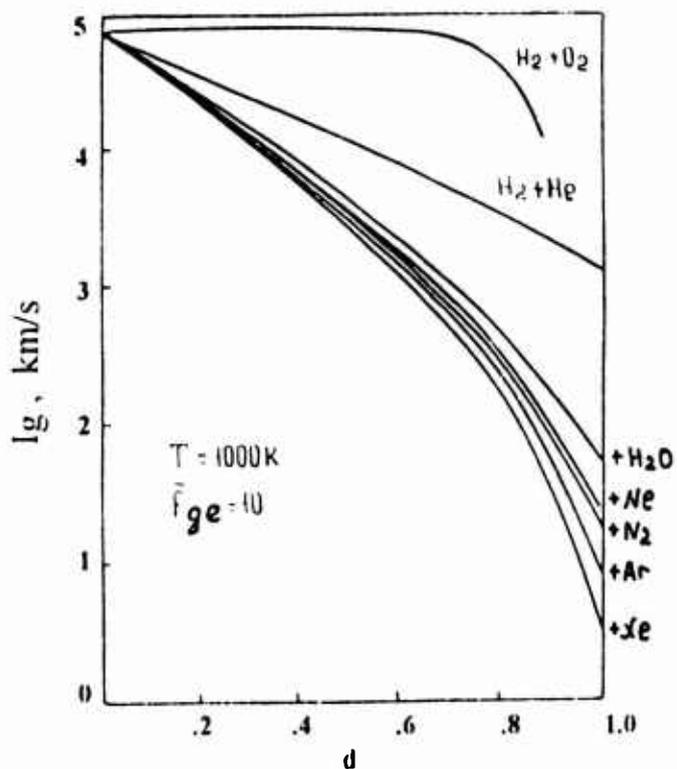
Fig. 1.4. Gas generator exhaust specific impulse as function of relative additional component consumption for different propellant additions.
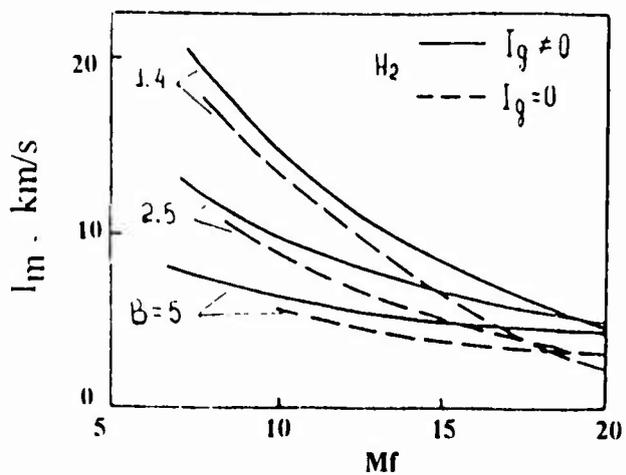
Fig. 1.6. Specific impulses of hydrogen scramjet for normal and tangential fuel injection with different fuel flow ratios.
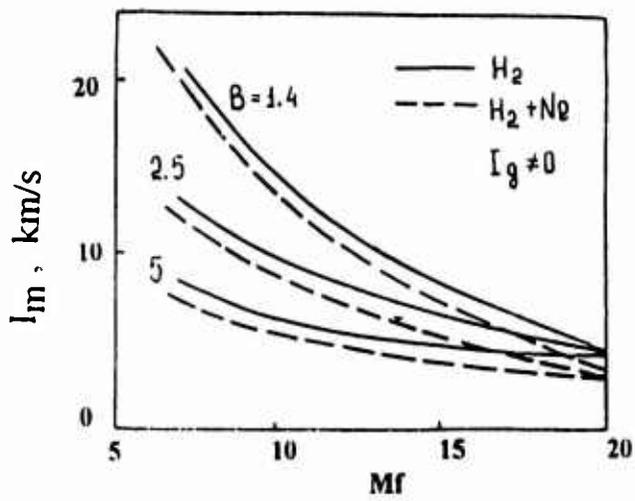
Fig 1 7. Specific impulses of hydrogen scramjet and
hydrogen-neon scramjet with different fuel
flow ratios.
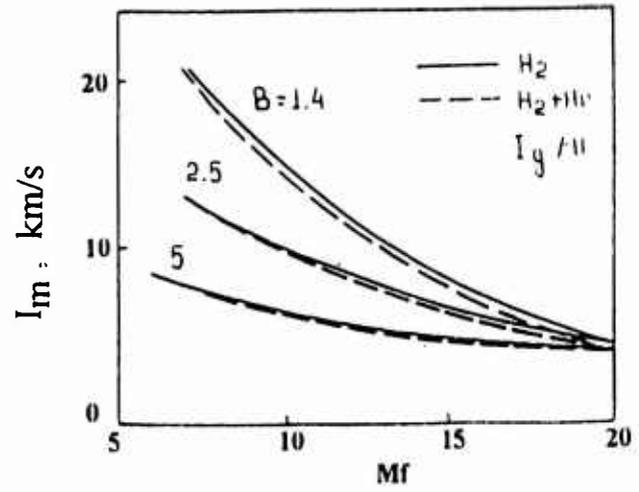
Fig 1 9 Specific impulses of hydrogen scramjet and
hydrogen-helium scramjet with different fuel
flow ratios.
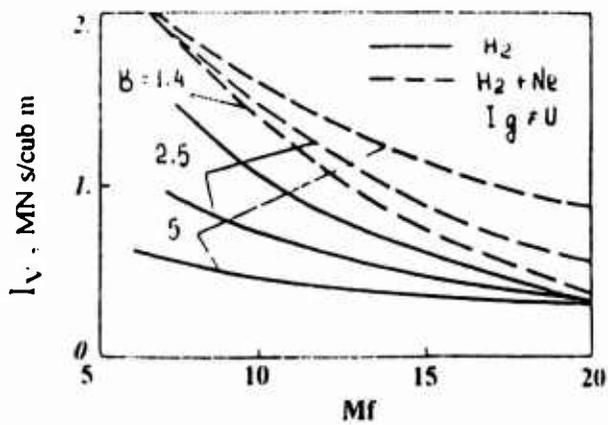
Fig. 1.8. Density impulses of hydrogen scramjet and
hydrogen-neon scramjet with different fuel
flow ratios
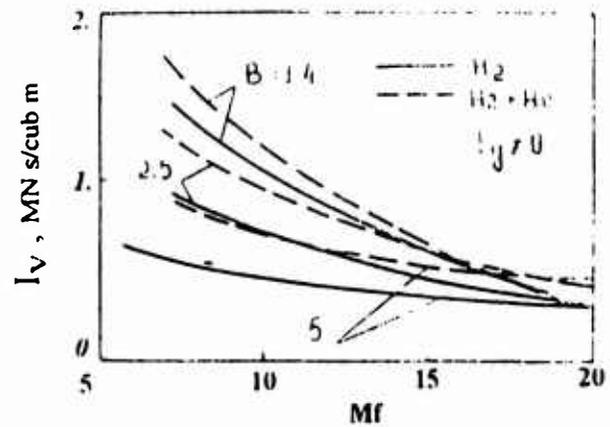
Fig. 1.10. Density impulses of hydrogen scramjet and
hydrogen-neon scramjet with different fuel
flow ratio.
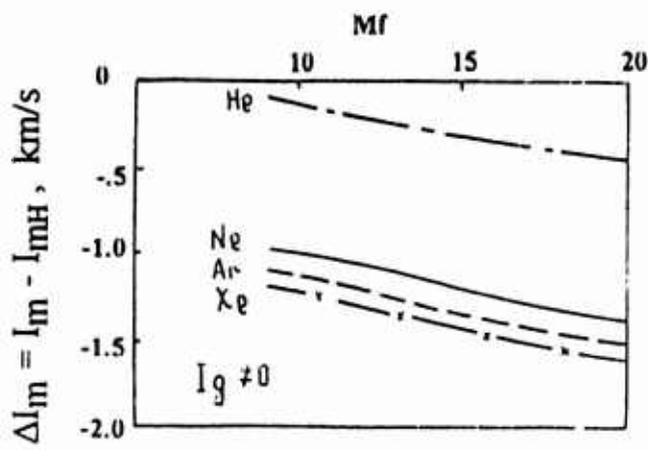
Fig. 1.11. Specific impulses differences of bipropellant scramjet and pure hydrogen scramjet for tangential fuel injection at B = 2.5.
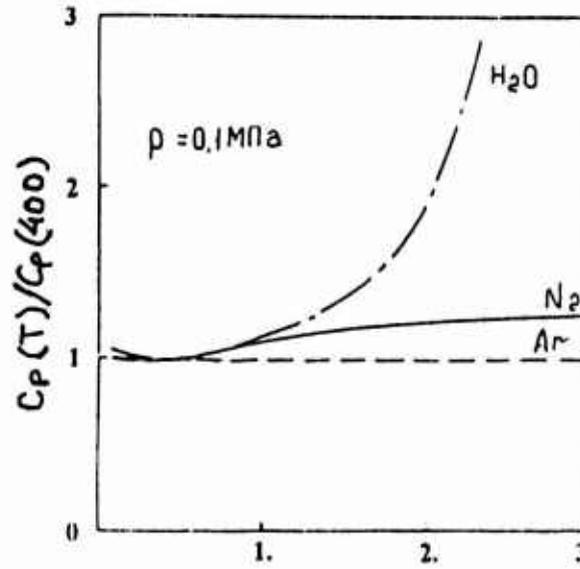
Fig. 1.13. Specific heat variations (divided by that at 400 K).
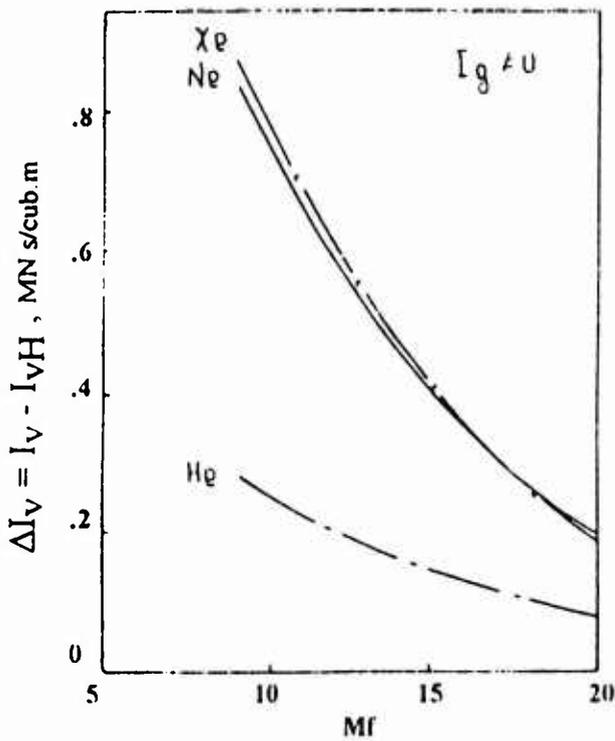
Fig. 1.12. Density impulses differences of bipropellant scramjet and pure-hydrogen scramjet for normal fuel injection at B = 2.5
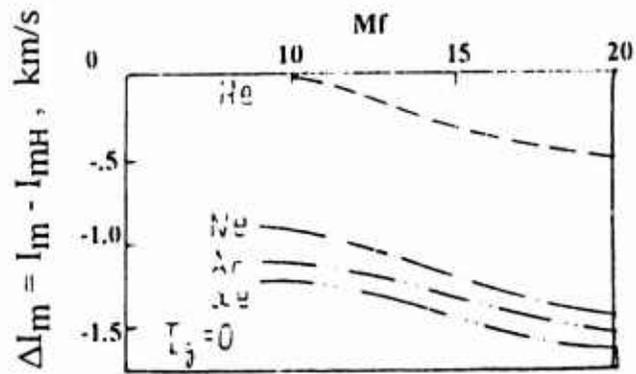
Fig 1.14. Specific impulses differences of bipropellant scramjet and pure-hydrogen scramjet for normal fuel injection at B = 2.5.
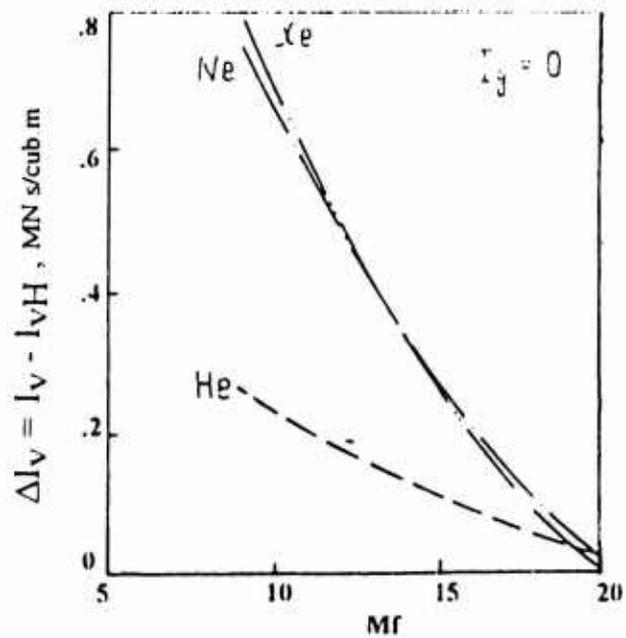
Fig. 1.15 Density impulses differences of bipropellant scramjet and pure-hydrogen scramjet for normal fuel injection at B = 2.5.
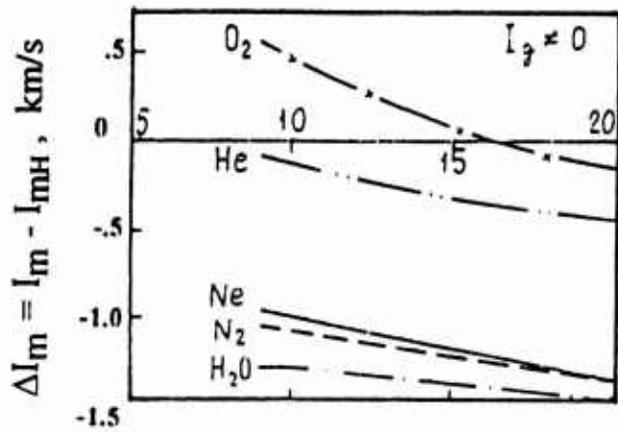
Fig. 1.16. Specific impulses differences of bipropellant scramjet and pure-hydrogen scramjet for tangential fuel injection at B = 2.5.
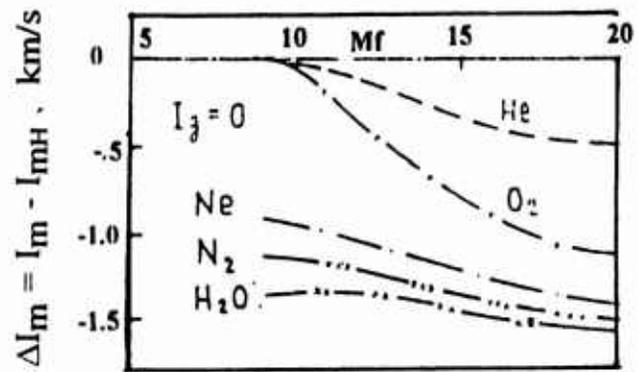
Fig. 1.18. Specific impulses differences of bipropellant scramjet and pure hydrogen scramjet for normal fuel injection at B = 2.5.
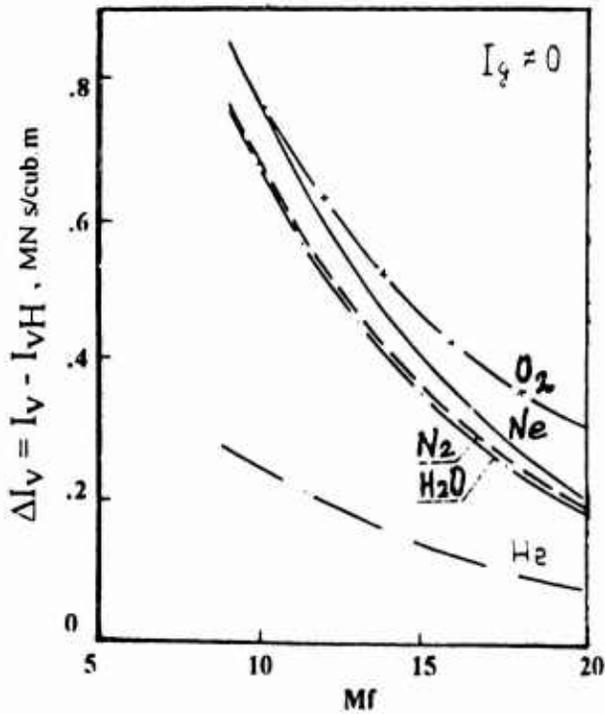
Fig. 1.17. Density impulses differences of bipropellant scramjet and pure hydrogen scramjet for tangential fuel injection at B = 2.5.
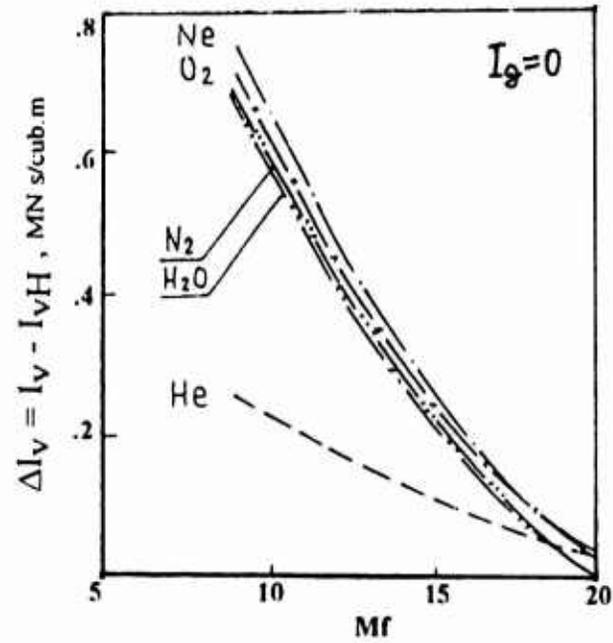
Fig. 1.19. Density impulses differences of bipropellant scramjet and pure-hydrogen scramjet for normal fuel injection at B = 2.5.
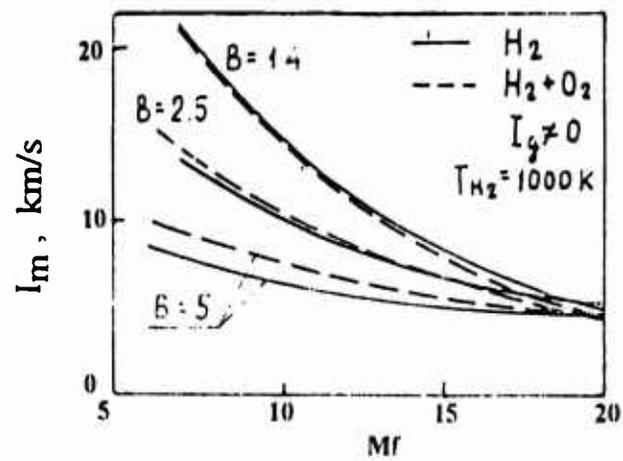
Fig. 1.20. Specific impulses of hydrogen scramjet and
hydrogen-oxygen rocket scramjet for
hydrogen temperature 1000 K.
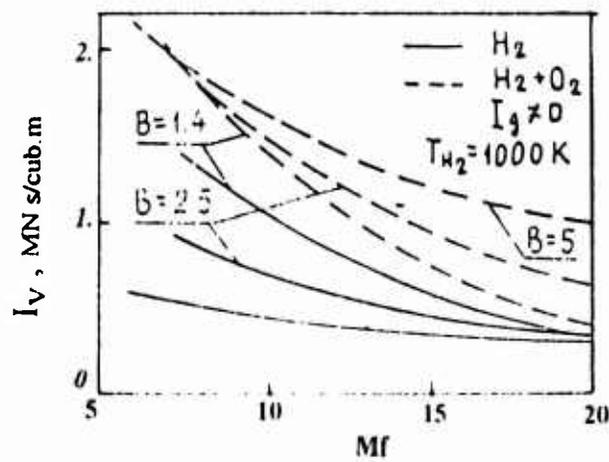
Fig. 1.21 Density impulses of hydrogen scramjet and
hydrogen-oxygen rocket scramjet for
hydrogen temperature 1000 K
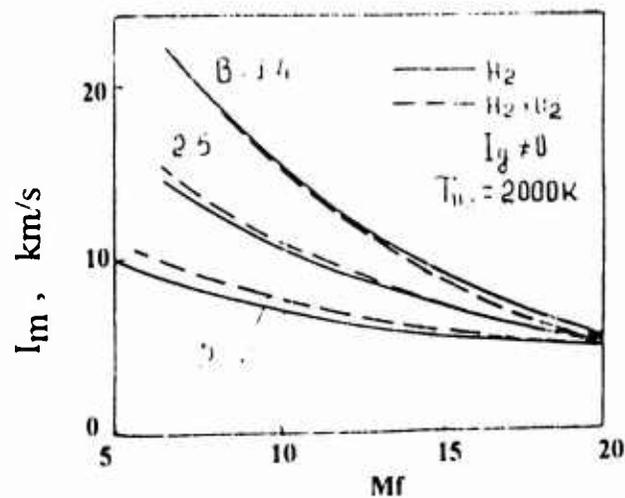
Fig. 1.22. Specific impulses of hydrogen scramjet and
hydrogen-oxygen rocket scramjet for
hydrogen temperature 2000 K.
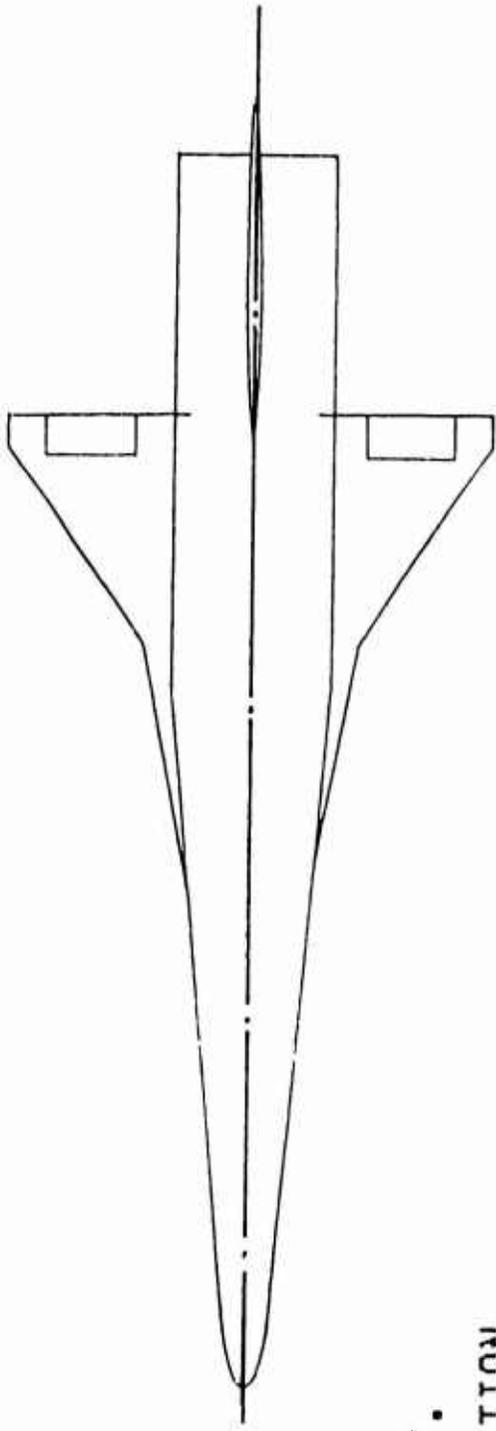
The A.S.P.
CONFIGURATION
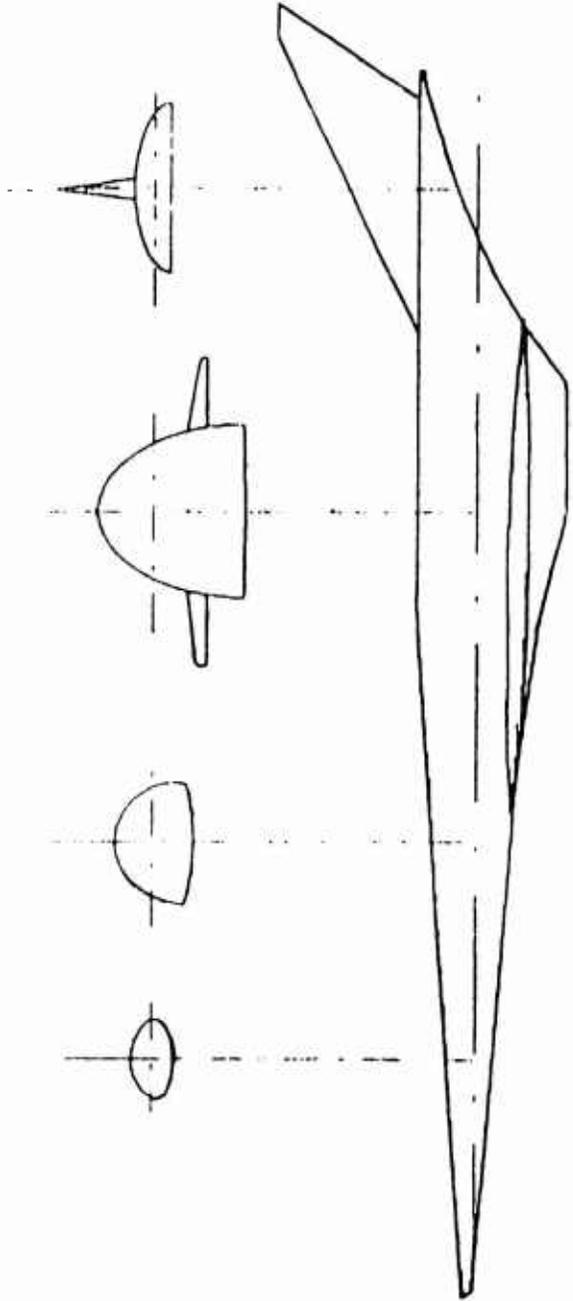
Fig. 1.23

The A.S.P.
DRAG FACTOR

FLIGHT MACH NUMBER
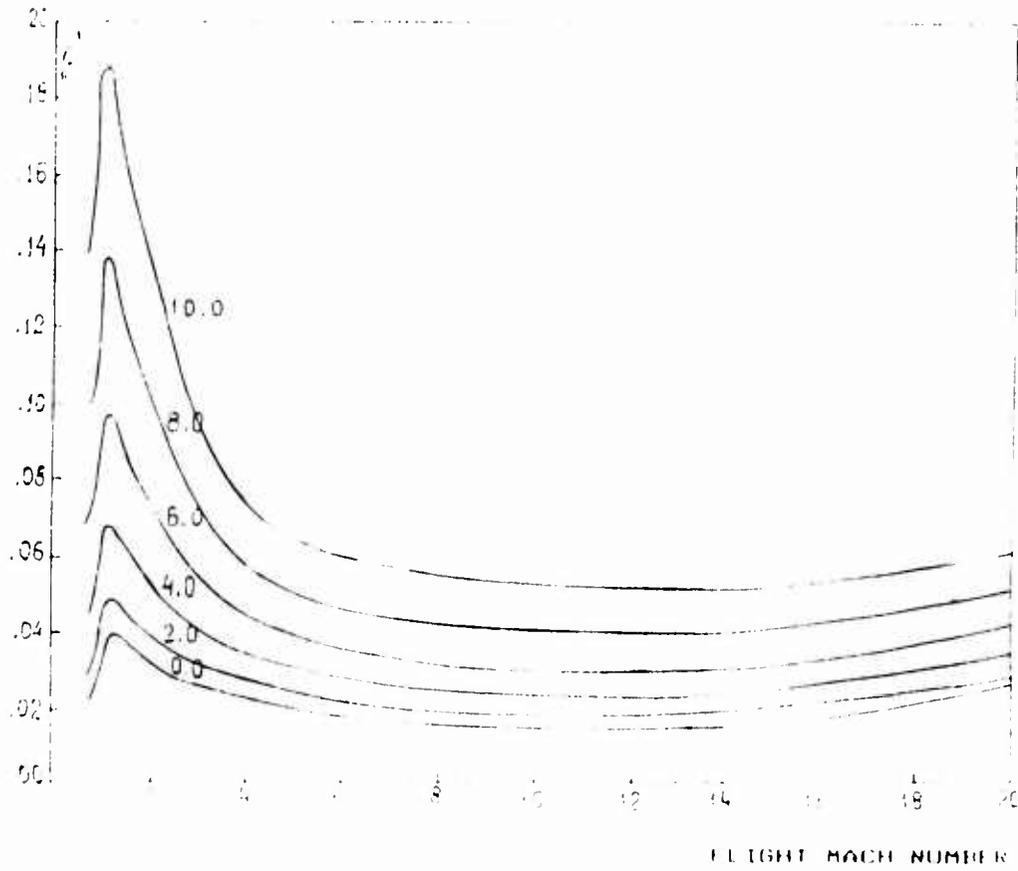
Fig. 1.24

The A.S.P.
LIFT FACTOR

FLIGHT MACH NUMBER
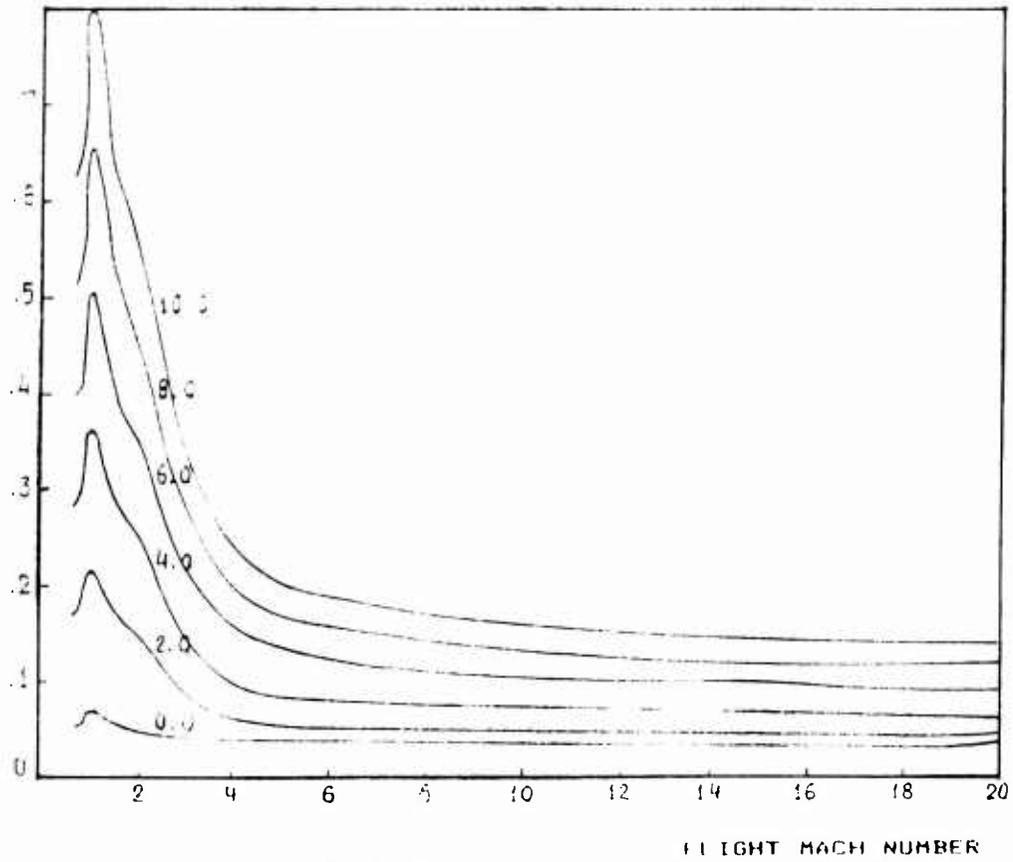
Fig. 1.25

The A.S.P.
AERODYNAMIC
FINENESS FACTOR
MAXIMUM   and
CORRESPONDING
ANGLE OF ATTACK
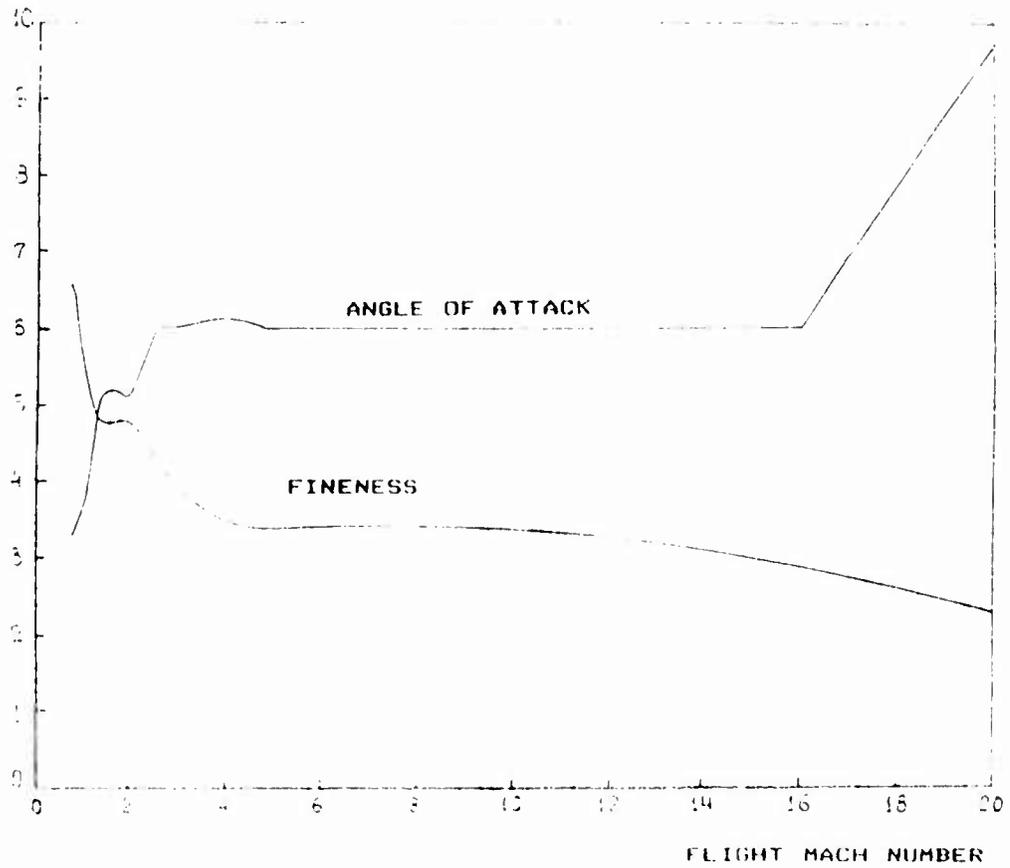
Fig. 1 26

SCRAMJET CFD METHODS AND ANALYSIS
PART 1. SCRAMJET CFD METHODS

NUMERICAL SIMULATION OF THE FLOW IN SCRAMJET DUCT

by

V. KOPCHENOV,
K. LOMKOV, L. MILLER, V. KRJUKOV, I. RULEV,
V. VINOGRADOV, V. STEPANOV, N. ZACHAROV,
R. TAGUIROV, M. AUKIN

CIAM (Central Institute of Aviation Motors)
Aviamotornaya street 2
111250 MOSCOW
RUSSIA

1.1 Introduction
1.2 Forebody and inlet flow model
1.3 Combustor CFD model structure
1.4 Nozzle and afterbody CFD model

1.1 Introduction

The computer analysis of scramjet flow became of great importance because of the limited possibilities of ground tests and difficulties of measurements in high speed/enthalpy flows. This fact is a powerful stimulus in CFD development on the other hand. The short description and examples of applications of the mathematical model for scramjet duct flow developed in CIAM are presented in this paper.

Before formulating the main requirements to the mathematical model it is necessary to take into account the following circumstances. The airbreathing hypersonic vehicle is characterized by high level of integration of airframe and propulsion system. Therefore, the correct prediction of propulsion system performances demands to consider the forebody pre-compression of air entering the scramjet engine. The afterbody of the vehicle is a nozzle extension. Thus, the mathematical model of the scramjet duct flow must include the description of the forebody and afterbody flows.

At the numerical simulation of scramjet duct flow, it is necessary to take into account the three-dimensional effects, the real gas effects, viscosity influence, turbulent mixing processes, chemical reactions. The complex gasdynamical structure of the flow and viscosity influence require to use the most general hydrodynamic model - the Navier-Stokes equations with Reynolds averaging. The turbulence model adequate to high supersonic Mach numbers flows is required. It is necessary to take into account the complex physical-chemical processes in air flow over the forebody and in inlet. It becomes necessary to incorporate the model of hydrogen-air combustion. Air-hydrogen chemical processes simulation is important in considering the flow in combustor and nozzle. Thus, it is desirable in general case to solve the three-dimensional Reynolds-averaged Navier-Stokes equations for multicomponent flow with adequate system of chemical reactions and turbulence model.

This level of numerical simulation requires the usage of the most powerful modern supercomputers. We have used the computers with like personal one power in our work. Therefore, the system of sufficiently simple models has been developed to evaluate the influence of the main processes, regime and design parameters on performances of propulsion system elements. This way leaves some questions open, but seems to be justified as really possible for preliminary design evaluations.

Recently some surveys about CFD in SCRAMJET applications were published [1-6]. We describe our own experience in this line in this report. The system of mathematical models and codes developed in CIAM has the modular structure and includes such elements: forebody, inlet, combustor, nozzle and afterbody. Comparatively simple, engineering models are used on the first step of the propulsion system performance evaluations. This is the level "0" in accordance with [5]. Another models allow to evaluate the influence of three-dimensional effects, real gas effects, to estimate the role of physical-chemical processes. The most part of these codes is based on the Euler and boundary layer equations and some procedures of viscous-inviscid interaction. This is level "1" in accordance with [5]. Several codes are based on the Reynolds-averaged parabolized Navier-Stokes equations and may be attributed to level "2" in

classification mentioned above. Finally some codes are developed for the numerical solution of the full Navier-Stokes equations in 2-D case. These codes may be used in local regions where strong viscous-inviscid interaction is significant. Besides, they allow to evaluate the influence of effects neglected in the models of lower level. It can be done on the examples of special test problems.

It is necessary to note, that dividing on the levels is conventional in our case. Indeed, the more simple physico-chemical model may be used with more complex hydrodynamic model (Navier-Stokes equations versus Euler equations for example) and vice-versa. Moreover, the combustion model of higher level may be used in 2-D case in comparison with 3-D case in codes for the numerical solution of Reynolds averaged parabolized Navier-Stokes equations.

The development of alternative versions of mathematical models and the comparison of the results obtained with the aid of various models are useful, because the most part of models is approximate. The experimental testing of existing mathematical models is very important problem. This is necessary to establish the credibility of CFD results used in design [7].

1.2 Forebody and inlet flow model

The main requirements to the airspace plane forebody design may be formulated. The forebody must have the minimal drag at fixed volume. The lower surface of forebody must precompress the flow with minimal losses, to provide the required massflow and uniform, as far as possible, air flow at the inlet entrance. The forebody must have blunt nose part. Bluntness of the nose must be chosen on the base of compromise between demands to be stable to the action of high heat fluxes and to decrease the wave drag and to provide the uniform air flow at the entry of inlet. From practical point of view, it seems to be justified to choose the minimal acceptable bluntness from the heat fluxes analysis and then to shape a forebody in order to satisfy other requirements.

Thus, the numerical model for the forebody must provide the opportunity to analyze the influence of blunt nose, the three-dimensional effects, the influence of physico-chemical processes in high temperature air, and effects of viscous-inviscid interactions.

The existing system of codes is based on numerical solution of the 3-D Euler equations. These codes are modified to include real gas effects in local equilibrium approach. It is supposed that gas composition, molecular mass, heat capacity and specific enthalpy are functions of local pressure and temperature. To complete the problem it is necessary to use the system of equations for the thermodynamic

equilibrium in addition to usual Euler equations [8,9]. More simple method is based on the use of analytical approximations for the air properties [10]. This method is implemented in combination with Euler equations in some CIAM codes for forebody and inlet flows.

Alternative method was proposed in [11] for approximations of gas properties in equilibrium approach. In this case effective specific heat ratio ($\kappa = a^2\rho/p$ where a is a frozen speed of sound, p is pressure and ρ is density), specific enthalpy h and molecular mass μ are represented as functions of two successfully chosen independent variables. One of them is the decimal logarithm of pressure, and another - the special function of pressure and density. It is possible to obtain the values of κ, h, μ as functions of chosen independent variables with the aid of approximation procedure, based on some "node" points. These "node" points are stored as tables, in which the main parameters κ, h, μ are represented in sufficient number of points in the space of independent variables to provide the acceptable approximation accuracy. The proposed method provides the accuracy 1-2% in wide range of pressures (from 100 Pa up to 10^8 Pa) and temperatures (from 200° K up to 20000° K).

Two codes are used for the numerical simulation of the flow over forebody (developed by V.Kopchenov, V.Krjukov, K.Lomkov and L.Miller). The first code for the computation of sub-, tran- and supersonic flows is based on time relaxation method. The region near the blunt nose is calculated with the aid of this code. The numerical method is the modified version of the well-known Godunov's scheme [12]. The piecewise linear distributions of the main parameters in all spatial directions instead of piecewise constant distributions in each computational cell are supposed [13]. The modified minimal increments principle [14] is used to provide the monotonicity condition [15]. The explicit higher order accuracy scheme proposed in [16] for hyperbolic systems of equations is realized as predictor-corrector scheme in accordance with [17].

The modified version of shock fitting procedure, which is based on some principles proposed for 2-D case in [18] is developed for 3-D case. The proposed method provides the second order accuracy on a regular uniform grids and conserves approximation on arbitrary nonuniform irregular grids. The local time step is chosen for each cell to decrease the run time necessary to obtain the steady state solution with the aid of the time relaxation procedure. The experience shows that local time step marching provides almost the twice gain in run time, when the transition from one flight Mach number regime to another is accomplished. Moreover, this method with local time step is comparable by the number of time iterations with the implicit method [19], based on the scheme with space directions and physical processes splitting and with global time integration step.

The marching method is used in the regions with supersonic longitudinal velocity component. This method is the higher order accuracy version of the steady analogy of Godunov's scheme [12]. The same model [11] of equilibrium air is incorporated. The modified version of the scheme for 3-D steady supersonic flows is based on the same principles as the scheme for the unsteady case [13, 14, 16-18]. The base version of this scheme for 3-D steady flows of perfect gas was proposed by A.Kraiko and S.Schipin.

It is necessary to evaluate the influence of the viscous effects on the flow fields. The simplified method was implemented until recently. The boundary layer displacement thickness is evaluated in approximate manner along generatrices of the body in each cell nearest the wall. Then the body surface is corrected on the boundary layer thickness and new "external" inviscid flow is calculated and so on. Such iterative procedure must be repeated up to convergence in some sense. This iterative procedure was developed and realized in [20]. The integral turbulent boundary layer method [21] allows to estimate the boundary layer displacement thickness, the momentum thickness, the skin friction coefficient and the specific heat flux to the wall.

The flowfield is calculated up to the inlet entrance. It is possible to evaluate in this cross-section the entropy layer thickness, the extent of parameters nonuniformity, the possible inlet area, the boundary layer thickness, and forces acting on the forebody and additional forces acting on the streamtube captured by inlet. The last is necessary for the analysis of control volume forces.

Typical forebody solutions are illustrated in following figures. The flow over the sphere is calculated for two hypersonic regimes with flight Mach numbers M_f=10 for the altitude H=10 km (Fig.1.2.1) and with M_f=20 for H=20 km (Fig.1.2.2). Results are compared with the primary standard results obtained in [9]. The pressure and density distributions on the surface of sphere are compared. The pressure and density are related accordingly to dynamic pressure and density in the free flow. The results are obtained on the grid containing the 10x10x10 nodes by means of the base Godunov's scheme and its modified version. The distance from the sphere surface to the bow shock along the sphere radius direction is also shown as a function of the polar angle in Fig. 1.2.1-c and 1.2.2-c. It is necessary to note the higher level of accuracy of modified scheme in comparison with original base version scheme.

The second example corresponds to the inviscid forebody flow. The geometrical shape of the blunted forebody is presented in Fig. 1.2.3. The calculations were performed for M_f=10 at an angle of attack 3.9° for the altitude 30 km. The pressure fields are presented in

Fig. 1.2.4 in four cross-sections to illustrate the influence of the shape change on the flow parameters distributions. One can see the generation of the internal shock and region of high compression within the shock layer connected with the deformation of the upwind side of the forebody. Therefore the visible nonuniformity in parameters distribution may be obtained at the entry of inlet.

The entropy layer which is formed on blunt nose part is also unfavorable factor for the inlet operation. The conventional "total pressure" is introduced to distinguish the entropy layer. This value is calculated for locally frozen flow parameters. Such "total pressure" distributions in some cross-sections are shown in Fig. 1.2.5. It is necessary to note, that the entropy layer occupies the all shock layer in cross-sections near the nose. But at the end of the conical part of the forebody, the major part of the entropy layer flows on the leeward side of the vehicle.

The calculation with the boundary layer estimation shows the following. The boundary layer displacement thickness in the last cross-section (see Fig. 1.2.4-d) constitutes approximately 5% from the shock layer thickness on the upwind side of the forebody. These estimations were obtained by N.Zacharov.

It is necessary to note that all these calculations were performed on the IBM PC/AT-486. The blunt nose flow was simulated on the grid containing 5000 nodes and it was required for this calculation about 2 hours of run time. The run time with the marching method up to the inlet entry constitutes approximately 5 minutes on the same computer.

The numerical simulation of the inlet flow is difficult task. This may be explained by several reasons. One of them is a wide range of operational regimes at flight Mach numbers variance from 0 up to 20-25. It is necessary also to note the essential part of viscous-inviscid interaction in the flow with deceleration. This part is most important on regimes of starting and unstarting. Besides that, the large nonuniformity in parameters distributions may exist at the entrance because it is impossible to control actively the boundary and entropy layers.

But on the other hand, it is necessary to analyze large number of inlet alternative schemes at the stage of preliminary design. Therefore it is desirable to use some simplified mathematical model of inlet flows. Nevertheless it is necessary to take into account the main factors influencing the inlet performances at simplification of mathematical model. These main factors are: the flow spreading over a forebody and additional drag concerned with this effect; the three-dimensional effects in the inlet flow; the real gas effects in high temperature flow; the boundary and entropy layer nonuniformity at the inlet entrance; the boundary

layer influence.

In accordance with the forebody flow model, it is possible to take into account the major part of the factors mentioned above by using the following inlets flow mathematical model. This mathematical model includes: the code for the 3-D calculations of steady supersonic flow in inlet on the base of marching Godunov's type scheme [22]; the real gas effects in high temperature flow are analyzed with the aid of equilibrium air model [10]; the boundary layer estimations on wetted surfaces are performed assuming that the flow is attached with the aid of integral method [21] in accordance with procedure proposed in [20]. Some examples of proposed mathematical model applications for inlet flow fields and performances predictions are presented in [20,22].

It is necessary to note that mathematical model is approximate and following justification is required for the recommendations have been made on the base of this model. But it is possible to "optimize" inlet configuration on the stage of preliminary design with the aid of this simple and computationally fast model and to diminish the number of variants for the following investigations.

The applicability of this configuration must be justified by experimental investigation or with the aid of some more full (if possible) and more expensive mathematical models. Numerous examples of proposed method application to solve various gasdynamic problems show that local and integral flow characteristics are defined with an accuracy sufficient for practical applications. Particularly, the computational errors in the definition of integral characteristics (inlet capture ratio that is equal to ratio of areas of captured stream tube at the inlet face and inlet frontal area, mass averaged total pressure recovery factor, additive drag coefficient) do not exceed 0.5 - 3 %.

The calculation of the single inlet performances was made [22]. The inlet configuration is shown in Fig. 1.2.6. The computational region is divided into some subregions. The computational region at zero slip angle is presented in Fig. 1.2.6-a. The inlet sidewall that begins in section x=0 has a sharp leading edge with sweep angle χ. The cutback cowl (x=L_c) has also a sharp leading edge with sweep angle α=45° . The sidewall and cowl are wedges with angles θ=5.3° and β=1° in planes XOZ and XOY (Fig. 1.2.6-a). Cowl internal surface coordinates (upper duct wall) and base plate (lower wall) are specified and, in our case, correspond to planes y=h and y=0 respectively.

The struts dividing the inlet into central and side passages (for the half of the inlet) have the same sweep angle as side walls. To reduce the excessive flow compression near the cowl, the central strut height is

reduced. Relative inlet throat area A_t (ratio of the area of captured stream tube at the inlet throat to the inlet frontal area) was about 0.21 taking into account the mentioned expansion.

Numerical investigation of inlet flow was carried out for M_f=4-8 with the grid in the plane ZOY containing 24*80 nodes. Calculations of integral characteristics were made according to the conservation equations written for control volume, which was defined by base plate, cowl, side wedges, entry and exit sections and upper surface limiting the freestream tube. While calculating C_{Dad} (additive drag coefficient), it was assumed for convenience in defining the airframe - integrated inlet drag, that the additive drag force includes not only the force acting on the liquid surface but also the force acting on parts of sidewalls (marked region in Fig.1.2.6-b) wetted by the flow that does not enter the inlet. Averaging was made with conservation of the flow rate, total enthalpy and entropy in real and averaged flows.

The total inlet characteristics are shown in the Fig.1.2.7 for three-strut inlet with sweep angle 48°. One can see a varying behavior of η=f(M_f) connected with the increased recovery losses at $M_f \approx 5$ because of critical flow regime in the central passage near the cowl. But it is necessary to note, that the evaluation of the possible influence of the viscous-inviscid interaction on the main inlet performances is required. Then it is necessary to use the reliable experimental data or more full, complex and expensive mathematical models. This fact is confirmed by the comparison of experimental and computational pressure distributions along the base plate and side wedge of considered inlet (see Fig. 1.2.8). Unfortunately, there is no acceptable mathematical model now to evaluate the inlet performances for regimes near starting and unstarting. The experimental investigations are the single possible method in this case.

1.3 Combustor CFD model structure

The numerical simulation of the combustor flow requires to take into account: the turbulent mixing; the physico-chemical processes in hydrogen-air mixtures; the complex gasdynamic structure of the flow; the three-dimensional effects.

It is necessary to note, that two characteristic combustion regimes can be considered in the scramjet combustor. The combustion process in duct at small supersonic combustor entrance Mach numbers corresponding to flight Mach numbers 6-7 realizes basically at subsonic velocity. This is caused by the pseudoshock wave system existing due to the mass-heat supply. The effects of interaction of shock wave system with boundary layer are of the great importance in the flow regime realization. Combustion regime with the

creation of extensive subsonic regiones and recirculation zones takes place as a result. The estimations of the combustion efficiency are made in CIAM for these regimes on the base of experimental data generalization.

At high flight Mach numbers combustion occurs in supersonic stream, when the velocity remains supersonic everywhere including combustion zone with the exception of wall boundary layers. The estimations of the combustion efficiency for these regimes are carried out using mathematical model, which is based on Reynolds averaged parabolized Navier-Stokes equations.

It seems to be justified to develop the system of mathematical models and a number of codes to evaluate the performances of scramjet combustor and the influence of the regime and design parameters on combustor performances. This system must include both the simple engineering models, based on generalization of experimental data, and the most full models, which are based on modern numerical simulation of supersonic combustion.

Apparently, the most general model must be based on the 3-D Reynolds averaged Navier-Stokes equations with acceptable for high Mach numbers flows turbulence model, for multicomponent mixtures with sufficiently detailed scheme of chemical reactions. But this level is inappropriate to the available computers. At the same time, some simplifications may be used, if only regimes with combustion in supersonic regions are considered . Then parabolized Navier-Stokes (PNS) equations may be used for the numerical simulation. It is possible to use effective marching numerical methods and to realize these models on available computers.

It seems that the most realistic way is to develop the hierarchy of models including:
- engineering models based on one-dimensional calculations of combustor duct flows with known curve of combustion efficiency obtained by experimental data generalization (see, for example, [23]);
- codes for 2-D calculations with turbulent mixing and combustion simulation;
- codes for 3-D effects evaluations.

The second and the third levels may be based on the PNS equations. But the more detailed combustion models may be incorporated into 2-D codes. In codes for 3-D flows, it is justified to use the more simple combustion models on the first stage. For example, the diffusion flame sheet model seems rather attractive. But the opportunity to estimate the applicability of this simplified model and to evaluate the influence of the finite rates of chemical reactions on the combustion process must be provided.

The more detailed description of the mathematical model is presented in the second part of

this paper. Some results obtained with the aid of the developed system of codes are presented in Fig.1.3.1-1.3.3. The combustion efficiency versus longitudinal distance is presented in Fig.1.3.1 for axisymmetric flow in the cylindrical duct. The regime is characterized by following parameters in the initial cross-section:

hydrogen jet - M_a=2.9, T_a=373° K;

air stream - M_e=4.8, T_e=1500° K;

pressures ratio in the hydrogen jet to air stream is equal to 1.92. This regime corresponds to conditions at the entry of supersonic combustor chamber for conventional vehicle at flight Mach number 12. The calculations were performed for two levels of turbulent viscosity (ε_0=3*10^{-4} and 2.5*10^{-3}) in initial cross-section. The turbulent viscosity is referred to the hydrogen velocity and the hydrogen jet radius in initial cross-section. It is interesting to point out the higher level of combustion efficiency for higher level of turbulent viscosity. This example demonstrates the influence of the mixing process on the combustion efficiency. Therefore the mixing enhancement becomes of primary importance for combustion efficiency augmentation.

The influence of the heat release on the gasdynamical structure of the flow in the duct is illustrated in Fig.1.3.2 and 1.3.3. The calculation was performed in the first case (Fig.1.3.2-a and 1.3.3-a) only with turbulent mixing without combustion. In the second case, the turbulent combustion was simulated with the aid of the flame sheet model (Fig.1.3.2-b and 1.3.3-b). The pressure (Fig.1.3.2) and Mach number fields (Fig.1.3.3) are shown. It is interesting to note, that the system of shocks in duct is much more distinct in the case of heat release. Moreover, the longitudinal dimensions of "periodical" structures becomes smaller.

The developed mathematical model may be used for the comparative study of various methods of mixing and combustion enhancement. This model may be implemented to evaluate the influence of the flight regime parameters on the combustor efficiency. It is possible to perform the efficiency comparison for some versions of injection system in combustor. Some CIAM experience in supersonic combustion model applications is presented in the second part of this report.

1.4 Nozzle and afterbody CFD model

The exhaust system of airspace plane is characterized by the following features: the integral scheme of the nozzle and airframe; the principle of combined propulsion system; the 3-D schemes.

In the integral scheme of exhaust system and airframe, the surfaces of the nozzle are at the same time the airframe surfaces. Therefore the exhaust system performances must be determined taking into account the afterbody flow. The principle of combined propulsion system supposes that various engines or their

combinations may be used on some sections of flight trajectory. In this case the exhaust system is a nozzles combinations of various engines (liquid rocket, turbojet, scramjet), operating simultaneously or sequentially in time. The mathematical model must provide the determination of longitudinal and transverse forces, moments of forces, skin friction forces and heat fluxes on the walls of the exhaust system, thrust direction and its location point.

The proposed mathematical model may be used to evaluate the influence of two factors mentioned above. This simplified mathematical model for 2-D flows is based on the following principles. The computational region is divided into several subregions. The supersonic inviscid flow is described by the steady Euler equations, which are solved numerically with the aid of Godunov's type marching scheme. The version of the scheme is used, which was proposed in [24]. The integral method is used to describe the boundary layer and mixing layer flows. The skin friction and wall heat fluxes are evaluated with the aid of the integral method [21].

The method [25,26] was developed to determine the base pressure and base enthalpy behind the backward step, which is flowed by two different supersonic streams. The method allows to determine the base pressure and enthalpy taking into account the influence of Mach numbers, Reynolds numbers, initial boundary layers thicknesses in main streams. The total pressures and temperatures are different in two flows. The gas is considered as perfect with different specific heat ratios in two streams. The method permits to estimate the influences of mass blowing into the base region and heat flux through the wall of the base face on the base pressure and enthalpy. The model of viscous-inviscid interaction [25,26] was used to determine the parameters in the base region. The original condition in reattachment point was proposed [25].

In general case, the configuration of the exhaust system-afterbody involves the base face. Moreover, the exhaust system is considered as uncontrolled. Therefore, large base regions may arise in exhaust system flow on the acceleration part of flight trajectory, when scramjet engine does not operate, and some additional engines of combined propulsion system operate. It is known that large thrust losses may exist in this case.

The possibilities of the proposed mathematical model are illustrated in Fig.1.4.1-1.4.5. These results are obtained by R.Taguirov and M.Aukin. Some estimations were performed for conventional vehicle exhaust system in the case of turbojet engine operation. The flow field is illustrated in Fig.1.4.1 for supposed regime, corresponding to flight Mach number 1.3. The bypass of the gas was realized through the duct of the non operating scramjet engine. Two base regions in the exhaust system flow take place. The thrust losses constitutes in this case more than 30 % from the ideal thrust.

The flow picture is shown in Fig.1.4.2 for another conventional regime. It is supposed that the combined propulsion system operates at flight Mach number $M_f=2$ in such manner: the liquid rocket and turbojet engine are operating, and massflow bypass is realized through the scramjet duct. The external flows over afterbody and nozzle cowl are also considered in this case. Besides that, the base region exists near the base face of afterbody-exhaust system configuration. The thrust losses constitutes in this case approximately 20 %.

The Mach number contours are shown in Fig.1.4.3 for conventional regime, corresponding to $M_f=10$. Only scramjet engine operates in this case. The performances of the exhaust system were evaluated for the conventional regimes of M_f from 4 up to 16. The exhaust system configuration presented in Fig.1.4.3 is considered. The thrust losses are obtained in comparison with ideal thrust as function of flight Mach number and are shown in Fig.1.4.4. The dependence of the slope of the thrust vector on flight Mach number is presented in Fig.1.4.5.

It is necessary to note, that the developed mathematical model is approximate and has serious restrictions. This model is being modified now to include the three-dimensional and real gas effects. The experimental investigations are required especially for regimes with large separation zones to verify the numerical codes.

References

1. White M.E., Drummond J.P., Kumar A., "Evolution and Application of CFD Techniques for Scramjet Engine Analysis", J. of Propulsion and Power, V.3, N 5, 1987, pp.423-439

2. Schetz J.A., Billig F.S., Favin S., "Modular Analysis of Scramjet Flowfields", J. of Propulsion and Power, V.5, N 2, 1989, pp.172-180.

3. Barber T.J., Cox G.B.,Jr., "Hypersonic Vehicle Propulsion: A Computational Fluid Dynamics Application Case Study", J. of Propulsion and Power, V.5, N 4, 1989, pp.492-501.

4. Povinelli L.A. "Advanced Computational Technology for Hypersonic Propulsion", ISABE 89-7106, 1989, pp.993-1008.

5. McClinton C., "CFD Support of NASP Design", AIAA 90-5249, 1990.

6. Anderson G., Kumar A., Erdos J., "Progress in Hypersonic Combustion Technology with Computation and Experiment", AIAA 90-5254, 1990.

7. Mehta U., "The Aerospace Plane Design Challenge: Credible Computational Fluid Dynamic Results", AIAA 90-5248, 1990.

8. Бабенко К.И., Воскресенский Г.П., Любимов А.Н., Русанов В.В., "Пространственное обтекание гладких тел идеальным газом", Москва, Наука, 1964, 506 с.

9. Любимов А.Н., Русанов В.В., "Течения газа около тупых тел", Части 1 и 2, Москва, Наука, 1970.

10. Крайко А.Н., "Аналитическое представление термодинамических функций воздуха", АН СССР, Инженерный Журнал, Т.4, вып.3, 1964, с.548-550.

11. Дьяконов Ю.Н., Пчелкина Л.В., Сандомирская И.Д., "Сверхзвуковое обтекание затупленных тел", Издательство Московского Государственного Университета, 1971, 406 с.

12. Годунов С.К., Забродин А.В., Иванов М.Я., Крайко А.Н., Прокопов Г.П., "Численное решение многомерных задач газовой динамики", Москва, Наука, 1976, 400 с.

13. Колган В.П., "Конечно-разностная схема для расчета двумерных разрывных нестационарных газодинамических решений", Ученые Записки ЦАГИ, Т.6, N 1, 1975, с.9-14.

14. Тилляева Н.И., "Обобщение модифицированной схемы С.К.Годунова на пространственно неоднородные сетки", Ученые Записки ЦАГИ, Т.17, N 2, 1986, с.19-26.

15. Годунов С.К., "Конечно-разностный метод для численного расчета разрывных решений уравнений гидродинамики", Математический Сборник, Т.47, N 3, 1959, с.271-306.

16. Копченов В.И., Крайко А.Н., "Монотонная конечно-разностная схема второго порядка точности для гипер-болических систем с двумя независимыми переменными", Журнал Вычислительной Математики и Математической Физики, Т.23, N 4, 1983, с.848-859.

17. Родионов А.В., "Монотонная схема второго порядка аппроксимации для сквозного расчета неравновесных течений", Журнал Вычислительной Математики и Математической Физики, Т.27, N 4, 1987, с.585-593.

18. Крайко А.Н., Макаров В.Е., Тилляева Н.И., "К численному построению фронтов ударных волн", Журнал Вычислительной Математики и Математической Физики, Т.20, N 3, 1980, с.716-723.

19. Ковеня А.А., Яненко Н.Н., "Метод расщепления в задачах газовой динамики", Новосибирск, Наука, 1981, 304 с.

20. Виноградов В.А., Дуганов В.В., Степанов В.А., "Применение численных методов к расчету характеристик сверхзвуковых и гиперзвуковых воздухозаборников ВРД", Ученые Записки ЦАГИ, Т.13, N 2, 1982, с.62-68.

21. Авдуевский В.С., "Метод расчета пространственного турбулентного пограничного слоя в сжимаемом газе", АН СССР, Механика и Машиностроение, N 4, 1962, с.3-12.

22. Vinogradov V.A., Stepanov V.A., Alexandrovich E V., "Numerical and Experimental Investigation of Airframe-Integrated Inlet for High Velocities", J. of Propulsion and Power, V.8, N 1, 1992, pp.151-157.

23. Аннушкин Ю.М., "Основные закономерности выгорания турбулентных струй водорода в воздушных каналах", Физика Горения и Взрыва, Т.17, N 4, 1981, с.59-70.

24. Аукин М.К., Тагиров Р.К., "Конечно-разностная схема второго порядка точности для расчета трехмерных сверхзвуковых течений идеального газа", Журнал Вычислительной Математики и Математической Физики, Т.29, N 7, 1989, с.1057-1066.

25. Масалов В.К., Тагиров Р.К., "Расчет донного давления и энтальпии за уступом, обтекаемым двумя сверхзвуковыми потоками, с учетом влияния пограничных слоев и тепловых потоков", Известия АН СССР, Механика Жидкости и Газа, N 5, 1991, с.167-176.

26. Тагиров Р.К., "Расчет критического перепада давлений на скачке уплотнения, возникающего при отрыве турбулентного пограничного слоя", Известия АН СССР, Механика Жидкости и Газа, N 4, 1985, с.38-45.

PRESSURE DISTRIBUTION ON SPHERE SURFACE

$\dfrac{\rho}{\int_{\infty}V_{\infty}^2}$

0.5

--- --- 1-ST ORDER SCHEME
——— 2-ND ORDER SCHEME
●●● |9|

ω

0   20°   40°   60°   80°

$M_f = 10$, $H = 10$ km

Fig.1.2.1 - A.

DENSITY DISTRIBUTION ON SPHERE SURFACE

$\int/\int_{\infty}$

7.5

5

2.5

--- --- 1- ST ORDER SCHEME
——— 2 - ND ORDER SCHEME
●●● |9|

ω

0   20°   40°   60°   80°

$M_f = 10$, $H = 10$ km

Fig.1.2.1 - B.

BOW SHOCK DEPARTURE

$M_f = 10,$ $H = 10$ km

$- \cdot - \cdot$ 1 - ST ORDER SCHEME
—— 2 - ND ORDER SCHEME
o o o [9]

Fig.1.2.1 - C.

PRESSURE DISTRIBUTION ON SPHERE SURFACE

$M_f = 20,$ $H = 20$ km

Fig. 1.2.2 - A.

DENSITY DISTRIBUTION ON SPHERE SURFACE

$M_f = 20,$ $H = 20$ km

Fig. 1.2.2 - B.

BOW SHOCK DEPARTURE

$M_f = 20,$ $H = 20$ km

- - - 1 ST ORDER SCHEME

——— 2 ND ORDER SCHEME

o o o [9]

ω

Fig.1.2.2   C.

THE FOREBODY SCHEME

$X = X_1$ X_2 X_3 X_4 X_5 X_6
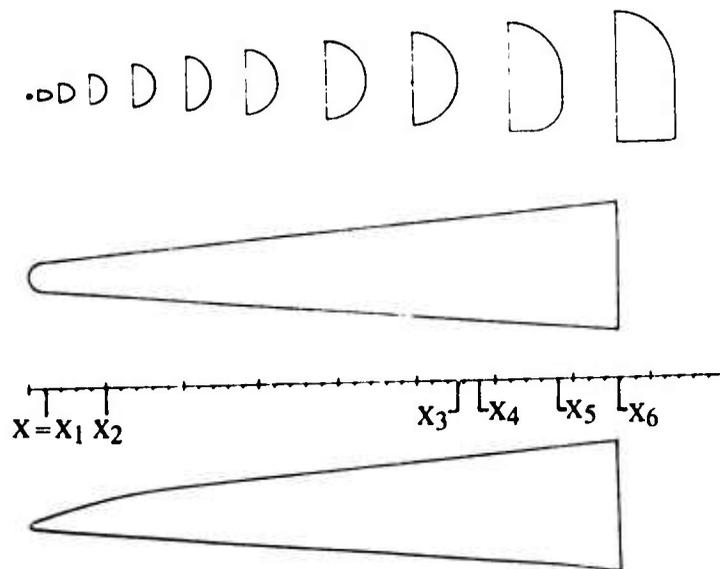
Fig.1.2.3.

THE PRESSURE FIELDS

MH= 10.00
ALFA= 3.90
BETA= .00

CNN 10=40
P/PH=CONST
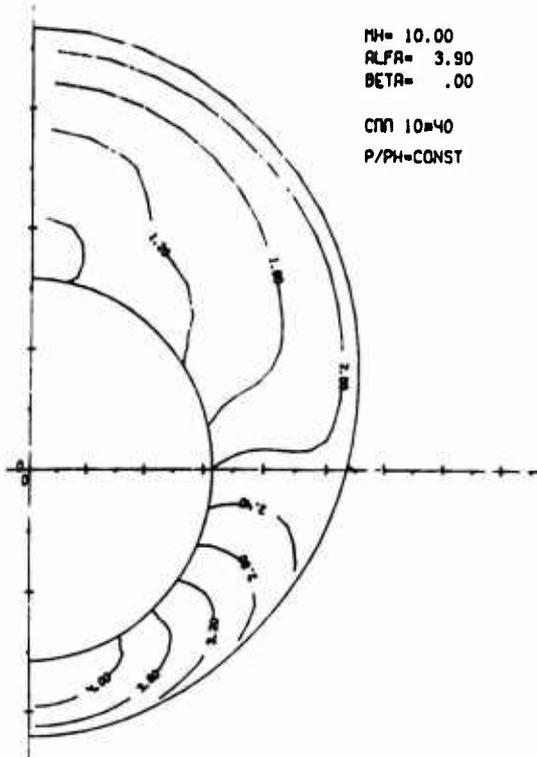
Fig.1.2.4 - A.   THE CROSS-SECTION $X = X_3$

MH= 10.00
ALFA= 3.90
BETA= .00

CNN 10=40
P/PH=CONST
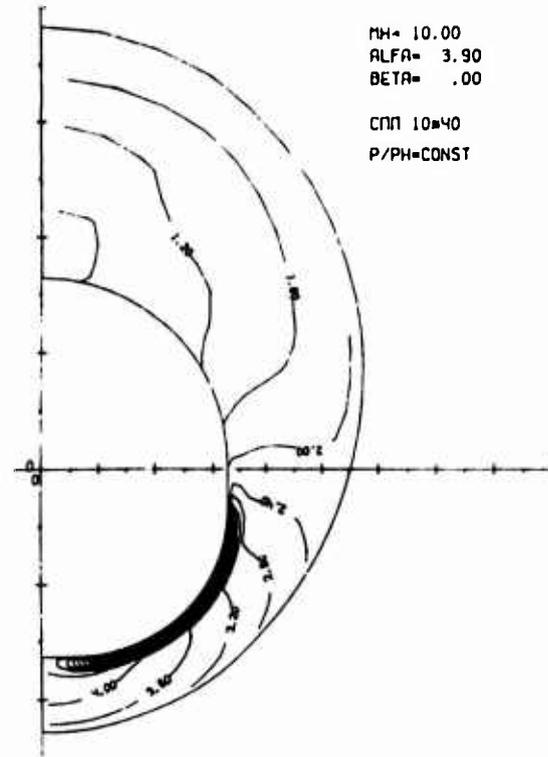
Fig.1.2.4 - B.   THE CROSS-SECTION $X = X_4$

THE PRESSURE FIELDS

MH= 10.00
ALFA= 3.90
BETA= .00

CNN 10=40
P/PH=CONST
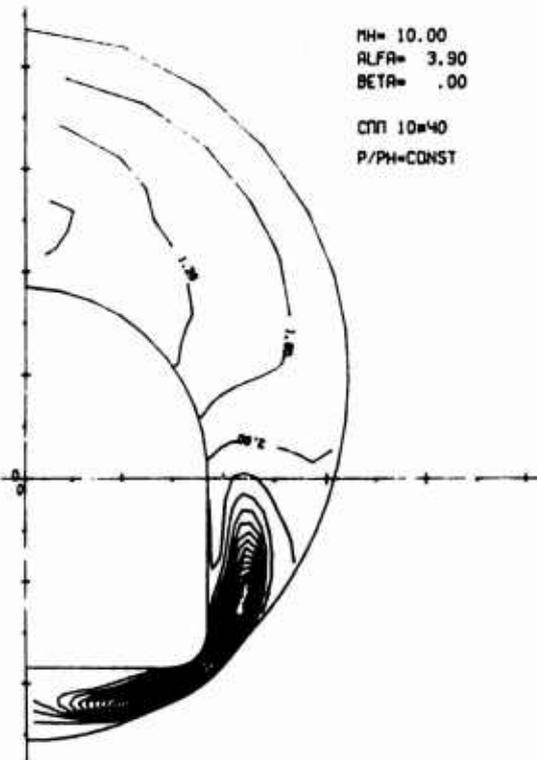
Fig.1.2.4 - C.   THE CROSS-SECTION $X = X_5$

MH= 10.00
ALFA= 3.90
BETA= .00

CNN 10=40
P/PH=CONST
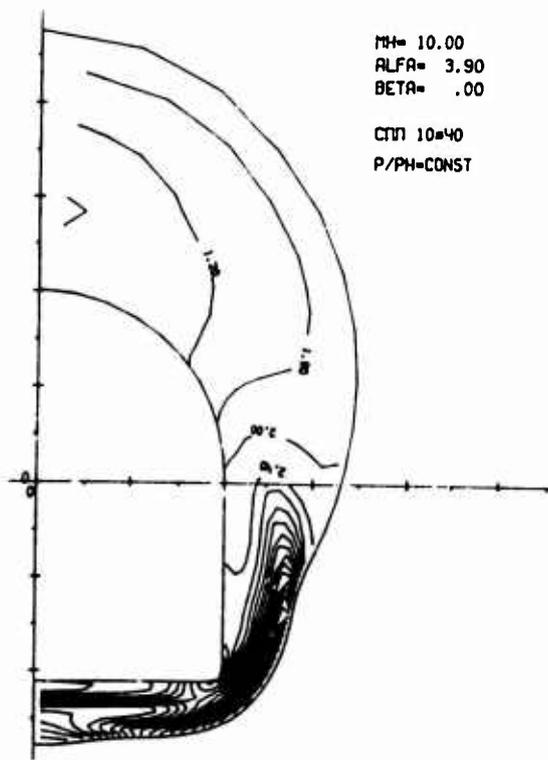
Fig.1.2.4 - D.   THE CROSS-SECTION $X = X_6$

THE "TOTAL" PRESSURE FIELDS

MH= 10.00
ALFA= 3.90
BETA= .00

Cr 10=40
P= =CONST
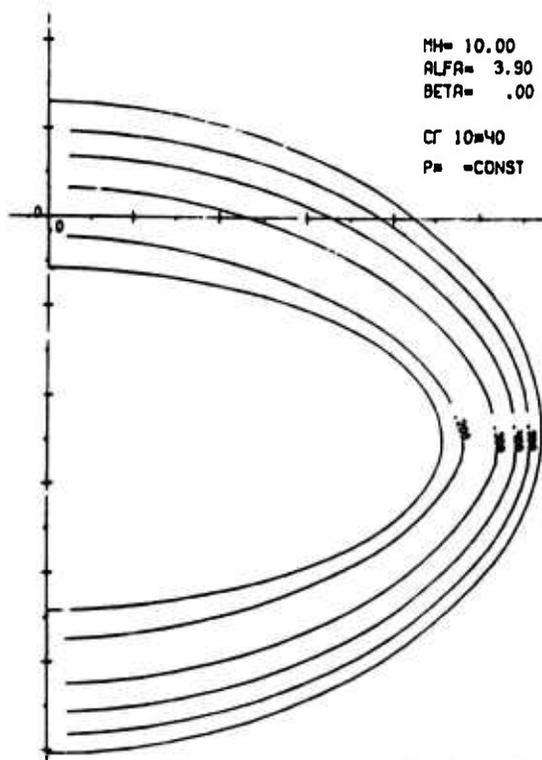
Fig.1.2.5 - A.   THE CROSS-SECTION $X = X_1$

MH= 10.00
ALFA= 3.90
BETA= .00

Cnn 10=40
P= =CONST
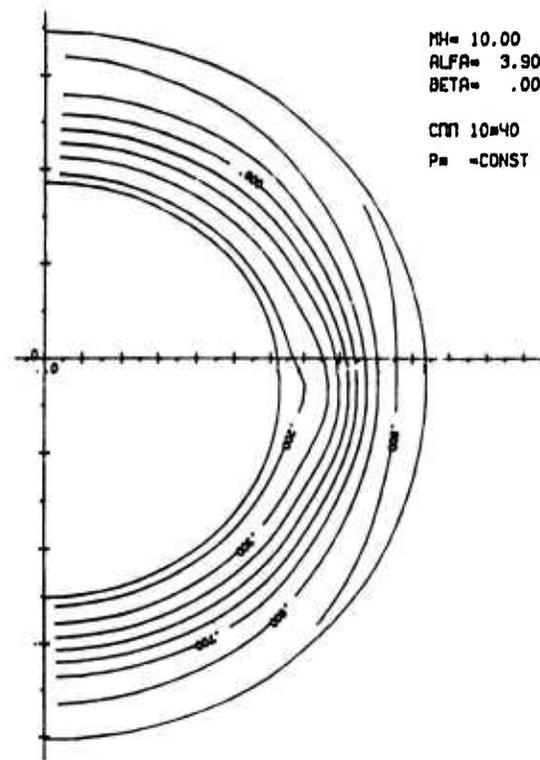
Fig.1.2.5 - B.   THE CROSS-SECTION $X = X_2$

THE "TOTAL" PRESSURE FIELDS

MH= 10.00
ALFA= 3.90
BETA= .00

Cnn 10=40
P= =CONST
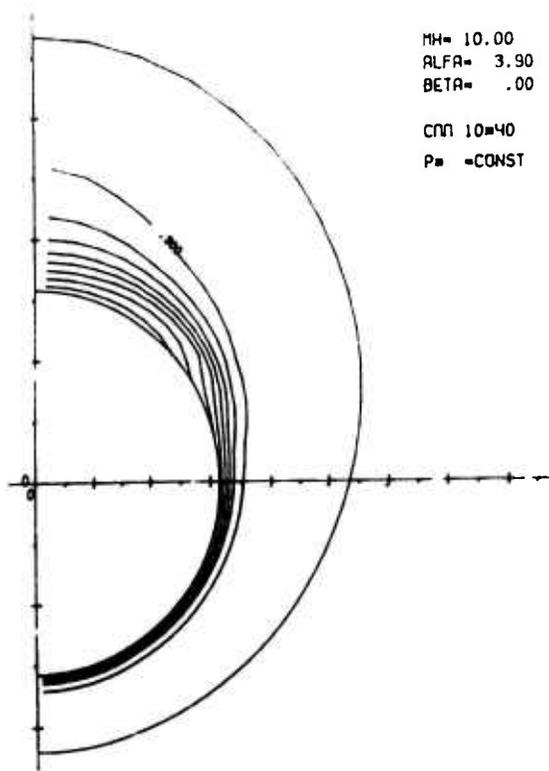
Fig.1.2.5 - C.   THE CROSS-SECTION $X = X_3$

MH= 10.00
ALFA= 3.90
BETA= .00

Cnn 10=40
P= =CONST
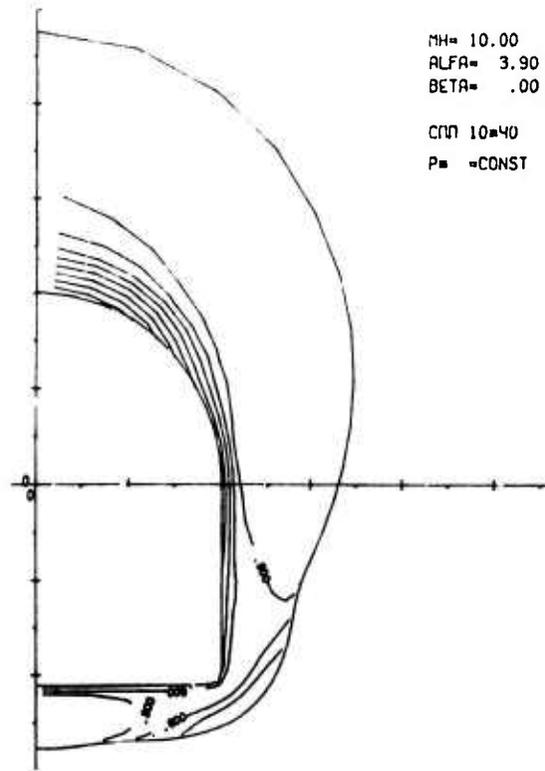
Fig.1.2.5 - D. THE CROSS-SECTION $X = X_6$

THE HYPERSONIC INLET SCHEME
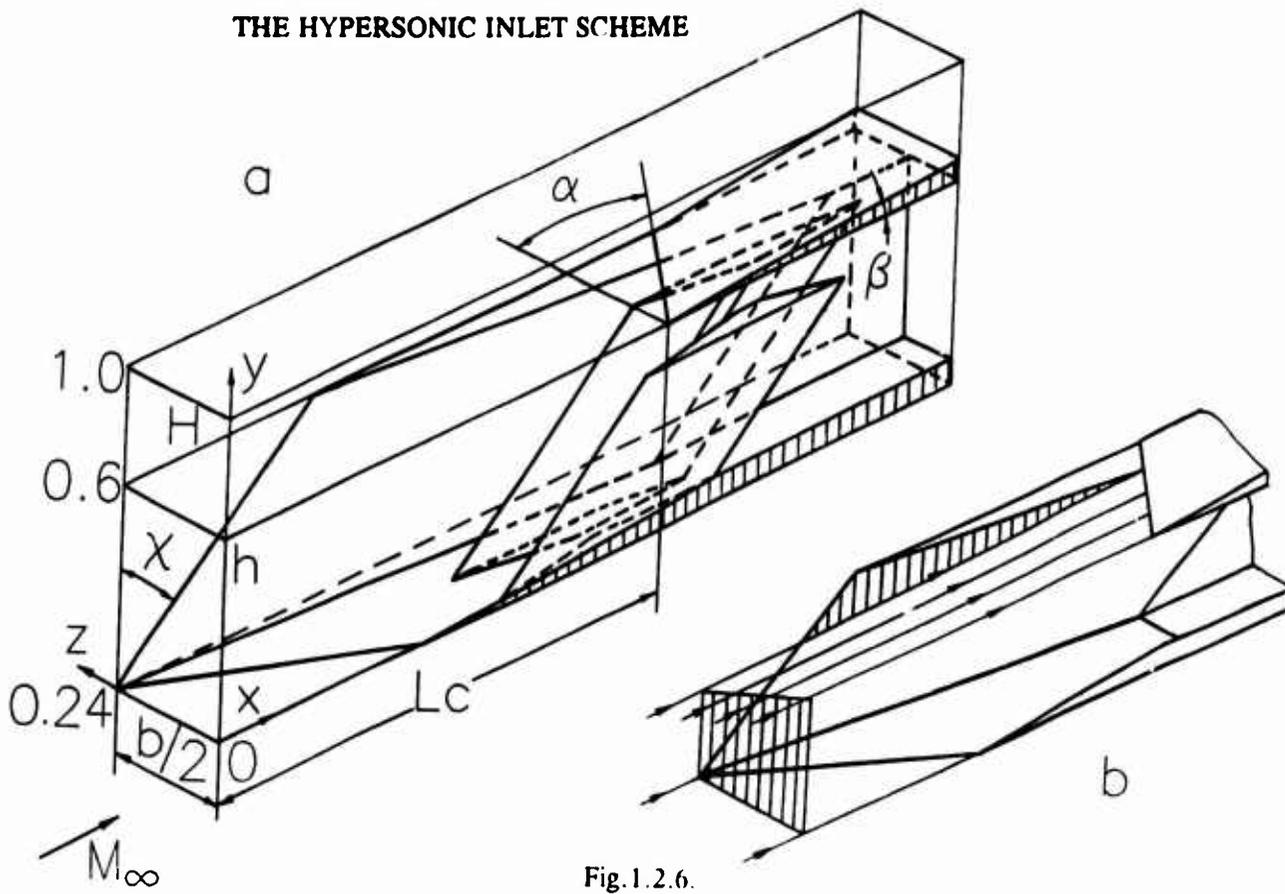
Fig.1.2.6.

THE PERFORMANCES OF THE THREE - STRUT INLET
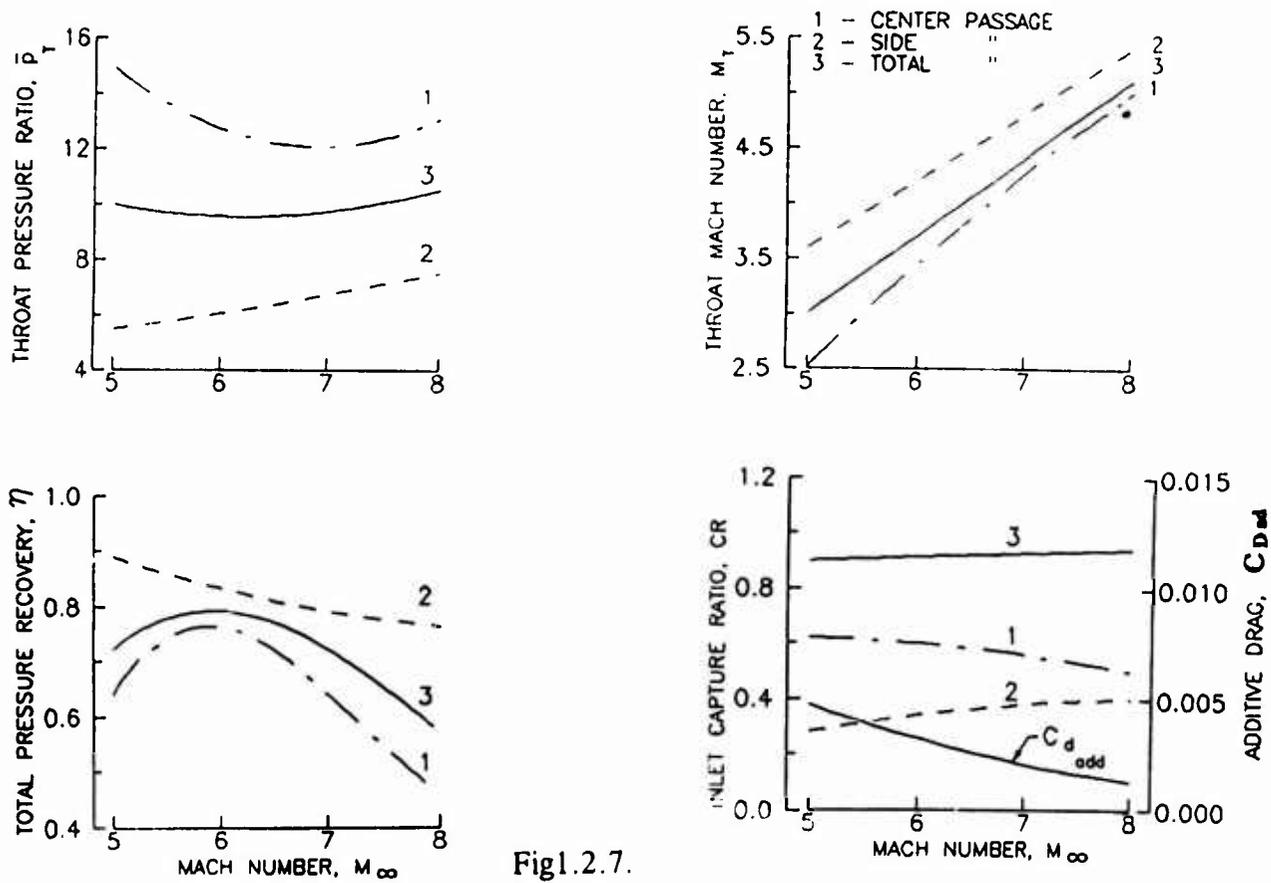
Fig1.2.7.

STATIC PRESSURE DISTRIBUTION ALONG THE BASE PLATE
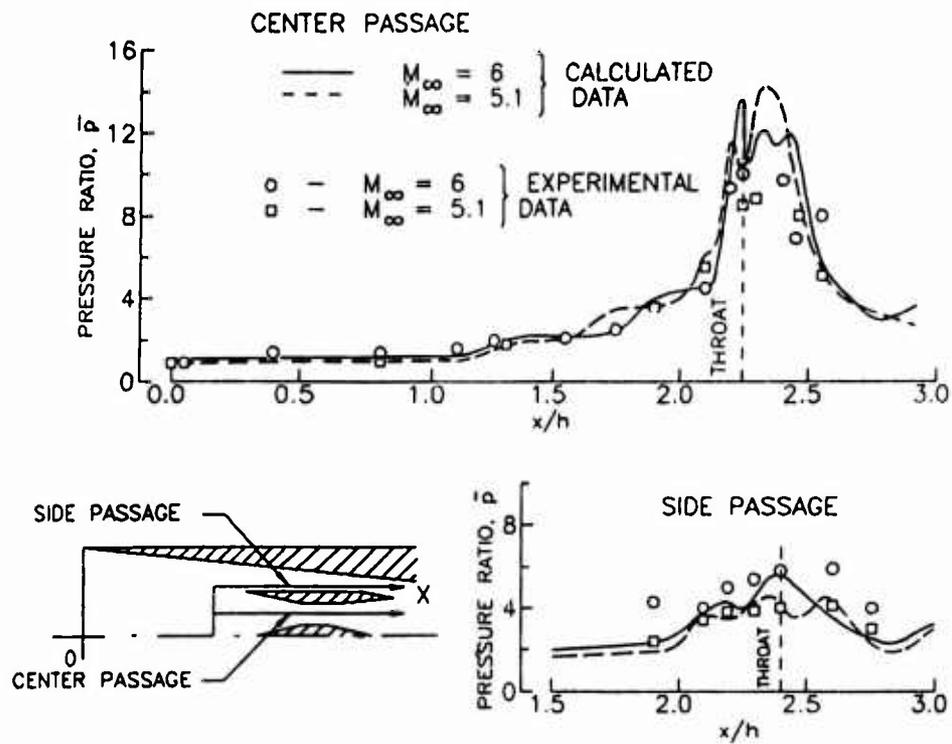
Fig.1.2.8 - A.

STATIC PRESSURE DISTRIBUTION ALONG THE SIDE WALL
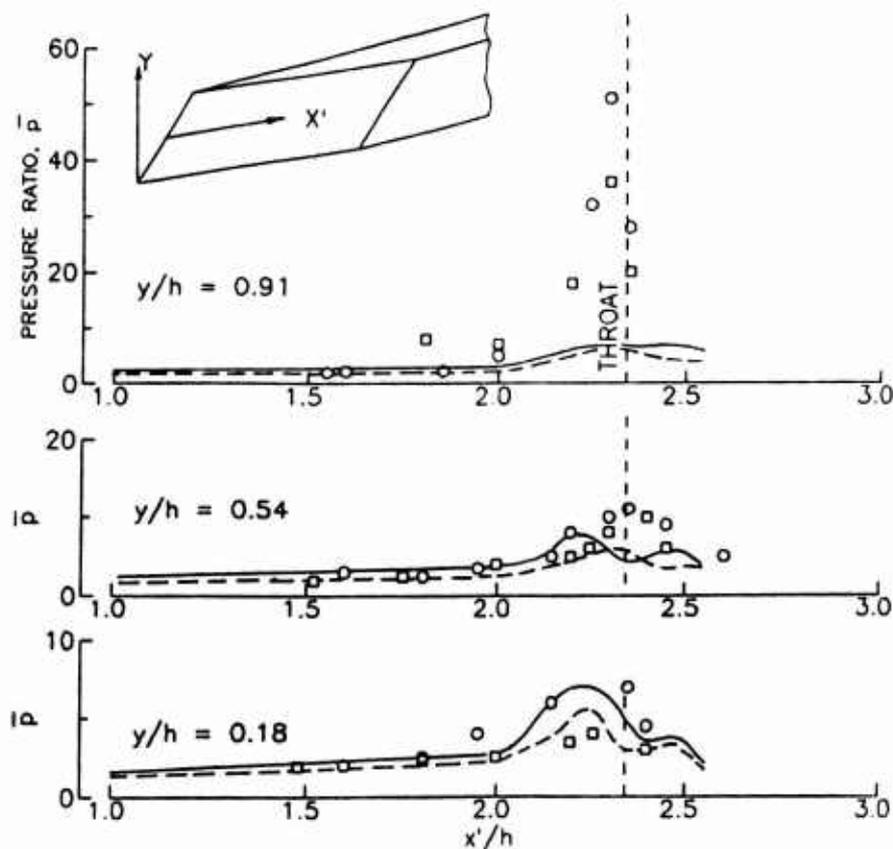
Fig.1.2.8 - B.

THE COMBUSTION EFFICIENCY FOR TWO INITIAL
LEVELS OF TURBULENT VISCOSITY
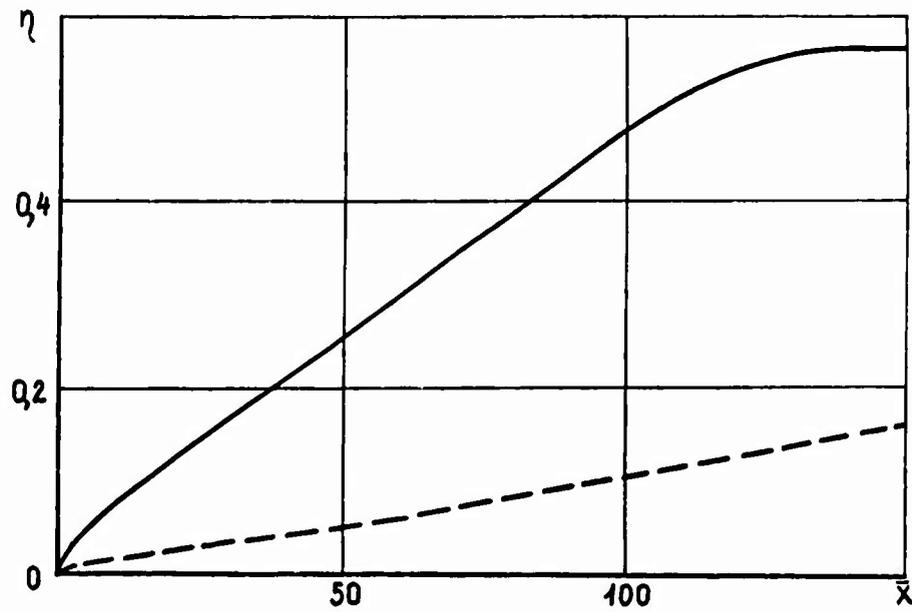
THE FUEL - AIR EQUIVALENCE RATIO $\phi = 1.66$

Fig.1.3.1.

A   MIXING ONLY
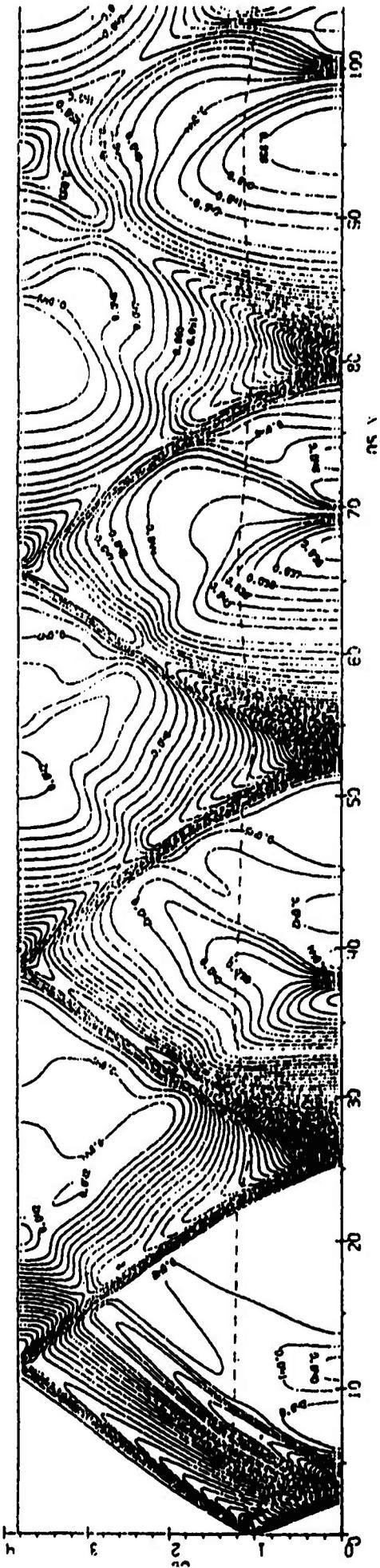
B   MIXING WITH HEAT RELEASE ON FLAME FRONT
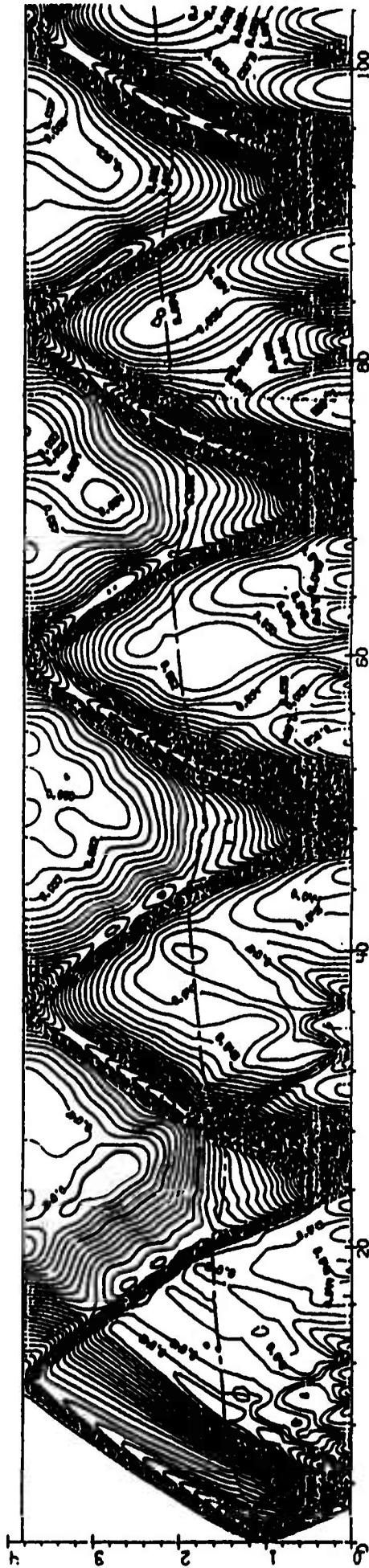
Fig. 1.3.2.   THE PRESSURE FIELD IN AXISYMMETRIC DUCT

4-17

A   MIXING ONLY
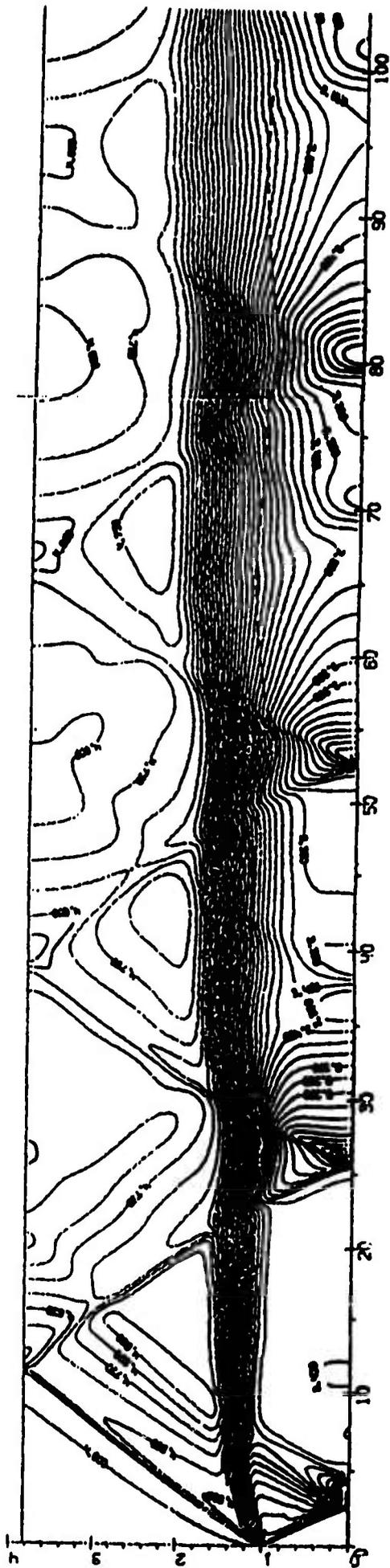
B   MIXING WITH HEAT RELEASE ON FLAME FRONT
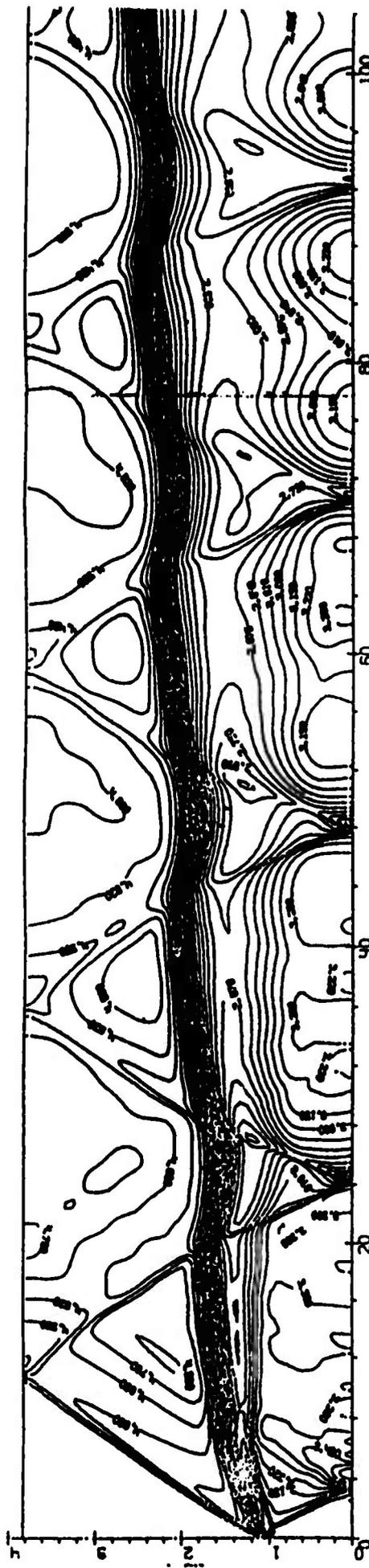
Fig. 1.3.3.   MACH NUMBERS CONTOURS

COMBINED NOZZLE
SMALL SUPERSONIC FLIGHT MACH NUMBER

$M_f = 1.3$
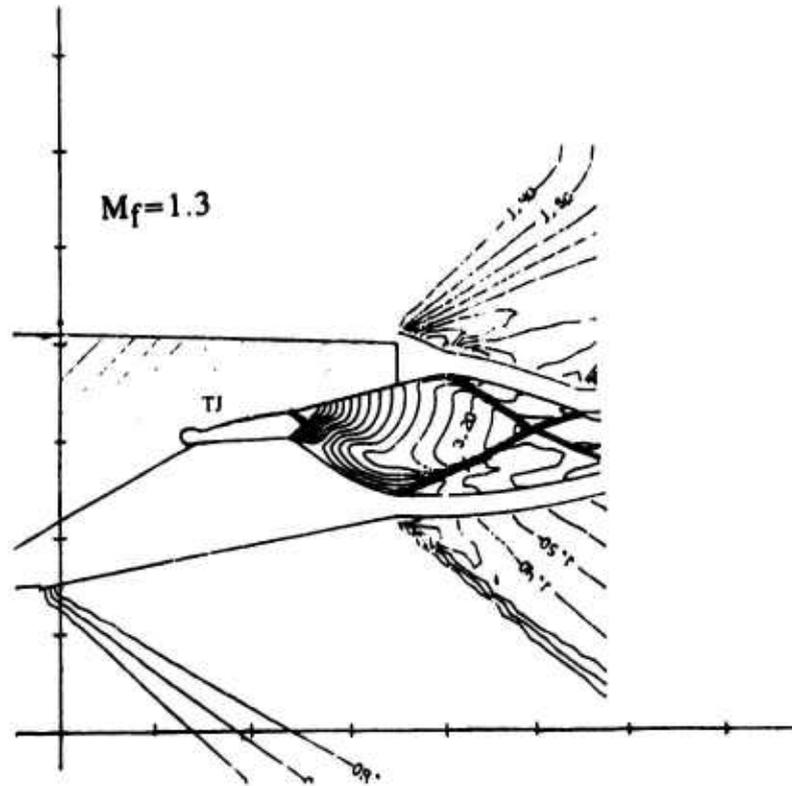
Fig.1.4.1. MACH NUMBERS CONTOURS

COMBINED NOZZLE
SMALL SUPERSONIC FLIGHT MACH NUMBER

$M_f = 2.0$

BASE PRESSURE

LR

TJ
SCRJ   BYPASS

BASE PRESSURE
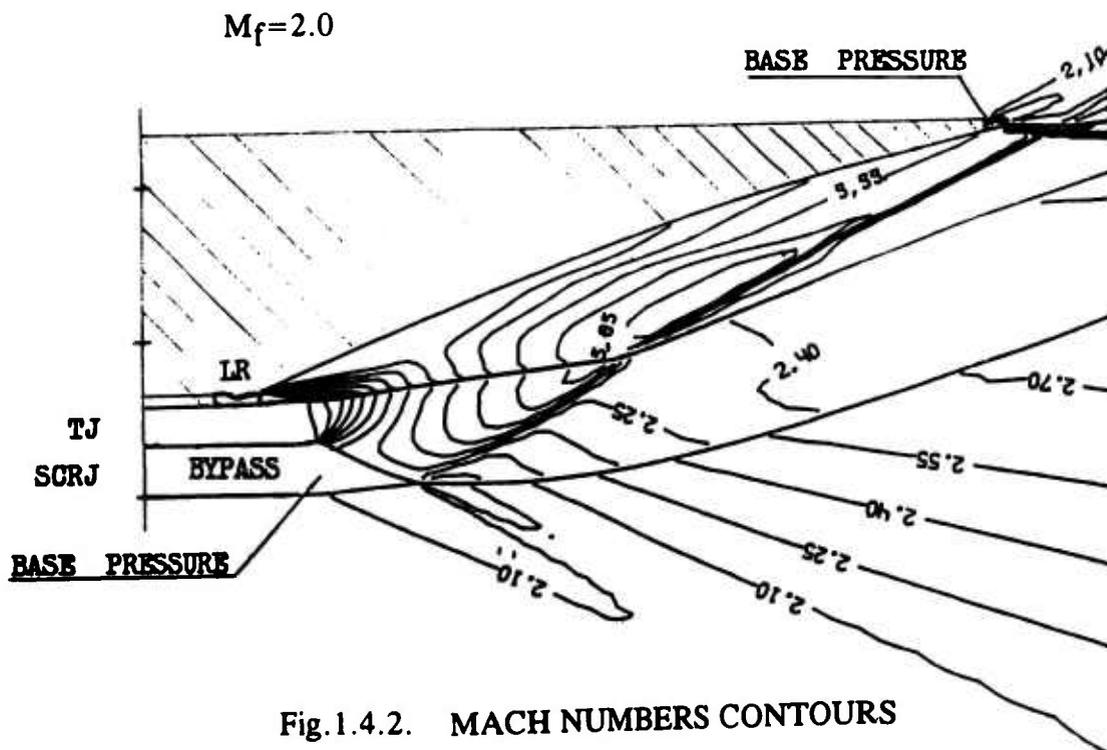
Fig.1.4.2. MACH NUMBERS CONTOURS

HYPERSONIC NOZZLE

$M_f = 10$

10.03

4.41

18.4

3.41 3.61 3.61 4.01 4.21 4.41

18.4

8.02

Fig. 1.4.3.   MACH NUMBERS CONTOURS
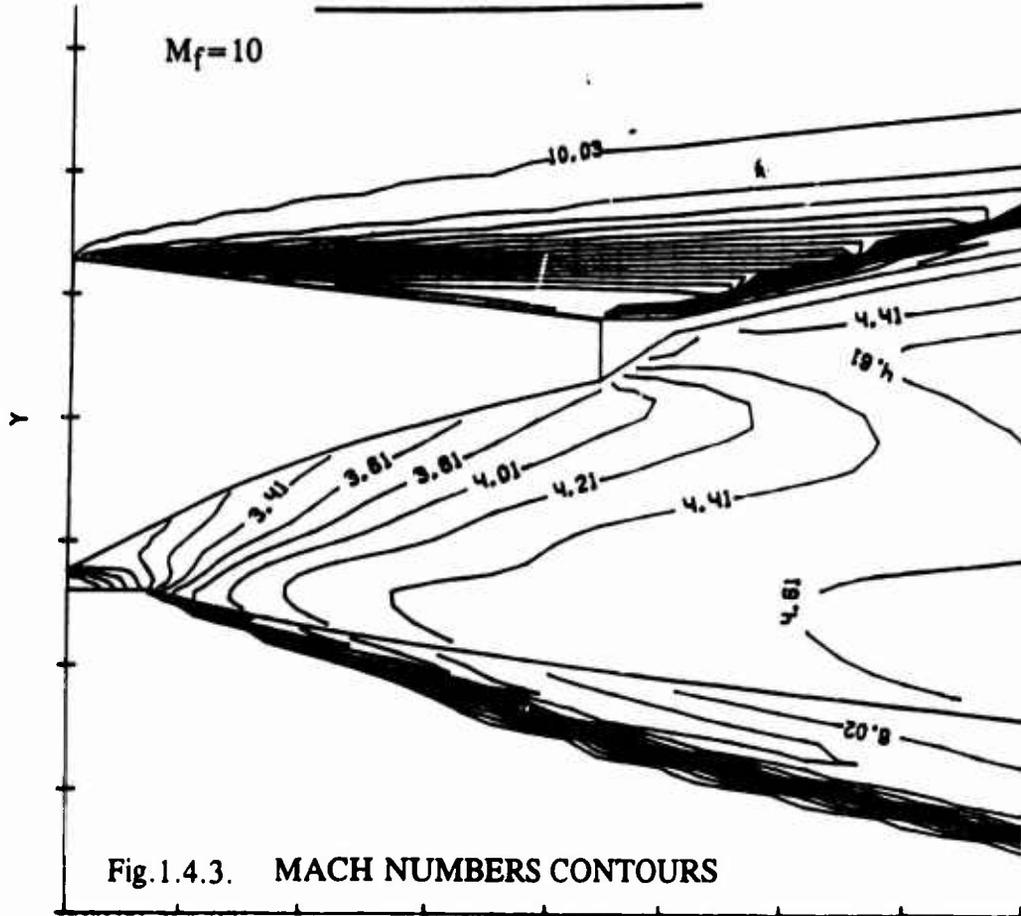
NOZZLE PERFORMANCES

THRUST LOSSES

$\Delta \bar{R}_c$

0   5   10 M_f
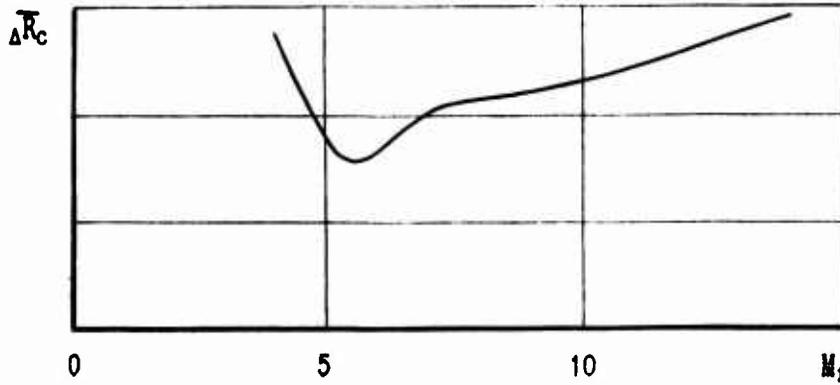
Fig. 1.4.4.

THRUST VECTOR ANGLE

α, deg

0

0   5   10 M_f
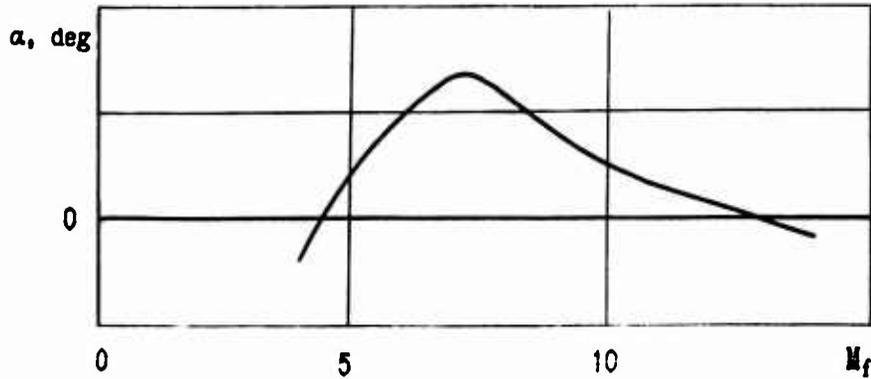
Fig. 1.4.5.

RESEARCH AND DEVELOPMENT OF RAMJETS/RAMROCKETS
PART II   INTEGRAL LIQUID FUEL RAMJETS

by

Prof., D.Sc. V.SOSOUNOV

CIAM (Central Institute of Aviation Motors)

2, Aviamotornaya St. 111250 MOSCOW

RUSSIA

S U M M A R Y

Integral liquid fuel ramjets have some specific features influencing on their arrangement and construction. Among such features are: mostly bigger size and working duration than by SPRR, the necessity of fuel manifolds and flameholders, and also wall cooling system arrangement in combustion chamber, the possibility of fuel flow and nozzle position control during flight on different speed/altitude trajectories. In this lecture there will be discussed some items, concerning the mentioned LFRJ features:

- The integration of ram combustor and booster.
- Duct flow instability during the ejection of booster case.
- Fuel supply device and effective combustion in ramjet.
- Adaptive control of ramjet on different flight trajectories.

NOMENCLATURE

A	- area;
d	- diameter;
G	- mass flow rate;
H	- altitude;
M	- Mach number;
$q = \rho_0 V_0^2/2$	- dynamic pressure;
r	- range;
T	- temperature;
t	- time;
V	- flight velocity;
α^0	- angle of attack;
λ	- dimensionless velocity coefficient;
ρ	- density.

INDICES

f	- fuel;
o	- ambient atmosphere;

ABBREVIATIONS

AB	- after burner;
ABE	- air breathing engines;
LFRJ	- liquid fuel ramjet;
LH_2	- liquid hydrogen;
LR	- liquid rocket;
RJ	- ramjet engine;
SPRR	- solid propellant ramrocket;
SR	- solid rocket.

1. INTEGRATION OF LIQUID FUEL RAMJETS WITH BOOSTER

The concepts of the missiles integration with liquid fuel ramjets (LFRJ) and SPRR as propulsion systems have their features, specific to the conditions of using each missile type. As known by practice, the solid propellant ramrocket engines are the most preferable on small "air-to-air" and "ground-to-ground" missiles, the liquid fuel ramjets are preferable on larger "air-to-ground" and "ground-to-ground" missiles. The main characteristic sections of the integral ramjets (solid or liquid fuels) are given in Fig. 3.1.

The relative low gross take-off weight and low operation times of "air-to-air" and "ground-to-air" missiles predetermine using on them the SPRR with fixed gas-air flow passage as a propulsion system of the second missile stage. The cast or ramjet case-well-bonded grain of a solid propellant booster with ejectable nozzle (or nozzleless solid booster) is used to fill at most the volume in the SPRR.

Fig. 3.2 shows the principle schemes of the integral ramjets of different class and application.

Opposed to the missiles with the SR the integration of the missiles with ramjets is associated with solving some problems caused, first of all, by high structural complexity of separate elements and components of the combustor and jet nozzle as well as of the fuel and vehicle actuator control systems.

The type of the start (air, ground and submarine) defines a booster grain mass, which may highly differ, due to a significant difference in time from the missile start to the ramjet operation initiation.

When designing the ramjets for "air-to-ground" small missiles (d = 350-450 mm) due to the severe restrictions in a free volume, they are used, where possible, the simplest solutions in terms of the structure: the organization of burning process stabilized on a bottom without flameholders, a fixed frontal unit at the combustor inlet with a fixed supersonic nozzle (the missile of Kh-31type) and using, where possible, thermal barriers of the combustor walls (of ASALM type) instead of air-film ones (see Fig. 3.2).

The other concept of the integration - the location of the solid propellant booster together with a case in the liquid fuel ramjet combustor is used for the high gross take-off weights and high engine operation time of "ground-to-ground" and "air-to-ground" missiles. In this case the compact location of the engine elements, components and units complicated in the structural manufacturing (unfolding fuel manifolds and flameholders, nozzle flap control mechanism) in the limited volume of combustor is needed to fill the combustor volume by inserted solid propellant booster the most fully.

Using the inserted solid propellant booster has its advantages and allows:
- independently to develop a booster and ramjet on the specialized test beds;
- to use a light ramjet combustor with air-film cooling, the most reasonable for high operation time;
- to use the same module of the ramjet on missiles of different application with significantly different flight paths and different solid propellant booster engines such as in ASM MSS missile of double application.

A wide range of using such an engine for flight altitude and velocity is provided by also a stepped or smooth control of the nozzle throat area after the solid propellant booster ejection as well as by a wide range of fuel flow control that is possible with liquid fuel.

The type of launchers (or the location of missiles on a carrier), as well as launching conditions influences directly the integration of a vehicle with a ramjet. Both these factors define, first of all, the type of the air intake and its placement on a missile. At present, as known, the missiles with air intakes of different types are developed: nose (frontal), removable (two-dimensional, circular, segmented) and ventral. Their location is determined by the type of a launcher.

The individual suspension under a fuselage, as a rule, does not limit the choice of intake type. The missiles with ventral intake are the most rational for cassette launchers of a drum type; using the nose air intake is the most reasonable for missiles of submarine start.

Fig. 3.3 illustrates the scheme of the integral liquid fuel ramjet with the inserted solid propellant booster. Fig. 3.3 shows also all possible types of intakes that are used on existing and developable missiles.

Fig. 3.4 shows longitudinal section of the integral liquid fuel ramjet, in which the frontal unit and flameholders are unfolded after booster ejection and the supersonic nozzle throat section is variable.

The possible schemes of integration of the ramjet and solid propellant booster, presented in Fig. 3.1, 3.2, and 3.3, to a considerable extent are associated with the size of the vehicle and engine, depend on the velocity, up to which a solid propellant booster operates, the starting conditions, etc.

So, the problem of solid propellant booster structure matching with cruising ramjet is a key question in designing the whole of propulsion system and means a reasonable compromise in the selection of the configuration and the vehicle.

2 INTEGRATION OF LFRJ WITH BOOSTER AND DUCT FLOW INSTABILITY

Unsteady processes, such as booster ejection, inlet start - unstart, combustor start - unstart, change of fuel injection, self - excited oscillation in inlet or combustor, ramjet response on external shock waves and so on, are very important part of integral ramjets functioning, because they can lead to the engine distruction.

Numerical simulation is the only way of investigations of this processes, as a rule, because experimental researches are very expensive, need perfect equipment, and can lead to experimental model destruction.

Therefore, the mathematical models and numerical codes for unsteady processes simulation were worked out in CIAM. This models based on 1D and 2D unsteady Euler equations for reacting gas mixture. They include various experimental and empirical dates, and take into account different construction peculiarities of researched ramjet. Numerical

codes are based on the second order accuracy Godunov - Kolgan algorithm.

Now, let me present you some results of unsteady processes numerical simulation, fulfilled in CIAM. In Fig. 3.5 you can see the scheme of Liquid Fuel Ramjet with the ejected booster, used as the first stage of missile. All investigation, I'll tell you, were fulfilled for such type of ramjets.

Gas oscillation in closed inlet during missile acceleration. On the first part of missile trajectory the ramjet's inlet is closed by the booster. If flight Mach number is greater then 1.5 - 2.0, then selfexcited oscillations in ramjet's inlet appear very often. They can lead to ramjet distruction. We use numerical simulation to predict the appearance of selfexcited oscillations, to calculate their amplitudes and frequencies, to predict the efficacy of different ways of this oscillation amplitude decreasing. In Fig. 3.6 you see the example of such numerical simulation. Flight Mach number equals 2.5, the maximal undimensional amplitude is about 0.4.

Booster ejection. The next problem, we deal with, is the booster ejection - see fig 3.7. Mathematical model, we use, describes booster motion and gas dynamic flow in ramjet's duct together. Aerodynamic and inertial forces, friction, external airflow around ejected booster and other effects are taken into account. You see in Fig. 3.7 the time evolution of booster velocity and its location. So we can predict the possibility of blow interaction between the booster and ramjet nozzle.

In Fig. 3.8 the time evolution of self - excited oscillation during the booster ejection is presented. And in Fig. 3.9 you can see the comparison of experimental (curve 1) and numerical (curve 2) simulation of gas dynamic flow, induced by the moving booster. You see a good agreement between numerical and experimental results. So, we can calculate the values of dynamic loads, applied to the internal surface of ramjet and initiated by moving shocks and supersonic zones. It's a very important result, because the unsteady aerodynamic loads can tear off the defense screens in combustor.

All this results can be summarized as a safe ejection area, presented in the space of parameters: flight Mach number, flight altitude in Fig. 3.10. Curve 1 is a boundary of blow interaction between booster and ramjet nozzle; curve 2 is the boundary of combustor destruction due to high pressure in front of booster, curve 3 - the missile trajectory. The missile's trajectory

part, picked out in Fig. 3.10, is possible the booster ejection.

The combustor start. In Fig. 3.11 you can see some results of the next unsteady process numerical simulation - the combustor start. Mathematical model, which we use, bases on unsteady Euler equation for reacting gas mixture. We suppose, that there exist an equilibrium state in subsonic combustion chamber. We take into account experimental dates for the length of burning zone, coefficient of combustion completeness and so on. We find the dynamic loads, the maximum temperature in combustor and other parameters of unsteady flow. The main and very important effect, we've found, is follow. The initiation of air-fuel mixture leads to appearance unsteady stress waves, that move from combustor to ramjet inlet and decreases during short time the total airflow through ramjet duct. In Fig. 3.11 you can see the time evolution of air excess coefficient. Curve (1) is quasi steady approximation, when total airflow is constant and only fuel weight flow changes. Curve (2) describes a real unsteady process, curve (3) is a stable combustion boundary.

You see, that unsteady decrease of air-excess coefficient can be very strong (from steady value 1.8 to minimal value about 0.9). Therefore, if the optimal value of air excess coefficient on the start part of missile's trajectory is about $\alpha = 1.2-1.3$ and the stable combustion boundary is about $\alpha = 0.9$, the automatic control system must provide combustor start with $\alpha = 1.8$, and only after that increases slowly the weight fuel flow to necessary value $\alpha = 1.2-1.3$. And during combustor restart regime, automatic control system work must be organized by the same way - see Fig. 3.11.

Self-excited oscillation in combustor. In Fig. 3.12 you can see the numerical simulation results of self-excited oscillation in combustor, working on near-stoichiometric air-fuel mixture. The physical nature of this oscillation is follow. Lets suppose, that we increase fuel injection so, that air-excess coefficient decreases to the value $\alpha = 1.0$. Then the combustor heat increase too. At the same moment the stress wave appearances in combustor and moves to the ramjet inlet, decreasing the total airflow. Therefore the value of α becomes less than 1.0, for example $\alpha = 0.8$. Than combustor heat decreases, the stress wave becomes weaker, the total airflow increases for the short time to value $\alpha = 1.2$. But very soon the constant value of fuel injection leads air-

excess coefficient to it's steady value $\alpha=1.0$, and all process, described above, repeats.

Ramjet response on external shock wave and atmospheric nonuniformities. In Fig. 3.13 you can see the result of numerical simulation of shock wave motion through the ramjet. The moving shock increases the total airflow through the ramjet duct. Therefore air excess coefficient α increases too. New value of α must be less than stable combustion boundary.

All this numerical researches were fulfilled in the CIAM and were used for development of different Russian ramjets.

3. FEATURES OF THE COMBUSTION PROCESS ORGANIZATION IN RAMJET

The scheme selection of the combustion process organization in the straight-through-flow type combustors (ram combustors) is mostly defined by the flow parameters at a combustor inlet such as pressure P_t, temperature T_t and λ - velocity coefficient.

A possible range of change in these parameters in modern afterburners and ramjet combustors is tabulate in Table 1.

Table 1.

Combustor type	P_t kPa	T_t K	λ
Turbojet afterburner	40-600	900-1200	0.20-0.25
Turbofan afterburner with flow mixing	40-600	600-850	0.15-0.22
Ramjet combustor	40-600	350-1300	0.20-0.22

It follows from the Table that feature of the booster-sustainer ramjet combustors is a wide range of variations in a combustor inlet air temperature which covers a possible change of the temperature in all existing afterburners.

When the turbojet afterburners were creating the combustion process organization scheme with consecutive realization of fuel mixing, vaporization and combustion processes along the combustor was developed. In such a scheme of combustion process organization the fuel is supplied to flow upstream flameholders in a distance sufficient to its practically full vaporization and mixing with gases entering to the afterburner. Under conditions typical to afterburners the fuel burning length L_b depends mainly on mutual arrangement of fuel stabilizers

and is equal to $L_b = (10-12)B$, where B is an average distance between the axes of two adjacent flameholders. The given scheme of the combustion process organization has proved itself and at present is being used widely in turbofan afterburners with flow mixing. Fig. 3.14 shows the typical arrangement of fuel manifold and flame stabilizers for the turbojet and turbofan afterburners.

Using the mentioned scheme for the combustion process organization in the ramjet combustors led, as a rule, to significant problems with providing the stable operation of these combustors at low inlet air temperature ($T_t \leq$ 500K). These problems were associated with the fact that the combustors of the mentioned scheme of the combustion process organization show a great tendency to the excitation of the regular longitudinal gas pressure fluctuation in them, particularly in fuel reach mixtures.

Studying the combustion process of the atomized liquid fuel at low flow temperatures showed that a decrease in combustion process stability was due mostly to a reduction in a degree of the fuel vaporization ahead of flameholders, the deposition of fuel droplets on the flameholder walls and, hence, a significant enrichment of the gas with fuel, being in the recirculation zones after them [3]

Fig. 3.15 gives the experimental dependence of the air excess coefficient in the flameholder recirculation zone α_{RZ} on the fuel vaporization degree z upstream the flameholder. It follows from the presented data that at $z \to 0$ the gas composition in the recirculation zone is approximately 2.2 as rich as the mixture approaching to the stabilizer.

At high air temperature ($T_t \cdot 1100$-$1200K$) the fuel self ignition is possible upstream flameholders. The burn-out and destruction of flameholders in this case are inevitably.

Therefore, for the ramjet combustors operating at the low inlet air temperature CIAM suggested the other scheme of combustion process organization, so-called scheme with the separate fuel supply, in which the processes of fuel mixture, vaporization and burning take place simultaneously.

The proposed scheme of the combustion process organization with separate fuel supply allows to provide:
- a stable combustor operation at low air inlet temperature ($T_t \leq 500K$);

- a high reliability of the combustor operation at high air inlet temperatures ($T_t > 900K$);
- maximum possible stability of the combustion process under high altitude conditions;
- the maximum simplicity of the structure when developing the combustor with unfolding flameholders.

However, there are some problems in providing high combustion efficiency at low air temperatures and, besides, the special requirements are made on consumption characteristics of fuel manifolds at such scheme of the combustion process organization.

Schemes of Combustors of Liquid Fuel Ramjet Integrated with Booster Engine

Let us consider now the possible schemes of the flameholder mounting in the air cooled combustors of booster-sustainer ramjet. In the case when the length of the booster engine, that is placed into combustor, is less than the extent of fuel burning zone length or equal to it, the flameholders and fuel manifolds are stationary located in the combustor as in the turbofan afterburners.

In case when the length of the booster engine exceeds the extent of the burn-out zone, the unfolding (turning) flameholders are needed to install. This is associated with the fact that the enlargement in combustor length beyond required for the fuel burning out leads to the increase in air flow to its cooling system and in this connection to a reduction in fuel combustion efficiency in the fuel rich region.

Fig. 3.16 presents the schematic diagram of such a combustor. At the initial moment of time the flameholders are located close to the combustor wall as the booster engine occupies practically the whole volume of the combustor. After its jettison the flameholders are unfolded (turned) and are set into operating position. After that the ramjet combustor is started. Scheme of such unfolding radial flameholder is shown in Fig. 3.17.

Characteristics of Burning Process in LFRJ Combustors

To compare the characteristics of the fuel combustion process in the modern accelerating-sustaining ramjet combustor and turbofan afterburner with flow mixing is of interest, when the combustion process in the latter is organized by the traditional scheme.

Two combustion chambers with the same relative length of the hot section ($L_h/H = $ const) and approximately the same scheme of the inter combustor process control were selected to compare.

Fig. 3.18 and 3.19 illustrate the regions of the stable burning in these combustion chambers. It follows from the data presented in Fig. 3.18 that at $T_{tmin} = 770$-820 K, $\lambda = 0.15$ and P_t/P_o 0.5 the burning in afterburner is stable in the range of the air excess coefficient variation of $0.9 \leq \alpha \leq 6.7$. The minimum value of pressure in afterburner, at which the fuel combustion is possible under these conditions is $P_t/P_o = 0.27$ ($\alpha = 2.0$) [4].

Decrease in afterburner inlet temperature to $T_t = 500$ K leads to the fact that at $P_t/P_o = 0.5$ the combustion is stable only at $\alpha > 1.25$ and the minimum pressure at this temperature is $P_t/P_o = 0.32$ and corresponds to $\alpha = 3.0$.

The rather complicated curve, bounding the region of the stable burning in the afterburner with obviously marked minimum, is transformed for the ramjet combustor into a straight line above which the burning is stable and below which it is impossible (see Fig. 3.19).

At the same values of T_t and λ the minimum gas pressure when the combustion is still possible is much the same in both combustion chambers. The difference is in fact that under the minimum gas pressure condition the burning in the afterburner is possible at practically the same value α, whereas in the ramjet combustor it is possible in a wide range of α variation.

Fig. 3.20 compares the combustion efficiency for two considered schemes of the combustion process organization in combustion chambers with close relative length of hot section (L_h/B) [5]. It follows from the diagram that if the combustor inlet air temperature lies in the range typical to the afterburners, the combustion efficiency is practically the same in both schemes.

Increase in flow temperature up to $T_t = 1170$ K in the ramjet combustor slightly influenced the combustion efficiency value in it. Decrease in ramjet combustor inlet air temperature to $T_t = 360$ K with a simultaneous reduction in fuel temperature to $t_f = -50°C$ led to the fact that the maximum combustion efficiency in it did not exceed the value $\eta = 0.68$.

So, the use of the developed scheme of the combustion process organization with separation fuel supply allows to create the booster-sustainer ramjet combustor operating in more wide range of inlet air temperature in comparison with combustors designed according to traditional scheme.

Features of the LFRJ Combustor Start

In conclusion it should be said several words about the features of the combustor starting in the modern booster-sustainer ramjet.

If the ramjet has a fully-variable nozzle, the combustor may be started under the same conditions as the afterburner of modern turbofans and practically by the same means. If the ramjet is equipped with the nozzle, having a constant throat area, or two-position nozzle, the combustor starting under these conditions becomes a more complicated problem.

The point is that in this case, after the booster engine jettison and unfold of the flameholders in their operating position, such a flow regime in the combustor is set when the flow velocity between the flameholders becomes equal to the sonic one ($\lambda = 1.0$). The combustion process stabilization with such velocities of the flow in the combustor, using hydrocarbon fuels, is impossible.

Therefore, the special starting devices of high heat power with rather high time of operation are used to start the ramjet combustor. In this case after switching on the starting device, firstly, the gas flow in the combustor is transformed to the subsonic one due to heat release in flow as a result of the fuel portion combustion, delivered to the combustor, in hot jet of the starting device. Only thereafter the combustor is ignited.

4. CONTROL OF LIQUID FUEL RAMJET (LFRJ)

Solid propellant ramrockets have limited possibilities of in-flight control. In comparison with them liquid fuel ramjets can be widely controlled. Control stages of SPRR in comparison with LFRJ are shown schematically in Fig. 3.21.

The automatic control system (ACS) is one of the basic components of LFRJ on manufacturing quality of which the flight performance of aircraft depends. It is necessary to provide the LFRJ missile flight on different

and rather complicated flight paths (see Fig. 3.22), over the course of which the flight altitude and speed are varied in a wide range. It requires the change in wide ranges of the engine thrust and fuel consumption delivered to it on different segments of flight path. As the engine thrust depends on the atmospheric conditions, they must be taken into consideration in controlling the fuel consumption through the engine. In connection with the fact that LFRJ are used, as a rule, on unmanned aircraft the engine ACS must be algorithmically integrated with the aircraft flight control system to provide the required thrust on all the flight path segments. In this case both inter-engine parameters and also the parameters used in the aircraft flight control system are utilized to control the fuel consumption through the engine [2].

The necessity of rational using all the volumes on unmanned aircraft leads to the advisability not only of algorithmic but also hardware integration of the engine ACS with the flight control system under which all the calculations are performed by the same onboard computer and only the transducers and actuators are installed in the engine.

Target of LFRJ Control

In selecting the control parameters and program, in addition to the provision of the required engine thrust on all the flight path segments, the main task is also provision of the best flight characteristics of aircraft on all check flight path, namely, the most effective use of sustain fuel reserve. Besides, the LFRJ control tasks involve the limitation of the engine operation regimes and aircraft flight, providing the conditions for no-failure operation of the main engine and aircraft components. Among such restriction are:

for the aircraft

- the minimum ram determining the possibilities of aircraft maneuver;
- the maximum ram determining the loads on aircraft components and elements;
- the maximum air stagnation temperature defining the material strength of the aircraft structure;

for the engine

- the provision of adequate margins of fuel combustion stability;
- the provision of adequate margins of intake operation stability (stall margin);
- the prevention of reduction in flight Mach number below the minimum Mach number under which the flight becomes impossible at all values of fuel consumption and air excess coefficient.

5-7

The LFRJ control tasks involve also the provision of its reliable starting.

The mentioned restrictions of the engine operation regime and vehicle flight determine the boundaries of the latter application, area in the M-H coordinates. Fig. 3.23 depicts the application area of the "air-to-surface" missile as an example. The left bottom of the area boundary of "air-surface" missile application is defined by the minimum Mach number. The left upper part of the application area boundary is determined by the minimum ram, surge boundary of the intake, combustion instability and again by surge boundary of the intake. The right upper part of the application area boundary is defined by maximally admissible stagnation temperature of air flow and the right lower part of the boundary - by the maximally permissible values of air ram.

The boundaries of the vehicle application area depend on the parameters of the vehicle and engine as well as the engine control program atmospheric conditions.

The flight control program is selected so that Mach number - flight altitude dependencies (operating modes lines) were not beyond the boundaries of the vehicle application area during the whole flight for all possible trajectories and atmospheric conditions (see Fig. 3.23). In this case the conditions of no-failure operation of all the basic components of the engine and vehicle are provided.

Structure and Control Loops of ACS

Fig. 3.24 shows diagram-scheme of the ramjet ACS. The control system generally involves the control loops of fuel consumption, nozzle thrust area and intake geometry.

The fuel consumption control loop performs all the above mentioned functions. The fuel consumption control loop is made as hydraulic fuel metering unit controlled by electrical signals from the aircraft computer.

The control loop of the nozzle throat area is used in the control system to match the intake and engine operation regimes as well as to provide the adequate margins of the intake stability at high thrust levels necessary on aircraft climb and acceleration regimes.

The control loop of the intake geometry is used for improving the engine fuel efficiency if it

is required to provide a wide range of variation in flight Mach number.

The control loops of the nozzle and intake may be made both with uninterrupted change of its geometry and as two-position ones - with relay change of the intake and nozzle geometry. In the first case the aircraft flight characteristics is only little more than the aircraft characteristics with relay control of the nozzle and intake. At the same time in the second case the gas dynamics forces may be used to move flops of the nozzle and intake that significantly decreases the cost, dimensions and weight of the control system and makes it possible to place some additional quantity of the sustain fuel on board and to improve the aircraft flight characteristics.

Using the control loops of the nozzle and intake is more effective, the larger the aircraft sizes (the more the fuel reserve) and the wider the range of variation in aircraft altitude and speed.

Fig. 3.25 gives as an example the effect of the nozzle control introduction on the flight characteristics of the "air-surface" missile. Curve 1 shows the missile flight range - launch altitude dependence only with the fuel consumption control according to the program

$$G_f = f(P_{dm}, M).$$

Curve 2 in Fig. 3.25 illustrates the similar dependence with the fuel consumption control and two-position control of the nozzle according to the program

$$G_f = f_1(P_{dm}, M, A_n^*)$$
$$A_n^* = f_2(H, M)$$

Curve 3 in Fig. 3.25 displays the missile flight range with the fuel consumption control and two-position control of the nozzle and intake according to program

$$G_f = f_1(P_{dm}, M, A_n^*)$$
$$A_n^* = f_2(H, M)$$
$$A_{in} = f_3(M, \alpha)$$

It is seen that the flight range, depending on a launch altitude, with the introduction of the two-position nozzle control increases by 40-68% and with the introduction of the intake control loop - by 13-17% more.

To provide high flight aircraft characteristics with sufficiently reliable operation of all the main airframe and engine components, it is necessary very carefully to select the command parameters and to optimize the engine control program. The engine control program is to be optimized in close mutual trade-off with the selection of the aircraft flight control program. Developed for this purpose are the characteristics calculation program complex of the engine and aircraft as a whole and also a number of service and auxiliary programs, facilitating significantly and reducing process and time of the control program optimization respectively.

During the optimization of the aircraft flight and engine control programs the command signals ACS parameters are selected in such a way as to provide rather wide area of aircraft application, covering all the required regimes of its flight, including the most economic ones and at the same time to obtain such thrust-economic engine characteristics which permit the flight to be made along the all check paths (see Fig. 3.23).

The complex selection method of the program of the ramjet and vehicle flight control permits all the possibilities of the engine and vehicle to be used and so to improve the flight characteristics of vehicles with LFRJ. Besides, the developed method makes it possible to select such directions of works on the main engine and vehicle components that will lead to the maximum improvement of the flight characteristics of vehicles with LFRJ. The calculations show that the flight characteristics of the modern vehicles with LFRJ may be improved by a factor of 2-3 as a result optimizing the characteristics of the main engine and vehicle components as well as the program of the engine and flight control.

CONCLUDING REMARKS

The integral liquid fuel ramjets are the most promising propulsion for missiles of quite big size and long distance flight because of their exclusive energetic effectiveness and compactness. In comparison with SR missiles, which thrust values are permanent during the flight, the thrust of liquid fuel ramjets is depend on airflow, i.e. velocity and altitude, and on fuel, i.e. control system and on intake/nozzle control, and can therefore change in wide range under required flight conditions.

So LFRJ-missiles are very effective on low-altitude trajectories, on high altitude and on trajectories of combined type. Because of thrust control flexibility the LFRJ-missiles has bigger mean trajectories speed then the SR missiles.

As the rather new propulsion the liquid fuel ramjets this system has many possibilities of future development: fuel energetic, more effective control system modes, new materials and light structure, improved external gas dynamics.

Many successfully acting in service LFRJ-missiles show that advantages.

REFERENCES

1. Бондарюк Б.С., Ильяшенко С.М. Прямоточные воздушно-реактивные двигатели. М., Оборонгиз, 1958, 392 с.

2. Орлов Б.В., Мазинг Г.Ю., Рейдель А.Л., Степанов М.Н., Топчеев Ю.И. Основы проектирования ракетно-прямоточных двигателей для беспилотных летательных аппаратов. М., Машиностроение, 1967, 424 с.

3. Раушенбах Б.В. и др. Физические основы рабочего процесса в камерах сгорания воздушно-реактивных двигателей. М., Машиностроение, 1964.

4. Теория воздушно-реактивных двигателей. Под ред. С.М. Шляхтенко. М., Машиностроение, 1975.

5. Зайцев С.А., Кузнецов В.Р., Кунцев Г.М. Влияние прогрева и испарения жидкого топлива на процесс горения в модельной камере сгорания. Физика горения и взрыва. Т.27, №6, 1991, с. 45-52.
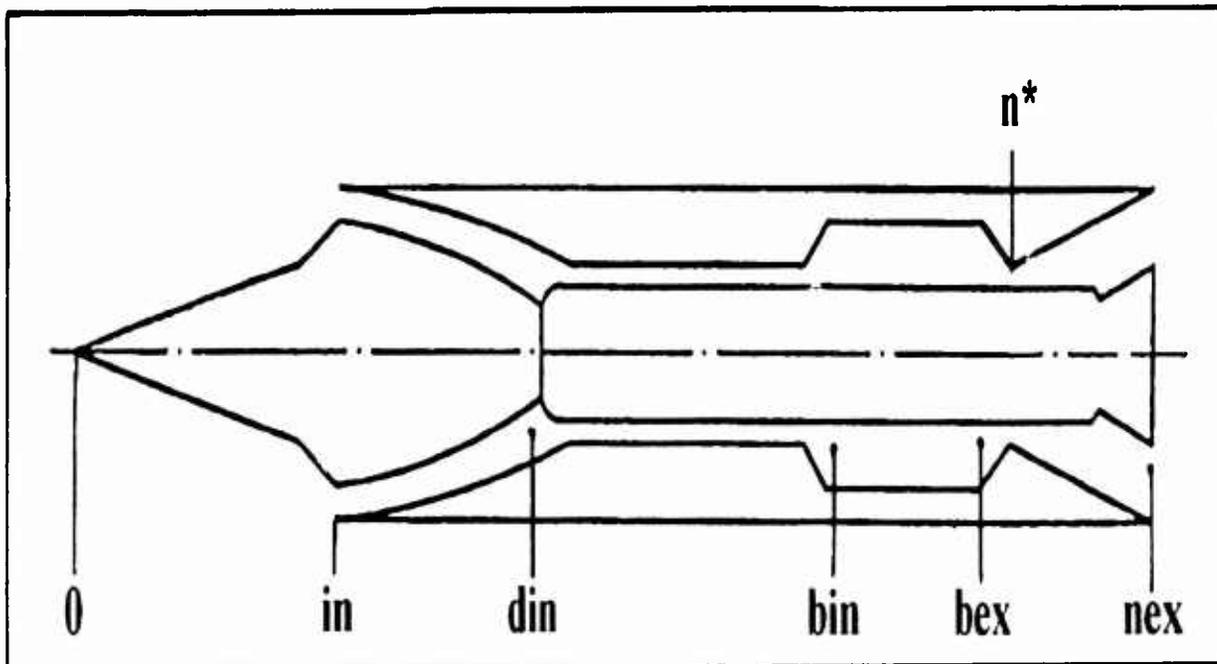
Fig. 3.1. Liquid fuel ramjet with inserted booster. Base crossections.
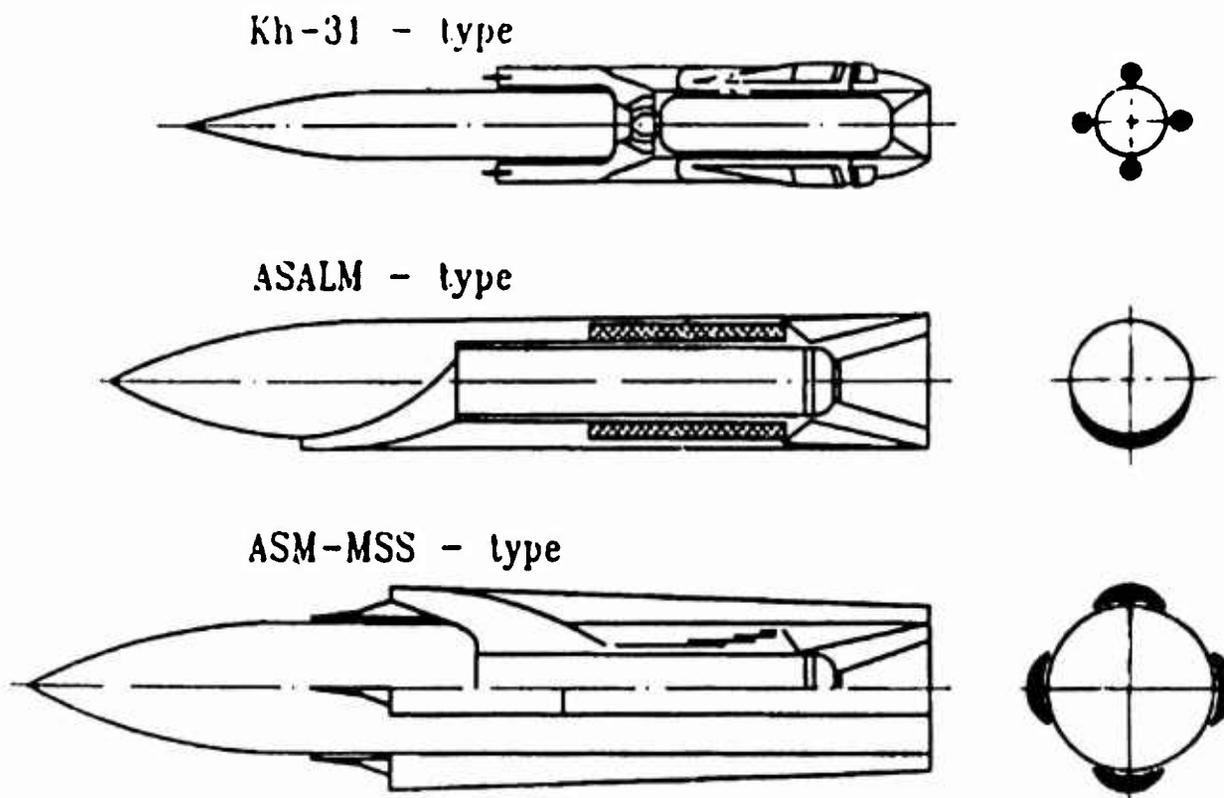
Fig. 3.2. Typical layouts of different classes missiles with integral liquid fuel ramjets.

Inlets type

circular nose
air inlet

separated
air inlets

underfuselage
air inlet

Integration problem

- SR ejection
- choise of air inlet type
- folding flame stabilizer
- variable nozzle
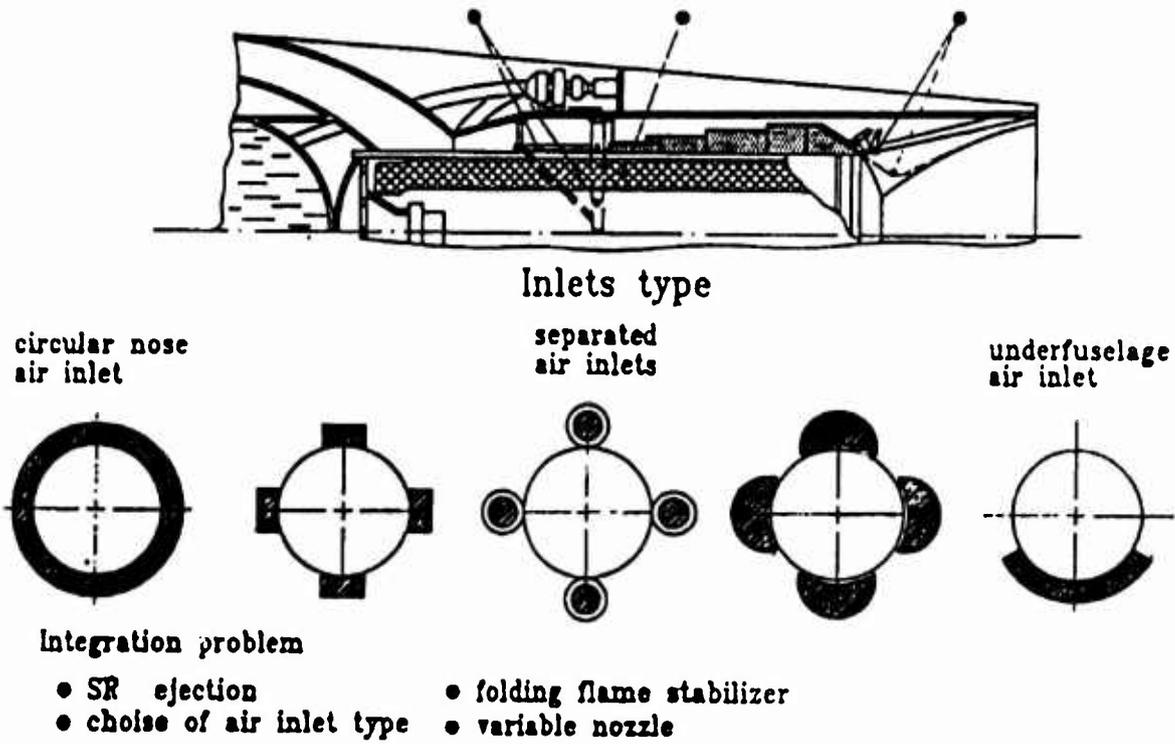
Fig. 3.3. The LFRJ and booster integration main features.
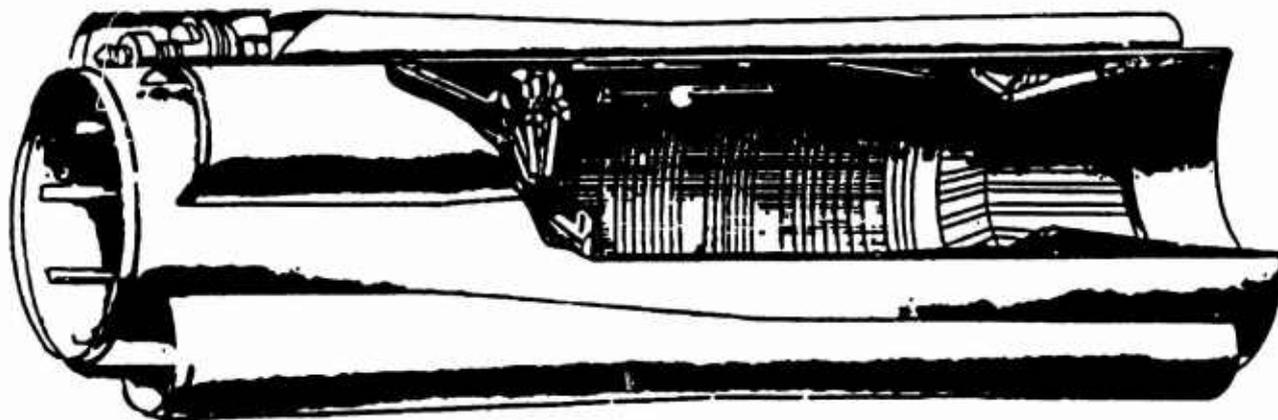
Fig. 3.4. The view of LFRJ combustion chamber (the folding fuel manifolds and stabilizators, and variable nozzle are seen).
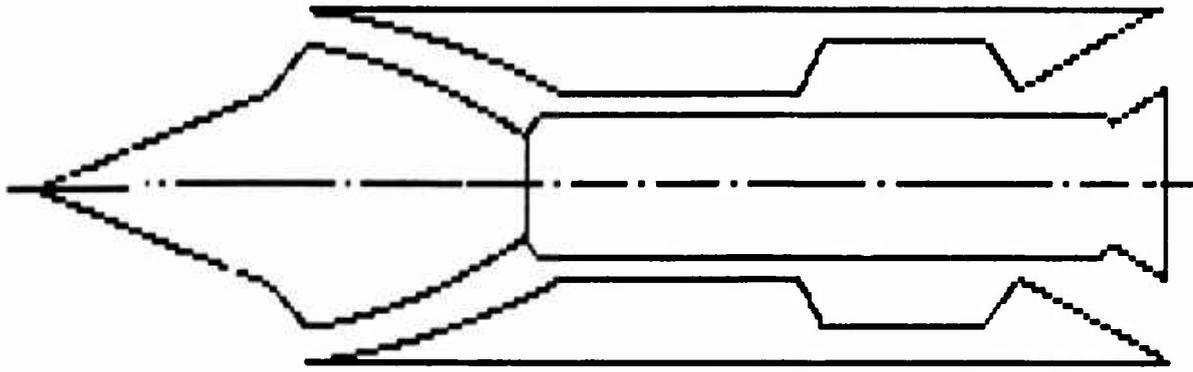
Fig. 3.5. Liquid fuel ramjet with separated solid fuel engine.
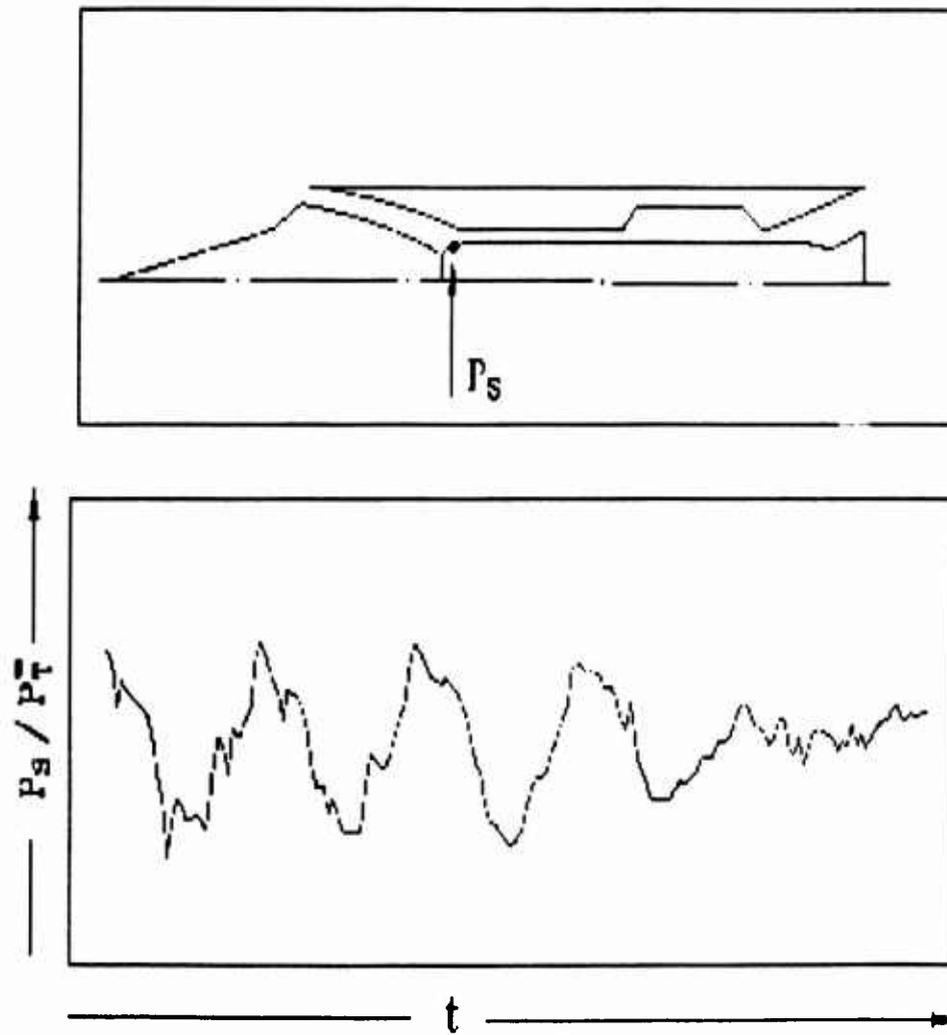
Fig. 3.6. Self-excited oscillation in ramjet's inlet, closed by solid fuel engine.
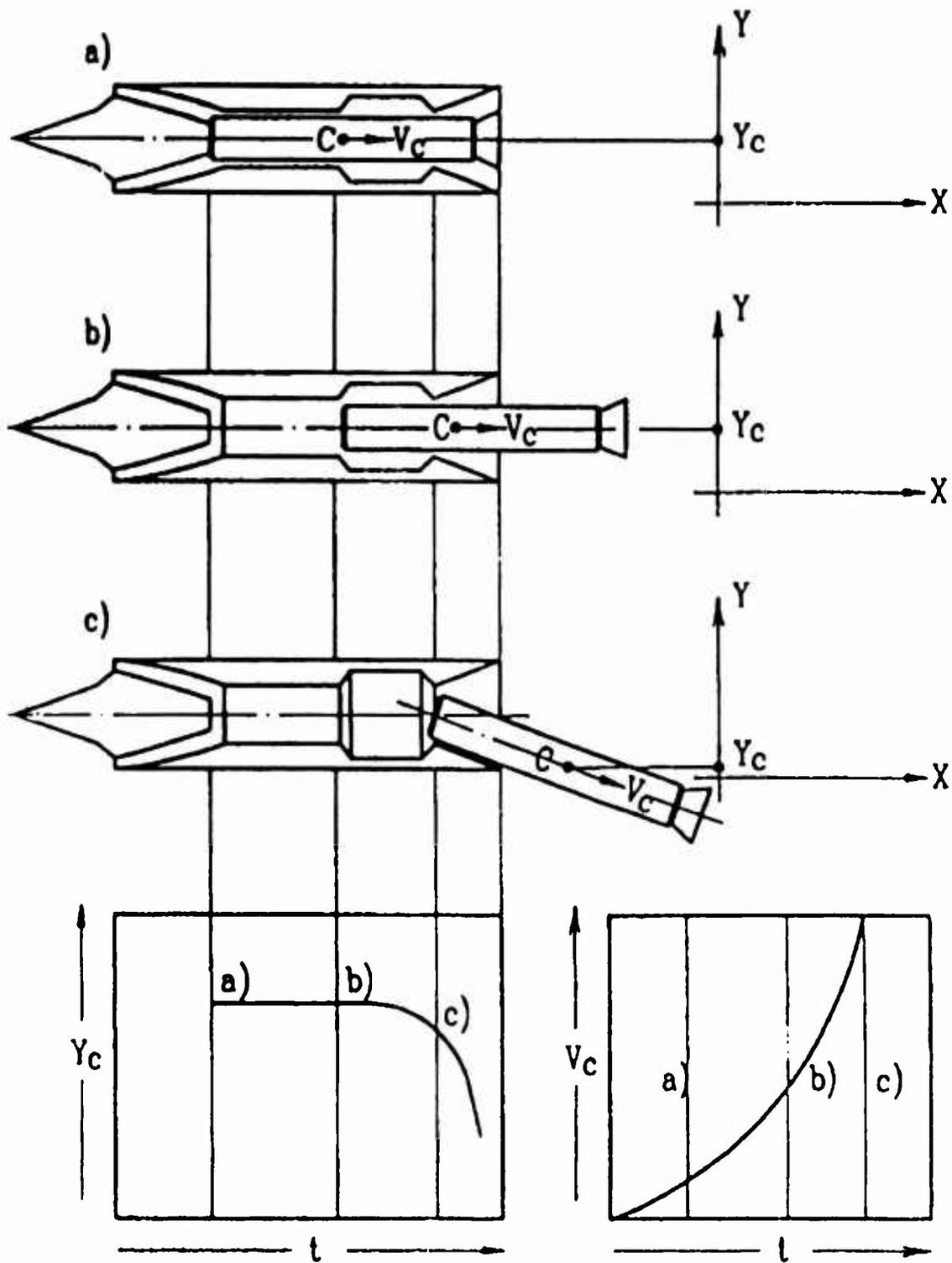
Fig. 3.7. Numerical simulation of stage separation. Time evolution of solid fuel engine's velocity.
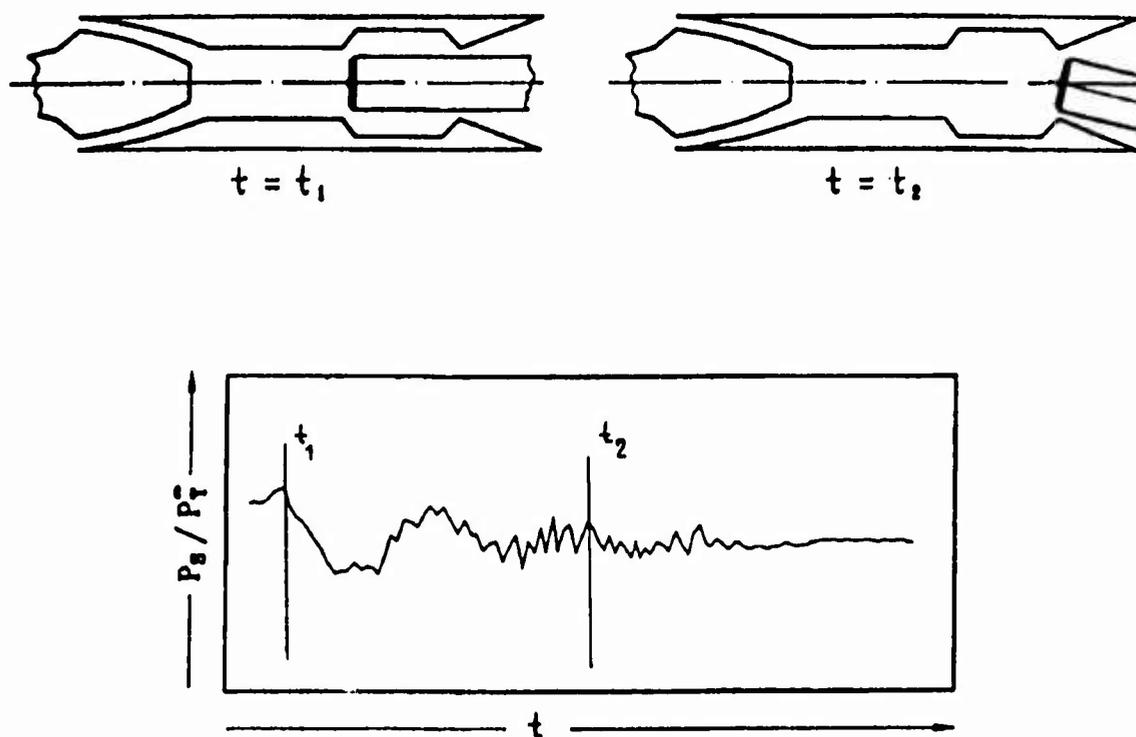
Fig. 3.8. The evolution of self-excited oscillatio in ramjet inlet during the stage separation.
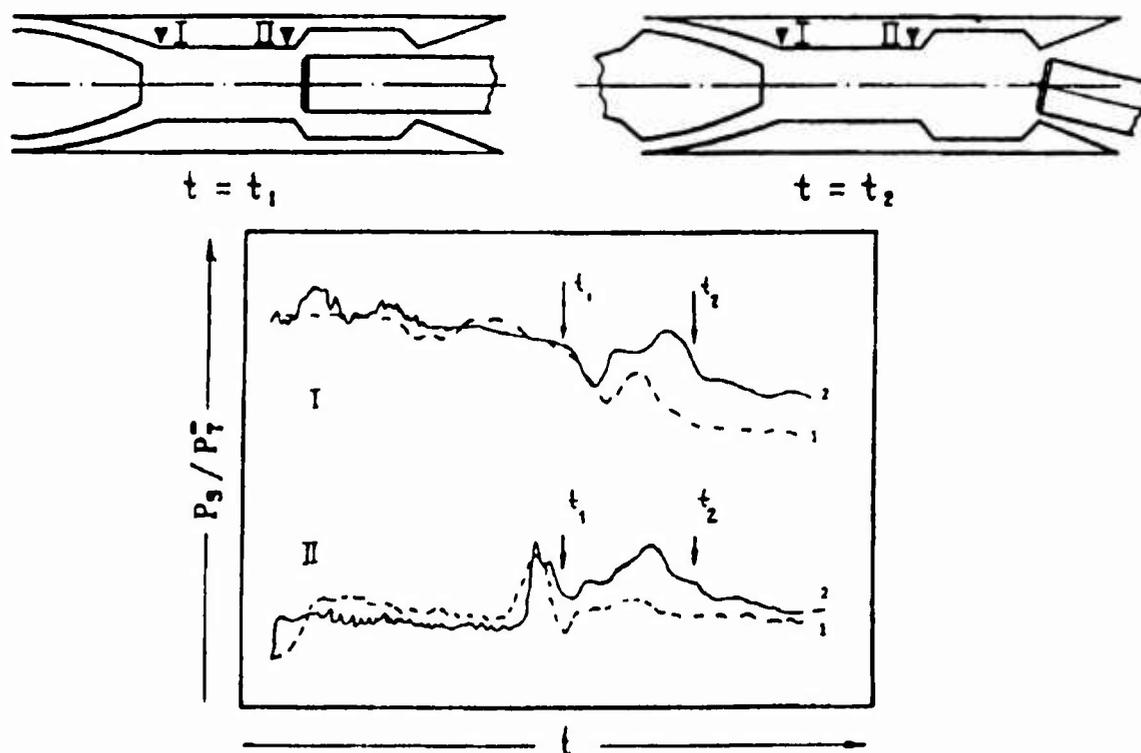
Fig. 3.9. Experimental (1) and numerical (2) simulation of gas dynamic flo in ramjet duct, induced by the stage separation.
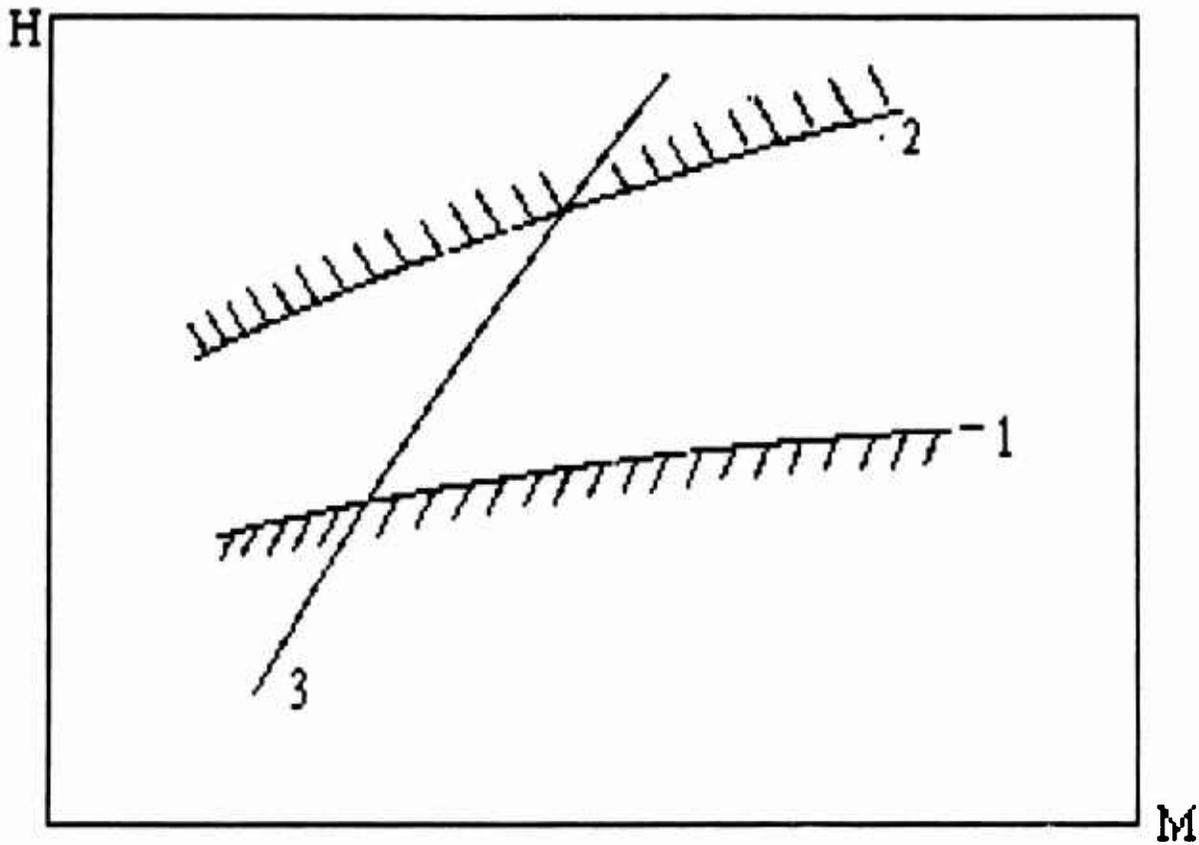
Fig. 3.10. The stage separation area in the space of parameters: flight mach number, flight altitude

curve (1) - boundary of blow interaction between solid fuel engine and ramjet's nozzle;
curve (2) - boundary of combustor destruction, due to high pressure in front of solid fuel engine;
curve (3) - missile's trajectory.
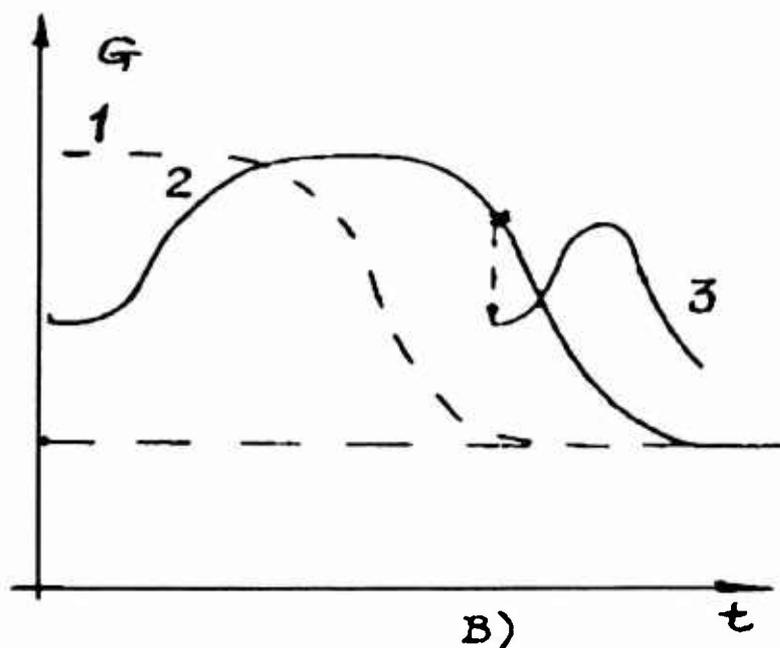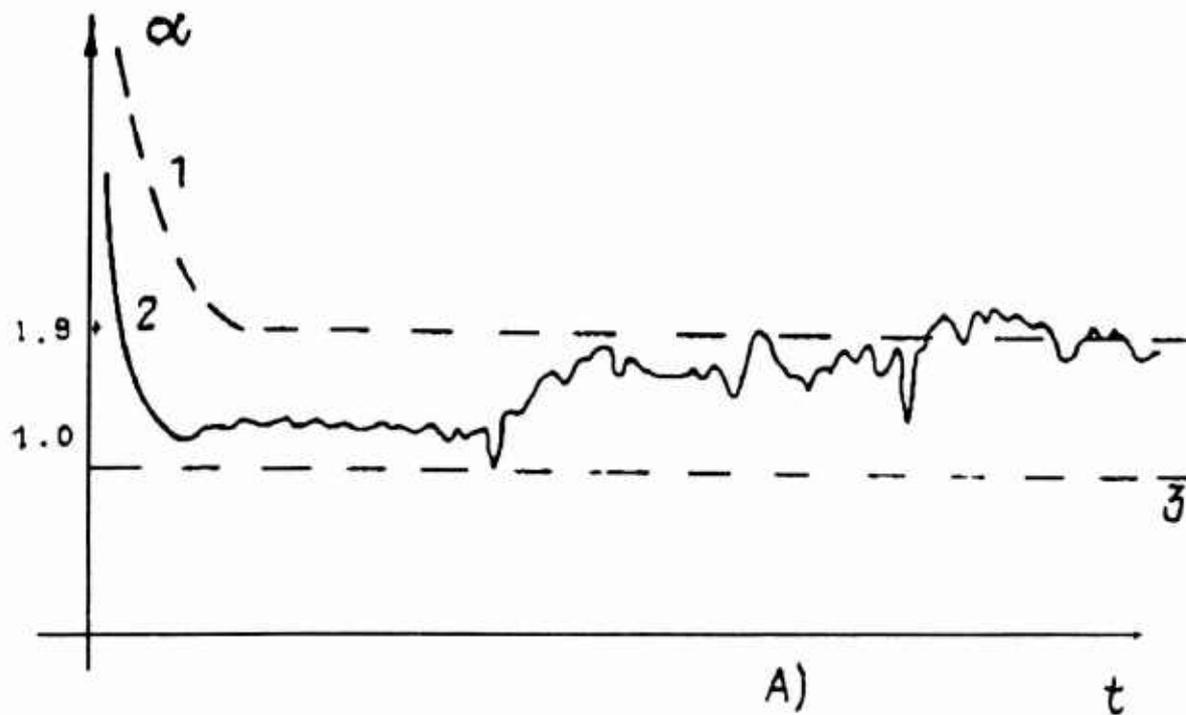
Fig. 3.11. Combustor start numerical simulations

a) Time evolution of air excess coefficient

curve (1) - quasisteady approximation;
curve (2) - unsteady process;
curve (3) - stable combustion boundary;

b) Fuel weight flow along the missile trajectory

curve (1) - optimal regime;
curve (2) - the fuel weight flow, governed by automatic control system;
curve (3) - combuster restart.
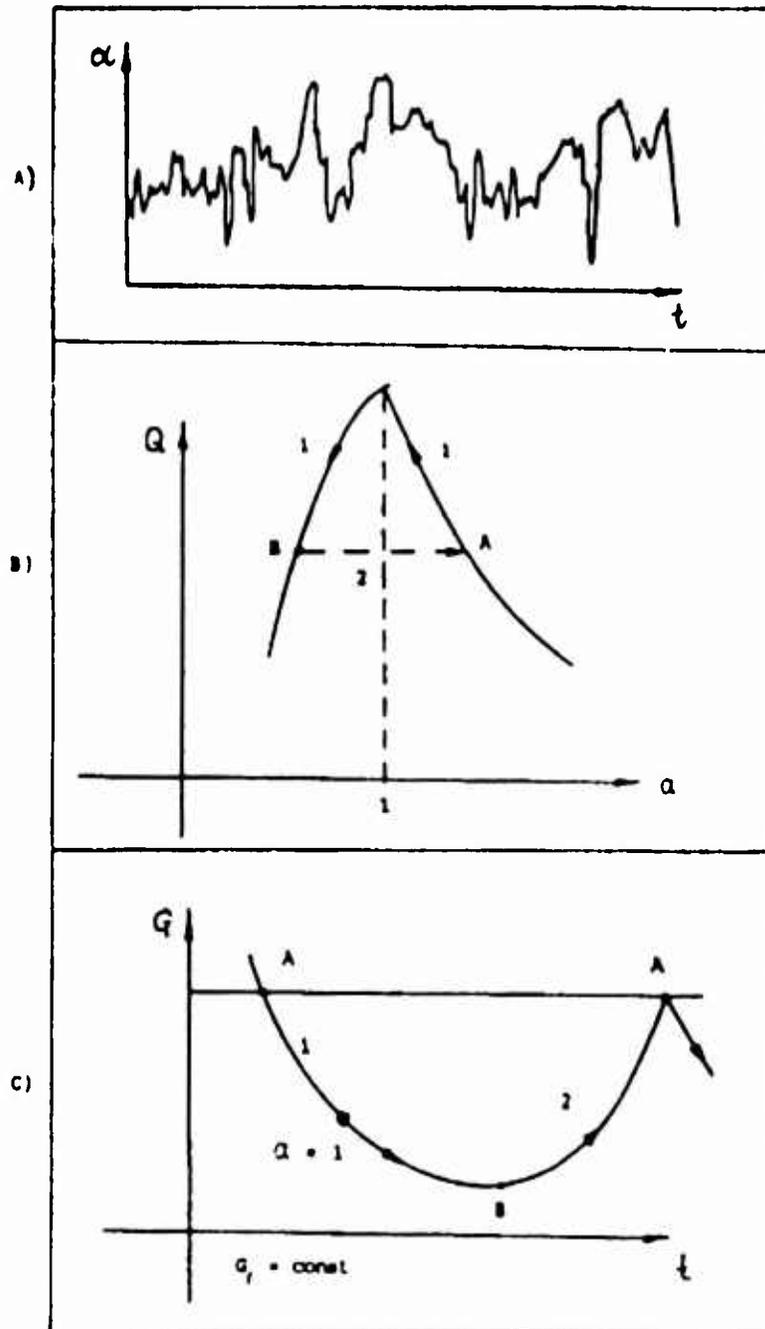
Fig. 3.12. Numerical simulation of self-excited in combustor, using near-stoichiometric air-fuel mixture.

a) Time evolution of air exess coefficient;
b) Mass heat combustion dependance on air exess coefficient;
c) The total airflow change during self-exited oscillation.
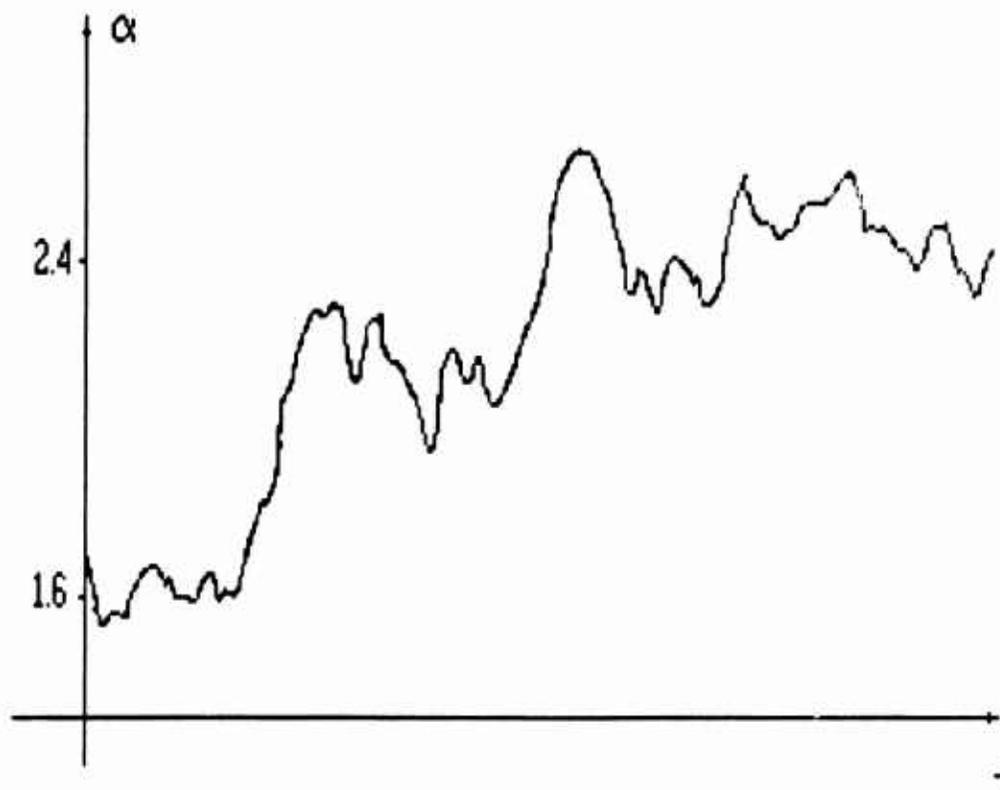
Fig. 3.13. The air excess coefficient change, induced by the shock wave, passing throw the ramjet.
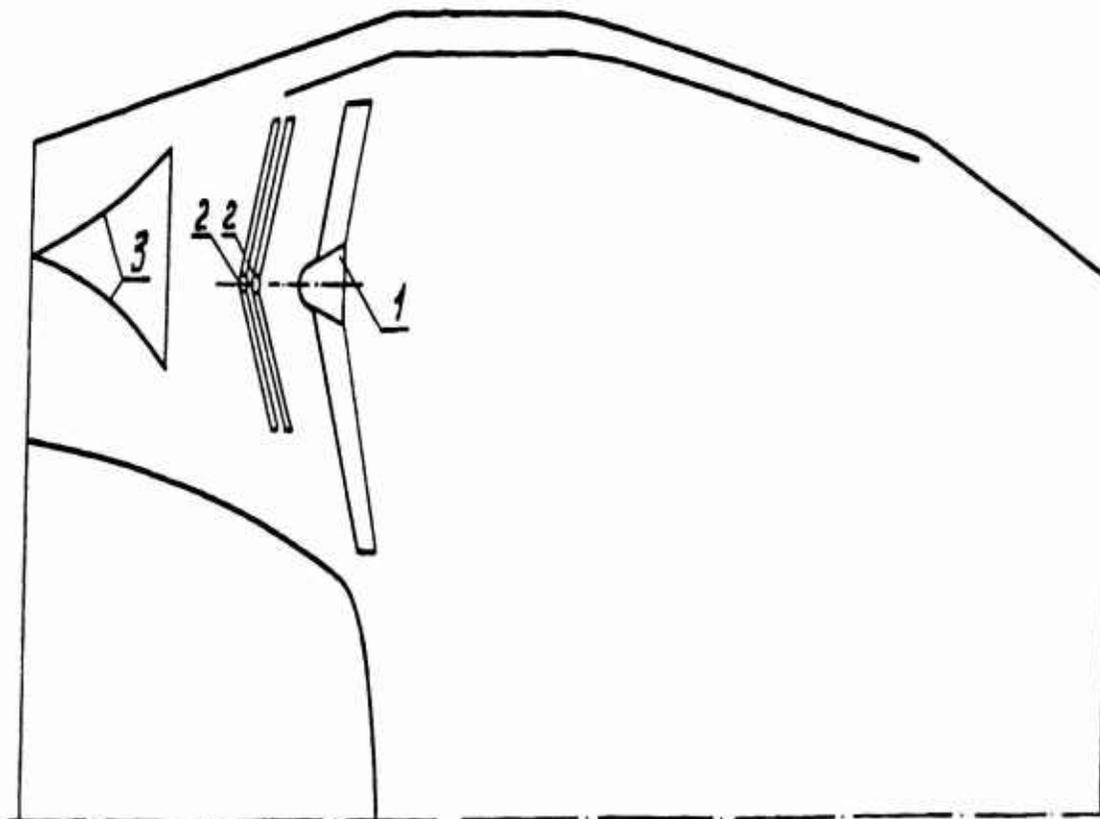
Fig. 3.14. Scheme of modern turbofan afterburner.
1 - flameholders, 2 - manifolds, 3 - flow mixing device.
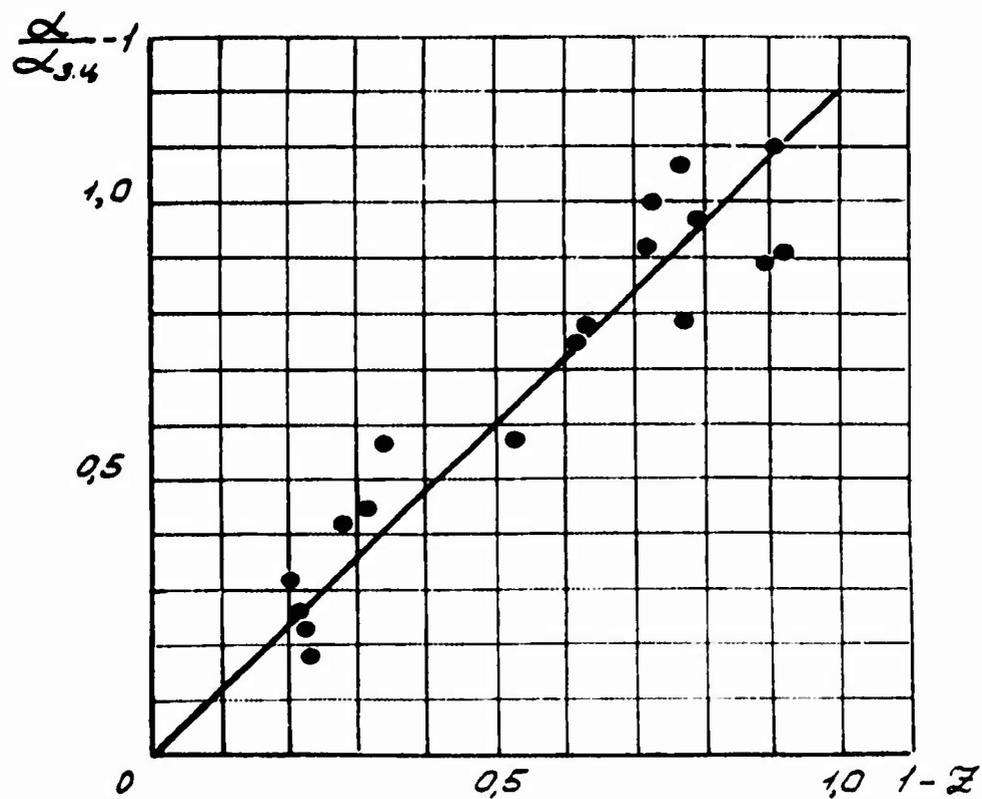
Fig. 3.15. Experimental dependence of air excess coefficient in recirculation zone on fuel vaporization level.
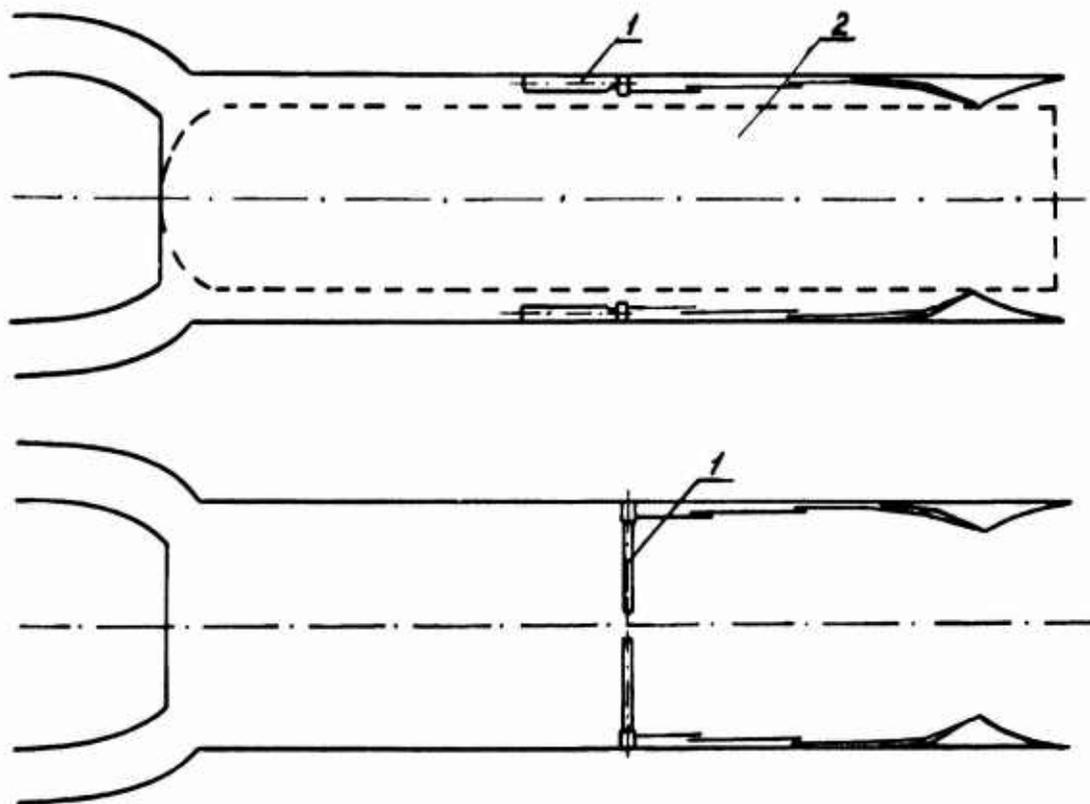
Fig. 3.16. Scheme of combustor of the ramjet integrated with a booster.
a - before booster ejection, b - after booster ejection;
1 - flameholders, 2 - booster engine.

A-A
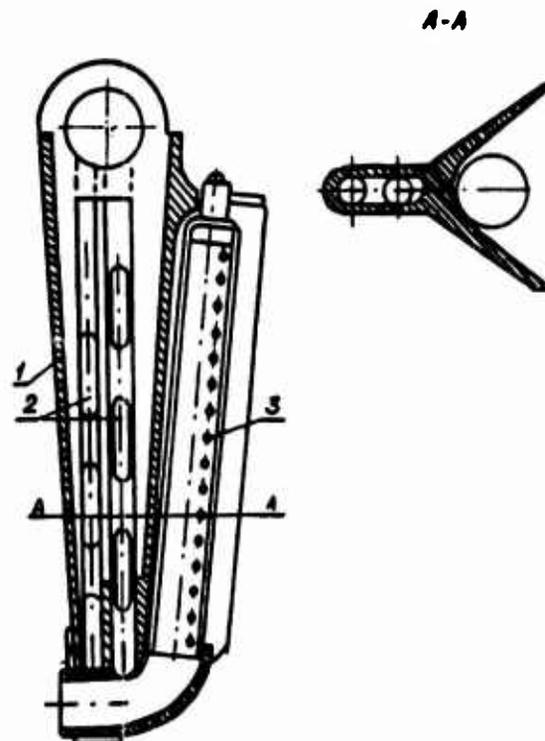
Fig. 3.17. Scheme of an folding radial flameholder with "carburator".
1 - flameholder, 2 - fuel manifolds,
3 - "carburator"
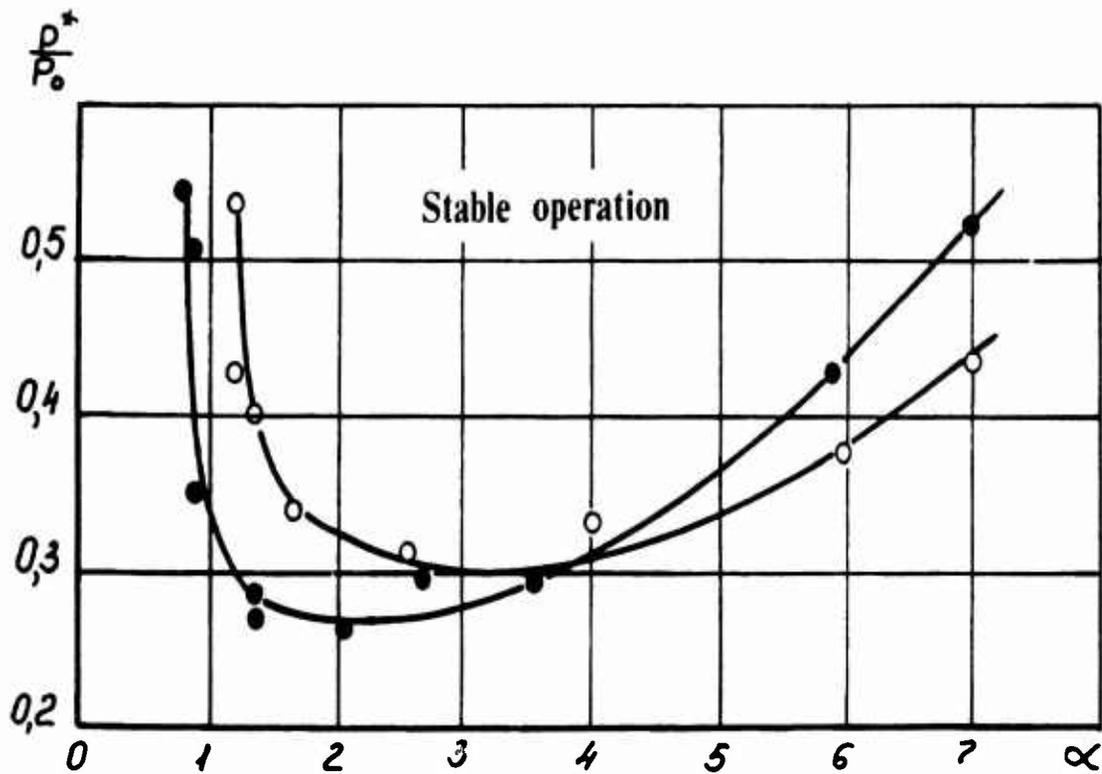
Fig. 3.18. The boundaries of stable combustion region in turbofan afterburner.

● - T_t = 770 - 820 K, λ = 0.15;
○ - T_t = 500 K, λ = 0.14 - 0.15.
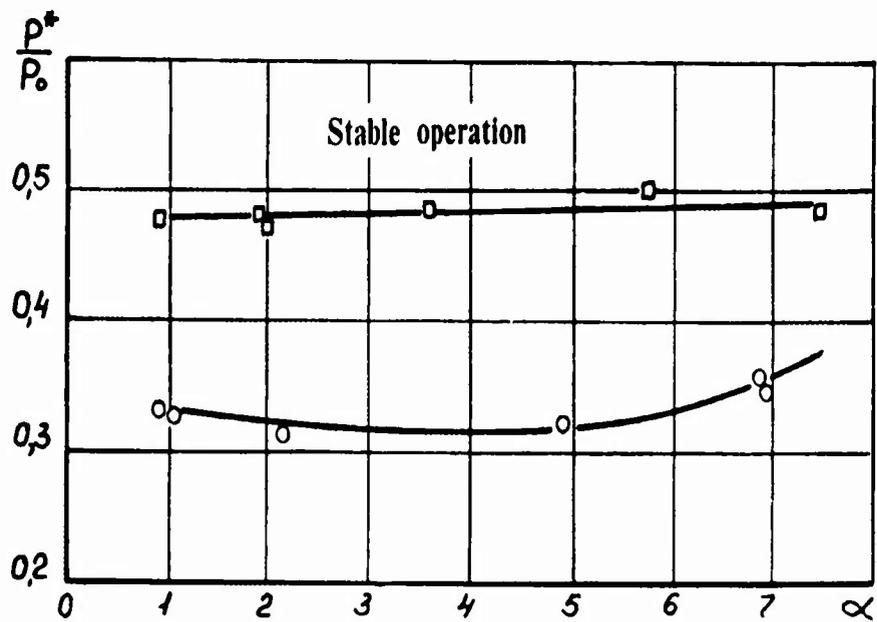
Fig. 3.19. The boundaries of stable combustion region in ramjet combustor.
O - T_t = 500 K, λ = 0.14 - 0.15;
□ - T_t = 360 K, λ = 0.15 - 0.16.
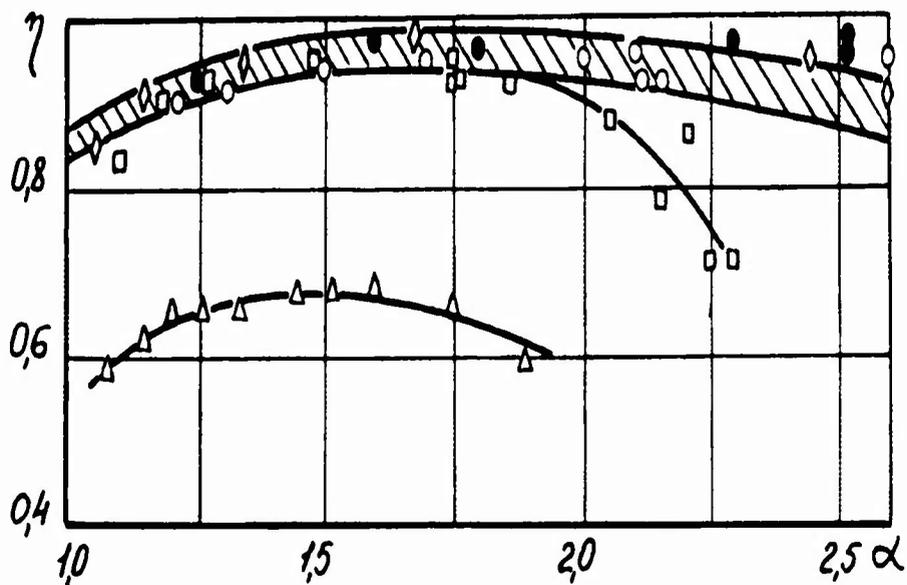
Fig. 3.20. Combustion efficiency of modern afterburners and ramjet combustors.

\\\ - afterburners, L_b/B = 10.5, T_t =600 - 850 K, P_t = 70 - 100 kPa, $\lambda \approx 0.15$.
Ramjet combustor, L_b/B = 9.5;

O - T_t = 990 K, P_t = 65 kPa, λ = 0.17 - 0.22;

● - T_t = 1170 K, P_t = 60 kPa, λ = 0.25;

◊ - T_t = 700 K, P_t = 50 - 60 kPa, λ = 0.2;

△ - T_t = 360 K, P_t = 300 kPa, λ = 0.2.

Fig 3.21. Control stages of SPRR/LFRJ.
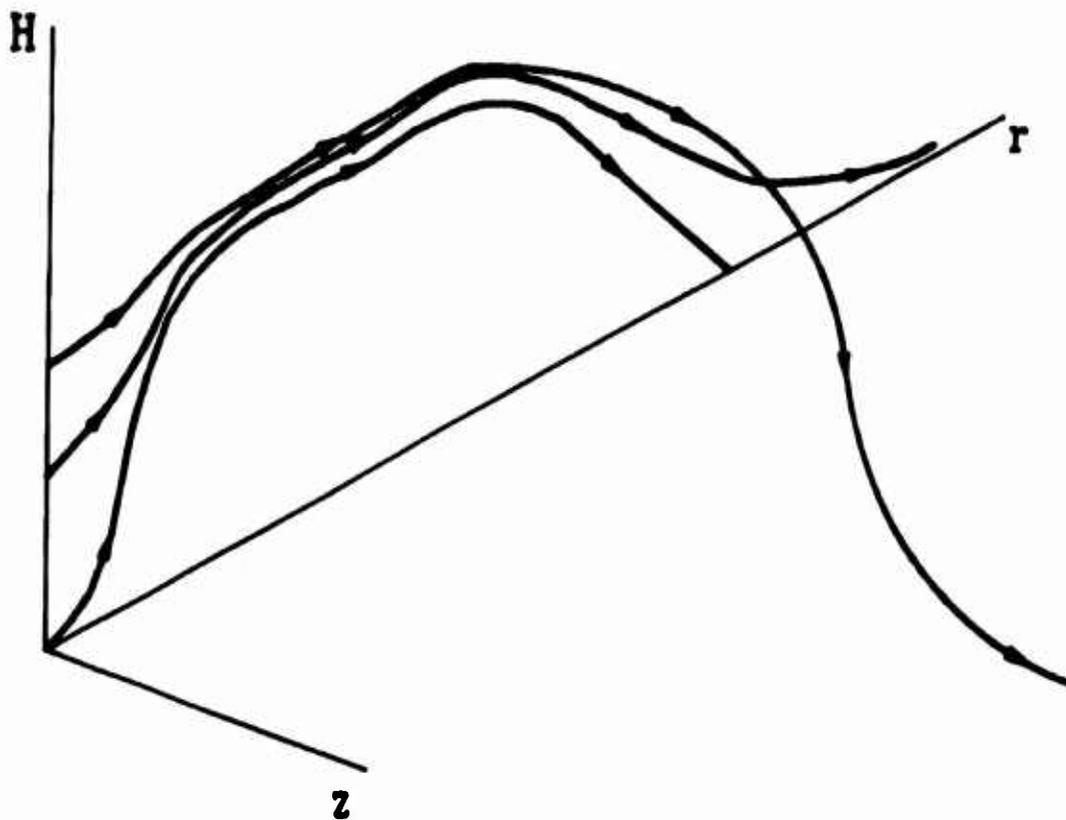
Fig. 3.22. Typical flight trajectories of air-surface missile.
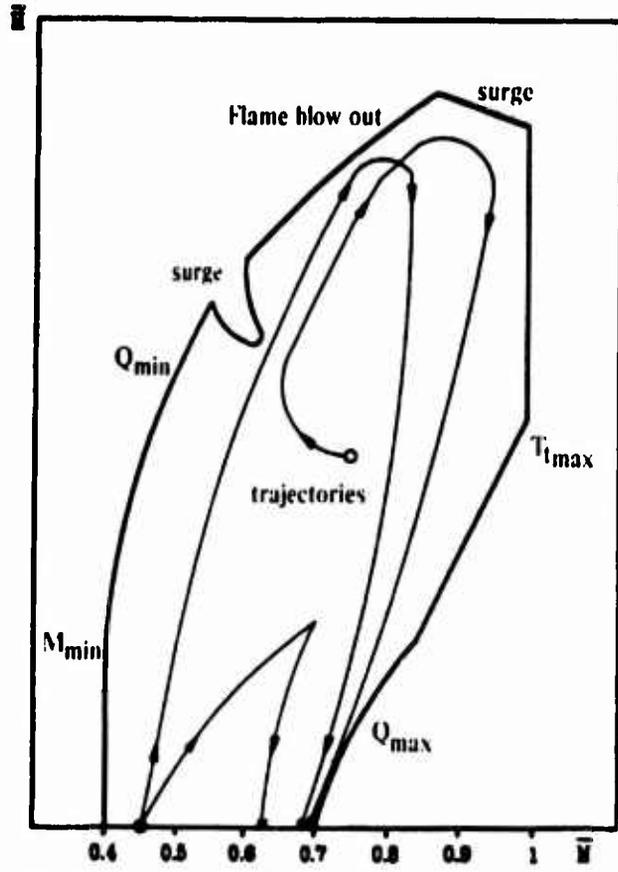
Fig. 3.23. Air-surface missile envelope with typical trajectories.

O - start, * - finish.
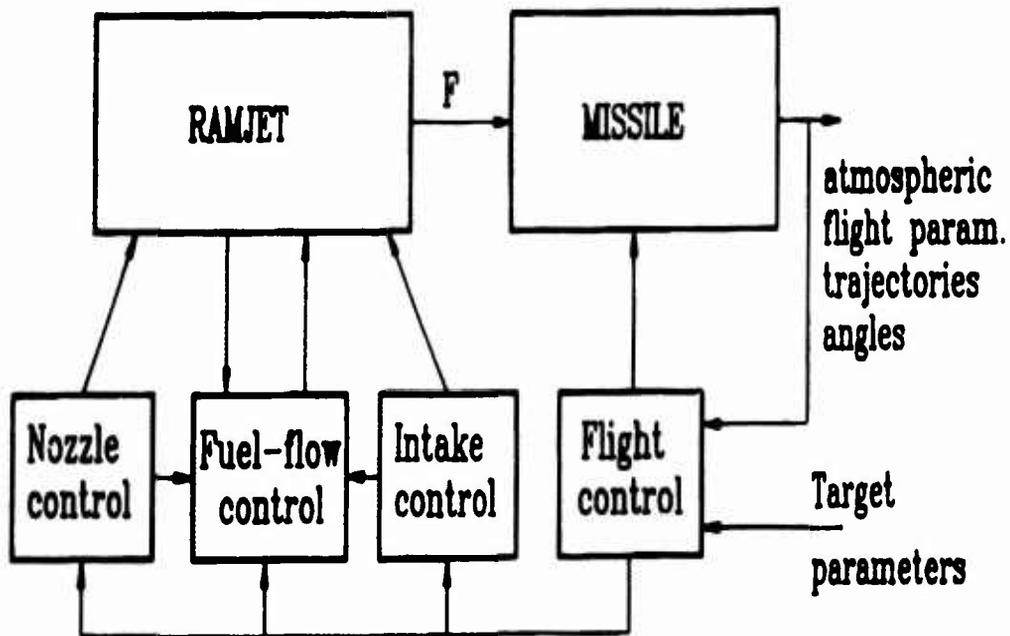
Fig. 3.24. Automatic control system diagram.
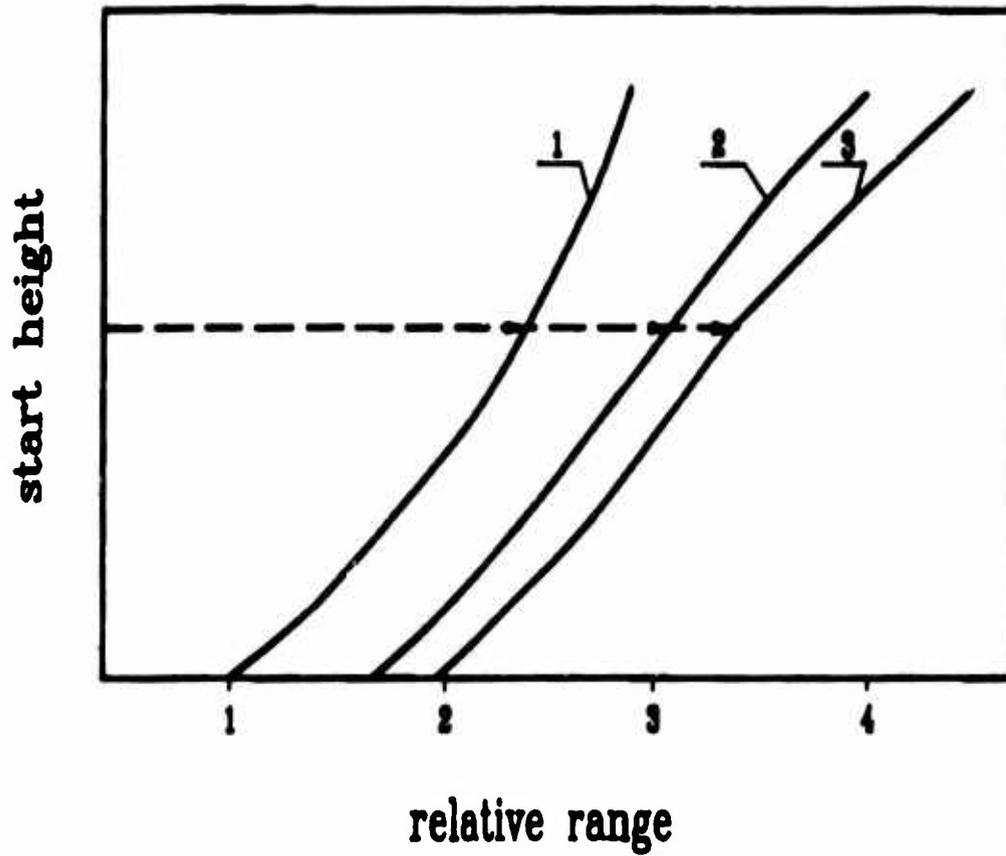
Fig. 3.25. Dependence of air-surface missile flight of the ramjet control complication, by different start height.

1. Fuel flow control.

2. Fuel+nozzle control.

3. Fuel+nozzle+intake control.

RESEARCH AND DEVELOPMENT OF RAMJETS/RAMROCKETS PART III. THE STUDY OF GASEOUS HYDROGEN RAM COMBUSTORS

by

Prof., D. Sc. V.A. Sosounov,
CIAM (Central Institute of Aviation Motors),
2, Aviamotornaya St.,
111250 Moscow,
Russia

SUMMARY

The peculiarities of H_2 ramjet turboramjet high efficiency ram combustors are discussed, which include some special questions, such as:

- flame stabilization behind nozzle edge;

- increase of number of nozzles and ram combustor length reduction;

- separate combustion without mixing of flames;

- uniform spread of fuel and air in chamber section;

- the experiment on model burner series;

- methods of effective H_2 combustion in short combustor.

NOMENCLATURE

A   - area;
d   - diameter;
G   - mass flow;
L   - length;
M   - Mach number;
N   - number of nozzles;
P   - pressure;
S   - distance between nozzles;
T   - temperature;
W   - speed;
β - equivalence fuel/air ratio;
δ - nozzle edge thickness;
η - fuel combustion completeness;
ρ - density.

INDICES

a   - air;
b   - combustor, combustion;
f   - fuel;
fl   - flame;
n   - nozzle.

ABBREVIATION

A   - air;
AB   - afterburner;
ABE   - air-breathing engine;
B   - combustor;
C   - compressor;
F   - fan;
FV   - flying vehicle;

GH_2 - gaseous hydrogen;
GH_2 T - gas (vapour) hydrogen turbine;
HE   - heat exchanger;
LA   - liquid air;
LH_2 - liquid hydrogen;
P   - pump;
R   - reduction gearbox;
T   - turbine;
TF   - turbofan;
TJ   - turbojet;
TR   - turborocket engine.

INTRODUCTION

Unique properties of hydrogen allow to study and develop a great number of new types of engines with complex thermodynamic cycles having a substantially better characteristics and parameters in comparison with the conventional gas turbine engines.

These unique properties of hydrogen enable to significantly improve the parameters and characteristics of the air-breathing engines:

- to increase the specific thrust (per 1 kg/s of air flow) by 1.5 - 2.0 times;

- to increase the specific impulse at maximal thrust by 1.2 - 1.5 times;

- to increase thrust/weight ratio by 1.5 - 2.0 times;

- to increase the maximum speed use of the gas turbine engine by using of cooling capacity of LH_2 till M_{max} = 5-7.

These advantages are gained in different types of the LH_2 - ABE. At present in different countries and companies there is under way an extensive work for searching of the optimal types of the LH_2 - air-breathing engines suitable for the initial acceleration phase of the aerospace system - the third generation of space vehicles. This significant theme is not a main subject of that report. Therefore one may confine to the demonstration of some ABE proposed by a number of engineers and companies and using the cooling and energy capacity of the hydrogen or both these properties (Fig. 4.1). Morphological research by Zwicky [1] shows that such types of the LH_2 - ABE can be more than 10000. Using

the liquid oxygen if it is abroad permits additionally to improve thrust and weight of the turborocket engines.

All of LH$_2$ - ABE, which are developed for high Mach numbers flight vehicle, have reheat or ram combustor chamber (for example, turboramjet engine for Zänger). The operational behaviour of H$_2$ combustion chamber is significantly differ from ram combustors, using liquid or solid fuels.

1. MAIN PROBLEMS

There are considered ABE designed for subsonic and supersonic FV. The special problems for scramjet are not discussed further.

Liquid hydrogen in tanks as a result of cooling of hot engine components or in special heat exchangers must be gasified and enters the combustion chamber as a gaseous state.

The experiments shows that the effective burning of the hydrogen in the primary combustion chambers of the gas turbine engines (ahead of the turbine) presented no special problems: it is necessary to increase the air supply to the primary zone of the chamber and to ensure an intensive mixture of the hydrogen with the air, for example, with the help of the swirling of these component flows in the injectors and combustor domes.

A wide range of problems is posed while burning the hydrogen in the reheat and ramjet direct-flow combustion chambers of a small length (Fig. 4.2). Such combustors are specific to reheated turbojet and turbofan engines and also to high-speed ramjet, turboramjet and turborocket engines with subsonic speed of the air and the gas in the ram combustors. In such chambers there occurs the diffusion combustion of the hydrogen flowing out of many nozzles as opposed to the burning of the homogenized mixture of the kerosene with the air in the conventional combustion chambers.

Research series of the burning of the hydrogen in such combustors carried out in CIAM by the author together with collaborators [2, 3, 4, 5] found out the conditions the hydrogen flame stabilization at the nozzles and also the possibilities of nozzle number increase to reduce the combustor length in the event of isolated combustion without confluence of flames. While meeting these conditions the reheat and ramjet combustion chamber using the hydrogen can be made 2 - 2.5 times as short as a combustor using the kerosene.

2. STABILIZATION OF THE HYDROGEN FLAMES

The first problem is a stabilization of the hydrogen flames at the nozzles (Fig. 4.3). The experiments in the open air flow showed that the nozzles must have a sufficient edge thickness to realize the condition of the flame stabilization in the recirculation zone (RZ) behind the edges, namely the time of air-fuel mixture staying in it must be more than the time of burning. Obtained in the experiment the relationship generalized in correlating parameters, shows that stability of the hydrogen diffusion flame is well above than of methane flame. Received dependencies allow to select the required area ratio of the fuel nozzles and its edges thickness to obtain the stabilization of the hydrogen flame in the required operating range.

3. RELATIVE HYDROGEN FLAME LENGTH

There are examined the variations of the relative hydrogen flame length L_n/d_n from the speed ratio of the air to fuel W_a/W_f in the open air flow (Fig. 4.4).When the nozzle edge thickness is equal to 0, the maximum flame length is observed following the theory of G N Abramovich [6] at W_a/W_f = 1. With the finite nozzle edge thickness the flame length decreases continually with the air speed increasing that is related to more intensive hydrogen burning in the recirculation zones. The rate of decreasing in the flame length growth with the relative edge thickness increasing.

One can obtain the generalized relationship of the relative flame length on the complex parameter involving the speeds and densities ratio of air and fuel at the finite nozzle edge thickness (in Fig. 4.4 below, left).

4. FUEL NOZZLE NUMBER

It is known [2] the idea about the diffusion flame reduction with fuel nozzle number increasing. In this case at the same fuel flow the flame length L_n as against that of a single flame L_n^* decreases with

$$L_n = L_n^* / \sqrt{N_n} \qquad (1)$$

where N_n - is a nozzle number (Fig 4.4, right).

This dependencies used for designing the combustion chambers. However, nozzles in pylons must be located so that the flames did not interact with each other and did not confluent into one common flame (Fig. 4.5).

The minimal critical distance between nozzle axes S^* was determined by experiment. This distance decrease with increasing of the relative air speed and the nozzle edge area.

5. HYDROGEN COMBUSTION CHAMBER-NOZZLE SYSTEMS

In Fig. 4.6 are given the results of the experiment on a model burner having some lateral fuel manifolds located in one plane or separately. The number of the nozzles in the manifolds is varied as well as an inclination of their axes. Spacing between the nozzles met the requirements $S > S^*$. The separate disposition of manifolds with an axial fuel feed proved to be best in combustion efficiency and hydraulic resistance (burner 3).

In accordance with the relationship (1) one may introduce the concept of the <u>equivalent relative length of multi-nozzle chamber</u> $\overline{L}_h^*$. This length resembles the relative one of a single nozzle chamber of the same length L_h and diameter d_{heq} [2] in the combustion efficiency

$$\overline{L}_h^* = \frac{L_h}{d_{heq}} = \frac{L_h}{2}\sqrt{\frac{N_n \pi}{A_h}} \qquad (2)$$

By means of the parameter $\overline{L}_h^*$ one can compare the chambers with different nozzle number such that $\overline{L}_h^*$ can be varied both by chamber length L_h or the nozzle number N_n.

The combustion efficiency η, derived from the heat combustion Hu, depends on the equivalent chamber length and fuel-air ratio β. One may select on the basis of the experimental data the type of the function $f(\beta)$ at which the parameter $Z \sim \overline{L}_h^* f(\beta)$ will define a unique fashion of the combustion efficiency η. The function $f(\beta)$ has a different form at $\beta < 1$ (air excess) and $\beta > 1$ (fuel excess). Obtained in such a way the generalized relationship of burning completeness of hydrogen (Fig. 4.6) enables to estimate by calculation the combustion efficiency characteristic at a different number of the nozzles or chamber length, namely at $\overline{L}_h^* = $ var (Fig. 4.6 on the right). Here is shown the combustion efficiency η, determined from the maximally possible heat generation, therefore at $\beta < 1$: $\eta^* = \eta$ (left part), and at $\beta > 1$: $\eta^* = \eta\beta$ (right part).

These data show the possibility to achieve very high H_2 combustion efficiency. In the usual operation region $\beta = L_0 G_f / G_a = 0.2 - 1.0$ by using the special nozzle devices with great number of nozzles i.e. by long equivalent relative combustor chamber (2) the experimentally achieved value of η were 0.9 - 0.99 in an absolutely short combustion chamber.

CONCLUSION

The results of investigation of hydrogen combustion chamber give us the methodology of developing a short combustion chambers (decreasing of length more than two times) with stable operation in wide region of fuel/air ratio, the possibility of developing of CDF-codes and design engine with hydrogen ram combustor.

REFERENCES

1. F. Zwicky Morphology of Propulsive Power. Monographs on Morphological Research, № 1, Society for Morphological Research, Pasadena, Calif., 1962, 382 pp.

2. V.A. Sosounov. Some problems concerning optimal ducted rocket engine with secondary burning. Proceedings of the 2d ISABE, 1974.

3. Ю.М. Аннушкин, Г.Ф. Маслов Е.Д. Свердлов. Стабилизация горения диффузионного факела водорода в спутном потоке воздуха. Новосибирск, АН СССР. Физика горения и взрыва, № 6, 1983, сс. 14-20.

4. Ю.М. Аннушкин, Е.Д. Свердлов. Закономерности изменения длинны диффузионных пламен газообразных топлив в спутном потоке воздуха. Новосибирск, АН СССР. Физика горения и взрыва, № 3, 1984, сс. 46-51.

5. V.A. Sosounov, Yu.M. Annushkin, E.D. Sverdlov, D.G. Pagy. Investigation of hydrogen diffusion flames in direct-flow combustors. Hydrogen Energy Progress. VII Proceedings of the 7th World Hydrogen Energy Conference. Vol. 3. Pergamon Press, 1988, pp. 2009-2024.

6. G.N. Abramovich. The theory of turbulent jets. Trans. from Russian. The M.I.T. Press, Cambridge, Massachusetts, 1963.
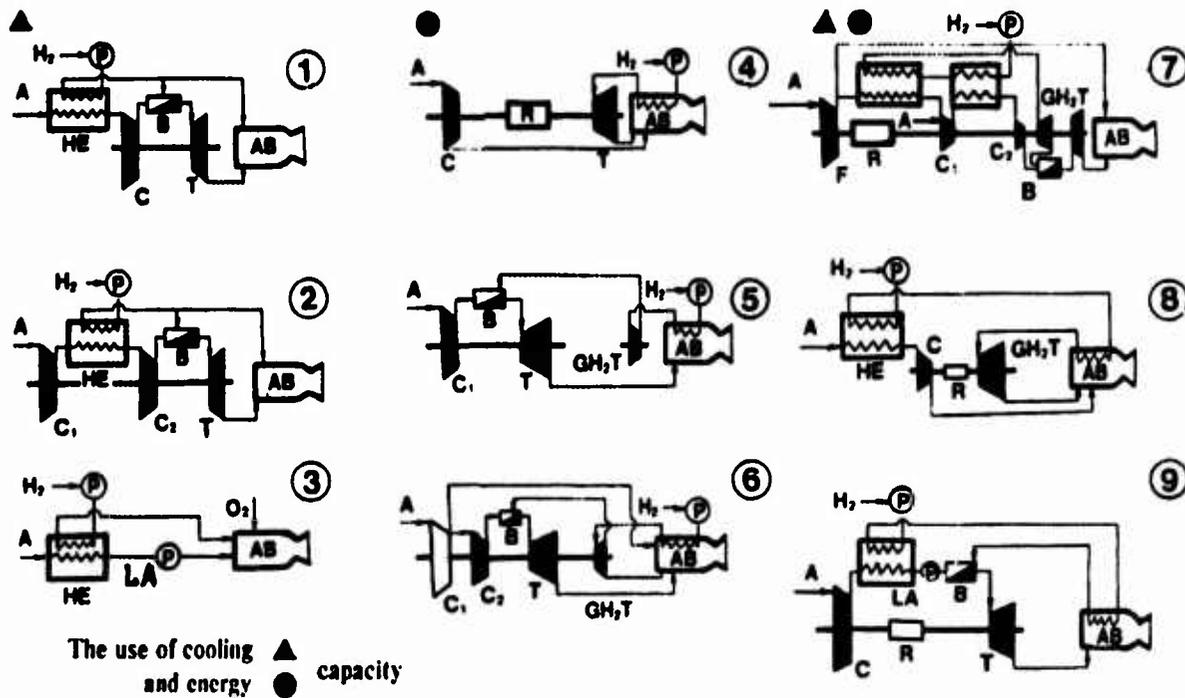
Fig. 4.1. New types of LH$_2$ air-breathing engines.

1- TJ with precooling; 2 - TJ with intercooling; 3 - liquid rocket engine whith air liquefaction; 4 - turborocket engine (TR) with a gaseous hydrogen turbine GH$_2$T; 5 - TJ with GH$_2$T; 6 - TF with the GH$_2$T; 7 - TF with the intercooling and GH$_2$T; 8 - TR with precooling; 9 - TR with air liquefaction.

$$L_{r.ch.JP} = (2 - 2.5)L_{r.ch.h}$$
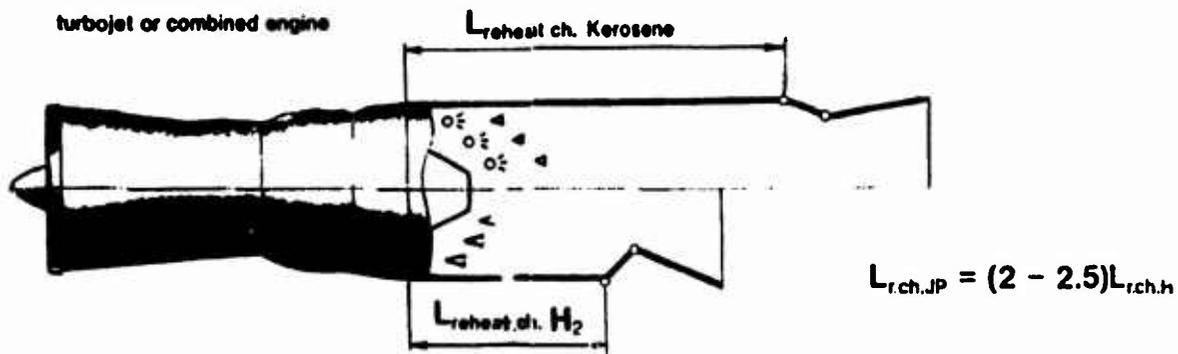
● JP – homogenized mixture combustion
● H$_2$ – gaseous fuel diffusion combustion

Problems
– flame stabilization behind nozzles edge
– ignition and flame spread in all nozzles
– increase of number of nozzles and reheat chamber length reduction
– separate combustion without mixing of flames
– even spread of fuel and air in chamber section

Fig. 4.2. Implementing the burning in reheating and ramjet combustion chamber.

Fig. 4.3. Hydrogen flame stabilization.

$$K_S = \frac{W_\beta}{\delta P_a T_a}$$
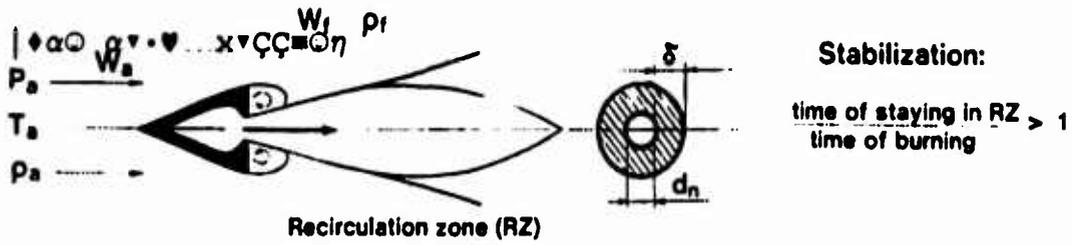
Hydrogen:

● **Reliable stabilization of burning on edges**

● **Broad range of burning without flameout**

▶ **Selection of required nozzles edge thickness**

Stabilization:

$$\frac{\text{time of staying in RZ}}{\text{time of burning}} > 1$$

Recirculation zone (RZ)
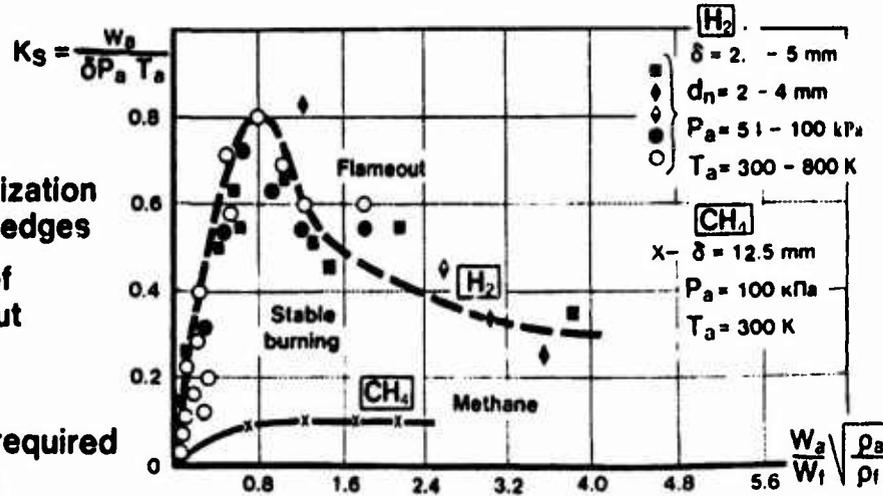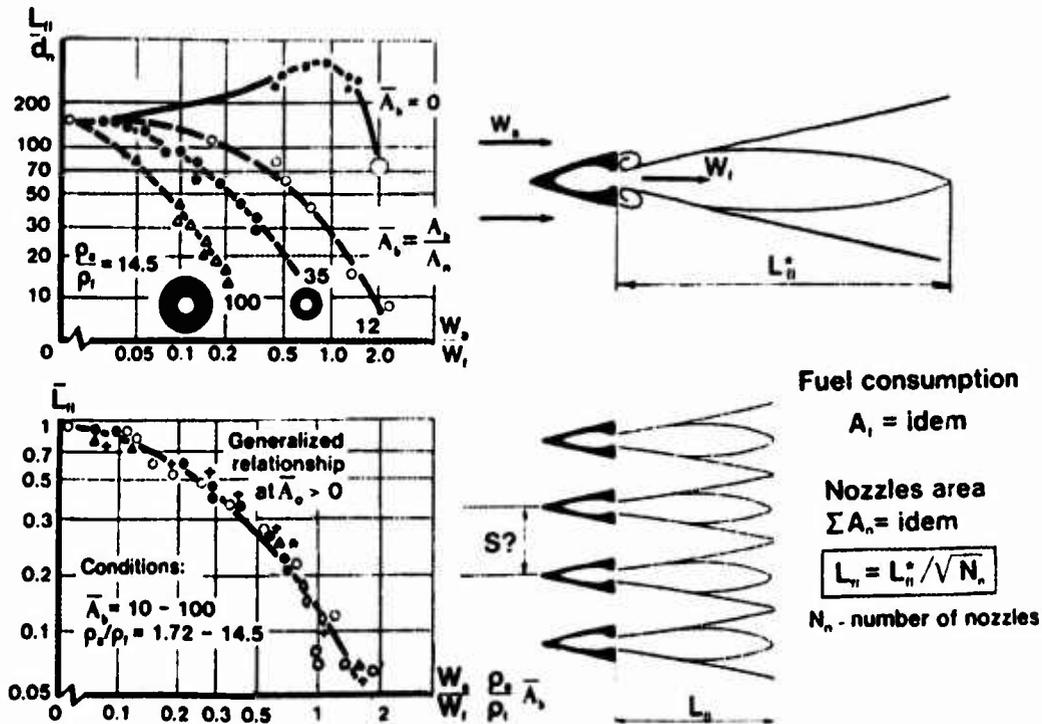
Fig. 4.4. Hydrogen flame length in an open air flow.

Fuel consumption

$A_t = $ idem

Nozzles area

$\sum A_n = $ idem

$$L_n = L_n^* / \sqrt{N_n}$$

N_n - number of nozzles
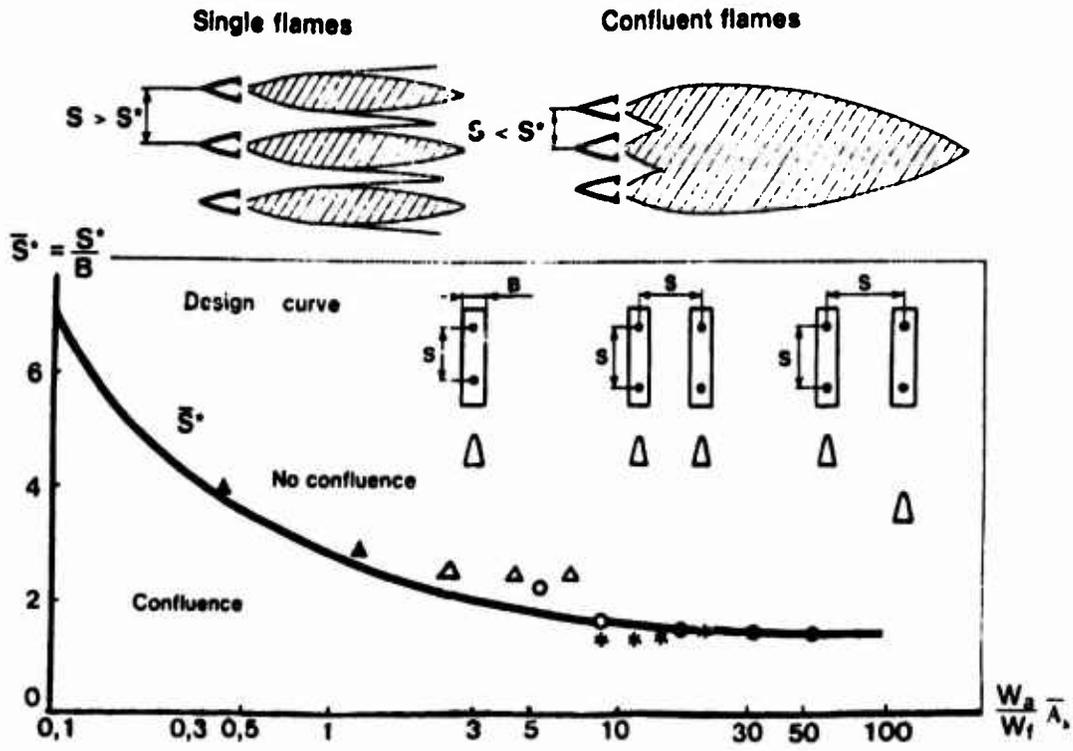
Fig. 4.5. Disposition of nozzles in pylons.
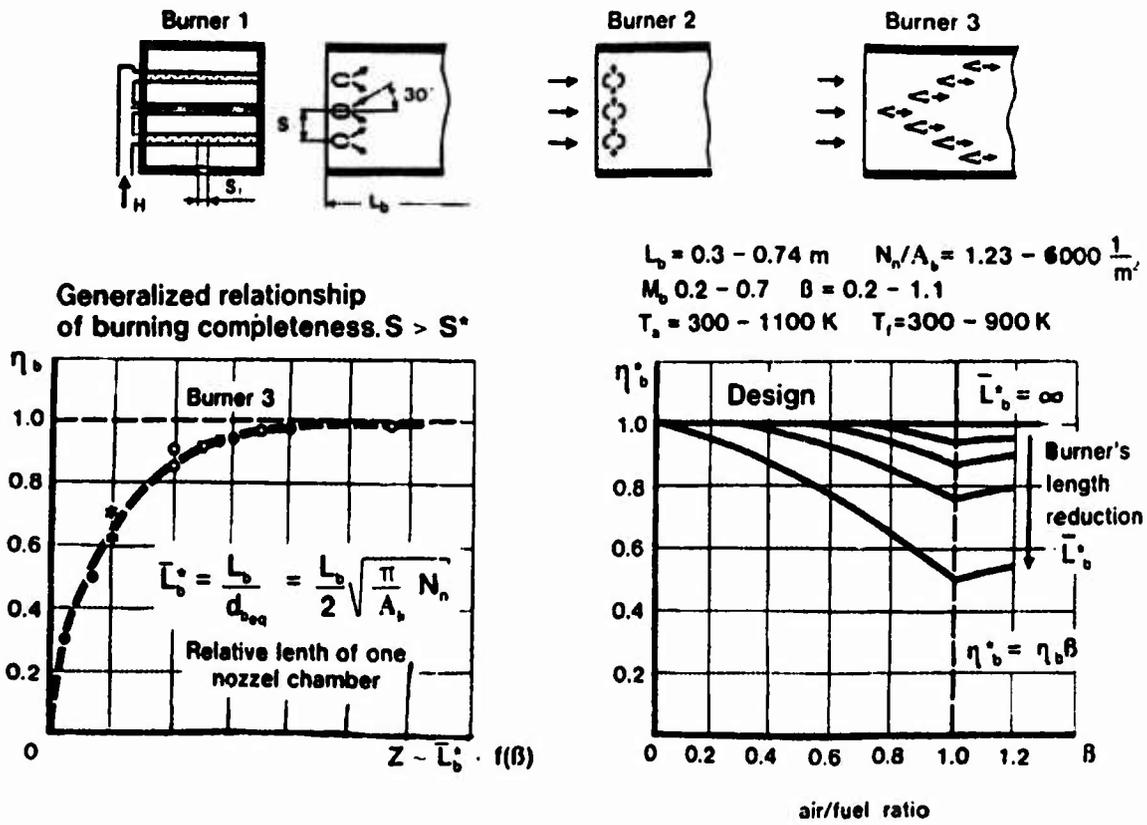
Fig. 4.6. Experimental investigations of model burners.

CIAM EXPERIMENTAL TURBORAMJETS

by

Dr M.M.TSKHOVREBOV
V.I.SOLONIN . P.A.KADJARDOUZOV

CIAM (Central Institute of Aviation Motors)
2, Aviamotornaya st.,
111250 MOSCOW,
RUSSIA

ABSTRACT

In this report some results of the TRE operating process including those performed on specially developed demonstrator engines are considered. Essential technical requirements and design features of the experimental TRE designed and developed at CIAM for investigatory study on a test bench are shown. Test facilities for experimental investigations of TRE in "connected tube" manner and experimental work technology features are presented. Some results of the CIAM TRE experimental study including engine parameters on changing to ramjet operation mode variation, working parameters in the windmilling (ramjet) mode of operation, and flow characteristics in the afterburner-ramjet combustion chamber are shown. A TRE based on TF parts characteristics matching on changing to ramjet operation mode and engine working parameter variations when going to windmilling in the ramjet mode are discussed.

NOMENCLATURE AND ABREVIATIONS

A	- area.
Ard	- TRJ outer duct area.
ABE	- air-breathing engine.
ARCC	- augmented-ramjet combustion chamber.
a	- air - to - fuel stoichiometry ratio coefficient.
$b = \dfrac{m}{m+1}$	- relative airflow in RJ duct or TF outer duct.
C	- flow absolute velocity in compressor or turbine flowpath.
FV	- flight vehicle.
fin	-ratio of free stream cross section area to inlet area.
k	- adiabatic exponent.
M	- Mach number.
Mx	- flow M at the ARCC inlet.

m	- bypass ratio.
N	- RPM.
P	- pressure.
Pa	- ambient air pressure.
PS	- propulsion system.
PRC	- compressor pressure ratio.
q	- dynamic pressure.
RJ	- ramjet engine.
R	- gas specific work.
SFC	- specific fuel consumption.
Sin	- intake recovery coefficient.
T	- temperature, K.
T	- engine thrust.
Ta	- ambient air temperature.
t	- time.
TF	- turbofan engine.
TFRJ	- turboramjet with TF as a core.
TFRJs	- TRE with TF as a core and bypass ARCC.
TJ	- turbojet engine.
TRE	- turboramjet engine.
TRJ	- TRE with TJ as a core.
TRJs	- TRE with TJ as a core and bypass RJ combustion chamber.
Vx	- flow velocity at ARCC inlet.
	- mass airflow.

SUBSCRIPT

a	- ambient air.
c	- compressor.
col	- cooling system, air.
cor	- corrected parameters.
ex	- exit.
f	- fan.
g	- gas, turbine inlet.
in	- intake, inlet.
m	- mean value.
n	- nozzle.
oil	- oil.
r	- ARCC, reheat.

rd	- Ram duct.
s	- screen.
t	- total parameters.
u	- tangential component.
v	- flight conditions.
w	- windmilling mode.
x	- ARCC inlet.
o	- sea level static conditions.
*	- throat; critical

*) Dr., Senior Scientist, Head of Division. **) Dr., Senior Scientist, Head of Department. ***) Dr., Senior Scientist.

parameters.

INTRODUCTION

In the second half of the fifties in connection with the successful launch of the first Earth satellite there was a significant growth of interest in advanced high supersonic and hypersonic flight technology. CIAM began fundamental studies of combined ABE whose operation process is based essentially on evolution of the concept of the bypass engine with reference to flight conditions at high supersonic speeds. At the same time the foundation of their theory was laid.

Studies were conducted on a variety of TRE types based on TJ and TF as a core and useful fields of application were determined. For the first time, methods of engine configuration selection were determined, which is essential in the case of the TRE for optimum matching of the parameters of gas gas turbine and ramjets. A theory of TRE operation was developed when switching from one operation mode to another, operation in ramjet mode at maximum flight speed under conditions of high kinetic heating, including the modes with turbofan (turbocompressor) windmilling. The extensive theoretical research into turboramjet performances, structures and application possibilities was carried out before experimental work began.

Bench tests of experimental full-scale turboramjets were carried out at CIAM in the 70-s [1]. For experimental work the TRE types on the basis of TJ (with common ARCC) and TF (Fig.1) were chosen.

Investigations into real operation and performance of the TRE were conducted within the programme of development, together with test bench studies of several versions of full-scale TRE demonstrators, created in production TJ's. There were studied Performances on switching for various operation modes, in the ramjet mode, with cooling of the heat stressed components; also studied were the operation conditions of rotor supports etc. For the first time tests were conducted on an experimental TRJ under simulated flight conditions at M = 3 - 4 (Tin = 300 - 600 C) over a long period (several hours) [1].

All these investigations were intended for development of a cruise mission FV using kerosene. However, the results obtained and the Russian experience of liquid hydrogen use [2] open up possibilities for development of TRE for FV using liquid hydrogen as fuel.

Experimental demonstrator engine investigations are part of an advanced power plant design methodology created in CIAM - the national scientific centre of the engine industry. CIAM carries out scientific supervision of the work conducted in engine and accessories design bureaus and related research institutes [1]. The principle of this methodology, which assumes stage-by-stage development,

consists of building a scientific-technical base prior to the engine development phase. This principle includes development of new construction materials and technologies, design and testing methods, design and development of experimental parts, components, gas generators, engines with gas-dynamic, duration and cyclic testing. Although this initial phase is characterized by relatively low costs with respect to the total programme it is however very important in providing new engine high quality and efficiency (Fig.2). Application of the methodology favours aircraft and engine development matching.

CIAM has the largest rigs to investigate engines and their components in altitude conditions. The unique experimental base of CIAM allows performance of comprehensive tests of engines of practically any thrust and power.

As an example of an up-to-date powerful facility for investigation of supersonic engines there is an altitude facility with a multimode generator of flow disturbances at engine entry, an automated system for monitoring experimental processes, up-to-date means of data processing (Fig.3), which enable the investigation of non-uniform flow effects on engine performance under conditions closest to those in flight at steady-state and transient regimes. The facility imitates the flight dynamic conditions along the trajectory, simulating non-uniformity of pressure distributions and pulsations at engine entry which correspond to inlet operation at different angles of attack and slip [3].

Some results of the TRE operating process experimental investigations are presented below [4,5, 6,7,10].

1. EXPERIMENTAL TURBORAMJETS AND SPECIALIZED TEST CELL

Investigations into real operation and performance of the TRE were conducted at CIAM as part of the programme of development and test bench studies of several versions of full-scale TRE demonstrators, based on production TJ's and their parts. The experimental TRJ was developed on the basis of two TJ and AB engines of the R-11-300 family (Fig.4) [5].

To provide a simple solution to the problems of maintain ability, service, preparation, manufacturing, and controlling the unified ram-duct with a shut-off device with remoted control was used. The ram-duct consists of front and back manifolds and four connecting side tubes; replaceable after-turbine nozzles which provided different exit turbine areas were used (Fig.5).

During the TRJ heat state problems study the ARCC was equipped with a perforated screen along its length, a distribution system of manifold fuel supply and a separate air cooling system. This cooling system could provide variable parameters of cooling air (Wcol, Pcol, Tcol) to the cooling duct i.e. into the space between the external case and the perforated screen of ARCC. The bearing supports of TRJ were reconstructed too. To provide operability of engine transmission, thermo-protective screens were located over support cases. Air cooling system with variable parameters (Wcol, Pcol, Tcol) and oil system with variable oil feed were used for bearing support cooling.

The main goals of the experimental research were as follows:

- complex study of operation process;
- afterburning ramjet combustor operation;
- engine switching modes and operation stability;
- windmilling and ramjet operation mode characteris- tics;

- passage hydraulic characteristics;
- power output possibilities;
- ramjet combustor and nozzle cooling at $M = 3.5-4.5$;
- cooling system impact on operating parameters;
- structure heat state and transmission operability.

Tests on experimental TRE engines were conducted at the facility with an attached air pipeline, with the air parameters behind the inlet reproduced at the engine entry (Fig.6). The maximum entry air temperature realised at the facility corresponds to approximately $M = 5$. It is provided by heat exchanger and flame heaters (with recovery of normal air composition by oxygen replenishment) and, in case of need, may be increased. Air pressure at entry reaches 900 kPa. The facility has several hundred channels for temperature and pressure measuring in static and dynamic modes. The facility dimensions allow testing of any current supersonic engine. This cell was also equipped with an injector exhaust system. The test facility was equipped with separate controlled air cooling and oil systems.

The parameters of air flow at the engine inlet were changed in the range:
- $Ptin = 0.1...0.2$ MPa,
- $Ttin = 270 - 900$ K.

The variable parameters of cooling air for ARCC cooling were changed in the range:

- $Ttcol = 400...900$ K,
- $Ptcol/Ptr = 0.95...1.40$,
- $Wcol/Wxin = 0.03...0.23$.

The bearing cooling air pressure was varied in range up to 0.5 MPa and oil pressure on entrance to bearing supports was changed in the range:

- Poil = 0.16...0.22 MPa.

The air mass flows through ram-duct and ARCC cooling air tube were controlled by changing the shut-off device damper angles. During the experimental investigations measuredthe following parameters :

- total and static pressures and total temperature at the engine inlet;
- total/static pressures and total temperature at the compressor inlet and outlet, at the turbine outlet;
- total and static pressures in the ARCC and in ARCC cooling duct;
- total and static pressures in the ram duct;
- total and static pressures and temperature at the outlet section of both engine parts ducts;
- total temperatures in both the ARCC and the cooling air streams;
- wall temperature of perforated screen along its length;
- cooling air flows through both the cooling duct and the bearing supports;
- temperatures of bearing support cases;
- cooling air temperatures at entrance and exit of supports;
- oil temperatures at entrance and exit of supports;
- oil flow through bearing supports;
- engine rotational speed and some other parameters.

The layout of the engine and ARCC preparation is shown in Fig.6. Engine continuous operation time at M =4...4.5 was about 3 hours.

2. THE EXPERIMENTAL INVESTIGATIONS OF TRJ TRANSITION TO RAMJET MODE

The transition from gasturbine to ramjet mode (also windmilling mode) is of great interest for TRJ. The first part of tests were directed just to these modes [6]. Some results of these investigations will be discussed. The rational value of flight speed for transition to ramjet mode depends on the design operating parameters, the TJ control mode and the size correlation between typical propulsion system duct areas. The transition Mach number is usually in the range 2.5 - 3.5 [8].

The working lines on the compressor map for different modes of operation are shown on Fig.7. The gasturbine mode corresponds to the curve A. The joint operation of TJ and RJ is realized in the transition mode. In these conditions the pressure behind the turbine is greater than that at the ram-duct entrance. If the shut-off device opens, the control system of TRJ must respond in such a way

that stable operation of the inlet and the engine is ensured [4].

The RJ starting mode corresponds to zero air flow through the ram-duct. The curves B and C (Fig.7) correspond to this mode for different values of turbine exit duct area (this area for curve C is bigger than one for curve B). A certain engine nozzle throat area at the selected turbine exit corresponds to this condition. The region above the curves B and C corresponds to the reverse flow of the gas part from behind the turbine to the entry of the engine. Such reverse flow occurs if the engine nozzle throat area An * is less than the value An*o corresponding to the curve Wrd = 0. With lower values of An* unstable operation of TRJ and propulsion system is possible. The points below the curves Wrd = 0 correspond to the direct air flow through the ram-duct. Such flow occurs if the engine nozzle throat area An* is bigger than the An*o. If An* is increased additionally, there is an increase of air flow through the ram-duct at practically the same air flow through TJ. The experimental points in the joint operation mode are located nearly the curves B and C.

At definite values of corrected RPM the curves Wrd = 0 cross the curve A and approach the compressor stall curve. But usually for TRJ the corrected RPM for the transition to RJ-mode is located right of the curve crossing point. Therefore, an error of control at the start of RJ (the shut-off device prematurely open) presents a danger rather for stable operation of the inlet (Fig.8). As follows from the Figure, the forestalling shut-off device opening leads to lowering of the TJ inlet corrected airflow with corresponding consequences. This was confirmed by tests of TRJ [5].

The rational control of an engine on transition to RJ-mode process must provide not only stable operation of the propulsion system but also thrust onset without significant drops.

Investigations have revealed a rather narrow operation interval, inside which a stable working process of the power plant with parallel operation of TJ and RJ parts could be realized. Maintaining the TJ operating parameters with respect to the limitations provides propulsion system reliability on transition to RJ mode. In transition operation the profile of ARCC inlet flow velocity changes considerably. The transition to RJ-mode finisheds with TJ windmilling, which may be used to drive engine accessories.

In the transient mode the structure of flow at the ARCC entry is strongly changed (Fig.9). The results of TRJ tests show that ARCC inlet flow velocity increases at constant rotation speed approximately in proportion to the increase in engine nozzle area. In this case a considerable distortion of flow takes place. For example, in the TJ-mode the distortion of flow is not more than 10 - 20% (the curve A in Fig.9), but in the engine parts joint mode

the maximum flow speed can exceed the mean flow velocity by about 2 - 2.4 times (the curves B and C in Fig.9). Therefore, special measures possibly would be demanded for stable combustion in ARCC in the transition mode.

3. THE RJ-MODE OF TRJ WITH WINDMILLING TJ

In the RJ-mode TRJ can operate with either open or closed gas turbine part of the engine. The curve D on Fig.7 corresponds to the windmilling mode of the TJ turbocompressor. The pressure losses in TJ in windmilling mode depend very much on compressor corrected air flow (the curve A in Fig.10 with the ram-duct closed). In the RJ-mode the TRJ pressure losses do not exceed 5 - 7% if TJ is closed (the curve C in Fig.10) or operated in the windmilling mode (the curve B in Fig.10). Application of the TJ windmilling mode provides an increase of engine air flow as the additional part of the air flow is passed through TJ and gives some possibilities for accessories drive. However these possibilities depend on TJ efficiency in the windmilling mode. On Fig.11 the experimental curve for TJ efficiency in windmilling with energy output is presented [4].

In the RJ-mode the ARCC inlet flow has relatively little speed distortion. At the begining of transition mode the region of maximum speed is located in the central part of the ARCC, and very strong distortion takes place, but in the windmilling mode it moves to the peripheral part of ARCC (the curve D in Fig.9). The unevenness of ARCC inlet flow decreases if the corrected air flow also decreases.

4. COOLING OF THE AFTERBURNER-RAM COMBUSTION CHAMBER

The ARCC and nozzle are one of the most heat loaded units of the TRE operating in the ramjet mode. To provide reliability of these units, it is natural to use an air cooling system in which a part of the air is taken away from the engine flowpath to the ARCC cooling duct (i.e. a space between the ARCC case and the perforated screen).

In the experimental TRJ, an air cooling system with a perforated screen was used for cooling the ARCC and the slot system was used for cooling the nozzle (Fig.12).

Experimental investigations of heat state and operability of high heat loaded TRJ units were carried out in the ramjet mode operation with windmilling of gasturbine core and simulation of Mach numbers in the range of 2.5...4. The next heat state problem tasks investigated

were: - ARCC combustion performance with the distortion of ARCC inlet total pressure and flow velocities fields;
- joint operation of ARCC and its cooling system;
- heat state of ARCC structure; - heat state of bearing supports in the ramjet operation mode. Some results of experimental investigations on full-scale ARCC in the ramjet mode working process and estimation of cooling system operation influence on engine performance are discussed below.

4.1. Operation of ARCC cooling system in RJ modes

The operation of TRJ is characterized by a wide range of ARCC inlet parameter change with significant distortion of inlet total pressure fields. The value of inlet total pressure distortion depends on the operating mode and the value of the corrected air flow through the engine. In the course of the experimental investigations of TRJ the ARCC inlet parameters of flow were characterized by the values:

$Ttx = 450...900$ K,
$Mx = 0.1...0.25.$

The radial distortion of ARCC inlet total pressure was 6...12% with the gasturbine core wind- milling and 7...14% with the closed gasturbine core. Nozzle flap location and the cooling air blowing through perforated screen slightly influence the shape of the total pressure fields in the nozzle throat section. Inlet total pressure distortion decreases along the ARCC and corresponding to estimates, in the throat nozzle section it is not more 2...3% when combustion takes place. ARCC combustion efficiency under the conditions considered depends mainly on the air-to-fuel ratio coefficient and is in a range typical for afterburners.

The length of the combustion zone significantly influences distribution of cooling air along the perforated screen of ARCC. Combustion zone length can be characterized indirectly by the static pressure drop on the ARCC screen measured along the ARCC. As experiments show (Fig.13), fuel combustion is finished in a distance of less than 2/3 of ARCC length.

The cooling air flow variation and its distribution along the ARCC are defined by very complex processes in non-uniform flow with combustion in ARCC. The hydraulic characteristics of the ARCC cooling duct depends on the discharge coefficient of the holes and duct pressure loss coefficient. These factors variation was examined in the course of the investigation [7].

Analysis of the cooling air parameters in the ARCC cooling duct has revealed that the cooling air temperature along the cooling duct changes slightly. When the total pressure ratio is Ptcol/Ptx < 1 the cooling air temperature

at the duct exit is 20...30% higher than the value of the duct inlet temperature (Fig.14). This temperature variation is explained by penetration of hot gas into the cooling duct through the holes in the perforated screen part of the duct. However, the change of cooling air temperature in this case is not great. It should be noted that a small change of Ttcol along the ARCC has no practical influence on the hydraulic characteristics of the ARCC cooling duct, and it is possible to use an assumption about the constant value of the cooling air temperature along the ARCC cooling duct.

The results of experimental investigations showed that distribution of cooling air along the ARCC perforated screen depends on the variation of both the cooling air and the ARCC gas parameters in a wide range. The variations of the corrected airflow in the underscreen duct and the gasflow in ARCC as a function of the ratio of total and static pressures in the characteristic sections were obtained.

The results of experimental investigations enabled definition of the hydraulic characteristics of the cooling duct and ARCC in joint operation. In this case the following reasons were adopted as a base :

- For pressurec defining characteristi cross section which is located at approximately half length of ARCC was adopted; in this section the combustion is mainly completed and main part of pressure losses is realized; - air total pressure in cooling duct characteristic cross section is taken as equal to the mean value between the values for inlet and exit of cooling duct; ARCC total pressure is taken as equal to the ARCC exit total pressure.

- one part of the cooling air from the cooling duct blows out through the perforated screen and the other part of the cooling air is used for nozzle cooling. Obtained by means of experiment and calculation, the hydraulic characteristic of ARCC and its cooling system is shown in Fig.15 in the form of the dependence of the ratio of the corrected airflow in the cooling duct to the gasflow in the ARCC, on the corresponding total pressures ratio. The curves are given at constant values of corrected flow density in the duct and ARCC. The hydraulic characteristic obtained helps to form the principles governing coolant flow.

The hydraulic characteristic of the cooling system shows, that when the total pressure ratio is near to 1, the mass flow ratio change is rather small in a wide range of both ARCC and cooling duct parameter variation.

These data enable an approach to the development of an optimally controlled cooling system for ARCC. For the development of a controlled air cooling system with the possibility of cooling air flow change in different engine operating modes it is necessary to select the total pressure ratio somewhat higher than 1.

4.2. Heat state of ARCC

The heat state of ARCC, which is characterized by the perforated screen temperature Ts, depends on the engine operating mode, flight conditions, parameters and flow of cooling air. Using the hydraulic characteristic of the air cooling system, one can consider the correlation between relative cooling air flow Wcol/Wx, mean screen temperature Tsm and flight M number bearing in mind, for example, the non controlled cooling system of ARCC without conditioning of cooling air (Ptcol.in = Ptx, Ttcol.in = Ttx). The two possible laws of PS control in RJ operating mode are characteristic:

- with a constant value of engine inlet corrected air flow, which corresponds to the constant value of ARCC inlet Mach numbers Mx independently of flight conditions;

- with a decreasing value of inlet engine corrected air flow .vs flight M number, which corresponds to a drop in ARCC inlet Mach numbers; in this case the air flow through the engine is limited by maximum inlet productivity.

The variation of mean screen temperature and relative cooling air flow is shown in Fig.16 depending on flight Mach numbers in ramjet mode operation and the air-to-fuel ratio coefficient a = 1.2.

It follows that the relative cooling air flow changes very little, although the change of TRJ parameters for these two laws of PS control is significant. At flight Mach number M = 4 the mean screen temperature is Tsm = 1150...1230 K and the relative cooling air flow is 12% approximately.

At flight Mach numbers M < 4 the cooling air flow in an uncontrolled cooling system is significantly higher than necessary for optimum cooling. Because of this the mean screen temperature at lower flight Mach numbers is rather low. For the two laws of PS control there is very little distinction between the mean screen temperatures. For example, at M = 4 the increase of Mx from 0.13 to 0.18 provides a decrease of Tsm by 80 K. In this case, the cooling airflow decreases by 2% approx.

TRJ throttling at flight Mach number M = 4 by decrease of fuel supply to ARCC causes a decrease in Wcol because of lower heat pressure losses. However, the decrease of air cooling flow is lower than necessary for an optimum cooling system. In this case, bigger coolant flow also provides low screen temperature.

The results of full-scale TRJ experimental investigations in simulated flight conditions at Mach numbers M = 2.5...4 have shown that with an uncontrolled ARCC air cooling system with perforated screen in non-design flight conditions (lower flight Mach numbers or engine

throttling at M = 4) the relative cooling air flow is significantly higher than the required value. This leads to thrust performance aggravation in these modes. Improving per- formance is possible by choosing rational cooling air parameters and using the controlled cooling air flow system.

The results of TRJ experimental investigations enabled development of a method to compute the engine thrust performance characteristics taking account of the influence of cooling air flow mixing with the main stream. Performance estimations were made according to the two types of ARCC which are used in different types of TRE [9]: ARCC in engine common exit duct ("cylindrical" ARCC) and ARCC in separate ramduct ("coaxial" ARCC). In performance definition account was taken of the nonuniformity of total pres- sure and temperature in ARCC and nozzle and the screen heat state.

It was considered that the cooling system was operating in optimum mode, in which the necessary value of cooling airflow is defined by the limit value of screen temperature. The ratio of thrust and SFC values to their conditional quantities, without accounting for cooling air flow output (fig.17) was used as a measure of the degree of influence of cooling air flow output. The performances given are dependent on flight Mach number along the trajectory with dynamic pressure q = 5000 kg/m2 and at air-to-fuel ratio coefficient a = 1.2 for screen materials with different temperature limits.

A significant increase of cooling air flow takes place at flight Mach numbers M = 4...5. At the higher flight Mach numbers the necessary value of the cooling air flow becomes very high with significant increase of loss of performance (Fig.17).

It is possible to decrease the amount of cooling air at high flight Mach numbers by the use of a conditioning system. which decreases the cooling air temperature. Fig.18 as an example shows the influence of cooling air temperature Ttcol on both thrust and SFC for two different types of ARCC using the same screen material in the flight conditions M = 5, H = 25 km. TRE with common ARCC has a higher thrust value of 7...18% and lower SFC of 2% than TRE with separate ramduct because of the latters larger area of cooling surface. To provide equal values of cooling air flow output in both engine types the cooling air temperature in TRE with "coaxial" ARCC must be lower by 100...150 K than in another type of ARCC. The SFC variation vs Ttcol is rather small.

To ensure ARCC operability up to flight Mach numbers M = 4...4.5 there is no need for a conditioning system. At higher flight Mach numbers the use of such a system is a necessity. A rational type of cooling air conditioning system depends on duration of cruise flight at the maximum flight speed, fuel cooling capacity (hydrocarbons, LH2) etc.

5. BEARING SUPPORTS HEAT STATE IN RAMJET MODE OPERATION (WINDMILLING CORE)

The bearings which are used in the supports of the TRJ gas turbine core define the engine's reliability to a high degree. Reliable and long-term operation of bearings is possible only when the bearing temperature is lower by 40...50 C than the tempering temperature of the bearing's material [7].

Synthetic oils are used for cooling and lubrication of aviation engine bearings. Increased flight speed leads to the increase of inlet engine air temperature and heat loads on units and construction elements of the engine. The heat flow into the engine's supports increases if an oil with limited operating temperature is used. When flight speeds are higher than M = 2.5...3, operability of gasturbine engine supports should be achieved using special structural measures.

One of the most effective methods to ensure bearing support operability is the use of active thermo-protection. This comprises the setting up of a protective screen over the support case under which conditioned air from the engine cooling system is supplied. The layout of an experimental TRJ support is shown in Fig.19. All supports for experimental TRJ had autonomously controlled oil supply and thermo-protective screen under which cooling air with controlled parameters was supplied.

Some results of heat state investigation of experimental TRJ bearing supports in ramjet operation mode with windmilling of gas-turbine core are discussed below.

The summary value of heat flow into the oil cavity of supports depends on:
- heat of friction in bearings and seals;
- heat flow through the details of the bearing supports;
- heat flow from hot air, which penetrates from the engine flowpath through the seals into the oil cavity.

The experimental investigation of TRJ support heat state showed that along with the TRJ transition to ramjet mode with windmilling of gasturbine core the redistribution of relative values of each of the above mentioned heat components takes place. It has been determined that part of the friction heat in the bearings decreases because of the decrease of both the rotor RPM and the axial forces. Heat flow through the details of supports and heat coming from hot air penetrating into the oil cavity components rises because of inlet temperature increase and aggravation of seal operating conditions. The total heat flow into the supports rises as compared with gas-turbine mode

(Fig.20), so the exit support oil temperature rises too and achieves its limit at certain flight Mach numbers (Fig.21).

Autonomous oil supply to each engine support in combination with air cooling supply have enabled investigation of the influence of both oil and cooling air parameters on TRJ support operability. The experimental data for relative cooling air flow and relative support exit oil temperature depending on relative cooling air pressure are shown in Fig.22. At the relative pressure ratio (Ptcol/Ptin) > 1.7 the cooling air flow ceases to rise and the support exit oil temperature also stabilises.

A cooling air supply under screen space enables a significant decrease in the support exit oil temperature and ensures engine transmission operability at flight Mach numbers M > 2.5...3. The use of a thermo-protective screen, under which cooling air is supplied, ensures engine support operability up to M = 4...4.5 (Fig.21).

6. TFRJ PERFORMANCE IN THE RJ OPERATING MODE

The operating parameters, thrust and SFC performances and control principles of TRE types based on TF core (TFRJ and TFRJs) at higher flight M numbers (transition and ramjet operation modes), including some experiments with imitation of these conditions, are considered below.

6.1. Fan performance in the RJ operating mode

To maintain low losses in the air intake with flight Mach number increase the fan corrected airflow should be decreased, as follows from the equality of airflows in the stream at infinity before the air intake and in the fan at the area ratio fin . Ain / Af:

$$(Wfcor/Wfcor \; o) = \frac{Po \cdot \left[\dfrac{k}{R \cdot To}\right]^{0.5} \quad M \cdot \left[\dfrac{Tt*}{Ta}\right]^{0.5}}{(Wfcor \; o/Af) \quad Sin \cdot (Pt*/Pa)} \cdot \frac{fin \cdot Ain}{Af}$$

where (Wfcor/Wfcor o) is the relative corrected airflow in the fan. This tendency is particularly clear when the area ratio becomes constant (Fig.23).

For example, when area ratio is equal to Ain/Af = 1.5, up to certain flight M numbers, the airflow in PS is defined by the fan working at the maximum RPM (fin < 1, the part A-B of the operating line). At higher flight M numbers the airflow is limited by air intake maximum productivity (fin = 1, the B-C part). The typical area ratio would be approximately equal to 1...2 [9]. As follows from Fig.23, at M = 4...5 , corresponding to such area ratios corrected airflow decreases to nearly 20...40% of

the maximum design value. The fan corrected RPM decreases by the same order.

Let us consider the peculiarities of fan operation at low rotational speed (Ncor/Ncor o<0.4). On Fig.24 (curve A) the typical fan characteristic at low rotational speed is shown (it is implied in the conditional fan stage which reflects the low staged fan operating process). At point 1 the flow angle of attack at mean radius is of some positive value, the difference of tangential velocity components Delta Cu > 0, fan expended work is positive and the fan pressure ratio value is near 1. When the counterpressure behind the fan reduces, the operating point is shifted to the right on the characteristic, and this is followed by "stretching" of the velocity triangles, decreased of angle of attack, Delta Cu, ex- pended work and PRCf. The point 2 corresponds to the case when the Delta Cu and expended work values are equal to 0, i.e. the fan operates in the free wind- milling mode and presents hydraulic drag in the air flow (PRCf < 1). The combination of such points at various rotational speeds gives a line of fan windmilling mode operation (curve B). With further shift of the operation point down along the characteristic (up to exit section choking) the transition to "turbine" operation mode takes place. At point 3 the Delta Cu and expended work values are negative, and the fan can provide some power.

The example of zero work (free windmilling) performance lines for fans with different design pressure ratio values is shown in Fig.25. The less PRCfo, the less pressure loss and the wider the range of air flow in the fan on windmilling. At design pressure ratio values 2...2.5 and (Wcor/Wcor o) < 0.4 the total pressure decrease in windmilling fan flowpath is of the same order as that of the pressure losses in the separate ramjet duct of the TRE [9].

In the RJ operating mode the airflow in the engine inner part (gasturbine core flowpath) is near to zero. Under these conditions the fan turbine becomes the consumer of power being produced by the windmil- ling fan. The turbine resistance to rotation is defined by so called ventilation losses, which arise as a result of energy feed to the airflow in the turbine flowpath and also by the turbine disc friction losses. The turbine driving work is proportional to the air density and to the rotational speed value in the power of about 2.7. A turbofan working in typical RJ operating mode condition analysis has showed that because of low rotational speed ad- ditional pressure decrease in the fan driving the turbine is usually small [9].

Experimental investigations of TFRJ models based on production TFs with replaceable nozzles (Fig.26) and external oil supply unit were performed on the special CIAM test facility on the connected tube scheme (see above).

The higher the flight Mach number and inlet pressure recovery and the lower the design fan pressure ratio, the less the pressure loss in the fan on windmilling. Experiments on full-scale TFRJ models have demonstrated the possibility of RJ mode performance with rather low losses with a windmilling fan (Fig.27). It is possible to use a windmilling fan for driving engine accessories in the RJ operating mode. The expediency of using the fan to drive the power plant accessories in the ramjet mode of operation depends on its efficiency as a "turbine", values of the work taken-off, thermal conditions and other factors.

If a windmilling fan is loaded by external energy consumers the operating points on the performance map lie beneath the zero work line. However in the TFRJ ramjet operating mode this deflection is usually insignificant and it is possible to adopt the zero work line as an operating line for the engine RJ operating mode.

The possibility of using a windmilling fan to drive the accessories in the RJ operating mode is a significant advantage of TFRJ and TFRJs.

In some cases, particularly when the fan design pressure ratio is rather high it is possible for TFRJ thrust performance in the RJ operating mode to be improved by arranging the bypass duct around the fan case with a corresponding controlled shut-off device.

6.2. TFRJ transition to RJ mode

Engine transition to RJ operating mode essentially consists of switching off the gasturbine part without engine thrust loss. For the TFRJ and TFRJs a gradual transition process is typical at a certain range of flight Mach numbers. The transition process begins at Mach number Mb when engine airflow at maximum rating approaches the inlet maximum airflow capacity (point B on Fig.23) and finishes at flight M = Me when the whole (or practically whole) airflow is feeding through the outer (ramjet) engine part (b = 1). As flight speed increases in the range of Mb < M < Me it is necessary to gradually decrease the fan corrected airflow by decreasing the core combustion chamber fuel supply and the throat areas of air-inlet and nozzle thus maintaining minimum intake pressure losses. In the transition proceeding the operating process in the ARCC is carried out at maximum inlet flow velocity Vx and minimum air-to-fuel ratio value.

To lower the TF airflow it is necessary to decrease the engine RPM. It is expedient to use a rather simple method of RPM reduction by gradually decreasing the turbine inlet temperature until the engine goes into windmilling mode. In this case the nozzle throat areas or the common nozzle throat area must decrease just after cessation of the combustion chamber fuel supply.

An example of engine parameter and performance variations in transition to RJ operating mode is given firstly for TFRJs (solid lines on Fig.28...30). As a characteristic value the area ratio Ain/Af = 1.3 was adopted in this case. The points B and E correspond to the start and finish of the transition to RJ mode process; the point W corresponds to the TFRJ parameters just at the moment of going to the windmilling mode.

At M = 2.7 the inlet maximum airflow capacity is reached. With further flight speed increase the engine-inlet matching for maintaining fin.max is provided by a corresponding decrease of the combustion chamber fuel supply. For the first time, the inner and outer nozzle throat areas An*1, and An*2 are maintained constant. As a result at M > Mb the temperature ratio Ttg/Ttin and the turbo-fan RPM quickly decrease. Maintaining the maximum ARCC flow capacity in conjunction with decreasing the airflow in the engine gas-turbine part leads to a rapid increase in the bypass ratio and the b value, i.e. the engine operating mode approaches the RJ mode (Fig.29). As a result the overall heat supply in the engine increases because of maintaining the ARCC rating at minimum air-to-fuel ratio. However, reduction of the engine nozzle expanding ratios is found to be a prevailing factor in this case, and as a result the engine specific thrust slightly decreases. For this reason the thrust increase rate is somewhat lower when M > Mb; the SFC increases simultaneously (the section B-W on Fig.30).

After going to windmilling mode (point W at M = 3) engine governing is provided by optimum variation of the nozzle throat areas. Under the flight conditions corresponding to Mw the b value is equal approximately to 0.9, i.e. about 10% of the overall airflow goes through the engine inner part (Fig.29). When the flight M number is higher than Mw it is expedient to decrease the airflow in the engine gasturbine part and the latter's drag by decreasing the An*1. For this purpose it is possible, for example, to shift the inner nozzle central body. The nozzle area decreases, which corresponds to inlet engine matching with minimum pressure losses and the ARCC inlet flow velocity limitations; the outer nozzle throat area being constant as is shown in Fig.29 (section W-E).

Along with An*1 decrease the turbine expansion ratio and work fall off, which leads to a decrease in fan RPM and pressure ratio (Fig.28). When the flow in the fan turbine becomes sub-critical, the inner nozzle area decrease leads to a decrease in compressor turbine work along with core RPM and corrected airflow lowering. As a result the engine airflow redistributes in favour of RJ part, and with full gas-turbine part shut-off (An*1 = 0) b = 1. At this moment (M = 3.4 on Fig.29.30) the transition to RJ operation mode is being completed. The corres- ponding operating point on the fan performance map is found practically on the zero work line (point E on Fig.28).

Along with inner nozzle area lowering the engine specific thrust increases because of the decrease in core losses and increase of the overall heat supply. For this reason in the range Mw-Me engine thrust rises, and SFC varies slightly. At M = Me flight conditions the TFRJs parameters differ from the "pure" RJ parameters by the value corresponding to the additional pressure losses in the windmilling fan.

In the RJ operation mode (M > Me) inlet/engine matching is provided by a corresponding decrease of the RJ part nozzle throat area An*2. The fan RPM and pressure losses are gradually decreasing (PRCf -> 1), and the engine thrust performance is approaching RJ performance.

Now let us consider some peculiarities of the TFRJ operating process when transition to RJ mode is carried out. using as an example the engine with the same cycle parameters and transonic (M = 1.3) to hypersonic (M = 4...5) thrust ratio as discussed above. For this condition the area ratio Ain/Af would be somewhat higher than for the TFRJ engine type (in correlation of transonic specific thrust values). In this case the area ratio for TFRJ would be about 1.4. as against 1.3 for TFRJs.

The TFRJ operating parameter variation peculiarities are conditioned mainly by the mutual influence of gas and air flows in the common ARCC inlet. As a result of core pressure ratio decrease vs flight speed. which is not compensated by fan duct outlet pressure variation. fan turbine specific work decreases. Because of the fan duct flow influence the fan operating line on the performance map deflects down from the corresponding line for TFRJs. and the bypass ratio vs flight M number rises more rapidly (Fig.28.29). Meanwhile corrected airflow variation vs flight M number is approximately the same as for the TFRJs.

As a result of the higher Ain/Af ratio the TFRJ propulsion plant approaches the maximum inlet capacity conditions at a higher flight M number than that of TFRJ (Fig.29). and corresponding fan pressure ratio is nearer to 1. Then. since the transition beginning the TFRJ operation mode is nearer to the RJ mode. Lowering of the turbine inlet temperature at M > Mb leads to b value increasing to almost 1 when TFRJ approaches the windmilling mode. The corresponding fan operating point lies practically on the fan zero work line (Fig.28). Then. in the case of TFRJ the completion of transition to RJ mode practically coincides with cessation of the fuel supply to the combustion chamber. As a result. the Mc number for TFRJ is lower than that of the TFRJ (in the example considered respectively Mc = 3.1 against 3.4. Fig.29).

A rather fast TFRJ transition to RJ mode is a consequence of the simultaneous effect of the turbine inlet temperature decrease and the gas dynamic influence of fan duct flow on gasturbine part performance.

TFRJ thrust performance variation vs flight M number is nearly the same as in the case of TFRJs. Any difference is connected with fan efficiency decrease and higher fan duct pressure losses. In the RJ operation mode (M > Me) inlet/engine matching is provided by a corresponding nozzle area decrease, and this is accompanied by RPM and engine flowpath pressure losses decreasing (dotted lines on Fig.29,30).

When analysing engine parameter variation on transition to RJ mode it was assumed that the air inlet operates at maximum capacity rating. This approach, although it does not account for possible inlet capacity limitations when M < Mmax, still enables simplification of the analysis and reveals the main correlations. The taking into account of real variable geometry inlet performance characteristics would not change engine parameter variation principle. but in the event of lower inlet capacity the transition flight M numbers range would shift to lower flight speeds.

The thrust performances of TRE in the RJ operation mode differ from that of the "pure" RJ and are conditioned mainly by additional pressure losses in the engine flowpath. The TRE performance aggravation in comparison with "pure" RJ at hypersonic flight speeds is possible also in connection with higher airflow or other agent expenditure for engine structure cooling.

Some engine thrust performance aggravation is also possible in connection with the part of airflow energy used for driving auxiliaries. In this case the use of a windmilling turbofan would be possible. When power take-off is low. this type of auxiliaries drive would be expedient in spite of rather low fan efficiency when running in the turbine mode (Fig.31).

CONCLUSION

The set of problems posed in connection with the application of the new types of ABE. concern the need to increase flight speed to M = 4...6.

Broad programmes of investigation of engines for high speed flights were carried out in Russia from the 60's to the 80's.
In the framework of these programmes an investigation of advisable engine concepts and operating process parameters of TRE were conducted. Test programmes on experimental full-scale TRE of different types were carried out at CIAM. The experimental TRE were assembled from units of production gasturbine engines. Flight conditions corresponding to Mach numbers M = 4.0...4.5. were simulated at the facility.

The results of theoretic and experimental investigations of TRE allow us to define:

- rational methods of transition from gasturbine to ramjet mode;
- the conditions of stable operation of the propulsion systems with TRE in the transition mode;
- performance characteristics and pressure losses in the windmilling mode for TRJ and TFRJ turbo-compressors;
- the expediency of the application of windmilling mode in the RJ operation mode;
- the performance of ARCC with distortion of ARCC inlet total pressure fields;
- the conditions of joint operation of ARCC with an air cooling system and the hydraulic characteristics of the cooled ARCC;
- the heat state of ARCC with perforated screen and of the bearing supports;
- the influence of ARCC air cooling on TRE thrust performance;
- the possibilities of heat protection of bearing supports by controlled oil and cooling air supplies.

Solving the complicated problems posed by the development of new aviation techniques requires high expenditure. International cooperation in the building up of a scientific-technical base for advanced powerplants is one of the important factors in the successful realisation of projects for 21st century air transport.

ACKNOWLEDGEMENTS

REFERENCES

1. ЦИАМ - 60 (месть десятилетий прогресса и традиций) М., ЦИАМ. 1991г.

2. V.A.Sosounov,"Some Aspects of Hydrogen and Other Alternative Fuels for Application in Air-Breathing Engines" IX ISABE, Athens, Greece, September, 1989.

3. В.А.Скибин и др. Отраслевой центр для исследований авиационных двигателей. Доклад на XV научных чтениях по космонавтике. М., 1991.

4. Д.А.Огородников. Силовые установки гиперзвуковых самолетов. Доклад на симпозиуме, на выставке "Авиадвигателестроение - 92". М., ЦИАМ, 1992.

5. V.A.Sosounov,"Study of Propulsion for High Velocity Flight." X ISABE, Nottingham, UK, September, 1991.

6. V.A.Sosounov, M.M.Tskhovrebov, V.I.Solonin, V.A.Palkin,"The Study of Experimental Turboramjets". AIAA PAPER 92-3720, 28th Joint Propulsion Conference, July, 1992.

7. V.A.Sosounov, V.I.Solonin, M.M.Tskhovrebov, P.A.Kadjardouzov, V.A.Palkin,"The Study of Experimental Turboramjets: Heat State and Cooling Problems". AIAA PAPER 93-1989, 29th Joint Propulsion Conference, June, 28-30, 1993, Monterey, CA.

8. M.M.Tskhovrebov, V.A.Palkin,"Combined Engines for Hypersonic Flight". ICAS-92-3.4.3. 18-th ICAS Congress, 21-25 September, 1992, Beijing, PRC.

9. "Теория двухконтурных турбореактивных двигателей". Под ред. С.М.Шляхтенко, В.А.Сосунова. М., Машиностроение, 1979, 432с.

10. Турбопрямоточные двигатели для гиперзвуковых скоростей полета. Под ред. В.А.Сосунова, М.М.Цховребова. Вопросы авиационной науки и техники. Серия Авиационное двигателестроение. Вып.3, 1993. М., ЦИАМ.

	Without energy transfer to ramjet part	With energy transfer to ramjet part
Separate ramjet combustion chamber		
Augumentor-ramjet combustion chamber		

Fig 1 TRE types [8]

- Forecasts
- "Lessons learned"
- Propulsion requirements
- R&D programmes

− gasdynamics, combustion, structural durability fundamental investigations
− engine configuration research
− aircraft-propulsion system optimisation

Engine design & developement process

CIAM
engine DB's
TsAGI
VIAM
IEPT
serial production plants
AS institutes

− advanced stages, parts, systems, gasgenerators
− quality level standards (reliability, fuel effectiveness, life time, expluatation technology, ecology)
− test facilities

− turbomachines 3-D design methods
− advanced engines experimental components
− critical components reliability
− environmental problems solutions
− engine control systems

− new materials and technologies
− experimental core engines and demonstrators
− aircraft-propulsion integration
− new generation engine conception

Fig 2 Scientific base for AE development [8]

1 RECEIVER
2 ALTITUDE TEST CHAMBER
3 COLD AIR PIPE
4 HOT AIR PIPE
5 INLET
6 HEAT EXCHANGER
7 CONTROL PANEL
8 MEASURING SYSTEM
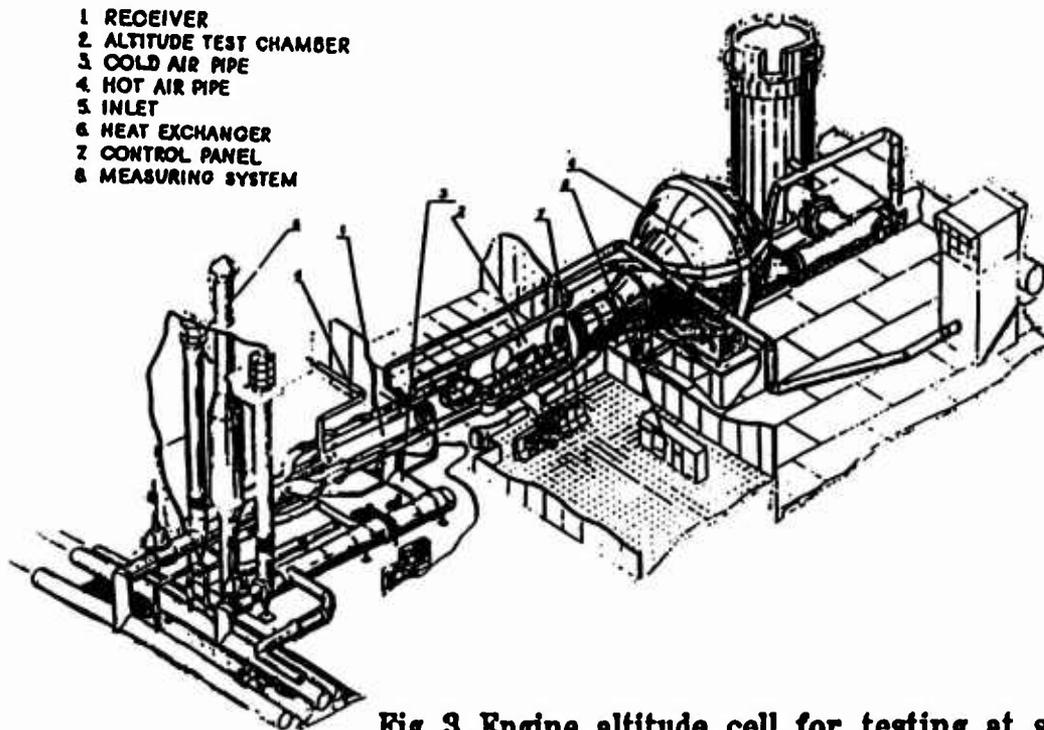
Fig 3 Engine altitude cell for testing at steady state and transient conditions [3]

- Complex Study of operation
- Engines switching modes
- Afterburning and ramjet combustor (ARC) operation
- Ramjet operation mode characteristics (M > 2.5)
- Windmilling mode
- Power output
- Passage hydraulic characteristics
- Structure heat state
- ARC and nozzle cooling at M ~ 3.5 – 4.5
- Transmission operability
- Cooling system impact on T and SFc

Fig 4 CIAM experimental TRJ [1,4,5,10]

Cooling air

Gas turbine engine mode

Ramjet engine mode

Fig 5 Experimental TRJ layout [5]

Controlled temperature

P,T
Cooling air

Water

Controled shut-off device   P,T   P,T, tcT   Water injection

P,T

P,T

$P = 1...2$ кг/см^2
T⩽1000 К

FAHE   FOU   FOP

Water (fuel)

Fig 6 Test facility schematic layout [6]

PRC

Stall line   A

TJ mode

B

C $\bar{N}_{cor} = 1$

Transition mode

0.8

Windmilling mode   0.6   **Fig 7 Compressor performance map [6]**

1.0   D

Compressor corrected air flow

Fig 8 TRJ performance at
transition mode [5]
1   – stable operation
2,3 – unstable operation
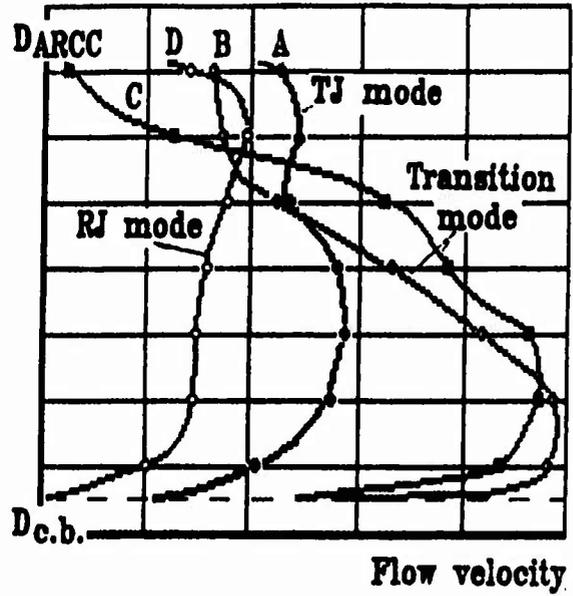
Fig 9 Flow velocity at ARCC entry
distortion [4.6]
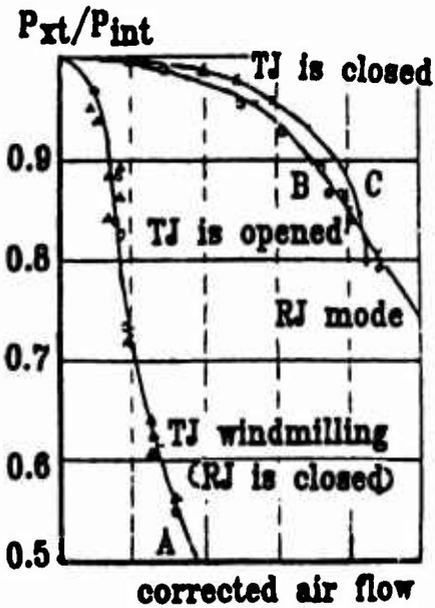
Fig 10 TRJ pressure losses at
RJ mode (windmilling core) [6]
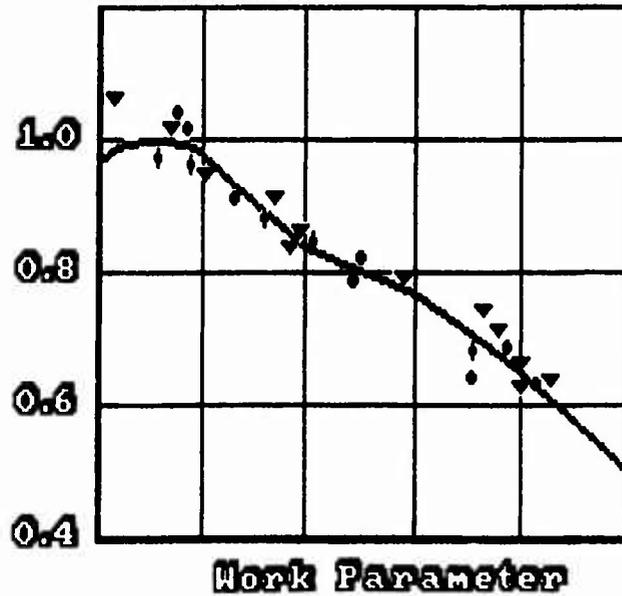
Fig 11 Windmilling TJ with power offtake
relative efficiency [4]
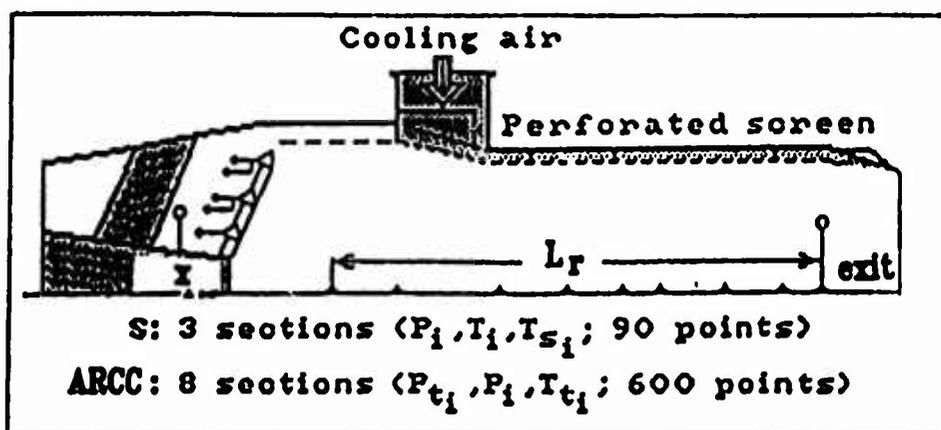
Fig 12 ARCC schematic layout [7]
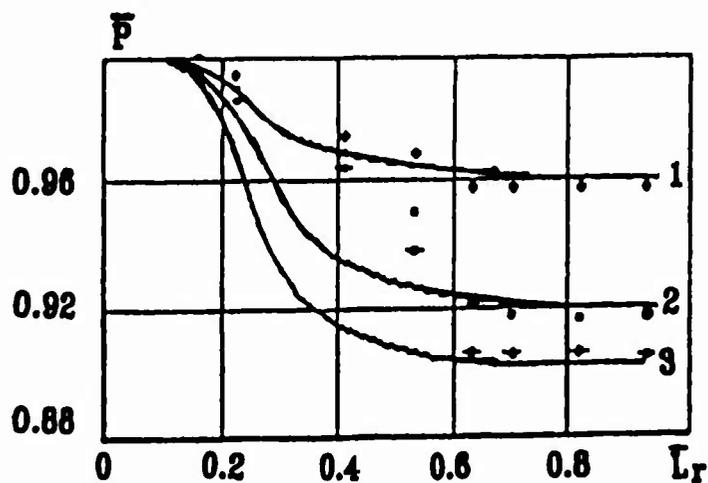
Fig 13

Static pressure variation along ARCC [7]

1 - $T_{ex}/T_x=2$; $M_x=0,16$
2 - $T_{ex}/T_x=2$; $M_x=0.2$
3 - $T_{ex}/T_x=2,6$; $M_x=0.22$
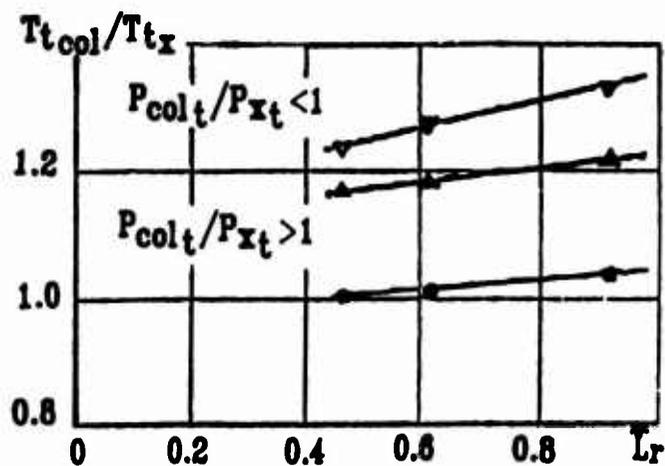
Fig 14 Cooling air temperature variation along cooling duct [7]
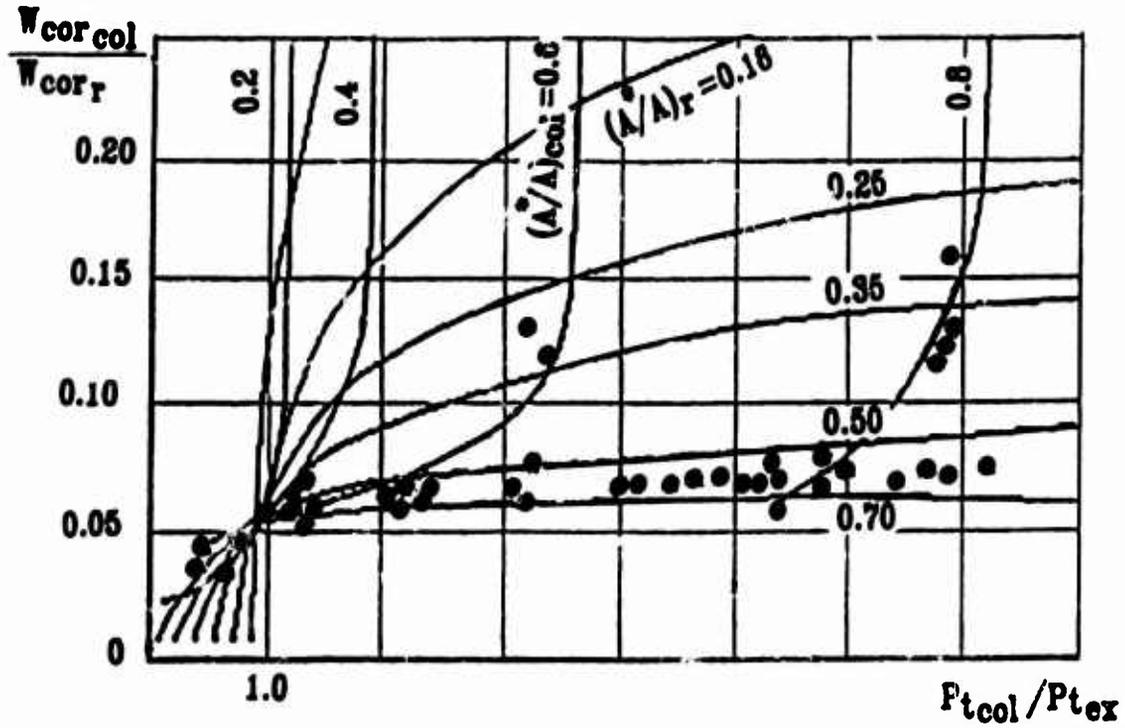
Fig 15 ARCC hydraulic characteristics cooling duct [7]
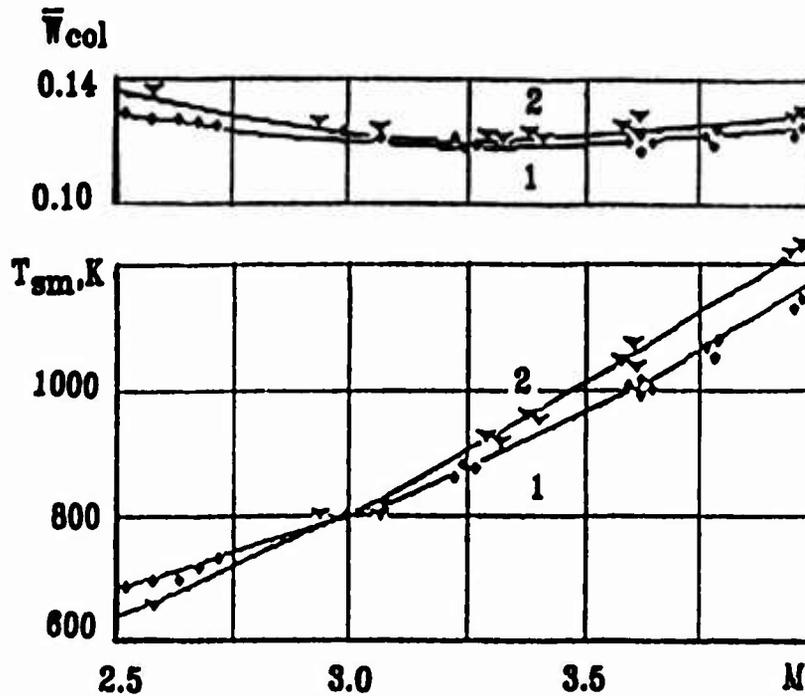
Fig 16 Relative cooling airflow and mean screen temperature vs flight Mach number [7]

$1 - W_{cor_X} = \text{const}$ $2 - W_{cor_X} = \text{var}$
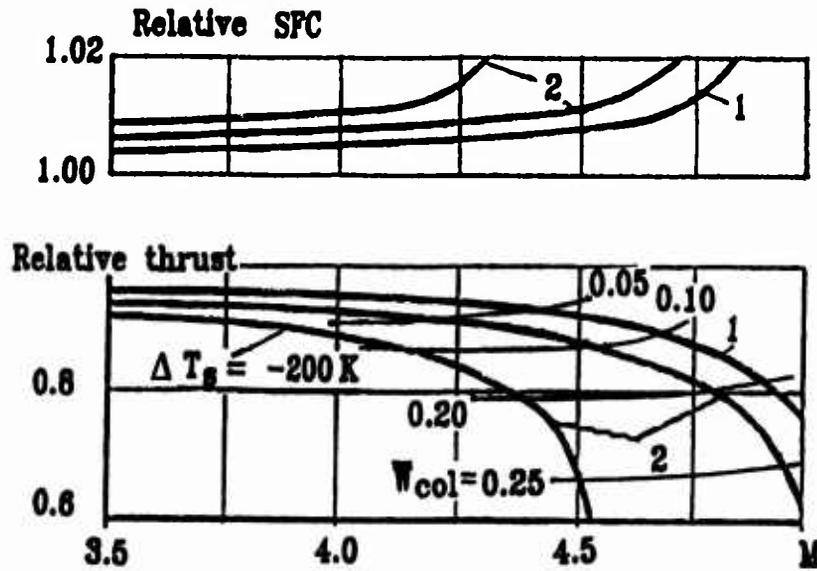
Relative SFC

Fig 17 Relative thrust and SFC variation
vs flight M number [7]
1-common "cylindrical" ARCC
2-separate "coaxial" ARCC
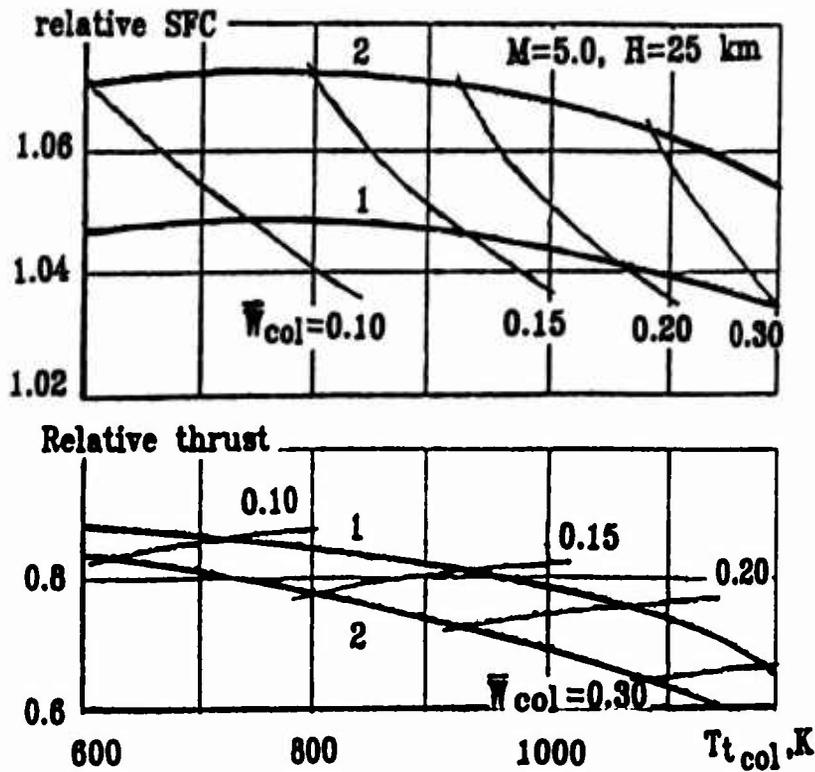
Fig 18 Relative thrust and SFC variation vs
cooling air temperature [7]
1-common "cylindrical" ARCC
2-separate "coaxial" ARCC
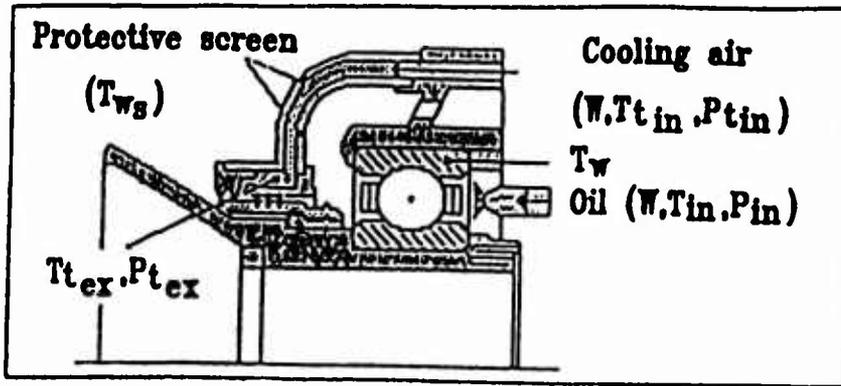
Fig 19 Bearing unit shematic layout [7]

Fig 20 Bearing support heat flows [7]
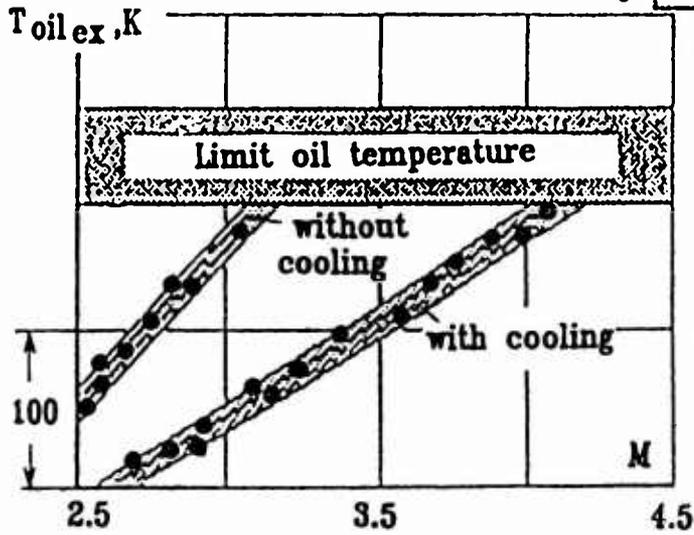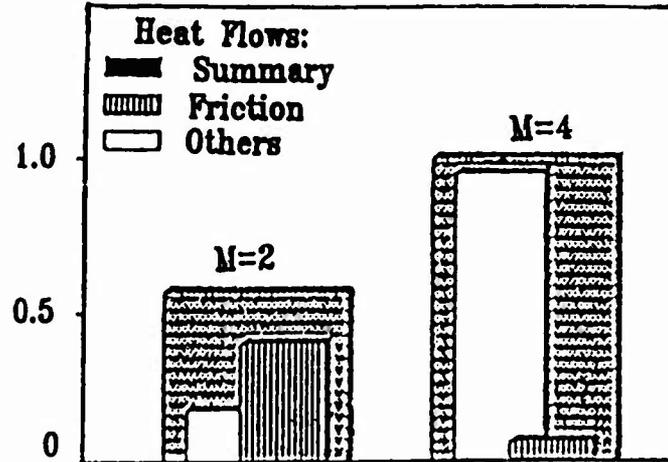
Fig 21 Influence of flight Mach number on support exit oil temperature [7]

Fig 22 Relative support exit oil temperature and cooling air flow in dependence of air pressure ratio [7]
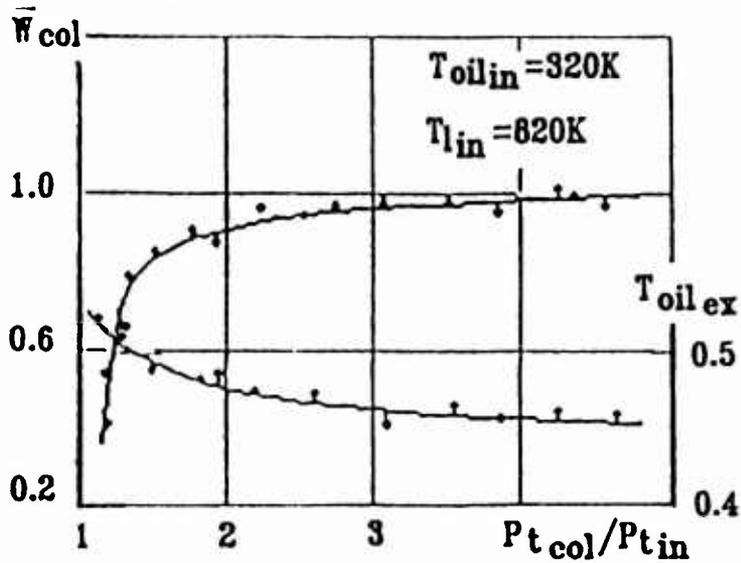
Fig 23
Relative fan corrected airflow in
dependence on free stream to fan
areas ratio and flight M number [9]
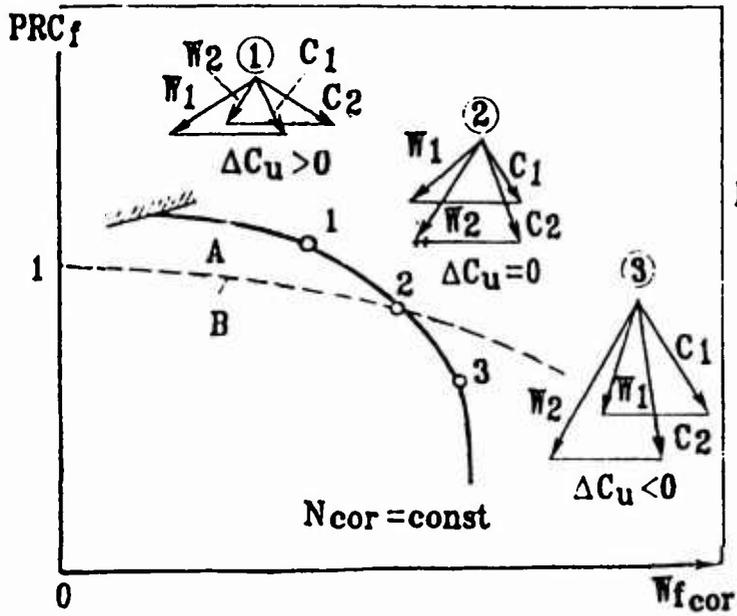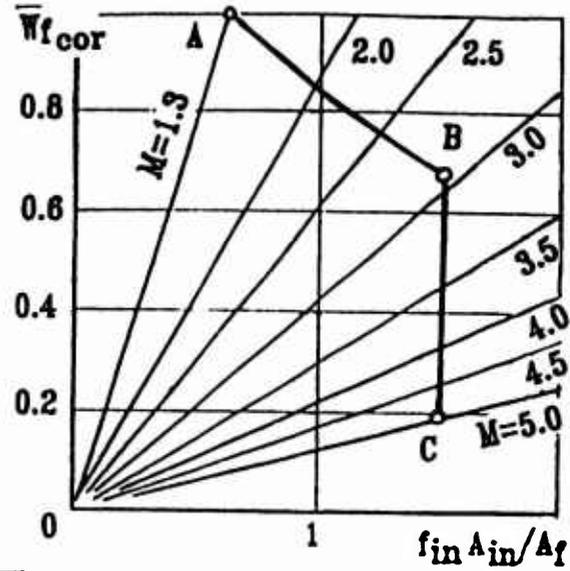
Fig 24 Fan stage parameters
variation along
the fan characteristic
(low RPM region) [9]
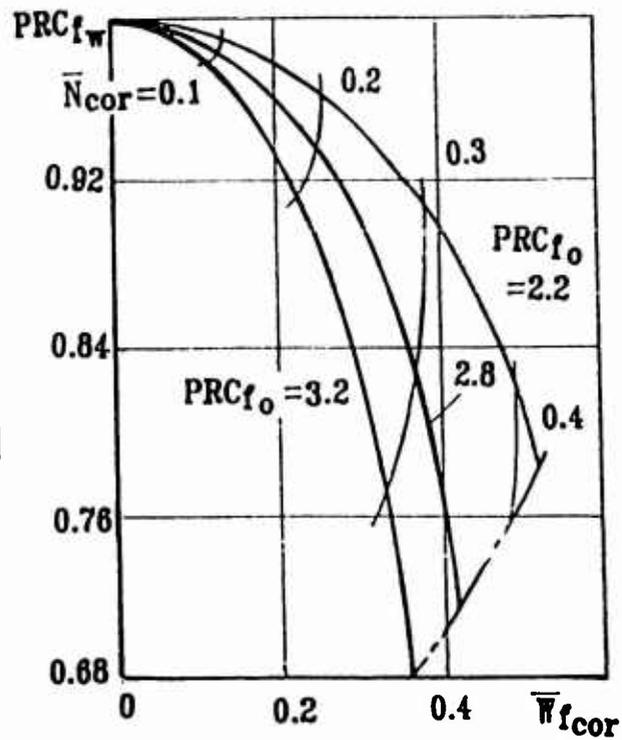
Fig 25
Zero work lines for fans with
different design pressure ratios [9]
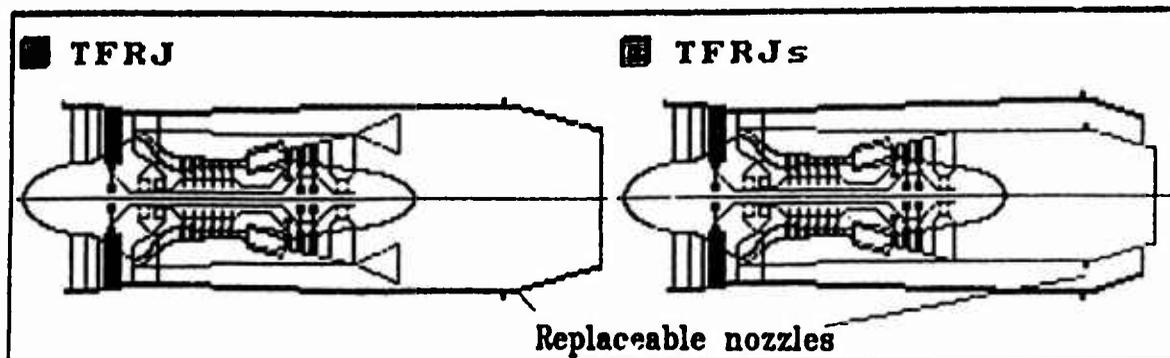
Fig 26 TFRJ models shematic layout [6]
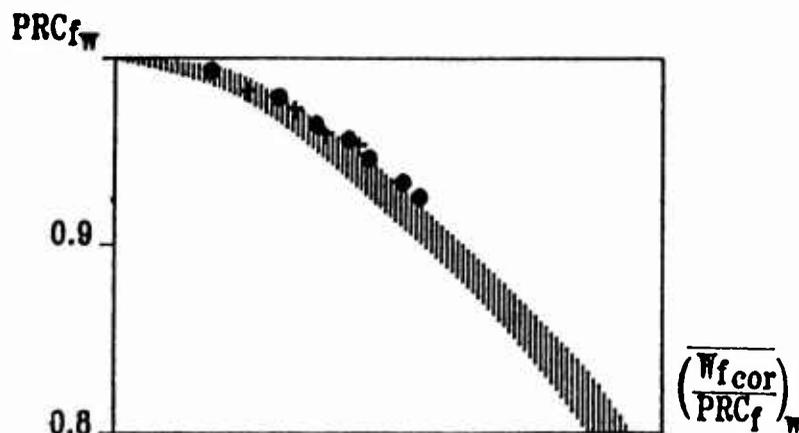
Fig 27 Fan pressure ratio at
windmilling mode [10]
$\bullet \, ^+PRC_{f_0}=1.8...2.6$
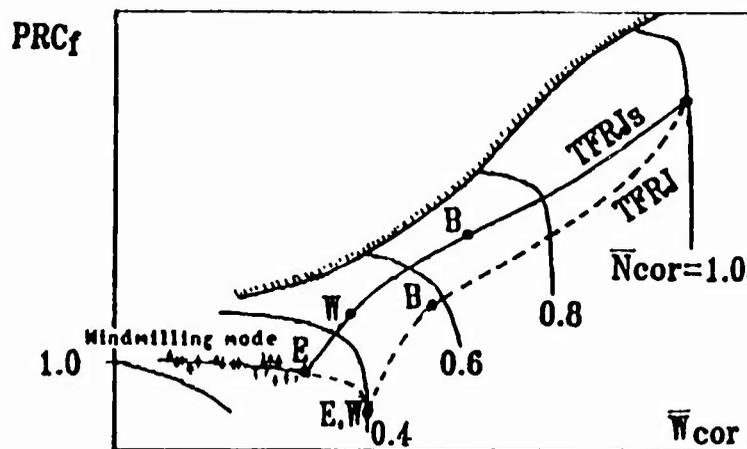
Fig 28 TFRJ fan characteristics map [6]

$\bar{A}_{n*}$

$\bar{A}_{n*_{II}}$

$\bar{A}_{n*_{I}}$ $\bar{A}_{n*}$

$b = m/m+1$

$\bar{N}_f$

B

W

B

E

E

Tt_g/Tt_{in}

Fig 29 TFRJ parameters variation when going to RJ mode [9]
—— TFRJs
--- TFRJ ►
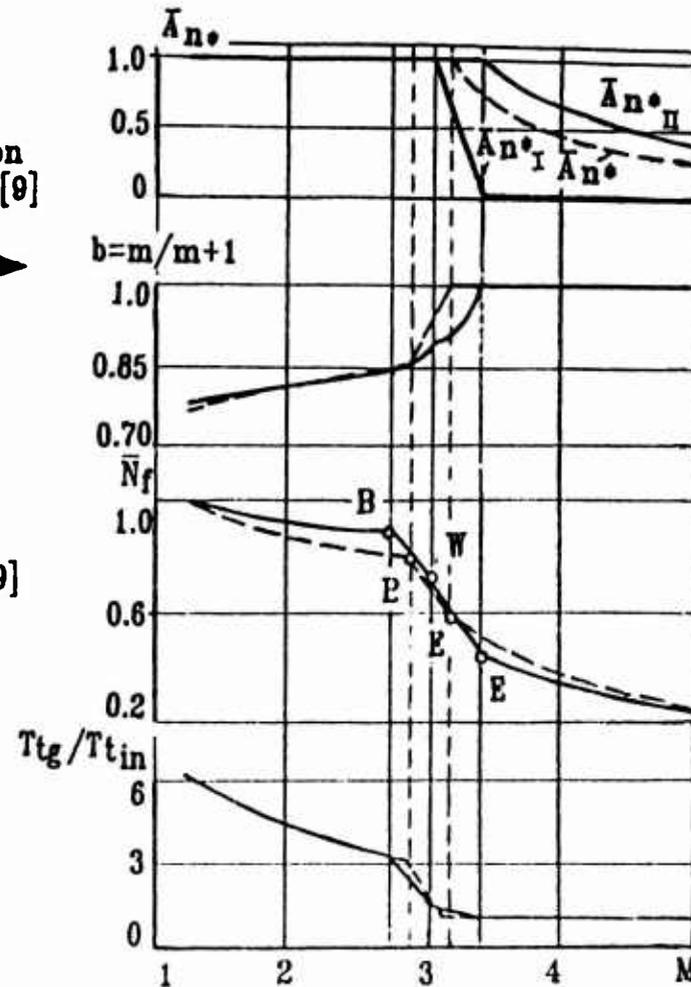
Fig 30

TFRJ relative thrust and SFC variation vs flight M number [9]
—— TFRJs
--- TFRJ ▼

SFC, $\dfrac{kg}{N \cdot h}$

E

E

B

W

B

Relative thrust
(H = c)

SFC $T_a = 216.6\,K$
   $M = 4$

2...4%

"pure" RJ

thrust
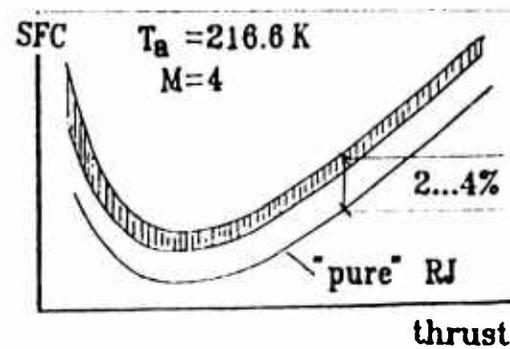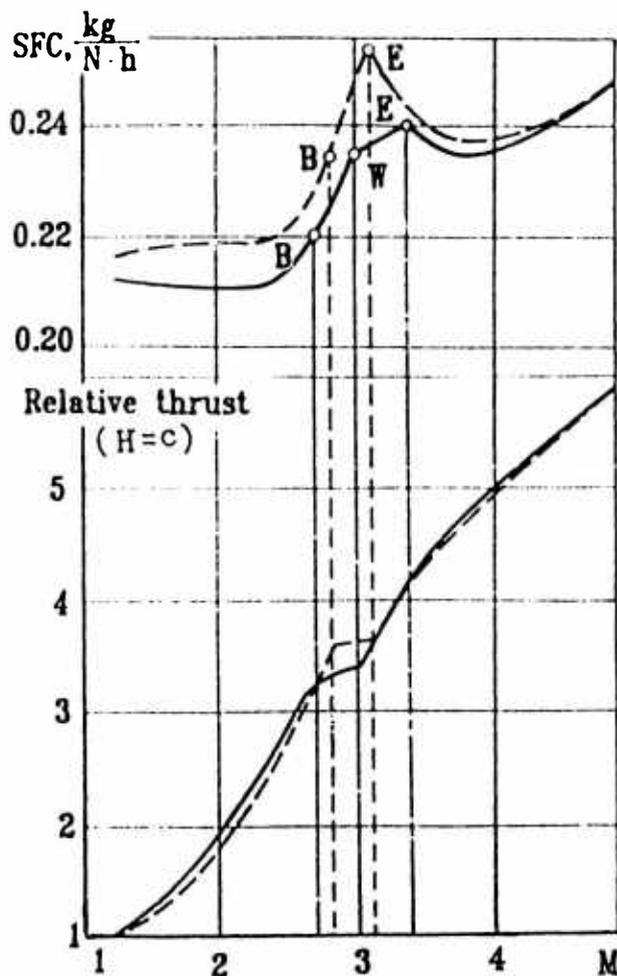
Fig 31 Power offtake influence on engine SFC at RJ operation mode [10]

SCRAMJET CFD METHODS AND ANALYSIS
PART 2. SCRAMJET CFD ANALYSIS

NUMERICAL SIMULATION OF SUPERSONIC MIXING AND COMBUSTION APPLIED TO SCRAMJET COMBUSTOR

by

V.KOPCHENOV,
K.LOMKOV, S.ZAITSEV, I.BORISOV

CIAM (Central Institute of Aviation Motors)
Aviamotornaya street 2
111250 MOSCOW
RUSSIA

2.1 Introduction
2.2 Mathematical model and numerical method
2.3 The main results of the CIAM investigations on supersonic mixing and combustion enhancement
2.4 Some notices about the jet/shock interaction and mixing enhancement
2.5 Evaluation of combustion efficiency and choice of acceptable design parameters for combustor
2.6 Estimation of the role of chemical kinetics

2.1 Introduction

It is necessary to note, that the problem of supersonic combustion of hydrogen in air stream was investigated in Russia both experimentally and numerically. It is not possible to give the full survey of publications about investigations concerning with numerical simulation in short description. As an example, monographs [1,2] may be pointed out. The boundary layer model was used in [1]. The experience in numerical simulation of supersonic combustion within the scope of Reynolds averaged Navier-Stokes equations and their parabolized version is presented in [2].

The influence of finite rates of chemical reactions and concentrations fluctuations on combustion efficiency in duct was investigated in [3-5] with the aid of boundary layer model. By this, the diffusion flame sheet model was used in [3], and sufficiently detailed kinetical scheme, including 20 reactions for 9 components was considered in [5]. The influence of duct geometry factors on combustion efficiency was also analyzed.

The supersonic combustion process near the wall was numerically simulated within the boundary layer approach [6-8]. The necessity to take into account the fluctuations of scalar parameters was shown. The model of unmixedness [9] was used to describe the influence of concentrations fluctuations on the chemical kinetics.

The system of mathematical models and numerical codes using the boundary layer and parabolized Navier-Stokes equations for two-dimensional flows was developed in [10-12] for the

numerical simulation of supersonic combustion. The modified k-ε turbulence model of Launder-Jones was used. The equilibrium and nonequilibrium combustion models were realized. The influence of the concentrations fluctuations on the reactions rates was also taken into account with the aid of the model [9].

The numerical investigation of supersonic combustion of hydrogen jet, injected tangentially along the wall into supersonic air stream, was performed within the scope of two - dimensional parabolized Navier-Stokes equations [13-15] . The system of 13 reactions for 9 components was considered. The algebraic turbulence models were used (modified Prandtl and Baldwin-Lomax).

Detailed survey of modern numerical investigations of the supersonic combustion on the base of three-dimensional Reynolds averaged Navier-Stokes equations or their parabolized version is presented in [16-19]. It is necessary to note, that simplified kinetical scheme [20] was most commonly used. The possibility to include more detailed kinetical mechanism into this class of mathematical models is directly dependent upon the progress in computer power.

The short description of the mathematical model developed in CIAM for numerical simulation of supersonic mixing and combustion, which permits to analyze the three-dimensional effects, is presented in this paper. Some aspects of mixing and combustion enhancement will also be considered on the base of CIAM experience.

The scramjet combustor efficiency depends strongly upon the efficiency of the mixing process

between fuel and oxidizer. There are two reasons for this effect. The first reason is that the mixing efficiency of supersonic flows decreases with Mach number increase because of the influence of compressibility [21-23]. The increase of the so called convective Mach number is accompanied by the essential mixing efficiency decrease in comparison with the incompressible fluid at the same velocities and densities ratios. This decrease observed in the experimental investigations for the plane shear layer spreading rates at supersonic convective Mach numbers may be near 70% of that value in incompressible case [24]. The similar data for axisymmetrical coflowing jets were obtained, for example, in [29].

Second reason consists in the decrease of the residence time in the combustor as the flight Mach number increases. It is obvious that the problem of mixing and combustion enhancement is very important to create high effective scramjet combustor.

The following factors must be taken into account at estimation of possible mixing and combustion enhancement methods. It is necessary to evaluate the additional losses connected with the mixing augmentation process and the influence of this losses on the overall performances of the propulsion system such as momentum or thrust [25]. It is desirable to use the own momentum of hydrogen jet injected into the air stream as better as possible. This hydrogen has been heated by using in the inlet and airframe cooling systems. This circumstance is particularly important for high flight Mach numbers and makes advantageous the axial hydrogen injection. Moreover, the possibility to use injection struts is doubtful at high hypersonic flight Mach numbers [26] and then it is necessary to analyze the opportunity to apply the near wall injection system.

One can distinguish the following control methods for the mixing enhancement at present :
1) direct influence on the hydrogen jet shape with the aid of the hydrogen injector nozzle design or use of special heads to distort the jet [27-34];
2) the shock-jet or mixing layer interaction [35-42]. Some enhancement mechanisms including the unsteady effects may exist in this case;
3) the hydrogen strut design in such manner to create intensive secondary flows with the convective mixing mechanism [43-47];
4) the swirling of the hydrogen jet [48 - 49];
5) the wall jet injection at some angle to the main air stream as an alternative to the slot injection in axial direction. The permissible angles of injection must be evaluated from the compromise between mixing enhancement and hydrogen momentum and gasdynamical losses [50-53];
6) the use of unsteady effects, including acoustic influence on hydrogen jet (see, for example, [54]).

It must be pointed out that the following

mechanisms responsible for the mixing enhancement may be revealed when using the above mentioned mixing control methods: the increase of the mixing surface; the vorticity generation in the flow; the influence on the stability characteristics; the influence on the large and small-scale turbulent structures. This mechanisms revealing in the specific control method is very difficult task and requires using of very sensitive modern measuring techniques and complex mathematical models elaboration. At the same time it seems to be justified to use more simple measurements and existing mathematical models to predict the efficiency of special mixing control methods and to evaluate the additional losses. Such evaluations for the special mixing control methods make possible the analysis of the efficiency of the real injection systems, which include several control methods simultaneously as a rule. But the physical investigations of the mixing enhancement mechanisms are of primary importance.

2.2. Mathematical model and numerical method

The 3-D parabolized Navier-Stokes equations are used for the numerical simulation of two supersonic flows mixing. These equations are derived from the full 3-D Navier-Stokes equations with exception of the second derivatives with differentiation in longitudinal direction [55]. The equations are written in cartesian coordinates X,Y,Z and longitudinal X-axis coincides with the air stream direction. The multicomponent flow of perfect gases is considered. The heat capacity of components depends upon temperature. The chemical reactions are not taken into account at mixing calculations. The turbulent regimes are considered in the quasilaminar approach. In this case the turbulent viscosity is introduced. The turbulent heat and mass transfer coefficients are expressed through turbulent viscosity coefficient using Prandtl and Schmidt numbers. The differential turbulence model with one equation for turbulent viscosity is used [56,57].

The approximate diffusion flame sheet model is used for the numerical simulation of flows with combustion. This approach [58,59] is based on the assumption that the combustion is controlled only by the mixing of fuel and oxidizer. Additionally, it is assumed that one global infinitely fast reaction takes place with formation of reaction products from fuel (hydrogen) and oxidizer (oxygen) and with heat release. The instantaneous reaction occurs at the surface of the front where the diffusion fluxes of fuel and oxidizer are in stoichiometric relation. Only fuel is contained on one side of the flame sheet, only oxidizer - on the another . The products of combustion diffuses in both sides from the flame front surface [58].

It is known for the flame sheet model that if diffusivities of all components are the same, and initial

concentrations profiles and boundary conditions for them are self-similar, it is possible to introduce the mixture fracture and to solve the single equation for this value with following definition of fuel, oxidizer and reaction products mass fractions taking into account their initial profiles.

The total enthalpy profile may also be obtained by use mixture fracture profiles with some additional assumptions. It is assumed that Prandtl and Lewis numbers are equal to unit, and the initial profile for enthalpy is piecewise constant as for the component mass fraction. Also it is necessary to omit some terms from the energy equation of PNS system, which are not essential in inviscid region and in shear layers.

Thus, in the case of diffusion flame sheet model, it is necessary to solve numerically the continuity equation for the mixture, three momentum equations, and equation for the mixture fracture. Then the total enthalpy and components mass concentrations are calculated on the base of mixture fracture.

In supersonic regions the marching procedure may be used in downstream direction for the numerical solution of PNS equations [55]. In initial cross-section the distributions of all parameters must be predetermined. The conditions on the lateral boundaries of computational region depend upon the physical problem. Some boundary conditions will be discussed later. But it is necessary to note that the boundary layers on the channel walls with subsonic regions are not taken into account, because it requires special consideration including global pressure iterations [55]. The wall boundary layer effects were neglected because the mixing process is the main object of our consideration.

The governing equations are solved numerically using the method, which is based on the higher order accuracy monotone Godunov's finite volume scheme for the steady supersonic flow [60-62], generalized to three-dimensional case by A.Kraiko and S.Schipin. This explicit predictor-corrector scheme including the modified [63] principal of minimal increments of functions [64] provides the monotonicity condition, the second order accuracy on regular uniform grids, and approximation on arbitrary nonuniform grids. The generalization of this method on the multicomponent flows taking into account variable heat capacities for PNS equations was performed by V.Kopchenov and K.Lomkov.

The proposed method permits to use the adaptive and regular grids. When the mixing layer is thin, the adaptive grid is used. This grid is matched to the dividing stream surface. When the shear layer becomes thick, the regular grid is used. In this way the accuracy of the results obtained is increased and the run time is reduced.

The mathematical model presented here is based on the assumption that the chemical processes are infinitely fast and the combustion is controlled only by mixing rate (flame sheet model). Nevertheless there is a number of scramjet operational regimes with the residence time in combustor is the same order as characteristic time scale for chemical processes. There are two different cases here. The first one is the "low" flight Mach number operational regimes (M_f=6-8). As a rule the air flow temperature at the entrance of combustor is not sufficiently high for self-ignition at these regimes. The combustion is possible in this case only if reliable flameholders and igniters are available.

The second case is more important for high flight Mach numbers. The residence time dramatic decreasing in this case may lead to incompleteness of sufficiently slow relaxation processes, because these processes are controlled by third order slow reactions. On the other hand these are the processes responsible for main part of energy release. Hence the combustion inefficiency controlled by chemical kinetics may be observed.

It is obviously seen that in both cases the flame sheet model is not valid and more complex, based on detailed kinetics approach, mathematical model is needed. To detect such kinetically controlled operational regimes and to avoid the possible errors connected with the usage of the flame sheet model, the simplified mathematical model for reacting gas flow in combustor was suggested by S.Zaitcev and I.Borisov. Here it is.

Let us suppose, that the flow field is one dimensional, and the static pressure is constant in combustor. The heat transfer from the reaction zone is neglected. The variation of the axial velocity u along the combustor is supposed to be negligible (the results of calculations show that u remains nearly the same and equals U along the combustor length unlike the Mach number decreases dramatically). Hence, the equations for species concentrations and the energy conservation law are to be taken into account

$$U \, dC_i/dx = W_i.$$

$$H = const.$$

Here, C_i is the species concentrations, W_i - chemical production rate, H - total enthalpy including species formation specific heats. The initial conditions at the entrance of combustion chamber have to be formulated to complete this problem. Two different sets of initial conditions were used for calculations. The first set corresponds to infinitely fast fuel and air mixing with conservation of the total mass, momentum and energy (MIX). The second set of initial conditions corresponds to assumption that the chemical processes take place at the stoichiometric mixture surface placed closely to the external boundary of jet. It was assumed

that initial temperature and pressure here are equal to the air parameters, and the hydrogen concentration is stoichiometric (DIF). The Dimitrov's detailed kinetics scheme was used in calculations [65]. It includes 30 elementary reactions between 8 reactants: H_2, O_2, H, O, OH, HO_2, H_2O_2, H_2O. The specific enthalpies of species were approximated. The Gear-based numerical code was used to solve the problem [66].

There were two values of main interest in the calculations. The first one is the $L_i = U * t_i$ - the characteristic ignition length scale (estimated for 5% enlarges of the temperature from its initial value). The second one is the $L_e = U * t_e$ - characteristic length scale for energy release (estimated as the length for temperature reaches 99% of its equilibrium value). The results of calculations are presented in section 2.6.

2.3 The main results of the CIAM investigations on supersonic mixing and combustion enhancement

The three-dimensional effects due to the interaction of the supersonic H_2 jet with supersonic air flow were analyzed as possible mechanism for mixing and combustion enhancement [67]. The design of supersonic part of the nozzle for hydrogen injection is considered as one of the possible passive control methods. The second method includes injection of hydrogen jet at an angle to the main air stream.

The mixing efficiency calculations were performed for four cases. In the first case, the hydrogen was injected through the axisymmetric nozzle with conical supersonic part (the reference case C_1). In the second case (C_2), the hydrogen was injected as circular uniform jet at an angle 10° to the air flow in horizontal direction, and in the third case (C_3) - at an angle 10° in vertical direction. In the fourth case (C_4), the nonaxisymmetric hydrogen injection nozzle is used. The nozzle has elliptical exit cross-section with 2:1 aspect ratio. The walls take straight-line form in meridional planes. The elliptical and axisymmetric nozzles have the same expansion ratio.

The test problem is formulated in the following manner. It is assumed that the cascade of struts is placed in the combustor without skew angle. The H_2 is injected in the air flow from the base surface of each strut through individual nozzles. The number of nozzles is large enough. Therefore, the influence of the wall on the "central" jet may be neglected. Approximately, it is possible to divide the flow field into the elementary regions with some symmetry or periodicity conditions on the elementary computational region boundaries. The computational regions for each of considered cases (C_1-C_4) are shown in Fig.2.3.1-a-d. The direction of transversal injection component is indicated by pointer. It is supposed, that the air flow in initial section is

uniform. When the jet is injected at an angle to main air flow (Fig.2.3.1-b,c), the jet parameters are given as uniform, including constant vertical or horizontal velocity component. At the investigation of the cases C_1 and C_4, (Fig.2.3.1-a,d) the hydrogen jet parameters in initial cross-section are obtained from the calculations of the inviscid supersonic nozzle flow.

To investigate possibilities of the mixing enhancement two series of calculations were performed. The design Mach number for the hydrogen axisymmetric nozzle was equal to 3.05 and the temperature T of the hydrogen at the nozzle exit is equal to 340° K. The air flow parameters for three regimes are shown in table 2.3.1. The ratio of longitudinal velocity components of hydrogen and air approaches to unit for the second regime. The turbulent viscosity generation mechanism is switched off according to the turbulence model, and the mixing efficiency is determined in this case by the initial turbulent viscosity level. Let us consider some results, obtained for regime R_1 .

The mixing efficiency is evaluated with the aid of the following characteristics. The value q is introduced as

$$q = (1 - C_m)/(1 - <C>).$$

Here C_m is maximum value of H_2 mass fraction in cross-section and $<C>$ is massflow averaged H_2 mass fraction

$$<C> = \iint_F \rho u C \, dF / \iint_F \rho u \, dF ,$$

where F is the channel cross-section area. This value varies from zero in the initial cross-section up to one at full mixing. This characteristic permits to determine accurately the initial region length and the mixing efficiency on transition and main regions. To evaluate the mixing efficiency in the whole region the second characteristic is introduced

$$D = \iint_F \rho u \, (C - <C>)^2 dF / \iint_F \rho u \, dF / <C>^2 ,$$

which defines the nonuniformity of mass fraction distribution in the channel cross-section. The mixing efficiency characteristic q, plotted as a function of streamwise coordinate X, is shown in Fig.2.3.2. The curves 1-4 correspond accordingly to investigated cases C_1-C_4.

The mixing process itself is connected with irreversible losses. It is necessary to analyze the influence of the mixing control method on the additional losses. For example, the additional losses origin may be concerned with shock generation in supersonic flow. The losses are estimated by the total

pressure averaged by the massflow. The value ζ is defined as the ratio of the averaged total pressure to the same parameter in the initial cross-section. The dependence of losses upon mixing efficiency θ is presented in Fig.2.3.3. The value θ is introduced as

$$\theta = (1 - D/D_0),$$

where D_0 is value D in initial cross-section. It varies from zero in initial cross-section to unit at full mixing. The total pressure losses level for ideal full mixing is designated by a marker. The results comparisons for these four cases confirms that the total pressure losses are approximately the same for identical mixing efficiency, determined by θ. But it is necessary to note, that identical mixing efficiency is achieved on different distances from initial cross-section (see Fig.2.3.2). Hence, the mixing is enhanced for this regime without noticeable additional total pressure losses. The mixing enhancement is also illustrated in Fig.2.3.4, where the H_2 mass fraction fields are shown for cases C_1 - C_4 in different cross-sections.

The H_2 jet injection at an angle $10°$ is accompanied by momentum losses of hydrogen jet of 1.5%, these losses are equal to 2.2% for conical axisymmetric nozzle, and for elliptical nozzle - 3.5%. Thus, the additional momentum losses for elliptical nozzle in comparison with axisymmetrical nozzle are equal 1.3%, and are approximately the same, as in the cases C_2 and C_3. Hence, providing the superior mixing level, the mixing enhancement using elliptical nozzle does not introduce visible additional losses in comparison with others alternative mixing control methods investigated at this paper.

It is important to reveal the cause of mixing enhancement. As follows from the analysis of the numerical results, presented in Fig.2.3.4, the hydrogen jet strongly changes its form with increase of "mixing" surface in the cases C_2-C_4. The hydrogen mass fraction fields give evidence about mixing enhancement. But for cases C_2, C_3, the confluence of neighboring hydrogen jets takes place at smaller distances from initial cross section than in the case of elliptical nozzle. Moreover, the lateral eruption of hydrogen jet is less intensive in the case C_3 in comparison with elliptical jet.

The second effect, arising at the three-dimensional fluid dynamic interaction of hydrogen jet and air flow, is concerned with intensive secondary flows formation. The fields of the transverse velocity components are shown for all cases in Fig.2.3.5. It is evident, that the axial vortices are formed as a result of three-dimensional interaction for cases C_2-C_4. These vortices are observed far from the initial cross-section and provide the convection mechanism for mixing enhancement. Significance of longitudinal vortices for mixing and combustion augmentation was also mentioned for example in [33]. But the nature of

vortices arising is different. In our case, the longitudinal vortices are the result of three-dimensional fluid dynamic interaction behind the nozzle exit cross-section. This vorticity is not generated in the nozzle flow.

In order to illustrate the influence of the mixing enhancement on the combustion efficiency, the same regime was calculated using the flame sheet model. The combustion efficiency as a function of streamwise coordinate is shown in Fig.2.3.6 for axisymmetric nozzle (N_1), and for two elliptical nozzles with 2:1 (N_2) and 3:1 (N_3) aspect ratio in the exit cross-section. The location of the flame front is presented in different cross-sections of the channel in Fig.2.3.7. The change of the flame front surface and its "interaction" with computational region boundaries may explain the dependence of the combustion efficiency upon the longitudinal distance, and, in particular, the reduction of the "combustion rate" at some distance, and also the superiority of the nozzle N_3 in comparison with nozzles N_2 and N_1.

Thus, it is seen, that the three-dimensional effects, arising due to interaction of the supersonic hydrogen jet from nonaxisymmetric nozzle with coflowing air stream, provide the mechanisms for the mixing and combustion enhancement. The first mechanism is connected with the increase of mixing and combustion surfaces. The second convective mechanism is the formation of intensive secondary flows with longitudinal component of vorticity. It is necessary to note, that for the mathematical model, presented in this paper, the investigated mixing and combustion enhancement effects are not connected with additional turbulent viscosity generation. Therefore, it is interesting to verify the role of the investigated effects for regimes with weak turbulent viscosity generation and simultaneously with low initial turbulent viscosity level.

For the regime R_2 the turbulent viscosity generation is small, because the ratio of longitudinal velocity components approaches to one, and the turbulent mixing efficiency is determined by the initial turbulent viscosity level. The dependence of the mixing efficiency q upon the longitudinal distance for axisymmetric and elliptical nozzles is represented in Fig.2.3.8 by curves 1 and 2 respectively. The initial dimensionless turbulent viscosity level is equal to $3*10^{-4}$ (the ratio of the turbulent viscosity to hydrogen velocity and radius of axisymmetric nozzle in the initial cross section). The curve 1 shows, that at small initial turbulent viscosity levels the turbulent mixing is unessential. It is obvious, that in this case the elliptical nozzle provides much more superior mixing characteristics relative to axisymmetric one.

In order to investigate the influence of the nozzle design on combustion efficiency for regime R_2, some

calculations were performed for axisymmetric N_1 and elliptical N_2 nozzles with two different initial levels of turbulent viscosity (10^{-4} and $2*10^{-3}$) and for elliptical nozzle N_3 with small initial turbulent viscosity level. The combustion efficiency as a function of streamwise coordinate is shown in Fig.2.3.9. The curves 1,2 correspond to axisymmetric nozzle with small and high levels of turbulent viscosity. The similar results for the elliptical nozzle N_2 are represented by curves 3,4 and curve 5 corresponds to the nozzle N_3 and low initial level of turbulent viscosity. The elliptical nozzle provides superior mixing characteristics relative to circular nozzle for both initial levels of turbulent viscosity. In the case of elliptical nozzle N_2 with small initial level of turbulent viscosity, the combustion efficiency is higher at large distances from initial section, than in the case of circular nozzle with large turbulent viscosity level. Taking into account the influence of the initial turbulent viscosity level on the combustion efficiency for the elliptical nozzle, it is possible to assume, that the mixing and combustion surface increase has the main significance for this regime. Possibly, the convective mechanism, provided by the secondary flows, is less essential in any case for the higher initial level of turbulent viscosity. The comparison of curves 1,3,5 shows, that the nozzle N_3 provides superior combustion efficiency.

At the third regime, air flow has high Mach number, hydrogen jet is strongly underexpanded, besides that the air flow velocity exceeds jet velocity. The comparison was made for three nozzles: N_1, N_2 and N_3. One can see from Fig.2.3.10 that the nozzle N_3 provides the best combustion efficiency again.

Thus, it may be noticed, that the elliptical nozzle for hydrogen injection provides the superior combustion efficiency in wide range of regimes in the duct with the rectangular cross - section. It seems, that it is possible to choose the nozzle aspect ratio, which provides the best level of combustion efficiency for this duct.

2.4 Some notices about the jet/shock interaction and mixing enhancement

The problem of hydrogen jet passage through an oblique shock wave was investigated in [39-42,68]. It was pointed out that a strong interface distortion and baroclinic torque take place as a result of shock-impingement [39-42] except the possible jet compression [68]. This distortion and baroclinic torque are connected with the generation of the vorticity located along the fuel/air interface [39-41].

The goal of this study was to investigate numerically the process of shock-impingement itself and conditions, providing mentioned effects. Free air stream conditions corresponded to $M_2=6$, $T_2=2000°K$.

The ramp with angle of $7.1°$ produced the oblique shock with pressure ratio about 2.5. Computational grid consists of 75x50 cells in cross-section. In the base (reference) case the hydrogen jet Mach number M_1 was equal to 2, and jet/air density ratio ρ' was equal to 0.5.

The density ratios 0.125, 0.5, 1.0 and 2.0 (corresponding to hydrogen temperatures $1120°$ K, $280°$ K, $140°$ K and $70°$ K) were studied in the first series for the inviscid case (Fig.2.4.1 and table 2.4.1). In this series M_1 was equal to 2. The peculiarity of the case with $\rho'=1$ consists in the absence of the baroclinic source term in the vorticity equation [40], because the normal component of density gradient on the jet boundary is turned off, and in unviscid case the density gradient as the pressure gradient is caused only by wave structure if the numerical scheme dissipation is negligible. However, the patterns of density fields (see Fig.2.4.2, 2.4.3) show, that jet shape deformation doesn't depend on ρ', and remains even if the density gradient is parallel to the pressure gradient.

In the second series, ρ' was fixed and equal to 0.5, but jet Mach number M_1 was changed: $M_1=2,4,6$. Air stream Mach number was equal to 6. To provide the identical shock slope in the jet and in the air in the last case, the air and hydrogen specific heat ratios were set equal to 1.4. The rapid interface deformation is proved to be reduced with the increase of jet Mach number. Fig.2.4.4 shows, that jet is only compressed by the shock in vertical direction at equal Mach numbers and then retains its shape. The non-dimensional circulation is presented in Fig.2.4.5 for the investigated cases. It is interesting to note, that there is no switching of circulation sign with reversing of density ratio, as it would be supposed according to [40]. Moreover, the essential influence of the density ratio on the circulation level is not observed. But the level of circulation diminishes with the rise of jet Mach number. So one can suppose that just the Mach number difference but not the density ratio is responsible for the rapid jet distortion.

Some explanation may be proposed on the base of the detailed pattern of density contours obtained with the grid 95x70 for the reference ((see Fig.2.4.6). After the jet and shock touching the part of shock inside the jet "moves" faster than shock in air due to the Mach numbers difference. Besides, the expansion wave arise on the lower part of jet boundary and moves toward the ramp surface. Probably, these waves result in secondary flows with longitudinal vorticity. At some distance, these flows induce jet dividing on two parts and considerable increase of the mixing surface. The jet dividing effect is clearly discernible in the Fig. 2.4.3.

The next series of computations was run for the reference regime with turned on viscosity terms to obtain information about mixing enhancement: a) for free jet without any shock, b) for the base case, when the

ramp leading edge is in the same section where jet is injected ($X_{ramp}=0$), and c) for $X_{ramp}=30$. Density contours for cases b), c) are shown in Fig.2.4.7, 2.4.8 and concentration fields in section x=120 - in Fig.2.4.9. One can see, that in spite of different X_{ramp} the resulting concentration fields are similar. Only the height of the jet center is slightly larger in the case of $X_{ramp}=0$. This fact can be explained by longer lifting action of vortices. As for the mixing efficiency, it is seen in the Fig.2.4.10 that the presence of the shock provides the superior mixing and the final effect is weakly dependent on the place of the shock impingement.

But two others curves in Fig.2.4.10, corresponding to hydrogen/air mixing in the case of equal Mach numbers with and without shock, also demonstrate some mixing enhancement by shock. The reduction of length, where the mixing efficiency 0.4 is achieved, constitutes 37% for jet Mach number 6 and 63% for jet Mach number 2 (comparisons of lengths are made for cases with and without shock impingement). It is difficult to divide the influence of general compression in the shock (the decrease of the jet cross-section area) and jet distortion on mixing enhancement, but the quantitative comparison allows to suppose, that the jet distortion may provide the additional mixing enhancement.

It is necessary to note that numerical simulation of shock/jet interaction was performed in CIAM by V.Vasiljev and S.Zakotenko [68]. They point out that the compression of the jet at processing through the shock is followed by decrease of the jet cross - section area. At the same time, the turbulent viscosity does not change its level after processing through the shock. The decreased cross - section area and the unchanged level of turbulent viscosity at the shock/jet interaction provide the main mechanism of the mixing enhancement from the point of authors view [68]. The secondary flows with vortical structure were observed. But from the authors of paper [68] opinion, this mechanism does not influence mixing process.

Thus, from our point of view, the rapid jet/air interface distortion and intensive secondary transversal flows are promoted by the difference of Mach numbers in the hydrogen jet and air stream, but not only by the density gradients in the baroclinic torque effect. This distortion increases the mixing enhancement. The jet contraction may become the prevailing enhancement mechanism at small Mach number difference.

2.5 Evaluation of combustion efficiency and choice of acceptable design parameters for combustor

Let us consider the question about the injector design parameters choice. It is necessary to choose the number of struts for hydrogen injection, the number of

nozzles for hydrogen injection in each strut, and to contour the nozzle for hydrogen injection. The injector design, the struts and nozzles disposition must provide the uniform hydrogen jet distribution in the combustor cross-section. For example, it is desirable to divide the combustor cross-section on the elementary square regions of the air stream and to inject the circular hydrogen jet to the center of this region with the aid of injection system. The uniform hydrogen jet distribution in air stream is realized in this case. But the following circumstances should be taken into account. The strut system induces the drag, besides it is necessary to solve the strut cooling problem. Therefore, the number of struts is limited and is comparatively small. Thus, it is necessary to design the effective injection system with a fixed, as small as possible number of struts. But the dimension of the square elementary region is large in the case of small number of struts. The combustion length at given parameters in initial cross-section is defined by chemical reaction rates and by mixing process. If the combustion process is limited by mixing, then the absolute flame length increases as the hydrogen jet radius or elementary region dimension are increased (at given air/fuel equivalence ratio they are correlated). Therefore, really the absolute combustion length is large in the case of uniform distribution of circular hydrogen jets for small number of struts.

It seems to be useful to increase the number of nozzles on the strut in order to decrease the absolute combustion length. But when the number of struts is fixed, the elementary air region becomes rectangular. The partial confluence of hydrogen jets may cause the decrease of the mixing and combustion efficiency in this case. In fact, as the ratio of hydrogen and air mass flows is fixed, then the distance h between nozzles is decreased as 1/N when the number of nozzles N in strut is increased. At the same time the axisymmetric nozzle radius r is decreased as $1/\sqrt{N}$, so that h/r $\sim 1/\sqrt{N} \rightarrow 0$ as $N \rightarrow \infty$. The confluence of hydrogen jets prevents from the effective combustion of circular hydrogen jet in rectangular elementary region. This effect was shown in the previous section. But it is possible to use the potential opportunity to decrease the absolute combustion length with increased number of nozzles and decreased hydrogen jet absolute dimensions by choosing the "optimal" elliptical nozzle for rectangular elementary channel. As it was demonstrated in the previous section, the elliptical nozzle provides the decrease of relative mixing and combustion lengths in comparison with axisymmetric nozzle for the case of increased number of hydrogen nozzles with rectangular elementary channel. The gain in combustion efficiency may be obtained in this case for equivalent absolute combustor length and identical number of struts in comparison with the base injector version, providing the uniform distribution of circular hydrogen jets in the cross-section.

Thus, it is possible to fix the number of struts

and to choose the number of elliptical nozzles on the strut with the "optimal" axis ratio. The previous investigations showed, that it is possible to increase the combustion efficiency with the increasing the elliptical nozzle axes ratio up to value 3 and more. The simultaneous variation of the number of nozzles in order to obtain the best number for each ellipticity is needed too. But such two - parameters "optimization" procedure seems to be very expensive task, because it is necessary to perform direct calculations with two parameters variation. But some practical limitations allow to reduce the volume of calculations. If the elliptical nozzle aspect ratio is too large, the excessive expansion angles in the large axis direction, and possible converging of nozzle with circular throat in the small axis direction result in high losses in comparison with axisymmetric nozzle. Besides, some design restrictions may exist on the nozzle shape and dimensions. For example, it may be the overall dimensions restriction.

Taking into account the aforementioned circumstances, the following design procedure seems to be justified. For a given number of struts the base injector version is considered, providing the uniform distribution of axisymmetric hydrogen jets. The injector with greater number of elliptical nozzles is investigated as alternative version. The general hydrogen mass flow through the elliptical nozzles is equal to that in the axisymmetric nozzles case. The overall dimensions of the nozzle and strut for the alternative injector do not exceed that for base version. The minimal cross-section of the modified nozzle remains circular, but it has some times lesser diameter in comparison with base axisymmetric nozzle. The length of nozzle supersonic part remains the same in both cases. The supersonic part of the modified elliptical nozzle has the rectilinear generatrices. These generatrices connect throat and exit cross-sections. The maximal generatrix inclination angle is obtained taking into account not only the geometrical considerations but also the desire to provide the acceptable level of nozzle performances. This configuration is considered as alternative injector version.

But simplified method of preliminary injector design may be proposed, which provides efficiency results equivalent to two times larger numbers of struts and axisymmetrical nozzles on each strut in comparison with base injector version. The corresponding schemes, illustrating the suggested method are shown in Fig.2.5.1-a and 2.5.1-d.

The base injector configuration ensures uniform distribution of hydrogen jets over combustor cross section, but absolute dimensions of jets and / or elementary duct falling on one jet are too great to realize acceptable combustion efficiency levels on chosen combustor length with chosen number of struts (see Fig.2.5.1-a) . The most simple solution is to increase the number of hydrogen injection nozzles and the number of struts and to decrease simultaneously absolute dimensions of jets and elementary ducts maintaining the uniform distribution of hydrogen jets over combustor cross section. The corresponding scheme, illustrating the case of two times greater number of strut and hydrogen nozzles on each strut is shown in Fig.2.5.1-b. In this case it is possible to realize more high combustion efficiency levels on the same combustor length or to decrease required combustor length due to reduction of absolute dimensions of jets and elementary ducts under condition that combustion process is controlled by mixing rather than by chemical kinetics.

But under some conditions we can't select this way, because of increase of struts number. On the other hand the simple increase of nozzles number on strut at constant struts number may be ineffective due to quick confluence of jets for neighboring elementary ducts with rectangular cross-section. The situation, corresponding to doubled number of nozzles on strut at constant struts number is shown schematically in Fig. 2.5.1-c. It is possible to avoid negative influence of jets confluence for rectangular elementary duct by use of elliptical nozzles elongated in the direction of greater side of elementary rectangular duct. The results presented above (see, for example section 2.3) show that jet from the elliptical nozzle divides into two parts at some distance from injection section. This provides practically uniform distribution of jets over duct cross-section, similar to distribution with two times greater struts number and simultaneously two times greater number of axisymmetric nozzles on each strut. The latter is shown schematically in Fig. 2.5.1- d (the jets, into which breaks down the jet from elliptical nozzle are shown schematically by two circles near the ellipse). But it is necessary to select axes ratio of elliptical nozzles providing the best dividing of hydrogen jets from the considerations of their mixing and burning.

As an example some combustion efficiency estimations were performed for the model combustor schematically presented in Fig.2.5.2. The strut system for hydrogen injection is located in combustor within the symmetrical angle in horizontal plane, which is equal to $36°$. The number of struts was chosen to be equal to 15. The air parameters at the combustor entrance are presented in the table 2.5.1. The Mach number at the exit of hydrogen nozzle and the parameters (pressure and temperature) are also shown in table 2.5.1.

Some injection schemes were tested to compare their relative efficiency. In the first case the hydrogen is injected through the slot in the backward face of the strut. The slot vertical dimension is equal to strut height. In the second case the high slot is divided into several sections. The hydrogen is injected through the each section at an angle $10°$ to the main air flow

direction with alternation of lateral directions of injection in neighboring sections. In the third case the injection is realized through the individual axisymmetric nozzles, which are placed inside strut with nozzle exit section on the strut backward face. Then using the number of struts, the number of hydrogen jets injected from each strut, the elementary region per one jet was obtained in accordance with combustor duct geometry (see Fig. 2.5.2). All estimations were performed for a single jet in the elementary channel with coflowing air flow. It is obvious that such evaluation method is approximate. But probably it is possible to compare alternative injection schemes efficiency in such manner.

Let us consider some results about the combustion efficiency, which are presented in Fig.2.5.3. It is necessary to note, that the injector with individual nozzles was chosen to provide the uniform distribution of hydrogen jets in the injector control cross-section. Therefore the number of nozzles is equal to 20 on each strut. The curves 1,2,3 in the Fig.2.5.3 show the combustion efficiency as the function of longitudinal coordinate for test cases 1-3 (correspondingly for slot, section slot and axisymmetric nozzles injection schemes). It is necessary to note the low combustion efficiency in the cases of slot and section slot injection. The better results are obtained in the third case for injection with the aid of individual axisymmetric nozzles.

The proposed scheme of combustion enhancement due to doubled number of elliptical nozzles at the same number of struts was also tested. In this case the elliptical nozzles with aspect ratio 2:1 in exit cross-section were used. The results obtained in this case are shown in Fig.2.5.3 by curve 4. The obtained results demonstrate the possibility to reduce the necessary combustor length with the aid of this injection system with doubled number of elliptical nozzles. So, if the combustion efficiency value 0.9 is reached on the distance approximately one conventional length unit for injector with elliptical nozzles, it is needed approximately 2.14 units for the injector with axisymmetric nozzles, and the distance more than 2.85 units is necessary to reach the combustion efficiency level 0.9 in the case of section slot and slot injectors.

2.6 Estimation of the role of chemical kinetics

To estimate the role of chemical kinetics at the different scramjet operational regimes, the set of parameters at the entrance of combustor presented in table 2.6.1 was used. The characteristic ignition length L_i versus flight Mach number is presented in Fig.2.6.1. It is seen that L_i is sufficiently smaller then the typical combustor length scale (~1m), and the self-ignition can be the limitation mechanism only if the flight Mach number $M_f < 8$-9.

The characteristic energy release length scale L_e versus flight Mach number is presented in Fig.2.6.2. It is seen that the heat release zone length is small in both (MIX and DIF) approaches at $M_f<12$. The role of recombination processes at M_f increase ($M_f>12$) is dramatically increased too and at flight Mach numbers $M_f=14$-20 these processes can substantially influence combustor operation.

The obtained results indicate that the reliable mathematical model for scramjet combustor has to be developed taking into account the detailed chemical kinetics. Nevertheless, the usage of the developed simplified mathematical model for kinetics effects estimations makes it possible to apply the flame sheet model in scramjet combustor flowfield calculations more argumentally.

References

1. Баев В.К., Головичев В.И., Ясаков В.А., "Двумерные турбулентные течения реагирующих газов", Новосибирск, Наука, 1976, 264 с.

2. Баев В.К., Головичев В.И., Третьяков П.К., Гаранин А.Ф., Константиновский В.А., Ясаков В.А., "Горение в сверхзвуковом потоке", Новосибирск, Наука, 1984, 302 с.

3. Мещеряков Е.А., Сабельников В.А., "Горение водорода в сверхзвуковом турбулентном потоке в канале при спутной подаче горючего и окислителя", Физика Горения и Взрыва, N 2, 1981, с.55-64.

4. Зимонт В.Л., Левин В.М., Мещеряков Е.А., Сабельников В.А., "Особенности горения неперемешанных газов в каналах", Физика Горения и Взрыва, N 4, 1983, с.75-78.

5. Мещеряков Е.А., Сабельников В.А., "Роль смешения и кинетики в уменьшении тепловыделения при сверхзвуковом горении неперемешанных газов в расширяющихся каналах", Физика Горения и Взрыва, N 5, 1988, с.23-32.

6. Громов В.Г., Ларин О.Б., "Тангенциальный вдув водорода в турбулентный сверхзвуковой пограничный слой", Известия АН СССР, Механика Жидкости и Газа, N 3, 1982, с.189-191.

7. Громов В.Г., Ларин О.Б., Левин В.А., "Применение модели "несмешанности" для расчета турбулентной пристенной струи водорода в спутном сверхзвуковом потоке воздуха", Химическая Физика, Т.3, N 8, 1984, с.1190-1195.

8. Громов В.Г., Ларин О.Б., Левин В.А., "Турбулентное горение водорода в пристенной струе, истекающей в спутный сверхзвуковой поток воздуха", Физика Горения и Взрыва, N 6, 1987, с.3-9.

9. Spiegler E., Wolfshtein M., Manheimer-Timnat Y., "A model of unmixedness for turbulent reacting flows", Acta Astronautica, V.3, N 3-4, 1976, p. 265.

10. Барановский С.И., Левин В.М., Надворский А.С., Турищев А.И., "Экспериментально-теоретическое исследование спутных сверхзвуковых реагирующих струй", Сборник "Турбулентные течения в реагирующих потоках", Минск, Наука, 1986, с.84-98.

11. Барановский С.И., Надворский А.С., Перминов В.А., "Расчет горения турбулентной сверхзвуковой неизобарической струи водорода в спутном сверхзвуковом потоке воздуха", Физика Горения и Взрыва, N 4, 1986, с.14-18.

12. Барановский С.И., Перминов В.А., "О применимости модели диффузионного горения к расчету сверхзвуковых турбулентных реагирующих струй", Физика Горения и Взрыва, N 3, 1987, с.85-88.

13. Колесников О.М., "Расчет повышения давления при горении плоской сверхзвуковой струи водорода в сверхзвуковом спутном потоке", Ученые Записки ЦАГИ, Т.13, N6, 1982, с.49-58.

14. Колесников О.М., "Влияние пульсаций концентрации на воспламенение пристенной струи водорода в сверхзвуковом потоке", Физика Горения и Взрыва, N 1, 1985, с.53-57.

15. Колесников О.М., "Влияние инжекции водорода на взаимодействие неравновесного пограничного слоя с внешним сверхзвуковым потоком", Ученые Записки ЦАГИ, Т.18, N 6, 1987, с.101-106.

16. White M.E., Drummond J.P., Kumar A., "Evolution and Application of CFD Techniques for Scramjet Engine Analysis", J. of Propulsion and Power, V.3, N 5, pp.423-439

17. Barber T.J., Cox G.B., Jr., "Hypersonic Vehicle Propulsion: A Computational Fluid Dynamics Application Case Study", J. of Propulsion and Power, V.5, N 4, 1989, pp.492-501.

18. McClinton C., Bittner R., Kamath P., "CFD Support of NASP Design", AIAA 90-5249, 1990.

19. Anderson G., Kumar A., Erdos J., "Progress in Hypersonic Combustion Technology with Computation and Experiment", AIAA 90-5254, 1990.

20. Rogers R.C., Chinitz W., "Using a Global Hydrogen-Air Combustion Model in Turbulent Reacting Calculations", AIAA J., V.21, N 4, 1983, pp.586-592.

21. Papamoschou D., Roshko A., "Observation of Supersonic Free Shear Layers", AIAA 86-0162, 1986.

22. Bogdanoff D.W., "Compressibility Effects in Turbulent Shear Layers", AIAA J., Vol.21, N 6, 1983, pp.926-927.

23. Samimy M., Erwin D.E., Elliott G.S., "Compressibility and Shock Vawe Interaction Effects on Free Shear Layers", AIAA 89-2460, 1989.

24. Gilreath H.E., Sullins G.A., "Investigation of the Mixing of Parallel Supersonic Streams", ISABE 89-7060, 1989.

25. Swithenbank J., Eames I., Chin S., Ewan B., Yang Z., Cao J., Zhao X., "Turbulent Mixing in Supersonic Combustion Systems", AIAA 89-0260, 1989.

26. Hewitt F.A., Ward B.D., "Advanced Airbreathing Powerplant for Hypersonic Vehicles", ISABE 89-7107, 1989.

27. Gutmark E., Wilson K.J., Schadow K.C., Parr T.P., Hanson-Parr D.M., "Combustion Enhancement in Supersonic Coaxial Flows", AIAA 89-2788, 1989.

28. Schadow K.C., Gutmark E., "Rewiew of Passive Shear Flow Control Research for Improved Subsonic and Supersonic Combustion", AIAA 89-2786, 1989.

29. Schadow K.C., Gutmark E., Wilson K.J., "Passive Mixing Control in Supersonic Coaxial Jets at Different Convective Mach Numbers", AIAA 89-0995, 1989.

30. Schadow K.C., Gutmark E., Koshigoe S., Wilson K.J., "Combustion-Related Shear-Flow Dynamics in Elliptic Supersonic Jets", AIAA J., Vol.27, N 10, 1989, pp.1347-1360.

31. Schadow K.C., Gutmark E., Wilson K.J., "Noncircular Jet Dynamics in Supersonic Combustion", J. of Propulsion and Power, Vol.5., N 5, 1989, pp.529-533.

32. Gutmark E., Schadow K.C., Bicker G.S., "On the Near Acoustic Field and Shock Structure of Rectangular Supersonic Jets", AIAA 89-1053, 1989.

33. Gutmark E., Schadow K.C., Parr T.P., Parr D.M., Wilson K.J., "Combustion Enhancement by Axial Vortices", J. of Propulsion and Power, Vol.5, N 5, 1989, pp. 555-559.

34. Zaman K.B.M.Q., Reeder M.F., Samimy M., "Supersonic Jet Mixing Enhancement by "Delta-Tabs" ", AIAA 92-3548, 1992.

35. Drummond J.P., Carpenter M.M., Mukunda H.C., "Mixing and Combustion Enhancememt in Supersonic Reacting Flows", Proceedings of the Fifth International Symposium on Numerical Methods in Engineering, Vol.1, Springer-Verlag, 1989, pp.175-184.

36. Drummond J.P., Mukunda H.S., "A Numerical Study of Mixing Enhancement in Supersonic Reacting Flow Fields", AIAA 88-3260, 1988.

37. Shau Y.R., Dolling D.S., "Experimental Study of Spreading Rate Enhancement of High Mach Number Turbulent Shear Layers", AIAA 89-2458, 1989.

38. Menon S., "Shock-Wave-Induced Mixing Enhancement in Scramjet Combustors", AIAA 89-0104, 1989.

39. Marble F.E., Hendricks G.J., Zukoski E.E., "Progress Toward Shock Enhancement of Supersonic Combustion Processes", AIAA 87-1880, 1987.

40. Waitz I.A., Marble F.E., Zukoski E.E., "Vorticity Generation by Contoured Wall Injectors", AIAA 92-3550, 1992.

41. Waitz I.A., Marble F.E., Zukoski E.E., "A Systematic Experimental and Computational Investigation of a Class of Contoured Wall Fuel Injectors", AIAA 92-0625, 1992.

42. Drummond J.P., "Mixing Enhancement of Reacting Parallel Fuel Jets in a Supersonic Combustor", AIAA 91-1914, 1991.

43. Northam G.B., Greenberg I., Byington C.S., "Evaluation of Parallel Injector Configurations for Supersonic Combustion", AIAA 89-2525, 1989.

44. Drummond J.P., Carpenter M.H., Riggins D.W., Adams M.S., "Mixing Enhancement in Supersonic Combustor", AIAA 89-2794, 1989.

45. Riggins D.W., McClinton C.R., "A Computational Investigation of Flow Losses in a Supersonic Combustor", AIAA 90-2093, 1990.

46. Northam G.B., Capriotti D.P., Byington C.S., Greenberg I., "Mach 2 and Mach 3 Mixing and Combustion in Scramjets", AIAA 91-2394, 1991.

47. Riggins D.W., McClinton C.R., Rogers R.C., Brittner R.D., "A Comparative Study of Scramjet Injection Strategies for High Mach Number Flows", AIAA 92-3287, 1992.

48. Naughton J., Cattafesta Z., Settles G., " An Experimental Study of the Effect of Streamwise Vorticity on Supersonic Mixing Enhancement", AIAA 89-2456, 1989.

49. Naughton J.W., Settles G.S., "Experiments on the Enhancement of Compressible Mixing via Streamwise Vorticity, Part 1-Optical Measurements", AIAA 92-3549, 1992.

50. Mays R.B., Thomas R.H., Schetz J A., "Low Angle Injection into a Supersonic Flow", AIAA 89-2461, 1989.

51. Fuller E.J., Mays R.B., Thomas R.H., "Mixing Studies of Helium in Air at Mach 6", AIAA 91-2268, 1991.

52. Fuller E.J., Walters R.W., "Navier-Stokes Calculations for 3-D Gaseous Fuel Injection with Data Comparisons", AIAA 91-5072, 1991.

53. Wood C.W., Thomas R.H., Schetz J A., "Effects of Oscillating Shock Impingement on the Mixing of a Gaseous Jet in a Mach 3 Air Stream", AIAA 90-1982, 1990.

54. Kumar A., Bushnell D.M., Hussaini M.Y., "A Mixing Augmentation Technique for Hypervelocity Scramjets", J. of Propulsion and Power, Vol.5, N 5, 1989, pp.514-522.

55. Андерсон Д.,Таннехилл Дж., Плетчер Р., "Вычислительная гидромеханика и теплообмен", Т. 1-2, Москва, Мир, 1990.

56. Козлов В.Е., Секундов А.Н., Смирнова И.П., "Модели турбулентности для описания течения в струе сжимаемого газа", Известия АН СССР, Механика Жидкости и Газа, N 6, 1986, с.38-44.

57. Козлов В.Е., "Упрощенный метод численного расчета трехмерной турбулентной свободной струи", Известия АН СССР, Механика Жидкости и Газа, N 1, 1989, с. 170-173.

58. Зельдович Я.Б., Баренблатт Г.И., Либрович В.Б., Махвиладзе Г.М., "Математическая теория горения и взрыва", Москва, Наука, 1980, 478 с.

59. Кузнецов В.Р., Сабельников В.А., "Турбулентность и горение", Москва, Наука, 1986, 287 с.

60. Годунов С.К.,Забродин А.В., Иванов М.Я., Крайко А.Н., Прокопов Г.П.," Численное решение многомерных задач газовой динамики", Москва, Наука, 1976, 400 с.

61. Копченов В.И., Крайко А.Н., "Монотонная конечно-разностная схема второго порядка точности для гиперболических систем с двумя независимыми переменными", Журнал Вычислительной Математики и

Математической Физики, Т.23, N 4, 1983, с.848-859.

62. Родионов А.В., "Монотонная схема второго порядка аппроксимации для сквозного расчета неравновесных течений", Журнал Вычислительной Математики и Математической Физики, Т.27, N 4, 1987, с.585-593.

63. Тилляева Н.И., "Обобщение модифицированной схемы С.К.Годунова на пространственно неоднородные сетки", Ученые Записки ЦАГИ, Т.17, N 2, 1986, с.19-26.

64. Колган В.П., "Конечно-разностная схема для расчета двумерных разрывных нестационарных газодинамических решений", Ученые Записки ЦАГИ, Т.6, N 1, 1975, с.9-14.

65. Dimitrow V.I., "The maximum kinetic mechanism and rate constants in the H_2-O_2 system", React. Kinetic Catal. Lett., V.7, No.1, 1977, pp.81-86.

66. Полак Л.С., Гольденберг М.Я., Левицкий А.А., "Вычислительные методы в химической кинетике", Москва, Наука, 1984, 280 с.

67. Kopchenov V.I., Lomkov K.E., "The Enhancement of the Mixing and Combustion Processes Applied to Scramjet Engine", AIAA 92-3428, 1992.

68. Васильев В.И., Закотенко С.Н., "Об интенсификации смешения потоков за косым скачком уплотнения", Известия РАН, Механика Жидкости и Газа, N 2, 1992, с.61-66.

TABLE 2.3.1

HYDROGEN JET PARAMETERS :
$M_1=3.05,$ $T_1=340°$ K

AIR STREAM PARAMETERS:

Regime	T_2 °K	M_2	p_2/p_1	u_2/u_1
R_1	1050	2.8	0.98	0.41
R_2	1950	5.5	5.88	1.10
R_3	2300	6.6	6.37	1.35

TABLE 2.4.1

AIR STREAM $M_2=6.0,$ $T_2=2000°$ K

series	case	ρ_1/ρ_2	M_1	T_1 °K	u_1/u_2
1	1.1	2.0	2.0	70	0.25
1	1.2	1.0	2.0	140	0.35
1	reference 1.3	0.5	2.0	280	0.5
1	1.4	0.125	2.0	1120	1.0
2	reference 2.1	0.5	2.0	280	0.5
2	2.2	0.5	3.0	280	0.75
2	2.3	0.5	4.0	280	1.0
2	2.4	0.5	6.0	280	1.5

TABLE   2.5.1

air stream parameters			hydrogen parameters		
M_2	P_2	T_2	M_1	P_1	T_1
4.22	$0.83*10^5$ Pa	1076° K	2.6	$1.5*10^5$ Pa	425° K

fuel - air equivalence ratio
ϕ=0.98

TABLE   2.6.1

M_f	8	12	16	20
ϕ	0.91	1.66	5.0	5.0
T_{air} °K	1100	1500	1970	2300
P_{air} Pa	$1.8*10^5$	$1.2*10^5$	$0.8*10^5$	$0.65*10^5$
M_{air}	3.05	4.8	5.5	6.6
$n=P_{H_2}/P_{air}$	0.84	1.92	5.88	6.37
M_{H_2}	2.9	2.9	2.9	2.9
T_{H_2} °K	373	373	373	373
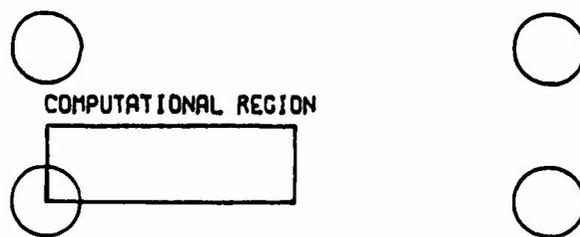
A) INITIAL CROSS-SECTION FOR CASE C_1
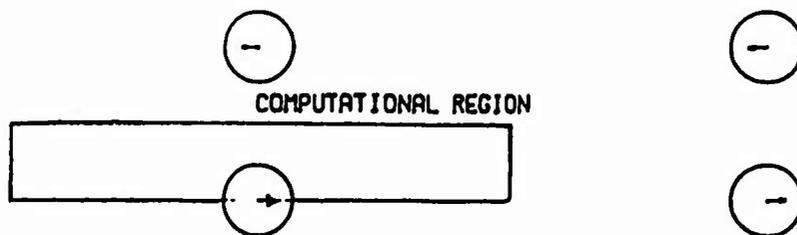
B) INITIAL CROSS-SECTION FOR CASE C_2
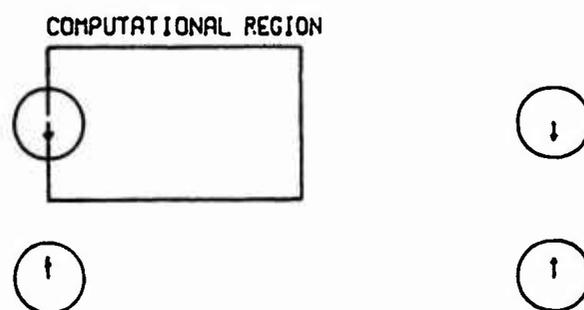
C) INITIAL CROSS-SECTION FOR CASE C_3
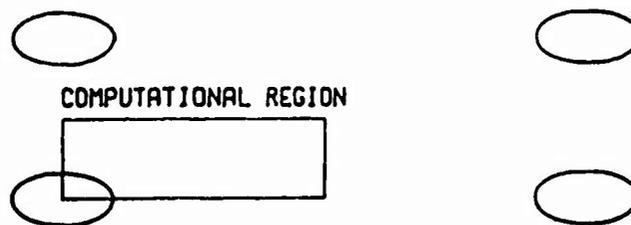
D) INITIAL CROSS-SECTION FOR CASE C_4

Fig.2.3.1 INITIAL CROSS-SECTIONS AND COMPUTATIONAL REGIONS FOR CASES C_1-C_4
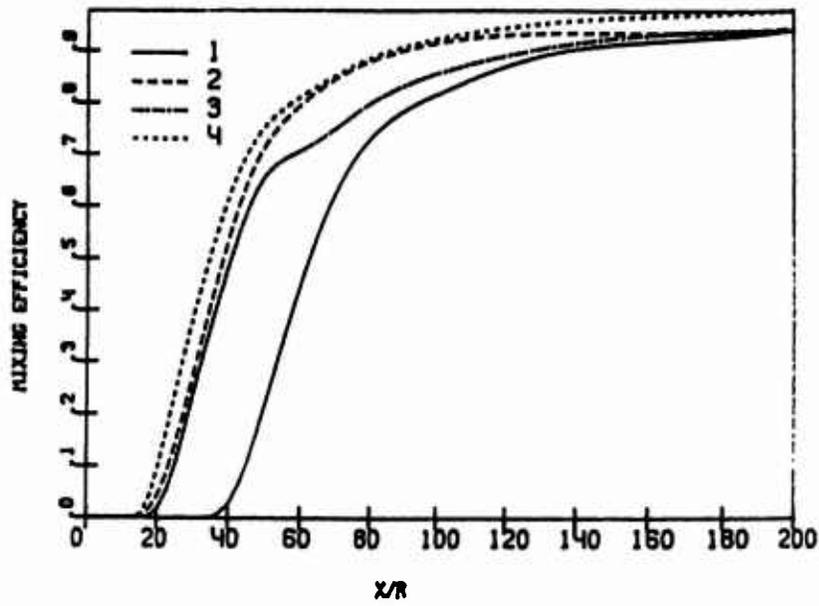
MIXING EFFICIENCY CHARACTERISTIC q FOR REGIME, R_1

Fig.2.3.2
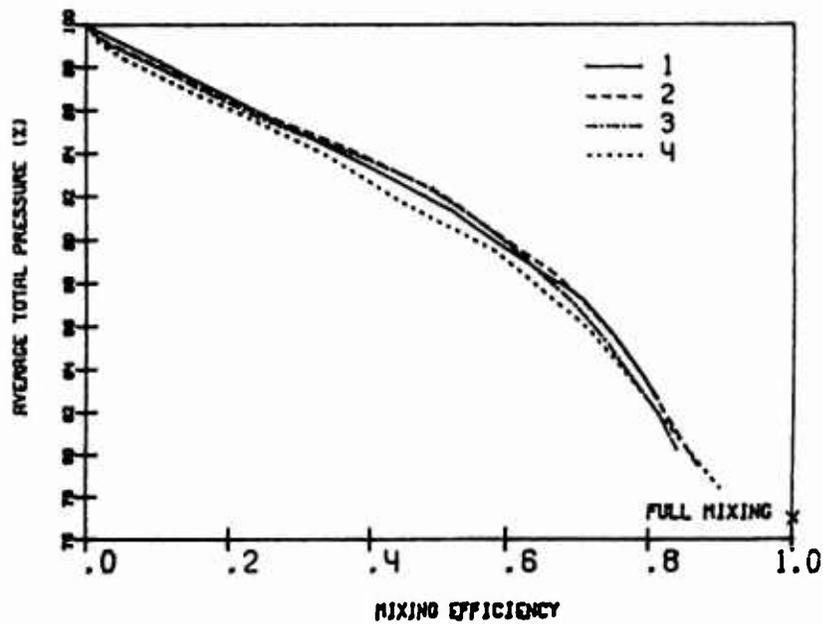
THE DEPENDENCE OF TOTAL PRESSURE LOSSES UPON MIXING EFFICIENCY

Fig.2.3.3

AXISYMMETRICAL NOZZLE

HORIZONTAL INTERACTION
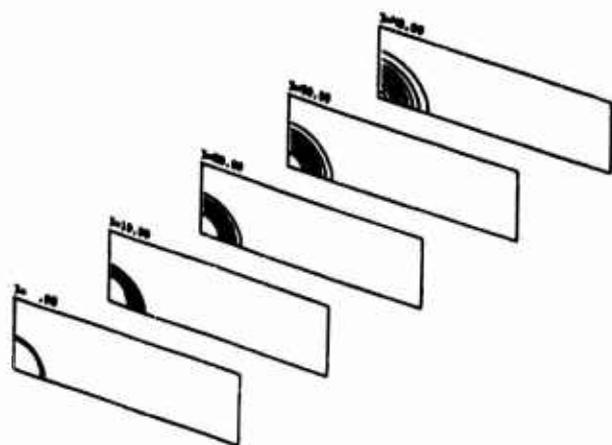
A) H$_2$ MASS FRACTION FIELDS FOR CASE C$_1$
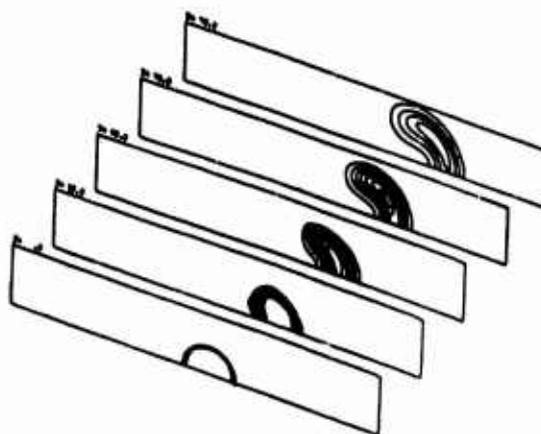
B) H$_2$ MASS FRACTION FIELDS FOR CASE C$_2$

VERTICAL INTERACTION

ELLIPTICAL NOZZLE

D) H$_2$ MASS FRACTION FIELDS FOR CASE C$_4$
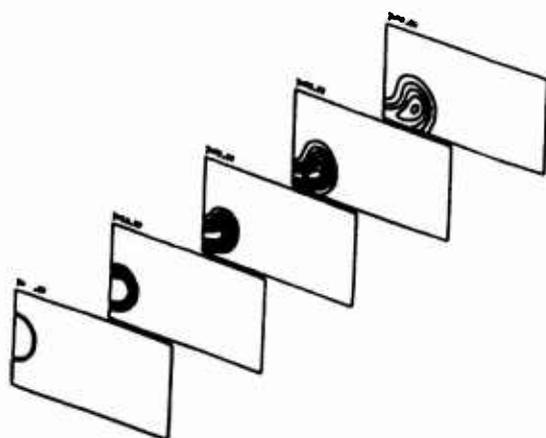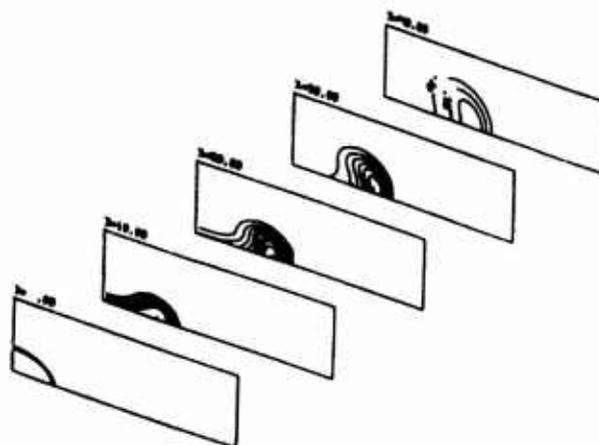
C) H$_2$ MASS FRACTION FIELDS FOR CASE C$_3$

H$_2$ MASS FRACTION FIELDS FOR CASES C$_1$-C$_4$
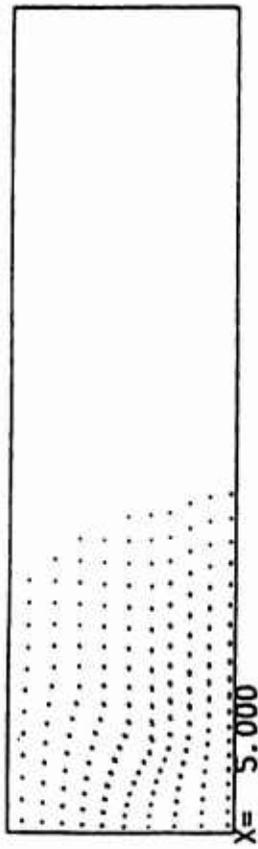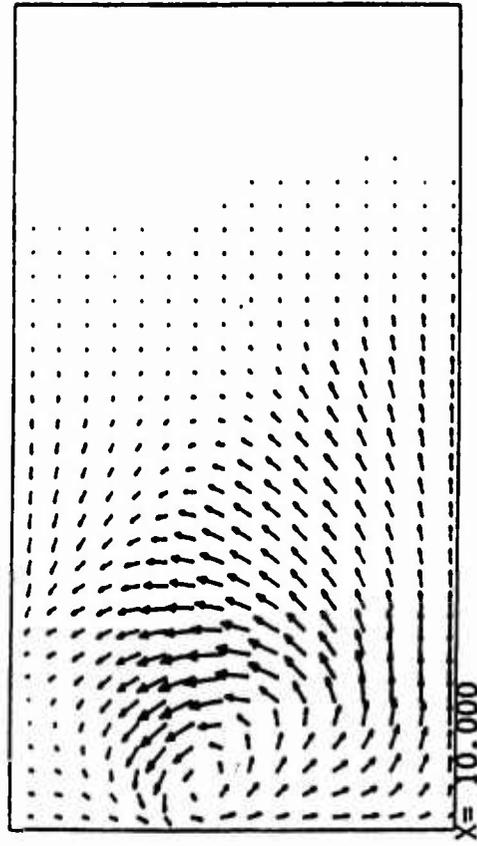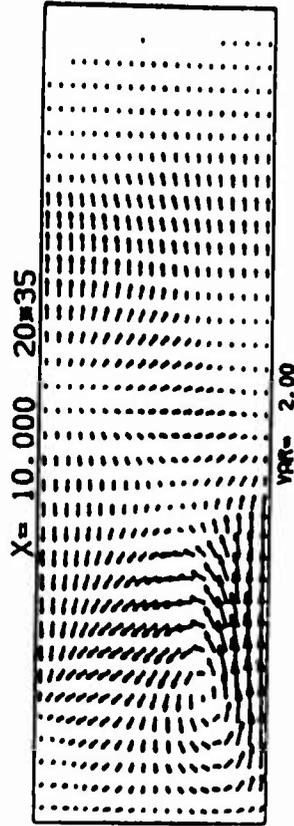
Fig.2.3.4

Fig. 2.3.5. TRANSVERSE VELOCITY COMPONENT FIELDS
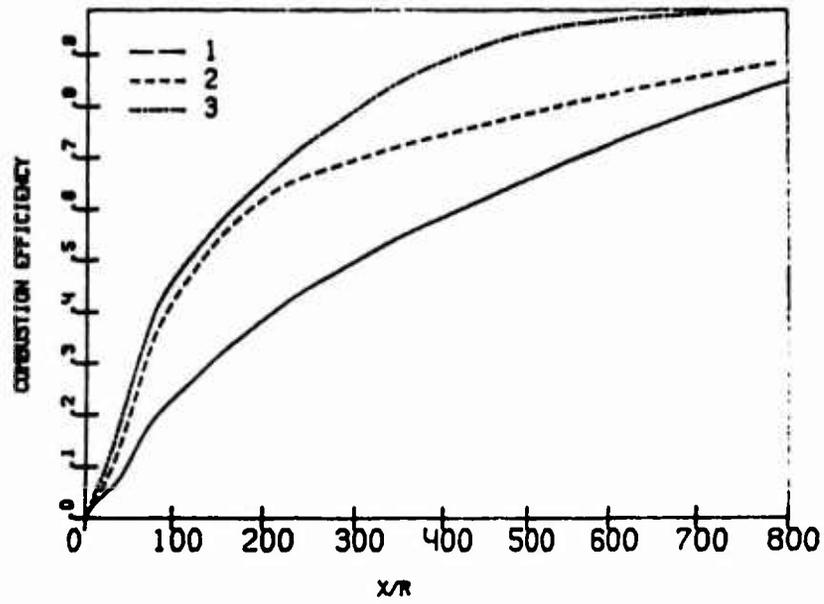
COMBUSTION EFFICIENCY FOR NOZZLES N_1, N_2 AND N_3 WITH ASPECT RATIO 1:1 2:1 AND 3:1

Fig.2.3.6

FLAME SHEET POSITIONS FOR NOZZLES:

N_1, N_2, N_3
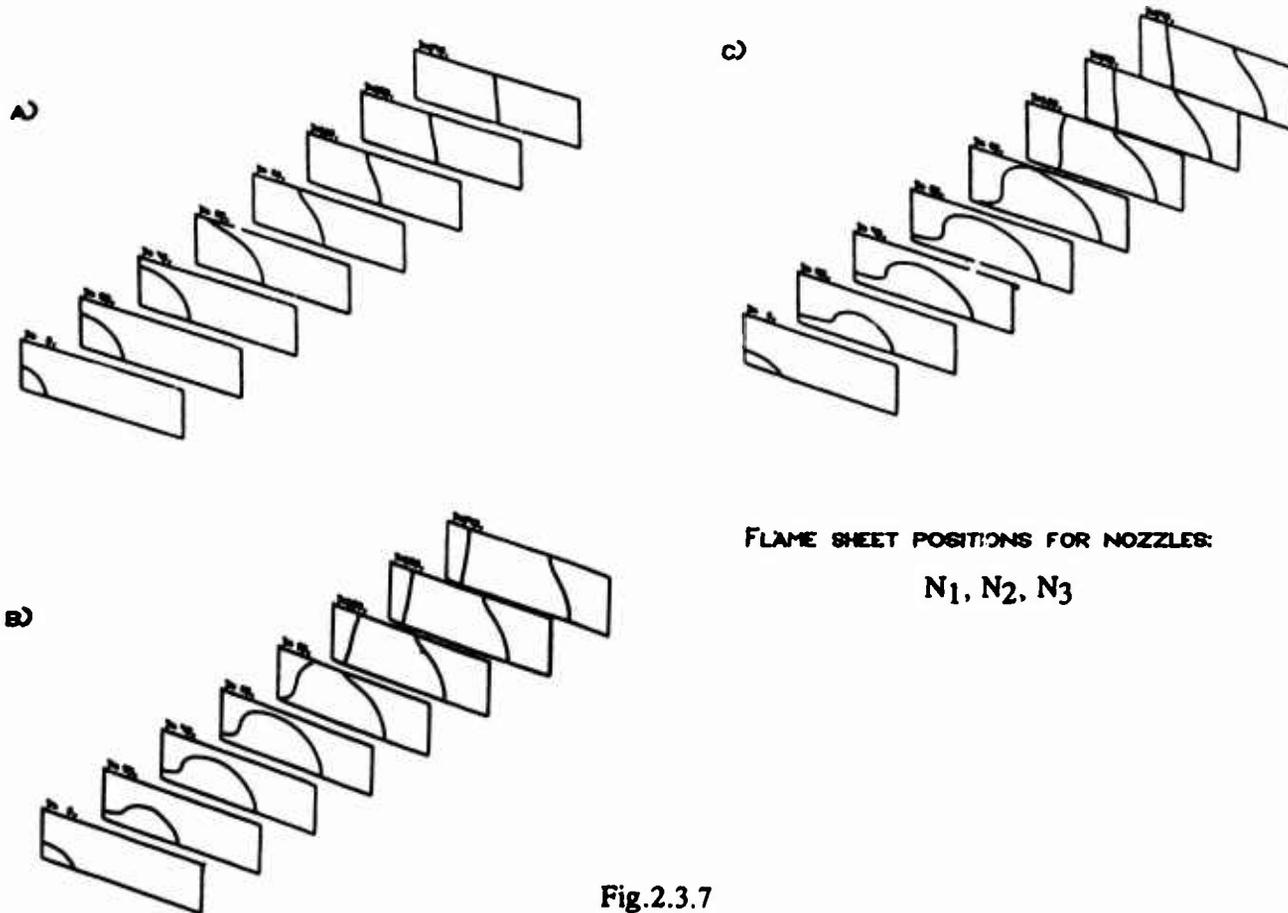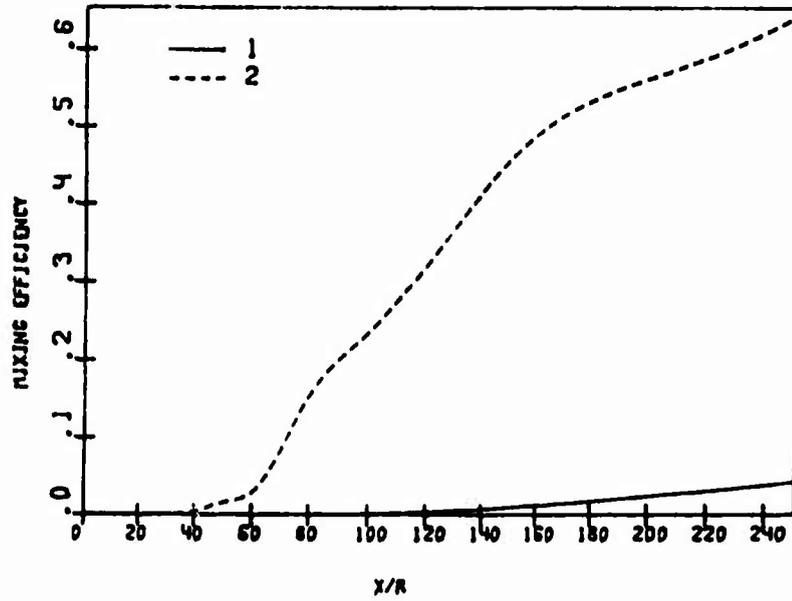
Fig.2.3.7

MIXING EFFICIENCY q FOR REGIME R_2

Fig.2.3.8
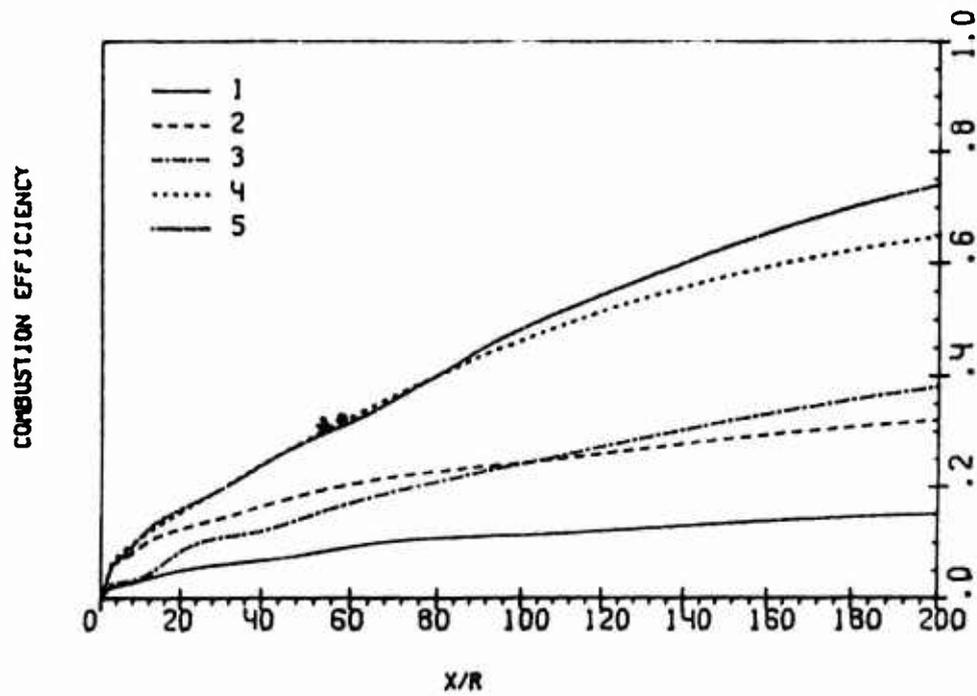
COMBUSTION EFFICIENCY FOR REGIME R_2

Fig.2.3.9
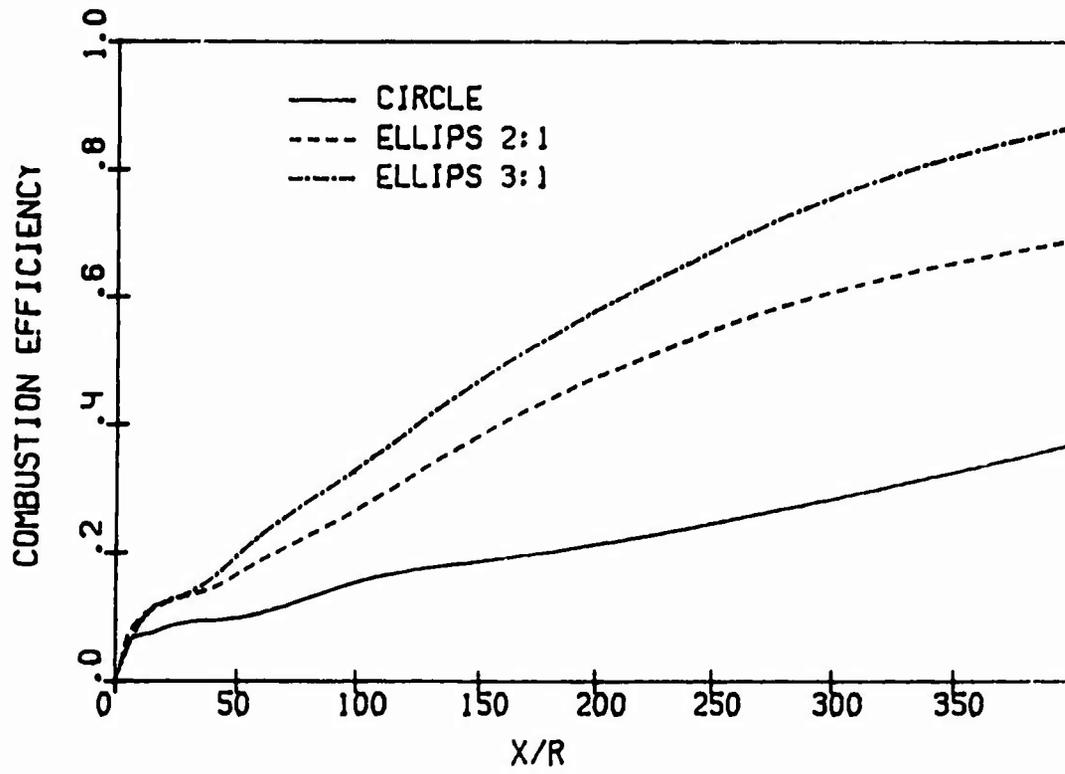
Fig.2.3.10. COMBUSTION EFFICIENCY FOR REGIME R₃
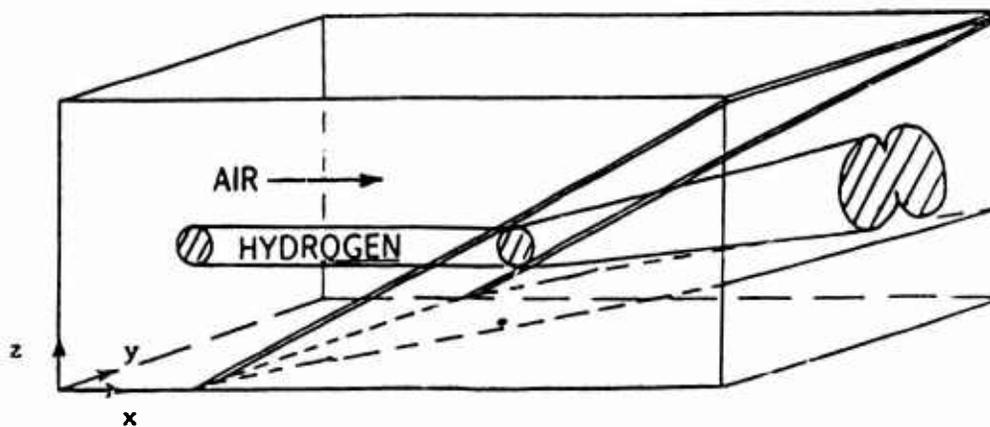
Fig.2.4.1   THE SCHEME OF SHOCK - JET INTERACTION
IN CHANNEL

SHOCK - JET INTERACTION

R/RH=CONST

Xm 18.0

Xm 16.0

Xm 14.0*

Xm 12.0

Xm 10.0

Xm 8.0

Xm 6.0

DENSITY FIELD

M1=2   M2=6   R1/R2=0.5   SERIES I
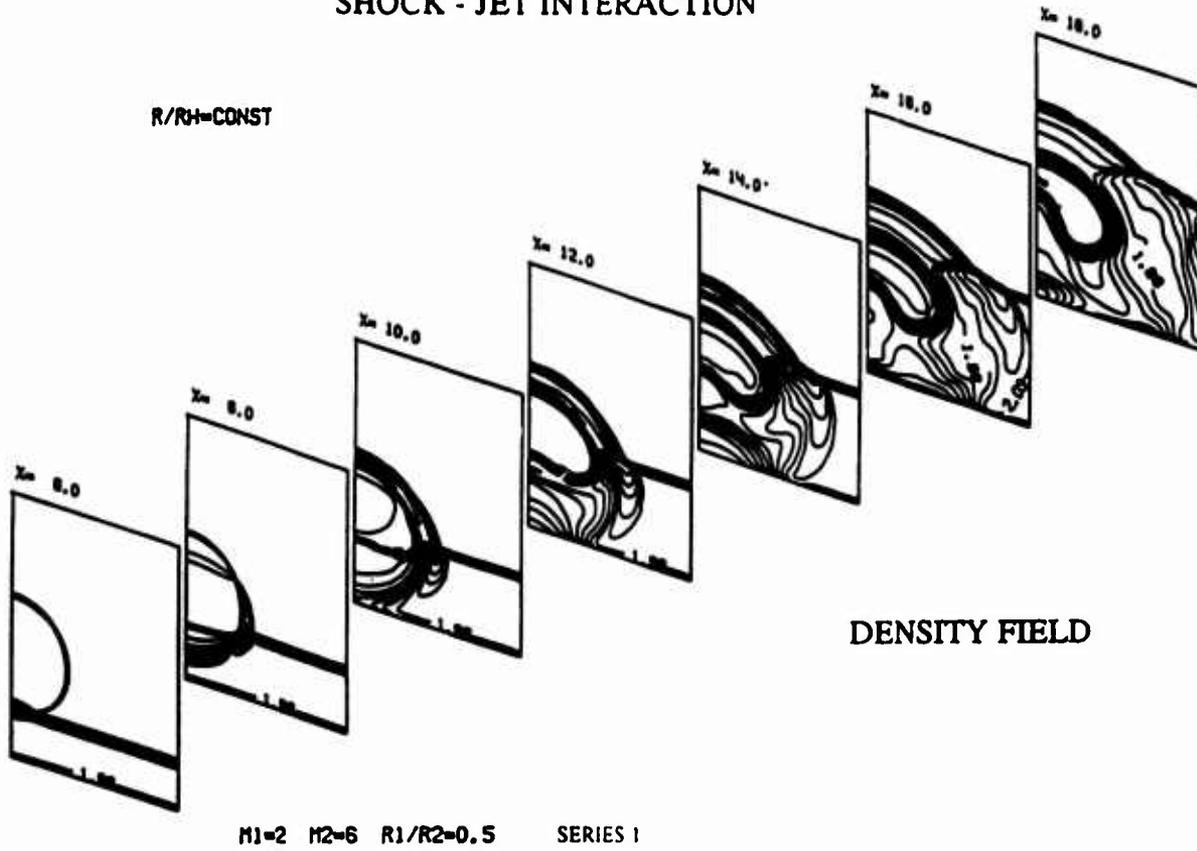
Fig.2.4.2 - A

SHOCK - JET INTERACTION

R/RH=CONST

Xm 18.0

Xm 16.0

Xm 14.0

Xm 12.0

Xm 10.0

Xm 8.0

Xm 8.0

DENSITY FIELD

M1=2   M2=6   R1/R2=1   SERIES I
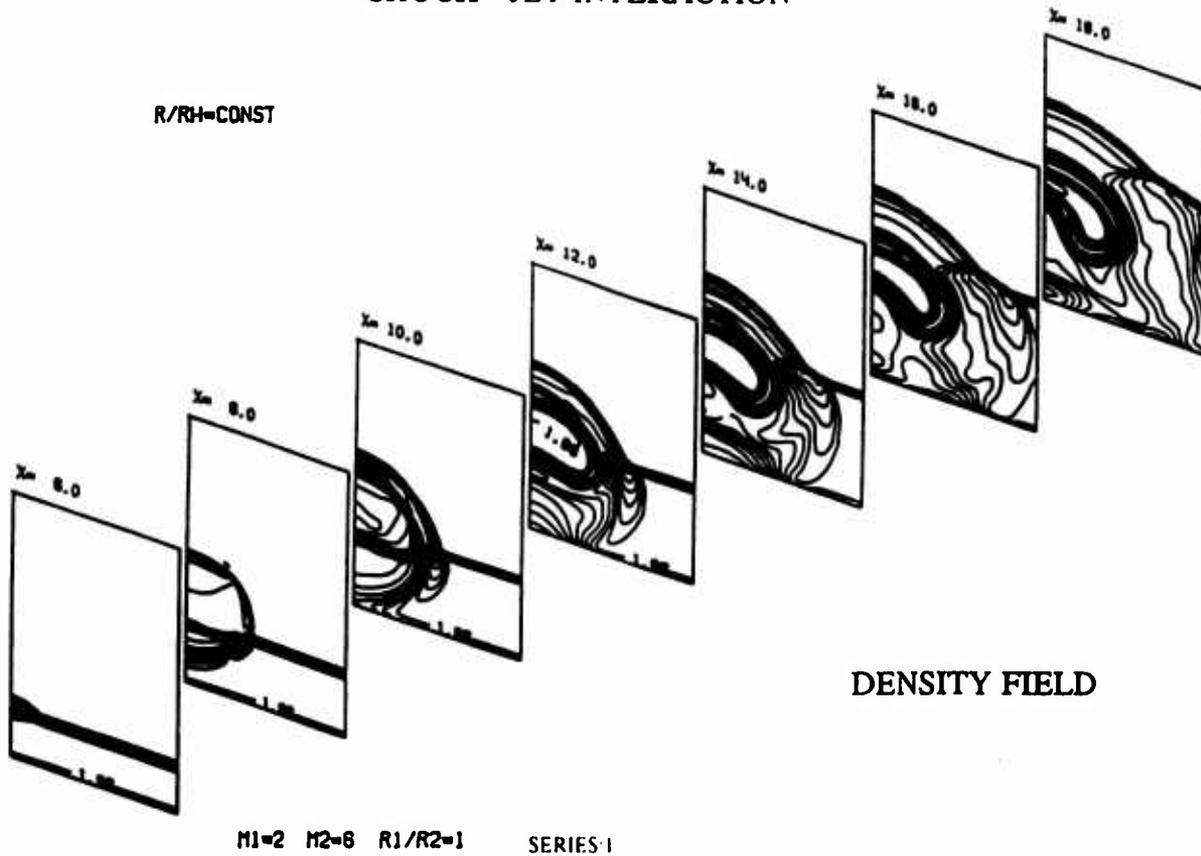
Fig.2.4.2 - B

SHOCK - JET INTERACTION

R/RH=CONST

DENSITY FIELD

M1=2 M2=6 R1/R2=2   SERIES 1
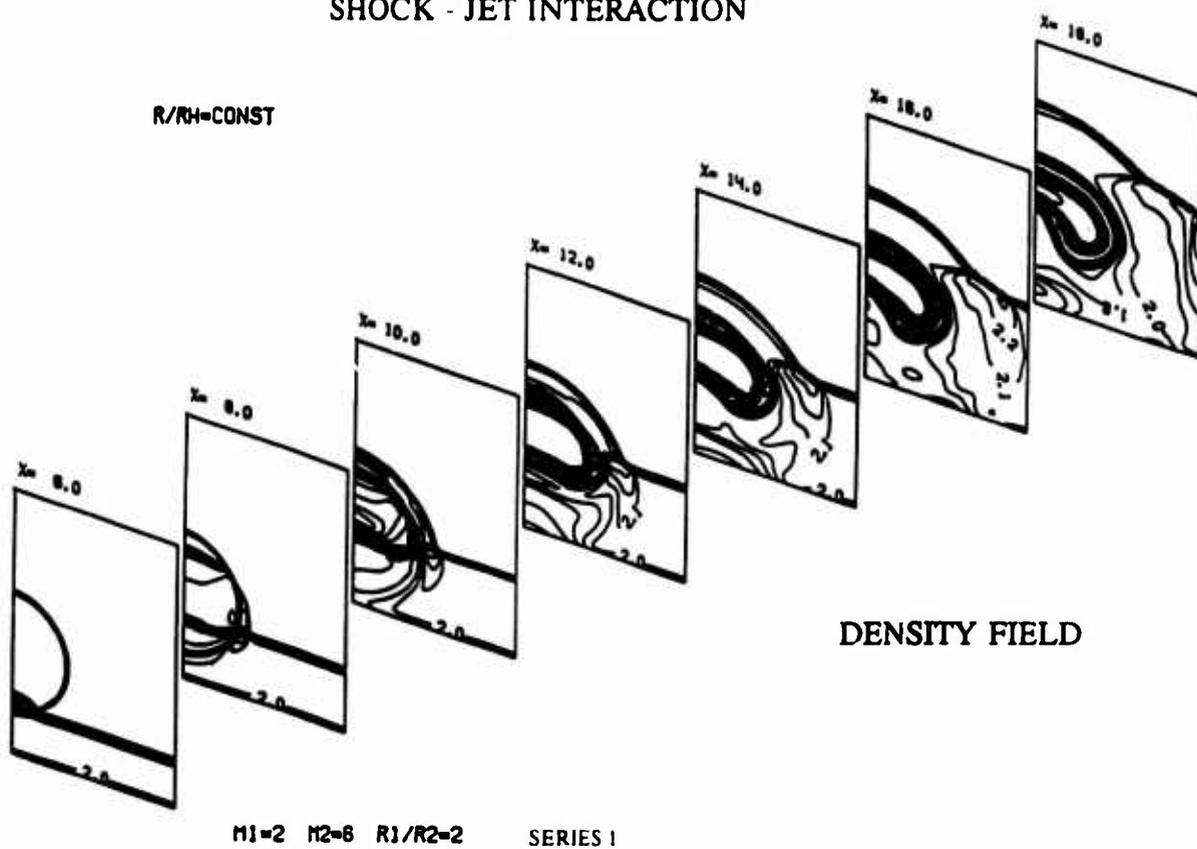
Fig. 2.4.2 - C

SHOCK - JET INTERACTION

R/RH=CONST

DENSITY FIELD

M1=2 M2=6 R1/R2=0.5
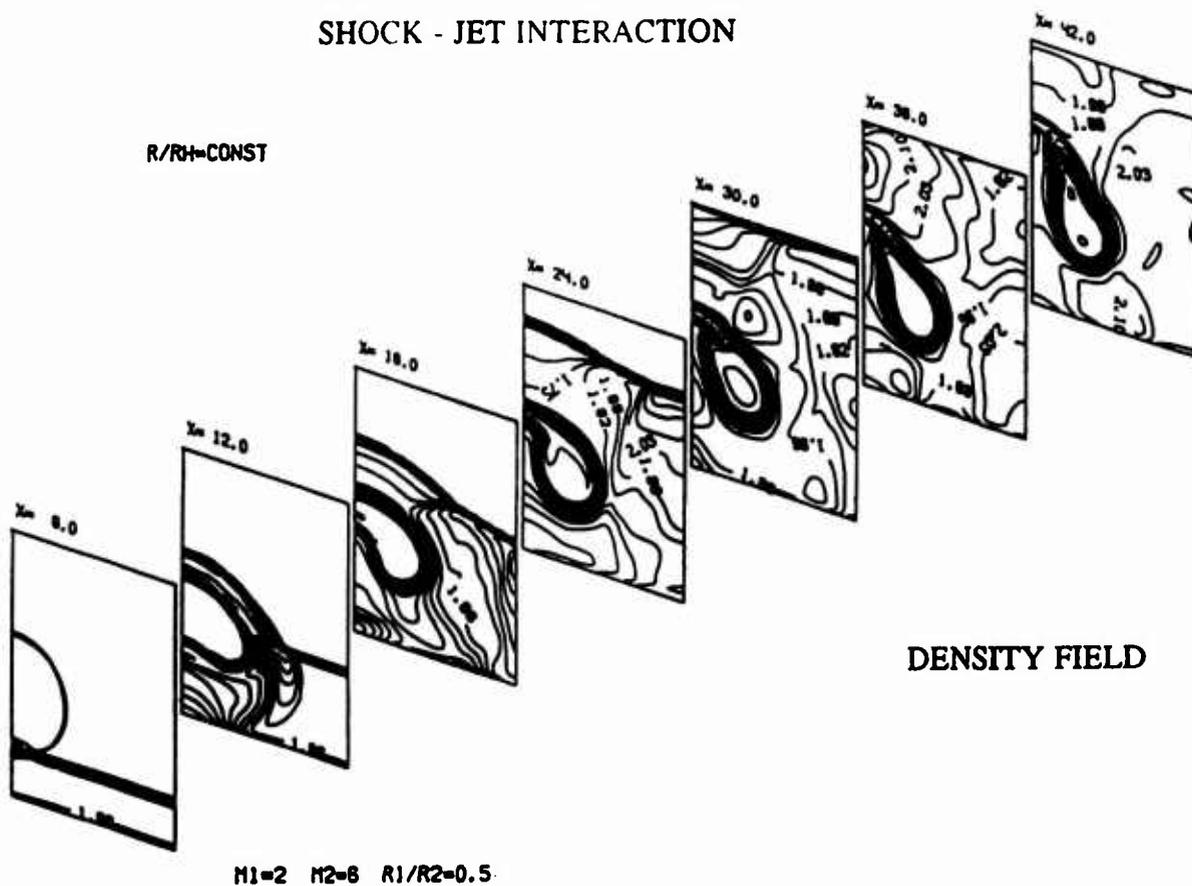
Fig. 2.4.3 - A

SHOCK - JET INTERACTION

R/RH=CONST

DENSITY FIELD

M1=2 M2=6 R1/R2=1
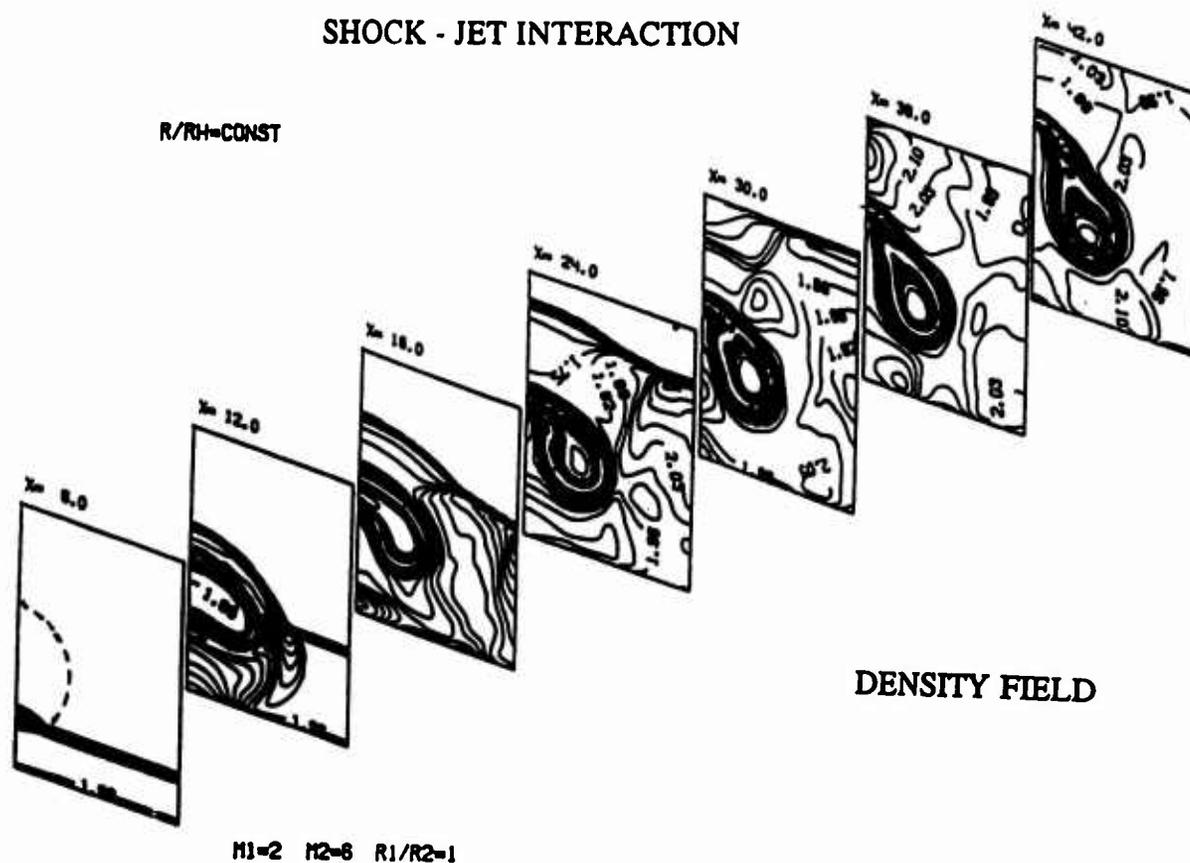
Fig.2.4.3 - B

SHOCK - JET INTERACTION

R/RH=CONST

DENSITY FIELD

M1=6 M2=6 R1/R2=0.5   SERIES 2
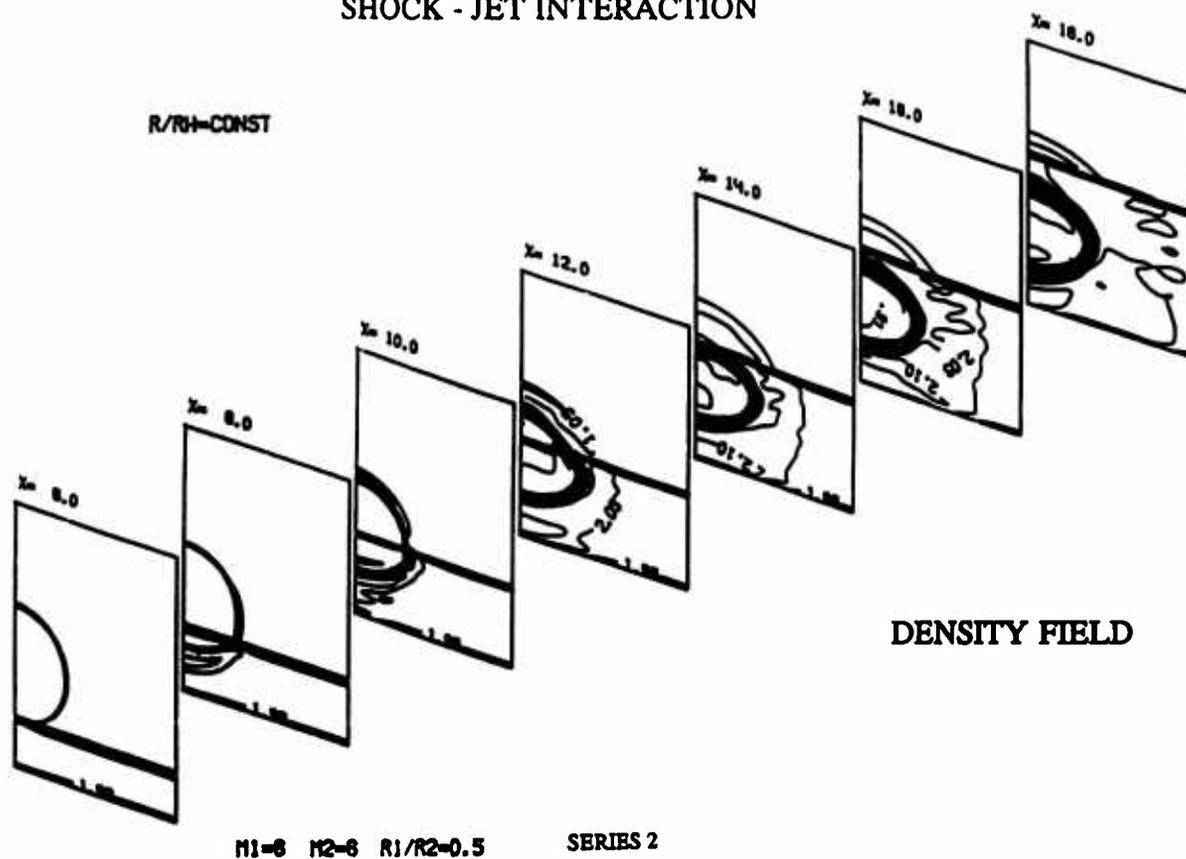
Fig.2.4.4

THE INFLUENCE OF THE DENSITY RATIO AND MACH NUMBER DIFFERENCE ON THE TOTAL VORTICITY LEVEL
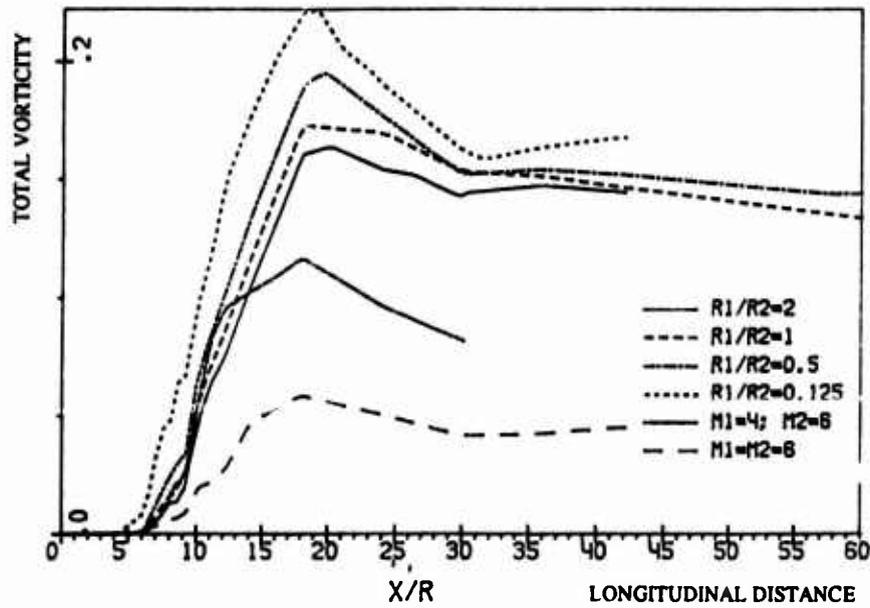
Fig.2.4.5

THE DETAILED STRUCTURE OF THE SHOCK - JET INTERACTION
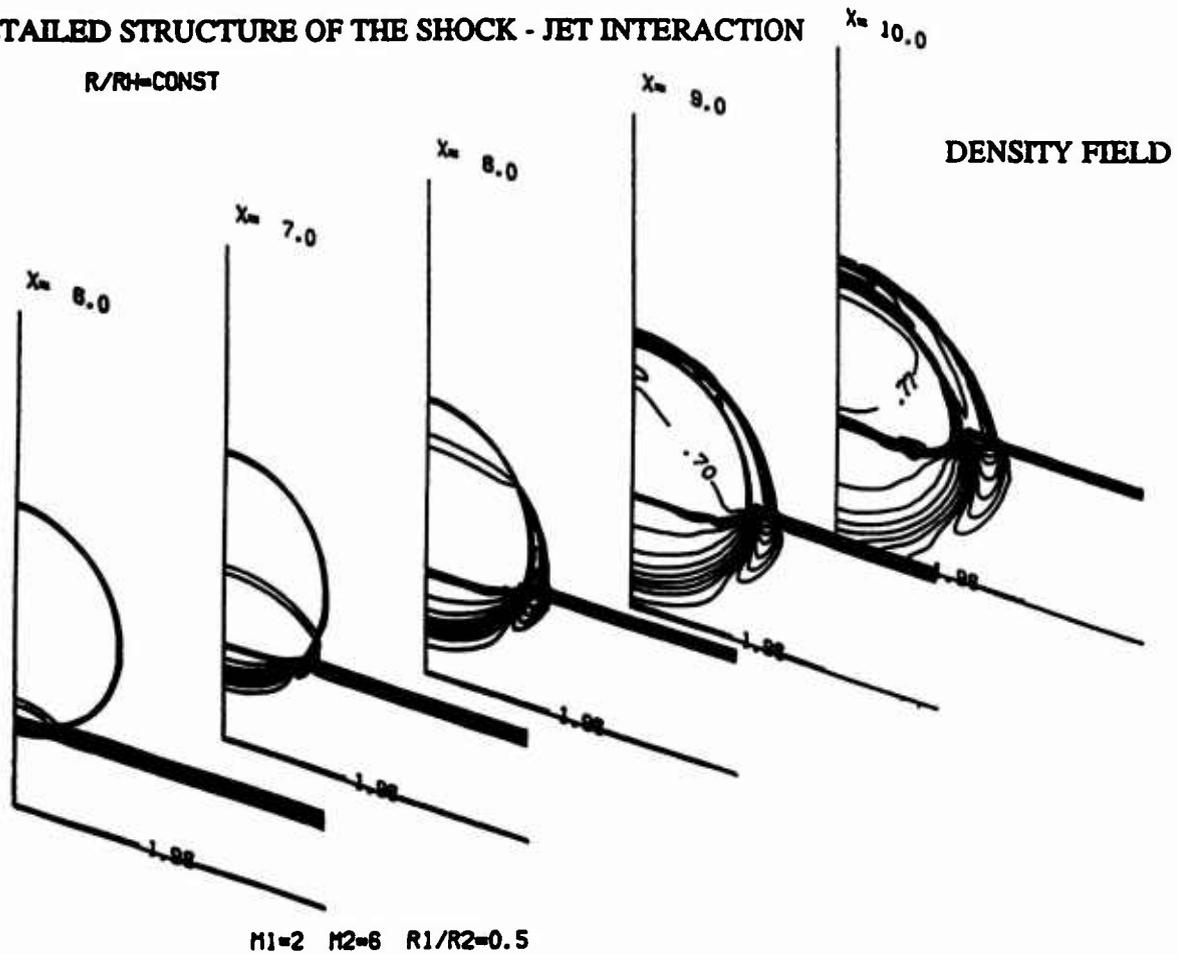
Fig.2.4.6

SHOCK - JET INTERACTION

R/RH=CONST

X= 8.0
Xm 10.0
Xm 14.0
Xm 18.0
Xm 24.0
Xm 30.0

DENSITY FIELD

M1=2   M2=6   R1/R2=0.5   CASE X ramp = 0
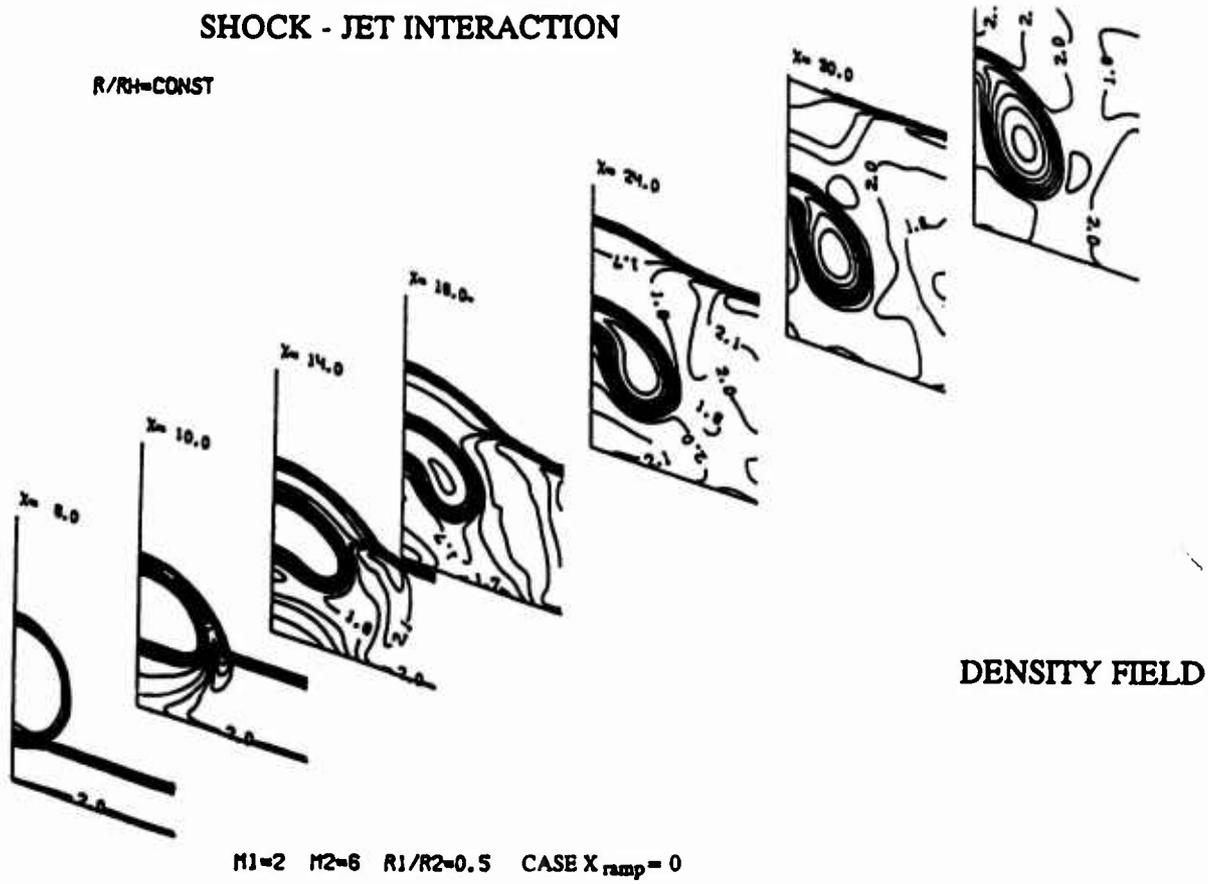
Fig.2.4.7

SHOCK - JET INTERACTION

R/RH=CONST

Xm 38.0
Xm 38.0
Xm 40.0
Xm 42.0
Xm 44.0
Xm 46.0
Xm 48.0

DENSITY FIELD

M1=2   M2=8   R1/R2=0.5   SHOCK   CASE X ramp = 30
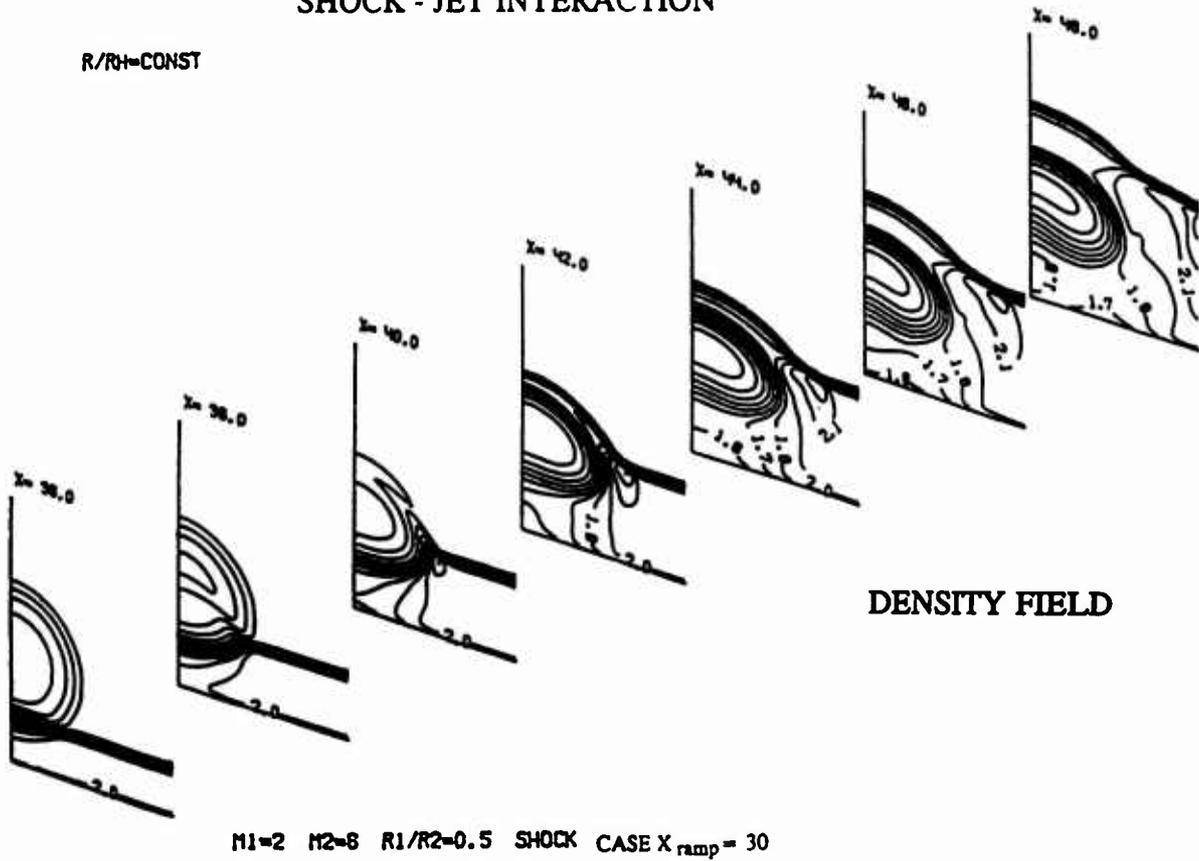
Fig.2.4.8

HYDROGEN MASS FRACTION FIELDS
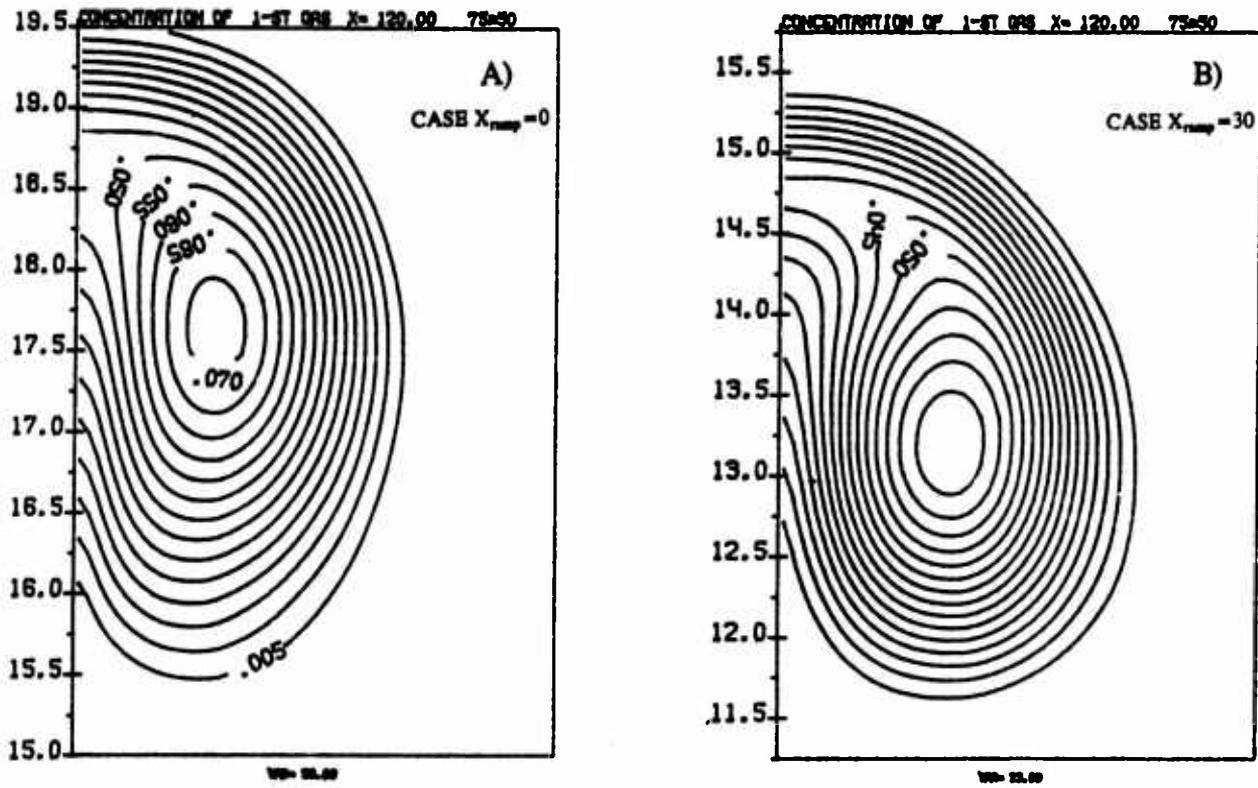
Fig.2.4.9
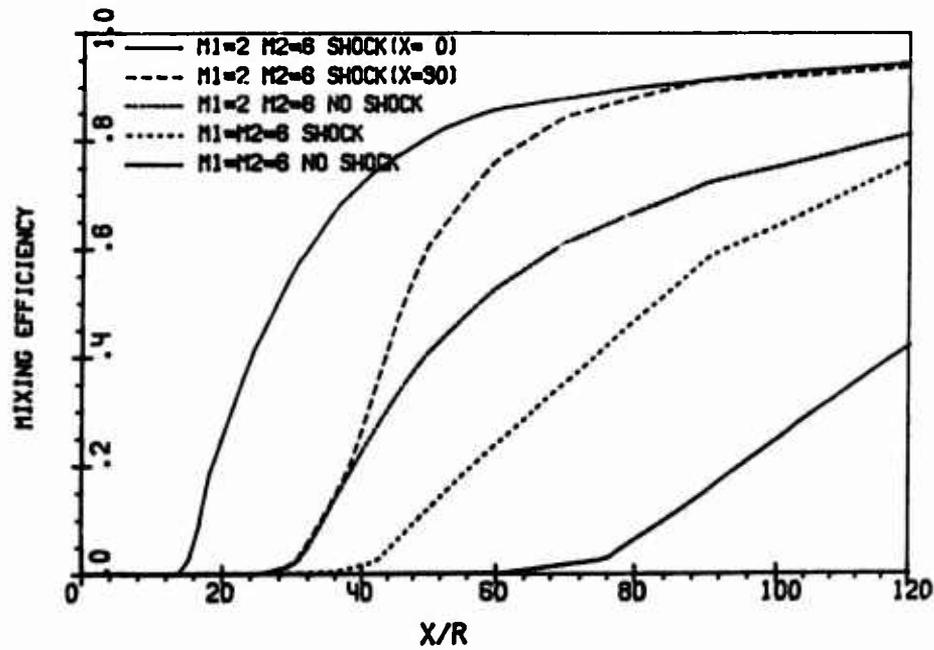
Fig.2.4.10.   THE MIXING EFFICIENCY
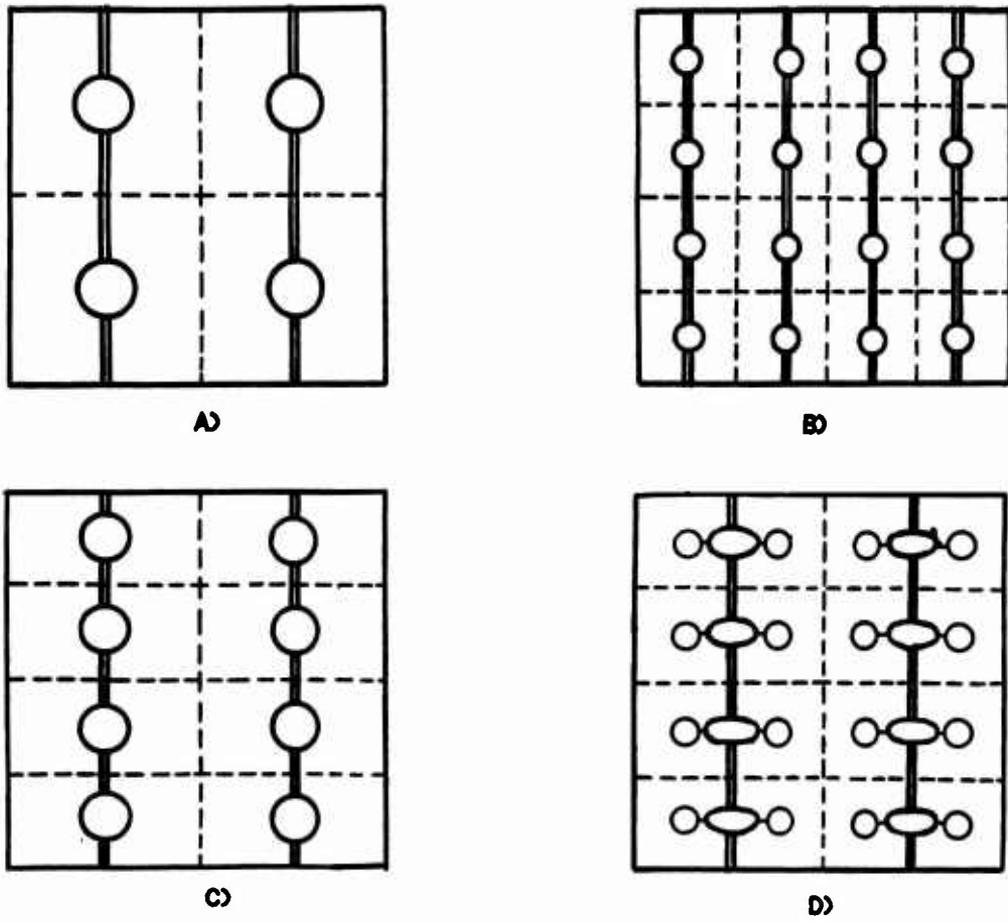
Fig.2.5.1

INJECTION SCHEMES.

THE COMBUSTOR SCHEME
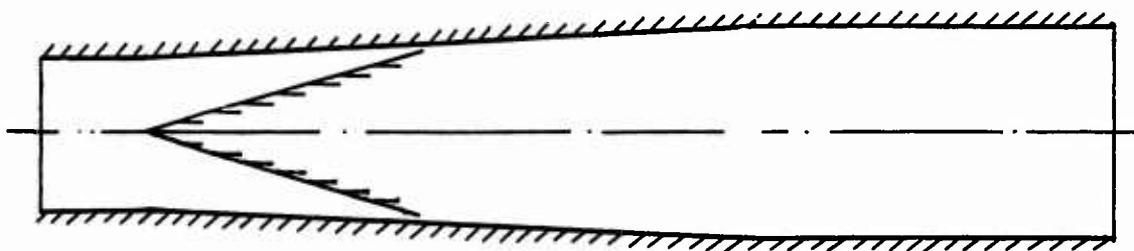
THE ELEMENTARY COMPUTATIONAL REGIONS
FOR VARIOUS INJECTION SCHEMES
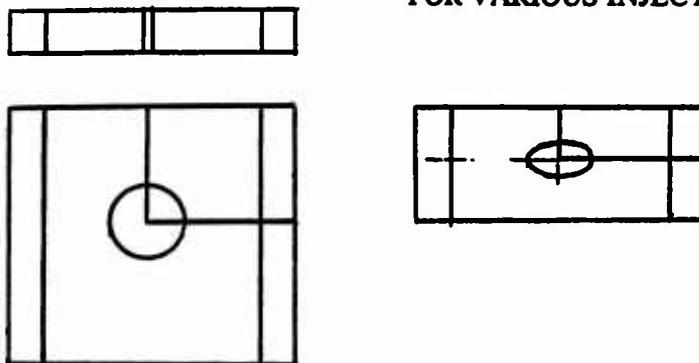
Fig.2.5.2
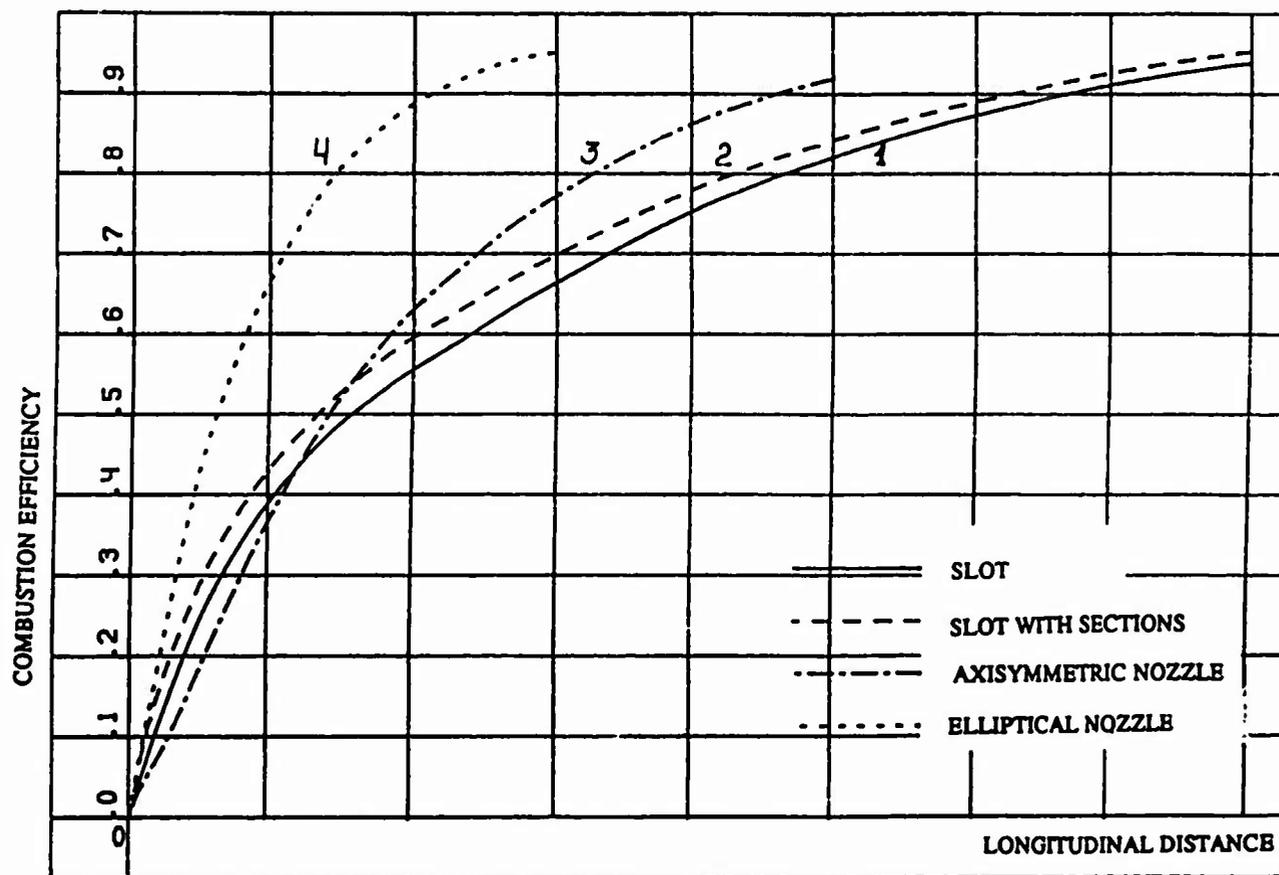
Fig.2.5.3 THE COMBUSTION EFFICIENCY FOR VARIOUS
INJECTION SCHEMES

MIX
DIF

L_i (meters)
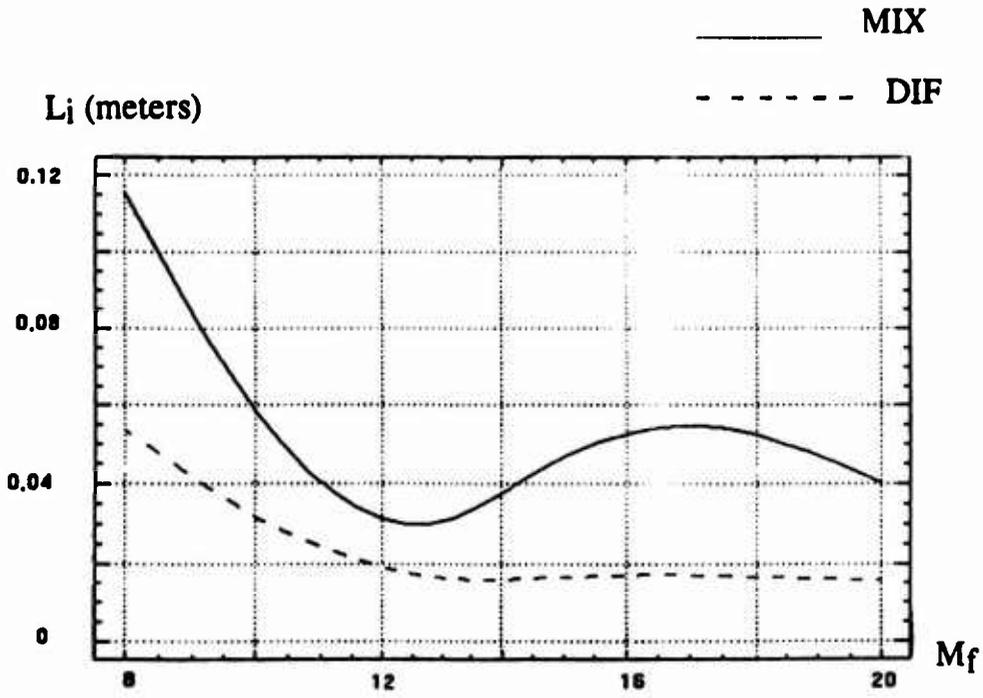
Fig.2.6.1. THE CHARACTERISTIC SELF - IGNITION LENGTH
V.S. FLIGHT MACH NUMBER

MIX
DIF

L_e (meters)
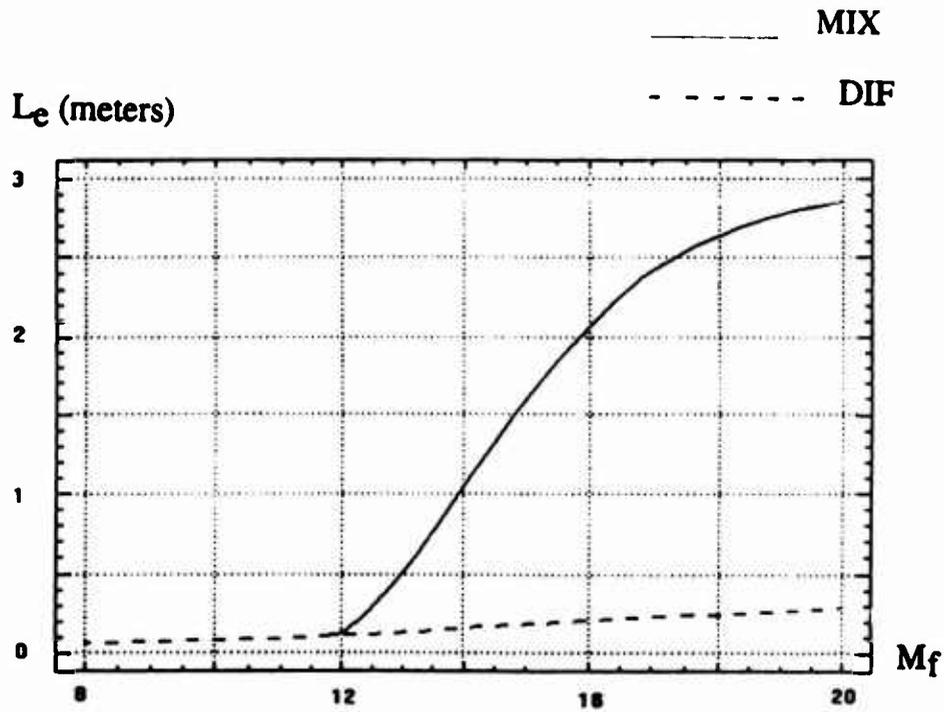
Fig.2.6.2. THE CHARACTERISTIC HEAT RELEASE LENGTH
V.S. FLIGHT MACH NUMBER

SOME PROBLEMS OF SCRAMJET PROPULSION FOR AEROSPACEPLANES
PART II. -- SCRAMJET: DEVELOPMENT AND TEST PROBLEMS
by
Dr A.ROUDAKOV
CIAM (Central Institute of Aviation Motors)
111250 MOSCOW
RUSSIA

Scramjet development strategy.

Scramjet is considered as the base of single stage aerospace plane propulsion system providing its acceleration from moderate supersonic (M_f 5) up to high hypersonic flight speeds (M_f 25)

The feature of scramjet scheme seems to be simple and comfortable for propulsion system and vehicle integration The method of scramjet specific parameter's computations seem to be also simple due to supersonic flow in scramjet (M 1) and configuration simplicity of scramjet duct and its elements inlet, combustor and exhaust nozzle.

But preliminary analyses of computation results show high difficulty of specific parameter's scramjet realization and rigorous demands to its design, operating process realization and its simulation in test facilities Aerospace plane flight scheme and main parameters of flow in its duct along the flight path presented in Fig. 2.1...2.4 illustrate it's fact. Conventional flight scheme is presented in Fig 2 1 in coordinates flight altitude H *(km)* and flight Mach number M_f V_a This flight scheme is limited in vertical direction by lines of maximum (q_{max} 2bar) and minimum (q_{min} 0 2bar) air ram value, and it is limited in horizontal direction by minimum (M_{min} 5) and maximum (M_{max} 22) Mach number values at which scramjet specific impulse exceed specific impulse of ramjet and liquid propellant engine respectively. The grid of constant total enthalpy and of engine entrance pressure is presented in the same Fig. 2.1. One can see, that total enthalpy change along the trajectory more than 20 times and reaches $20\ MJ\ kg$, that rouses large problem of scramjet design and creation

The lines of constant values of quasi equilibrium total temperature T_0 and equilibrium total pressure P_0 and the engine entrance computation with the assumption of thermodynamic equilibrium isotropic compression process are presented in Fig. 2.2 in the same coordinates H and M_f These parameters correspond to air parameters in high pressure cylinders that can be used at tests of scramjet duct and its element in test facilities. One can see, that since M_f 8 total temperature T_0 2500K and total pressure P_0 500bar exceed the possible values of these parameters that can be realized stationary at earth conditions.

The lines of constant value of the Reinolds number calculated for unit length of main stream (Re_l)

and temperature factor T $T_w T_0$ are presented in Fig 2.3 in coordinates H, M_f Wall temperature of scramjet duct is taken to equal $1000K$ One can see, that Reynolds number is approximately constant along the flight trajectory. When characteristic length of duct element L is about $10\ m$, real Reynolds number for all duct elements is very high, Re 10^7 10^8

Since M_f 12, temperature factor T_w values become lesser than that in liquid propellant engine combustors, T_w 0 2 In this case, overcooling wall layer corresponds to high enthalpy core flow Besides, flow in combustor and exhausts nozzle in characterized by high level of turbulence generated by shock waves The structure of these shock waves' changes along the flight trajectory and is determined by flight Mach number M_f and engine operating regime

The dependence of inlet throat Mach number M_H on the flight Mach number M_f is shown in Fig. 2 4 The values of Mach number at the exit of hydrogen combustor with constant cross section area at air-fuel ratio α 1 1 M^* are presented in the same fig.2.4. It is evident, that flow Mach number in such combustor remains approximately constant at given flight speed, changes strongly along the flight path and reaches value M^* 4 5 at high flight Mach number M_f 15

Scramjet specific parameters depend on given flight path optimized with taking into account restrictions concerned, in particular with ecology problems The restriction due to condition of minimum disturbance of atmospheric ozone layer is shown in Fig. 2.1 by section-lined belt.

Scramjet specific impulse this shown along the flight path corresponding to q 0 75 at α 1 1 in Fig. 2 5 with taking into account different components of losses The losses of specific impulse are taken into account by integral factors. inlet total pressure recovery factor σ $\sigma(M)$, combustion efficiency factor η_c nozzle impulse factor φ_n and nozzle under expansion factor n P_c/P_H 1. Solid line 1 shows calculated specific impulse of hydrogen scramjet with taking into account real losses of total pressure in inlet (σ $\sigma(M_f)$), losses due to combustion incompleteness (η_c=0.95) and impulse losses in nozzle (φ_n 0.97) at nozzle expansion ratio F_a 3. Solid line 5 presents specific impulse of ideal scramjet. The rest of dotted lines 2,3,4 show the values of components of specific impulse losses, describing perfection of scramjet duct elements. Influence

coefficients of every component of losses K_i, or particular logarithmic derivatives of specific impulse J on appropriate loss's factor f_i $(K_i \ (lnJ)/f_i)$ are shown by deshed lines. It should be noted that losses in exhaust nozzle and other's scramjet duct elements have strong effect on engine specific impulse and this fact imposes special requirement for physical or numerical simulation of scramjet operating process along the flight path

Thus, scramjet design and development demand realization of operating process in its duct with flow parameters in the range that can be realized in test conditions stationary only at $M_f \cdot \ 8$. Reliable data on physical chemical conversions in flow combustion, turbulence, three-dimensional and unsteady structure of flow wall flows and heat exchange and their coupling are absent for high Mach number at present. The extension of scramjet operating domain and improvement of scramjet performances is connected with duct complication and in particular with transition to multimode ducts with variable geometry, with use of gasgenerator like liquid propellant engine and so on. For this reason, the problems of new materials creation and development of active heat protection system of structure are of important significance

Thus, in spite of apparent simplicity of scramjet scheme, the development of this engine is extremely complex problem and solution is connected with working out some fundamental and applied scientific leads, methods of investigation and simulation of scramjet operating process scientific and methodical accompaniment of general conception of scramjet, which is fully integrated with vehicle and determines preliminary design of aerospace plane in general

If we take into account mutual interaction of considered problem elements, time and cost, which are necessary for developments, the possibility of appearance of new results, which can change former conceptions and technical approaches, it seems to be expedient to have scheme of scientific research and design works for scramjet development. This scheme is presented in Fig. 2 6

The whole of works, presented in Fig. 2 6 are divided into three different directions

-- hypersonic technology
-- scramjet conceptions
-- test base

The first of these directions is the most extensive. It is the complex of fundamental and applied scientific researches and design works with common purpose scramjet creation. It covers field of physical-chemical processes in high enthalpy supersonic turbulent flows, their physical and numerical simulation and methods of measurements and diagnostics, instruments materials and appropriate technical equipment and systems. These works create the basic of knowledge, data, and experience for new stage of scientific and technical advance, named conventionally hypersonic technology in parallel with solution of main problem (scramjet development)

The second lead is connected immediately with development and realization of scramjet starting with its preliminary design and including tests of engine, that determines lock of aerospace transport of XXI-st century

And finally, the third lead of works is connected with creation of industrial base for tests of full scale units of scramjet, their development and development of engine in general, including full scale service-life tests of scramjet in real range of parameters

On one hand, all three leads are sufficiently independent, and on the other hand, they interact essentially for a long time. This fact causes the necessity of coordination of effects in each of mentioned leads. The conception works on scramjet initiate works on leads 1 and 3. But new results in field of hypersonic technology, the time of appearance of which can't be predicted, can change essentially assumed design of scramjet. Long time high-cost design and development of test facilities can not give expected results without taking into account this fact

Hypersonic technology (see Fig. 2 7) includes 6 parts

  -- fundamental scientific investigations,
  -- applied scientific studies of scramjet
       operating process,
  -- experimental simulation of engine process,
  -- numerical simulation of operating process,
  -- new technical approaches and systems,
  -- control systems and units of scramjet

1 Fundamental scientific investigations (Fig. 2 8) will cover physical-chemical processes in high-enthalpy flows with shock waves, new materials creation and ecology problems. It seems to be very important to obtain new theoretical and experimental data on kinetics of chemical reactions in high-enthalpy flows with shock waves, detonation and combustion on turbulence structure in such flows and also on stability and control of these processes

These data are the necessary data base for mathematical simulation of processes of propagation of diffusion and detonation combustion in supersonic combustors and also for practical realization of energy supply to supersonic flow.

New material problem is the key problem for scramjet development because the use of existing and promising materials doesn't provide scramjet flight at

high flight Mach numbers M_f 16 due to restrictions caused by structure thermal state

Ecology problem of high-speed motion in atmosphere and, in particular, in ozone layer demands also in-depth study

2 Applied scientific studies of scramjet operating process (Fig. 2 9) will cover new sections of technical sciences, connected with selection of design scheme and parameters of scramjet inlet, combustor and exhaust nozzle and with organization and control of operating processes in them in a wide range of determining parameters and conception of reacting gas mixture

The development of computational model of operating process, of methods of duct unit's computation, representing the basis for technical approaches is connected with investigations in the fields of thermodynamics, gasdynamics, thermal physics and combustion, which are relied on new methods of measurements of supersonic reacting gas flow parameters and on results of numerical processing and simulation of three-dimensional and unsteady phenomena of various scale Wide use of super computers is necessary for mathematical simulation of scramjet operating process

3 Experimental simulation of scramjet operating process (Fig. 2 10) will be carried out in ground test complex and in flying test laboratories Ground test complex is the most prepared in spite of it is necessary to modernize it and equip it by laser methods of measurements of reacting gas parameters This complex includes of stationary supersonic wind tunnels, hypersonic facilities of short-time action, impulse tunnels, ballistic facilities and special equipment for production of high-enthalpy air flows with extremely clean composition with the aid of fire, plasma and electric heaters

The problems of diffusion and detonation combustion in supersonic flow, of control of boundary layer and wall flow at presence of shock waves and heat flux peaks can be considered in ground conditions at $M8$ and global Reynolds number $Re \sim 10^7$ Air chemical composition and initial turbulence levels do not practically correspond by this to conditions at flight in atmosphere almost always The use of flying laboratories is for this reason of extremely importance Wing flying laboratories of ballistic flying laboratories, launched by ballistic rocket can realize design flight path of aerospace plane in atmosphere H $H(M_f)$ both on separate parts and in a whole and to ensure the condition of scramjet vehicle interference without simulating real Reynolds numbers due to small dimensions of model scramjet duct The orbital laboratories with planning descent and following return to orbit or landing can be useful for studies of final period of scramjet operation at M_f 16.

4 Numerical simulation of scramjet operating process permits to generalize the whole experimental data accumulated in test studies and interpolate they on real conditions of engine operating in test facility and in flight (Fig 2 11)

Numerical simulation of operating process should be based on mathematical model of turbulence in high-enthalpy hypersonic flow of reacting gas mixture with taking into account the absence of equilibrium of physical-chemical conversions Supercomputers are necessary for computations of three-dimensional and unsteady interaction of shock waves with channel boundary layer determining thermal state of structure The problems of flow stability at combustion in bounded supersonic flow in essential in connection with combustor operating process control

5 New technical approaches (Fig 2 12) Scramjet realization is impossible without creation of new technical approaches It should be noted the followings
- the control of three-dimensional gasdynamic structure of supersonic flow in duct with the aim of its stabilizing, avoiding boundary layer separation and eliminating heat flux peaks.

- the control of combustion and mixing in supersonic flow with the aim of burning length reduction and combustion efficiency of hydrogen increase in wide range of Mach numbers

- the control of structure thermal state in high-enthalpy supersonic flow by use of active cooling system operating heat flux peaks moving along the scramjet duct surface.

- the use of hydrogen slush as coolant and fuel.

- the use of compact hydrogen-air heat exchangers.

- the use of light-weight structures of composites for controlled scramjet duct

6 Scramjet systems and elements (Fig 2 13) Unique systems and elements should be made on the base of new technical approaches, materials, technology diagnostic and control systems in the process of scramjet developing It is possible to point out for example the followings

- supersonic mixers on the base of gas-generators like liquid propellant engines for thrust creation and subsequent effective mixing of supersonic air flow with supersonic fuel jet in wide ranges of Mach numbers and fuel components ratios;

- multimode supersonic combustor, permitting

to realize conditions of subsonic and supersonic combustion in wide range of Mach numbers and fuel components ratios;

- active cooling system with system of diagnostic and control of coolant injection, ensuring structure thermal state at conditions of changing heat flux with high nonuniformity.

Scramjet conception, that will be developed jointly with aerospace plane conception, can be realized step by step in the form of modules, at first, in the form of sub-scale module and, then in form of full-scale module, and in the end-in form of full scale scramjet as a main engine of flying aerospace plane propulsion system (Fig. 2.14).

In the process of scramjet development, its elements and modules should be subjected to various tests with the aim of providing design parameters along the flight path, reliability and service life (Fig. 2.15). The necessary industrial base should have available specialized test facilities for development of each element and system for module development and for full scale scramjet tests. Let's cite as example specialized test facility for combustor development both in respect to thermal state and in respect to combustion efficiency and impulse. In particular, combustor impulse measurements, which is connected with appreciable error at test facility conditions. Let's cite as the second example supply system of liquid or slush hydrogen, which is connected with system of active cooling of duct. The main restrictions of ground tests are connected with restricted ranges of Mach number (M_f · 8) and Reynolds number (Re · 10^7) and incomplete simulation of interference of scramjet with vehicle. It is necessary to use the set of methods of scramjet study and development to eliminate these disadvantages: operating process simulation in the laboratory and in test facility, flying tests of models, mathematical simulation and full-scale flight tests.

This point is illustrated by comparison of various methods of scramjet duct operating process in Fig. 2.16. The objects of the investigation, merits and demerits of various methods and their interaction are formulated in presented Fig. 2.17...2.20.

1. Operating process investigation objects (Fig. 2.17). Tests in laboratory pursue the objects of revealing and elaborating of physical flow pattern and some characteristics of phenomena in scramjet duct elements (inlet, combustor, exhaust nozzle) with possible simulation of physical-chemical conversions in high enthalpy flow with taking into account influence of high cooled walls.

Simulation of operating process in test facility permits to investigate it at close to real conditions both for duct in whole and for its elements in possible range of M and Re corresponding to different parts of flight path.

Flight tests of sub-scale models permit to investigate operating process at conditions made more realistic as for duct in whole and for its elements along the flight paths close to real flight path.

Mathematical simulation of flows including physical-chemical conversions has as objectives the investigations of scramjet performances in whole range of external and internal parameters, the investigation various parameters influence on efficiency, economy and specific weight of scramjet, and the optimization of duct parameters for given goal function.

Full-scale flight test of modules and propulsion system on the whole permit to investigate all parameters of scramjet along possible flight paths

2. The advantages of various methods of investigations.(Fig. 2.18)

Experimental investigations in laboratory permit to' study non stationary and non equilibrium gasdynamic phenomena in detail including viscosity and turbulence and mechanism of flow stabilization at its separation and energy release diffusion and detonation combustion in range M_c 2...5 in core on the flow and in wall region. These studies permit to obtain experimental information with the aid of optics-electronic methods of measurements.

Operating process simulation in test facility permits to simulate phenomena on comprehensive in limited test duration. Flight tests of sub-scale models permit to simulate comprehensive the phenomenon for real air composition along the whole flight path of real scramjet in limited range of Re and at limited test duration. Flight test permit to simulate propulsion system-vehicle interference and to use independent methods of measurements of thrust balance and drag, and scramjet specific impulse.

Mathematical simulation of flows including physical-chemical conversions permits to calculate all parameters of problem in limitless ranges, gives necessary for design detailed data on flow patterns both on the whole and in the small, permits to generalize experimental result obtained in laboratory, test facility and flight tests and to simulate interference of propulsion system and plane.

Full-scale flight tests of modules and propulsion system on the whole permit to simulate all real conditions of scramjet operation.

3. The disadvantages of various methods of investigations (Fig. 2.19)

Unfortunately, each of mentioned methods

doesn't exhibit necessary completeness for comprehensive investigation of scramjet operating process. Experimental studies in laboratory don't comprehensive simulation of operating process both in scramjet duct on the whole and in its elements d e to impossibility to keep all similarity criteria, detailed duct configuration and initial and boundary conditions of flow. They permit to simulate only some characteristic features of flows and physicochemical phenomena and to obtain heterogeneous qualitative results.

Operating process simulation in test facility is possible only in limited range of M_f and Re (enthalpy and absolute flow velocity) and for limited model dimensions This leads to only partial simulation of physical-chemical composition of air, initial and boundary conditions of flow in model scramjet duct. Limited nature of information obtained by measurements in test facility, together with mentioned above disadvantages leads to necessity to use a set of facilities for parameter's simulation along the flight path.

Small dimensions of scramjet model duct and limited natures of measurements methods are the disadvantages of flight tests of sub-scale models.

Disadvantages of mathematical simulation of flows are connected with use of semi-empirical models of turbulence and physical-chemical phenomena and with impossibility of exact integration of motion equations for real numbers M_f and Re and gas composition.

Full-size flight tests of modules and propulsion system on the whole are possible only for limited number of tests. The disadvantage of this kind of tests in the limited information about operating process and extremely high cost and high risk of tests.

4. Interaction of investigation methods (Fig. 2.20) As to experiment in laboratory, the comparison of results obtained by different methods is necessary for estimations of their reliability and measurements' errors and to obtain reference data, verification and extrapolation of experimental results by use of all others (mentioned above) methods are necessary.

The use of results of experimental tests in laboratory and mathematical simulation of flows in necessary at operating process simulation in tests facilities.

The verification and extrapolation of test facilities results by methods of sub-scale flight tests are also necessary.

Flight tests of sub-scale models should use results of experimental laboratory studies, operating process simulation in test facilities, and mathematical simulation of flows.

The verification and extrapolation of obtained results are necessary a full-size flight test.

Mathematical simulation of flows including physical-chemical conversions permits to use the whole date base, obtained in experiments in laboratory, in test facility, at sub-scale model's flight tests and at full size flight tests. All previous results obtained by all methods of study are also used at pre starting procedure of full-scale flight tests and at their result's analysis.

Finally, it should be noted that scramjet design and development are the key problem for transorbital air transport. The solution of this problem will result in creation of hypersonic passenger into orbit enough space industrial opening up.

In accordance with high complexity and a large body of fundamental and applied problems, scramjet problem can be classified as one of the most difficult scientific-technical problems. Scramjet development is connected with parallel and interacting development of its conception, hypersonic technology and industrial test base.

The realization of scramjet duct operating process should be carried out on the base of all available scientific and technical means including ground, flight and orbital laboratories with comprehensive mathematical simulation.

The solution of considered problems, due to their importance, complexity, cost, and risk, are possible and expedient on the base of international collaboration and coordination of efforts of scientists, engineers and governments

Subscale Model SCRAMJET Flight Tests.

Ground test facility can not realize all condition of scramjet operations. The limitations of air enthalpy, air chemical composition breaking, turbulence conditions breaking and some other are typical features of hypersonic test facility. These defects can be corrected practically by flight tests only. But real size aerospace plane scramjet flight tests are extremely expensive and possible as final stage of system creation. But many necessitate data may be obtain due to flight testing of subscale model scramjet.

Subscale model scramjet flight test can not to use real size intake to save condition of boundary layer transition and limited sizes of nozzle don't permit to obtain good thrust efficiency of scramjet. All another conditions may be very close to real size flight vehicle and propulsion.

The first scramjet flight test could be X-15 scramjet flight test. But plane wreck disturbed this project.

Some preparation of scramjet flight test was beginning in Soviet Union by CIAM as head company in 70-ths beginning. The preliminary engineering by M.M. Bondarjuk and E.S. Schetinkov have effect on flight tests preparing. The works were conducted under leadership of R.I. Kursiner, D.A. Ogorodnikov and V.A. Sosounov.

Our model scramjet flight tests were planed as part of scramjet researches. A small surface-to-air rocket is suggested as booster. Ground tests of similar scramjet must be carried out before flight tests and many kinds of theoretical and computational investigated were planed too.

The axisymmetrical double mode scramjet was developed and created by Russia aviation specialists for flight tests specially. Due to strong financial limit the first unburning scramjet flights were in end of 80-ths. Flight tests of the Hypersonic Flying Laboratory (HFL) with hydrogen scramjet firing have been conducted on November 28 1991 on firing ground in Kazachstan for the first time. The preliminary analysis has shown that experimental scramjet had started in flight and was operating with fuel injecting corresponding to subsonic and supersonic combustion modes.

Due to high altitude and not enough ram value stable operating duration of supersonic combustion mode was several seconds only at the first flight test of scramjet.

The second flight test was in November 17, 1992. The works on the second flight test were conducted by Russian and French aviation specialists

jointly. The purpose of the second flight test was to define more exactly engine inside parameters at subsonic and supersonic combustion modes in during HFL flight along the trajectory with higher ram values. Stable operation of scramjet on both subsonic or supersonic combustion modes was in during more than 23 seconds of the second flight test.

Hypersonic Flying Laboratory and Experimental Double Mode SCRAMJET.

To provide the HFL flight trajectory, close to a standard flight trajectory of the vehicles with the propulsion system incorporating the scramjet, was one of the main causes due to which "Surface-to-Air" missile SA-5 was chosen as the HFL "Kholod" booster. This missile flight trajectory is very close to the required trajectory of the HFL "Kholod". Proceedings from the requirements of aerodynamics, stability and control ability of SA-5, experimental scramjet and all on-board service modules were manufactured in a form of axisymmetrical circular body; their diameter did not exceed 750 mm diameter of the standard SA-5 modules (Fig. 2.21).

Experimental hydrogen scramjet of axisymmetrical configuration was installed in the HFL forebody. The casing of the section N1 is an intermediate section between the experimental scramjet and on-board tank, occupying the section N2

The section N 1 is washed from the outside by high temperature jet emerging from the scramjet annular nozzle and for this reason it is protected by *12 mm* thermal-insulating layer. Hydrogen consumption controller (RPST-2) with actuating units and regulating flaps, ignition system electronics, flow meter devices and transducers to measure the parameters in the experimental scramjet were installed within the section N 1. Hydrogen supply lines, measuring tubes for pressure transducers, thermocouples and electric cables are also installed in the above section.

On-board hydrogen tank (section N 2) has shield-vacuum heat insulation with residual pressure lesser than 0.1 mm Hg. The operational pressure within the internal vessel at hydrogen supply to the scramjet is 2,2 MPa. Hydrogen level monitoring during on-board tank filling is carried out by capacitance level transducer and by internal vessel wall temperature sensor.

Expulsion system of hydrogen supply from the on-board tank to the scramjet combustor is installed in section 3A. Hydrogen expulsion system incorporates high pressure helium spherical container (37 MPa), the volume of which is 42 liters, pressure reducers, isolating and safety valves, and sensors for parameters monitoring in the hydrogen supply system.

High pressure nitrogen spherical container (37 MPa) is also located in section 3A. The volume of this container is 17 liters. Nitrogen is used for functioning of pneumatic actuated valves and hydrogen supply system units in flight. Joining units of on-board tank filling by hydrogen and spherical containers by helium and nitrogen are placed in the same section; electropneumatic joints to fulfill the technological and control operation on maintenance position and on launching pad during integrated checks of on-board systems and hydrogen filling is also installed in section 3A. Telemetry system units, electric power batteries, automatic pilot, warning indicator of scramjet combustor wall hazardous temperature and the ignition equipment of SA-5 missile control system are located in the section 3B.

HFL measuring complex together with RTS (radio telemetry station) makes available recording signals of boost rocket systems transducers, pressure transducers, temperature transducers and indicators of scramjet and HFL equipment operation from the start time up to *144-th s* of flight. HFL was equipment by 83 transducers of pressure, vibration and overload detectors, 58 temperature sensors and 46 indicators of equipment operation. Engine and its elements' parameters were measured by 68 pressure transducers, 49 thermocouples and temperature sensors and by 20 indicators of equipment operation. Information from the measuring complex was transmitted to telemetry station with 50 Hz sampling rate (from temperature sensors it was transmitted with 1,5 Hz sampling rate) through on-board telemetry station. External trajectory measurements were fulfilled by radar and phase direction finder complex.

The experimental dual mode scramjet of axisymmetric configuration consists of the uncooled three-shock inlet, the combined cooled combustor and the exhaust nozzle with one-sided expansion. The design of the mentioned engine was carried out as four basic units: intake central body, combustor central body, lips of combustor and outside shell (Fig. 2.22).

The engine is designed to operate in a wide range of flight conditions ($M_f = 3,5...6$ and $H = 15...35$ km) at subsonic and supersonic combustion modes experimental scramjet is made with constant duct dimensions to simplify engine structure and to ensure more high reliability.

The first part presents a small divergence and includes at its beginning a row of injectors followed by a flame stabilization. The second one, which is divergent, comprises at its entrance a step and two rows of injectors, each followed by a flame stabilizing cavity. The last one has a constant area. For subsonic combustion mode, ($M_f = 3,5...5,0$) the fuel is supplied through the injectors of the collectors with fuel burnout in the second and in the third part of the

combustor. At supersonic combustion mode ($M_f \geq 5.0$), part of a fuel is additionally supplied through the first collector with combustion in the first part of the combustor. The injectors are located uniformity along the circle and their number is the same in all collectors (N=42 holes). The injector nozzle diameter is 1,7 mm for the first row of injection, the injector diameter is 2.1 mm for the second and the third rows of injection. Hydrogen is injected into the flow at angle 30 degrees in the first and the second row of injection and it is injected at angle 90 degrees in the third row of injection.

The walls of both the central body and the external ring are cooled by the hydrogen used for combustion. At the exit of the tank, hydrogen first flows along the combustor double walls and then is sent to the injection valve supplying the last two collectors and to that supplying the first injectors' row. If necessary, the third valve permits to increase the hydrogen flow rate in the cooling jacket and to exhaust the extra hydrogen out of the combustion chamber.

The chart of fuel supply system and basic principles of fuel consumption control system design are presented in Fig. 2.22. As operating regimes change should be ensured only by fuel consumption variation and by fuel redistribution over fuel injector rings, basic requirements to computer-aided control system of dual mode scramjet are concerned only with fuel consumption control and change of fuel injection position in accordance with flight Mach number. The requirements of providing necessary cooling of engine structure elements and engine stable operation at maximum heat supply regimes are also important

As it is shown in Fig. 2.22a, engine internal parameters, i.e. static pressures P_1, P_4, P_5, P_{H_1} and P_{H_2} and total pressure P_0 determines fuel consumption and temperatures of structure elements (there can be several elements) determine coolant consumption through cooling jacket. By this, inlet first cone pressure determines incoming flow Mach number

$$P_0/P_1 = f(M_H)$$

pressures P_{H1} and P_{H2} determine real performances of combustor operating process,

$$P_{H1}/P_4 = f(M_H, a) \text{ and } P_{H2}/P_4 = f(M_H, a)$$

and pressures P_4 and P_5 characterize flow regime at duct entrance. If $P_4 < P_5$, then designed flow without detached shock wave takes place, if $P_4 > P_5$, then flow with detached flow shock wave and decrease air flow mass rate occurs.

Incoming Flow Parameters.

The main parameters of the incoming flow, necessary for analysis of engine operation in flight, are the following: pressure P_H , temperature T_H and density ρ_H, as well as the angle of attack of the incoming flow. External trajectory measurements and special meteorological measurements.are used to determine these parameters (H,W)

Mach number was calculated by the typical relation $M=W_H/(kgRT_H)1/2$ The change of M, H and ram value q_H depending on HFL flight time are presented at Fig. 2.23. Presented data show that the maximal flight Mach number value was M =5.3 and the maximal altitude was $H \cong 22.4km$.

SCRAMJET Operation in Flight Conditions.

The changes of combustor wall temperature near fuel injection positions and hydrogen temperature measured at cooling system exit are shown in Fig. 2.24. The presented data testify to active hydrogen combustion in dual mode scramjet combustor. The analysis has shown that the highest wall temperature at subsonic combustion regime $T_W=1140K°$ was recorded on cowl near 2 cavity stabilizer real wall. The maximal values of T_W at supersonic combustion regimes T_W =1400 ...1450 K° were recorded on central body of the first part of combustor near cavity stabilizer rear wall at $\tau=70$ ...72 s. Measured value of hydrogen temperature at cooling system exit was maximal in the end of dual mode scramjet operation duration and constituted $T_{H2}=950$ K° (Fig. 2.24).

We can see from considering T_W and T_{H2} dependence on time that thermal state of combustor structure elements at engine operation at subsonic combustion regimes was close to steady state after coolant consumption increase at $\tau=49$ ...52 s. But after transition to supersonic combustion regimes with additional heat release in the first part of combustor, the thermal instability increased, gradients $dT_W/d\tau$ and $dT_{H2}/d\tau$ increased too, that resulted in dual mode scramjet construction break-down. The complete analysis of experimental data, taking into account combustor walls thermal state, combustion efficiency and pressure losses in cooling system channels, has shown that the first symptoms of combustor walls' burnout have appeared already at $\tau=63$ ...64 s. The appearance of regimes with detached shock wave subsequently was caused evidently by this. For this reason, the analysis of dual mode scramjet main parameters was made for HFL flight time from 39 till 63 s.

Effective hydrogen combustion in combustor and producing thrust by experimental dual mode scramjet is corroborated by HFL overload factor Nx measurements. The difficulties of such integral measurements are caused by rocket engine operation till 57 s of flight and after its termination -- by small value of dual mode scramjet thrust in comparison with air drag force of the whole complex HFL-dual mode scramjet. But overload sensor has recorded dual mode scramjet thrust in the initial period of test at $\tau=40$ 44 s (Fig. 2.25).

Experimental Dual Mode SCRAMJET Parameters.

Gas-air flow parameters engine duct and scramjet inlet and combustor performances were determined by use of measured values of static pressure and wall temperature, incoming flow parameters, air mass flow rate, fuel and coolant consumption's. The calculations were carried out on one-dimensional gas dynamic equations including real thermodynamic properties of combustion products, drag forces of struts and cavity stabilizers, friction and heat removal into duct walls. Heat fluxes q_W accumulated by wall substance was calculated with use of unsteady heat conduction method. In accordance with this method, q_W is proportional to $dT_W/d\tau$ ($q_W \sim dT_W/d\tau$) Heat amount removed by coolant in cooling system channels' cowl and central body were calculated with the assumption that coolant consumption on cowl constitutes 80% of coolant consumption on central body.

The typical data on changes of flow pressure increase ratio $P=P/P_H$, wall temperature T_W, and total heat fluxes Q_{SW} along experimental dual mode scramjet duct at subsonic and supersonic combustion regimes are presented in Fig. 2.26. One can see from considering dependencies $P(X)$ that pseudo-shock, in which air stream deceleration from supersonic velocity to subsonic one, accompanied by sharp pressure increase (Fig. 2.26a) occurs, lies at subsonic combustion regime in initial part of combustor. Disturbances caused by heat release in 2 and the second parts of combustor don't extend upstream in the first part of combustor farther than till 1 cavity stabilizer. At the third part of combustor with constant cross section area, pressure decreases due to intensive heat supply and reaches minimum value at combustor exit. Unusual for such regimes' non monotonous change of pressure P in zone $X=6.5$...7.5 can be explained apparently by combined effect on the flow of fuel jets system of the second and the third injection rows, cavity stabilizers, active heat supply and change throat are of the second part of combustor.

The analysis has shown that pseudo-shock moves downstream at flight speed increase accompanied by decrease of relative heat supply, and static pressure in the second and the third parts of combustor increases. The maximum pressure increase ratio in engine duct is reached values $P = 30$...32 at

subsonic combustion regimes.

The flow field in engine duct changes fundamentally at supersonic combustion regimes with additional hydrogen supply through the first injection row in combustor beginning (see Fig. 2.26b). The region with maximum pressure is located in the first part of combustor and the pressure in the second and the third parts of combustor decrease by a factor 1.5...2. The maximum pressure increase ratio in duct is at this operation mode appreciably higher than that at subsonic combustion regimes and reaches values $P/P_{1F} \cong 55$ and greater $\tau > 63$ s.

P(X) considering in other flight moment has shown that the flow in the second and the third combustor parts during the initial period of engine operation at supersonic combustion mode is close to isobaric one. The flow field, characteristic for subsonic combustion mode , with flow deceleration and subsequent flow acceleration, is reached after 58-th second of flight at flight Mach number decrease in the third part of combustor ($X > 7.8$). Therefore, it is possible to suppose that both completely supersonic flow along the duct and that combined with subsonic zone in the third part of combustor are realized at fuel supply corresponding to supersonic combustion regimes.

It should be noted, that the pressure in the first part of combustor increases appreciably at engine operation with detached shock wave ($P \cong 72$) and disturbances spread upstream and give rise to average pressure increase more than 2 times

$T_W(X)$ distributions, shown in Fig. 2.26 give additional insight into thermal loads of dual mode scramjet inlet and combustor as compared with data of Fig. 2.24. One can see those heat fluxes on inlet compression surfaces ($X < 4$) are small and values of wall temperature T_W of central body increase during time interval $\tau = 43.5...57.5$ s not higher than by $\Delta T_W = 50...100$ K°. The comparison of $T_W(X)$ and $Q_{SW}(X)$ shows that specific heat fluxes in the first part of combustor increase appreciably at feed of fuel part through the first row of injection. This fact together with distributions P(X) change testifies to hydrogen combustion along the whole engine duct at subsonic combustion regimes at $\tau > 52$ s.

As the analysis has shown, static pressure values P measured on inlet compression surfaces are close to design values and experimental data obtained in ground test conditions. For this reason, calculated experimental dependencies of inlet coefficient φ and liquid streamline additional drag force factor Cx upon incoming flow Mach number and angle of attack were used to determine engine air mass flow rate and flow parameters in inlet throat (section X=4.2, before the first injection ring). Experimental dual mode

scramjet inlet parameters determined in flight test conditions are shown in Fig. 2.27. The first flight test data are presented in the same figure for comparison Reynolds numbers calculated on incoming flow parameters and cowl sharp edge diameter $D_a = 0.226$ m varied within the limits $Re = (0.5-2.1)10^6$ and $Re = (1.4-2.7)10^6$ in the first and the second flight tests, respectively. One can see a good agreement of inlet parameters (pressure increase ratio P_i, Mach number M_i and total pressure recovery factor σ_i) obtained in both tests are in good agreement.

Some distinction between M_i and σ_i values, obtained in different tests, appreciable at supersonic combustion regimes $M_{II} > 5$ is caused, apparently, by heat release in the first part of combustor effects on boundary layer and separation zone in inlet throat It is possible that pressure increase on central body compression surfaces is caused by the same reason, at least near pressure P5 points of measuring.

Flow Mach number M, total pressure losses and hydrogen fuel combustion efficiency distributions along the dual mode scramjet combustor on characteristic subsonic and supersonic combustion regimes are illustrated in Fig. 2.28 Flow Mach number change in the first part of combustor at subsonic combustor regime (Fig. 2.28a) characterizes flow deceleration in pseudo-shock wave zone. The mentioned above peculiarity of pressure distribution along the length at combustor second part (see Fig. 2.26a) becomes apparent in flow acceleration up to transonic velocity in section x=7.0 with two strongly pronounced subsonic flow zones at the second and the third part of combustor Main losses of total pressure at these regimes are concentrated in the first part of combustor and in the beginning of the second part in the region of air flow deceleration. Combustion efficiency, for an air to fuel ratio of 1.2 reaches 0.8 The most active fuel jets burning occur till x=8.7, in the second and in the beginning of the third part of combustor (Fig. 2.28a)

The results presented in Fig. 2.28b example of operation regime for which supersonic flow is achieved all along the engine duct. Here the main total losses occur in the first part of the chamber, where combustion takes place in a supersonic flow with high initial velocity (about Mach 2.2) and also in the second and third flame stabilizers zone. The total pressure decrease is about 50% in both regions. It does not exceed 30% or 40% in the rest of the combustor

Non monotonous variations of Mach number M in the first part of combustor is explained by combined effect of heat release and cross section area increase. It is obvious, that the effect of heat release is prevailing in stabilizer's region due fuel burns in the circulation zone and heat release is maximum at the beginning of hydrogen jets combustion.

The analysis results also show that the total pressure recovery ratio σ_{chamb} is constant behind the stabilizer cavity at that combustion efficiency, for the first injection, η_1, is about 0.7 at the end of the first combustor part. This can lead to the conclusion that probably, for small fuel mass flow rate combustion mainly takes place in the flame stabilizer operates not in flame regime. The global combustion efficiency at the combustor exit is about 0.7--0.8.

Data scatter at combustion efficiency factor variation along the combustor in both examples presented in Fig. 2.28 is explained by approximates of one-dimensional approach to the analysis of experimental data on pseudo-shock zone and high flow nonuniformity near fuel jets burnout beginning, including region near the second and the second cavity stabilizer. But the results of comparison of gas dynamic method used in present paper with thrust method of η determination results, obtained at experimental investigations of scramjet bed models, have corroborated the authenticity of determining averaged flow parameters in region with moderate nonuniformity extent: at combined combustor exit and in the end of its first part.

The generalization of the first and second flight tests experimental data related to combustion efficiency is presented in Fig 2.29 The symbols indicated experimental data and the solid lines the approximation of these data. The leading parts of diffusion processes in hydrogen combustion are corroborated by typical shape of correlation's between combustion efficiency and equivalence ratio β, with efficiency decrease near $\beta = 1$ and increase when β greater or low then 1. The higher values of efficiency in supersonic combustion regimes are explained by increase of fuel injectors' number and by the larger combustor length over which fuel jets mixing with air and combustion occurs.

Some Conclusion.

During the second flight test of the duel mode scramjet in the Hypersonic flight Laboratory "Kholod", the engine operated in the range of flight Mach number running from $M_{1f}=3.5$ to $M_{1f}=5.35$ and between altitude of 15 km and 24 km is subsonic and supersonic combustion operating modes. Hydrogen combustion in a flow that was supersonic all along the scramjet duct was achieved for the first time in flight test conditions, between Mach number of 5.1 and 5.3 and with air to fuel ratio of about 1.8.

For subsonic combustion regime, with air to fuel ratio running from 1.2 to 2.5, combustion efficiency varied from 0.65 to 0.88. In supersonic combustion mode, and for air to fuel ratio comprised between 1.7 and 2, it varied from 0.7 to 0.95.

The cooling system was able to ensure normal scramjet operation without structure break-down during 23 s. Hydrogen supplying system and engine regulation could also achieve engine starting and it's in two different combustion modes.

Thus, results have demonstrated technical feasibility of flight tests with rocket boosters and their ability to provide significant information about scramjet operation.

Bibliograthy

1. Курзинер Р.И. "Реактивные двигатели для больших сверхзвуковых скоростей полета" М. *Машиностроение*, 1989.

2. Ogorodnikov D., "Engines for Hypersonic Aircraft", *"Aviadvigatelestroenie-92" International Symposium*, 1992

3. Contensou P., Marguet R., Huet Ch., "Etude Theorique et Experimentale d'un Statoreacteur a Combustion mixte (domaine de vol Mach 3.5/7)" *La Recherch Aerospatiale* - No. 5, 1973.

4. Hirsinger F. "Optimisation des Performances d'un Statoreacteur Supersonique - Etude Theorique et Experimentale", *TP ONERA* No. 1106, 1992.

5. Vinogradov V., et.al. "Experimental investigation of 2-D Dual mode Scramjet with Hydrigen Fuel at Mach 4-6", *AIAA Paper* 90-5269,1990.

6. Албегов О., Курзинер Р., и др., "Некоторые особенности рабочего процесса в камере сгорания с дозвуковым и сверхзвуковым потоками", "Теория двигателей летательных аппаратов", АН СССР, 1986.

7. Roudakov A., Novelli Ph., et.al., "Flight testing an Axisymmetric scramjet - Russian Recent Advances." *IAF- 93*-S.4.485, 1993

8. Sosounov V. "Study of Propulsion for High Velocity Flight" *ISABE*. 1991.

9. Kleinau W., Koelle D., "Evolutionary Develoopment to a Reusable Single-Stage-to-Orbit Launcher", *IAF-93*-V.3.619, 1993.

10. Kuczera H., et.al., "The German Hypersonics Technology Programme - Status 1993 and Perspectives", *IAF-93*-V.4.629, 1993.

11. Koelle D., "Launch Cost Assessment of Operational Winged Launch Vehicles", *AIAA Paper* 92-5021, 1992.

12. Vandenkerckhove J, Barrere M , "Energy Managment", *ISABE* - 1993.

13. Billig F., "Research on Supersonic Combustion," *Jornal of Propulsion and Power,...* Vol 9, No. 4, 1993.

14. Heppenheimer. "The national Aerospace plane" *Pasha Publications*, 1989

15. Escher W.J.D., Teeter R.R, Rice E E "Airbreathing and Rocket Propulsion Synergism: Enabling Measures for Tomorrow's Orbital Transports" *AIAA Paper*, 86-1680, 1986

16. Murthy S.N.B., Czysz P.A. "Energy Analysis of High speed Vehicle Systems" *AIAA Paper*. 90-0089,1990.

FLIGHT PATH REGION, ENTHALPY CONSTANT LINES AND RAM CONSTANT LINES
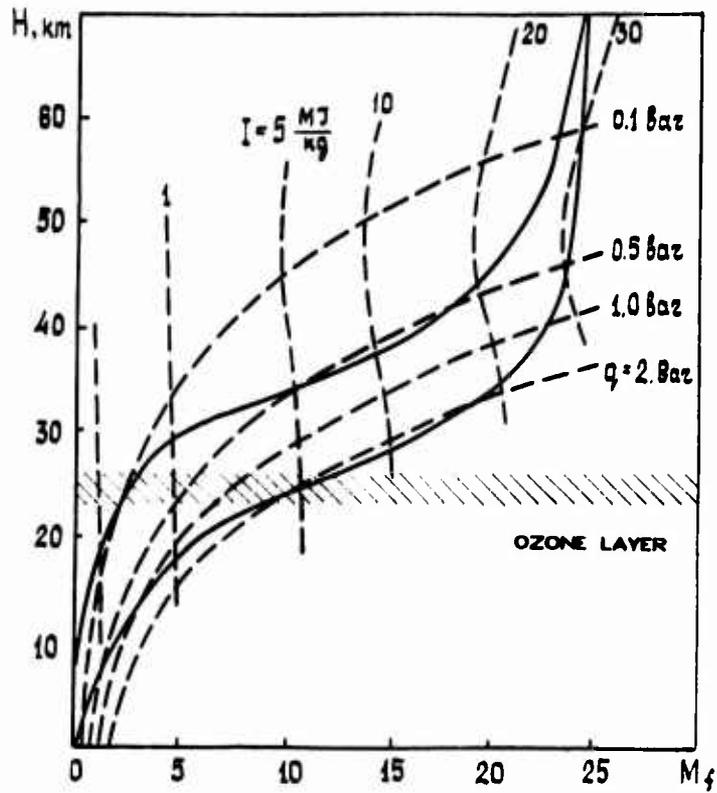
Fig 2.1

LINES OF CONSTANT QUASI-EQUILIBRIUM TOTAL TEMPERATURE T_t, TOTAL PRESSURE P_t AT SCRAMJET ENTRANCE AND THE FLIGHT PATH REGION
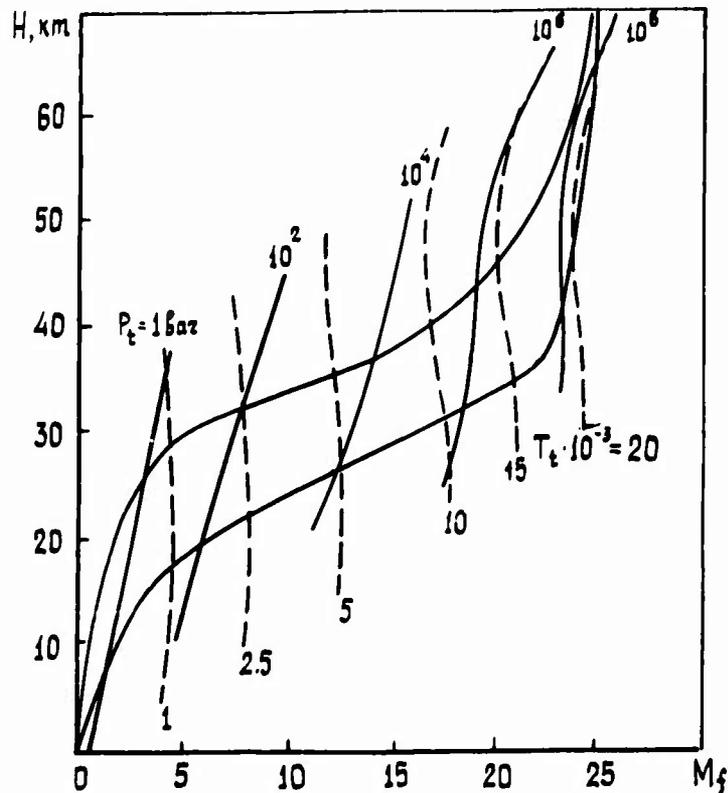
Fig 2.2

LINES OF CONSTANT REYNOLDS NUMBER Re_1, AND TEMPERATURE FACTOR
$\bar{T}_w = T_w/T_t$ AT SCRAMJET ENTRANCE AND THE FLIGHT PATH REGION
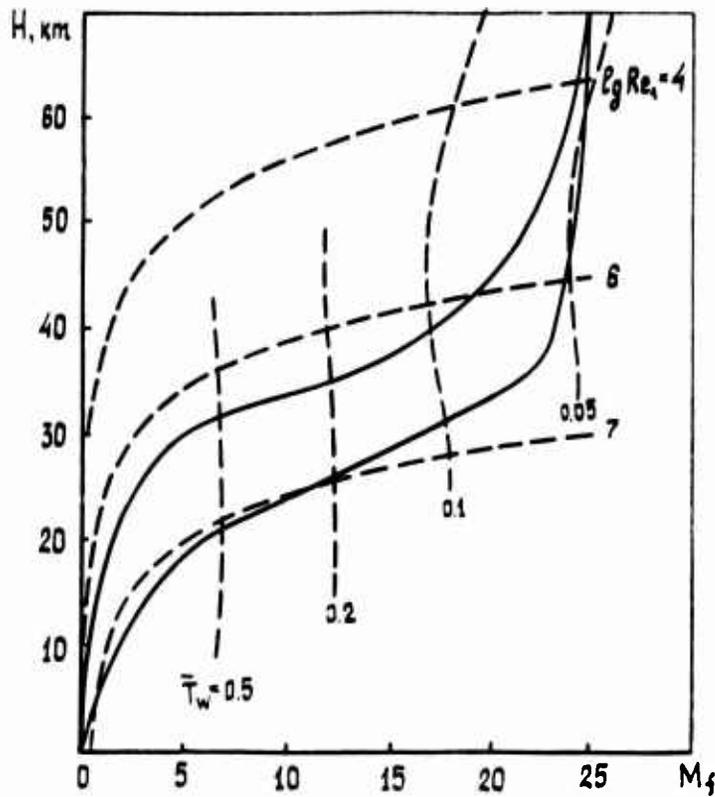
Fig. 2.3

INLET THROAT MACH NUMBER M_{th} AND COMBUSTOR EXIT MACH NUMBER M_*
DEPENDING ON FLIGHT MACH NUMBER M_f
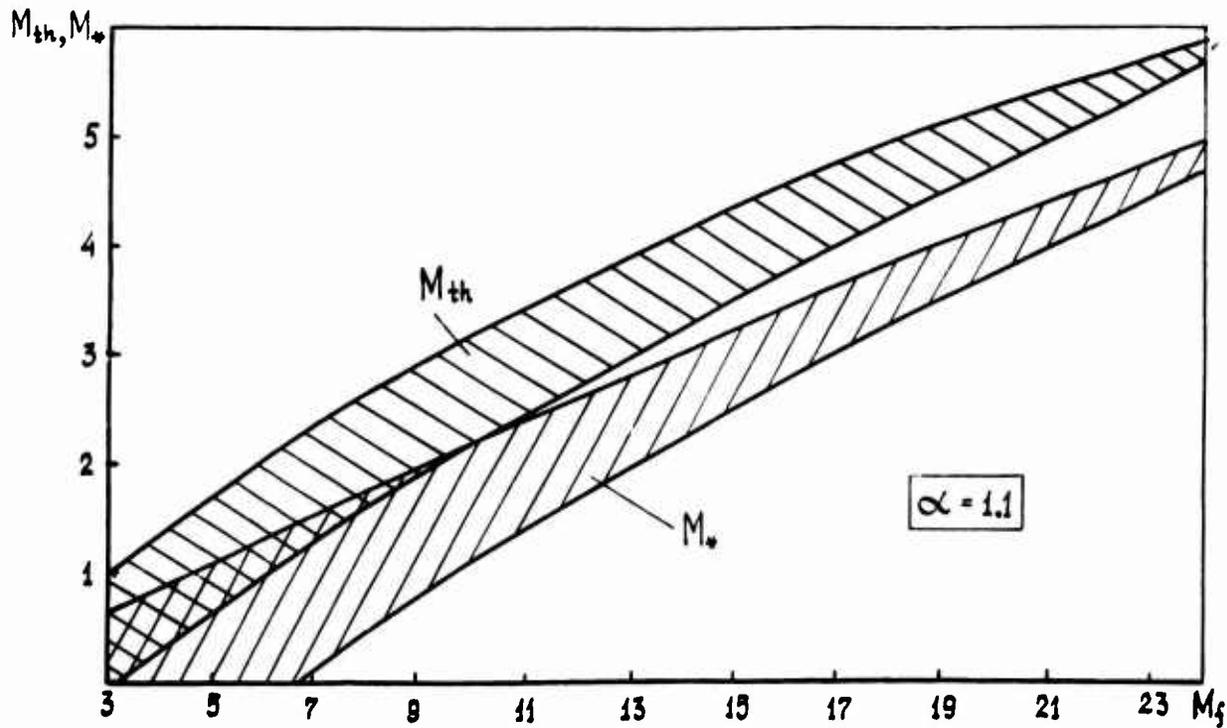
Fig. 2.4

INFLUENCES OF VARIOUS LOSSES ON SCRAMJET SPECIFIC IMPULSE ALONG THE FLIGHT PATH
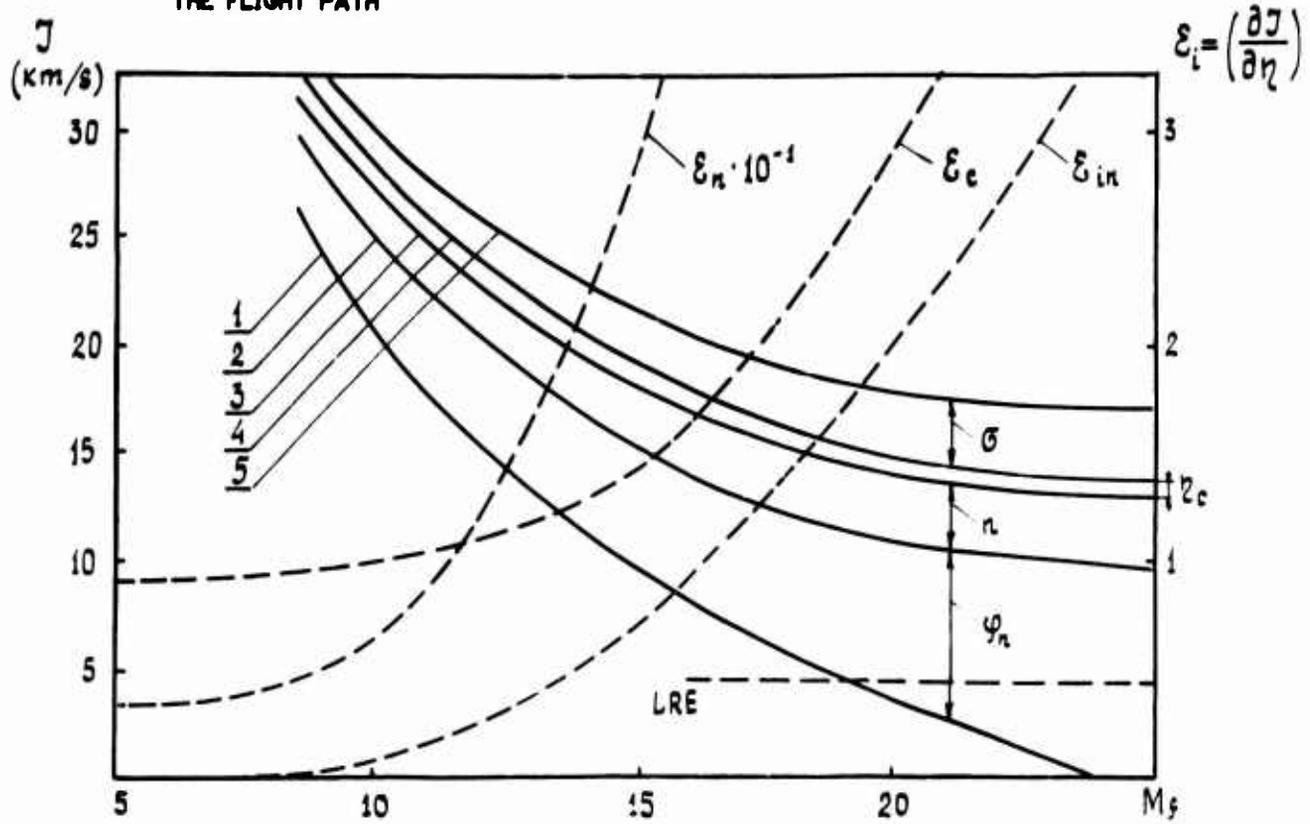
Fig. 2.5

Scheme of Research and Design Work for Scramjet Development
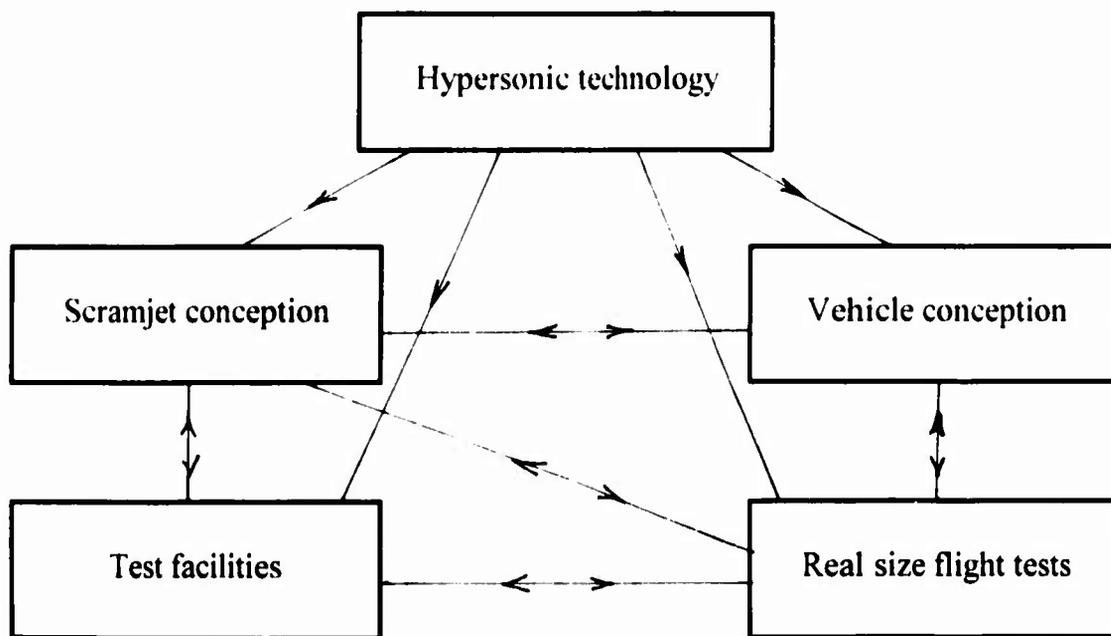
Fig. 2.6

Hypersonic Technology Development Directions

```
┌───────────────────────────────────────────────────────────┐
│                    Hypersonic technology                    │
└───────────────────────────────────────────────────────────┘
```

| Fundamental studies | Experimental simulation of engine process | New technical approaches |

| Applied scientific studies of engine process | Numerical simulation of engine process | Scramjet systems and elements |

Fig 2 7

Fundamental Studies
Applied Scientific Studies of Engine Process
Experimental Simulation of Engine Process
Numerical Simulation of Engine Process
New Technical Approaches
Scramjet Systems and Elements

--Physical process and turbulence.
--Materials
--Ecology.

Fig 2 8

Fundamental Studies
Applied Scientific Studies of Engine Process
Experimental Simulation of Engine Process
Numerical Simulation of Engine Process
New Technical Approaches
Scramjet Systems and Elements

--Thermodynamics.

--Thermal physics and combustion.

--Gas dynamics and turbulence.

--Numerical simulation.

--Diagnostics and measurements methods.

--Super computers.

Fig 2.9

Fundamental Studies
Applied Scientific Studies of Engine Process
Experimental Simulation of Engine Process
Numerical Simulation of Engine Process
New Technical Approaches
Scramjet Systems and Elements

--Ground test facility:

--gas dynamics;

--combustion and detonation;

--heat exchange.

--Flying laboratories:

--ballistic;

--winged 3<M<8.

--Orbital 10<M<25 operating process and propulsion system plane interference.

Fig 2.10

Fundamental Studies	--Mathematical models of turbulence in hypersonic high-enthalpy flow.
Applied Scientific Studies of Engine Process	--Nonqulibrium physical-chemical reactions in supersonic flow.
Experimental Simulation of Engine Process	--Three-dimensional and unsteady interaction of shock waves with boundary layer in channel.
Numerical Simulation of Engine Process	--Detonation combustion.
	--Direct numerical simulation of scramjet flow.
New Technical Approaches	--Scramjet thermal state simulation.
Scramjet Systems and Elements	--Operating process control.

Fig 2 11

Fundamental Studies	--Structure.
Applied Scientific Studies of Engine Process	--Materials.
Experimental Simulation of Engine Process	--Technology.
Numerical Simulation of Engine Process	--Efficiency.
	--Diagnostics and control.
New Technical Approaches	--Supersonic mixers on base of liquid rocket engine.
	--Multimode supersonic combustor.
Scramjet Systems and Elements	--Automatic control system.

Fig 2 12

Fundamental Studies	
Applied Scientific Studies of Engine Process	
Experimental Simulation of Engine Process	
Numerical Simulation of Engine Process	
New Technical Approaches	
Scramjet Systems and Elements	

--Flow gas dynamic structure control.

--Flow mixing and combustion control.

--Structure thermal state control in supersonic high--enthalpy flow. Active cooling system.

--Hydrogen slush use.

--Compact hydrogen--air heat exchanges.

--High temperature composite structures.

Fig. 2 13

Scramjet Development.

Scramjet conception.	← →	Vehicle conception.

Scramjet sub-scale model	→	Real-size scramjet model	→	Real-size scramjet

Fig. 2.14

Test Facilities Development

```
                    ┌─────────────────────┐
                    │   Test facilities   │
                    └─────────────────────┘
```

Development of scramjet units and systems	Scramjet module	Real-size scramjet service life tests
-- Combustor: 1. Thermal state 2. Combustion efficiency 3. Thrust impulse --Supply system	--Demonstration and service life tests, $3 < M_f < 8$ -- Scramjet module and plane interference	$3 < M_f < 8$

Fig 2 15

Methods of Scramjet Duct Operating Process Study

Mathematical Simulation of Flows Including PhysicalChemical Conversions
Test Facility Simulation of Operating Process
Flight Tests of Sub--Scale Models
Experimental Studies in Laboratory
Real--Size Flight Tests of Modules and Propulsion System on The Whole

Fig. 2.16

Scramjet Duct Operating Process Study Methods

Experimental Studies in Laboratory	Test Facility Simulation of Operating Process	Flight Tests of Sub--Scale Models	Mathematical Simulation of Flows Including PhysicalChemical Conversions	Real--Size Flight Tests of Modules and Propulsion System on The Whole
Investigation Objects				
--Revealing and elaboration of physical flow pattern and some characteristics of phenomena in scramjet duct elements (inlet, combustor, exhaust nozzle) with possible simulation of physicalchemical conversions in high--enthalpy flow including influence of high cooled walls	--Investigation at conditions close to real both for duct on the whole and for its elements in possible range of M and Re numbers, corresponding to different parts of flight path	--Investigation at conditions close to real both for duct on the whole and for its elements along fligh. paths close to real	--Investigation of scramjet performances on the whole range of external parameters. --Investigation of various parameters influence on scramjet efficiency, economy and specific mass. --Optimization of duct parameters for given goal function.	--Investigation of all scramjet duct parameters along possible flight paths.

Fig. 2 17

Scramjet Duct Operating Process Study Methods

Experimental Studies in Laboratory	Test Facility Simulation of Operating Process	Flight Tests of Sub--Scale Models	Mathematical Simulation of Flows Including PhysicalChemical Conversions	Real--Size Flight Tests of Modules and Propulsion System on The Whole
Various Investigations Methods Advantages				
--The opportunity of detailed investigation of unsteady and non equilibrium gasdynamics phenomena including flow viscosity and turbulence and mechanics of flow stabilization and energy release --The same for diffusion and detonation combustion process in range $M = 2$. 6 in flow core and wall region --The grater information obtained by optic--electronics measurements	--Comprehensive simulation of phenomena in limited ranges of M and Re numbers and at limited test duration	--Comprehensive simulation of phenomena for real air composition along the whole flight path of real scramjet in limited range of Re number and limited test duration --Simulation of propulsion system plane interference --Independent methods of measurements of scramjet thrust and drag balance and specific impulse	--Unlimited range of parameters --Detailed data on flow pattern on the whole and in the small. --Generalization of experimental results, obtained in laboratory, test facility and flight test. --Simulation of interference of propulsion system and plane.	Simulation of all real conditions of scramjet operation.

Fig. 2.18

Scramjet Duct Operating Process Study Methods

Experimental Studies in Laboratory	Test Facility Simulation of Operating Process	Flight Tests of Sub--Scale Models	Mathematical Simulation of Flows Including PhysicalChemical Conversions	Real--Size Flight Tests of Modules and Propulsion System on The Whole
Various investigations methods disadvantages				
--Incomplete simulation of operating process both in scramjet duct on the whole and in its elements due to impossibility to keep all similarity criteria, detailed duct configuration, initial and boundary conditions of flow. --Simulation of only some characteristic features of flows and phenomena. --Heterogeneous qualitative results.	--Limited ranges of M and Re numbers(enthalpy and absolute flow velocity), model dimensions, incomplete simulation of physical--chemical compositions of flow in model scramjet duct. --Limited nature of information obtained by measurements. --Necessity to use a set of test facilities for simulation of parameters along the flight path.	--Small dimensions of model scramjet duct. Limited nature of measurements methods.	--Use of semi-- empirical models of turbulence and physical--chemical phenomena in connection with impossibility of exact integration of motion equations for real Re and M and gas composition.	--Limited number of tests --Limited information on operating process. --Extremely high cost and risk of tests.

Fig. 2 19

Scramjet Duct Operating Process Study Methods

Experimental Studies in Laboratory	Test Facility Simulation of Operating Process	Flight Tests of Sub--Scale Models	Mathematical Simulation of Flows Including PhysicalChemical Conversions	Real--Size Flight Tests of Modules and Propulsion System on The Whole
Investigation Methods Interaction				
--Comparison of different laboratory methods is necessary to estimate measurements reliability and errors and to obtain reference data. --Verification and extrapolation of laboratory methods results by methods 2...5 is necessary.	--Results of methods 1 and 4 are used. --A set of measurements methods is necessary to obtain reference results. --Verification and extrapolation of results by methods 3,4,5 are necessary.	--Results of methods 1,2,4 are used. --Verification and extrapolation of results by methods 2,4,5 are necessary.	--The whole data base obtained by methods 1,2,3,5 is used, especially data of methods 1,2.	--Results of methods 1...4 are used.

Fig. 2.20

EXPERIMENTAL DMSCRAMJET

COMPARTMENT N 1

COMPARTMENT N 2

COMPARTMENT N 3A

COMPARTMENT N 3B
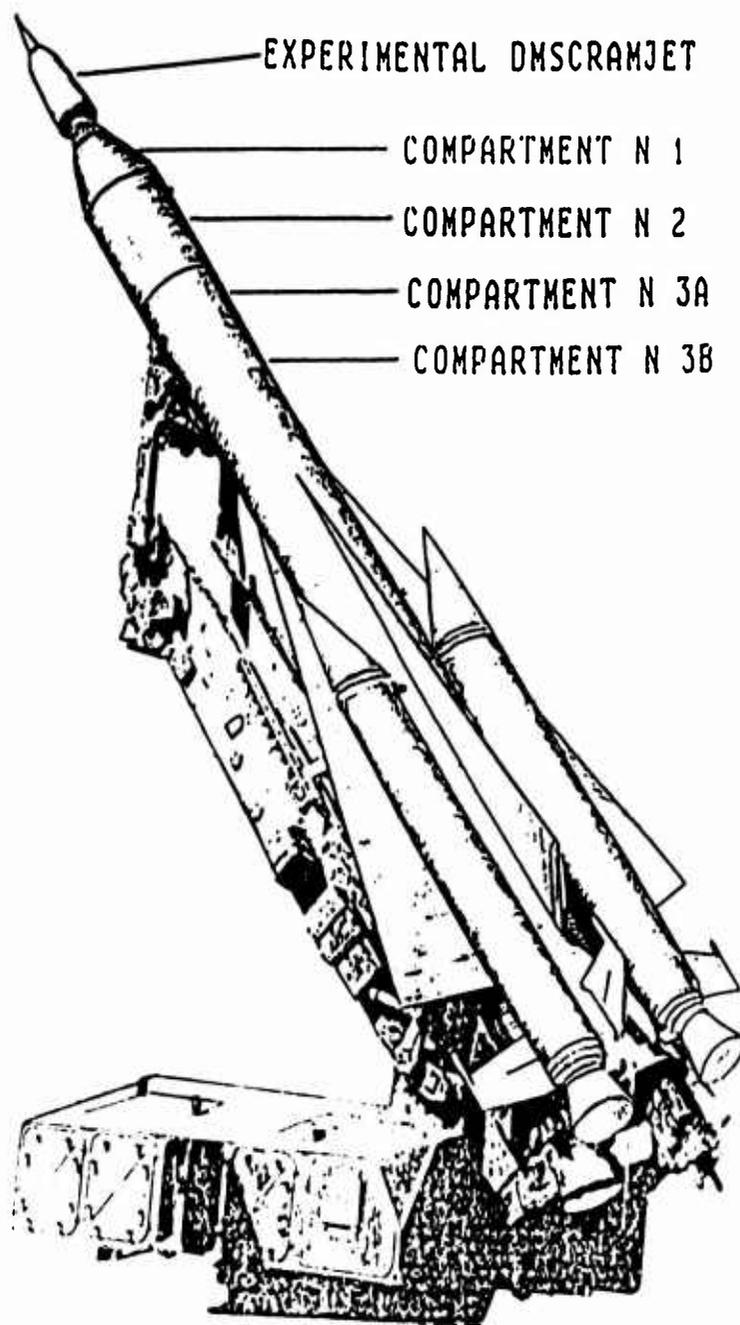
Fig. 2.21. Hypersonic flying laboratory with the experimental
dual mode scramjet on start position
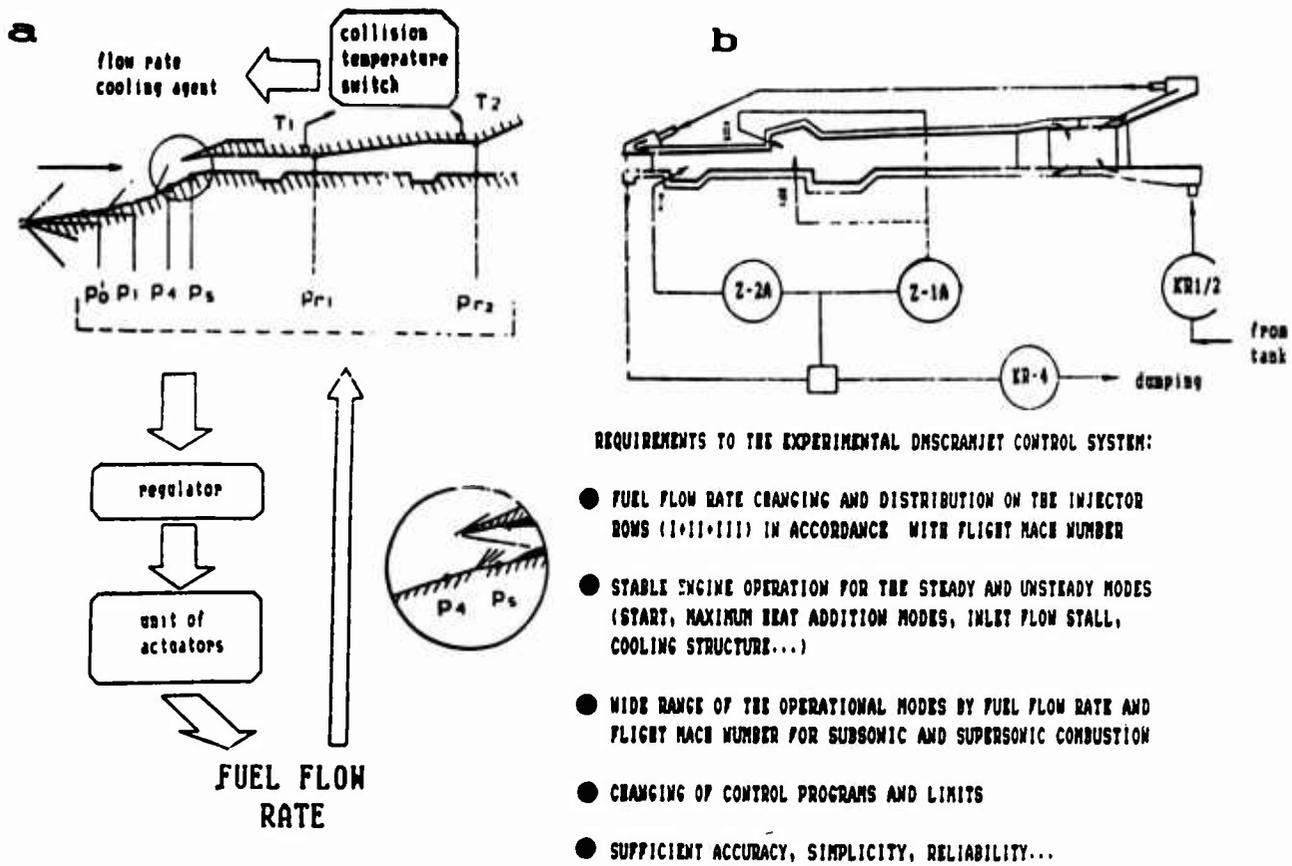
Fig. 2.22. Conception of the experimental dmscramjet control system
a - functional scheme of the control system;
b - scheme of the fuel feed and cooling system

REQUIREMENTS TO THE EXPERIMENTAL DMSCRAMJET CONTROL SYSTEM:

● FUEL FLOW RATE CHANGING AND DISTRIBUTION ON THE INJECTOR ROWS (I+II+III) IN ACCORDANCE WITH FLIGHT MACH NUMBER

● STABLE ENGINE OPERATION FOR THE STEADY AND UNSTEADY MODES (START, MAXIMUM HEAT ADDITION MODES, INLET FLOW STALL, COOLING STRUCTURE...)

● WIDE RANGE OF THE OPERATIONAL MODES BY FUEL FLOW RATE AND FLIGHT MACH NUMBER FOR SUBSONIC AND SUPERSONIC COMBUSTION

● CHANGING OF CONTROL PROGRAMS AND LIMITS

● SUFFICIENT ACCURACY, SIMPLICITY, RELIABILITY...

Fig. 2.23. HFL trajectory parameters (external trajectory measurements
EM - flight Mach number; EH:- altitude (km) ; QH - dynamic pressure (kg/m^3)

T, K
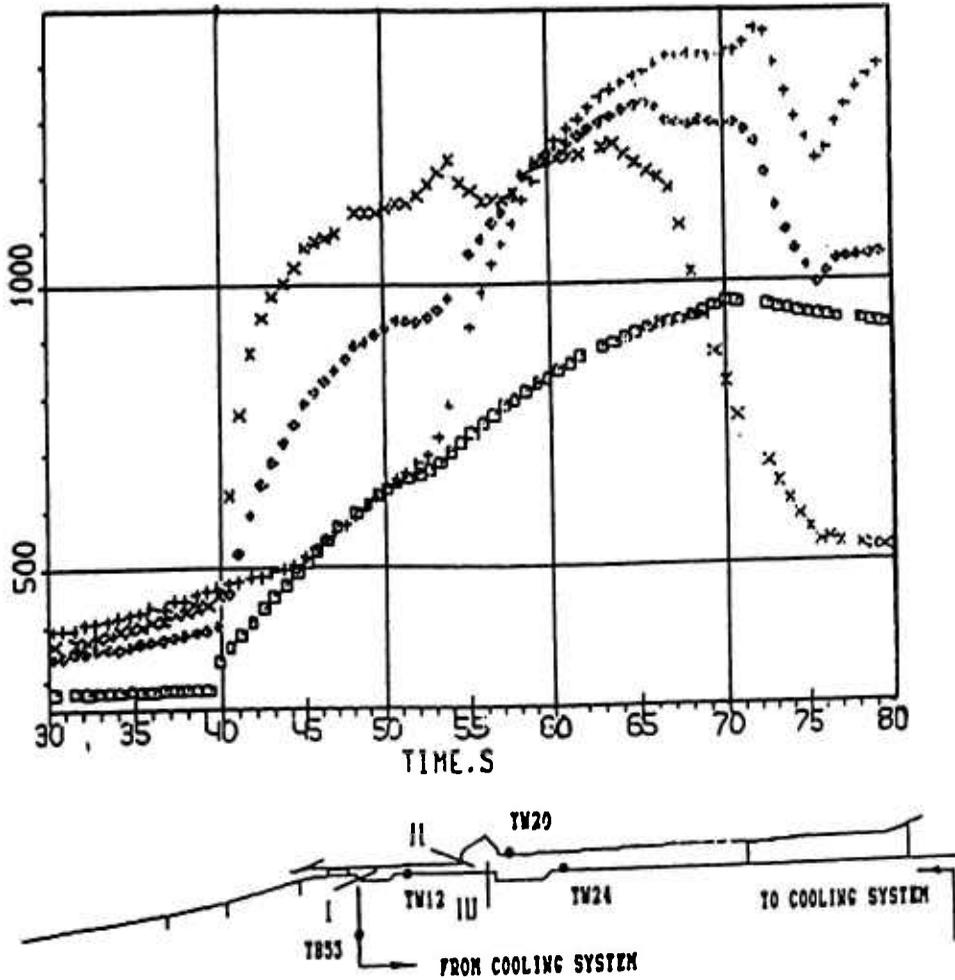
Fig. 2.24.   Wall temperatures (TW12, TW20, TW24) and hydrogen
temperature at cooling system exit (TB53) in the
dmscramjet operational time
+ – TW12, × – TW20, ◊ – TW24, □ – TB53
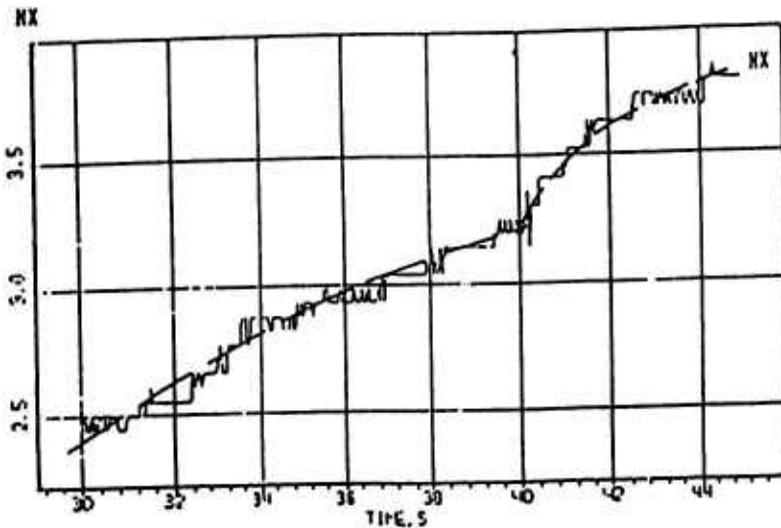
Fig. 2.25   Axial overload factor Nx
t = 40 s beginning of engine operation
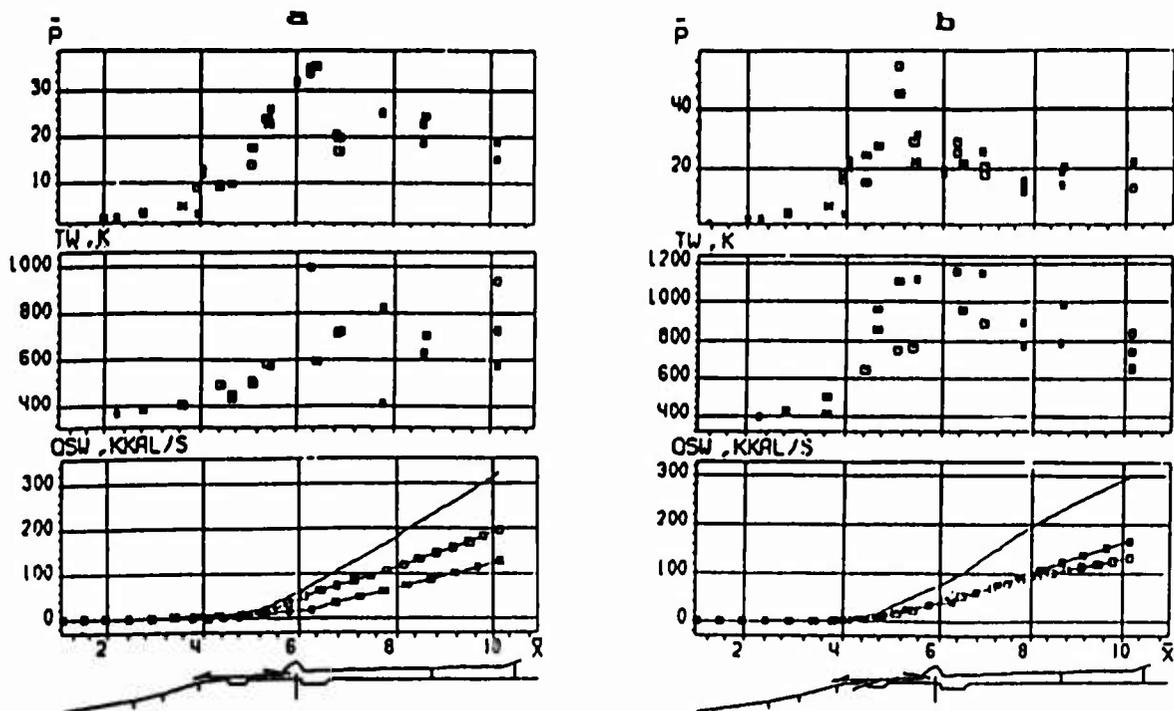
Fig. 2.26 Change of dascramjet parameters by engine length (P - pressure ratio, TW - wall temperature, QSW - heat flux; light symbols - cowling, dark symbols - central body. - regulator measurements)

a - subsonic combustion, TAU=43.5 s, MH=4.32, H=17.4 km, ALFA=1.18;

b - supersonic combustion, TAU=57.5 s, MH=5.33, H=21.7 km, ALFA=1.95
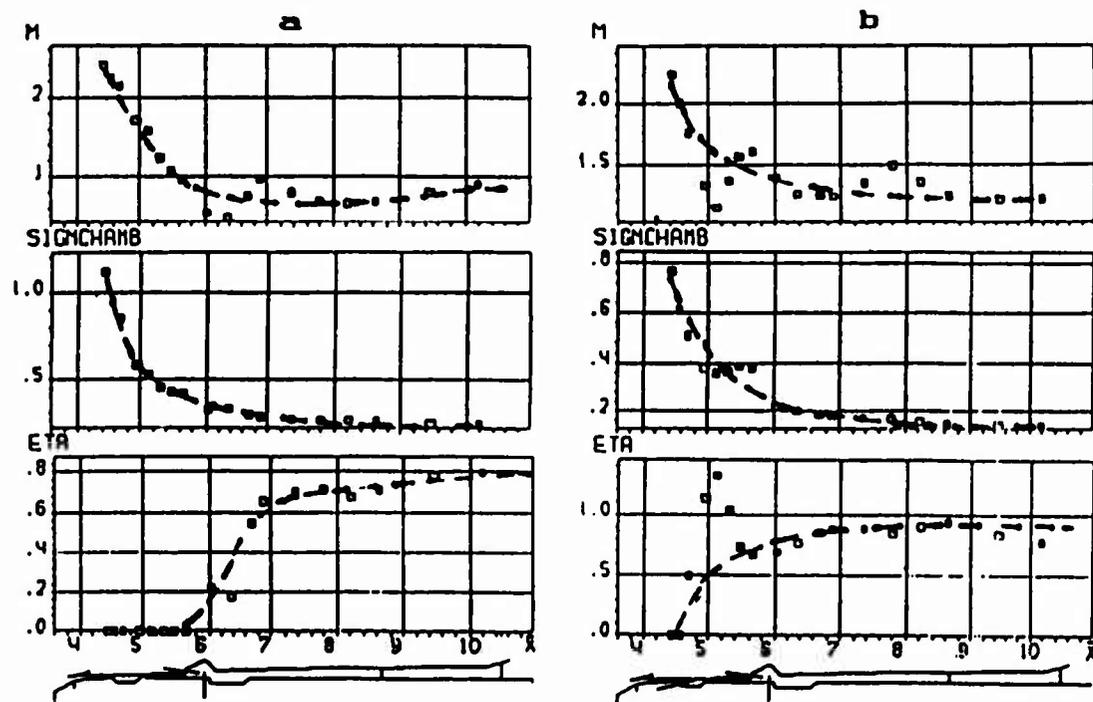
Fig. 2.28 Flow parameters in the dascramjet combustion chamber (M - Mach number, SIGMCHAMB - total pressure recovery coefficient, ETA - combustion efficiency, modes as Fig.8)
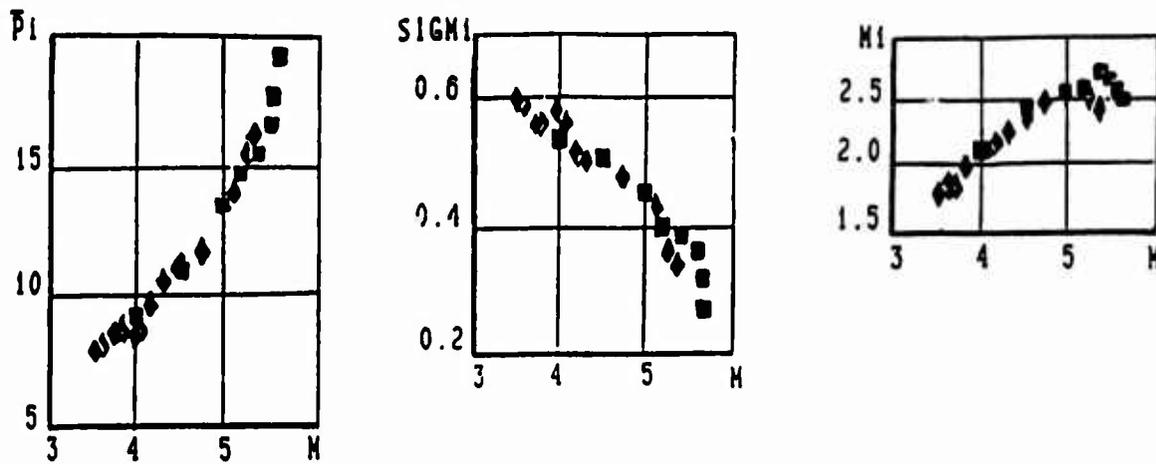
Fig. 2.27 Dual mode scramjet parameters in flight conditions
P_i static pressure ratio - M_i Mach number in the inlet throat -
σ_i total pressure recovery coefficient
■ first flight ◆ second flight
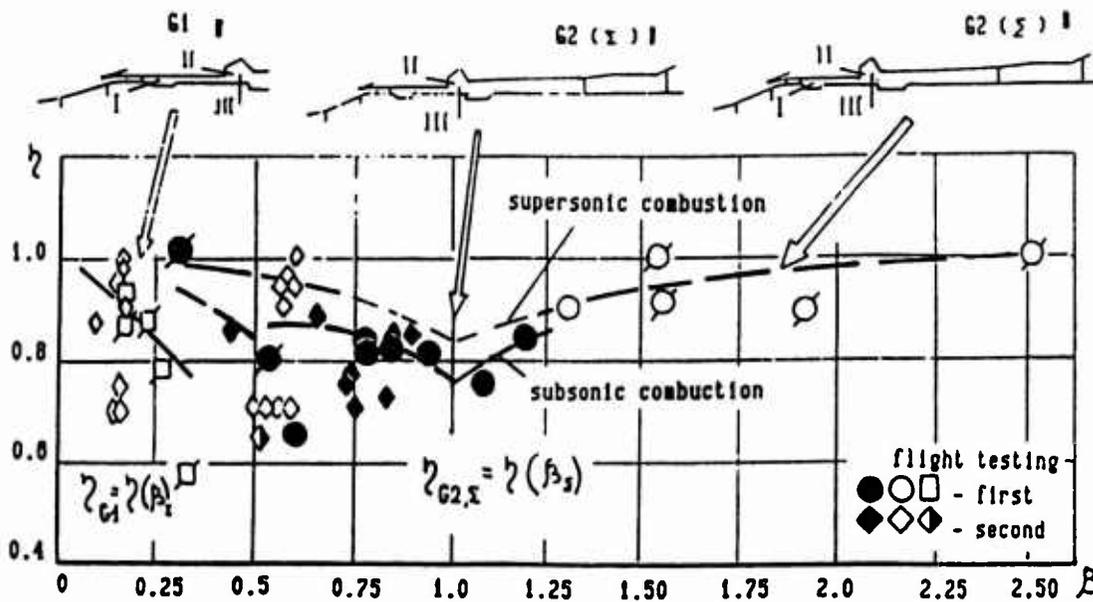
Fig. 2.29 Hydrogen combustion efficiency coefficients at the experimental scramjet
● ◆◈ - fuel feeding for subsonic combustion mode through II and
III injector rows; ○◇□ - fuel feeding for supersonic combustion
mode through I, II and III injector rows; ◗⬤□ - start chamber modes
or near "shock out" modes

REPORT DOCUMENTATION PAGE

1. Recipient's Reference	2. Originator's Reference	3. Further Reference	4. Security Classification of Document
	AGARD-LS-194	ISBN 92-835-0732-0	UNCLASSIFIED/ UNLIMITED

5. Originator	Advisory Group for Aerospace Research and Development North Atlantic Treaty Organization 7 rue Ancelle, 92200 Neuilly sur Seine, France

6. Title	RESEARCH AND DEVELOPMENT OF RAM/SCRAMJETS AND TURBORAMJETS IN RUSSIA

7. Presented on	1st—2nd December 1993 in Laurel, Maryland, United States, 13th—14th January 1994, in Köln, Germany and 17th—18th January 1994 in Paris, France.

8. Author(s)/Editor(s)	9. Date
Various	December 1993

10. Author's/Editor's Address	11. Pages
Various	232

12. Distribution Statement	This document is distributed in accordance with AGARD policies and regulations, which are outlined on the back covers of all AGARD publications.

13. Keywords/Descriptors	
Ramjet engines	Computational fluid dynamics
Solid rocket propellants	Russia
Liquid rocket propellants	Flight tests

14. Abstract

Russia has a long tradition of achievement in ramjet research and development. This tradition, and aspirations toward new and effective products, have led to establish Russian priority in the ramjet field.

This Lecture Series will present and discuss the scientific problems of the development of ramjets/ scramjets and turboramjets.

Some specific aspects of liquid/solid ramjet development, the concepts of LH2 high efficiency RAM combustors, the results of full scale turboramjet testing, scramjet or CFD analyses and their ground flight tests will be studied.

This Lecture Series, endorsed by the Propulsion and Energetics Panel of AGARD, has been implemented by the Consultant and Exchange programme.

AGARD Lecture Series 194
Advisory Group for Aerospace Research and Development, NATO
RESEARCH AND DEVELOPMENT OF RAM/SCRAMJETS AND TURBORAMJETS IN RUSSIA
Published December 1993
232 pages

Russia has a long tradition of achievement in ramjet research and development. This tradition, and aspirations toward new and effective products, have led to establish Russian priority in the ramjet field.

This Lecture Series will present and discuss the scientific problems of the development of ramjets/scramjets and turboramjets.

P.T.O.

AGARD-LS-194

Ramjet engines
Solid rocket propellants
Liquid rocket propellants
Computational fluid dynamics
Russia
Flight tests

AGARD Lecture Series 194
Advisory Group for Aerospace Research and Development, NATO
RESEARCH AND DEVELOPMENT OF RAM/SCRAMJETS AND TURBORAMJETS IN RUSSIA
Published December 1993
232 pages

Russia has a long tradition of achievement in ramjet research and development. This tradition, and aspirations toward new and effective products, have led to establish Russian priority in the ramjet field.

This Lecture Series will present and discuss the scientific problems of the development of ramjets/scramjets and turboramjets.

P.T.O.

AGARD-LS-194

Ramjet engines
Solid rocket propellants
Liquid rocket propellants
Computational fluid dynamics
Russia
Flight tests

AGARD Lecture Series 194
Advisory Group for Aerospace Research and Development, NATO
RESEARCH AND DEVELOPMENT OF RAM/SCRAMJETS AND TURBORAMJETS IN RUSSIA
Published December 1993
232 pages

Russia has a long tradition of achievement in ramjet research and development. This tradition, and aspirations toward new and effective products, have led to establish Russian priority in the ramjet field.

This Lecture Series will present and discuss the scientific problems of the development of ramjets/scramjets and turboramjets.

P.T.O.

AGARD-LS-194

Ramjet engines
Solid rocket propellants
Liquid rocket propellants
Computational fluid dynamics
Russia
Flight tests

AGARD Lecture Series 194
Advisory Group for Aerospace Research and Development, NATO
RESEARCH AND DEVELOPMENT OF RAM/SCRAMJETS AND TURBORAMJETS IN RUSSIA
Published December 1993
232 pages

Russia has a long tradition of achievement in ramjet research and development. This tradition, and aspirations toward new and effective products, have led to establish Russian priority in the ramjet field.

This Lecture Series will present and discuss the scientific problems of the development of ramjets/scramjets and turboramjets.

P.T.O.

AGARD-LS-194

Ramjet engines
Solid rocket propellants
Liquid rocket propellants
Computational fluid dynamics
Russia
Flight tests

Some specific aspects of liquid/solid ramjet development, the concepts of LH2 high efficiency RAM combustors, the results of full scale turboramjet testing, scramjet or CFD analyses and their ground flight tests will be studied.

This Lecture Series, endorsed by the Propulsion and Energetics Panel of AGARD, has been implemented by the Consultant and Exchange programme, presented on 1st—2nd December 1993 in Laurel, Maryland, United States, 13th—14th January 1994 in Köln, Germany and 17th—18th January 1994 in Paris, France.

ISBN 92-835-0732-0

Some specific aspects of liquid/solid ramjet development, the concepts of LH2 high efficiency RAM combustors, the results of full scale turboramjet testing, scramjet or CFD analyses and their ground flight tests will be studied.

This Lecture Series, endorsed by the Propulsion and Energetics Panel of AGARD, has been implemented by the Consultant and Exchange programme, presented on 1st—2nd December 1993 in Laurel, Maryland, United States, 13th—14th January 1994 in Köln, Germany and 17th—18th January 1994 in Paris, France.

ISBN 92-835-0732-0

Some specific aspects of liquid/solid ramjet development, the concepts of LH2 high efficiency RAM combustors, the results of full scale turboramjet testing, scramjet or CFD analyses and their ground flight tests will be studied.

This Lecture Series, endorsed by the Propulsion and Energetics Panel of AGARD, has been implemented by the Consultant and Exchange programme, presented on 1st—2nd December 1993 in Laurel, Maryland, United States, 13th—14th January 1994 in Köln, Germany and 17th—18th January 1994 in Paris, France.

ISBN 92-835-0732-0

Some specific aspects of liquid/solid ramjet development, the concepts of LH2 high efficiency RAM combustors, the results of full scale turboramjet testing, scramjet or CFD analyses and their ground flight tests will be studied.

This Lecture Series, endorsed by the Propulsion and Energetics Panel of AGARD, has been implemented by the Consultant and Exchange programme, presented on 1st—2nd December 1993 in Laurel, Maryland, United States, 13th—14th January 1994 in Köln, Germany and 17th—18th January 1994 in Paris, France.

ISBN 92-835-0732-0

AGARD

NATO ⊕ OTAN

7 RUE ANCELLE · 92200 NEUILLY-SUR-SEINE

FRANCE

Télécopie (1)47.38.57.99 · Télex 610 176

DIFFUSION DES PUBLICATIONS
AGARD NON CLASSIFIEES

Aucun stock de publications n'a existé à AGARD. A partir de 1993, AGARD détiendra un stock limité des publications associées aux cycles de conférences et cours spéciaux ainsi que les AGARDographies et les rapports des groupes de travail, organisés et publiés à partir de 1993 inclus. Les demandes de renseignements doivent être adressées à AGARD par lettre ou par fax à l'adresse indiquée ci-dessous. *Veuillez ne pas téléphoner*. La diffusion initiale de toutes les publications de l'AGARD est effectuée auprès des pays membres de l'OTAN par l'intermédiaire des centres de distribution nationaux indiqués ci-dessous. Des exemplaires supplémentaires peuvent parfois être obtenus auprès de ces centres (à l'exception des Etats-Unis). Si vous souhaitez recevoir toutes les publications de l'AGARD, ou simplement celles qui concernent certains Panels, vous pouvez demander à être inclu sur la liste d'envoi de l'un de ces centres. Les publications de l'AGARD sont en vente auprès des agences indiquées ci-dessous, sous forme de photocopie ou de microfiche.

CENTRES DE DIFFUSION NATIONAUX

ALLEMAGNE
Fachinformationszentrum,
Karlsruhe
D-7514 Eggenstein-Leopoldshafen 2

BELGIQUE
Coordonnateur AGARD-VSL
Etat-Major de la Force Aérienne
Quartier Reine Elisabeth
Rue d'Evere, 1140 Bruxelles

CANADA
Directeur du Service des Renseignements Scientifiques
Ministère de la Défense Nationale
Ottawa, Ontario K1A 0K2

DANEMARK
Danish Defence Research Establishment
Ryvangs Allé 1
P.O. Box 2715
DK-2100 Copenhagen Ø

ESPAGNE
INTA (AGARD Publications)
Pintor Rosales 34
28008 Madrid

ETATS-UNIS
NASA Headquarters
Attention: CF 37, Distribution Center
300 E Street, S.W.
Washington, D.C. 20546

FRANCE
O.N.E.R.A. (Direction)
29, Avenue de la Division Leclerc
92322 Châtillon Cedex

GRECE
Hellenic Air Force
Air War College
Scientific and Technical Library
Dekelia Air Force Base
Dekelia, Athens TGA 1010

ISLANDE
Director of Aviation
c/o Flugrad
Reykjavik

ITALIE
Aeronautica Militare
Ufficio del Delegato Nazionale all'AGARD
Aeroporto Pratica di Mare
00040 Pomezia (Roma)

LUXEMBOURG
Voir Belgique

NORVEGE
Norwegian Defence Research Establishment
Attn: Biblioteket
P.O. Box 25
N-2007 Kjeller

PAYS-BAS
Netherlands Delegation to AGARD
National Aerospace Laboratory NLR
P.O. Box 90502
1006 BM Amsterdam

PORTUGAL
Força Aérea Portuguesa
Centro de Documentação e Informação
Alfragide
2700 Amadora

ROYAUME UNI
Defence Research Information Centre
Kentigern House
65 Brown Street
Glasgow G2 8EX

TURQUIE
Millî Savunma Başkanlığı (MSB)
ARGE Daire Başkanlığı (ARGE)
Ankara

Le centre de distribution national des Etats-Unis ne détient PAS de stocks des publications de l'AGARD.

D'éventuelles demandes de photocopies doivent être formulées directement auprès du NASA Center for Aerospace Information (CASI) à l'adresse suivante:

AGENCES DE VENTE

NASA Center for
Aerospace Information (CASI)
800 Elkridge Landing Road
Linthicum Heights, MD 21090-2934
United States

ESA/Information Retrieval Service
European Space Agency
10, rue Mario Nikis
75015 Paris
France

The British Library
Document Supply Division
Boston Spa, Wetherby
West Yorkshire LS23 7BQ
Royaume Uni

Les demandes de microfiches ou de photocopies de documents AGARD (y compris les demandes faites auprès du CASI) doivent comporter la dénomination AGARD, ainsi que le numéro de série d'AGARD (par exemple AGARD-AG-315). Des informations analogues, telles que le titre et la date de publication sont souhaitables. Veuiller noter qu'il y a lieu de spécifier AGARD-R-nnn et AGARD-AR-nnn lors de la commande des rapports AGARD et des rapports consultatifs AGARD respectivement. Des références bibliographiques complètes ainsi que des résumés des publications AGARD figurent dans les journaux suivants:

Scientifique and Technical Aerospace Reports (STAR)
publié par la NASA Scientific and Technical
Information Program
NASA Headquarters (JTT)
Washington D.C. 20546
Etats-Unis

Government Reports Announcements and Index (GRA&I)
publié par le National Technical Information Service
Springfield
Virginia 22161
Etats-Unis

(accessible également en mode interactif dans la base de données bibliographiques en ligne du NTIS, et sur CD-ROM)

AGARD

NATO ⊕ OTAN

7 RUE ANCELLE · 92200 NEUILLY-SUR-SEINE

FRANCE

Telefax (1)47.38.57.99 · Telex 610 176

DISTRIBUTION OF UNCLASSIFIED AGARD PUBLICATIONS

AGARD holds limited quantities of the publications that accompanied Lecture Series and Special Courses held in 1993 or later, and of AGARDographs and Working Group reports published from 1993 onward. For details, write or send a telefax to the address given above. *Please do not telephone.*

AGARD does not hold stocks of publications that accompanied earlier Lecture Series or Courses or of any other publications. Initial distribution of all AGARD publications is made to NATO nations through the National Distribution Centres listed below. Further copies are sometimes available from these centres (except in the United States). If you have a need to receive all AGARD publications, or just those relating to one or more specific AGARD Panels, they may be willing to include you (or your organisation) on their distribution list. AGARD publications may be purchased from the Sales Agencies listed below, in photocopy or microfiche form.

NATIONAL DISTRIBUTION CENTRES

BELGIUM
Coordonnateur AGARD — VSL
Etat-Major de la Force Aérienne
Quartier Reine Elisabeth
Rue d'Evere, 1140 Bruxelles

CANADA
Director Scientific Information Services
Dept of National Defence
Ottawa, Ontario K1A 0K2

DENMARK
Danish Defence Research Establishment
Ryvangs Allé 1
P.O. Box 2715
DK-2100 Copenhagen Ø

FRANCE
O.N.E.R.A. (Direction)
29 Avenue de la Division Leclerc
92322 Châtillon Cedex

GERMANY
Fachinformationszentrum
Karlsruhe
D-7514 Eggenstein-Leopoldshafen 2

GREECE
Hellenic Air Force
Air War College
Scientific and Technical Library
Dekelia Air Force Base
Dekelia, Athens TGA 1010

ICELAND
Director of Aviation
c/o Flugrad
Reykjavik

ITALY
Aeronautica Militare
Ufficio del Delegato Nazionale all'AGARD
Aeroporto Pratica di Mare
00040 Pomezia (Roma)

LUXEMBOURG
See Belgium

NETHERLANDS
Netherlands Delegation to AGARD
National Aerospace Laboratory, NLR
P.O. Box 90502
1006 BM Amsterdam

NORWAY
Norwegian Defence Research Establishment
Attn: Biblioteket
P.O. Box 25
N-2007 Kjeller

PORTUGAL
Força Aérea Portuguesa
Centro de Documentação e Informação
Alfragide
2700 Amadora

SPAIN
INTA (AGARD Publications)
Pintor Rosales 34
28008 Madrid

TURKEY
Millî Savunma Başkanlığı (MSB)
ARGE Daire Başkanlığı (ARGE)
Ankara

UNITED KINGDOM
Defence Research Information Centre
Kentigern House
65 Brown Street
Glasgow G2 8EX

UNITED STATES
NASA Headquarters
Attention: CF 37, Distribution Center
300 E Street, S.W.
Washington, D.C. 20546

The United States National Distribution Centre does NOT hold stocks of AGARD publications.
Applications for copies should be made direct to the NASA Center for Aerospace Information (CASI) at the address below.

SALES AGENCIES

NASA Center for
Aerospace Information (CASI)
800 Elkridge Landing Road
Linthicum Heights, MD 21090-2934
United States

ESA/Information Retrieval Service
European Space Agency
10, rue Mario Nikis
75015 Paris
France

The British Library
Document Supply Centre
Boston Spa, Wetherby
West Yorkshire LS23 7BQ
United Kingdom

Requests for microfiches or photocopies of AGARD documents (including requests to CASI) should include the word 'AGARD' and the AGARD serial number (for example AGARD-AG-315). Collateral information such as title and publication date is desirable. Note that AGARD Reports and Advisory Reports should be specified as AGARD-R-nnn and AGARD-AR-nnn, respectively. Full bibliographical references and abstracts of AGARD publications are given in the following journals:

Scientific and Technical Aerospace Reports (STAR)
published by NASA Scientific and Technical
Information Program
NASA Headquarters (JTT)
Washington D.C. 20546
United States

Government Reports Announcements and Index (GRA&I)
published by the National Technical Information Service
Springfield
Virginia 22161
United States
(also available online in the NTIS Bibliographic
Database or on CD-ROM)